FIC domain toxins are the origin of intra- and inter-kingdom effectors of *Bartonella*

Inauguraldissertation

zur

Erlangung der Würde eines Doktors der Philosophie

vorgelegt der

Philosophisch-Naturwissenschaftlichen Fakultät

der Universität Basel

von

Alexander Harms

aus Deutschland

Basel, 2016

Originaldokument gespeichert auf dem Dokumentenserver der Universität Basel

edoc.unibas.ch

Dieses Werk ist lizenziert unter einer Creative Commons

Namensnennung – Keine Bearbeitungen 4.0 International Lizenz.

Genehmigt von der Philosophisch-Naturwissenschaftlichen Fakultät

auf Antrag von

Prof. Christoph Dehio

Prof. Urs Jenal

Basel, den 09.12.2014

Prof. Dr. Jörg Schibler

(Dekan)

für Julia

“Natural selection (…) does not work as an engineer works. It works like a tinkerer - a tinkerer who does not know exactly what he is going to produce but uses whatever he finds around him whether it be pieces of string, fragments of wood, or old cardboards (…). In contrast with the engineer's tools, those of the tinkerer cannot be defined by a project. What these objects have in common is ‘it might well be of some use.’ For what? That depends on the opportunities.”

François Jacob, French biologist and Nobel laureate, in “Evolution and tinkering”. Science, Volume 196, Number 4295, 10 June 1977, 1161-1166 (quotation continues ahead of the *Perspective* section).

Statement to my Thesis

This work was carried out in the group of Prof. Christoph Dehio in the Focal area Infection Biology at the Biozentrum of the University of Basel. My PhD thesis committee consisted of:

Prof. Christoph Dehio

Prof. Urs Jenal

Prof. Tilman Schirmer

I constructed my thesis in a cumulative format. It contains a broad introductory section followed by results chapters that are each dedicated to one article or coherent sets of unpublished data. My thesis contains in total six articles of which two are published review articles, another two are published research articles, and each one additional research article has been submitted or is under preparation, respectively. The different threads of research are taken up in a concluding “perspective” section that combines them in a working model and proposes the direction of future studies.

1. Abstract

Abstract

Bacterial secretion systems are machineries that allow one cell to take direct control of molecular processes in another one so that they are ubiquitously involved in the host interaction of mutualistic, commensal, and pathogenic bacteria. However, the evolutionary origin of these systems lies in genuine bacterial machineries. One of the most well-studied host-interacting secretion systems is the type IV secretion system (T4SS) that originally evolved to mediate bacterial conjugation, i.e., the interbacterial transfer of DNA. During conjugation, the DNA is transferred covalently linked to a protein called relaxase that is the actual substrate of the type IV secretion machinery.

It is the common focus of most studies that come together in this thesis to unravel the adaptive path by which the host-interacting VirB/D4 T4SS of *Bartonella* and its secreted effectors evolved from conjugative ancestors. In short, these studies allowed to propose a two-step model in which an ancestral conjugation machinery first acquired an interbacterial effector protein and was later exapted for host interaction which resulted in the evolution of the VirB/D4 T4SS.

In *Review article I* we comprehensively reviewed available literature regarding the molecular pathogenesis of the α-proteobacterial pathogen *Bartonella* and concluded that different phylogenetic lineages of this genus use partially divergent sets of virulence factors for essentially the same stealth infection strategy. Though the overall course of infection in their respective mammal reservoir hosts is similar, the bartonellae showed major differences in their host adaptability that correlated with the presence of the VirB/D4 T4SS in the promiscuous lineages. This machinery contributes to *Bartonella* virulence by secreting a cocktail of effector proteins (Beps) into mammalian host cells where they manipulate cellular signaling processes in favor of the pathogen. Previous studies had shown that all effectors of the VirB/D4 T4SS evolved from a single common ancestor that consisted of a FIC protein domain fused to a conserved type IV secretion signal which is also the most prevalent domain architecture among extant Beps. FIC domains are enzymatic domains that typically mediate adenylylation, the transfer of an adenosine 5'-monophosphate onto target proteins, suggesting that a prototypic effector of the VirB/D4 T4SS may have targeted host proteins by post-translational modification. Interestingly, a bacterial conjugation system called Vbh T4SS had been discovered in *Bartonella* and is encoded on a plasmid together with a Bep-like protein consisting of FIC domain and type IV secretion signal that had been named VbhT.

In *Research article I* we investigated the phylogeny and regulation of Fic proteins (i.e., proteins containing FIC domains) and found that their adenylylation activity is controlled by a conserved mechanism of active site obstruction via an inhibitory α-helix (α_{inh}). Depending on the positioning of α_{inh} either in a separate polypeptide or N- or C-terminally of the FIC domain in the same protein we classified FIC domain proteins as class I, class II, and class III,

respectively. Fic proteins have repeatedly evolved into bacterial virulence factors, but the far majority of them are genuine bacterial proteins of unknown function. We showed that the mutational activation of bacterial Fic proteins of all three classes by abrogation of active site obstruction results in bacterial growth inhibition, suggesting that most Fic proteins may be some kind of toxins. Interestingly, the elusive Bep-like VbhT protein of the Vbh T4SS was found to inhibit bacterial growth via target adenylylation unless it is inhibited by a small protein VbhA that contains the α_{inh}.as a hallmark of class I Fic proteins. This arrangement is reminiscent of toxin-antitoxin (TA) modules that are genetic elements consisting of a toxin that inhibits bacterial growth and an antitoxin that suppresses the toxin's activity but can unleash it in order to induce a phenotypic switch to the dormant persister state.

In *Review article II* we firmly established that class I Fic proteins form a new toxin-antitoxin (TA) module FicTA with FicT toxins being homologous to the VbhT FIC domain and FicA antitoxins being homologous to VbhA. A follow-up study described in *Research article III* characterized the FicTA toxin-antitoxin module and discovered that FicT toxins inhibit bacterial growth via the adenylylation and concomitant inactivation of DNA gyrase and topoisomerase IV (topo IV), the two bacterial type IIA topoisomerases. The resulting disruption of cellular DNA topology induced a phenotypic switch to the persister state. Although an important role of TA modules in persister formation is well established, previously known TA systems invariably induced dormancy by inhibiting translation or unsetting the proton-motive force. Our results therefore uncovered a new physiological path to the persister state that is likely involved in the inherent physiological heterogeneity of persisters as a main obstacle to their eradication. Furthermore, we found that the Vbh T4SS in *Bartonella* is sometimes associated to a functional FicTA module that is encoded at the locus where VbhTA would be expected but shows no trace of a type IV secretion signal.

The concluding *Perspective* section of this work combines the results of the aforementioned articles with a considerable amount of unpublished data and proposes a model that can explain the evolution of the VirB/D4 T4SS and its effectors in *Bartonella* from conjugative ancestors. In short, it is evident that an ancestral conjugative T4SS as well as a FicTA module (supplying the FIC domain for effector evolution) entered the genus *Bartonella* via horizontal gene transfer, though likely not together. After sequence reshuffling events had resulted in a *ficAT* locus encoded next to a conjugative Vbh-like machinery (like in some extant bartonellae), one of the two type IV secretion signals of the relaxase was transferred onto the FicT toxin via terminal reassortment and created a situation identical to the Vbh T4SS with VbhT. Based on additional evidence, we propose that extant Vbh T4SS and VbhT represent such an ancestral evolutionary state as a "living fossil". Furthermore, we suggest that VbhT is an interbacterial effector that is secreted via the Vbh T4SS during bacterial

conjugation in order to promote complementary strand synthesis in the recipient. Like this, the Vbh T4SS with VbhT constitutes a “missing link” in the evolution of the host-interacting, effector secreting VirB/D4 T4SS from purely conjugative ancestors. The remarkable sequence similarity between Vbh T4SS and VbhT on one side and the VirB/D4 T4SS and Beps on the other side suggests that such a conjugative machinery with interbacterial effector may have been exapted for host interaction in a second step. During that process, a primordial *vbhT*-like effector gene served as the template for a series of gene duplication and diversification events that created the extant effector repertoires by gradual evolution. The different paralogous effectors created by this process were generally suspected to have different roles in host interaction. Among other evidence, I could show earlier that one effector (Bep1) targets the host protein Rac1 by adenylylation. In *Research article II* we followed up on these results and identified the adenylylated target of another effector, called Bep2, as vimentin. For this purpose we had developed a new technique that identifies adenylylated target proteins by mass spectrometry using a characteristic pattern of peaks upon adenylylation with a mixture of heavy-isotope labeled ATP. Together with additional data of others and myself, these results suggest that the diversified effector repertoires of the VirB/D4 T4SS evolved to promote the stealth infection strategy of *Bartonella* by fine-tuned manipulations of host cell signaling. In particular, the modular architecture of both the type IV machinery and its effectors conferred an inherent evolvability that is likely involved in the remarkable host adaptability of those bartonellae that encode VirB/D4 T4SS and effectors.

The most important open point in this model is the biological function of VbhT as the first *bona fide* interbacterial type IV secretion effector. Future studies should address a possible role of VbhT in bacterial conjugation in order to strengthen the claim of a “missing link”.

In *Research article IV* we expanded the understanding of FIC domain proteins without obvious connection to *Bartonella.* This study was focused on NmFicT of *Neisseria meningitidis* as a model for class III Fic proteins that encode the α_{inh} at their C-terminus, but contain no additional domains or modules for their regulation. We reported strong evidence for a model in which NmFicT is controlled by a double-lock mechanism where the first level of control is tetramerization that generates an inactive storage form of the protein. Upon an unknown trigger, NmFicT monomers would be freed from oligomerization and then remove the second lock via intermolecular auto-adenylylation which abolishes α_{inh} –mediated active site obstruction and unleashes the full catalytic activity of NmFicT. Furthermore, we showed that activated NmFicT adenylylates DNA gyrase at the same residue as FicT toxins, though these also adenylylate topo IV and primarily inhibit the latter target *in vivo*. The biological function of NmFicT is unclear, but may be related to DNA repair and protection as described for other proteic gyrase inhibitors.

2. Table of content

3. Aim of the Thesis

I started my PhD work in February 2011 with the aim to understand the explosive radiations of *Bartonella* species that had been triggered subsequent to the acquisition of host-interacting type IV secretion systems (T4SS). More precisely, it was my aim to unravel the adaptive path that transformed an ancestral conjugative T4SS into the effector-secreting and host-interacting VirB/D4 type IV secretion system.

For that purpose, I performed a biochemical and functional analysis of effectors secreted by the VirB/D4 T4SS as well as the more ancestral Vbh (VirB-homologous) T4SS. Furthermore, I traced back the evolutionary origin of these effectors to a group of bacterial FIC domain proteins with no connection to type IV secretion and investigated the effectors and their ancestors using a wide range of microbiological techniques and structure-function analyses. Finally, I combined and interpreted my results to form a coherent model that describes how a primordial effector of an ancestral Vbh-like T4SS was generated *de novo.* Additionally, the model delineates how the secretion machinery and its effector repertoire co-evolved with their *Bartonella* host in two major steps into the extant VirB/D4 T4SS that promoted *Bartonella* evolution as a superior tool for host interaction.

4. About this work

The broad scope of my PhD project and its somehow paleo-microbiological topic implied that a wide range of techniques would be used and that, with increasing distance to *Bartonella* effectors, also a wide range of poorly connected fields of research were to be explored.

In consequence, the theoretical and practical focus of this project shifted over time and comprised diverse topics such as toxin-antitoxin systems, protein evolution, DNA topology, and bacterial persistence, on top of research directly targeting *Bartonella*. For this reason I chose to assemble my PhD thesis in a cumulative format. Furthermore, the *Introduction* section had to be more selective and less comprehensive as it would have been appropriate in a contentually more restricted work, though a certain ample thoroughness inherent to the thesis format was of course implemented. The different *Research articles* forming the *Results* section each have a separate, more comprehensive introduction and are accompanied by *Review articles* that go deeper into their respective subjects. Readers with a primary interest in the big picture may appreciate the short *Summary* preceding each article, but should still have a brief look at *Unpublished Results* presented after the different sections. A concluding *Perspective* at the end of this work combines the different threads of research to form a coherent model of *Bartonella* / type IV secretion system coevolution.

5. Introduction

5.1.Toxin-antitoxin modules

5.1.1. Biological functions and classification of TA modules

5.1.1.1. Classification and general features

Bacterial toxin-antitoxin (TA) modules comprise a toxin that blocks bacterial growth via the inactivation of essential cellular functions and an antitoxin that protects the cell from the toxin's activity. So far, five general types of TA modules have been defined based on the mode of action of the antitoxin (Figure 1A):

- In type I TA modules the antitoxin is an RNA that prevents translation of the toxin, typically by antisense interaction with the toxin mRNA (e.g., Hok/*sok*[12] or TisB/*istR*[13]).
- In type II TA modules the antitoxin is a protein that inhibits the toxin's activity via a direct interaction (e.g., RelBE[14] or Doc/Phd[15]).
- In type III TA modules the antitoxin is an RNA that inhibits the toxin's activity via a direct interaction (e.g., ToxIN[16] or TenpIN[17]).
- In type IV TA modules the antitoxin is an RNA that interferes with the inactivation of cellular functions by the toxin in the absence of a direct interaction (e.g., CbeA-CbtA[18] or AbiEi/ii[19])
- In type V TA modules the antitoxin is a protein that prevents translation of the toxin by degrading its mRNA (GhoST[20]).

Within the most abundant group of type II TA modules the nomenclature is systematically oriented at the different classes of toxins according to their fold and primary sequence, though a more simple terminology just by locus or toxin-antitoxin combination is prevalent in the literature. It is important to note that the same toxin "superfamily" can exhibit different molecular activities (e.g., poisoning of gyrase and cleavage of mRNAs for the CcdB / MazF family) and that toxin-antitoxin associations are rather flexible on a global scale[21] (Figure 1B).

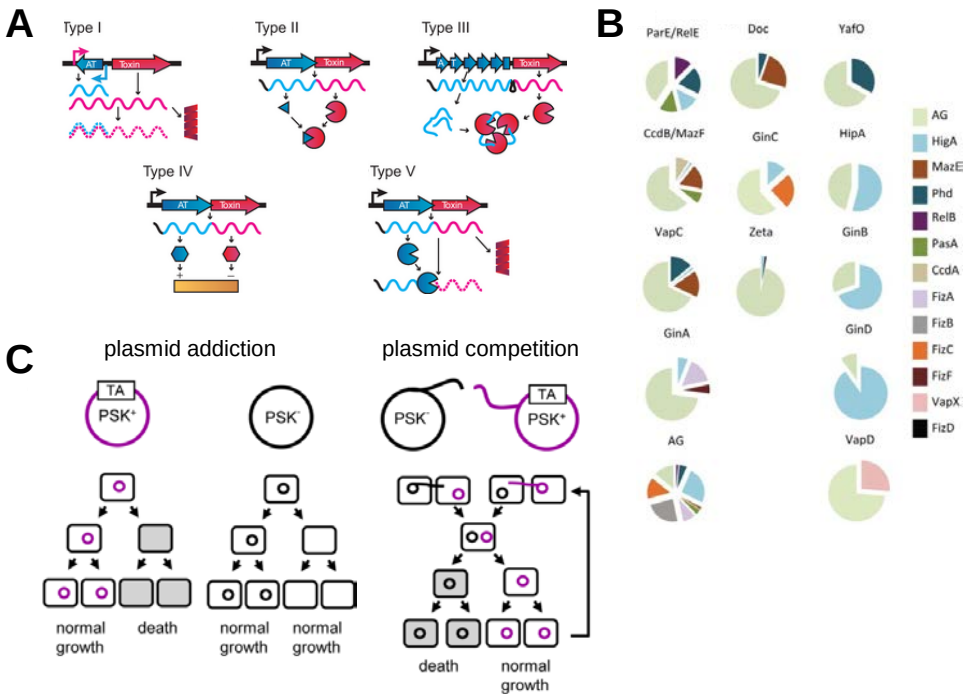

Figure 1: Introduction to toxin-antitoxin modules. A) Nomenclature of TA modules by the mechanism of antitoxin inhibition. Toxin and antitoxin (AT) are depicted in red and blue, respectively. See the running text for details (adapted from Schuster and Bertram[22]). **B)** Toxin-antitoxin associations of the twelve type II TA toxin superfamilies identified by a comprehensive bioinformatics study[21]. Toxin classes are shown as pie diagrams with the different antitoxin classes identified by color code (taken from Leplae *et al.*[21]). Novel toxin superfamilies that the authors identified *in silico* and validated experimentally are shown as GinA-D (growth inhibition). AG (associated by guilt) denotes novel, smaller families of toxins or antitoxins that are genetically associated to given toxin or antitoxin families. **C)** Plasmid addiction and plasmid competition model of post-segregational killing (taken from Van Melderen and de Bast[23]).

The toxins of TA modules interfere with various aspects of bacterial physiology by manipulating a plethora of cellular targets in any imaginable molecular way (see table I and the recent review by Unterholzner *et al.*[24]). Of those systems that have been investigated in detail, many act via the inhibition of translation at any step which has also been proposed to be the predominant type in general[21], but this conclusion may also be a sign of sampling bias or simply our limited understanding of the diversity of toxin-antitoxin modules. Typically, toxin and antitoxin are encoded together in a two-gene operon with the antitoxin being upstream, often featuring a few nucleotides of overlap between the open reading frames[25]. Together with transcriptional autoregulation via conditional cooperativity (see below) these genetic arrangements ensure that the antitoxin is always produced in excess of the toxin under usual conditions so that the default state of a TA module is “off”[26].

Name	type	Molecular activity of toxin	General concept	Biological function
RelBE[27] **YefM/YoeB**[28]	II	Ribosome-dependent mRNA endonuclease	Inhibition of translation	Persister formation
HicAB[29] **MazEF**[30] **MqsRA**[31]	II	Ribosome-independent mRNA endonuclease		
Doc/PhD[a,33,34]	II	Phosphorylation and inhibition of elongation factor TU (EF-Tu)		
HipAB[35]	II	Phosphorylation and inhibition of glutamyl-tRNA synthetase (GltX)		
VapBC[36]	II	Cleavage of initiating tRNA(fMet)		
VapBC20[37]	II	Cleavage of 23S rRNA at sarcin-ricin loop		
RatBA[38] **PasTI**[39]	II	Prevention of 70S ribosome assembly		
TisB/*istR*[13]	I	Disruption of membrane potential / proton-motive force	Abrogation of ATP synthesis	
GhoST[20]	V			
Hok/*sok*[40]	I			Post-segregational killing
CcdBA[41] **ParDE**[42]	II	Gyrase poisoning	DNA fragmentation	
AbiEii/AbiEi[19] **SanaTA**[43,44]	IV	Unknown (likely guanylylation)	Unknown	Abortive infection
AbiQ[45] **ToxIN**[46]	III	Ribosome-independent mRNA endonuclease	Inhibition of translation	
CptIN[17]	III	Unknown	Unknown	
TenpIN[17]	III	Unknown	Unknown	
ζ/ε[47] **("zeta / epsilon")**	II	Phosphorylation of peptidoglycan precursor UNAG	Cell lysis	unknown
CbeA/CbtA[18] **CptBA**[48]	IV	Interaction with MreB and FtsZ and inhibition of their polymerization	Inhibition of cell division	Stress tolerance (?)
SocAB[49]	n.a.	Binding to β sliding clamp DnaN	Inhibition of DNA replication	unknown

Table 1: List of diverse TA modules and their molecular activities and biological functions. The formal type of the TA module is indicated in Roman numerals. This table is by far not exhaustive (e.g., in listing type II TA endonucleases) and the degree of how safely biological functions have been assigned to different TA modules varies (e.g., abortive infections with CptIN have not been directly demonstrated). Further information is provided in the following paragraphs of the *Introduction* section and the reader is referred to a rich literature of dedicated reviews[22,24,26,50].

[a] The most well-investigated Doc-Phd module of bacteriophage P1 was described as a post-segregational killing system[32], but the homolog in *Salmonella* Typhimurium plays an important role for persister formation[33].

A switch to the "on"-state is achieved by a massive drop of the antitoxin / toxin ratio that frees a sufficient number of toxin molecules from antitoxin control. For example, the type I TisB/*istR* system is activated by the SOS response (see Box 1) which promotes degradation of the *istR* RNA antitoxin and in parallel up-regulates the expression of the TisB toxin[13] (compare Figure 1A). In case of type II TA modules the activation occurs via antitoxin degradation by specific proteases that respond to cellular signaling (recently reviewed by Brzozowska and Zielenkiewicz[51]). Most type II TA modules in *Escherichia coli* and related bacteria are under control of the protease Lon that is classically activated by starvation signaling via the second messenger ppGpp[52] (Figure 3B). However, the activation of Lon can also be triggered by other clues where the path of molecular signaling is less clear such as oxidative stress[53] or bacteriophage infection (see recent work by the Sorek lab and literature cited therein[43]). Apart from Lon, a minority of type II TA modules in *E. coli* are under the control of the ClpP protease[54,55], and dual degradation by both proteases has also been reported[56,57]. Notably, in other organisms such as gram-positives, ClpP and not Lon seems to be the main player in antitoxin degradation[58,59].

Box 1: The bacterial SOS response. The SOS regulon is a transcriptional program that gets activated in response to single-stranded DNA (ssDNA) in the bacterial cytoplasm which is an indicator of DNA damage. The SOS response is induced by the RecA protein that gets loaded on ssDNA by one of two presynaptic complexes, the RecBCD complex (acting on double-stranded DNA (dsDNA) ends) and the RecFOR complex (acting on ssDNA gaps). RecA loading results in the formation of a RecA-nucleofilament that promotes the auto-proteolysis of the LexA transcriptional repressor. LexA prevents the expression of SOS genes by tight binding to a cognate LexA box sequence in their promoters with different affinity. Therefore, increasing or persisting DNA damage causes the continuous degradation of LexA which activates more and more genes of the SOS response depending on the potency of their LexA box. In *E. coli*, approximately 40 genes belong to the SOS response and encode factors that are primarily involved in different pathways of DNA repair and recombination. Furthermore, the lytic programs of lysogenic bacteriophages as well as the activation of various other mobile elements are typically wired to the SOS response (see reviews by Baharoglu and Mazel[7] or Erill *et al*.[9]. Note that the formation of RecA filaments does not only trigger the SOS response but also initiates homologous recombination as part of the recombinational repair program[11].

5.1.1.2. Biological functions of TA modules

The first function of toxin-antitoxin systems described in literature was the stabilization of mobile replicons via post-segregational killing (PSK) as so-called addiction modules[60]. The concept of this "addiction" was envisioned in a way that, upon loss of a replicon encoding an addiction module, the rapid degradation of an intrinsically labile antitoxin would activate the more stable toxin and kill the host (see the scheme in Figure 1C and the comparative work of Jensen *et al.*[61]). Though intuitive at first glance, the general concept of acting as a plain "addiction module" has been refuted in more recent days in favor of a competitive function

where the TA module does not act in host-plasmid competition, but in plasmid-plasmid competition to eliminate incompatible replicons[62,63] (see Figure 1C). Some TA modules acting in this context (e.g., CcdBA[64]) are the only ones where a bactericidal mode of action *in vivo* is more or less undisputed.

In any case, the concept of PSK is unable to explain the remarkable abundance of TA loci on the chromosomes of all free-living bacteria which suggests that the action as "addiction modules" cannot be the primary function of toxin-antitoxin systems[65,66]. Instead, the field has now come to the conclusion that TA modules have important biological functions as abortive infection systems (triggering an altruistic suicide upon bacteriophage infection) or by promoting bacterial persistence, the ability to endure theoretically lethal conditions in a dormant state (see below). On top of these two main functions it is not surprising that secondary, specialized adaptations of some TA modules to other biological roles have been described, e.g., the control of gene expression via the differential degradation of mRNAs in the case of RNA endonuclease toxins (recently reviewed by Bertram and Schuster[67]) or different direct and indirect mechanisms influencing biofilm formation (see the review of Wang and Wood and rich literature cited therein[68]).

Bacteriophages are ubiquitous in the environment and constitute a major evolutionary pressure for the bacteria that they infect, particularly since their rapid evolution allows them to frequently outpace their hosts in a coevolutionary arms race (see also the essay by Stern and Sorek[69]). Therefore, it is not surprising that bacteria evolved a whole arsenal of systems to block any step of phage infection from initial adhesion to the takeover of cellular machineries[44,70,71]. Among these, abortive infection (Abi) systems get activated upon bacteriophage infection and then prevent host takeover via elimination of the infected cell in some kind of altruistic "scorched earth strategy" (see Figure 2A). Interestingly, it has become clear that a number of Abi systems are simply specialized TA modules responding to bacteriophage infection[16,17,19,43,45,56,72] (see Figure 2B), but the nominal discrimination between "Abi systems" and "toxin-antitoxin systems" acting in phage defense is maintained by some authors in the field for historical reasons (see, e.g., the recent review by the Fineran lab[44]). In most cases it is not known how bacteriophage infection provides a signal for the activation of Abi toxins, but some Abi systems were shown to respond to the presence of specific phage proteins or phage-induced changes in cellular physiology[44]. Mechanistically, a few Abi toxins have activities similar to those of other TA module toxins including mRNA degradation[46,56] and unsetting of the proton-motive force[73], but the molecular function of most Abi toxins is unknown. Ecological studies found that the Abi concept of altruistic suicide is quite effective in limiting the spread of phage infections[74], but bacteriophages have evolved master key antitoxins[75] as well as potent protease-inhibitors that prevent toxin

activation[43,76,77] to overcome abortive infection. Furthermore, even the *de novo* evolution of an Abi antitoxin in a phage genome has been reported[78], suggesting that Abi modules can always be only one piece in the bacterial defense line next to restriction-modification systems and different other active or passive strategies[44,79]. In addition to these TA modules that evolved for bacteriophage defense, a number of TA modules that are believed to have distinct primary functions can also exert abortive infection, likely because signaling triggered upon phage infection happens to inactivate their antitoxin[80,81].

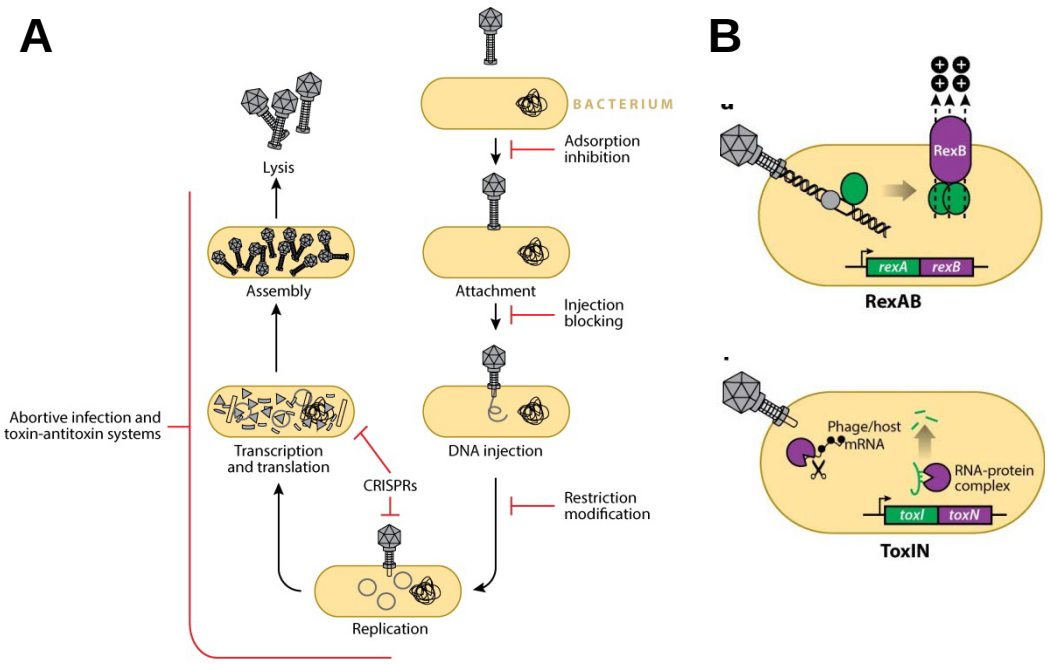

Figure 2: Abortive infection by TA modules. A) Action of abortive infection (Abi) systems during phage infections compared to other mechanisms of antiviral defense. **B)** Two examples of Abi systems of which RexAB (top) acts different from TA modules in that RexA senses phage infection and then activates RexB, an ion channel disrupting the membrane potential. ToxIN is a type III TA module that gets activated upon bacteriophage infection and causes abortive infection via the RNA endonuclease activity of the ToxN toxin. Both panels were adapted from the recent review by Dy *et al.*[44].

Next to abortive infection, the second main biological role of TA modules is to act as phenotypic switches into the persister state (see *Toxin-antitoxin modules and bacterial persistence* below). In short, the activation of TA modules in response to certain triggers or stochastically in the population can induce a state of dormancy in which the bacteria do not grow but are highly tolerant to perturbations such as antibiotic treatment or immune functions[82]. Sacrificing a small subpopulation for stochastic persister formation constitutes a pre-adaptation of the community to sudden threats as a bet-hedging strategy and can thus be seen as a "social trait"[83]. Therefore, it is interesting to note that - although they had initially been described as mediators of "selfish" behavior in different ways – TA modules appear to mostly promote altruistic behavior in form of abortive infection and persister formation.

During my PhD project I got interested in toxin-antitoxin systems because proteins representing a deeply ancestral state to effectors secreted by Vbh and VirB/D4 machineries of *Bartonella* turned out to show features of TA modules (see details in *Research article I*). Further investigations revealed a new class of toxin-antitoxin modules and biological functions in the context of bacterial persistence (see *Review article II* and *Research article III*).

5.1.2. TA modules and bacterial persistence

Bacterial persisters are phenotypic variants that display vastly increased stress tolerance via perseverance in a slow- or non-growing state which has been described as "dormancy"[35,42] (Figure 3A). Persister cells are notorious for their multidrug tolerance and, particularly if arising within biofilms, their resilience to clearance by the immune system[84-87]. Although persistence is a purely phenotypic phenomenon[a], the ability to form persister cells is genetically programmed in toxin-antitoxin modules that act as the switches into dormancy[b,33,91]. Importantly, persisters do not only survive lethal concentrations of antibiotics in laboratory test tubes but are important for the strategy of various pathogens to sustain chronic infections inside a hostile host. Many examples of TA-driven persistence of bacterial pathogens *in vivo* have been published, e.g., for *Salmonella* Typhimurium[33,92], *Haemophilus influenzae*[93,94], and uropathogenic *E. coli*[39]. It is likely that these cases are merely the proverbial tip of the iceberg, since the frequent redundancy of TA modules in a given bacterium often makes it difficult to pinpoint causal relationships. One example for such an organism is *Mycobacterium tuberculosis* whose around 80 TA modules have been proposed to play a critical role during its infamously persistent infections[95,96]. As a prerequisite for improved treatment options it is therefore important to understand how persisters are generated by toxin-antitoxin modules and which physiological changes in the bacterial cell allow persisters to survive under lethal conditions.

[a] Though persistence itself is by definition phenotypic, persisters can „behave as an evolutionary reservoir from which (genetically, A.H.) resistant organisms can emerge" (discussed by Cohen *et al.*[88]).

[b] Depending on the organism and the environmental circumstances, factors beyond TA modules can play more or less important roles. For example, *Pseudomonas aeruginosa* – notorious for its persistent infections – encodes only very few TA modules and seems to primarily rely on other mechanisms for persister formation[65,89,90].

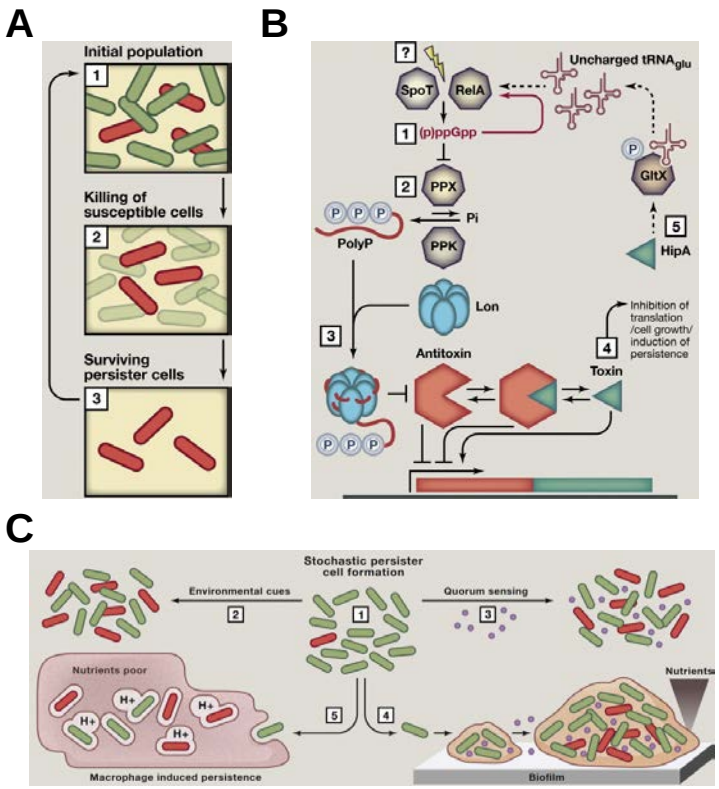

Figure 3: Bacterial persister formation. A) Persister cells (red) are rare phenotypic variants that ensure survival of the population by tolerance to lethal stresses ("bet-hedging strategy"). **B)** Type II TA modules in *E. coli* and related bacteria are typically under the control of protease Lon. Lon gets activated by polyphosphate (PolyP) which is produced in response to the second messenger (p)ppGpp, a mediator of starvation signaling. The HipA toxin induces ppGpp signaling, making it a powerful switch to the persister state. **C)** Stochastic (1) and deterministic (2-5) stimuli inducing persister formation. Persistence can be triggered by environmental signals (2), quorum sensing (3), biofilm formation (4), or phagocytosis by host cells (5). All illustrations were taken from the recent review by Maisonneuve and Gerdes[82].

5.1.2.1. A switch to dormancy is genetically programmed in TA modules

Both the dormant state that is characteristic of persisters and the transient as well as bistable nature of persistence in bacterial populations can be explained with inherent features of toxin-antitoxin modules: Beginning in the "off" state of the TA module, upstream signaling can induce a massive drop of the antitoxin / toxin ratio (e.g., by promoting antitoxin degradation) and consequently shift the cellular level of toxin activity above the threshold required for a phenotypic switch to dormancy. In this state, the bacteria persist until the recovery of antitoxin inhibition resuscitates growth[97,98]. Persister cells are constantly generated as a small subpopulation in bacterial communities in response to stochastic internal stimuli like the fluctuation of ppGpp levels in *Escherichia coli* which control the activity of the antitoxin-targeting protease Lon[52] (see Figure 3B). The resulting bistability between a majority of growing cells and a few non-growing persisters is maintained by transcriptional control via conditional cooperativity which enables low random induction, strong amplification of stochastic signals, and quick removal of free toxin once the inducing signal is gone[5,6,98] (see Box 2). This heterogeneity ensures survival of the bacterial population in form of pre-

formed persisters that can endure rare, unpredictable threats following a "bet-hedging strategy" that is favored over adaptive "sensing" strategies under these conditions[97,99,100]. In addition to stochastic stimuli, persisters can also be generated in a deterministic manner by any signaling that causes the activation of TA modules, particularly sublethal levels of stress. As an example, the type I toxin TisB of *E. coli* is part of the SOS regulon and can therefore initiate persister formation in response to DNA damage[101,102] (see also Box 1). Similarly, a whole arsenal of TA modules is activated in *Salmonella* Typhimurium upon entry into phagocytic vesicles in response to starvation and vacuole acidification to promote intracellular persistence[33] (Figure 3C). Another important trigger of TA module activation and persister formation is oxidative stress (via the activation of proteases Lon and ClpP)[53,103]. Additionally, the rate of persister formation is dependent on the bacterial growth state with elevated frequencies of persisters in stationary phase and within biofilms where persisters appear to be responsible for their notorious drug tolerance[52,86,104,105]. The concept of stochastic and deterministic persister formation is illustrated in Figure 3C.

Box 2: Conditional cooperativity. The joint regulation of type II TA locus expression by toxin-antitoxin complexes of different stoichiometry is called conditional cooperativity. Depending on the ratio of toxin and antitoxin, the toxin can either act as a co-repressor (excess antitoxin) or a net-activator (excess toxin) of TA transcription, though the precise molecular mechanism differs between TA modules[1-3]. Consequently, conditional cooperativity dampens the expression of TA loci in the absence of activating stimuli to minimize their metabolic cost[4]. The onset of antitoxin degradation does not only result in toxin activation, but at the same time induces expression of the TA locus (thereby producing more toxin) because transcriptional repression is relieved. Strong transcription of TA loci in turn promotes rapid resuscitation of cellular growth by efficient toxin sequestration as soon as antitoxin degradation is abolished. Recent advances in the understanding of conditional cooperativity have been published by Cataudella *et al.*[5,6].

The most well investigated class of toxin-antitoxin systems are type II TA modules where the antitoxin is a protein that inhibits the toxin via direct interaction, and bacterial chromosomes often encode multiple different ones[65]. Interestingly, it has been noted that obligate intracellular bacteria lack type II TA loci, while free-living generalists or pathogens contain vast arsenals. This contrasting pattern can be explained with the propensity of toxin-antitoxin modules to spread via horizontal gene transfer[a] among bacterial communities and their function in the protection against diverse stresses and unpredictably changing environments that are typical threats for free-living prokaryotes[66]. One study even found that a strong accumulation of TA modules in the genome was associated with particularly dangerous, pandemic bacterial pathogens[107], but this could also be a secondary consequence of the infestation with mobile genetic elements during progressing genome deterioration[66,108]. The

[a] Interestingly, dedicated studies showed that type II[21] and type III[17] TA modules are frequently transmitted via horizontal gene transfer, while type I TA modules are not[106]. The reason for this discrepancy is unclear.

model organism *Escherichia coli* K-12 as a host-associated generalist contains at least 37 TA modules of different types[109] and bacteria of the genus *Bartonella* as obligate host-associated parasites typically encode between ten and twenty (type II) TA modules per genome[65] (but see Figure 36 in the *Perspective*). Although some degree of redundancy between TA modules has been observed in *E. coli* and was proposed for organisms with large numbers of them (like *M. tuberculosis*)[91,95], comparative analyses often revealed that even closely related TA modules can have additive effects in various organisms which supports the adaptive role of accumulating TA modules in free-living bacteria[33,39,110] (Figures 4A and 4B). In addition to the different molecular functions of their toxins, the cumulative behavior of TA modules has been proposed to be a consequence of specialization to different upstream signaling[68], though this remains to be shown on a broader scale. However, the main open question in the field of TA-dependent persistence is the nature of the "persistent" state itself beyond its phenotypic outcome of remarkable stress tolerance.

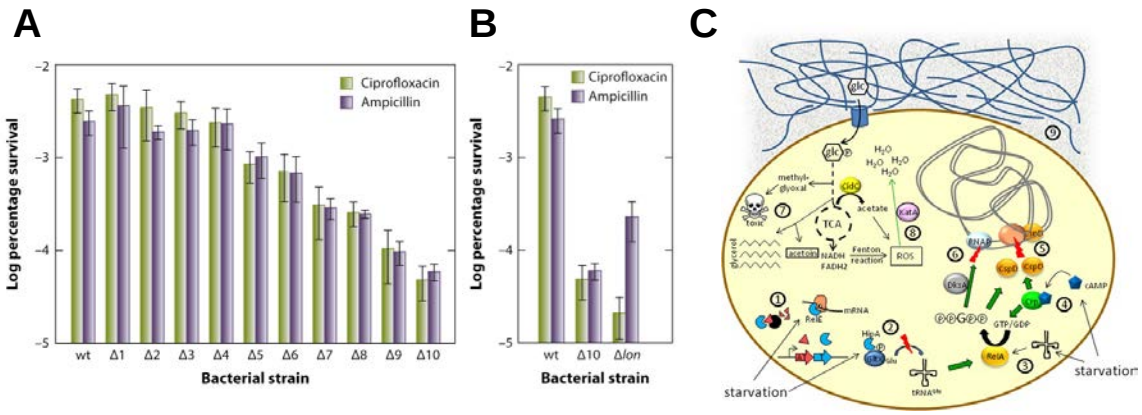

Figure 4: Mechanisms of bacterial persister formation. A) The sequential deletion of ten RNA endonuclease TA toxins in *E. coli* K-12 reveals both redundant (Δ1-4) and cumulative (Δ5-10) behavior of TA modules. **B)** The deletion of *lon* results in a decrease in the proportion of persister cells similar to the deletion of the ten TA modules, illustrating the important role of Lon in type II TA module activation in *E. coli*. **C)** The figure illustrates the various metabolic aspects that have been related to persister formation. Panels (A) and (B) were adapted from Gerdes and Maisonneuve[26] and panel (C) from Prax and Bertram[111].

5.1.2.2. Physiological basis of bacterial persistence

Despite the first description of bacterial persisters already in 1944[112], the physiological basis of this phenomenon has still remained elusive, although our understanding of TA modules as phenotypic switches and their upstream signaling has progressed remarkably (recently reviewed by Maisonneuve and Gerdes[82]). Precisely, it is completely unclear which changes in the cellular physiology would allow bacteria to survive a plethora of unrelated and clearly lethal conditions (discussed in a recent "Viewpoint article" by experts in the field[85]).

In this respect, it is important to note that "persisters are not simply non-growing cells"[87] but represent an evolved, specialized phenotypic state[113]. Transcriptomic studies on persister cells isolated from *E. coli*[114] or *M. tuberculosis*[115] revealed that persisters appeared similar to

exponentially growing cells rather than stationary phase cells, but displayed a strong downregulation of genes related to energy production, while the expression of various TA modules was increased[a]. Consistently, mutants showing sustained upregulation of metabolic functions in both organisms exhibited considerably decreased frequencies of persister formation[116,117]. These results are in line with an important role of TA modules as well as some kind of metabolic rearrangements during persister formation, but they do not point towards the molecular mechanism(s) of multidrug tolerance. Initially, it was proposed that the targets of bactericidal antimicrobials may be inactive in dormant cells and thus not available for lethal poisoning[113]. However, this model appears too simplistic, because it is not supported by the exponential-cell like transcriptomes of persisters and cannot explain why, e.g., TA modules targeting translation can generally protect cells from fluoroquinolones that corrupt DNA gyrase[52,113,118].

Our lack of a conceptual understanding regarding the physiological basis of the persister state is not caused by a lack of studies on the topic: To cite only a few, it was found that different factors such as glycerol-3-phosphate metabolism (though only during stationary phase[119]) and indole signaling[120] are involved in bacterial persistence. Furthermore, protein aggregation can play a role[121], and persistence can be artificially induced by the overexpression of diverse "toxic" proteins[118]. The alternative sigma factor RpoS was shown to be involved in persistence for different organisms (though not under all conditions)[122,123] and is wired to TA modules in *E coli*[103]*.* Additionally, spread-out networks involving the small RNA regulator Hfq, DNA replication inhibitor CspD, and various other factors were reported to mediate persister formation induced by the MqsRA TA module of *E. coli*[53,124]. To add even more complexity, it has recently been shown that a considerable number of these variables are involved in persister formation exclusively in aged or only in fresh cultures of *E. coli*[125]. Clearly, it is impossible to reconcile the results of these studies in the frame of a single "big picture" that would conclusively represent the molecular basis of the persister state (see the recent review on this topic by Prax and Bertram[111] and Figure 4C). Therefore, it has been reasonably argued that there is likely not a single "persister state" and that bacteria employ different, parallel pathways to persistence[126,127], even if one subtracts persisters formed by general cell malfunctioning ("persistence as stuff happens" model (PaSH)[128]). For example, it was shown that metabolic vitalization of the proton-motive force via different sugars enables the killing of persisters by aminoglycosides but not quinolones or β-lactams[129,130]. Similarly, the characteristic metabolic inactivity of persisters is neither necessary nor sufficient for persistence, but simply seems to be a shared feature of many persister cells[33,131].

[a] Interestingly, Shah *et al.* found other TA modules to be upregulated than a second study that investigated a technically different population of persister cells[87].

It is somehow intuitive that the multitude of molecular mechanisms by which TA modules flip the switch to persister formation may be the basis of this heterogeneity of persister cells. This idea is further supported by the observation that, under laboratory conditions, the ectopic expression of various “toxic” proteins and the treatment with diverse drugs can trigger persister formation via mechanisms both related and completely unrelated to the mode of action of known TA modules[118,132]. However, and despite the plethora of different molecular functions that have been reported, the conceptual way by which TA modules induce bacterial persistence have so far been limited to the inhibition of translation or, in a few cases, the abrogation of the proton-motive force[20,27,34,133]. This surprising result suggests that the function of TA modules as a phenotypic switch into dormancy may be defined by a number of physiological constrains so that not various paths, but rather only a few beaten tracks to the persister state exist within bacterial cells. The systematic, comparative analysis of the processes connecting the inhibition of translation or the depolarization of the membrane potential (and possibly others that remain to be discovered) with stress tolerance will reveal the nature of the persister state(s) in molecular details. These findings will be of critical value for the development and improvement of silver bullet drugs that hit persisters based on recent breakthroughs in the field[134].

During my PhD project I contributed to the discovery of a new type II toxin-antitoxin module (see *Research article I* and *Review article II*) that promotes bacterial persistence via a novel molecular pathway, the disruption of cellular DNA topology (see *Research article III*). An additional, toxin-antitoxin-like system with a similar biochemical (and biological?) function is presented in *Research article IV*.

5.2.FIC domain proteins

5.2.1. "filamentation induced by cAMP" in *Escherichia coli*

The acronym "fic" has been introduced by Utsumi *et al.* more than thirty years ago to describe the phenotype of a peculiar mutant of *E. coli* which exhibited "filamentation induced by cAMP"[135] (Figure 5A). Precisely, the temperature-dependent gain-of-function allele *fic-1* of the *fic* gene[136] causes a G55R substitution[137] in the corresponding protein Fic and suppressed cell division at 43°C in the presence of 1.5 mM cAMP. Although a clean deletion of the *fic* gene had no phenotype and revealed that *fic* is "dispensable to the cell"[136], findings that a *fic* deletion mutant became auxotrophic for p-aminobenzoate, a precursor of folic acid, let some researchers speculate that the *fic* gene may be involved in its biosynthesis[138]. Clearly, there is no tenable connection between *fic* and p-aminobenzoate, but the promoter of the downstream gene *pabA* (p-aminobenzoate synthetase) lies partially within the *fic* gene[139]. Although this trivial fact easily explains the auxotrophy of some *fic* deletion mutants (dependent on their construction), an involvement of *fic* homologs in p-aminobenzoate synthesis persists in databases like Pfam (Fic/DOC family being PF02661; accessed last on November 20th 2014) and diverse gene annotations. In addition to *pabA*, the *fic* gene is encoded together with a small ORF called *yhfG* that is positioned upstream of *fic* with a few nucleotides of overlap. This genetic arrangement is immediately reminiscent of TA modules, and while *fic* and *yhfG* homologs generally appear to be encoded together, the local synteny between *yhfg-fic* and *pabA* is only found in *Enterobacteriaceae* (see Figure 19A in the *Unpublished Results related to Research article III*). Consistently, a bioinformatics study explicitly proposed that *yhfG-fic* loci encode a novel type II TA module[140], but this notion had remained speculative (particularly with respect to the *E. coli* homolog), though a direct interaction between YhfG and Fic has been demonstrated[141].

A lot of purely descriptive results have been published in the course of attempts to unravel the physiological basis of "filamentation induced by cAMP" and revealed that, e.g., *fic* expression is induced in stationary phase[142] or that the phenotype is sensitive to high salt concentrations[136] and correlates with the upregulation of an obscure membrane protein[143]. More importantly, it was shown that 1) the mutant Fic-1 protein as well as elevated temperature are necessary for fic, proving that *fic-1* is a gain-of-function allele[136], that 2) signaling triggered by CRP (cAMP receptor protein) bound to cAMP is necessary for the phenotype[135], and that 3) the phenotype is sensitive to the addition of folate[138]. The latter finding indicates that "filamentation induced by cAMP" may not be caused by any biochemical activity of the Fic protein itself, but rather by a repression of *pabA* expression. It is tempting to speculate that the G55R substitution, being far from active site and target interaction surfaces of FIC domains (see below), may somehow influence the transcriptional

autoregulation of a TA-like *yhfG-fic* module and thereby affect transcription of *pabA*. However, further research would be necessary to understand the enigmatic "filamentation induced by cAMP" phenotype and connect the plethora of old data with fresh studies.

During my PhD project we described a novel toxin-antitoxin module composed of *yhfG-fic* homologs, but not including *fic* and *yhfG* of *E. coli* themselves (see *Research articles I* and *III*). In *Review article II* we therefore introduced a nomenclature calling the Fic homologs "FicT" (for "Fic toxin", e.g., "EcFicT" for Fic of *E. coli*) and the YhfG homologs "FicA" (for "Fic antitoxin", e.g., "EcFicA" for YhfG of *E. coli*). So far, *yhfG-fic* of *E. coli* ("*ecficAT*") has resisted all attempts to demonstrate "filamentation induced by cAMP" in *E. coli* K-12 (see *Unpublished results related to Research article III*) or any other biological activity reminiscent of TA models.

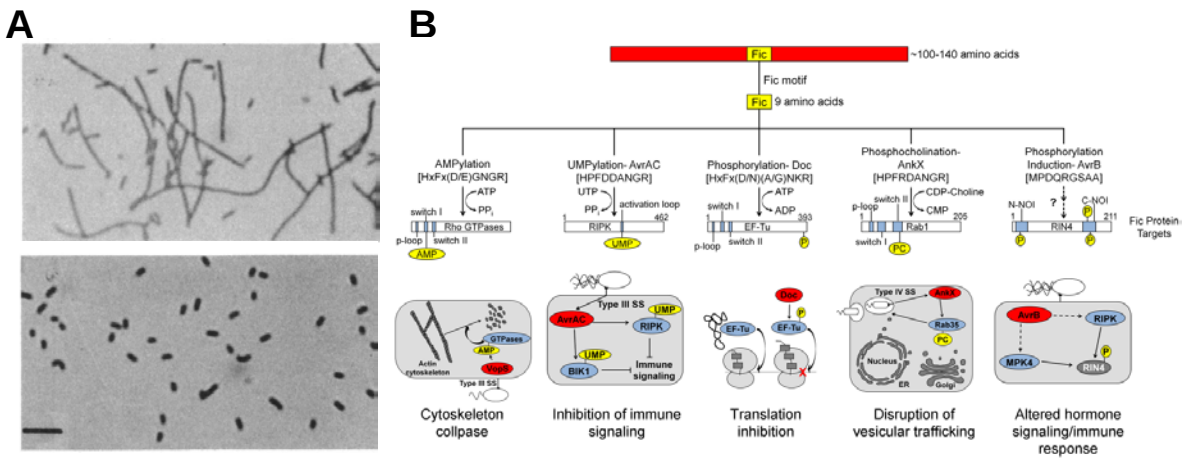

Figure 5: Introduction to FIC domain proteins. A) "Filamentation induced by cAMP" of a *fic-1* mutant of *E. coli* (top) and wildtype morphology (bottom) after two hours at 43°C with 10mM cAMP. The scale bar represents a length of 10 µm (taken from Utsumi *et al.*[135]). **B)** Biochemical plasticity and biological diversity of FIC domain proteins (adapted from Cruz and Woychik[144]). AMPylation (adenylylation) represents VopS and IbpA.

5.2.2. FIC domains in host-targeted virulence factors of bacterial pathogens

Fic of *E. coli* comprises a single protein domain that was accordingly named FIC (consistently written in capital letters in this work to avoid confusion with protein names). Although the far majority of FIC domains are found in genuine bacterial proteins (see the phylogenic distribution of the Fic/DOC family (PF02661) in the Pfam database or of Fido (IPR003812) in the InterPro database), the majority of research after the initial studies on "filamentation induced by cAMP" has focused on host-targeted virulence factors of bacterial pathogens. Though these proteins are clearly not representative for the bulk of FIC domains with regard to biological function, they were instrumental to the understanding of the biochemistry and structure-function relationship of Fic proteins.

The type III secretion (T3SS) effector protein VopS of *Vibrio parahaemolyticus* and the type V secreted surface protein IbpA of *Histophilus somni* both induce a collapse of the actin cytoskeleton and cell death upon translocation into eukaryotic host cells[145,146]. VopS and IbpA contain one and two closely related FIC domains, respectively, and studies by the Orth and Dixon labs revealed that both proteins target small GTPases of the Rho family via adenylylation (also called AMPylation), the transfer of an adenosine 5'-monophosphate, and established adenylylation / AMPylation as the conserved biochemical activity of FIC domains[125,126] (Figure 5B). The adenylylation of small GTPases causes the cytotoxicity of VopS and IbpA by blocking the binding of downstream signaling partners and thereby also disrupts multiple cellular pathways besides the control of the actin cytoskeleton[147]. A considerable number of small GTPases including RhoA, Rac1, and Cdc42 are nearly indiscriminately adenylylated by VopS and IbpA[148,149]. Already the first study on VopS showed that its adenylylation activity is dependent on an invariant histidine within a conserved FIC domain signature motif HPFx(D/E)GNGR[150]. This sequence motif was later shown to constitute the active site of FIC domains with the histidine likely serving as a general base during the catalysis of target adenylylation[151-153] (frequently referred to as "catalytic histidine" of FIC domain proteins[151,154,155]).

Like VopS or IbpA, the FIC-domain containing T3SS effector protein AvrAC of *Xanthomonas campestris* is secreted into host cells to subvert signaling in favor of the pathogen, but in this case the target are plant cells. A study on AvrAC revealed that this effector lacked any detectable adenylylation activity and instead acts via the uridylylation ("UMPylation") of two receptor-like kinases of plant cells that are involved in the sensing of pathogen-associated molecular patterns (PAMP)[156] (see Figure 5B). Uridylylation occurs on a pair of neighboring serine / threonine residues that would need to be phosphorylated for the activation of the targets, so that AvrAC prevents the induction of immune responses by *Xanthomonas*.

The FIC domain containing T4SS effector AnkX of *Legionella pneumophila* had long been known to induce fragmentation of the Golgi apparatus as well as to cause defects in vesicular transport in host cells[157]. These phenotypes depended on the integrity of the AnkX FIC domain and its active site histidine[155,158]. During the course of my PhD work, others showed that AnkX targets the small GTPases Rab1 and Rab35 via phosphocholination using CDP-choline as the substrate[159] (Figure 5B). Phosphocholination blocks the interaction of the Rab GTPases with activating GTP/GDP exchange factors (GEFs) or GDP dissociation inhibitors (GDIs) and therefore results in their functional deactivation, since the active GTP-bound form cannot be regenerated[160].

The *Pseudomonas syringae* T3SS effector protein AvrB does not show significant sequence similarity to FIC domain proteins, but harbors a structural fold that is clearly related[161]. Upon

infection of plant cells, the AvrB protein interacts with a number of host proteins like the MAP kinase MPK4 and immune regulator RIN4[162,163]. It had therefore been suggested that AvrB may act in host plant immunomodulation, e.g., via disturbance of hormone signaling[163], but this had remained speculative for a long time. Biochemically, the interaction of AvrB with RIN4 causes RIN4 phosphorylation by RIPK1, and this modification can induce effector-triggered immunity in plant cells[164]. Such an activation of immune responses upon sensing of the activities of bacterial effectors is a common theme in the co-evolutionary arms race between plants and their pathogens[165], but did not help to unravel the molecular function and biological role of AvrB. It has been revealed only very recently that the AvrB-mediated phosphorylation of RIN4 impairs the activation of plant immune responses. More specifically, this modification counteracts the immune-stimulatory signaling triggered by phosphorylation of RIN4 on another residue upon recognition of bacteria[166] (Figure 5B). Intriguingly, a potential kinase activity of AvrB itself that may target RIN4 directly (instead or on top of phosphorylation by RIPK1 and other kinases) has been proposed repeatedly based on the structure of AvrB in complex with ADP and a peptide of RIN4[152,162,167], but is now considered to be rather unlikely (discussed and reviewed by Roger W. Innes[168]).

Similar to VopS, AnkX, or AvrAC, the far majority of effectors secreted by the host-interacting VirB/D4 T4SS of *Bartonella* (called Beps for *Bartonella* effector proteins) contain FIC domains that are likely involved in the manipulation of host cell functions[169] (see below). Though no phenotypes of *Bartonella* infection could yet be unambiguously traced to the FIC domain of one or more effectors, research in our laboratory could demonstrate the adenylylation activity of a truncated construct of BepA of *B. henselae* that results in the modification of host factors of approximately 40 kDa and 50 kDa[152]. In parallel, I had developed a biochemical assay capable of the mid-throughput analysis of full-length effectors and demonstrated the adenylylation activity of two orthologous groups of effectors Bep1 and Bep2 that are only distantly related to BepA. Different orthologs of Bep1 all specifically modify Rac1 and a few closely related small GTPases at the same residue as IbpA, but with considerable target specificity (see *Appendix: Further results*). Bep2, a paralog of Bep1, modifies a different host target of approximately 50 kDa size (identified in *Research article II*), suggesting that effectors within one orthologous group may have the same activity while those from different orthologous groups have different activities. However, an additional *in silico* analysis performed during my Master project indicated that the far majority of *Bartonella* effectors with FIC domains may not act via adenylylation due to considerable deviations from the canonical FIC domain active site sequence (see Figure 28 in the *Appendix: Further results* section).

5.2.3. The Doc / Phd toxin-antitoxin module

The Doc (*death on curing*) protein has first been described as the toxin of a post-segregational killing system that enforces maintenance of the P1 lysogenic plasmid in bacteria ("plasmid addiction")[32]. This toxin is characterized by an incomplete Fic core that can be complemented by the binding of its antitoxin Phd (prevents host death) which restores a complete FIC domain fold, but at the same time inhibits its activity[15,170]. Though the well-studied Doc/Phd homolog encoded by *E. coli* phage P1 acts as an addiction module, Doc/Phd is abundant as a chromosomal TA module, e.g., in *Salmonella* Typhimurium where it was found to be the involved in macrophage-induced persister formation[33]. While the results in *S.* Typhimurium suggest that Doc/Phd would be activated by Lon like most TA modules in *E. coli* and related bacteria[33], the homolog of phage P1 is under the control of ClpP[55]. Doc is a very potent toxin and inhibits growth via the inhibition of translation, but not transcription or chromosome replication[171]. A molecular mechanism in the context of ribosomes had been suspected for a long time[171], and the dependence of Doc-mediated growth inhibition on the histidine within its FIC domain signature pointed towards a post-translational modification[15]. However, it has only recently been revealed that Doc is a kinase that uses the FIC domain active site to phosphorylate translation elongation factor EF-Tu. Phosphorylation makes EF-Tu unable to bind aminoacylated tRNAs and thus immediately stops the translation process[34] (Figure 5B). Therefore, Doc is another TA module toxin that inhibits translation, but gives an important example how new catalytic functionalities can evolve from the FIC domain core (see below). Interestingly, it was proposed that Doc evolved via the deterioration of adenylylating FIC domain proteins and that Phd acquired the missing α-helix via a sequence shuffling event of illegitimate recombination[15,170].

5.2.4. Metazoan FIC domain proteins

Proteins containing FIC domains are not restricted to prokaryotes, but can also be found in eukaryotic organisms. Interestingly, metazoans encode each one copy of a FIC domain protein with an N-terminal transmembrane helix followed by tetratricopeptide repeats[172]. An auto-adenylylation activity was shown *in vitro* for the homologs of humans (called HypE or FicD)[173] and *Drosophila melanogaster* (CG9523)[161]. CG9523 is essential for the recycling of the visual neurotransmitter histamine in capitate projections of glia cells[174]. A recent study showed that CG9523 (and HypE) adenylylate BiP/GRP78, a chaperone of the endoplasmic reticulum, but it has remained elusive whether this activity is causal to the blindness of mutant flies or if additional targets exist[175]. Additionally, HypE has been found to adenylylate the same residue in small GTPases as IbpA[173] as well as an unknown residue in histone H3[176], but the relation of these activities to potential biological function(s) have remained elusive so far.

5.2.5. General features and structure-function relations of FIC domain proteins

From a technical point of view, all FIC domain proteins share a conserved enzymatic core that can be extended via different accessory modules to guide substrate and target specificities (Figure 6). This molecular machinery has been recently reviewed by Garcia-Pino *et al.*[170] who defined the minimal Fic core as a set of six α-helices containing the active-site loop with the Fic signature motif HxFx(D/E)GNGRxxR[177]. The FIC domain active site has evolved to perform the transfer of a phosphoryl group generated from the cleavage of a pyrophosphate bond onto a hydroxyl side chain of the target protein. A “catalytic histidine” within the active site of FIC domain proteins is critical for efficient catalysis because it deprotonates the target hydroxyl group in order to enable its nucleophilic attack on the pyrophosphate bond[18,127,129].

On top of this enzymatic core, FIC domain proteins can contain inserted accessory elements at three typical “grafting points” that serve to direct the enzymatic activity of the Fic core[170]. Modules responsible for target recognition are typically found at the N- and / or C-terminus of the enzymatic core and are largely unique for individual groups of FIC domain proteins, e.g., the N-terminal “arm subdomains” of IbpA and VopS FIC domains that bind to small GTPases[151,153]. Additionally, a β-hairpin between helices α2 and α3 (the “flap”) that is shared between all FIC domains *sensu stricto*[170], but absent in Doc[15], constitutes a target protein docking site that forms intermolecular antiparallel β-strand interactions with the target and thereby positions the attacking hydroxyl side chain towards the FIC domain active site[152,153,162]. These β-β-interactions are generally sequence-independent and can therefore be seen as part of the enzymatic machinery rather than a way of target recognition[152,178]. The different crystal structures of FIC domain proteins confirm this role of the β-hairpin flap in target accommodation by showing diverse conformations ranging from a partly disordered loop[152] in a solitary Fic structure to a solid a β-sheet engaged in the interaction with stretches of target or surrogate target[153,162,179].

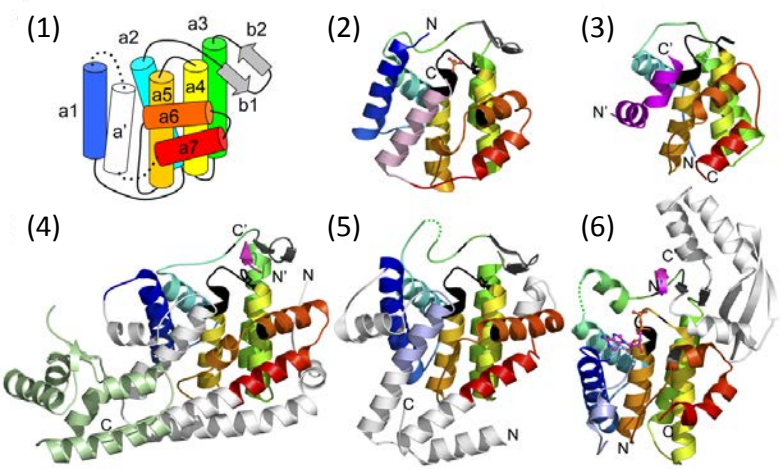

Figure 6: FIC domain proteins comprise an enzymatic core with different functional extensions. The conserved FIC domain core is sketched in (1) with rainbow coloring of it secondary structure. Structures (2) to (6) show the Fic core of each protein (rainbow) with different accessory modules in white. Particular elements like the β-hairpin flap (b1-b2 in (1)) or a helix-turn-helix domain (4) are highlighted in grey and light green, respectively. The figure was adapted from Kinch *et al.*[161] and the structures represent HpFicT of *Heliciobacter pylori*[a] (2), Doc with Phd (3; Phd in magenta), SoFicT of *Shewanella oneidensis* (4), BtFicT of *Bacteroides thetaiotamicron* (5), and AvrB of *P. syringae* (6) in complex with a peptide of its target RIN4 (magenta). Note that the definition of the "Fic core" in the source of this figure[161] is slightly different from the one used by the new review of Garcia-Pino *et al.*[170], but this divergence does not affect its illustrative power. The discussion of different opinions regarding the FIC domain "core" and a comparison of *sensu stricto* Fic proteins with the FIC domains of Doc or AvrB is mostly semantic and beyond the scope of this work.

The conserved phosphoryl transfer machinery in the Fic core can catalyze diverse chemical reactions dependent on the small molecule substrate that donates the phosphoryl group. For the most prevalent group of FIC domains that mediate nucleotidyl transfer ("NMPylation") the binding of their nucleotide substrate has been investigated in detail and involves parts both of the Fic signature motif as well as the β-hairpin flap[152,153,178]. For Doc (acting as a kinase) and AnkX (performing phosphocholination), their peculiar biochemical activities are catalyzed by basically the same enzymatic machinery as with classical nucleotidyl transfer, but the small molecule substrate binds in an inverted conformation relative to the nucleotide in their adenylylating FIC domain cousins. Consequently, the leaving group of the nucleophilic attack changes and a phosphate is transferred from ATP by Doc and a phosphocholine is transferred from CDP-choline by AnkX[34,154].

In addition to target modification, all FIC domains investigated so far also perform auto-modification reactions like auto-adenylylation / auto-AMPylation, but the functional relevance of this phenomenon has not been explored in detail[152,153,161]. So far, only the hypothesis that

[a] For reasons of consistency I used a universal nomenclature of genuine bacterial FIC domain proteins throughout this thesis that follows one possible path of common sense in protein biology. For example, this Fic protein of *Helicobacter pylori* is called HpFicT with "Hp" denoting the species, "Fic" denoting the protein family, and "T" as the final capital letter giving information regarding the protein's activity (compare "EcFicT" introduced above or "SoFicT", "NmFicT", and "YeFicT" appearing in later sections). However, the primary authors of different articles that are part of this work decided to apply different, more open nomenclatures (*Research articles I* and *IV*).

auto-adenylylation may represent the first step of an enzymatic ping-pong mechanism has been refuted by enzyme kinetics of VopS in favor of the formation of a ternary complex during catalysis[151].

Prior to the beginning of my PhD project and also over the course of it the field of FIC domain research has been repeatedly and comprehensively reviewed, particularly with respect to structure-function relations[144,158,170,180]. I had already contributed to the field during my Master project by an analysis of *Bartonella* effector proteins *in silico* and proposed auxiliary modules that may be involved in their remarkable target specificity and diversity (see *Research article II* and *Appendix: Further results*). Furthermore, I was involved in the elucidation of a conserved mechanism that regulates the adenylylation activity of the majority of FIC domain proteins (*Research article I*) and guided or contributed to different projects that largely expanded our biochemical and functional understanding of FIC domain proteins (*Research articles I-IV* and *Review article II*).

5.3.Control of cellular DNA topology in bacteria

5.3.1. Basics of bacterial DNA topology

The concept of two complementary strands of DNA that anneal to form the well-known helical structure of dsDNA is a brilliant answer to conceptual questions arising for the storage, transcription, and transfer of genetic information. However, it causes major topological problems that are inherent to the structure of the dsDNA helix (see the magnificent review by Deweese *et al.* for an introduction into DNA topology[181]).

In short, the topology of a classical circular and covalently closed dsDNA molecule is described with three parameters twist (Tw), writhe (Wr), and linking number (Lk). While twist means the total number of helical turns, writhe describes the wrapping and buckling of the DNA strand and is numerically defined as the number of crossings upon 2D projection. Simply, Lk is the sum of Wr and Tw and cannot be changed as long as the DNA molecule stays intact, while Wr and Tw are interconvertable (see an example in Figure 7A). The storage of genetic information within a single strand of the double-stranded molecule makes it necessary to open up the dsDNA helix whenever the information is to be accessed. Therefore, the DNA in bacterial cells is by default underwound (i.e., „negatively" supercoiled[a]) which promotes its manipulation because the „negative" writhe can be converted into local unwinding, i.e., a reduction in twist. Conversely, the progressive dsDNA melting inherent to DNA replication and transcription is a forced reduction of twist that causes compensatory overwinding or „positive" supercoiling, an increase in writhe. This is big part of the dilemma of the DNA double helix: Its constant manipulation by vital processes consumes negative supercoils and produces positive supercoils that impede further manipulation (recently reviewed by Koster *et al*.[182]).

[a] By convention, overwinding and underwinding (relative the relaxed state with one helical turn per 10.5 base pairs) are referred to as „positive" and „negative" supercoiling, respectively.

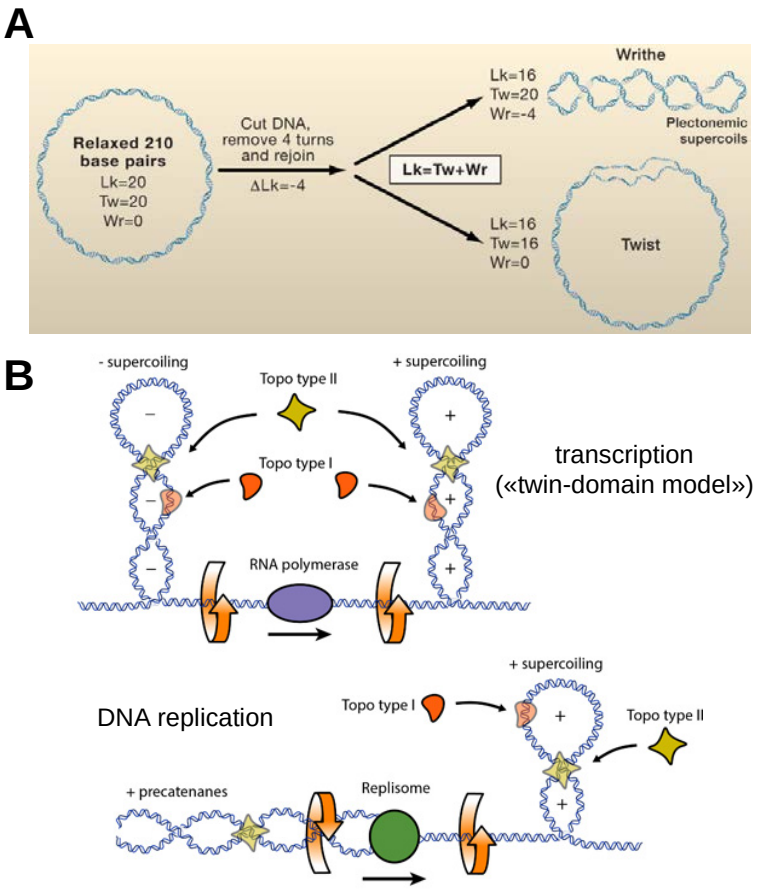

Figure 7: Introduction to DNA topology. A) Exemplary illustration of the topological parameters Lk, Tw, and Wr of dsDNA molecules (taken from Koster *et al.*[182]). The dsDNA molecule with a length of 210 base pairs contains 20 helical turns in a torsionally relaxed state (10.5 bp / turn) – the twist (Tw) is 20, writhe (Wr) is 0, and therefore Lk (linking number) is 20. A reduction in Lk to 16, e.g., via dsDNA breakage, four rotations, and resealing, can either partition to a reduction of Wr (top: "negative" supercoiling" with Wr = -4) or to a reduction of Tw (bottom: DNA unwinding with Tw = 16, i.e., only 16 instead of initially 20 helical turns). Note that the two dsDNA molecules shown to the right are topologically equivalent, i.e., negative supercoiling is interconvertible with local unwinding. **B)** Distortions of dsDNA topology upon DNA transcription (top) or DNA replication (bottom). The DNA rotation imposed by RNA polymerase causes positive supercoiling ahead of the transcription site and negative supercoiling behind it. Similarly, DNA replication causes positive supercoiling ahead of the progressing replisome, and the intertwining of the daughter chromatids results in (pre-)catenanes. The illustrations also show where type I and type II topoisomerases can intervene and remove topological distortions (see below). Figures adapted from the Website of Dr. Michelle Wang[a].

More precisely, the rotational drag imposed by transcribing RNA polymerase causes DNA to fold up to positive supercoils ahead of the transcription machinery and generates corresponding negative supercoils behind it („twin-domain effect"[183]). Similarly, the unwinding of the DNA duplex during DNA replication results in positive supercoiling ahead of the replication fork[184] (Figure 7B). At first glance, the separation of bacterial chromosomes and other large dsDNA molecules into independent topological loops[b] (ca. 400 with each around 10'000 base pairs for the chromosome of *E. coli*[185]) may confine such distortions to the DNA

[a] available on http://www.hhmi.org/research/dynamics-accessing-dna (last accessed on November8th, 2014)

[b] The organization of chromosomal DNA into such topologically independent, negatively supercoiled loops is also a major aspect of nucleoid compaction that allows to fit the chromosomes into bacterial cells as discussed by Postow *et al.*[185], though the causalities are likely more complex as previously assumed[186].

locus where they arouse. However, the ubiquity and simultaneity of DNA transcription is such a strong drain of DNA underwinding that it can even consume negative supercoils from adjacent loops, while positive supercoiling generated by DNA replication is more a local obstacle to fork progression itself[187]. But constant overwinding is not the only problem arising from cellular DNA manipulations: Additionally, the rotation of the replication complex relative to the DNA causes intertwining of the sister chromatids behind the replisome[184,188] (Figure 7B). It is intuitive that already a single crossing of these entanglements or „catenation“ would be sufficient to prevent chromosome segregation. Furthermore, intramolecular knots that arise from accidents during processes of DNA manipulation directly block unwinding of the dsDNA helix (recently reviewed by Schvartzman *et al.*[189]). DNA supercoiling, catenation, and knotting are illustrated in Figure 8.

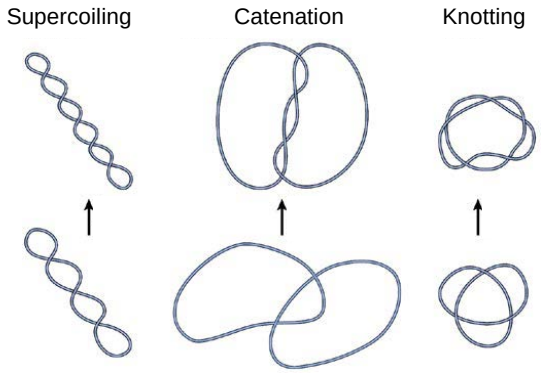

Figure 8: DNA supercoiling, catenation, and knotting. The three topological forms of circular dsDNA molecules are shown in comparison (catenated and knotted DNA can also be supercoiled in addition; adapted from Cozzarelli *et al.*[190]). While positive supercoiling stops DNA replication and transcription, excess negative supercoiling promotes the formation of harmful structures like R loops (annealing of a transcribed RNA with its template DNA behind the RNA polymerase; summarized by Pommier *et al.*[191]). Catenation impairs DNA segregation, while DNA knotting inhibits DNA unwinding and thereby productive manipulation of the dsDNA helix.

In conclusion, it is clear that the constant assault of positive supercoiling, excess negative supercoiling, catenation, and knotting on the functionality of bacterial (as well as eukaryotic, for that matter) DNA needs to be counteracted by cellular machineries that can itself manipulate and adjust the topology of dsDNA – since they interconvert different isomers of DNA topology, they are called DNA topoisomerases.

5.3.2. Control of DNA topology in bacterial cells

Conceptually, DNA topoisomerases remove distortions in cellular DNA topology via manipulations of Lk during transient breaks in the double helix (recently reviewed by Vos *et al.*[192]). They are generally classified as type I or type II dependent on whether their mechanism involves the formation of a transient single-strand or double-strand DNA break which has different functional implications[193] (Figure 7B). Since topoisomerases are generally essential for life as we know it, an “intelligent designer would have probably invented only

one ubiquitous Topo I and one ubiquitous Topo II"[a]. Instead, the different domains and even lineages of life contain a zoo of topoisomerases with complex patterns of homology[194].

Type I topoisomerases cut a single strand of the dsDNA, move it around the complementary strand via controlled rotation, and religate the dsDNA helix which changes the linking number in increments of one[192]. *E. coli* contains two type I topoisomerases that are called topoisomerase I (topo I) and topoisomerase III (topo III). It is the main function of topo I to relax the flood of negative supercoils that are typically generated locally behind RNA polymerase at sites of strong transcription, but it also plays a role in the adjustment of global DNA topology via the relaxation of any excess of negative supercoiling[195,196]. The function of topo III was long debated, but it appears to be involved in the resolution of Holliday junctions during recombination and can participate in the decatenation of daughter chromosomes[197,198]. Structurally, topo I and topo III are nearly identical over most of their primary sequence, and minor differences in their biochemical properties underlie their different biological functions[199]. Next to the type IA family of type I topoisomerases (comprising topo I, topo III; and reverse gyrase) a type IB family (mostly eukaryotic) and type IC (only a single representative in an archaeon) exist[192].

Additionally, two types of type II topoisomerases have been described so that in total five distinct families of DNA topoisomerases are known today[194]. The type IIB family is mostly found in archaea and plants where they relax excess negative as well as positive supercoils and act in decatenation[192,200]. Type IIA DNA topoisomerases are found in all domains of life as well as viruses and comprise three homologous families of enzymes, eukaryotic topo II as well as prokaryotic topo IV and DNA gyrase. While eukaryotic topo II and prokaryotic topo IV share the ability to act as strong decatenases, DNA gyrase is unique in its ability to introduce negative supercoils[193,194].

DNA gyrase and topo IV are paralogous heterotetramers assembled from each two A and B subunits ($GyrA_2$-$GyrB_2$ respectively $ParC_2$-$ParE_2$) of which – in short – the A subunits contain the active site responsible for DNA manipulation while the B subunits contain an ATPase domain whose activity is generally required for the reaction mechanism[193,201] (Figure 9A). While DNA gyrase is universally essential, a few bacteria are known to lack topo IV, but it appears that in these cases DNA gyrase may have taken over the functionality of its paralog[202].

DNA gyrase and topo IV act via a conserved "three-gate mechanism" involving transient double-strand breakage of a closed-circular DNA molecule via transphosphorylation onto

[a] … „to facilitate the task of future biochemists", as the authors feel obliged to add with some bitterness. Interestingly, they argue that the diversity of DNA topoisomerases among the phyla of cellular life is a strong hint that DNA topoisomerases as well as, ultimately, DNA itself are of viral origin.

active site tyrosines of the topoisomerase. The formation of this covalent complex is followed by unidirectional passage of the same (supercoiling / relaxation and knotting / unknotting) or a different (catenation / decatenation) DNA molecule through the resulting cleft. Finally, the phosphodiester bonds of the DNA backbone are resealed and the enzyme is reset for a new cycle of topoisomerisation (Figures 9A and 9B). Despite their different biological outcome, the activities of DNA gyrase and topo IV are therefore "based on the same structural and mechanistic framework (and) achieved by different fine-tuning of a common theme" (recently reviewed by Gubaev and Klostermeier[203]). In the case of DNA gyrase, the topoisomerase wraps ca. 150bp[204] of the double strand around a gyrase-specific C-terminal β-pinwheel domain of GyrA and can thus pass it through a transient dsDNA break in the same molecule (Figures 9B). The wrapping around GyrA produces a dsDNA crossover with positive node sign that is inverted by the strand passage, thereby reducing the linking number in increments of two[205]. The canonical "GyrA-box" in the first blade of the GyrA β-pinwheel is essential for the functioning of DNA gyrase because it guides DNA wrapping and the formation of the positive node at the crossover[206-208]. The C-terminal domain of ParC lacks β-pinwheel and GyrA-box, but analogously controls the directionality of strand passages by topo IV via specificity for certain crossover geometries as substrates[209,210].

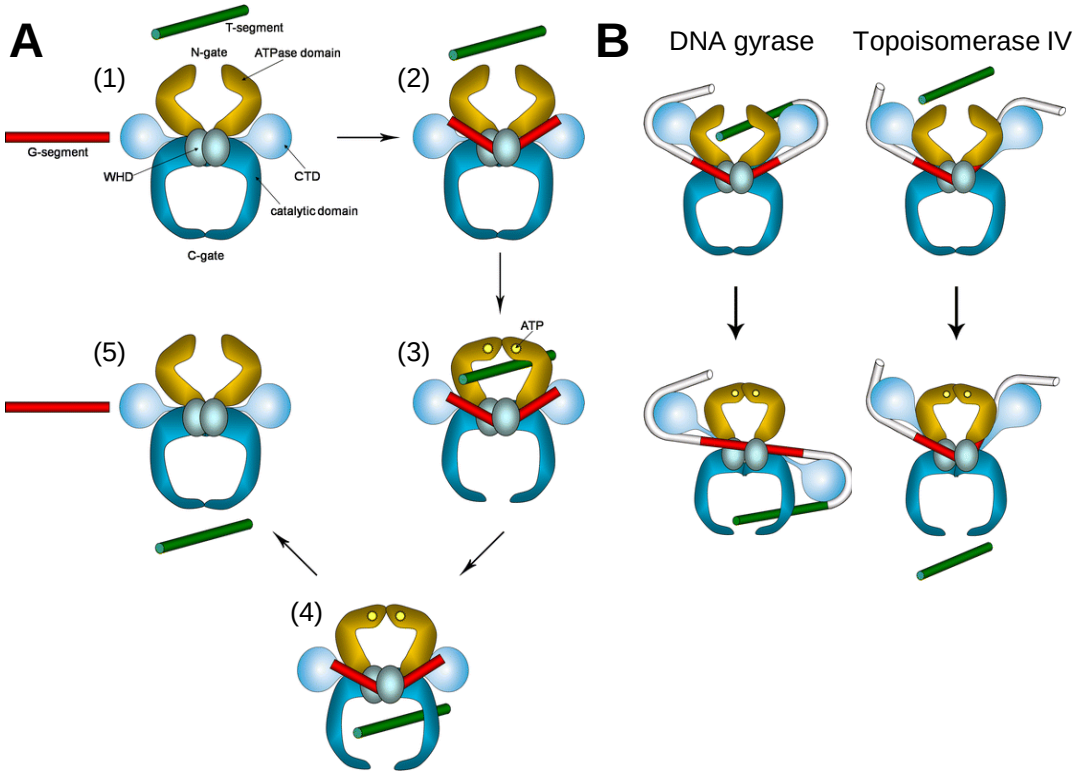

Figure 9: Bacterial type IIA topoisomerases as molecular machineries. A) In short, type II topoisomerases mediate the transfer of one piece of dsDNA (T-segment, green) through a cleft in another one (G-segment, red) via a "three-gate mechanism". The T-segment enters the topoisomerase II holoenzyme (1) via the N-gate between the ATPase domains of the B subunits (2). Upon ATP binding, the N-gate closes (3). In coordination with ATP hydrolysis, the G-segment is cut open by the active site in the winged-helix domains (WHD) of the A subunits ("G-gate") and strand passage takes place (4). Finally, the T-segment is released through the C-gate (5). **B)** In case of gyrase (left), T- and G-segment are part of the same dsDNA molecule that is wrapped around the C-terminal domain (CTD) of GyrA to allow strand passage. For decatenation by topo IV (right), T- and G-segment belong to different dsDNA molecules. Both panels were taken from Sissi and Palumbo[211].

Importantly, all biologically relevant activities of type II topoisomerases depend on concurrent ATP hydrolysis, though the mechanistic basis for this requirement is still under investigation[212,213]. In case of DNA gyrase it is clear that the ATPase activity of GyrB fuels the energetically unfavorable negative supercoiling activity of the enzyme, but the precise mechanochemical basis of this requirement is not well understood. Others have shown that ATP binding is necessary to overcome a kinetic barrier in the wrapping of a positive supercoil but that ATP hydrolysis may be rather loosely coupled to the individual mechanical transitions of the strand passage[214]. Recently, Stanger *et al.* from our laboratory proposed that ATP hydrolysis may induce DNA cleavage as well strand passage[215] (Figure 10A), but such a causal connection remains to be demonstrated experimentally. For topo IV (and also eukaryotic topo II) the strand passages itself are nearly isoenergetic[216] so that ATP hydrolysis may power the enzymes in other ways and, e.g., serve to control the large protein domain movements inherent to the reaction mechanism in order to prevent free double strand break formation[213].

The biological functions of DNA gyrase and topo IV are mostly non-overlapping, but show considerable cooperation. Both enzymes act together during chromosome replication to support replication fork movement by clearing positive supercoils produced in front of the fork and resolving daughter strand intertwining behind it[211]. While DNA gyrase reverts most of the positive supercoils[217], topo IV is the key player in daughter chromosome decatenation[218] (see in Figure 7B). Unsurprisingly, the inhibition of both enzymes in *E. coli* rapidly stops DNA replication, and inhibition of DNA gyrase alone leads to a drop of replication fork movement to ca. 1/3 as well as a slow stop of chromosome replication[217,218]. During transcription, DNA gyrase intermittently removes the positive supercoils accumulating in front of the RNA polymerase at heavily transcribed loci which is responsible for the characteristic “bursting” of bacterial transcription[219]. In addition to its activity in decatenation, topo IV is also responsible for the removal of inter- and intrachromatid knots. DNA knots continuously arise in the tangled nucleoid from random strand passages that occur whenever cellular DNA handling cuts open the chromosome, e.g., during processes of replication, recombination, or repair, and they cannot be removed in the absence of functional topo IV[220]. The propensity to form knots increases with the chain length of the circular DNA molecule (see recent work by Witz and Stasiak and literature cited therein[216]). Chromosomal knotting blocks DNA replication and transcription, i.e., it “interferes with genetic metabolism”[221]. Importantly, both the decatenation and unknotting activities of topo IV are linked to the functionality of DNA gyrase because the negative supercoiling of substrate DNA acts as a “magnet” to find detrimental crossovers of knots and catenanes as the proverbial “needle in the haystack”[216,222,223].

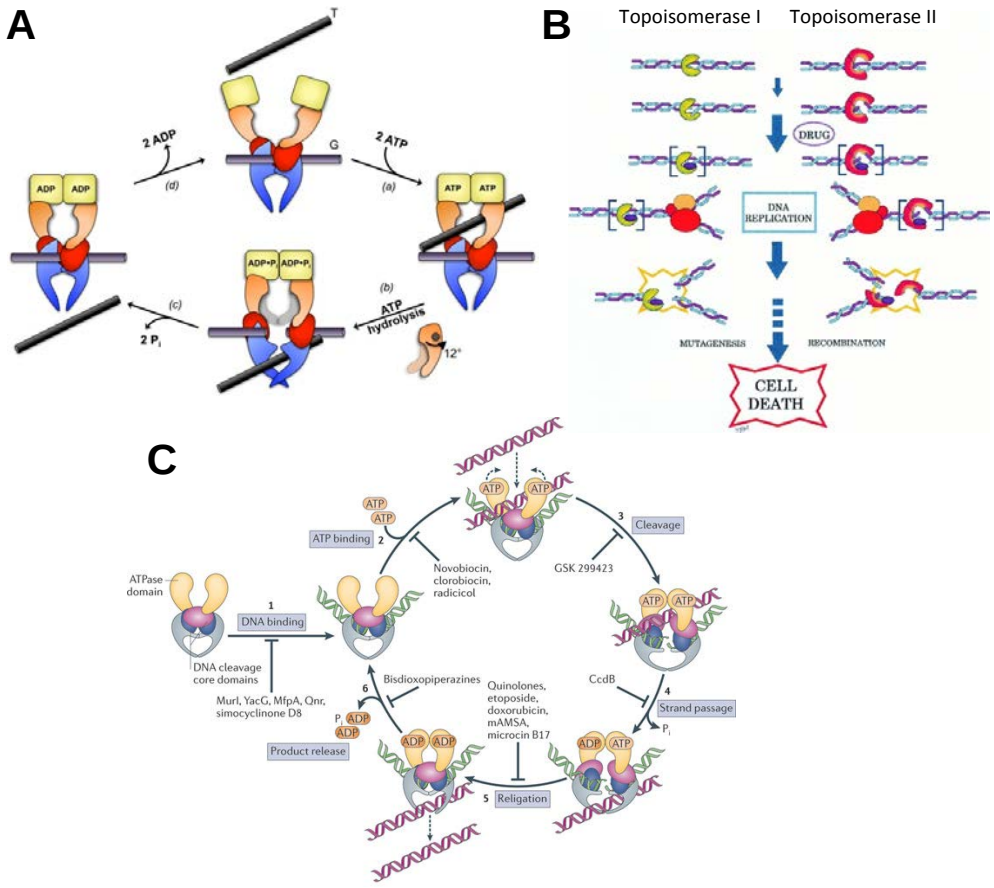

Figure 10: Further details of topoisomerase IIA mechanism and inhibition. A) The catalytic cycle of DNA gyrase (compare Figures 9A and 9B) as shown by Stanger *et al*[224]. They propose that ATP hydrolysis is coupled to strand passage via a concomitant 12° rotation of the transducer domains adjacent to the ATPase domains in GyrB. **B)** Topoisomerase poisoning traps the cleavable complex on the DNA template and causes dsDNA breaks upon collision of these "roadblocks" with DNA tracking complexes like replisomes. The illustration was uploaded by user Vtvu to the wiki commons[a]. **C)** Another representation of the topoisomerase II reaction cycle with the steps at which the various poisons and inhibitors act (taken from Vos *et al.*[225]). Topoisomerase poisons lock the cleavable complex by inhibition of DNA cleavage (3), strand passage (4), or religation (5), while inhibitors typically target DNA binding (1) or ATP binding and hydrolysis (2). Bisdioxopiperazines like ICRF-187 are anti-cancer drugs that inhibit eukaryotic topo II by bridging and stabilizing a dimer interaction between the two ATPase domains of the holoenzyme[226].

In addition to DNA topoisomerases that mostly adjust the DNA topology against perturbations, DNA supercoiling and nucleoid compaction are also controlled on a more global level by nucleoid-associated proteins ("NAPs" such as H-NS (forming negative supercoils; recently reviewed by Rimsky and Travers[227]) or the structural maintenance of chromosome ("SMC") proteins like MukBEF in *E. coli* (involved in nucleoid compaction and chromosome segregation; recently reviewed by Carter and Sjögren[228]). Multiple crosslinks between these layers of DNA organization and both DNA gyrase and topo IV have been described[229-232].

[a] available at http://commons.wikimedia.org/wiki/File:Topoisomerase_Inhibitor.JPG (last accessed on November 8th 2014)

5.3.3. The inhibition and poisoning of type IIA topoisomerases in bacteria cells

Due to their ubiquity in combination with essentiality and strong conservation[194] topoisomerases constitute important targets for inhibition and poisoning both as part of the coevolutionary warfare in natural environments and as drug targets for the treatment of human patients. While a bacteriostatic block of cellular DNA manipulations is intuitive as the consequence of topoisomerase inhibition, the concept of poisoning is different. Unlike inhibitors, poisons do not generally abolish the catalytic activity of their topoisomerase target, but instead use it to cause DNA damage. More specifically, topoisomerase poisons trap the normally only transient „cleavage complex“ in which the enzyme's polypeptide bridges a DNA break that will be exposed upon removal of the topoisomerase, e.g., after collision of a replication fork with the cleavage complex acting as a „roadblock“[233] (Figure 10B). Theoretically, the resulting double-strand breaks can be repaired, but their accumulation upon enforced topoisomerase poisoning easily overcomes the cellular repair pathways and causes cell death both in prokaryotes as well as in eukaryotes (see the article by Deweese *et al.* for an introductory summary[181]). Human topo I as well as topo II are targeted in anticancer chemotherapy by camptothecin and etoposide or anthracyclines (such as doxorubicin), respectively, that are all poisons (recently reviewed by Pommier *et al.*[191]).

Unlike for human topo I, no clinically approved drug targeting bacterial topo I as an antimicrobial is available[234], but the general feasibility of topo I poisoning with small compounds to kill bacteria has been demonstrated[235]. The situation is completely different for the bacterial type IIA topoisomerases DNA gyrase and topo IV that are targeted by a plethora of different drugs as well as bacteriocins and TA addiction toxins (recently reviewed by Collin *et al.*[236]). For an overview I catalogued the various poisons and inhibitors of bacterial type IIA topoisomerases in table II (see also Figure 10C).

Concept	Drug class	Examples	Mechanism of action
Inhibitors	Aminocoumarins	Novobiocin, coumermycin A1	Competitive inhibitors of ATP binding and therefore hydrolysis at GyrB[237,238] (and ParE)[239]
	Simocyclinones	Simocyclinone D8	Blocking the DNA binding site in GyrA (not ParC)[240]
	Cyclothialidines	Ro 09-1437, GR122222X	Competitive inhibitors of ATP binding and therefore hydrolysis at GyrB[241,242]
	Cinodin	Cinodin β	Inhibition of supercoiling by DNA gyrase (at GyrA?)[243]
	Pyrrolamides	*Compounds not named*	Competitive inhibitors of ATP binding and therefore hydrolysis at GyrB[244]
	Gyramides	Gyramide A	Competitive inhibitors of ATP binding and therefore hydrolysis at GyrB[245]
	Proteic inhibitors	Pentapeptide repeat proteins (PRPs), GyrI, YacG, glutamate racemase (MurI)	prevent enyzme DNA binding, interaction with gyrase (GyrI[246,247] and MurI[248]), gyrase / topo IV (PRPs[249,250]) or C-terminus of GyrB (YacG)[251,252]
Poisons	(Fluoro)quinolones	Nalidixic acid, ciprofloxacin	Stabilization of a covalent complex with GyrA (or ParC) being covalently attached to dsDNA break, resulting in chromosome fragmentation and cell death[253-255]
	Clerocidin	Clerocidin	Stabilization of covalent enzyme-DNA complexes causing dsDNA breaks and cell death by poisoning at A subunits of gyrase[256] and topo IV[257]
	Bacteriocine peptides	Albicidin[258], microcin B17[259]	Different mechanisms of cleavage complex stabilization of gyrase (microcine B17) or gyrase and topo IV (albicidin) at A (albicidin) or C-terminus of B subunit (microcine B17)
	Addiction module toxins	CcdB, ParE	Different mechanisms of cleavage complex stabilization at GyrA[42,260,261]
	GSK299423	GSK299423	"Bridging" between DNA and GyrA dimer to induce ssDNA breaks[262]

Table 2: The different classes of inhibitors and poisons of bacterial type IIA topoisomerases have been compiled based on the work of Collin *et al.*[236] and additional literature mining. Emerging conclusions are discussed in the running text.

Generally, it is the emerging picture that bacterial type IIA topoisomerases are either targeted by poisons or via one of two different mechanisms of inhibition, the prevention of DNA binding and the block of the ATPase cycle. Antimicrobial compounds are found in both major

classes with aminocoumarin drugs and quinolone antibiotics as the most important examples that both target DNA gyrase as well as topo IV. Aminocoumarins are bacteriostatic as competitive inhibitors of ATP binding to the targets' B subunit[237,238] and have either never been in clinical use (coumermycin A1) or are not in the market anymore (novobiocin). In direct contrast, quinolones and their derivatives act as topoisomerase poisons and "are among the most successful antimicrobials both clinically and economically"[234]. The molecular mode of action at the target for both classes of drugs has been well investigated on the atomic level[255,263], but the downstream processes leading to chromosome fragmentation and cell death after quinolone-mediated cleavage complex stabilization are not fully understood[253].

Unsurprisingly, the bacteriocins as well as the toxins of TA addiction modules uniformly employ a poisoning mechanism similar to quinolone-mediated cleavage complex trapping because an irreversible, lethal mode of action is elemental for their biological functions. However, there are some differences in the precise molecular mechanism of topoisomerase poisoning such that, e.g., the CcdB toxin requires ATP hydrolysis and probably strand passage for gyrase poisoning while new generation fluoroquinolone antibiotics do not, suggesting that they target a pre-transport state of the topoisomerase[208,264].

An increasing number of small proteins are known to inhibit bacterial type IIA topoisomerases via a tight direct interaction which typically blocks the target's DNA binding and therefore prevents topoisomerase poisoning. Among these proteins are biologically and mechanistically distinct factors such as GyrI that is part of the SOS response in *E. coli*[247] or the abundant pentapeptide repeat proteins that act as DNA mimics and mediate quinolone resistance (recently reviewed by Shah and Heddle[265]). Interestingly, also the target inhibition by aminocoumarins has been reported to protect bacteria from gyrase poisoning[266].

During my PhD project I discovered that the FicTA family of TA modules inhibits DNA gyrase and topo IV via adenylylation at the ATPase domain of the B subunits which causes a disruption of cellular DNA topology characterized by DNA knotting, catenation, and relaxation (see *Research article III*). Furthermore, I could show that a distinct class of FIC domain proteins acts via the same molecular mechanism (*Research article IV*).

5.4.Bacteria of the genus *Bartonella*

5.4.1. *General features and virulence factors*

The α-proteobacterial genus *Bartonella* forms a monophyletic group of mammal pathogens within the mostly plant-associated order of Rhizobiales and comprises a growing number of currently around 30 species[267]. *Bartonella* bacteria cause characteristic biphasic infections in their respective reservoir hosts and are transmitted by blood-sucking arthropods (reviewed by Chomel *et al.*[268]). These infections are shaped by the stealth infection strategy of the pathogen that uses sophisticated tactics of immune evasion and immunomodulation to first pass through an enigmatic "primary niche" (probably involving replication within vascular endothelial cells) and then achieve intraerythrocytic persistence (recently reviewed by Pulliainen *et al.*[269]; see Figure 11). By definition, the "reservoir hosts" of a given *Bartonella* strain are the host species in which it can reach the intraerythrocytic niche and therefore be further transmitted.

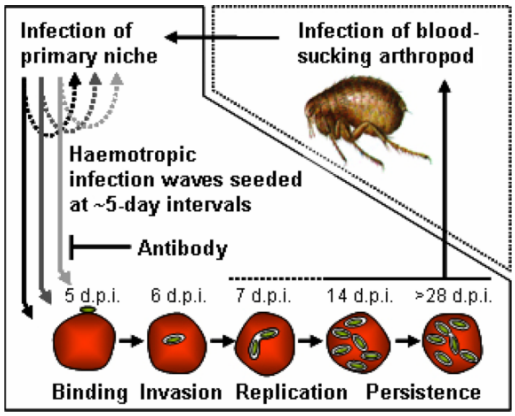

Figure 11: Common infection cycle of *Bartonella* spp. The model depicts the different stages of *Bartonella* infections in the mammalian reservoir host and the blood-sucking arthropod vector (adapted from Chomel *et al.*[268]; d.p.i. = days post-infection). Details are explained in the running text.

Characteristically, infections of reservoir hosts cause no or only negligible disease despite long-lasting bacteremia, while accidental infections of non-reservoir hosts with *Bartonella* can result in mild and self-limiting, yet discernable sickness for immunocompetent individiuals. The infection of immunocompromised hosts often presents with vasoproliferative lesions as well as a range of variable symptoms both in animals as well as in humans[270]. While occasional zoonotic infections with many different *Bartonella* species have been described, most infections of human patients are caused by cat-adapted *B. henselae* (self-limiting "cat scratch fever"), closely related[271] *B.quintana,* as well as *B. bacilliformis*[272]*.* Although the latter two species are both adapted to infect humans as their reservoir host, *B. quintana* typically causes only mild and self-limiting disease in immunocompetent patients ("trench fever"), while "Carrion's disease" caused by *B. bacilliformis* can be lethal during its acute phase if untreated[273]. However, *Bartonella* infections are typically responsive to antimicrobials, though

a lengthy treatment can be required (see the recent review on human bartonelloses and their treatment by Angelakis and Raoult[274]).

For the enforcement of their complex infection strategy the bartonellae use a wide range of different virulence factors most of which have been identified (or confirmed) in signature-tagged mutagenesis (STM) screens[275,276]. Most prominently, *Bartonella* features classical bacterial virulence factors like a considerable arsenal of diverse type V secretion systems, numerous outer membrane proteins with different functions in host interaction, a specialized lipopolysaccharide, and two different type IV secretion systems with distinct functions during the infection cycle (reviewed by Minnick and Battisti[277]). Alongside, a panel of more obscure factors such as secreted GroEL chaperone that acts as a potent mitogen[278] or deformin, an elusive small molecule that subverts the stability of red blood cell membranes[279] have been described. However, the precise molecular functions and biological roles of most *Bartonella* virulence factors are unknown, not to speak of a big picture that would combine the different threads of research and assign the various virulence factors of *Bartonella* to different steps of the infection cycle.

Only a few research groups in the *Bartonella* field are investigating the molecular aspects of *Bartonella* infections[a] with most contributions coming from the Kempf lab (focusing on a type V secretion system of *B. henselae*[280]), the Koehler lab (focusing on a group of type V secretion systems[281] and some outer membrane proteins[282] of *B. quintana*), the Andersson lab (focusing on the molecular evolution of *Bartonella*[283,284]), and our laboratory that uses *Bartonella* as a model system to study the coevolution of a bacterial pathogen and an effector-secreting type IV secretion system[169,276]. Some other research groups also made important contributions to our understanding of the molecular pathogenesis of *Bartonella*[278,285-287]. On the other side, most researchers in the *Bartonella* field are veterinarians and concerned with *Bartonella* as a frequent cause of disease in animals and an emerging pathogen of humans, though both aspects are typically seen as connected from the perspective of "One Health"[288]. These laboratories typically publish case studies[289-291], sampling studies[292-294], and occasionally also molecular biology research[295] or experimental infections[296-298] that are of particular importance because they allow to expand key concepts beyond small rodent models and their cognate *Bartonella* pathogens.

In conclusion, at the beginning of my PhD project the *Bartonella* field was highly fragmented and lacked a fully conclusive picture describing how the different virulence factors of *Bartonella* act together at different stages of the infection strategy. Additionally, the few

[a] During the course of my PhD project the laboratory of Dr. Katharina Dittmar (University of Buffalo, The State University of New York, Buffalo, United States) joined the field with a series of significant publications on the molecular evolution of *Bartonella* (see *Unpublished results related to Review article I*).

comprehensive reviews on this topic were several years old and did therefore not embrace recent developments in the field[277,299,300]. It is clear that this situation was problematic for researchers concerned with treatment strategies for human bartonelloses such as trench fever and Carrion's disease that are gaining ground due to alterations in society, ecology, and climate[301,302]. Furthermore, without a comprehensive understanding of how the different virulence factors of *Bartonella* act together during the infection strategy it was pointless for me to analyze the co-evolution of one of them, the VirB/D4 T4SS, with its bacterial host. I therefore started my PhD project with a systematic catalogization and analysis of *Bartonella* virulence factors based on available literature (see *Review article I* and a recent update in the *Unpublished results related to Review article I*).

5.4.2. *Bartonella* as a model for the evolution of type IV secretion systems

At the beginning of my PhD project it was the prevailing model in the field that the genus *Bartonella* is split into four phylogenetic lineages with lineage 3 (L3) and lineage 4 (L4) being sister clades and lineage 1 (L1) being the sister clade of a clade formed by the other three lineages (Figure 12). In this model, *Bartonella bacilliformis* as the only species in L1 represents an ancestral evolutionary state. Though it employs the same overall infection strategy as the other species, it is less proficient in precise manipulation of its human host and thus can cause severe illness in patients. In contrast to *B. bacilliformis* which is restricted to infect humans, the species in L2-4 adapted to a huge variety of mammal hosts through explosive radiations and cause no or only mild symptoms in their respective reservoir hosts. The deep split between L1 and L2-4 (the "modern" bartonellae) correlates with the presence of at least one of three type IV secretion systems (T4SS) in the radiating lineages, but their complete absence in *B. bacilliformis*, suggesting that type IV secretion systems may have facilitated the host adaptation of *Bartonella* (evolutionary model described in detail by C. Dehio[300])[169,275].

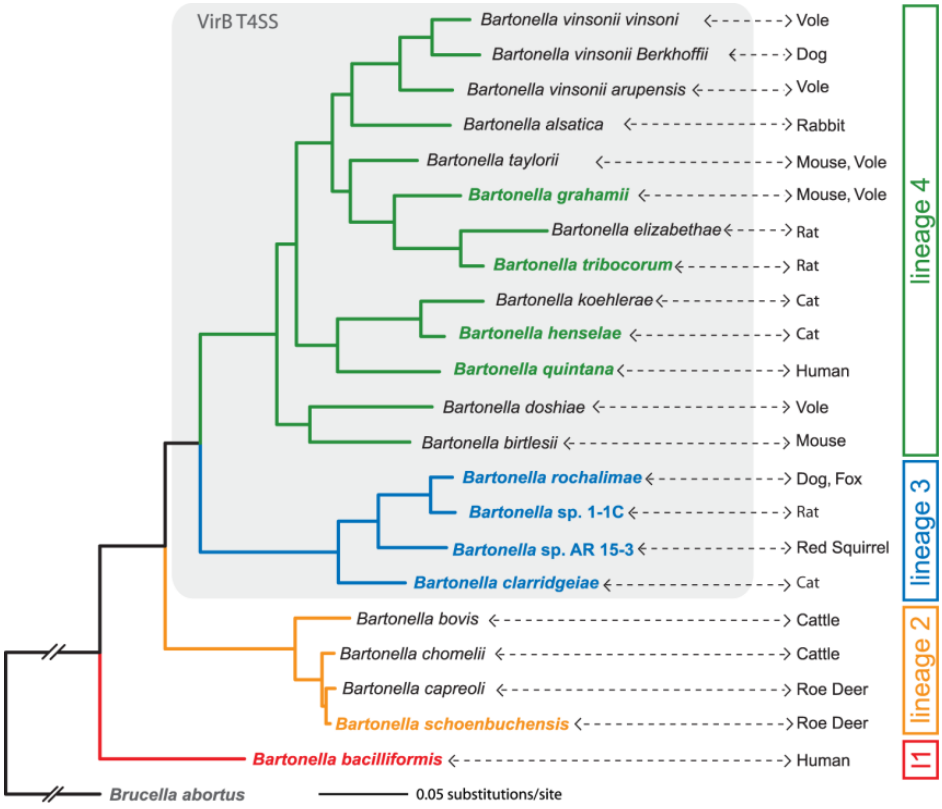

Figure 12: Phylogenetic tree of the genus *Bartonella* as published by Engel *et al.*[169]. The phylogeny was constructed using a maximum likelihood analysis of an alignment of 487 genes of ten sequenced *Bartonella* species (bold and colored) as well as *Brucella abortus* (outgroup). Additional species were included based on the sequences of a number of housekeeping genes. Grey shading indicates presence of a VirB/D4 T4SS, and the primary mammalian host of the respective *Bartonella* species is shown to the right. The four lineages described in the running text are shown by color code.

It is well known that host-interacting type IV secretion systems evolved multiple times independently from conjugative ancestors, i.e., from type IV secretion systems mediating the interbacterial transfer of genetic information typically in form of plasmids that encode the type IV machinery itself[303]. During bacterial conjugation, a protein called relaxase is covalently linked to a single strand of the conjugative plasmid and transferred from the donor bacterium to the recipient via type IV secretion, thus enabling DNA transfer[304] (see more details in the *Perspective* section). Interestingly, the by far most species-rich L4 of *Bartonella* encodes a T4SS called Trw that is closely related to the conjugative machinery of R388, an enterobacterial plasmid (see also Figure 35). However, the *Bartonella* Trw T4SS has evolved to mediate adhesion to red blood cells via its extracellular pili and lost the conjugative relaxase as well as the associated DNA processing and transfer machinery completely[305] (Figure 13). Therefore, no effectors evolved that could be secreted into host cells, but instead the extracellular subunits of the type IV secretion pilus were shaped by gene duplication and diversification to mediate host-specific adhesion to erythrocytes[276,283]. The presumed co-expression of the different copies suggests that their diversity may be an adaptation to the notorious polymorphicity of red blood cell surface structures in mammals rather than being

involved in some kind of phase variation or similar immune evasion mechanisms[305-307]. Interestingly, the presence of the Trw T4SS (in L4) is mutually exclusive with flagellation (in L1-3)[169], suggesting that flagellation as an ancestral trait has somehow been functionally replaced by the Trw T4SS in a common ancestor of L4[300]. The flagella of *Bartonella* have been shown to be involved in erythrocyte infection, but also represent a major target for the host's immune system despite TLR5 evasion[308-310]. Given the clear dominance of L4 within the genus *Bartonella* and their adaptation to diverse hosts it is tempting to speculate the modularity of the Trw machinery could make it superior to flagellation with regard to host adaptability and on top avoid the surface expression of a highly conserved bacterial protein[300].

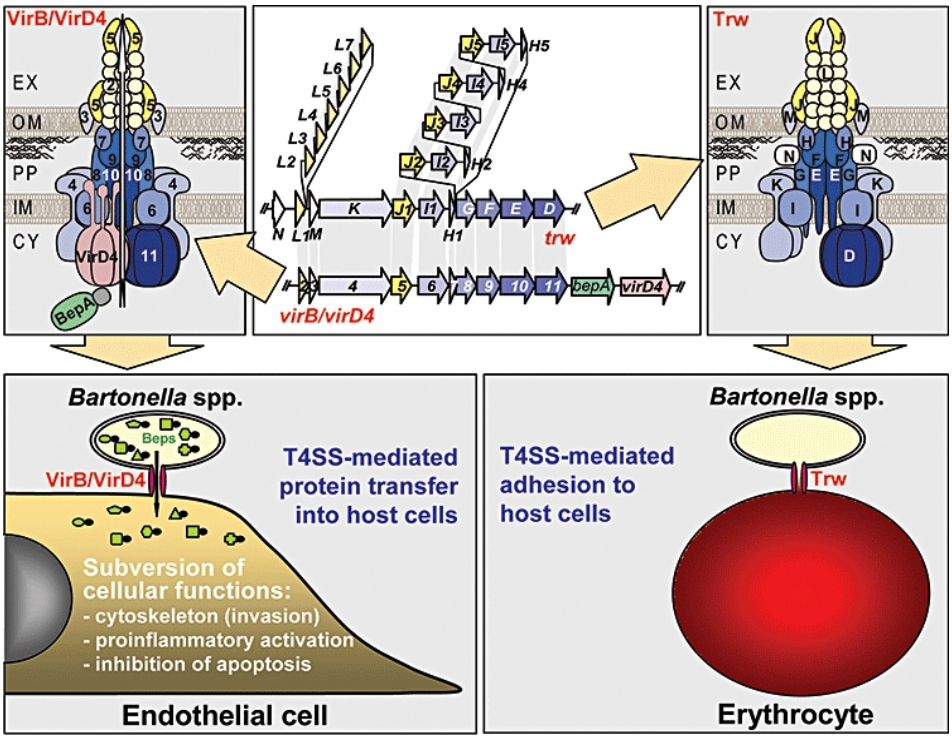

Figure 13: Virulence-associated type IV secretion systems in *Bartonella*. Their genetic organization as well as models of their architecture are shown for VirB/D4 T4SS (left) and Trw T4SS (right) in the upper half of the illustration (taken from the review of Christoph Dehio[300]). Note that the VirB/D4 T4SS comprises a complete type IV secretion system while the Trw T4SS lacks both the coupling protein and any identifiable substrates. Instead, it displays tandem duplications of extracellular pilus subunits. These differences reflect the divergent biological functions of the VirB/D4 T4SS (effector secretion into nucleated host cells; bottom left) and of the Trw T4SS (erythrocyte adhesion; bottom right). EX = extracellular matrix, OM = outer membrane, PP = periplasm, IM = inner membrane, CY = cytoplasm

The contribution of a type IV secretion system to host adaptation is particularly clear for L3 and L4 that are both species-rich and have adapted to a multitude of different host species in two recent adaptive radiations, while the host range of L1 (*B. bacilliformis* limited to infect humans) and L2 (limited to infecting ruminants) is highly restricted[169,268] (see Figure 12). In the prevailing model, two explosive radiations resulting in L3 and L4 were triggered by improvements of host-interaction after the acquisition of a host-interacting VirB/D4-like T4SS

and the evolution of host-targeted effector proteins called Beps (*Bartonella* effector proteins)[169] (see Figures 12 and 14A). This implies that common ancestors of L3 and L4 had each acquired similar versions of a primordial VirB/D4-like type IV secretion system with a single ancestral effector. Subsequently, this effector evolved into the extant repertoires with seven and ten orthologous Beps in L3 and L4, respectively, via two independent series of gene duplication and diversification[169,275] (see Figures 14A and 14B). The VirB/D4 T4SS is closely related to rhizobial conjugation systems like the AvhB type IV secretion machinery of *Agrobacterium*, suggesting that it initially evolved from such a machinery. Consistently, the secreted effectors of *Bartonella* employ a BID (Bep intracellular delivery) domain together with a positively charged C-terminus as their secretion signal, just like the relaxases of rhizobial conjugation systems[311]. On top of this secretion signal, the common ancestor of all Beps (and the majority of extant effectors) harbored a FIC domain as its putative "effector module" that may have served to manipulate host proteins by adenylylation[169]. Secondarily and independently in L3 and L4, a second class of effectors evolved in which the FIC domain was replaced with a block of sequence harboring tyrosine-containing motifs (Figure 14B). These tyrosine motifs get phosphorylated by host kinases and may serve as hubs to manipulate signaling in host cells[169,275]. Furthermore, the evolutionary pressure on the effector repertoires to mediate complex host interactions resulted in BID domains that, on top of serving as a secretion signal, took over functions in host interaction[224,312,313]. From a conceptual point of view it was generally assumed that orthologous groups of effectors share common biological functions, while paralogous effectors adapted to different roles in host cell manipulation.

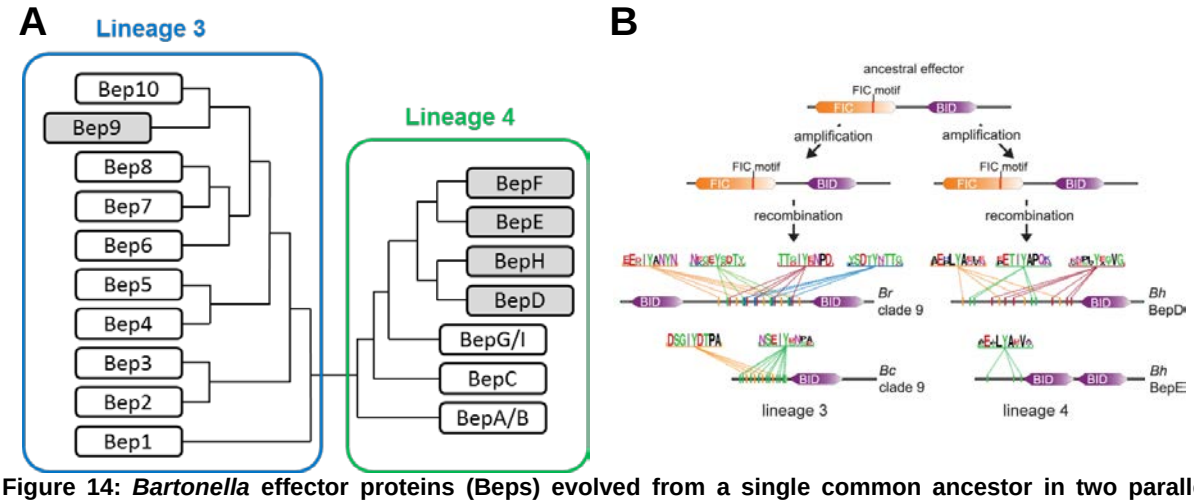

Figure 14: *Bartonella* effector proteins (Beps) evolved from a single common ancestor in two parallel series of gene duplication and diversification. A) The phylogeny of Beps was redrawn with arbitrary branch lengths from a maximum likelihood analysis that was based on the BID domain and the C-terminal extension that constitute the shared type IV secretion signal[169]. Different orthologous groups of effectors are shown as boxes and the typical functional architecture with an N-terminal FIC domain is indicated by a plain white box. The phylogeny shows that Beps of L3 (green frame) and L4 (blue frame) evolved independently from a common ancestor via series of gene duplication and diversification. Effectors containing tandem-repeated tyrosine-phosphorylation motifs instead of a FIC domain evolved independently in L3 and L4 (grey shading and lateral shift). **B)** The model illustrates our current understanding of Bep evolution with the amplification and diversification of FIC domain containing effectors and the secondary emergence of Beps with tyrosine containing motifs (*Br* = *B. rochalimae*, *Bc* = *B. clarridgeiae*, *Bh* = *B. henselae*). Both panels were adapted from Engel *et al.*[169].

Considerable knowledge on the individual functions of effectors secreted by species of L4 had already been gathered as my PhD project started, but it was considered a major riddle that none of them could be traced back to any effector's FIC domain. Even for BepA of *B. henselae* that harbors a FIC domain with a canonical active site motif and was shown to adenylylate (unknown) host target(s)[152] the leading phenotypes are solely mediated by its BID domain[312]. During my master project I systematically analyzed the FIC domains of *Bartonella* effectors *in silico* and started the functional investigation of effectors of L3 (see *Appendix: Further results*). My results showed that the most ancestral orthologous groups of effectors in L3 - Bep1, Bep2, and Bep3 – harbor a canonical FIC domain active site motif in every single known ortholog, suggesting that they act via adenylylation of host factors to subvert signaling in favor of the pathogen (see also Figure 28). Consistently, I demonstrated the adenylylation activity of Bep1 (targeting Rac1 and a few related proteins) and Bep2 (targeting an unknown protein of approximately 50 kDa size; identified in *Research article II*). These findings stand in contrast to most of the other orthologous groups in L3 and all effectors of L4 where at most scattered representatives harbor a canonical FIC domain active site motif and where I failed to detect adenylylation. Taken together, available data support the hypothesis that – at least as a general principle - different orthologs of L3 effectors share common activities or functions, while paralogous effectors have different molecular and biological functions. This emerging picture would be very similar to the situation in L4 (recently reviewed by Siamer *et al.*[314]) and could explain why the explosive radiations in both lineages had only been triggered *after* the evolution of a full effector repertoire. Furthermore, this principle of "specificity and diversification" of a fine-tuned repertoire of effectors is intuitive for a stealth pathogen like *Bartonella* as opposed to pathogens employing frontal attack strategies[315] that deal with host defenses like *V. parahaemolyticus*[316] (harboring VopS) or *H. somni*[317] (harboring IbpA).

As it is a common phenomenon among comprehensive models, the picture of *Bartonella* evolution that had been painted above has been obliterated in a number of details over the time of my PhD work. However, its general outlines were confirmed and even strengthened by new findings of others (see the considerations as part of *Unpublished results related to Review article I*). In any case, one of the most important questions had so far not been addressed – where did the ancestral VirB/D4-like machinery come from whose coevolution with *Bartonella* likely promoted the pathogen's host adaptability? One hint that had already been noted previously is the presence of an additional type IV secretion system called Vbh or Vbl (for VirB-homologous or VirB-like; the denomination as "Vbh" will be consistently used in this work) in all species of L2 and a number of species of L4[169]. The Vbh T4SS is closely related to the VirB/D4 T4SS and sometimes encoded together with a *bep*-like gene of unknown function that displays a clear FIC-BID domain architecture[169,275,318,319]. The high

sequence similarity between the BID domains of these Bep-like proteins associated with the Vbh T4SS and their cognate relaxase makes it obvious that they are secreted by the Vbh T4SS, suggesting that they may somehow be evolutionarily related to the inferred ancestral VirB/D4 T4SS with a single ancestral effector protein.

During my PhD project I characterized the molecular and biological function of genuine bacterial FIC domain proteins that are ancestrally related to secreted effectors of Vbh and VirB/D4 machineries in *Bartonella* (*Research articles I* and *III* as well as *Review article II*). Furthermore, my findings allowed to propose a coherent model that describes the *de novo* evolution of a secreted effector at an ancestral Vbh-like T4SS and the subsequent coevolution of effector, type IV secretion machinery, and *Bartonella* (see the *Perspective* at the end of this work).

6. Results

6.1.Review article I (published)

"Now what is the message here? The message is that there are no 'knowns'. There are things we know that we know. There are known unknowns. That is to say there are things that we now know we don't know. But there are also unknown unknowns. There are things we don't know we don't know. So when we do the best we can and we pull all this information together, and we then say well that's basically what we see as the situation, that is really only the known knowns and the known unknowns. (…)
It sounds like a riddle. It isn't a riddle. It is a very serious, important matter."

Donald H. Rumsfeld, 21st US Secretary of Defense, Press Conference at NATO Headquarters in Brussels, Belgium, June 6th 2002; last accessed on October 21st 2014 from the online transcript available at http://www.defense.gov/transcripts/transcript.aspx?transcriptid=3490.

Intruders below the radar: molecular pathogenesis of *Bartonella* spp.

Alexander Harms and Christoph Dehio

Clinical Microbiology Reviews, Volume 25, Number 1, January 2012, 42-78.

Summary

In this review article I compiled all available information on the pathogenesis of *Bartonella* bacteria with a focus on molecular mechanisms.

Phylogenetically, the genus is split into four lineages with lineage 1 (L1, comprising only *B. bacilliformis*) and lineage 2 (L2, infecting ruminants) representing evolutionarily ancestral states compared to the more species-rich lineages 3 and 4 (L3 and L4) that arose from recent explosive radiations and infect a wide array of mammals as their primary hosts. It is the prevailing view in the field that the parallel adaptive radiations of L3 and L4 were triggered by a more subtle and fine-tuned host interaction as a key innovation which had been enabled by the acquisition and subsequent adaptation of the effector-secreting VirB/D4 T4SS and the adhesin-like Trw T4SS.

Despite some differences in the repertoires of virulence factors, a careful analysis of available data from research and clinics suggested that all species of *Bartonella* share a characteristic stealth infection strategy involving passage through an ill-defined “primary niche” that probably includes the infection of migratory cells and the vascular endothelium. From there, the bacteria are seeded into the bloodstream where they invade erythrocytes and persist intracellularly to promote transmission by blood-sucking arthropods. Throughout the infection cycle the bartonellae employ diverse tactics of immune evasion and immunomodulation to avoid clearance by host immune responses.

Various *Bartonella* species that infect diverse primary hosts can cause accidental zoonotic infections in humans, but most human infections are caused by *B. henselae* (adapted to infect cats) and the two human-adapted species *B. quintana* and *B. bacilliformis*. Though infections with ancestral *B. bacilliformis* can be lethal if untreated, *Bartonella* typically causes only mild and self-limiting disease in accidental hosts and no or negligible symptoms in primary hosts (despite a long-lasting bacteremia), but infection rates far above 50% are not uncommon among wild mammals. Infections with *B. bacilliformis* and, particularly in immunocompromised hosts, also with other species can cause pathological angiogenesis as well as hemolytic anemia (rare beyond *B. bacilliformis*) that represent runaway consequences of improper host interaction during the two phases of *Bartonella* infections, respectively.

In the primary niche, *Bartonella* invades nucleated cells using a zipper-like mechanism that appears to involve an interaction with β1-integrins and possibly ICAM-1 and is generally independent of type IV secretion. The bacteria enter their host cells in small vesicles that accumulate in the perinuclear region, but mechanisms of cellular egress have not been

described. Interestingly, in case of some variants of the Houston-1 strain of *B. henselae* the strong anti-endocytic effect of effectors secreted by the VirB/D4 T4SS transiently prevents bacterial uptake despite major cytoskeletal rearrangements and causes their aggregation on the cell surface in form of structure called invasome. Subsequently, the whole bacterial aggregate is taken up by the host cell. Interactions with *Bartonella* induce a complex transcriptional reprogramming of nucleated host cells that involves the induction of Ca^{2+}, HIF-1, as well as NF-κB signaling and is caused by both secreted and contact-dependent activities of the pathogen which are amplified by auto- and paracrine signaling of the host. Furthermore, *Bartonella* promotes the secretion of immunomodulatory factors such as "master key" cytokine IL-10 to achieve a global attenuation of host defenses.

From the primary niche, the bacteria are seeded into the bloodstream where they infect erythrocytes in a sequence of adhesion, deformation (impairing membrane tightness), and invasion. The entry into red blood cells has been described as "forced endocytosis", but the molecular details of this process are not understood. Intracellular persistence of *Bartonella* for the remaining lifespan of the erythrocyte enables transmission by blood-sucking arthropods.

The molecular contributions of *Bartonella* virulence factors to pathogenesis can be summarized as follows:

- Trimeric autotransporter adhesins (TAAs) are found in all species of *Bartonella* and seem essential for productive infection *in vivo.* Single homologs were shown to mediate adhesion to the extracellular matrix, to manipulate host cells via β1-integrins to activate HIF-1 and NF-κB signaling, and to inhibit macrophage phagocytosis.
- The VirB/D4 T4SS is found in all species of L3 and L4, but the repertoires of effectors (Beps) in both lineages evolved independently from a single common ancestor in parallel series of gene duplication and diversification prior to the onset of the adaptive radiations. While no data had been published on Beps of L3, broad literature on the effectors of L4 demonstrated contributions to the inhibition of apoptosis and proinflammatory activation of host cells, the modulation of angiogenesis, and the inhibition of endocytosis.
- The chaperone GroEL appears to have a moonlighting function as a secreted mitogenic as well as anti-apoptotic factor and likely acts via the induction of Ca^{2+} signaling.
- Diverse outer membrane proteins (OMPS) of *Bartonella* were shown to interact with host cells, though their binding partners and biological functions are largely unknown. They may contribute both to adhesion and the manipulation of host cells, e.g., as obvious candidates for the invasin(s) causing *Bartonella* uptake in a zipper-like mechanism or as

the LPS-associated lipoprotein that manipulates cytokine secretion via toll-like receptor 2 (TLR2).

- The hemin binding proteins (Hbps) are one particular group of OMPs that is present as a series of paralogs in all species of *Bartonella*. Various molecular functions and biological roles have been proposed but not conclusively demonstrated, e.g., the participation in heme uptake, the formation of an antioxidant coat, or the direct participation in host cell manipulation.
- The Trw T4SS of L4 mediates host-specific adhesion to erythrocytes and forms variable surface structures using an array of pilus subunits that evolved via gene duplication and diversification likely to cope with host polymorphisms on the erythrocyte surface.
- Deformin is an elusive small molecule that causes the “pits” or “trenches” appearing on red blood cells upon contact with *Bartonella* and is believed to locally decrease the tightness of erythrocyte membranes as a prerequisite of “forced endocytosis”.
- Flagellation is an ancestral trait of *Bartonella* conserved in L1-3 and was shown to be involved in erythrocyte invasion. Though a role in erythrocyte adhesion had been proposed earlier, it seems most likely that flagella contribute to the invasion of red blood cells by providing mechanical force.
- The invasion-associated locus of *Bartonella* consists of *ialA* and *ialB* genes that are essential for erythrocyte invasion, but not adhesion. While IalA appears to be involved in cellular stress responses, IalB is an outer membrane protein and likely the factor directly responsible for the “forced endocytosis” of *Bartonella* into red blood cells.
- The LPS of *Bartonella* is mostly (but not exclusively and homogenously) deep rough and of peculiar chemical structure so that it is not recognized by TLR4 and even acts as an antagonist of TLR4 signaling.
- Classical autotransporters of *Bartonella* belong to two separate phylogenetic groups:
    - One of them (the *iba* group) is monophyletic in *Bartonella* but split into two subclades that diverged before the diversification of extant lineages. The first group comprises homologs of *B. henselae* Cfa and may be involved in the manipulation of membranes. The second group contains homologs of *B. henselae* Arp and may act as pertactin-like adhesins. Several representatives of the *iba* autotransporters were found to be individually essential for *Bartonella* infections *in vivo*.
    - The other, smaller group contains phylogenetically unrelated autotransporters that exhibit similarities to proteins found in *Enterobacteriales*.
- Filamentous hemagglutinins are secreted via the two-partner pathway and present in form of two separate clades that were acquired independently from different sources.

- In addition to this catalogization of known virulence factors I also reported the discovery of a machinery to produce and secrete cyclic β-(1,2)-glucans that is highly conserved within *Bartonella* and constitutes a major virulence factor of closely related *Brucella* bacteria.

In conclusion, the comprehensive compilation of available literature on the molecular pathogenesis of *Bartonella* in this review article was able to close some gaps in our understanding and connected many open threads of research to form a more coherent picture. However, this article also pointed at a disturbing number of open questions and even added a number of new ones that emerged from the systematic analysis of previous research.

Recent developments in the field are shortly summarized as *Unpublished results related to Review article I*.

Statement of the own participation

I contributed to this publication by analyzing the scientific literature on the pathogenesis of *Bartonella* and systematically catalogued and interpreted the content with a focus on molecular mechanisms. Furthermore, I closed some minor gaps of knowledge by sequence analyses *in silico* and proposed the cyclic β-(1,2)-glucan synthesis and export machinery of *Bartonella* as a potential virulence factor that had not been proposed before. I drafted the manuscript and sketched the figures.

Prof. Christoph Dehio mentored the work and gave hints regarding important publications that I had missed. Furthermore, he participated in the construction of the manuscript. Patrick Lane of ScEYEnce Studios performed the art enhancement on several figures prior to publication.

CMR
Journals.ASM.org

Intruders below the Radar: Molecular Pathogenesis of *Bartonella* spp.

Alexander Harms and Christoph Dehio

Focal Area Infection Biology, Biozentrum, University of Basel, Basel, Switzerland

INTRODUCTION

The genus *Bartonella* constitutes a group of facultative intracellular pathogens that share a unique stealth infection strategy aiming at persistence in an intraerythrocytic niche, thus enabling continuous transmission by bloodsucking arthropods and establishing a sanctuary protected from the assault of the host's immune system.

Each of the bartonellae infects only one or a few closely related mammal species as its reservoir host, a relation defined by the capability of *Bartonella* to establish an intraerythrocytic and typically asymptomatic bacteremia, although infections in incidental hosts may evoke discernible disease. Several species of the genus *Bartonella* are human pathogens, including both zoonotic agents and species that infect humans as their reservoir host. While most human infections, for example, with *Bartonella henselae* or *Bartonella quintana*, elicit only limited morbidity, *Bartonella bacilliformis* is unique as a deadly pathogen causing Carrion's disease, which can kill more than 80% of the patients during its acute phase but is restricted to the Andes region (reviewed in reference 272). Consistent with this, phylogenetic analyses identified *B. bacilliformis* as the only known representative of an ancient lineage that is widely separate from the other, so-called modern species of the genus (374).

Address correspondence to Christoph Dehio, christoph.dehio@unibas.ch.
Copyright © 2012, American Society for Microbiology. All Rights Reserved.
doi:10.1128/CMR.05009-11

Despite very limited public awareness of *Bartonella* outside the areas where *B. bacilliformis* is endemic, research over the last 20 years has uncovered the virtual ubiquity of *Bartonella* bacteremia among mammals, thus justifiably tempting other researchers to question the typical notion of blood as a sterile organ (51). Infection rates of higher than 50% are common among wild-living mammals, and, e.g., 15 to 30% of pet cats are infected, thereby constituting a large reservoir for zoonotic *Bartonella* infections that can cause considerable morbidity, especially in immunocompromised patients (see below). The bartonellae are currently classified as (re)emerging pathogens, since various species are increasingly found to elicit human disease, most likely due to changes in human society and medical practice but also thanks to improved diagnostics (46, 220, 301).

We are convinced that investigating the molecular and cellular bases of *Bartonella* infections *in vitro* and *in vivo* is crucial for understanding the pleiotropic pathology in human patients, because bacterial virulence strategies evolved not to cause disease in the host but to promote continuous spread and proliferation. It is therefore necessary to set the results from molecular and cellular microbiology into context with clinical as well as veterinary studies in order to understand the infection process as a whole. However, the assembly of a comprehensive picture is hampered by the obstacle that, as already stated by others, the bartonellae remain understudied (294) compared to more famous pathogens, and as a consequence, available knowledge often appears to be fragmented. This review therefore aims at compiling published work on the molecular pathogenesis of *Bartonella* and tries to highlight the various links to medical research in the field.

EPIDEMIOLOGY AND CLINICAL ASPECTS

Epidemiology

Striking evidence for the success of the bartonellae as stealth pathogens is that the majority of species have been discovered only very recently, although *Bartonella* infections are virtually ubiquitous among mammals (90). Remarkably, the infection rate may reach up to around 50% in feral cats or rodents and can be as high as 90% in wild ruminants (reviewed in reference 51). Apart from these groups of thoroughly investigated animals, *Bartonella* infections have been reported for diverse hosts such as bats (240), aquatic mammals (belugas [270]), and even nonmammal vertebrates (sea turtles [423]). Despite certain geographic differences that coincide with vector ecology, it is obvious that *Bartonella* infections are among the most prevalent bacterial infections worldwide.

Although the ubiquity of bartonellae in various mammals is an important reservoir of zoonotic infections, the majority of human disease is caused by only three species. *B. henselae*, whose reservoir host is the domestic cat, is well known to be the most common species infecting humans and characteristically causes cat scratch disease, a condition associated with only limited morbidity (see below). It was estimated at the end of the 20th century that 22,000 cases of cat scratch disease may appear every year in the United States, and roughly 10% of these were considered to require hospitalization (202). *B. quintana* is the only modern species of *Bartonella* that infects humans as its reservoir host, and it is known to cause trench fever, a louse-borne disease that was widespread in armies of the modern era such as Napoleon's Grand Army (350) and affected approximately 800,000 allied soldiers in France during World War I (66). The incidence of trench fever has dropped considerably since then, but infections with *B. quintana* are (re)emerging as urban trench fever, a condition that is associated with homelessness, alcoholism, indigence, and poor conditions of life, particularly health and hygiene, among individuals living on the fringes of society in developed countries (59, 189, 203, 399).

In contrast to the other species of the genus, *B. bacilliformis* is a deadly pathogen but endemic only in the high valleys of the Andes and apparently restricted to infecting humans (recently reviewed in reference 272). It can cause devastating disease and has been known as a pathogen among natives since the pre-Incan times (5) but apparently became a general health concern only with alterations in epidemiology due to climate change and increased migration into and out of the areas of endemicity in the last 150 years (81, 87, 131, 239). Disease caused by *B. bacilliformis* first received major attention around 1870 during the construction of the Oroya railroad through a region of endemicity, as approximately 70% of the (mostly nonlocal) workers died, to a large extent from the hemolytic anemia that is known today as Oroya fever (325). The seroprevalence of *B. bacilliformis* can be higher than 60% in natives of the areas of endemicity (230), and a considerable proportion of around 10% of the population was found to bear asymptomatic bacteremia, thus probably serving as a reservoir for infection (see various studies listed in reference 325).

Clinical Aspects

The most common malady associated with *Bartonella* in immunocompetent patients is cat scratch disease due to infection with *B. henselae*, a condition characterized by regional lymphadenopathy as the leading symptom, which may be accompanied by other unremarkable manifestations such as fever or fatigue (reviewed in reference 249). Cat scratch disease is usually self-limiting, though possibly long lasting, and can occasionally be caused by other *Bartonella* species such as *B. clarridgeiae* (237). Infections of immunocompetent individuals with *B. quintana* typically lead to a disease known as trench fever or 5-day fever, denoting the characteristic cyclic course of the symptoms with peaks of fever, bone pain, and headache that are accompanied by persistent bacteremia (66, 318). Both *B. quintana* and *B. henselae* are further able to elicit bacillary angiomatosis, i.e., the outgrowth of multiple vasoproliferative tumors, as a common complication of infection, primarily but not exclusively in immunocompromised individuals such as AIDS patients. While these lesions are most often found on the skin, bacillary angiomatosis or related conditions may also affect the liver ("bacillary peliosis"), spleen, bone marrow, eyes, or other parts of the body (304, 339). The dissemination of *Bartonella* infections is a complication observed mostly in highly immunocompromised patients, but it can also occur in apparently immunocompetent individuals. Such systemic infection not only with *B. henselae* or *B. quintana* but also with various other zoonotic species can lead to a plethora of symptoms, including extraerythrocytic bacteremia, neuroretinitis, or endocarditis (55, 94, 143). In addition, various moderate neurological symptoms such as insomnia or memory loss have been reported (53, 56, 73).

The classical course of infections with *B. bacilliformis* is known as Carrion's disease and consists of Oroya fever as the acute phase with hemolytic anemia and a subsequent chronic phase hallmarked by multiple vasoproliferative lesions on the skin (verruga peruana for "Peruvian wart") (Carrion's disease was recently reviewed in reference 272). The devastating hemolytic

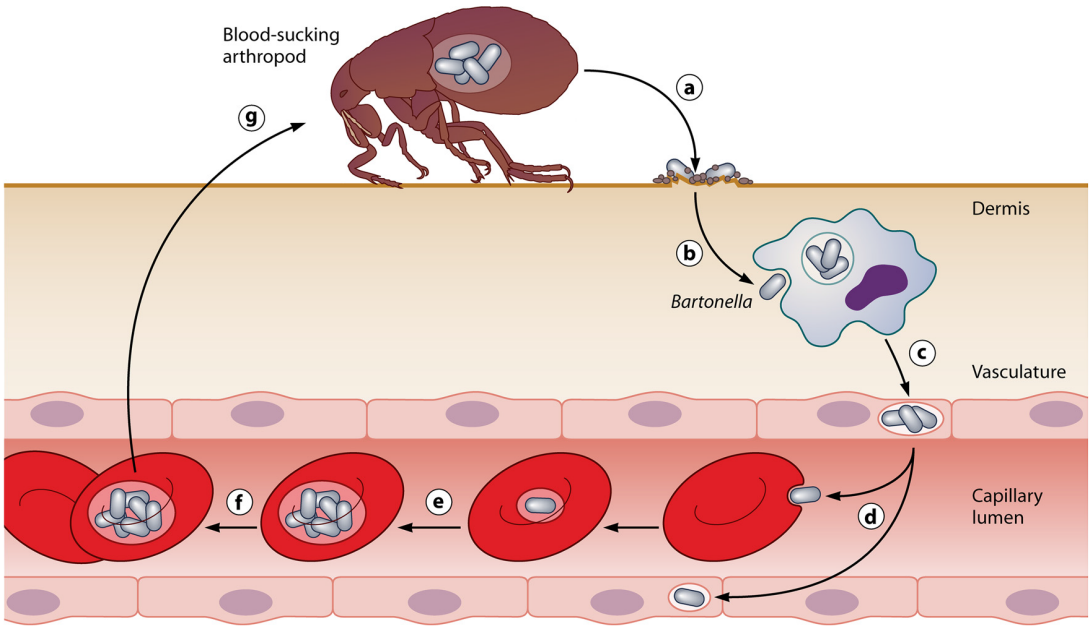

FIG 1 Common infection strategy of the bartonellae. The drawing illustrates the general concept of reservoir host infections with *Bartonella*. Following transmission by an arthropod vector (a), the bartonellae colonize the primary niche, which probably involves entry into migratory cells (b) and transport to the vascular endothelium (c), where the bacteria persist intracellularly. From the primary niche, the bacteria are seeded into the bloodstream (d), where they invade erythrocytes and reinfect the primary niche. After limited replication inside the red blood cell (e), they persist in the intraerythrocytic niche (f) competent for transmission by a bloodsucking arthropod (g).

anemia during Oroya fever is a critical difference between the pathologies of *B. bacilliformis* and the other bartonellae, since severe morbidity and hemolytic anemia are usually not observed during infections with the modern species. A recent compilation of various studies concluded that the mortality during Oroya fever ranges from close to zero in the case of hospitalized patients receiving antibiotic treatment to up to 88% in untreated cases (325). Approximately 70% of patients suffering from Oroya fever develop complications of the disease, of which approximately half are of an infectious and half of a noninfectious nature. Noninfectious complications such as fever, anorexia or an altered mental status have been suggested to be primarily a consequence of systemic infection (271). The impairment of immunity during Oroya fever favors secondary infections that contribute prominently to morbidity and mortality by provoking septicemia, most often with *Salmonella* (271, 325, 359). During Carrion's disease, the abrogation of hemolytic anemia is characteristically followed by massive pathological angiogenesis as hallmark of the chronic tissue phase called verruga peruana. It is crucial to note that the nodules observed over the course of this phase are "clinically and histologically indistinguishable" from the tumors arising during bacillary angiomatosis with the modern *Bartonella* species (67, 254). Like these, the pathological angiogenesis during the verruga peruana phase usually occurs in the skin, but atypical cases involving other organs such as the spleen (266) have been reported. In striking contrast to the acute phase of Carrion's disease, verruga peruana is associated with only negligible mortality (325). Notably, the name of this biphasic infection and the discovery of the link between its two phases derive from Daniel Alcides Carrion, who died from Oroya fever after he inoculated himself with blood from a verruga peruana nodule (396). However, it is known today that this classical course of Carrion's disease is not the only possible outcome of a *B. bacilliformis* infection, since natives in the areas of endemicity exhibit a significant baseline of asymptomatic bacteremia (see above) and suffer from Oroya fever relatively rarely (359) but frequently develop verruga peruana without prior hemolytic anemia (150).

LIFE CYCLE AND INFECTION STRATEGY

The infection cycle of *Bartonella* is initiated with the inoculation of a mammal reservoir host, characteristically following transmission via bloodsucking arthropods. Upon inoculation, the bartonellae are not capable of directly colonizing erythrocytes. Instead, a preceding period of residence in a primary niche is apparently necessary to make the bacteria and/or the host competent for this step. From the primary niche, the bartonellae are seeded into the bloodstream and infect erythrocytes in a sequence of steps ranging from adhesion to eventually invasion and intracellular persistence that enables continuous vector transmission (Fig. 1).

During the whole course of infection, the lack of an effective host immune response and a globally moderated inflammatory profile are highly beneficial for *Bartonella* and are promoted by the pathogen via both passive immune evasion and active immunomodulation. The infection cycle of *Bartonella* has been extensively studied and reviewed elsewhere (see references 89 and 403). Importantly, although it is obvious that certain differences from species to species do exist and probably arose due to specific paths of pathogen-host adaptation, it is generally believed that the overall concept of this infection cycle is conserved among members of the genus *Bartonella*.

Host Specificity

It is apparent from the epidemiology of *Bartonella* infections that host specificity must be a determining factor for the selective prevalence of these bacteria in various mammals (51, 121). Furthermore, the multistep infection strategy of *Bartonella* suggests that host specificity could be a complex phenomenon, because every step may involve critical interactions of the bacterium with its hosts that could require fine-tuned manipulations on the molecular level.

Since inoculation of a naive host individual with *Bartonella* classically requires transmission via a bloodsucking arthropod, it is obvious that vector ecology has a major impact on host specificity. However, direct transmission between mammal hosts has occasionally been reported, e.g., via cat bites (57), and the release of *Bartonella* into the saliva of infected cats has been demonstrated (311).

It is well known that the sand fly (*Lutzomyia verrucarum*) is the most important vector for *B. bacilliformis*, and the geographic range of *L. verrucarum* prevalence is roughly congruent with the areas where Carrion's disease is endemic (325). However, certain differences in the distributions as well as recent epidemics in areas outside the geographic range of *L. verrucarum* indicate that other *Lutzomyia* species may serve as additional vectors (4, 68, 325). The role of human body lice (*Pediculus humanus corporis*) and their feces in the transmission of trench fever was well known already more than half a century before the discovery of *B. quintana* (66), but other vectors such as cat fleas (*Ctenocephalides felis*) have been occasionally reported as well (368). Cat fleas are the natural vector of *B. henselae*, and their potency to transmit the pathogen between cats has been demonstrated experimentally (93). Transmission to humans is thought to occur mostly indirectly via contaminated flea feces that are inoculated via a cat scratch ("cat scratch disease") (89). It was shown for both human body lice and cat fleas that *B. quintana* and *B. henselae*, respectively, can replicate in their digestive systems and are shed in the arthropod feces (139, 145, 398). More general, it is obvious that other hematophagous arthropods are capable of transmitting *Bartonella* as long as the bacteria can survive within these vectors and make productive contact with new host individuals. For example, the long-debated capability of ticks to serve as vectors for *Bartonella* has recently been demonstrated (354), and biting flies are known to play an important role in the transmission of *Bartonella* among ruminants where they are predominant bloodsucking parasites (122, 279). Coincident with the prevalence of the common arthropod vectors, the *Bartonella* infection rate among mammals is usually higher in warm, humid areas than in cold, arid ones (29, 206) and higher in wildlife than in domestic animals (e.g., 15 to 30% in pet cats [91, 166, 167] compared to up to 50% in feral cats [173]). The relationship between *Bartonella* and the different vectors has been comprehensively reviewed elsewhere (89).

It is striking that the effects of vector ecology via selective transmission are not at all sufficient to explain current knowledge on the host specificity of *Bartonella*, especially since host specificity has been readily reproduced in experimental infections under laboratory conditions in the absence of any vector. In particular, persistent bacteremia as the hallmark of reservoir host infection was obtained only when using reservoir host models (134, 165, 233, 236, 242, 330, 394). Attempts to infect nonreservoir hosts with bartonellae resulted neither in verifiably intraerythrocytic bacteremia nor in persistent infection (92, 134, 195, 213). However, it is known that the host range of *Bartonella* does not strictly follow the taxonomic borders on the species level but may include a few closely related species, so that *B. quintana* has been reported to infect not only humans but also rhesus macaques, both naturally and upon experimental inoculation (190, 450). Since the *Bartonella* infection strategy involves complex interactions with both nucleated host cells and erythrocytes, it is apparent that host specificity can act on both of these levels. Strong evidence supporting an intricate host species/host cell type/*Bartonella* species specificity concerning phenotypes associated with the primary niche (see below) points toward a certain restriction already at this level, probably eliminating a considerable number of incidental infections due to improper immunomodulation. In addition, the establishment of intraerythrocytic bacteremia as the key step to enable continuous transmission is known to be critical for host specificity of the modern bartonellae. It has been demonstrated that the ability of these species to adhere to erythrocytes is highly restricted to those of reservoir hosts, while this step is apparently not limiting for *B. bacilliformis* to a similar extent (see "Infection of Erythrocytes" below). However, no considerable pathology of any experimental infection of nonprimates with *B. bacilliformis* has been reported (see references 195 and 313), strongly suggesting that further mechanisms in addition to vector ecology restrict the host range of this deadly pathogen.

The Primary Niche

Cellular nature of the primary niche. Little *in vivo* evidence is available that would allow us to draw a precise picture of the infection stage between the inoculation of *Bartonella* into the skin (e.g., from the feces of arthropod vectors) or the bloodstream (e.g., from ticks or sand flies) and the bacteremic stage of the infection. Intravenous inoculation of *Bartonella* does not lead to immediate infection of red blood cells (see below), strongly suggesting that the bacteria and/or the host needs to be primed in some way to enable erythrocyte colonization and implying that *Bartonella* persists in a primary niche prior to blood-stage infection (394). While the nature of this niche in the case of infections with the modern species constitutes one of the key controversies in the field, almost no research has been performed on the primary niche in infections with *B. bacilliformis*. However, the existence of such a niche for this species is widely accepted (271, 417) and may explain part of the remarkably long incubation time of Oroya fever (60 days on average [272]).

No conclusive evidence that would unambiguously reveal the cellular identity of the primary niche has been published. However, the abundance of accordant clinical conditions, the amount of *in vitro* data supporting extensive interactions with the pathogen, and their obvious proximity to the circulation have established endothelial cells as an important target of *Bartonella in vivo* and a likely candidate to be part of the primary niche (reviewed in reference 113). However, it is likely that additional cell types are involved in this niche and bring in properties or abilities that cannot be supplied by endothelial cells. Most obvious is that the apparent need for bacterial transport within the host (e.g., from typical intradermal inoculation) implies that migratory cells may play an underestimated role in the establishment of *Bartonella* infections. It seems reasonable to assume that the bartonellae could enter migratory cells after inoculation and travel passively to a remote location in the host's body where they would persist and

multiply, most probably in the microvasculature. The frequent affliction of lymph nodes during *Bartonella* infections may indicate that such transport might occur via the lymphatic system, and it has been proposed that lymphocytes or mononuclear phagocytes could be the vehicles of *Bartonella* transport as part of the primary niche (236). The long life span of these cells and their circulatory migration between tissues and vasculature not only may be part of the classical course of *Bartonella* infection but also could promote the dissemination of the pathogen in the host's body as a common complication of cat scratch disease (see above). A possible role of migratory cells as part of the *Bartonella* infection strategy is striking, considering that *B. henselae* can resist macrophage killing for at least 3 days (236) and establish an intracellular niche in these cells that is distinct from the endocytic pathway (246). Consistent with this, a murine model of *B. henselae* infection revealed that bacteria are detectable in liver and lymph nodes within 6 h after intraperitoneal inoculation (219), which is difficult to explain without transport of the pathogen by a host mechanism.

Other studies proposed hematopoietic progenitor cells or erythroblast cells, nucleated progenitors of erythrocytes, as part of the primary niche (162, 274, 366). Since mature red blood cells are nonendocytic (see below), it is an interesting hypothesis that *Bartonella* could infect erythrocyte progenitors and then enter the bloodstream coincident with their maturation. However, it has been demonstrated for *B. tribocorum* that *Bartonella* can invade mature red blood cells *in vivo* (394). It is therefore not necessary to assume that erythrocyte progenitors are part of the primary niche, although it seems clear that *Bartonella* can infect these cells *in vivo* and that they, when mobilized, may contribute to (re)infection of the bloodstream as well as dissemination of the pathogen, as suggested by others (376).

The frequent relapse of *Bartonella* infections in reservoir and incidental hosts after antibiotic treatment and/or apparent clearance of bacteremia by the immune system (examples in references 66, 155, 236, and 339) indicates that the bacteria in the primary niche and potentially in disseminated niches would be protected from such assault, for example by persisting intracellularly from where they may reinfect the bloodstream. A periodic seeding of bacteria from the primary niche into the circulation at intervals of several days has been demonstrated in the *B. tribocorum* rat infection model (403) and may very well explain the cyclic relapse of symptoms ("5-day fever") that is the hallmark of *B. quintana* infection in humans (66, 114). However, it is not clear if such regularity is a general feature of *Bartonella* infections.

Intracellular bartonellae in nucleated cells *in vivo* have been frequently reported, e.g., *B. bacilliformis* in littoral cells lining lymphatic sinuses (359) or *B. quintana* in the cardiac endothelia of patients suffering from infective endocarditis (60, 351), although the relationship of these compartments to the primary niche is unclear. A number of *in vitro* studies showed that *B. henselae* can invade diverse cell types such as endothelial cells (120), endothelial progenitor cells (376), epithelial cells (24), hematopoietic progenitor cells (274), monocytes/macrophages (223, 309) (including microglial cells [307]), and even tick cells (40). The ability to manipulate such a variety of cell types is very likely to contribute to the highly diverse illness with a plethora of different symptoms that can arise in human patients suffering from systemic cat scratch disease. A wide range of different cell types have also been found to be invaded by *B. bacilliformis*, including HeLa cells as well as human dermal fibroblasts, human laryngeal epithelial cells, and human umbilical vein endothelial cells (HUVECs) (182).

Interaction with nucleated host cells. The interaction of *Bartonella* with nucleated host cells (particularly endothelial cells) has been thoroughly studied *in vitro*, revealing a set of leading phenotypes: cellular invasion, activation of NF-κB and HIF-1 signaling, inhibition of apoptosis, and mitogenic stimulation (360, 385). Though likely to play a key role in the colonization of the primary niche, it is obvious that the underlying mechanisms will also be involved in the colonization of secondarily infected sites, which may be identical to the primary niche or feature additional cell types, especially during disseminated infection at various sites of the host's body. Several virulence factors of *Bartonella*, such as the trimeric autotransporters or the VirB/D4 type IV secretion system (T4SS), have been shown to participate in the interaction with nucleated host cells, and it appears as if they would not contribute to strictly separated aspects of infection but rather would manipulate a set of cellular responses together (Table 1).

(i) Cellular invasion. The entry of *B. henselae* into human endothelial cells can occur via two mutually exclusive pathways, either as single bacteria using an apparently zipper-like mechanism (224) or in form of large aggregates in a remarkable structure that is known as the invasome (120). The uptake of single bacteria or small conglomerates in the zipper-like mechanism yields *Bartonella*-containing vacuoles (BCVs) that fail to acidify and to fuse with lysosomes but instead accumulate in the perinuclear space (246). Residence in perinuclear vacuoles was also reported for *B. bacilliformis* (429) and *B. quintana* (60, 395), indicating that this mode of intracellular persistence may be a common property of the bartonellae and possibly reflect a cellular niche colonized during infection *in vivo*. The entry of *B. bacilliformis* was found to be fully or partially dependent on the activation of the small GTPases Rho, Rac, and Cdc42, on an altered pattern of tyrosine phosphorylation, and on $\alpha5\beta1$-integrins. Furthermore, the invasion process was dependent on a bacterial surface protein and involved actin rearrangements that manifested, during the course of intracellular persistence, as a massive formation of stress fibers anchored to focal adhesions (182, 428, 439). Interestingly, the intracellular vacuoles colonized by this species were shown to be associated with the Golgi complex, whose functions the pathogen could possibly manipulate in its favor, although intracellular replication has not been demonstrated (429, 430).

Because invasome formation has been the main focus of studies investigating the entry of *B. henselae* into host cells (see below), much less is known about the zipper-like uptake process and, in particular, if it is directly or indirectly related to the uptake of *B. bacilliformis*. One study suggested that *B. henselae* would replicate inside human endothelial cells, and the inhibition of host cell protein synthesis with cycloheximide seemed to impair intracellular replication, indicating that the pathogen would obtain nourishment from resources supplied by the host cell metabolism (224). Consistent with this, the stimulation of endothelial cell proliferation via vascular endothelial growth factor (VEGF) significantly raised the growth rate of *B. henselae* during experimental infection (225). In apparent congruence to the findings with *B. henselae* and *B. bacilliformis*, *B. quintana* was shown to interact with membrane ruffles and to invade endothelial cells within 1 min, where it then divides in intracellular vesicles (60).

(ii) Pathological angiogenesis. Bacillary angiomatosis and verruga peruana lesions are key elements of the pathology related to

TABLE 1 Virulence factors of *Bartonella* spp.

Virulence factor(s)	Direct function(s)	Contribution(s) to pathogenesis
Trimeric autotransporter adhesins (BadA, Vomps)	Bacterial autoaggregation, attachment to extracellular matrix, host cell binding via β1-integrins, activation of HIF-1 and NF-κB, inhibition of macrophage phagocytosis	Stable interaction with host cell as basis for further manipulation, secretion of proangiogenic cytokines
VirB/D4 type IV secretion system, *Bartonella* effector proteins	Inhibition of apoptosis, proinflammatory activation, modulation of angiogenesis, invasome formation	Setup and control of intracellular niche
Unknown factor (probably surface protein)	Activation of cellular signaling via β1-integrins	Triggering host cell invasion in course of invasome formation
Outer membrane proteins	Activation of NF-κB signaling, host cell adhesion	Secretion of MCP-1 and upregulation of E-selectin and ICAM-1 (as part of proangiogenic signaling?)
Secreted factor (GroEL)	Unknown, activation of Ca^{2+} signaling?	Inhibition of apoptosis and mitogenic stimulation of host cells
Trw type IV secretion system	Adhesion to erythrocyte surface	Enabling erythrocyte invasion (lineage 4)
Deformin	Formation of invaginations in erythrocyte membranes	Enabling erythrocyte invasion
Flagellation	Mechanical force?	Invasion of erythrocytes (lineages 1-3)
Invasion-associated locus (IalAB)	Unknown	Invasion of erythrocytes
Lipopolysaccharides	Invisibility to TLR4, antagonizing TLR4 signaling	Immune evasion and immunomodulation
Autotransporters	Unknown, cohemolysin activity (Cfa)?	Unknown
Filamentous hemagglutinins	Unknown	Unknown
Hemin binding proteins	Hemin binding, fibronectin binding (HbpA)	Host cell adhesion?, formation of a heme surface layer (antioxidant barrier? nutritive reservoir?)
OMP43	Fibronectin binding, host cell binding	Host cell adhesion?

Bartonella in human patients and appear as macroscopic symptoms corresponding to the remarkable angiogenic activities of these pathogens that have been detected *in vitro* (113, 150). Histologically, the pathological angiogenesis during *Bartonella* infection results in tumor-like lesions packed with lobes of immature capillaries that are lined with a swollen endothelium. Bacterial aggregates as well as dispersed bacteria can be found in close proximity to the proliferating endothelium, and the lesions are characteristically infiltrated by phagocytes such as macrophages and neutrophils (39, 97, 273). Maintenance of these peculiar tumors is fully dependent on the presence of live bacteria, since eradication of the pathogen by antibiotic treatment is known to efficiently resolve the lesions (365). The striking similarity of clinical and histological features and the strong association of both bacillary angiomatosis and verruga peruana with preceding immunosuppression generated the hypothesis that these conditions may be caused by similar means of molecular pathogenesis (86).

The angiogenic properties of *Bartonella* can be subdivided into a direct mitogenic and antiapoptotic stimulation of endothelial cells and the triggering of autocrine and paracrine cytokine secretion that synergizes with the direct effects. Current knowledge indicates that the angiogenic properties of *B. henselae* proceed through at least two apparently distinct pathways, one via a secreted factor that stimulates Ca^{2+} signaling (283) and another via a certain proinflammatory activation involving NF-κB that is possibly contact dependent (223). Similarly, a secreted mitogen or antiapoptotic factor as well as an activation of NF-κB has been reported for endothelial cells infected with *B. bacilliformis* (297, 430). However, most studies did not separate secreted and contact-dependent activities, and it is very likely that the results under normal infection conditions *in vitro* reflect the cumulative effect of both.

Histological analysis of verruga peruana nodules revealed that *B. bacilliformis* infection stimulates the production of VEGF, its receptors VEGFR-1 and VEGFR-2, and angiopoietin-2 in host cells (80). Immature vasculature is known to require a constant supply of VEGF as a survival factor (30), and VEGF and angiopoietin-2 together have a strong, synergistic effect on angiogenesis that is linked to both mitogenic and antiapoptotic activities (264, 445). Remarkably, the endothelium in the verruga peruana lesions was found to produce all of these factors except VEGF, which seemed to be supplied by the surrounding epidermis, suggesting that vascular tumor formation during verruga peruana would be driven by the cooperation of several cell types (80). The secretion of VEGF has also been demonstrated in vasoproliferative tumors that arose during human infection with *B. henselae* (225), and an angiogenic mechanism involving other cell types in addition to endothelial cells is strongly supported by published work on the modern species as well.

The infection of human endothelial cells with the two most prevalent lab strains of *B. henselae* induces a prominent transcriptional reprogramming that involves the activation of inflammatory pathways and leads to elevated expression levels of various factors supporting angiogenesis, such as ICAM-1, angiopoietin-2, interleukin-8 (IL-8), or Bcl-2-related protein A1 in response to the Houston-1 typing strain (ATCC 49882^T) (124) and a closely related set of genes in response to the Marseille strain (see below). Remarkably, although both strains also induced a significant transcriptional upregulation of VEGF, neither the Houston-1 nor the Marseille strain was able to trigger any considerable secretion of VEGF in infected endothelial cells (124, 225). These results are in contrast to the fact that VEGF was detected in bacillary angiomatosis tumors *in vivo* (225) and thus confirm that other cell types in the vasculoproliferative lesions would produce VEGF to drive angiogenesis. However, massive secretion of IL-8, a potent proangiogenic cytokine, was readily detected in endothelial cells upon infection with *B. henselae* (284). Further experiments in the same study revealed a critical role of autocrine IL-8 signaling in the stimulation of endothelial cell proliferation and angiogenic phenotypes in response to *B. henselae* infection. The mitogenic stim-

ulus was accompanied by a potent antiapoptotic effect via a strong increase in the ratio of Bcl-2 to Bax, and both cell proliferation and inhibition of apoptosis were dependent on IL-8, thus confirming published work that IL-8 heavily promotes angiogenesis by stimulating endothelial cell proliferation and inhibiting apoptosis via pathways including the aforementioned ones (257). It is also known that an upregulation of Bcl-2 can stimulate IL-8 secretion, suggesting that positive feedback may already play a role in this autocrine signaling (315), especially since *B. henselae* infection also triggered an increase in surface expression of an IL-8 receptor (284). As expected from the clinical similarity, both Bcl-2 upregulation and a parallel mitogenic effect have also been observed in endothelial cells infected with *B. quintana* (258). However, it is apparent that the investigation of endothelial cells infected with bartonellae *in vitro* does not fully represent the processes driving pathological angiogenesis *in vivo*, because VEGF secretion is missing.

In contrast to the results with endothelial cells, stimulation of VEGF secretion upon infection with *B. henselae* was readily detected in several other cell types, such as epithelioid or monocytic cells and macrophages (i.e., Mono Mac 6 cells) (223) and HeLa cells and Ea.hy926 cells (222); the latter were derived from a fusion of HUVECs with epithelial cancer cells and thus exhibit characteristics of both cell types (129). The secretion of VEGF from HeLa cells and human THP-1 macrophages was also evident upon infection with *B. quintana* (395). Although inhibition of apoptosis was apparent in monocytes, it was contact dependent and driven via NF-κB (223), suggesting that the secreted factor could not act on these cells. *B. henselae* further failed to inhibit apoptosis in human fibroblasts or epithelial cell-like dog kidney cells (MDCK), and although various strains of *B. henselae* as well as *B. quintana* inhibited apoptosis and stimulated proliferation of human endothelial cells, no such effect was detected in the parallel examination of *B. clarridgeiae*, *B. elizabethae*, or *B. vinsonii* (226). Unfortunately, the authors of that study did not test endothelial cells of species other than humans, but they conclusively suggested a certain host species/cell type/bacterium specificity as underlying the differential effects they observed. Importantly, these results are in line with other work reporting that *B. bacilliformis* extracts contained a mitogenic activity specific for endothelial cells (150). A recent study confirmed the relevance of host species and cell type by showing that *B. henselae* was unable to stimulate the proliferation of various feline cell lines, in contrast to the case for several human lines (37). Furthermore, the authors reported that human microvascular and macrovascular endothelial cells responded differently to infection with *B. henselae* (37). It is important to realize that vascular tumor formation *in vivo* is driven by proliferation of the microvasculature, although many experiments *in vitro* have been performed with human umbilical vein endothelial cells (HUVECs), which are macrovascular cells. Furthermore, the authors pointed out that human skin microvascular endothelial cells, unlike other endothelial cell types of humans as well as cats, produced VEGF upon infection with *B. henselae*, thus suggesting that additional autocrine signaling could play a role in vascular tumor formation *in vivo* and may be a reason why pathological angiogenesis as a symptom of *Bartonella* infection preferentially affects the skin. However, an earlier study reported that HMEC-1 cells, another human skin microvascular endothelial cell line (3), lacked VEGF secretion in response to *B. henselae* infection (355).

Since endothelial cells infected with *B. henselae* typically do not secrete VEGF, a key role for VEGF production in other cell types and paracrine signaling to endothelial cells in the vasoproliferative tumor seems very likely, especially when considering the histological findings for verruga peruana nodules (see above). It has in fact been demonstrated that culture supernatants of human cells infected with *B. henselae* (Ea.hy 926 cells [225] and THP-1 macrophages [355]) could stimulate the growth of endothelial cells, undoubtedly because they contained VEGF and possibly other proangiogenic factors such as IL-1β (355) or IL-8 (284). Similar to the direct effects of *B. henselae* infection and indicative of mutual amplification, this paracrine stimulation was shown to trigger the secretion of various proangiogenic and antiapoptotic factors, particularly IL-8 or monocyte chemoattractant protein 1 (MCP-1) (225, 284). These cytokines are known for their chemotactic properties, and the culture supernatants of endothelial cells infected with *B. henselae* were indeed able to induce chemotaxis in THP-1 macrophages, thus indicating that bartonellae in the vascular tumors could promote the immigration of VEGF-secreting cells (282).

Taken together, these results imply a model for pathological angiogenesis in which proangiogenic effects of both direct stimulation by *B. henselae* infection and autocrine IL-8 signaling drive endothelial cell proliferation and inhibition of apoptosis together with paracrine signaling from infected nonendothelial cells such as the surrounding epithelium or infiltrating macrophages. Macrophages, as potent VEGF-secreting effector cells, could be attracted by chemokine secretion from the infected endothelium and build up a paracrine loop of mutual positive feedback that keeps up the complex angiogenic programs and finally results in vascular tumor formation (discussed in references 113 and 221).

Pathological angiogenesis due to infection with *B. henselae* has so far not been demonstrated in cats (61, 62) but was found in dogs, for example, upon infection with *B. henselae* or *B. vinsonii* subsp. *berkhoffii* (227, 441). However, it is reasonable to assume that the pathological angiogenesis observed in certain hosts and in response to certain *Bartonella* species (including *B. bacilliformis*) may reflect bacterial activities that evolved in the genus *Bartonella* for the colonization of the primary niche in the reservoir host, possibly for the maintenance of a locally restricted shelter in the microvasculature. Assuming that these activities would be potent but tightly balanced and regulated in order to keep up the stealth infection strategy, it is easy to imagine that differences in the responsiveness of cells in distinct hosts may cause an imbalance and finally trigger escalating feedback loops that would drive vascular tumor formation around the bacteria.

Infection of Erythrocytes

After colonization of the primary niche during *Bartonella* infection, the bacteria are seeded into the bloodstream, where they infect erythrocytes, thus establishing a protected niche that is competent for vector transmission in order to proceed in the infection cycle (89).

Entry in three steps: adhesion, deformation, and invasion. Most experiments investigating the phenomenology of erythrocyte infection *in vitro* have been performed with *B. bacilliformis*, but the occasional use of *B. henselae* as a modern species and the wide conservation of most bacterial factors suggest that the overall process is probably similar among the bartonellae (see below). However, particular disparities in the arsenal of dedicated virulence factors and the comparison of *in vivo* infection models using

modern species (e.g., *B. tribocorum* [394] or *B. henselae* [1]) to the pathology of *B. bacilliformis* made it obvious that prominent differences must exist at least between *B. bacilliformis* and the other bartonellae as well as between flagellated and nonmotile species (see below).

In general, the seeding of *Bartonella* into the circulation seems to be followed by a sequence of adhesion, deformation, invasion, and finally intraerythrocytic persistence. Adhesion to erythrocytes as a first step of colonization was found to be a critical determinant of host specificity for the modern species (427) but apparently not for *B. bacilliformis*, since this species is known to adhere to cat erythrocytes (201), although it is restricted to infecting humans and closely related primates. Walker and Winkler reported that *B. bacilliformis* poorly adhered to human erythrocytes that had been treated with glucosidases, while the application of unspecific proteases (subtilisin or pronase) strongly favored adhesion (434). They thus concluded that *B. bacilliformis* might bind a glycolipid that would be uncovered from surface proteins by the proteases but might be destroyed by the glucosidases. Other studies focused on the interaction of *B. bacilliformis* with host proteins on erythrocyte membranes, although it is not clear which interaction partners might serve as receptors for adhesion and which ones might possibly be involved in the invasion process. A first report showed that the sets of erythrocyte proteins bound by *B. bacilliformis* and *B. henselae* are remarkably similar and clearly include actin and spectrin (201), while a second study provided solid evidence that *B. bacilliformis* interacts with the α and β subunits of spectrin, band 3 protein, glycophorin A, and monomeric as well as dimeric glycophorin B (63), thereby specifying the previous results. Binding of *B. bacilliformis* to glycophorin B from solubilized erythrocytes was considerably enhanced if these had been treated with trypsin or neuraminidase before, but chemical removal of the carbohydrate moieties from erythrocytes abolished binding to all proteins (63). These results indicate that the binding site of glycophorin B might be somehow masked under the conditions used and that binding of *B. bacilliformis* to erythrocyte proteins apparently involves their glycosyl chains. Interestingly, both trypsin and neuraminidase had only a slight, statistically insignificant effect on the adhesion of *B. bacilliformis* to whole erythrocytes, suggesting either that glycophorin B binding may not be critical for this process or that the bacterium could express a factor providing access to glycophorin B on red blood cells. Similarly, no significant effect of trypsin or neuraminidase treatment has been observed in an *in vitro* infection model with cat erythrocytes and *B. henselae*, but, just as for *B. bacilliformis* adhesion, the application of pronase led to an increased level of erythrocyte invasion (285).

Benson et al. showed that erythrocytes developed progressing indentations and invaginations at the sites where *B. bacilliformis* attached (31), a process that is known as deformation and was also confirmed for *B. henselae* (201). The molecular mechanism underlying deformation and the contribution of a dedicated, small molecule from *Bartonella* (see "Deformin" below) have not been resolved so far, but it seems as if the pits on the erythrocyte surface would provide entry sites for *Bartonella* (31).

Like that of deformation, the molecular mechanism of erythrocyte invasion is not well understood, but the interaction with band 3 protein, spectrins, and glycophorins seems conspicuous, since these proteins also serve as receptors for *Plasmodium falciparum*, the etiological agent of malaria (137, 158, 280, 418). Band 3 protein is part of a complex that connects the erythrocyte membrane to the underlying spectrin-actin cytoskeletal network (41, 209, 302), which is essential to maintain the shape and stability of red blood cells (for a recent review on erythrocyte membranes, see reference 303). Disconnecting this network from the membrane in order to locally weaken surface integrity (e.g., by degrading components like spectrin) is a common strategy of pathogenic parasites, including *Plasmodium* (112, 141, 171), and it seems reasonable to speculate that similar processes may also play a role at some stage of *Bartonella* infection. Importantly, mature erythrocytes are generally nonendocytic under physiological conditions and exhibit considerable resistance against the formation of endovesicles (discussed as a conceptual obstacle to *Plasmodium* infection in reference 308). However, the capacity of *B. tribocorum* to infect mature erythrocytes of its reservoir host has been demonstrated *in vivo*, and corresponding processes have repeatedly been observed *in vitro*, for example in an early study describing the phenomenology of *B. bacilliformis* invasion as "forced endocytosis" (31). A possible role for glycophorin B in the invasion process of *B. bacilliformis* could explain part of the host restriction of this species and cannot be directly conserved in many other bartonellae, since this protein evolved only in primates (352). In addition to direct interactions with the erythrocyte, bacterial motility was shown to be critical for the invasion process of *B. bacilliformis* and hence probably for the flagellated bartonellae in general (see below), potentially by providing mechanical force. It is apparent that erythrocyte invasion should be a relatively efficient process, since results with human serum and *B. henselae* revealed that the pathogen was efficiently killed by complement activation (362). Similarly, the preincubation of *B. bacilliformis* with different sera resulted in bacterial aggregates that were unable to deform or enter erythrocytes (287). Specific antibodies in the serum did not lead to increased killing of *B. henselae* but favored elimination of the bacteria by phagocytes (362), and antibodies against flagellin appear to inhibit erythrocyte invasion of the flagellated species (see "Flagella" below).

Intraerythrocytic persistence. It has not been resolved in great detail how erythrocyte infection proceeds after the invasion process, e.g., in what way the bacteria gain access to the nutrients inside the red blood cell. *B. bacilliformis* was reported to end up in intraerythrocytic vacuoles when the invaginations from membrane deformation bud off during "forced endocytosis." However, the bacteria also occasionally appeared in the lumen of infected erythrocytes *in vitro* (31), but it is not clear if the bartonellae are able to actively leave the vacuole under physiological conditions. The examination of rat erythrocytes from *in vivo* infection with *B. tribocorum* indicated that the bacteria remain inside a membrane-bound compartment (394).

Experiments on the rat model also indicated that red blood cells would be initially infected by not more than one or two bacteria, which divide two or three times, giving rise to eight bacteria per erythrocyte on average, and then persist for the residual life span of the red blood cell, which was apparently not shortened by infection (394). These results are supported by studies with other modern species reporting either five bacteria (*B. quintana* in human patients [367]) or only one bacterium (*B. henselae* in naturally infected cats [369]) per erythrocyte *in vivo*. Available data for *B. bacilliformis* confirm a similarly low ratio of ca. 4 bacteria per red blood cell (370). Interestingly, it seems as if not only the number of bacteria per infected erythrocyte but also the proportion of colonized red blood cells during *Bartonella* bacteremia would be

rather low, at least when considering infections caused by the modern species. The proportion of infected erythrocytes ranges from well below 1% in the cases of *B. quintana* in humans (367) and *B. tribocorum* in rats (394) to about 5% in cats infected with *B. henselae* (234, 369). The course of bacteremia caused by the modern species in reservoir hosts has been investigated extensively using various experimental models as well as naturally infected animals, and the bacteremia was shown to persist usually subclinically for several months or even for considerably more than 1 year in both settings (see references 1, 235, 238, and 443; see also literature cited in "Host Specificity" above). Bacterial titers in the blood can reach 10^6 or even 10^7 (241, 443) but are usually two or more orders of magnitude lower (21, 45, 78, 88, 92), a variation possibly dependent on both the *Bartonella* and host species, immunological characteristics, and infection phase. The duration of *Bartonella* bacteremia in nature is not known (51) and is difficult to determine due to relapsing bacteremia from the primary niche and reinfections promoted by the high prevalence of *Bartonella* bacteremia among most communities of wild mammals (see examples in reference 211 and above).

In contrast to the modern species, *B. bacilliformis* can infect up to 100% of the host's erythrocytes (around 60% on average [271]) and thereby trigger a devastating hemolytic anemia during Oroya fever, the acute phase of Carrion's disease (272). The processes underlying the induction of hemolytic anemia by this pathogen are not well understood, but several studies have brought consensus that the red blood cells are not directly destroyed by a bacterial factor but rather by a host response (356, 359, 434). Based on both the examination of human patients and *in vitro* data, it is apparent that hemolytic anemia arises due to the elimination of many infected erythrocytes by mononuclear phagocytes, possibly upon recognition of abnormal surface properties. Such hemophagocytosis usually occurs in spleen, lymph nodes, and liver and leads to fever, hepatosplenomegaly, lymphadenopathy, and anemia (142, 208), which are also commonly observed during Oroya fever (272). Strikingly, Reynafarje and Ramos could show by the inspection of human patients suffering from Oroya fever that infected erythrocytes are preferentially destroyed in liver and spleen (356), and hemophagocytosis of red blood cells infected with *B. bacilliformis* was demonstrated histologically (359). Furthermore, the mechanical stability of erythrocytes in patients suffering from Oroya fever appears to be frequently decreased, which may also contribute to hemolysis (356).

Importantly, immune-mediated hemolytic anemia has also been reported as a rare complication of infections with modern bartonellae (50, 159, 424), implying that the bacterial factor(s) or strategy triggering hemophagocytosis may be conserved but somehow masked or more tightly regulated in these species. On the other hand, persistent and asymptomatic bacteremia of *B. bacilliformis* seems to be relatively frequent in the areas of endemicity (see above), indicating that the devastating hemolysis during Oroya fever may not be a necessary part of the infection strategy of this species.

Immune Evasion and Immunomodulation

Bartonella characteristically avoids elicitation of a host immune response by means of passive camouflage and active deception as part of its stealth infection strategy (outlined in reference 288). This bipartite strategy of "anti-immunology" (see reference 140 for a review) aims at colonization of the intraerythrocytic niche, where the bacteria are protected from both innate and adaptive immunity and persist in a compartment competent for vector transmission. In short, hiding and modification of pathogen-associated molecular patterns (PAMPs) like lipopolysaccharides (LPS) or flagella (see below) allow *Bartonella* to prevent its recognition as a bacterial pathogen. Additionally, *Bartonella* manipulates the host immune system on a systemic scale to achieve a state of immunological attenuation. Although most research has been performed on only a few species, available evidence allows the assumption that the general mechanisms of how *Bartonella* deals with the host immune system might be similar throughout the genus. However, it is clear that certain details of immunopathology might differ from species to species due to peculiarities in the particular process of host adaptation. The examples of passive immune evasion during *Bartonella* infections are discussed together with the corresponding bacterial factors at a later point in this review, so we focus here on how *Bartonella* actively obstructs functions of the host's immune system and how the immune system may control or eradicate the pathogen.

Current knowledge strongly suggests that the stimulation of IL-10 secretion is an important part of the immune modulation by *Bartonella*. This cytokine is a key regulator of immunity and has a moderating effect on immune responses by suppressing functions of various immune cells, including T helper cells, monocytes/macrophages, and dendritic cells, thus interfering both with innate immunity and with the establishment of an adaptive immune response. Although the resulting low level of inflammation may counteract acute pathology in the host under some circumstances, it is obvious that the effects of elevated IL-10 secretion greatly favor an asymptomatic, persistent course of infection as it is advantageous for *Bartonella* (see reference 104 for a recent review on IL-10). It has been proposed that the IL-10 level during infections may pose a balance between consequences that are more in favor of the host (e.g., prevention of tissue damage) or the pathogen (e.g., dampening the immune system), and the stimulation of IL-10 production was proposed to be a common feature of many intracellular pathogens that establish persistent infections (106). The central role of IL-10 for *Bartonella* has been strikingly demonstrated in the murine model of *B. birtlesii*, since the pathogen was unable to establish bacteremia in IL-10 knockout mice (275). Consistent with this, humans infected with *B. quintana* showed elevated IL-10 levels and exhibited an "attenuated inflammatory profile" (72). *B. henselae* promoted the secretion of IL-10 in mice, cats, and humans *in vitro* or *in vivo* (215, 328, 431), although the additional pattern of cytokine secretion elicited in the different hosts was not consistent and may contribute to the distinct outcomes of infection in reservoir and incidental hosts.

With respect to reservoir host infections, the study investigating mouse mutants in the *B. birtlesii* infection model further found that bacteremia in CD4 knockout mice (i.e., lacking T helper cells) was longer and featured higher bacterial titers than infections in wild-type mice (275). The authors concluded that this effect may derive from the key roles of humoral immunity as well as professional phagocytes in clearing *Bartonella* infection, both of which would require T helper cells (see reference 436 for a review). In contrast to the case for the CD4 knockout mice, infections in CD8 knockout mice were indistinguishable from those in wild-type animals. These results are complementary to those of another study using a mouse reservoir host model but infecting with *B. grahamii* (233). In this study, the lack of B cells as well as the lack

of B and T cells considerably prolonged *Bartonella* bacteremia. Consistent with the findings previously mentioned, the authors proposed that mice lacking B cells would be unable to produce antibodies against *Bartonella* that could eliminate the bacteria seeded from the primary niche, similar to what was observed in the *B. tribocorum* rat infection model (394). Transferring immune serum from infected wild-type mice to B-cell-deficient mice was sufficient to restore a course of bacteremia congruent with the wild-type situation (233). A T_h2 response and corresponding activation of humoral immunity via IL-4 were also detected in cats naturally infected with *B. henselae* (212). The production of specific antibodies played a great part in removing *Bartonella* from the bloodstream but was apparently not suited to eliminate potentially intracellular bacteria from the primary niche, since relapsing bacteremia was observed. This finding is supported by another report showing that antibodies against *B. henselae* can prevent pathology in infected cats but fail to protect against the establishment of bacteremia (321). A further study proposed a central role for a T_h1 response involving the secretion of gamma interferon (IFN-γ) as well as tumor necrosis factor alpha (TNF-α) and stimulating cellular immunity in the eradication of *B. henselae* from experimentally infected cats (214). Studies investigating dogs infected with *B. vinsonii* subsp. *berkhoffii* revealed pleiotropic impairment of the host immune system coinciding with *Bartonella* bacteremia in the presence of considerable titers of specific antibodies (329, 330). The symptoms were deficiency in bacterial phagocytosis, an increase in major histocompatibility complex class II (MHC-II)-negative B cells (possibly due to hampered antigen presentation), an increase in naive $CD4^+$ T cells apparently deriving from abortive proliferation, and a decrease in $CD8^+$ T cells, which further seemed to be functionally handicapped. The effect of *Bartonella* infection on lymphocyte cell numbers appears to differ between the species, since cats infected with *B. henselae* were reported to exhibit a transient decrease in $CD4^+$ T-cell numbers (214), but the reason for or importance of these conflicting results is unclear. Taken together, instances of both cellular and humoral immunity seem to be necessary for complete eradication of *Bartonella* from reservoir hosts, and the pathogen apparently actively counteracts the establishment of such an immune response.

When comparing infections with modern *Bartonella* species in different hosts, a dichotomy between the usually self-limiting but possibly morbid course of infection in incidental hosts and the characteristic persistent but mostly asymptomatic infections in reservoir hosts is apparent. Various studies investigating infections of mice with *B. henselae* reported that the bacteria failed to cause bacteremia and elicited a T_h1 response with the secretion of IFN-γ that reliably eliminated the pathogen (16, 215, 219). The apparent importance of IFN-γ was interpreted to suggest a leading role for phagocytes and T-helper-mediated immunity in clearing *Bartonella* infections (220). These findings are supported by *in vitro* results showing that the activation of murine macrophages by IFN-γ prevented persistence of *B. henselae* in these cells and induced killing of intracellular bacteria, primarily by the production of nitric oxide (309). In humans, infections with *B. henselae* usually lead to cat scratch disease that elicits low to moderate morbidity and is typically self-limiting (see above). The characteristic swelling of lymph nodes derives from the formation of B-cell-rich granulomas that apparently feature continuous recruitment and stimulation of macrophages (397, 431). Similar lymphadenopathy could be observed in a mouse model for cat scratch disease, though no granuloma formation was evident and the swelling was mostly caused by the immigration and proliferation of B cells (244). Interestingly, the use of *B. grahamii* (infecting mice as its reservoir host) instead of *B. henselae* in the same study did not result in comparable lymphadenopathy unless the bacteria were sonicated before inoculation, though infecting IFN-α/β receptor-deficient mice yielded lymphadenopathy with both *Bartonella* species. These results suggest that the bartonellae may actively induce the secretion of IFN-α/β to counteract local immune responses via mechanisms that exhibit a certain host specificity.

In conclusion, these observations in mice and humans indicate that *Bartonella* immunomodulation may be impaired in incidental hosts and allow cellular immunity to clear the infection, especially since the inability to invade erythrocytes deprives the pathogen of its most important shelter.

The course of infection in general seems to critically depend on the ability of the host to launch an effective immune response against *Bartonella*: while most patients do not show signs of severe illness, cat scratch disease and other bartonelloses can develop into devastating, often systemic infections, particularly in immunocompromised individuals such as those suffering from AIDS but also in immunodeficient animals. It was thus proposed that an impairment of cellular immunity may enable *Bartonella* to colonize various sites of the mammal body due to its stealth properties (220). Reservoir host infections of the modern species seem to establish an antibody-mediated protective immunity that prevents reinfection once the bacteria have been eliminated (161, 444), but that apparently does not confer cross-protection against distinct bartonellae (442).

Although the molecular aspects of immune modulation during infections with *B. bacilliformis* have been scarcely investigated, a transient immunosuppression, including $CD4^+$ T-cell lymphopenia and an impairment of cellular immunity during Oroya fever, seems established in the field (150, 152, 191, 271) and is strikingly reminiscent of AIDS (417). Two studies confirmed increased levels of IL-10 in patients infected with *B. bacilliformis* (191, 192), strongly suggesting that enhanced secretion of this cytokine could participate in the immunosuppression as observed for the modern species. The most drastic difference in the immunopathology of *B. bacilliformis* compared to that of the modern species is that the majority of infected erythrocytes are usually destroyed by mononuclear phagocytes during Oroya fever, a condition rarely observed in infections with other bartonellae. Furthermore, the characteristic immunosuppression during Oroya fever makes the patients prone to secondary infections as a severe complication (see above). Secondary infections during infections with the modern *Bartonella* species have rarely been reported (412) and seem not to affect course or severity of infection (411), although coinfection with two or more different bartonellae is not uncommon (examples in references 54 and 336). Like for infections with the modern species, patients suffering from infections with *B. bacilliformis* seem to acquire antibody-mediated immunity against the pathogen, which is generally believed to abolish the acute phase of the disease. The considerable incidence of chronic carriers, the high seroprevalence of *B. bacilliformis*, and the relatively low rate of Oroya fever compared to verruga peruana among natives in the regions of endemicity seem to indicate that, like for the modern species, antibodies are not suited to eliminate the bacterium from

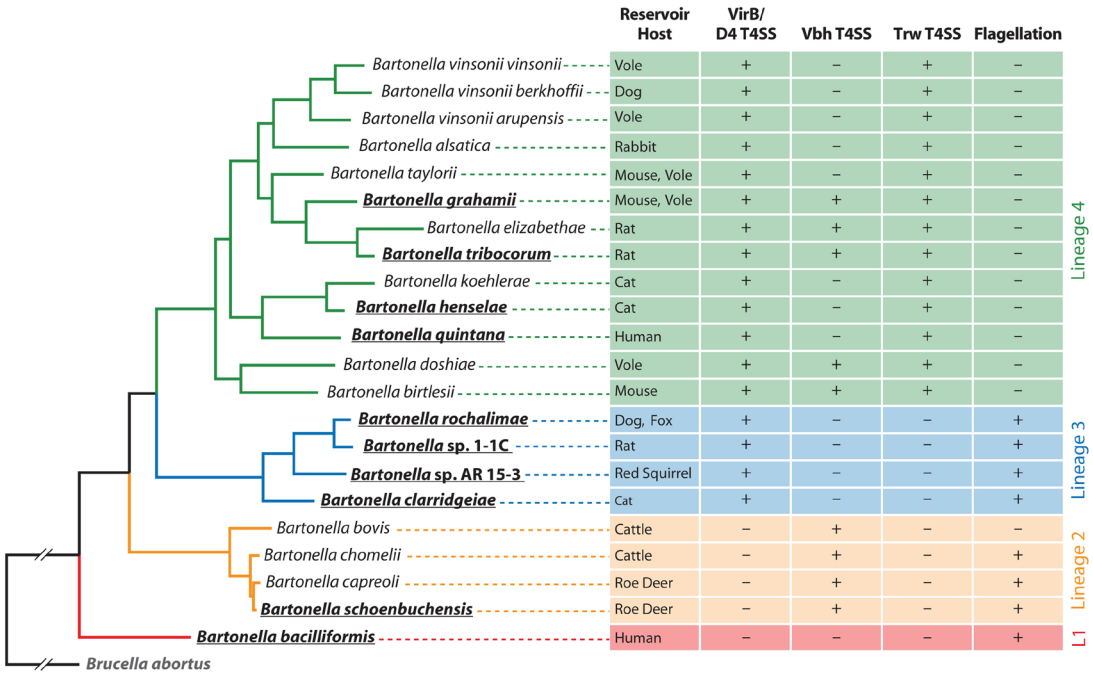

FIG 2 Phylogenetic structure and distribution of key virulence factors within *Bartonella*. The phylogenetic tree is based on a maximum-likelihood analysis of close to 500 genes of the 10 sequenced *Bartonella* species (bold and underlined) and *Brucella abortus*. Additional species were included using the sequences of a set of housekeeping genes (for details, see reference 134). The separation of the genus *Bartonella* into the three modern lineages 2 to 4 and the ancestral *B. bacilliformis* (lineage 1) is striking. Furthermore, type IV secretion systems are present in every modern species but not in *B. bacilliformis*, and flagellation as an ancient virulence determinant has apparently been replaced by the Trw T4SS in lineage 4. (Adapted from reference 134 with permission.)

niches outside the blood circulation and that maternal protection may exist (discussed in references 180, 218, and 220).

EVOLUTION OF THE GENUS *BARTONELLA*

The entry of *Bartonella* into the postgenomic era and the associated quantum leap in our understanding of *Bartonella* evolution has generated valuable knowledge not only for molecular microbiology but also for clinical science. Not only did it contribute to our awareness of the wide array of *Bartonella* virulence factors by enabling signature-tagged mutagenesis (STM) screens (373), but in addition it allowed us to get an idea of the evolutionary mechanisms underlying the remarkable host adaptability of this genus, which is of obvious interest in the context of its zoonotic potential. The complete genome sequences of 10 *Bartonella* species of all four phylogenetic lineages (see below) are available today and thus provide a broad basis for comparative analysis (134).

As a first result, genomic and phylogenetic analyses confirmed the disparity between *B. bacilliformis* as a deadly pathogen and the modern bartonellae, which exhibit a refined infection strategy that includes diminished morbidity and mortality. It was shown that *B. bacilliformis* is isolated within the *Bartonella* phylogeny as the only known representative of an ancient, deep-branching lineage (called lineage 1), while the other, modern bartonellae form three phylogenetic clusters of rather closely related species (lineages 2 to 4) (Fig. 2). These clusters apparently evolved rather recently via at least two independent adaptive radiations and thus contain groups of species that are adapted to infecting various mammalian reservoir hosts (134, 374). While the species of lineage 2 (e.g., *B. schoenbuchensis*) are still characterized by a certain limited host spectrum and have been isolated from different ruminants, the species of lineage 3 (e.g., *B. clarridgeiae*) and lineage 4 (e.g., *B. henselae*) infect diverse mammals as their reservoir hosts (134).

Genomic and pathogenomic analyses of the *Bartonella* genomes revealed that the different species share a core genome whose characteristics reflect the adaptation to a host-associated lifestyle, e.g., by a certain degree of genome reduction, although the genomes of some species have also been inflated, particularly by the acquisition of various phage-related elements (reviewed in reference 133). One striking example of a specific adaptation to the hemotropic lifestyle of the bartonellae is their apparent inability to synthesize heme (6), thus explaining why these bacteria are critically dependent on the availability of this compound that is usually abundant in the niches they colonize (see, e.g., reference 377). In addition, it has been shown that *Bartonella* (*B. henselae*) uses amino acids and not sugars such as glucose as its primary carbon source, probably because amino acids are more easily accessible in the host, for example, via extracellular proteolysis (85). Analyses on the level of *Bartonella* strains and populations revealed that the bartonellae seem to evolve in clonal complexes that exhibit considerable genome dynamics, particularly by excision and insertion of genomic islands, loss and acquisition of plasmids, and both intraspecies and interspecies horizontal gene transfer (32, 33, 133, 197, 335).

Genomic analyses also revealed the presence of type IV secretion systems in the modern species as the most obvious difference from *B. bacilliformis* and thus proposed that these systems may have served as host adaptability factors responsible for the adaptive radiations of the modern lineages (374). The current model suggests that the acquisition of (probably conjugative) type IV

secretion systems via horizontal gene transfer would have provided the raw material for the evolution of virulence factors that allowed common ancestors of the modern lineages to greatly refine their capabilities of host interaction. As a consequence, the emergence of such molecular tools apparently induced subtle changes in the common infection strategy of the bartonellae and thereby promoted elevated host adaptability and decreased morbidity as evolutionary key innovations that triggered the adaptive radiations (134, 374). The exact nature of this modulation of the common *Bartonella* infection strategy is not known, but it must affect one or more critical points of host interaction since functional inactivation of a type IV secretion system in different modern species has repeatedly resulted in avirulent strains (374, 427), although the *Bartonella* infection strategy had initially evolved in the absence of type IV secretion systems (115).

It is well known that *Bartonella* reservoir host infections characteristically feature more or less asymptomatic bacteremia but that infections in incidental hosts may manifest in certain morbidity. In conclusion, it seems reasonable to assume that those bartonellae causing discernible disease in their reservoir host may have emerged from a rather recent host switch and would not yet be fully adapted to the new reservoir host. Consistent with this, a recent evolutionary study on *Bartonella* proposed that incidental host infections may pose an appealing opportunity for a host shift (134), particularly since these infections can also be long lasting. It is apparent that *B. quintana*, the only modern species that infects humans as its reservoir host, is such a recently emerged species that evolved from *B. henselae*, and a comparative genomic analysis of both species concluded that they must have diverged less than 100,000 years ago (6). In addition, it has been repeatedly noted that *B. vinsonii* subsp. *berkhoffii* is a frequent cause of significant morbidity in its canine reservoir host and elicits symptoms that appear to be very similar to those observed during human infections with *B. quintana* or, particularly in immunocompromised patients, *B. henselae*. Infections with *B. vinsonii* subsp. *berkhoffii* in dogs were described to involve well-known conditions such as fever, lymphadenopathy, pathological angiogenesis, and endocarditis (49, 50, 52, 98, 441) and have thus even been proposed to serve as a model for human disease (330). It is apparent from the phylogeny of the bartonellae that the subcluster containing *B. vinsonii* subsp. *berkhoffii* exclusively contains rodent-infecting species such as the other subspecies of *B. vinsonii* or *B. taylorii*, while *B. koehlerae* and *B. henselae*, as the closest relatives of *B. quintana*, infect cats as their reservoir host (Fig. 2). The molecular mechanism of these host switches has not been resolved in detail, but the outstanding importance of host shifts for the zoonotic potential of the bartonellae cannot be underestimated. A recent study identified the adhesion to erythrocytes via the Trw type IV secretion system (T4SS) as one key element of host specificity, since erythrocyte adhesion is the necessary first step to intraerythrocytic persistence and appeared to be strictly host specific (427). However, the authors demonstrated that, as the only known exception to this rule, *B. quintana* was able to adhere to erythrocytes of both humans and cats, indicating that a mutation within the diverse array of Trw-associated surface structures (see below) may have allowed the *B. henselae* clone ancestral to *B. quintana* to close the infection cycle in humans.

When discussing the evolution of *Bartonella*, it is important to mention that the role of a gene transfer agent, i.e., a bacteriophage-like vehicle of horizontal gene transfer (described and reviewed in references 250 and 408), has been appreciated only recently and must not be confused with the occurrence of real bacteriophages in some species of this genus (for example, prophage I in *B. grahamii* [34] or another phage of *B. tribocorum* [374]). Corresponding bacteriophage-like particles (BLPs) with an icosahedral head that apparently pack ~14-kb pieces of linear, double-stranded DNA in a semirandom fashion were discovered early on and found to be morphologically similar in many *Bartonella* species, including *B. bacilliformis*, *B. henselae*, and *B. quintana* (11, 23, 47, 269, 421). The different reports showed that these particles may be found with or without a tail and not only in the bacterial supernatant but also attached to the bartonellae or intracellular. Furthermore, the BLPs seem to contain an invariable set of three proteins of approximately 32 kDa, 34 kDa, and 36 kDa as well as other minor constituents (11). The 36-kDa component has been termed PapA (for particle-associated protein A) and was revealed to be a phage tail protein (12). Remarkably, an early study described that BLPs inside the cytoplasm of *B. bacilliformis* lacked a tail, while those attached to the surface apparently adhered to the bacterium via their tail, indicating that PapA could be inserted into the outer membrane and somehow polymerize on the phage (421). A smaller protein of ca. 32 kDa was described as Pap31 (for particle-associated protein of 31 kDa) and subsequently revealed to be HbpA, a well-known virulence-factor of *Bartonella* (see "Hemin binding proteins" below). A recent study indicated that this protein might end up in the BLPs by coincidence because it is highly expressed under conditions of high hemin levels, and HbpA indeed was not detectable in BLPs of bacteria that had been cultured in the absence of hemin (34). Encouraged by the obvious relationship of the *Bartonella* BLPs to bacteriophages, extensive attempts to demonstrate a lytic release of these particles have been made, but bacterial lysis linked to BLPs could never be shown (11). However, the release of bacteriophage-like particles in liquid culture of *B. henselae* correlated with the entry of these bacteria into a post-exponential-phase "death phase" with a drop in bacterial viability and membrane integrity, but a causal relationship to the BLPs has not been established (85).

Although the semirandom nature of DNA incorporation into the BLPs of the gene transfer agent prompted other authors early on to propose these particles as a part or remnant of a mechanism for horizontal gene transfer (47), a conclusive model for such a process has been brought up only recently by Berglund et al. (34). Using *B. grahamii*, they could show that a highly variable region of the bacterial genome encoding various type V secretion systems as well as the VirB/D4 type IV secretion system was amplified by runoff replication and preferentially packed into the BLPs, thus providing at least one appealing mechanism that may account for the genomic diversity of the bartonellae in natural populations and the horizontal gene transfer of virulence factors.

VIRULENCE FACTORS

In order to draw a comprehensive picture of the molecular pathogenesis of *Bartonella* infections, we apply a broad definition of the term virulence factor and discuss bacterial factors that confer the "ability to enter, replicate and persist in a host" (105). We classify these factors in *Bartonella* according to the stage of infection at which their activity is mostly contributing to pathogenesis; i.e., we separate them depending on whether they are primarily involved in the interaction with nucleated host cells (see "The Primary Niche" below), contribute to blood-stage infection (see "Infection

of Erythrocytes" below), or cannot be sorted into one of these categories (see "Other Virulence Factors" below).

Decades of studies, continuous advances in the molecular biology of *Bartonella*, and the entry of this genus into the postgenomic era have greatly increased the number of bacterial factors that are assumed to participate in virulence, but comparably little is known about the molecular pathogenesis and the particular function of many of them (6, 119, 123, 267, 294). A comprehensive view of the molecular pathogenesis of *Bartonella* is further complicated by the fact that the two common lab strains of *B. henselae*, by far the most well-studied species, have different genotypic backgrounds and differ in their arsenals of virulence factors. Two subtypes of *B. henselae* (I and II) have been distinguished based on serotypic and genotypic characteristics, and the Houston-1 typing strain belongs to group I, while the Marseille strain belongs to group II (197, 198, 251). Importantly, a two-dimensional (2D) gel electrophoresis analysis revealed that 95% of the protein spots were identical in the Houston-1 and the Marseille strains (452), thus making it possible to imagine yet-unknown differences in the arsenal of virulence factors, especially since the genome sequence of the Marseille strain is not available. Strains of the two groups of *B. henselae* have been reported to exhibit certain differences in the interaction with endothelial cells (82), although these findings could not be confirmed by a more recent study (37). Furthermore, the two subtypes of *B. henselae* have also been suggested to differ in pathology (83) as well as in their association with feline or human infection (44). Most critically, the prevailing variant of the Marseille strain expresses a functional BadA trimeric autotransporter adhesin (TAA) but no VirB/D4 T4SS, while the situation is the opposite in the most common variant of the Houston-1 strain (382), although both factors are most likely essential for productive infection *in vivo*. The evaluation of the available literature further suggests that other variants of Houston-1 and, most likely, the original isolate exhibited surface expression of BadA (for example, "well piliated" Houston-1 in reference 245), while the variant used for genome sequencing did not (361).

The Primary Niche

TAAs. Trimeric autotransporter adhesins (TAAs) are well-known virulence factors of Gram-negative bacteria and typically contribute to pathogenesis by binding to host proteins on cell surfaces, in the extracellular matrix (ECM), or as circulating factors (recently reviewed in reference 260). They form extracellular filaments composed of head and stalk domains that are assembled on a C-terminal membrane anchor, thus resulting in a characteristic "lollipop-like" structural architecture (103, 185, 260, 322). The membrane anchor inserts into the outer membrane as a trimeric β-barrel and allows passage followed by trimerization of the exported filament. Unlike the case for classical (monomeric) autotransporters, the trimerization of TAAs is crucial for their folding, stability, and activity (102). While the head of TAAs usually constitutes the "business end," the stalk serves primarily as an extender that presents the head to its host binding partners, although it may also directly contribute to the interaction (260, 363). The head and stalk are built up from a repetitive array of a limited set of domain modules, hence favoring events of sequence reshuffling and recombination that can alter the length of the stalk by repeat contraction or expansion and modulate binding specificities of the head (260, 286).

TAAs play important roles in the infection strategies of various pathogens such as *Yersinia* (YadA) (132), *Haemophilus* (Hia) (247), or *Neisseria* (NadA) (71). They can be found in the genomes of all *Bartonella* species sequenced so far, usually featuring several paralogous copies and pseudogenes (34, 157, 216, 450), and related proteins are encoded in the genomes of other *Rhizobiales* such as *Brucella* (e.g., BruAb1_0072 in *B. abortus* [170]). It has been shown in experimental infections with *B. birtlesii*, *B. tribocorum*, and *B. quintana* that TAAs of *Bartonella* are important virulence factors and necessary for successful colonization of the primary niche (267, 374, 427).

(i) BadA, a trimeric autotransporter adhesin of *Bartonella henselae*. Most research on the TAAs of *Bartonella* has been performed on *Bartonella* adhesin A (BadA) of *B. henselae*, a giant protein composed of more than 3,000 amino acids per polypeptide chain. BadA trimers form hair-like filaments of ~240 nm length on the bacterial surface (306) (Fig. 3), and their appearance was initially misinterpreted as being related to type IV pili (24). The key role of BadA in the molecular pathogenesis of *B. henselae* has been thoroughly studied with the Marseille strain (i.e., in the absence of a functional VirB/D4 T4SS), which exhibits a plethora of BadA-dependent phenotypes: bacterial autoagglutination, adhesion to host cells as well as extracellular matrix (ECM), inhibition of phagocytosis, and induction of a proangiogenic transcriptional program in target cells (360) (Fig. 3). As expected, the head of BadA was found to be sufficient for most of these phenotypes (217). Structural analysis of the head revealed that it is composed of three subdomains featuring an N-terminal domain similar to the head repeats of *Yersinia* YadA as well as a Trp ring domain and a GIN domain that show remarkable structural similarity to elements present in the head of *Haemophilus* Hia, but the assignment of particular functions to these head subdomains has remained enigmatic (413).

Solid experimental evidence indicates that BadA-mediated adhesion to endothelial cells may target β1-integrins and involve bridging via ECM proteins such as collagens or fibronectin (217, 360). Consistent with this, it was shown that *B. henselae* binds these components of the ECM and several others, like hyaluronate, laminin, and vitronectin, in a BadA-dependent manner (306, 360). Although the head of BadA was sufficient to bind endothelial cells as well as collagens, the stalk was required to bind fibronectin (217), and a recent study investigating the effect of dynamic flow conditions revealed that BadA was particularly important for endothelial cell attachment in the presence of shear stress as expected *in vivo* (306).

In addition to host cell adhesion, the head of BadA was also found to be sufficient as a trigger for the proangiogenic transcriptional program that the Marseille strain of *B. henselae* induces in host cells (217). A study by Kempf et al. indicated that this reprogramming of gene expression is based primarily on the activation of NF-κB as well as hypoxia-inducible factor 1 (HIF-1) and involves the upregulation of 20 genes in infected HeLa cells (222). Similar to the well-known modulation of NF-κB by bacterial pathogens (349), HIF-1 activation has recently been recognized as a common theme in human infections (438) and is a key trigger of various angiogenic processes (344). Consistent with this, the majority of genes upregulated in HeLa cells upon infection with *B. henselae* Marseille could be linked to angiogenesis, cell metabolism, or growth and included genes for potent proangiogenic factors such as IL-8 (regulated by NF-κB) and VEGF (regulated by

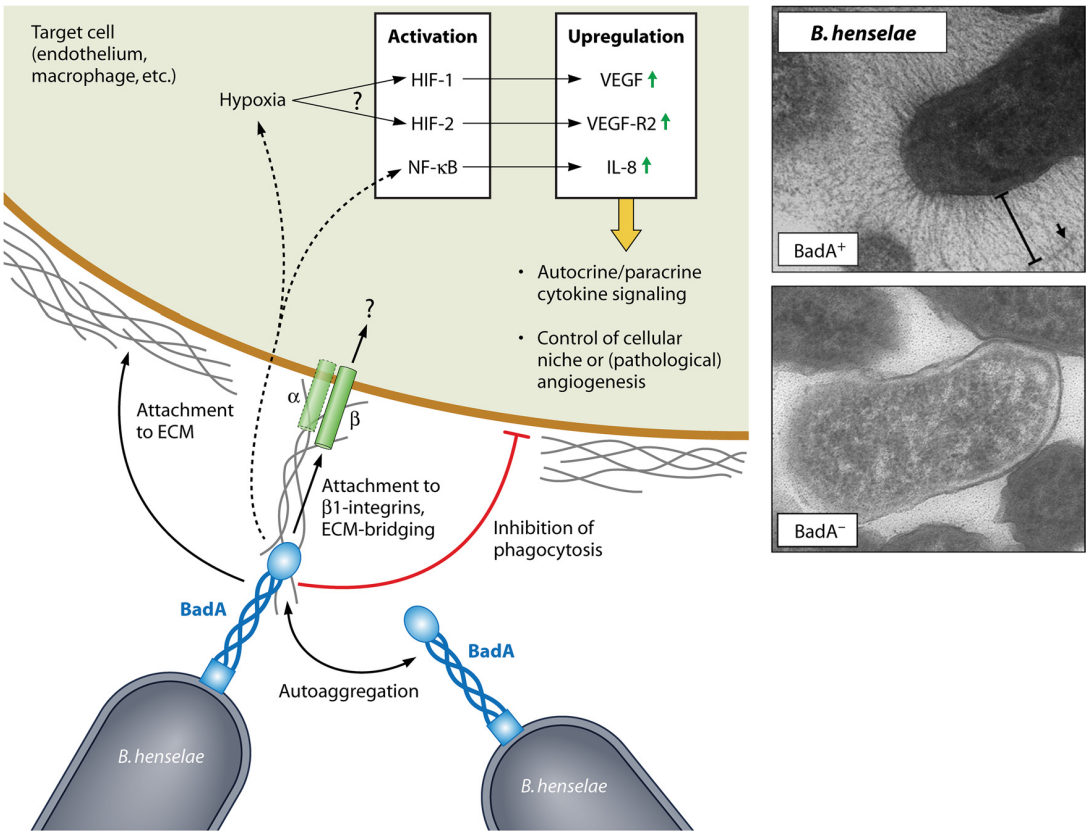

FIG 3 BadA, a trimeric autotransporter adhesin of *B. henselae*. Left, the different virulence phenotypes that have been attributed to BadA in experiments with the *B. henselae* Marseille strain are summarized in a schematic drawing. Note that a direct or indirect causal relationship between the attachment to β1-integrins and the activation of HIF-1/2 or NF-κB seems likely but has not been demonstrated. Right, transmission electron micrographs of wild-type *B. henselae* Marseille and a mutant lacking BadA expression. Not only is the remarkable size of the trimeric autotransporter adhesin obvious (bar, ca. 240 nm), but a close view also reveals spots of electron density that may be the head domains (arrow). (Right panels adapted from reference 306 with permission.)

HIF-1) (222). The activation of both NF-κB and HIF-1 was found to be dependent on BadA (217) but seemed to proceed independently (222), although considerable cross talk and interdependence between the NF-κB and HIF-1 pathways have been described in the literature (415, 426). Interestingly, the infection of HUVECs instead of HeLa cells resulted in the upregulation of more genes of the NF-κB regulon (e.g., that for MCP-1) and activated HIF-2 in addition to HIF-1, thus stimulating the expression of VEGF-R2. In line with the great majority of reports for *Bartonella*, both cell types secreted IL-8, while considerable VEGF secretion was detected only for HeLa cells, although corresponding transcriptional upregulation was observed in both cell types (222). In conclusion, it is apparent that the altered pattern of gene expression in response to BadA is part of the contact-dependent antiapoptotic and mitogenic effects of *B. henselae* (see above).

The molecular mechanism of how BadA mediates the activation of NF-κB and HIF-1/2 in host cells is not known, but Kempf et al. detected BadA-dependent hypoxia in infected cells that could trigger HIF-1/2 activation (222). Hypoxia was also shown to be a possible trigger of NF-κB activation (320), but it may also be induced by the interaction of BadA with β1-integrins via bridging of ECM proteins such as fibronectin. β1-Integrins are key players in angiogenesis (reviewed in reference 17), and the binding of fibronectin to α5β1-integrins was shown to induce expression of proangiogenic genes, including that for IL-8, in endothelial cells via an NF-κB dependent pathway (228). It is therefore conceivable that such an interaction of BadA would induce the NF-κB part of the proangiogenic transcriptional program, especially since other TAAs such as *Yersinia* YadA or NadA of *Neisseria* were also shown to bind β1-integrins and to trigger the expression of IL-8 in host cells (130, 147, 310, 386).

The multiple roles of BadA during infections with *B. henselae* have not been fully resolved, but the activation of HIF-1 was detected by immunohistochemistry in monocytic phagocytes that infiltrated bacillary angiomatosis lesions in human patients (222). This finding supports the hypothesis that *Bartonella* would trigger the secretion of proangiogenic cytokines from nonendothelial cells like these phagocytes as part of a paracrine loop that drives pathological angiogenesis (222) (see above), especially since BadA was also shown to protect *B. henselae* from phagocytosis by macrophages via an unknown mechanism (360).

Despite such detailed knowledge on the role of BadA as a virulence factor of *B. henselae*, a paralogous TAA encoded close by has been described only recently and appears to be intact both in the Marseille strain and the Houston-1 strain (216). However, no experimental evidence on any kind of functionality of this protein has been published so far, but it was found to contain several Trp

rings and GIN domains that are not present in some TAAs of other *Bartonella* species (322).

(ii) Trimeric autotransporter adhesins of other *Bartonella* species. Trimeric autotransporter adhesins can be found in every *Bartonella* species sequenced so far, but they vary considerably in length and show differences in their domain composition (recently reviewed in reference 322). Most research on the TAAs of *Bartonella* apart from BadA has been performed on the *B. quintana* homologs called Vomps (for "variably expressed outer membrane proteins") (450). The Vomp genes form a genomic locus of four genes (encoding VompA to -D), but frequent events of recombination between these genes apparently led to the inactivation of one or more of them in the different strains of *B. quintana*. Consistent with this, the deletion of several (but never all) Vomp genes was occasionally observed in strains isolated from experimentally infected rhesus macaques as well as from human patients. This phenomenon is most likely attributable to functional redundancy in combination with selective pressure of the host's immune system (450), since the Vomps are known to be immunodominant in human infection (43). However, a complete deletion of the Vomp locus resulted in an avirulent strain (267), consistent with the phenotype of TAA-deficient mutants in STM screens of *B. birtlesii* and *B. tribocorum* (374, 427). Regarding sequence diversity and similarity, VompA to -C appear to be very close and to lack the Trp ring domain and the GIN domain found in the BadA head, thus featuring only the part that is homologous to the YadA head repeats. In contrast to these three proteins, VompD also contains Trp ring and GIN domains (322, 413). Furthermore, the Vomps are much shorter than BadA (approximately 40 nm, compared to about 240 nm for *B. henselae* Marseille BadA [306]), which is mostly due to a considerably lower number of stalk repeats (322).

The biological role of the Vomps has been investigated in several studies, and they seem to play a role in adhesion and angiogenic reprogramming similar to that of *B. henselae* BadA. However, despite the presence of all four Vomp genes in the JK-31 strain of *B. quintana*, which is used as Vomp-positive wild-type strain, VompD seems not to be expressed in this strain (395), and thus no direct evidence for the function of this protein is available. A phenotypic comparison of the JK-31 strain with other strains lacking Vomp expression revealed that VompA to -C are apparently necessary for the induction of VEGF secretion in HeLa cells and THP-1 macrophages, but no significant contribution to attachment to these cells could be detected (395). Furthermore, VompC was found to bind collagen IV, while VompA was both necessary and sufficient for bacterial autoaggregation (450). However, a more recent study using the same strain revealed clear Vomp-dependent adhesion to endothelial cells under both static and dynamic flow conditions, and the authors speculated that this apparent discrepancy may be caused by the expression of a specific binding partner on endothelial cells but not on the other cell types (306). They further detected Vomp-dependent adherence of *B. quintana* to fibronectin (in contrast to a previous study [395]) and other ECM proteins such as collagens or laminins under static conditions, but this binding seemed to be rather unspecific. Under flow conditions, binding to most ECM components, except hyaluronate and vitronectin, was greatly decreased, indicating that these factors may be relevant targets of Vomp-mediated adhesion during human infection (306). In addition to obvious functions during infection of the mammal host, one or more of the Vomps may also play a role in transmission via the arthropod vector, for example, by contributing to adhesion in the flea gut (450).

The TAAs of other *Bartonella* species are less well characterized, but it appears as if one of the three homologs in *B. bacilliformis* contains a head similar to the shorter paralog of BadA, featuring several Trp rings and GIN domains, while the others seem more closely related to VompA to -C and lack these head subdomains (216). *B. tribocorum* encodes only one TAA, but this protein was described to be the longest TAA in *Bartonella* and features a BadA-like head with a Trp ring and GIN domain (322). The three TAAs of *B. vinsonii* subsp. *arupensis* (called BrpA to -C for *Bartonella* repeat protein) contain excessive repeats and were discovered in a study investigating *Bartonella* antigens because at least one of them, BrpA, seems to be immunodominant in a mouse infection model (157).

VirB-like T4SS. (i) The VirB/D4 T4SS and *Bartonella* effector proteins. Type IV secretion systems (T4SS) are macromolecular machineries prevalent among most groups of prokaryotes and originally mediated conjugation, i.e., the interbacterial transfer of genetic material (usually plasmids) in form of a nucleoprotein complex (7). Conjugation is a major mechanism of lateral gene transfer in bacteria and plays prominent roles in the dissemination of genes involved in virulence, antibiotic resistance, or other fitness traits among bacterial populations (317). Conjugative T4SS have repeatedly evolved into host-interacting machineries that are well known as bacterial virulence factors (146), typically contributing to pathogenesis by translocating effector proteins into eukaryotic target cells (19). Based on the nomenclature of the prototypic VirB/D4 T4SS of *Agrobacterium tumefaciens*, the type IV secretion (T4S) machinery consists of 10 essential components, VirB2 to -11, plus the type IV secretion coupling protein that serves as a substrate recognition module. The T4S machinery is assumed to assemble a translocation channel that spans both the inner and outer membranes and then merges into a surface filament. This filament mediates initial attachment to target cells and is thus called "sex pilus" in the context of conjugation. However, the precise mechanism of substrate translocation by T4SS remains poorly understood, although two major models propose either a piston mechanism or export through a pilus channel (77, 95, 435).

The VirB/D4 T4SS of *Bartonella* constitutes one of the most prominent virulence factors of this genus (115) and is present in all species of lineages 3 and 4 (134). It was discovered during the investigation of a 17-kDa antigen of *Bartonella henselae* that turned out to be a VirB5 homolog and encoded as part of a *virB2-virB11* operon (326, 387, 410). The two STM screens in *B. birtlesii* and *B. tribocorum* revealed that a functional VirB/D4 T4SS is essential for the pathogenicity of these species, and a segregation analysis with two T4SS complementation plasmids in the *B. tribocorum* infection model strongly indicated that it is required during colonization of the primary niche rather than for blood-stage infection (374, 392, 427). These results are further supported by *in vitro* infections with the *B. henselae* Houston-1 strain, which elicits various VirB/D4-dependent phenotypes in human endothelial cells (385). Taking the findings together, it is apparent that the VirB/D4 T4SS plays a major role in the manipulation of nucleated host cells during infections with a large group of modern *Bartonella* species.

(a) Bartonella effector proteins. The VirB/D4 T4SS contributes to *Bartonella* virulence by translocating Beps (*Bartonella* effector proteins) into host cells, where they subvert cellular functions in

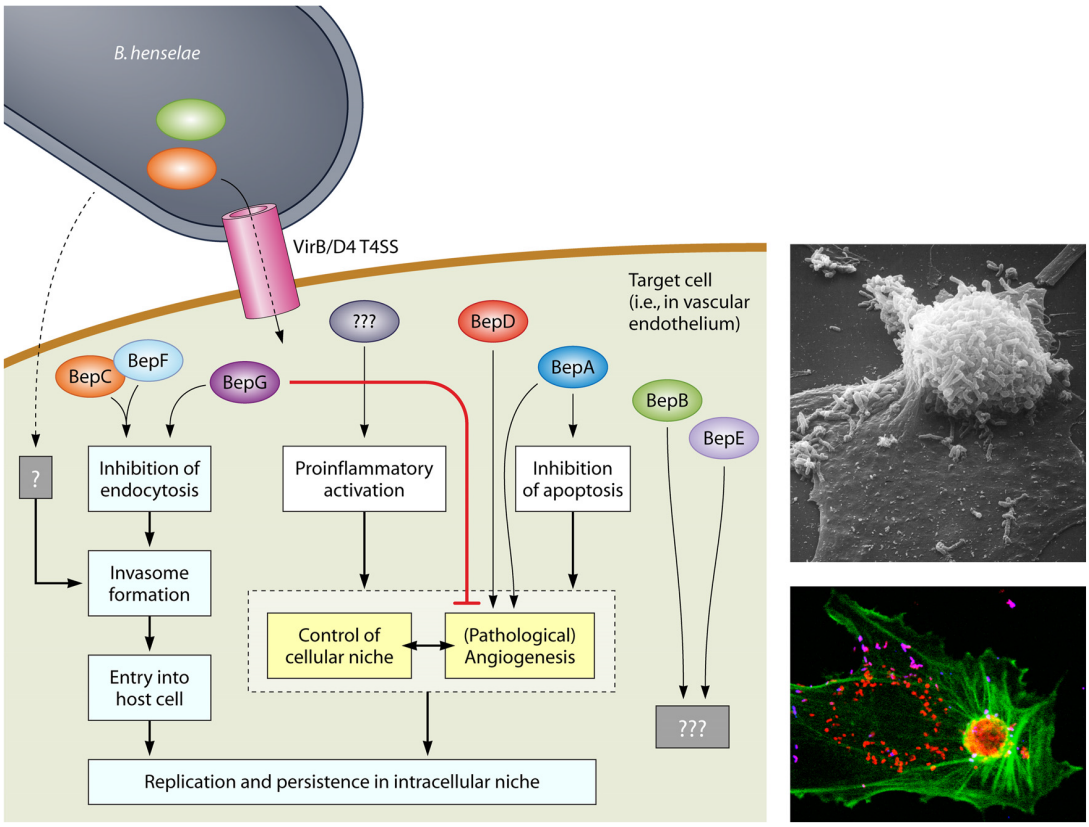

FIG 4 VirB/D4 T4SS and Beps of *B. henselae*. Left, the different virulence phenotypes of the VirB/D4 T4SS and the Beps are summarized in a schematic drawing. It becomes apparent that the diverse cellular activities converge toward the establishment, maintenance, and control of an intracellular niche. Right, the formation of an invasome on human endothelial cells infected with *B. henselae* is shown as visualized by different techniques (top, scanning electron microscopy; bottom, confocal microscopy and immunocytochemistry). In the bottom part intracellular bacteria appear red, extracellular bacteria appear purple, and the actin cytoskeleton is stained green. Note the remarkable actin ring structure forming around the bacterial aggregate. (Right panels adapted from reference 120 with permission.)

favor of the pathogen (Fig. 4). All known VirB/D4-dependent cellular phenotypes of *B. henselae* in the *in vitro* infection model are dependent on the delivery of at least one effector (385, 393). The Beps display a modular domain architecture with N-terminal host-interacting modules fused to a C-terminal secretion signal. This signal consists of a Bep intracellular delivery (BID) domain followed by a nonconserved tail sequence displaying a net positive charge as the only discernible feature (393).

The Beps of lineage 3 (e.g., *B. clarridgeiae*) and lineage 4 (e.g., *B. henselae*) can be sorted into 10 and 7 phylogenetic clades (i.e., orthologous groups), respectively. Most of these carry an N-terminal FIC (filamentation induced by cyclic AMP [cAMP]) domain that is usually followed by a small oligonucleotide/oligosaccharide binding (OB) fold and the C-terminal secretion signal (134). However, a subset of effectors in both lineage 3 and lineage 4 harbor other functional modules instead of FIC domains and feature either additional BID domains or tyrosine-containing motifs that are phosphorylated upon translocation into the host cell (374). Three of the seven Beps of *Bartonella henselae* (BepA to -C) display the FIC-OB-BID architecture, and four (BepD to -G) harbor other elements at their N termini, whereas in lineage 3, 9 of the 10 phylogenetic clades of Beps contain a FIC domain and only one bears tyrosine phosphorylation motifs instead (134).

Although various cellular phenotypes associated with single effectors or a subset of Beps have been reported (see below), comparatively little is known about interacting host factors or underlying molecular mechanisms. FIC domains as the putative host-interacting part of many *Bartonella* effector proteins are known to mediate AMPylation, i.e., the covalent transfer of an AMP moiety onto hydroxyl side chains of target proteins. This peculiar enzymatic activity has been examined using several virulence-associated proteins of other bacterial pathogens and was even detected for BepA of *B. henselae* (327, 371). However, no FIC domain of any *Bartonella* effector has so far been demonstrated to contribute to *Bartonella* virulence *in vitro* or *in vivo*.

Tyrosine phosphorylation motifs are a prevalent feature among bacterial effector proteins and usually promote infection by subverting host signaling cascades upon phosphorylation in the target cell (20). Consistent with this, Beps with tyrosine motifs from both lineage 3 and lineage 4 were shown to become phosphorylated in human cells (134, 393). Although their particular mode of action remains largely unknown, the phosphotyrosine motifs of BepD to -F were found to bind various SH2 domain-containing host proteins (400) that are key elements of cellular signaling (334). No phenotype during *in vitro* infection, however,

has yet been demonstrated to depend on the tyrosine phosphorylation motifs of any *Bartonella* effector protein.

In contrast to the FIC domains and tyrosine phosphorylation motifs of the *Bartonella* effectors, the BID domain of *B. henselae* BepA was found to be sufficient for elicitation of the strong antiapoptotic and proangiogenic phenotype that is the hallmark of this effector protein (381, 384) (see below). Because the same domain also mediates translocation of BepA, it is apparent that BID domains of *Bartonella* effector proteins can have dual functions and act in host interaction and as signals for the type IV machinery. Conspicuously, various effector proteins contain several BID domains, although, for example, in the case of *B. henselae* BepG the C-terminal one alone is sufficient for translocation (358). It is hence more than likely that direct functions of BID domains in the manipulation of host cells are more widespread among *Bartonella* effectors, further highlighting the evolutionary versatility of these fascinating proteins.

(b) Evolution. It is well established that the VirB/D4 T4SS played a major role in the evolution of the modern bartonellae, but its own evolution also constitutes a fascinating matter of research. Generally, the work by Frank et al. showed that protein-secreting type IV secretion systems evolved out of conjugative ancestors various times independently (146), and it is hence not surprising that the closest known relatives of the VirB/D4 T4SS outside *Bartonella* are conjugative T4SS encoded on plasmids found in other *Rhizobiales* (374). Remarkably, the relaxase secretion signal of one of these, the AvhB T4SS on the pATC58 plasmid of *A. tumefaciens*, was sufficient to direct VirB/D4-dependent translocation of fusion proteins from *B. henselae* into human endothelial cells (393), and another study found that the VirB/D4 T4SS of *B. henselae* could transfer a relaxase loaded with plasmid DNA into human cells (391). These results suggest that the bipartite secretion signal of *Bartonella* effector proteins (BID domain plus positively charged tail) may have evolved in relaxases of alphaproteobacterial conjugation systems and was then simply adopted during the evolution of *Bartonella* effector proteins to deliver host-interacting modules into target cells (393).

The two separate arrays of *Bartonella* effector proteins in lineages 3 and 4 evolved convergently from one common ancestor, suggesting that a primordial VirB/D4 T4SS would have initially operated with a single effector protein. Since FIC domain-containing effectors are closest to the root of the *Bartonella* effector phylogeny in both lineages (BepA and Bep1, respectively), it is likely that the ancestral effector harbored a FIC domain and contributed to *Bartonella* pathogenesis via the AMPylation of host targets (134). The striking similarity of the VirB/D4 T4SS and the Vbh T4SS, a third and mostly plasmid-encoded type IV secretion system found in several *Bartonella* species, makes it likely that both systems might have diverged from a common ancestor rather recently in evolution (374). After chromosomal fixation of a primordial VirB/D4 T4SS in combination with an ancestral effector, successive rounds of gene duplication, diversification, and reshuffling generated the distinct effector arsenals of lineages 3 and 4. The diverse cellular phenotypes of the Beps encoded by *B. henselae* strongly suggest that their rapid evolution was driven by functional diversification with the acquisition of different roles in host interaction (358, 381, 384, 420). Although most clades of effector proteins still display the ancestral domain architecture, the N-terminal FIC domain has secondarily been replaced with other functional modules in effectors of both lineages independently. This remarkable parallel evolution generated novel types of effector proteins containing tandemly repeated tyrosine phosphorylation motifs and/or additional BID domains as presumable host-interacting elements (134).

(c) Cellular effects. The Houston-1 strain of *B. henselae* was found to elicit a wide array of VirB/Bep-dependent cellular phenotypes in an infection model with human endothelial cells that may correspond to the manipulation of nucleated host cells *in vivo*, e.g., during primary niche infection (115). These phenotypes comprise inhibition of apoptosis, activation of proinflammatory signaling via NF-κB, modulation of angiogenesis, and reorganization of the actin cytoskeleton during invasome formation (381, 385) (Fig. 4), but the molecular contribution of each single effector protein has been only partially resolved so far.

The entry of *B. henselae* Houston-1 into host cells via invasome formation proceeds in three steps and starts with bacterial adhesion and aggregation on the cell surface, accompanied by effector secretion. Subsequently, the bacterial aggregate is engulfed by cellular protrusions and finally internalized as a whole (358). The term "invasome" denotes the host cell structure that takes up the bacteria, comprising mostly stress fibers that form a compact F-actin ring underneath the bacterial aggregate (Fig. 4). Invasome formation is a slow process and takes at least 16 to 24 h, while the alternative pathway yielding BCVs takes only minutes or a few hours (120, 358). It was found that invasome formation is fully dependent on the translocation of *Bartonella* effector proteins and can be elicited by BepG alone or BepC in combination with BepF (358, 420). Surprisingly, these effectors apparently do not trigger invasome formation directly but seem rather to contribute indirectly by inhibiting endocytic uptake of *B. henselae.* The ectopic expression of BepG in human cells did not induce any discernible cytoskeletal rearrangements, although it was sufficient to restore invasome formation of an effectorless mutant of *B. henselae*. Furthermore, the expression of BepG, as well as BepC and BepF, interfered with endocytic uptake of inert microspheres (358, 420). Rhomberg et al. thus suggested that the inhibition of endocytosis could be a prerequisite that enables *B. henselae* to aggregate on the cell surface and thereby cluster host receptors bound to the bacteria. This clustering of cellular receptors (and not the direct activity of any *Bartonella* effector protein) may then trigger the massive actin rearrangements that lead to invasome formation. Consistent with this, the effectorless mutant of *B. henselae* Houston-1 enters human endothelial cells into BCVs (358). Recent work showed that *B. henselae* Houston-1 binds β1-integrins on host cells and activates them in a fibronectin-independent manner via talin-1 inside-out signaling, indicating that integrins may be a major receptor for *B. henselae* on host cells (419). This hypothesis is further supported by the finding that an extended, activated conformation of β1-integrins on human endothelial cells is necessary for effector translocation and is recruited to the sites of invasome formation. Moreover, the same study suggests that β1-integrin outside-in signaling via focal adhesion kinase (FAK) and Src to paxillin and vinculin may control the actin rearrangements that are the basis of invasome formation. These include both the reorganization of preexisting F-actin and the *de novo* polymerization via pathways involving Rac1/Scar1/WAVE/Arp2/3 and Cdc42/WASP/Arp2/3. BepC/F-dependent invasome formation further required cofilin 1, a protein that controls actin turnover. Based on these results, Truttmann et al. proposed that BepC and BepF would manipulate host signaling at an intermedi-

ate stage of the cascade leading to invasome formation, while BepG would operate more downstream and potentially interact with actin itself, thus making cofilin 1 dispensable (358, 420). Although no direct evidence corroborates a role for the particular process of invasome formation in *Bartonella* infections *in vivo*, the similarity to the bacterial aggregates in the surrounding of proliferating endothelial cells in bacillary angiomatosis lesions is striking (117).

In addition to invasome formation, it was further noticed that *B. henselae* Houston-1 shows clear VirB/D4-dependent stimulation of angiogenesis in addition to a basal VirB/D4-independent proangiogenic activity and thus apparently contributes to the contact-dependent activities described above. Using an *in vitro* 3D model for angiogenesis that followed the cumulative length of capillaries sprouting out of endothelial cell spheroids, it was found that the VirB/D4-dependent stimulation was in fact the net effect of Beps with pro- and antiangiogenic properties: while BepA (heavily) and BepD (moderately) promoted sprouting when expressed in an effectorless mutant upon infection, BepG strongly inhibited angiogenesis in this model and even diminished the VirB/D4-independent stimulatory activity to the background of uninfected cells. Interestingly, the BID domain of BepA alone was sufficient to trigger the capillary sprouting phenotype (381). The authors also showed that *B. henselae* Houston-1 stimulated angiogenesis in their *in vitro* model to a similar extent as VEGF. Surprisingly, further investigation revealed that only the VirB/VirD4-independent angiogenic activity alone was cumulative with VEGF stimulation but that translocation of *Bartonella* effector proteins apparently made endothelial cells irresponsive to this growth factor (382). It could be shown that a protein tyrosine phosphatase (PTP) activity induced and/or provided by the Beps dephosphorylates at least two tyrosines in the cytosolic C terminus of VEGF-R2 (Tyr951 and Tyr1175). Phosphorylation of these tyrosines provides docking sites for downstream effectors of VEGF signaling, and both were shown to be either directly or indirectly involved in angiogenesis (187, 375, 449). In line with these findings, the authors demonstrated a corresponding obstruction of VEGF-R2 downstream signaling and further detected a considerable loss of cellular tyrosine phosphorylation at various molecular weights, indicating that VEGF-R2 would not be the only target of the effector-associated PTP activity. No single Bep was sufficient to restore the inhibition of VEGF signaling in an effectorless mutant, further highlighting that the effector proteins of *Bartonella* act together as a multifaceted cocktail that subverts host cell signaling.

In addition to its strong effect on angiogenesis, the BID domain of BepA was further shown to be responsible for an antiapoptotic activity observed during infections of human endothelial cells with *B. henselae* Houston-1 (384). Since endothelial cell proliferation is intimately connected to the inhibition of apoptosis (see above), it is likely that the two *in vitro* phenotypes of BepA arise from the same molecular activity. The particular mechanism underlying the effects of BepA has not been resolved, but inhibition of apoptosis correlates with its localization to the host cell plasma membrane and an increase in cellular cAMP levels (384). Experiments with drugs triggering elevated cAMP levels showed that such elevation could mimic the antiapoptotic effect of BepA, suggesting that the increase in cellular cAMP observed in the presence of BepA is no side effect but the actual signal that mediates its antiapoptotic activity. Interestingly, the authors further reported that the BID domain of *B. quintana* BepA, but not the ortholog of *B. tribocorum*, inhibited apoptosis in human endothelial cells. These results are in line with experiments of Kirby and Nekorchuk that revealed a certain host-pathogen specificity of *Bartonella*-derived antiapoptotic and mitogenic effects (226). Furthermore, a recent study reported that the stimulation of cAMP production in endothelial cells was observed only when the Houston-1 strain of *B. henselae* had been used to infect (immortalized) HUVECs and not with any other combination of bacterial strain and host cell line (37), thus confirming that the cellular effects of the Beps are apparently in a subtle balance with other bacterial and/or host factors.

The proinflammatory activation of endothelial cells via activities of *Bartonella* effector proteins comes in addition to a VirB/D4-independent activation of NF-κB, which has been linked to several virulence factors such as outer membrane proteins (OMPs) or BadA of *B. henselae* (385). The VirB/D4-dependent increase in NF-κB activation was evident in a corresponding elevation of ICAM-1 surface expression and IL-8 secretion, supporting the idea that the proinflammatory effect may overlap with or be part of the angiogenic activity of the *Bartonella* effector proteins and participate in the dedicated contact-dependent effects on endothelial cells.

Since *Bartonella* research in the last decades focused on *B. bacilliformis*, *B. henselae*, and *B. quintana* due to their role as human pathogens, suitable *in vitro* infection models for species of lineage 3 are not available. No evidence for the translocation of these Beps into host cells or for potential cellular activities or phenotypes (apart from the phosphorylation of tyrosine motifs) is available. However, future research may elucidate the role of the VirB/Bep system in infections of these species and allow us to explore the parallel evolution of *Bartonella* effector proteins at a cellular level.

(d) Possible functional interaction with TAAs. It has been speculated for *B. henselae* that BadA and the VirB/D4 T4SS might interact synergistically in a way that BadA would mediate initial attachment to target cells, facilitate effector secretion, and manipulate cellular functions together with the Beps (322). The concept of such a relationship between an adhesin and a T4SS is reminiscent of the case for *Helicobacter pylori*, where host cell binding via the BabA protein was shown to amplify phenotypes associated with effector secretion (199). Although one could imagine that the enormous size and the dense surface layer of BadA may interfere with *Bartonella* effector secretion, the T-pilus of the plant-targeting *A. tumefaciens* VirB/D4 T4SS is known to range from 1.4 μm length on average up to even 4.5 μm and would hence be much longer than BadA (8). It is true that the participation of a T4S pilus in *Bartonella* effector secretion has never been demonstrated, but conjugation of the prototypic *Escherichia coli* F plasmid occurs over a distance of up to 12 μm (18), confirming that T4S is able to bridge remarkable distances and may be able to cross the BadA surface layer. As an alternative to a functional interaction, it was hypothesized that BadA and the VirB/D4 T4SS may not be coexpressed in the bacteria (216). At least a certain regulatory antagonism is indeed evident from transcriptional data on *B. henselae* during infections *in vitro*, since under these conditions expression of the VirB/D4 T4SS was upregulated and that of BadA downregulated (347). In conclusion, it seems plausible that BadA and the VirB/D4 T4SS of *B. henselae* could somehow cooperate in the manipulation of host cells, but experimental evidence supporting this hypothesis is missing.

The direct investigation of the potential functional interaction between BadA and the VirB/D4 T4SS has so far been impeded by the use of strains that express only one of the two (see above). Since assembly of both macromolecular machineries is very costly for the bacterium, one factor is typically lost under nonselecting conditions in the laboratory, although published reports are available only for loss of BadA expression *in vitro* (225, 361).

(ii) The Vbh T4SS. The genome sequence of *B. tribocorum* revealed the presence of a third type IV secretion system in addition to those encoded by the *virB/D4* and *trw* loci that was, owing to considerable protein sequence identity of 40 to 80%, called the VirB-homologous (Vbh) T4SS. Subsequent phylogenetic analyses showed that the Vbh T4SS and the VirB/D4 T4SS cluster together in a clade that is clearly separate but most related to a set of conjugative machineries in other *Rhizobiales*, such as the AvhB T4SS in the pATC58 plasmid of *A. tumefaciens* (374). Close homologs of the Vbh T4SS were found in other *Bartonella* species (34, 134), and although no direct evidence corroborates a function in virulence, its presence in all species of lineage 2 as the sole T4SS has been interpreted as indicative of a role in pathogenesis (115, 374). This hypothesis was further supported by the discovery of genes coding for potential effectors with a FIC-BID domain architecture close to the *vbh* loci in *B. grahamii* and *B. schoenbuchensis* (34, 134). Elucidating a potential function of the Vbh T4SS in the pathogenesis of *Bartonella* will provide important insight into both the virulence and evolution of this genus.

Outer membrane proteins. A study with *B. henselae* revealed that various outer membrane proteins (of 28 kDa, 32 kDa, 43 kDa, 52 kDa, and 58 kDa in size) bind human endothelial cells *in vitro*, indicating that they could act as adhesins or somehow stably interact with cell surface moieties (64). While the 43-kDa protein was found to be the strongest adhesin and may very well be OMP43 (see "Other Virulence Factors" below), another study discovered that low-molecular-mass outer membrane proteins (3 to 33 kDa) of *B. henselae* Houston-1 were sufficient to trigger NF-κB activation independent of LPS and Toll-like receptor 4 (TLR4) and stimulated the secretion of MCP-1 by endothelial cells (282). Consistent with this, another group reported that outer membrane proteins of *B. henselae* Berlin-1 and *B. henselae* Houston-1 could activate NF-κB in HUVECs, leading to the upregulation of adhesion molecules (E-selectin and ICAM-1) that may promote the attachment of circulating leukocytes (148). The interaction partners of these *Bartonella* outer membrane proteins on the host cell surface are not known, but it has been suggested that ICAM-1 may be one of them, since this protein is enriched in the tips of host cell membrane protrusions that tightly associate with the bacterial aggregates during invasome formation (120). It is further tempting to speculate that one or more of the host cell binding outer membrane proteins would be the elusive factor of *B. henselae* Houston-1 that binds β1-integrins in the context of invasome formation and is regulated by the BatR/BatS system (419).

Taken together, current knowledge suggests that one or more outer membrane proteins of *Bartonella* contribute to host cell adhesion and the contact-dependent proinflammatory activation of endothelial cells that was observed *in vitro* and *in vivo*, although the identity of these proteins has remained elusive so far. More outer membrane proteins of *Bartonella* that are suspected to be virulence factors but whose particular roles during infection have not been worked out are discussed in "Other Virulence Factors" below.

GroEL. Bacterial GroEL heat shock proteins are a conserved group of chaperonins whose function to mediate protein folding has made them widely essential to resist various stressors such as extreme temperatures or nutrient limitation (164, 265, 348). Interestingly, although no member of the GroEL family bears any discernible secretion signal, overwhelming evidence indicates that surface-exposed or secreted GroEL plays a key role in the infection strategies of many bacterial pathogens (35, 181, 184; reviewed in reference 174). As an example, the corresponding homolog of *Legionella pneumophila* is known to be displayed on the bacterial surface, where it promotes an invasive phenotype, and the same protein apparently manipulates cellular trafficking, cytoskeleton, and signaling once it is released inside the eukaryotic host cell (recently reviewed in reference 153).

It is therefore not surprising that GroEL of *Bartonella* is strongly suspected to be a virulence factor, although its role during infection is not well understood. Most evidence derives from experiments with *B. bacilliformis*, where GroEL was found not only in the cytoplasm but also in the outer membrane and actively secreted into culture supernatants (297). These supernatants as well as lysates of *B. bacilliformis* triggered the proliferation of HUVECs, indicating the presence of a mitogen, and antibodies against GroEL or its partner GroES strongly reduced this activity. The presence of a dose-dependent mitogen in extracts of this species had already been discovered before (150, 151), and lysates of *B. bacilliformis* expressing different amounts of GroEL triggered cell proliferation in accord with GroEL levels (297). This stimulatory effect of GroEL on host cell proliferation is apparently a conserved element in the infection strategy of *Bartonella*, since lysates generated from *B. henselae* also showed mitogenic activity, albeit weaker than that of lysates of *B. bacilliformis*. These results are in line with other reports that *B. henselae* secretes an antiapoptotic and mitogenic activity into culture supernatants (226, 268) that may very well be GroEL. Interestingly, the antiapoptotic activity of these supernatants was weaker than the net effect of live *B. henselae*, hence confirming the role of additional factors that are known to act on the same phenotype and may account for an attenuation of GroEL potency during evolution (like the VirB/D4 T4SS). GroEL was further found to localize to the outer membrane not only of *B. bacilliformis* but also of *B. henselae*, and it is highly immunogenic in various *Bartonella* species (43, 84, 229, 357, 432). In addition, it was recognized that *Bartonella* GroEL harbors a C-terminal phenylalanine that is a general characteristic of outer membrane proteins, indicating that GroEL of *Bartonella* would be adapted to exposure on the bacterial surface (69, 409).

It remains enigmatic how GroEL of *Bartonella* would act as a mitogenic and antiapoptotic factor on the molecular level, but corresponding activity has been shown for GroEL of *Chlamydia pneumoniae*, which triggers the proliferation of human cells via TLR4-dependent activation of p44/p42 mitogen-activated protein kinases (MAPKs) (380). GroEL could hence be imagined to directly trigger proliferative signaling and/or to induce the secretion of factors that act as autocrine or paracrine mitogens such as IL-8. The latter hypothesis is consistent with findings that *E. coli* GroEL stimulates the expression of granulocyte-macrophage colony-stimulating factor (GM-CSF), IL-6, and ICAM-1 in HUVECs (149). A recent study indeed reported that the secreted mitogen of *B. henselae*, most likely GroEL, would act via an elevation of the intracellular Ca^{2+} levels (283). Alternatively, the effect

of *Bartonella* GroEL could be indirect, for example, by protecting the actual yet unknown bacterial mitogen from degradation.

Due to its essential role in cellular homeostasis, the importance of GroEL for *Bartonella* pathogenesis could not be assessed in the STM screens with *B. birtlesii* or *B. tribocorum*, but GroEL was found to be part of the BatR/BatS virulence regulon in *B. henselae* (347). Surprisingly, the *groEL* gene seems to be strongly downregulated during *in vitro* infection of endothelial cells, which is bizarre with respect to its major role both in stress responses and as a potential virulence factor, but could protect heavily infected cells from adverse effects. It was further reported that, while mitogenicity had initially been observed with lysates of *B. bacilliformis*, the coculturing of live bacteria stimulated HUVEC proliferation only with strains expressing low or moderate levels of GroEL. Expression of large amounts of GroEL appeared to induce apoptosis in HUVECs after long coculture (96 h), although all strains initially inhibited spontaneous apoptosis (407). The authors conclusively interpret the apparent contradiction to previous results with the homology of bacterial GroEL to eukaryotic HSP60 chaperonins that are known to stimulate apoptosis if present in huge excess. The proapoptotic effect in coculture would hence derive from intracellular bacteria releasing large amounts of GroEL, while the stimulatory effect on cell proliferation would most likely be triggered by extracellular GroEL (407). It is thus tempting to speculate that the potentially deleterious effects of intracellular GroEL secretion in heavily infected cells could be counteracted under physiological conditions by the downregulation of bacterial *groEL* expression that was described for *B. henselae*.

Taken together, solid evidence suggests that GroEL is the secreted mitogenic and antiapoptotic factor of *Bartonella* that has been described repeatedly, although the underlying molecular mechanism remains unknown.

Infection of Erythrocytes

The Trw T4SS. In addition to the VirB/D4 T4SS, the species of lineage 4 harbor the Trw T4SS as a lineage-specific virulence factor that mediates adhesion to red blood cells (427). It is not closely related to the other type IV secretion systems of *Bartonella* but has apparently been acquired independently. Sequence similarity of up to 80% at the protein level to the conjugative Trw T4SS of the IncW broad-host-range plasmid R388 suggests that it may have been obtained from such a conjugative plasmid via lateral gene transfer, especially since transcriptional regulation by the KorA/KorB repressor system is conserved in *Bartonella* (402).

The Trw T4SS was discovered using a differential fluorescence induction (DFI) screen for genes that are upregulated in *B. henselae* during infection of endothelial cells *in vitro*, and the STM screens in *B. birtlesii* and *B. tribocorum* confirmed its essentiality as a virulence factor for the species of lineage 4 (374, 427). Interestingly, a mutant devoid of a functional Trw system was found to appear in the bloodstream but was cleared shortly after infection, which provided the first evidence that the Trw T4SS is involved in erythrocyte infection rather than colonization of the primary niche (116). The upregulation observed during endothelial cell infection hence apparently constitutes a phenotypic adaptation of the bacteria for the infection of red blood cells, since expression and assembly of the Trw machinery only in the bloodstream would extend the time that the bacteria had to spend in this hostile environment. Further investigation revealed that the Trw T4SS not only is essential for the adhesion of *Bartonella* to erythrocytes but also dictates the host specificity of this process, most likely by adaptation to erythrocyte surface structures that are highly variable among the different host species of the bartonellae. Strikingly, ectopic expression of the Trw T4SS of one *Bartonella* species in another one was found to be sufficient for a corresponding extension of the host range in an *in vitro* erythrocyte infection assay (427).

In contrast to the VirB/D4 T4SS of *Bartonella*, the Trw T4SS apparently neither harbors a coupling protein nor translocates any known effectors, but it carries numerous tandem gene duplications coding mostly for surface-exposed subunits (401). Coduplicated gene copies encoding a core subunit are highly conserved, while the genes encoding putative minor and major pilus subunits have been shaped by diversifying selection. Diversification is thought to have occurred via intra- and intergenomic combinatorial sequence reshuffling and even led to potential subfunctionalization into two versions of the major pilus subunit. It is assumed that the polymorphicity of erythrocyte surface structures in mammals has been the driving force for this remarkable sequence dispersion (316), especially since the different copies of Trw surface proteins seem to be coexpressed (115). Such host polymorphisms have also been proposed to affect red blood cell invasion of *Plasmodium* parasites (289, 414, 437), but it remains unknown which host factors the Trw T4SS binds on the erythrocyte surface.

Deformin. Evaluation of human red blood cells infected with *B. bacilliformis in vitro* revealed deformations appearing as "pits" or "trenches" on the erythrocyte surface (31), which were proposed to serve as entry points for the invasion process (Fig. 5). It has been suggested that a secreted bacterial factor, deformin, would cause the membrane invaginations (440), but its molecular identity, mode of action, and secretion mechanism have remained elusive so far, although a well-documented phenomenology allows us to assemble a basic picture of its functionality. Importantly, deformation could also be demonstrated for *B. henselae*, making it likely to be a common feature of *Bartonella* erythrocyte infection (201).

Early reports describing deformin to be a protein of 65 kDa or 130 kDa (440) or implying physicochemical properties of proteins (e.g., heat inactivation [287]) arose from confusion with its tight binding to serum albumin. Instead, deformin was found to be a small (1.4-kDa) water-soluble but amphiphilic molecule that is resistant to heat, several proteases, α-amylases, and pH change in the range of 2 to 9.5 (126).

Filtered supernatants of *B. bacilliformis* cultured in certain media could reproduce the deformation phenotype in the absence of bacteria, since they apparently contained deformin bound to serum albumin (287). The pretreatment of erythrocytes with trypsin or neuraminidase greatly favored deformation, and without such pretreatment the deformation phenotype induced by deformin in filtered culture supernatant was very weak compared to that of whole, live bacteria (287). These results suggest that increased accessibility of erythrocyte membranes could facilitate the activity of deformin and that live bacteria may harbor additional factors, like a secretion machinery and/or hydrolytic enzymes, that would assist deformin delivery. It is worth noting that pretreatment with trypsin or neuraminidase also strongly enhanced the binding of *B. bacilliformis* to glycophorin B from solubilized erythrocytes (63), although the link to deformation is not clear. Additional evidence for a manipulation of erythrocyte membranes as underlying red

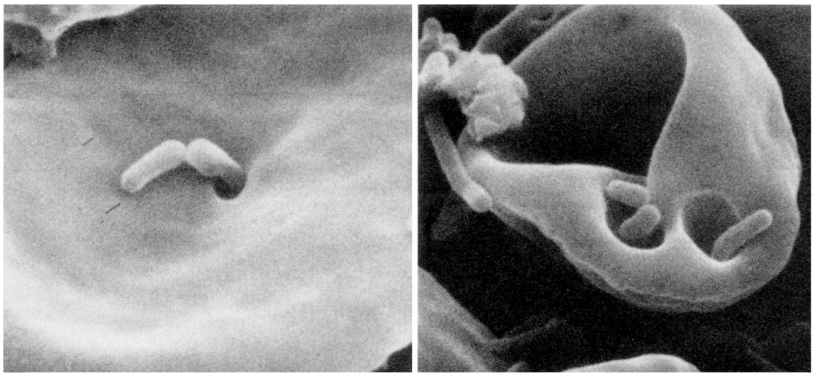

FIG 5 Entry of *Bartonella* into human erythrocytes. The scanning electron micrographs show *B. bacilliformis* first inducing indentations in the erythrocyte surface (left) and then invading at the resulting pits (right). Note that neither the deformation of erythrocyte membranes nor the actual invasion process appears to involve rupturing of the erythrocyte surface. (Adapted from reference 31 with permission.)

blood cell deformation comes from findings that phospholipase D (cleaving phosphatidylcholine) and vanadate (which inhibits the flippase that maintains membrane leaflet asymmetry [332]) dampen and prevent deformation, respectively (287, 440).

The function of erythrocyte deformation during blood-stage infection by *B. bacilliformis* has not been resolved experimentally, but the hypothesis of it being involved in the formation of some kind of entry site is convincing (295), especially since deformation was found to precede erythrocyte invasion (287).

No molecular mechanism has been demonstrated so far for *Bartonella*-induced red blood cell deformation, but the small size of deformin and the finding that it does not directly modify phospholipids (440) speak against a biochemical activity on membrane components. Interestingly, deformation is stable for some time but can be rapidly reversed by different compounds that interfere with the asymmetric distribution of phospholipids in the two membrane leaflets, indicating that deformin would exploit this asymmetry (440). Convincingly, these results let Xu et al. (440) speculate that deformin-induced membrane invaginations might arise in a way similar to what Sheetz and Singer proposed for erythrocyte stomatocytosis in their bilayer couple hypothesis (404). In short, invaginations on erythrocyte membranes could be induced by processes that would locally jumble the inner and outer leaflets (like intercalation of an amphipath), since active reconstitution of leaflet asymmetry occurs only from outside to inside (through the flippase mentioned above). This imbalance in lipid transport results in net extension of the inner leaflet, formation of an indentation, and finally vacuolization (259, 390). Although the molecular identity of deformin remains mysterious, a small peptide or lipid/LPS compound could be imagined to trigger deformation via processes like those described above. Importantly, deformation seems not to involve detectable rupturing of membrane integrity, because traversing diffusion of dyes or labeled proteins was never observed. Instead, the presence of deformin in the absence of bacteria was sufficient to trigger the uptake of extracellular fluid into intraerythrocytic vesicles, reminiscent of *Bartonella* "forced endocytosis" (31, 440). In further consistency with a mechanism involving integration of an amphipath into erythrocyte membranes, deformin seems to be consumed upon contact with red blood cells, since filtered supernatants with deformin were found to lose activity during serial addition and removal of erythrocytes (287). The whole process is strongly reminiscent of studies discussing the use of amphiphilic substances to trigger the uptake of drugs into intraerythrocytic vesicles (example in reference 389). Interestingly, such techniques were developed to deliver drugs to cells of the mononuclear phagocyte system, because these would selectively eliminate the abnormally vacuolized erythrocytes just as observed during Oroya fever.

Like most aspects of its activity, the mechanism by which deformin gets into the extracellular space has remained enigmatic. Remarkably, the apparent secretion of deformin into culture supernatants seems to depend on the presence of functional albumin or other serum components, because heating or dialysis of the culture medium after the addition of serum supplement made it incapable of acquiring deforming activity (287). It hence cannot be ruled out that the secretion observed *in vitro* may be nonphysiological. In any case, the presence of deformin in filtered supernatants was accompanied by bacterial outer membrane proteins appearing in association with membrane fragments or vesicles (440). Interestingly, the presence of bacterial membrane proteins of 31 to 36 kDa in supernatants generated with the KC583 strain of *B. bacilliformis* correlated with its ability to secrete deformin, while these proteins as well as deforming activity were missing in supernatants of the KC584 strain. Live bacteria of both strains induced deformation of erythrocytes (179), indicating that the discrepancy was due to differences in the secretion of deformin. The authors of the study proposed that the proteins missing in the supernatant of KC584 might be identical to deformin, involved in its secretion, or part of a "deforming protein complex" (179), but no direct link to deformation could be demonstrated experimentally. It is conceivable that these elusive proteins may derive from outer membrane vesicles (OMVs), which are a general phenomenon among Gram-negative bacteria (243) and often serve as vectors for the delivery of periplasmic or membrane-associated virulence factors to target cells (9, 290, 433). Alternatively, the proteins and membrane fragments may derive from bacteriophage-like particles, because their size and the association with some kind of membrane vesicles are immediately reminiscent of the BLPs that have been repeatedly described for *Bartonella* (see above). However, it remains enigmatic how the release of BLPs could be connected to the secretion of deformin, especially since both the KC583 and KC584 strains have been shown to harbor these particles (11).

In conclusion, it is apparent that membrane deformation is

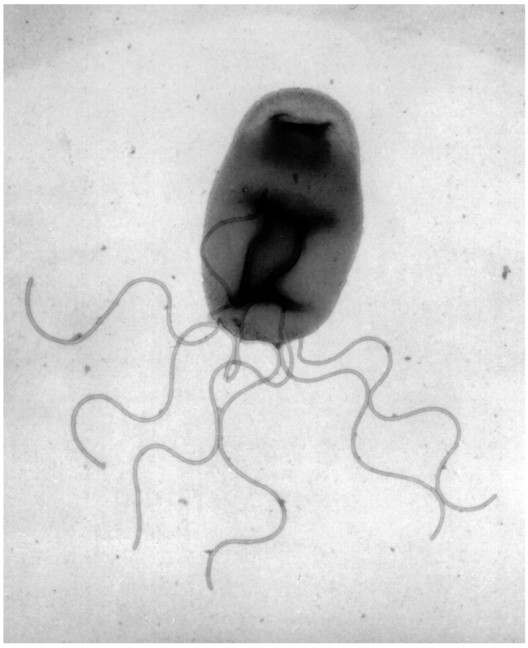

FIG 6 Flagellation of *Bartonella*. The transmission electron micrograph shows several unipolar (lophotrichous) flagella of *B. clarridgeiae*. Morphologically indistinguishable flagella have also been observed for other species of lineages 2 and 3 as well as *B. bacilliformis*, while the species of lineage 4 are not flagellated (31, 36, 118, 136). (Adapted from reference 13 with permission.)

important at an initial step of erythrocyte invasion during *Bartonella* infections, but the molecular mechanism and the identity of the deforming factor remain mysterious.

Flagella. In a remarkable difference from the species of lineage 4, the bartonellae of lineages 1 to 3 harbor a set of unipolar (lophotrichous) flagella and are thus motile (Fig. 6). Flagella are well established as bacterial virulence factors (210), and those of the flagellated bartonellae are known to play an important role during the infection of erythrocytes by these species. Early studies noted that nonmotile *B. bacilliformis* organisms were unable to invade red blood cells (287), and Benson et al. observed that bacteria were pushing into surface indentations with a "boring or twisting motion" (31), implying that the flagella might contribute mechanical force to the entry process. Nonmotile *B. bacilliformis* showed decreased erythrocyte attachment and deformation, indicating that motility would be beneficial but not necessary for these initial steps of red blood cell infection (287). Consistently, it was reported that antiflagellin antibodies decreased erythrocyte attachment but much more invasion of *B. bacilliformis* (383). It was further hypothesized that the flagella of *Bartonella* could play a role as adhesins like in the case of other pathogens (135), especially since fiber-like structures were apparent on bacteria attached to red blood cells (434). However, the differential effect of antiflagellin antibodies on adhesion and invasion makes such functionality unlikely (383), and it was reported that neither recombinant flagellin nor flagella isolated from *B. bacilliformis* could bind erythrocytes (193). Remarkably, a study using immunofluorescence to follow the flagella of *B. bacilliformis* during erythrocyte infection indicated that the flagella would be ejected for intraerythrocytic persistence (370), although the reasoning for this step remains unclear.

The apparent exchange of flagellation for the Trw T4SS in the species of lineage 4 and the common function of both virulence factors in erythrocyte invasion indicate that the Trw T4SS may have somehow functionally replaced the flagella directly or indirectly (115). Such a process could have been favored in evolution because the versatility of the Trw T4SS was of great advantage and/or because of disadvantages inherent to flagellation. It is particularly tempting to speculate that flagella would have been lost due to their role as major antigens of both innate and adaptive immune responses (253). Consistently, flagella of *Bartonella* may evade detection by the dedicated Toll-like receptor 5 (10), but they were found to elicit an antibody response (378) that would presumably heavily interfere with erythrocyte invasion (383) and clear the bacteria from the bloodstream.

Invasion-associated locus. The invasion-associated locus (*ial*), encoding IalA and IalB, is an essential virulence factor of *Bartonella* and critical for erythrocyte invasion but not adhesion (374, 427). Both proteins are conserved over the whole genus and were found to be sufficient for conferring a correspondingly invasive phenotype to ectopically expressing *Escherichia coli* (300).

IalA has been identified as a Nudix family nucleoside polyphosphate hydrolase (76, 101). These enzymes are involved in the catabolism of alarmones, and homologs of IalA in other pathogens were shown to be crucial for infectivity (38, 128, 200, 422). It is thus reasonable to assume that IalA may contribute indirectly to invasion, and a homolog in *Rickettsia prowazekii* was indeed suggested to "buffer" the bacterial homeostasis against stressful conditions during growth in a hostile, intracellular environment (154).

Conspicuously, the protein encoded directly upstream of IalA, CtpA, is a C-terminal processing protease that has initially been proposed to control levels of protein junk under stress conditions during infection (299). Homologs of CtpA are important virulence factors of other pathogens (27, 353), and the CtpA protein of *Borrelia burgdorferi* was found to process several outer membrane proteins known or thought to be involved in pathogenesis (323, 338, 451). However, the initial publication concerned with CtpA in *Bartonella* failed to detect processing of IalA or IalB by CtpA or any effect of CtpA on erythrocyte invasion (299), meaning that functional evidence for a contribution of this protein to *Bartonella* virulence is missing. A role for pathogenicity in *Bartonella* seems still likely, since, e.g., the ortholog in the closely related *Brucella suis* was shown to be necessary for survival in macrophages *in vitro* and infection of mice *in vivo* (22). Similarly, the *filA* gene just upstream of *ctpA* has also been suspected to encode a virulence factor, but no experimental findings that would confirm or discard this assumption have been published (293). It was, however, shown that the promoter of *filA* contains an H box that is indicative of transcriptional regulation by Irr together with other virulence factors such as the hemin binding proteins or OMP43 (26).

In contrast to IalA and CtpA, IalB is an outer membrane protein based on its signal sequence and findings in *B. henselae* (84), thus seeming to be the natural candidate for the host-interacting component of the invasion-associated locus. Initial results that IalB of *B. bacilliformis* was located in the inner membrane were surprising for the authors of the study as well and could have been caused by suboptimal growth conditions (100). The crystal structure of IalB of *B. henselae* was solved recently by Patskovsky et al. and revealed a β-barrel fold (Protein Data Bank [PDB] no. 3DTD), further confirming localization in the outer membrane

(232). Although homologs of IalB are widely conserved, especially among *Rhizobiales*, including the zoonotic pathogen *Brucella suis* (333), possible enzymatic capacities and/or host interaction partners remain elusive. However, IalB was described to exhibit considerable sequence similarity to the *Yersinia* Ail protein, which belongs to a family of bacterial outer membrane proteins whose members have frequently been associated with host cell attachment and invasion (172, 300). It is thus easily conceivable that IalB may be directly involved in erythrocyte invasion, possibly by interacting with one or more of the red blood cell surface proteins bound by *Bartonella*.

Transcriptional analysis of *B. bacilliformis* showed that IalB expression is strongly upregulated under conditions resembling the sand fly gut (20°C and acidic pH), suggesting that the bacteria would become "primed" for erythrocyte infection in the arthropod vector (99). Mutants lacking functional IalB both in *B. bacilliformis* (100) and in *B. birtlesii* (427) have been tested using *in vitro* assays for erythrocyte infection and were strongly attenuated compared to wild-type bacteria. Taken together, these results indicate that IalB and the invasion-associated locus are vertically inherited key virulence factors of *Bartonella* whose function is essential for erythrocyte invasion.

Hemolysins. The acute phase of infections with *B. bacilliformis* is characterized by severe hemolytic anemia that accounts for high mortality rates in untreated patients and is usually not associated with infections caused by the modern *Bartonella* species.

In apparent contradiction to several studies concluding that *B. bacilliformis* does not actively lyse erythrocytes during infection (see above), one study reported the discovery of a membrane-associated, proteic hemolysin in *B. bacilliformis* that was absent in *B. henselae* (178). The author states that hemolysis was contact dependent and not connected to the process of erythrocyte deformation. It apparently did not rupture erythrocytes but rather led to the formation of intact ghosts, indicating that hemolysis may derive from some kind of local puncture. However, other studies explicitly did not detect a loss of membrane integrity in infected erythrocytes (31). It is possible that this inconsistency derives from differences in the experimental conditions, since the author reporting hemolysis pointed out that such a phenomenon was not presentably detectable on blood agar plates but required an elaborate experimental procedure (178). We therefore suggest that hemolysis during Oroya fever may not be caused primarily by a bacterial hemolysin, although a membranolytic factor could allow *Bartonella* (*B. bacilliformis*) to escape from intracellular vesicles at any state of infection and still, under certain conditions, lyse red blood cells *in vitro*.

Although hemolysis has been reported as a typical feature only of *B. bacilliformis*, all species of the genus *Bartonella* seem to carry genes that are annotated as encoding putative hemolysins, such as, e.g., the *tlyA* or *tlyC* homologs in *B. henselae*. However, no evidence for a role of these elusive factors in the infection process of *Bartonella* has been published. More solid data are available for one autotransporter of *B. henselae*, termed Cfa (CAMP-like factor autotransporter), which was found to bear cohemolysin activity, i.e., the capacity to disrupt membranes of predestabilized erythrocytes (261). The fact that orthologs of this protein were shown to be essential for *Bartonella* pathogenesis in both STM screens confirms its importance as a virulence factor (374, 427). However, the Cfa mutant of the *B. birtlesii* screen was apparently not impaired in erythrocyte infection *in vitro*, indicating that it may act at a different stage of infection (427).

Other Virulence Factors

Lipopolysaccharides. It is a critical requirement for the stealth infection strategy of any Gram-negative bacterial pathogen that the host cannot detect its lipopolysaccharides (LPS), since these are among the universal properties of bacterial pathogens that are recognized by innate immunity. Stimulation of Toll-like receptor 4 (TLR4) with LPS triggers a strong inflammatory response (291) that would likely obstruct bacterial persistence. It is therefore not surprising that the LPS of *Bartonella* are adapted to virtual invisibility to the host's defenses and have even been shown to participate in the immunomodulation that is one of the most amazing features of this group of pathogens. In addition to these aspects directly linked to immunity, the low endotoxicity of *Bartonella* LPS was suggested to be critical for the intimate interaction with endotoxin-sensitive cells such as endothelial cells (448).

Most research on the LPS of *Bartonella* has been performed with *B. quintana*, and the LPS of this species were shown to stimulate TLR4 three to four orders of magnitude less than *Salmonella* LPS, so TLR4 apparently does not play a role in the recognition of this pathogen (277). TLR2, a peculiar receptor recognizing primarily lipoproteins and lipopeptides (447), was found to be unresponsive to *B. quintana* LPS but apparently reacts to LPS-associated bacterial components (see below). Furthermore, it was shown that the LPS of *B. bacilliformis*, *B. henselae*, and *B. quintana* do not elicit a specific humoral immune response in mammals (84, 292).

In apparent contradiction to their definitive role in immune evasion, the LPS of *B. quintana* reacted strongly in the *Limulus* amebocyte lysate assay, a standard tool to detect endotoxicity (278). However, no considerable secretion of TNF-α could be detected in human whole blood challenged with *B. quintana* LPS or upon intravenous injection of the LPS into rats (278). This striking lack of proinflammatory activation is likely based on the remarkable property of *B. quintana* LPS of not only being virtually undetectable by TLR4 but even acting as a potent antagonist of TLR4 signaling, leading to considerable transcriptional downregulation of the proinflammatory program triggered upon activation of this receptor (including TNF-α) (340). In addition to the silencing of TLR4, an apparently LPS-associated component of *B. quintana* stimulated the secretion of IL-8, IL-10, and (small amounts of) TNF-α in host cells (277, 278). Consistently, TLR2-dependent production of IL-8 was also observed for *B. henselae* crude LPS extracts but was not detected upon further purification (277), which could explain the stimulation of IL-8 secretion in rats injected with *B. quintana* LPS as reported in an earlier study (278). Taken together, the available evidence shows that the LPS of *Bartonella* have immunomodulatory properties by acting as TLR4 antagonists and that an LPS-associated factor (perhaps an outer membrane lipoprotein) can obviously trigger cytokine secretion via TLR2 as part of the contact-dependent proangiogenic activities of *Bartonella*.

These immunoevasive and immunomodulatory properties of *Bartonella* LPS apparently derive from their molecular architecture. The structure of the *B. henselae* LPS has been solved by Zähringer et al. and revealed a deep-rough chemotype, in line with findings for other *Bartonella* species such as *B. bacilliformis* or *B. quintana* (448). In addition, the LPS of *B. henselae* is pentaacylated

and contains a very small carbohydrate moiety and a long-chain fatty acid, which are well-known attributes of LPS of other stealth pathogens such as *Legionella* (446), indicating that these features may enable immune evasion by common mechanisms (448). It is worth noting that the *Bartonella* LPS do not seem to be homogenously deep-rough, since Zähringer et al. reported a certain proportion of smooth LPS and linked their finding to the smooth and dry colony phenotypes observed during growth of *Bartonella* on plates (448). The dimorphism between "dry agar-pitting" and "smooth non-agar-pitting" colonies has been observed for several *Bartonella* species, such as *B. henselae* (24), *B. schoenbuchensis* (118), and *B. bacilliformis* (434) and is believed to be caused by phase variation, although the molecular basis of this phenomenon has never been revealed (245). No function for the smooth LPS of *Bartonella* has been worked out so far, but a similar phenomenon of LPS heterogeneity is known from other *Rhizobiales* such as *Sinorhizobium*, where it was suggested to play a role in host interaction (163).

Autotransporters and filamentous hemagglutinins. In addition to trimeric autotransporter adhesins like BadA, the bartonellae also harbor classical autotransporters as well as two-partner secretion systems and hence feature representatives of each class of type V secretion systems (177).

Classical autotransporters are similar to TAAs in that an N-terminal passenger domain is translocated over the outer membrane through a C-terminal transporter domain, but they contain a full β-barrel transporter per monomer. The passenger domain is usually cleaved off from the transporter after translocation but typically stays attached to the bacterial surface (recently reviewed by Dautin and Bernstein [109]). Autotransporters are important virulence factors of various bacterial pathogens (176), but comparably little is known about the homologs in *Bartonella*. It is apparent that all *Bartonella* species encode a set of several autotransporters that belong to two distinct phylogenetic clades (personal observation). Representatives of the larger clade were first described as bacterial factors upregulated during *in vitro* infection of endothelial cells, and hence the genes were called *iba* (for inducible *Bartonella* autotransporters) (403). This clade of autotransporters was analyzed by Berglund et al. *in silico* and is again separated into two phylogenetic groups that seem monophyletic in *Bartonella* but separated before branching off of the *B. bacilliformis* lineage (34). Two representatives of the *iba* group were investigated by Litwin et al. and termed Arp (for acidic repeat protein) (262) and Cfa (for CAMP-like factor autotransporter) (261). While Cfa was found to exert cohemolysin activity (see above), the passenger domain of Arp shows sequence similarity to pertactin-like adhesins, which was interpreted as an indication of a potential related function of Arp (262). Notably, Arp and Cfa are representatives of the two distinct clades of *iba* autotransporters and were both found to stay attached to the outer membrane after cleavage from the transporter domain (261, 262), indicating that this may be a common feature of these proteins in *Bartonella*. Several *iba* autotransporters were confirmed to be upregulated during *in vitro* infections with *B. henselae* in a second study and were found to be essential for virulence in the two STM screens (e.g., Cfa) and immunogenic in infections (347, 374, 427, 432). Furthermore, representatives of this group in *B. quintana* were shown to contain an H box in their promoters, which indicates regulation in response to the transcription factor Irr together with other virulence-related genes, like those encoding the hemin binding proteins (26).

A second, smaller group of autotransporters (in *B. henselae* BH05490, BH05500, and BH05510) also features representatives in every *Bartonella* species but shows sequence similarity to autotransporters of *Enterobacteriales* such as *Yersinia* rather than to the *iba* proteins (personal observation). Like some *iba* genes, autotransporter genes of this group were upregulated during *in vitro* infection of human endothelial cells and were found to be immunogenic (347, 432), but they do not seem to be individually essential for establishing blood-stage infection as examined in the STM screens (374, 427).

Molecular functions or any particular contribution of both groups of autotransporters during *Bartonella* pathogenesis remain (with the partial exception of Cfa) to be uncovered. Other autotransporters of bacterial pathogens have been found to exert various functionalities, e.g., as adhesins (252) or as extracellular proteases for antibodies (298) or for hemoglobin (324).

The filamentous hemagglutinins (Fha) are an additional type V secretion system of *Bartonella* that is present only in *B. grahamii*, *B. henselae*, and *B. tribocorum* among the sequenced species (34). Filamentous hemagglutinins are secreted in a manner very similar to that for classical autotransporters, but the passenger domain (the actual filamentous hemagglutinin FhaB) and the transporter domain (FhaC or Hec for hemolysin activator protein) are encoded in separate genes. After translocation over the outer membrane, the passenger domain is usually subjected to further processing and finally either is secreted into the extracellular space or stays attached to the transporter or the outer membrane (96, 205, 281). The filamentous hemagglutinins of *Bartonella* can be separated into two clades that were apparently acquired independently from different sources. It is notable that the *fha* loci are associated with integrases and phage genes and that the distribution of their occurrence is very diverse even within closely related populations, pointing toward frequent exchange via lateral gene transfer (32, 34). Interestingly, *B. quintana* does not encode any filamentous hemagglutinins, although the closely related *B. henselae* harbors various copies of both passengers and transporters (34). The available data do not allow conclusive assignment of any function to the Fha proteins in *Bartonella* (322), but the genes coding for the outer membrane transporters were found to be regulated by the BatR/BatS system in *B. henselae* (347). One filamentous hemagglutinin and two transporters were immunogenic in cats infected with *B. henselae* (432), thus proving that at least some of these proteins are expressed inside the host. No *fha* gene is essential for the pathogenesis of *B. tribocorum* (374), but the presence of various *fhaB* and *hec* genes indicates potential redundancy that would impede detection by STM (322). The filamentous hemagglutinins may further be capable of extracellular complementation, especially since the passenger domain is potentially released from the bacterial surface.

Filamentous hemagglutinins are important virulence factors of other pathogens such as *Bordetella*, where they are necessary for optimal colonization of the respiratory tract (312) and may be key factors for host specificity (194). The *Bordetella* Fhas have been shown to mediate adhesion to various host structures (204) and to modulate the NF-κB pathway of immune cells (2). Similarly, an analysis of the filamentous hemagglutinins in *Erwinia chrysanthemi* revealed that they are required for full virulence and pointed

toward horizontal gene transfer as a common feature in the spread of these pathogenicity factors (364).

Hemin binding proteins. The hemin binding proteins (Hbps) of *Bartonella* are a group of porin-like outer membrane proteins that bind hemin on the bacterial surface, but lack any discernible homology to known bacterial heme receptors (25). Remarkably, Pap31, the first known member of this family in *Bartonella*, was discovered not as a virulence factor but as being a major protein component of the BLPs that *Bartonella* releases into culture media, although it is known today that its prevalence in the phage-like particles is rather coincidental (see above). Subsequent research established the alternative denomination of Pap31 orthologs as HbpA and identified the Hbps as a protein family (75, 296). Three to five representatives are present in the genome of every *Bartonella* species, and homologs are widespread among *Rhizobiales* but rare beyond this taxon (reference 294 and personal observation). The Hbps show considerable sequence similarity to members of the OMP25/31 family of *Brucella* (75), which are apparently crucial for several aspects of pathogenesis, although their molecular function is not known (74, 276). Furthermore, homologies to the well-known *Neisseria* Opa proteins, which are critical mediators of host cell interaction involving invasion and immunomodulation (372, 388), have been described (296). Comprehensive theories explaining the contribution of *Bartonella* Hbps to pathogenesis are lacking, although a plethora of experimental data are available and various (not mutually exclusive) hypotheses have been proposed. In short, the Hbps were suggested to be (part of) a heme uptake system, to form an antioxidant coat, to maintain a microaerobic intracellular environment, or to participate directly in host cell manipulation (26).

It is undisputed that the acquisition of heme is critical for *Bartonella*, since the bartonellae have an exceptionally high need for this compound (377). However, the hemin binding activity of the Hbps does not automatically imply a function in heme acquisition, especially since *Bartonella* harbors a distinct, dedicated hemin import system (HutABC/HmuV) (331) (see below). One study reported that HbpA of *B. henselae*, whose ortholog in *B. quintana* constitutes the strongest hemin binding activity of this species (75), could complement a *hemA* deficiency in *E. coli* and thus act as part of a hemin uptake machinery (453). However, these results have been decisively challenged by other authors (294), especially since the *hemA*-deficient *E. coli* strains are known to display a leaky phenotype (379). We hence conclude that a primary function of the *Bartonella* hemin binding proteins in heme acquisition seems unlikely, although an accessory role via the accumulation of substrate is conceivable.

In addition to this potential facilitation of heme acquisition, the hemin binding of the Hbps should lead to a coat of heme on the cell surface, whose properties and functions would depend largely on the properties of heme. Extracellular deposition of heme is also seen in *Yersinia pestis*, where efficient transmission by bloodsucking arthropods depends on outer membrane storage of this compound (183, 337). Most obviously, such a surface coat would provide a nutritive reservoir for *Bartonella*, especially as it has to compete with its arthropod vector for heme in the midgut (25). Furthermore, the intrinsic peroxidase activity of heme would make the coat a potent antioxidant barrier (25) and hence constitute a suitable protectant against reactive oxygen species (ROS) as key mediators of antimicrobial defense both in the arthropod gut (169, 305) and as part of mammal immune defenses (42). ROS release in the arthropod gut is highly regulated, for example, in order to protect symbionts (168), and was found to be decreased in bloodsucking arthropods upon perception of heme in the gut lumen (319). Such a mechanism would potentially allow *Bartonella* not only to tolerate but also to prevent certain challenge by ROS, though no experimental data are available. *Porphyromonas gingivalis* is an example of a pathogen that uses surface coating with heme and related compounds as a defense mechanism against ROS in humans (405, 406). Similarly, heme can also modulate the behavior of mammalian cells (15, 127, 138), making it conceivable that a coat of heme would also contribute to subvert responses of the vertebrate host.

Besides functions in host interaction, heme would also decrease oxygen levels around the bacteria. Battisti et al. speculated that bartonellae (exemplified by *B. quintana*) would lack aerobic respiration and could, similarly to other *Rhizobiales* such as *Agrobacterium* spp., be adapted to growth in microaerobic compartments. They further proposed that hemin binding via Hbps or their orthologs may be a common strategy for this purpose among different *Rhizobiales* (25, 26).

Finally, HbpA of *B. henselae* was shown to bind fibronectin, heparin, and HUVECs (107). Binding to these ECM compounds has been linked to the homologous OpaA protein of *Neisseria*, which also binds fibronectin and mediates invasion of epithelial cells via an integrin-dependent mechanism (107, 425). Additionally, a *B. henselae* HbpD mutant was deficient in escape from phagosome maturation (246), but the underlying direct or indirect mechanism has not been resolved.

In summary, the abundance of evidence makes it likely that the Hbps contribute prominently to *Bartonella* pathogenesis in several ways. It is thus not surprising that studies of *B. quintana* discovered sophisticated transcriptional control mechanisms guiding *hbp* expression and revealed a clear correlation between biologically relevant stimuli and altered expression patterns of the *hbp* genes (25). From a regulatory point of view, the Hbps seem to constitute two subgroups, with the first one (HbpB and HbpC) being preferentially expressed under conditions that resemble the arthropod midgut or feces (high hemin and 30°C) and the second one (HbpA, HbpD, and HbpE) being preferentially expressed under mammal-like conditions (37°C and low hemin) (25). Although this second subgroup was still predominant under bloodstream-like conditions (5% instead of 21% O_2), the decrease in oxygen led to significant downregulation of all Hbps, indicating that these proteins might not be of major importance in the intraerythrocytic niche. Alterations of pH and free iron concentrations did not have significant effects on *hbp* expression (25).

Several transcription factors were found to exhibit differential expression in response to the environmental cues known to influence *hbp* transcription and are hence obvious candidates for being involved in their regulation (26). One of these, Irr, reacted particularly strongly (to temperature change) and was found to bind a peculiar promoter element (the H box [for *hbp* family box]) that is conserved among *Bartonella hbp* genes and several other virulence factors (autotransporters and OMP43). Because expression of Irr seemed to antagonize HbpC transcription, Irr was suggested to be a repressor of HbpC expression. Consistently, Irr overexpression yielded a bloodstream-like expression pattern of *hbp* genes and generally seemed to amplify the effects of temperature (26). Battisti et al. further reported a certain influence of the major virulence regulator BatR, which was confirmed in a subsequent study

with *B. henselae* (347). Although this second study indeed reproduced the subgroups as identified in *B. quintana* when analyzing bacterial gene expression using the *B. henselae* Houston-1 *in vitro* infection model, HbpB and HbpC were upregulated in the course of infection, while HbpA and HbpD were downregulated (*B. henselae* lacks an apparent ortholog of HbpE) (347). Such a regulatory pattern seems counterintuitive when comparing it to the transcriptional data for the closely related *B. quintana* and indicates that *hbp* expression (and function) may be more complex than our current understanding.

Roles for the Hbps of the second subgroup in mammal host infection are strongly supported by phenotypic data (see above). Interestingly, the proteins of this subgroup seem to be structurally close, since an antibody raised against HbpA of *B. quintana* cross-reacted with HbpD and HbpE of the same species. The significance of the environmental stimuli simulated *in vitro* is confirmed by the finding that *B. quintana* infecting a rhesus macaque reproduced the "mammal-like" expression pattern (25). Consequently, those Hbps of the first subgroup very likely function predominantly in context of the arthropod vector. Although a contribution of HbpC seems very likely (it is more than 100-fold upregulated at 30°C compared to 37°C), the role of HbpB remains unclear. It was generally expressed at lower levels, reacted more weakly (hemin) or not at all (temperature) to the stimuli that were potent for HbpC, and has been reported to lack hemin binding properties (25). Furthermore, an insertion of approximately 500 base pairs makes HbpB larger than the other Hbps. This insertion is predicted to partition extracellularly and features tandem repeats as well as an abnormally high GC content, indicating that it may originate from lateral gene transfer (296). However, HbpB was the only hemin binding protein of *B. tribocorum* that was found to be essential for establishing bacteremia in the STM screen (374).

Potential antigenicity is an important feature particularly of surface-exposed proteins of bacterial pathogens and was assessed for the Hbps in several studies. Interestingly, HbpA of *B. henselae* seems to be immunogenic from live bacteria in rabbits (107), but firm evidence suggests the absence of an antibody response against any Hbp in cats seropositive for this species (84). Importantly, the latter finding was strongly supported by an independent study that tested a protein microarray of almost all predicted open reading frames (ORFs) of *B. henselae* against a large set of cat sera and failed to detect antibodies against any hemin binding protein (432). These results indicate that the absence of Hbp antigenicity may be part of *Bartonella* reservoir host adaptation or that events/strategies exclusive for the reservoir host could interfere with immune detection of the Hbps (e.g., downregulation of the humoral immune response). However, the hemin binding proteins of *B. quintana* were found to be immunogenic in human infections (43), but this species seems to be not yet fully adapted to its reservoir host (see above).

ABC systems. ATP binding cassette (ABC) systems are a superfamily of protein machineries that use ATP hydrolysis to energize the transmembrane passage of various substrates and were hence also called "traffic ATPases" (excellently reviewed in references 110 and 111). They share an architecture composed of two integral inner membrane domains and two periplasmic domains that typically constitute four independent polypeptide chains in ABC importers but are usually fused into one protein in exporters (111). Since ABC systems themselves cover translocation over only the inner membrane, transport across the outer membrane can be accomplished in different ways depending on the substrate. Importers usually rely on unspecific or specialized porins for substrates of small or moderate size, while very large or rare cargo is bound by high-affinity outer membrane receptors that also enable transport over the outer membrane. These particular receptors are typically powered by the TonB machinery, hence using the proton motive force stored over the inner membrane (314, 341). ABC exporters characteristically assemble a complex including the actual ABC transporter (paradigmatic *E. coli* HlyB) with a periplasmic membrane fusion protein (*E. coli* HlyD) and the outer membrane channel TolC, thus allowing one-step export in a mechanism referred to as type I secretion (reviewed in reference 186).

Several ABC import systems have been revealed to be essential for *Bartonella* virulence in the two STM screens. Not surprisingly, these comprise the uptake system for heme (HutABC/HmuV) and two iron uptake systems (FatBCD/CeuD and Sit/YfeABCD) whose role in the lifestyle of *Bartonella* had already been proposed before (25). The HutABC/HmuV system has been explored in more detail in *B. quintana* and is genetically associated with genes for a putative heme degradation enzyme (*hemS* [also known as *hmuS*]) and the *tonB* gene of the bartonellae (331).

Many other hits in the STM screens revealed that several ABC proteins involved in amino acid import are essential for virulence (374, 427), thus confirming the key role of amino acids as a carbon source for the bartonellae (85). In particular, the branched-chain amino acid import system (*liv* [for leucine-isoleucine-valine]) was required for establishing blood-stage infection in both screens. It is interesting in this context that other *Rhizobiales* drop biosynthesis of these particular amino acids during growth in bacteroids and then completely depend on their supply from the host plant ("symbiotic auxotrophy") (342, 343). However, one enzyme of the branched-chain amino acid synthesis pathway was also essential for virulence in *B. birtlesii* (427), indicating that not only import but also biosynthesis of these amino acids is necessary at one point of the infection. Additionally, several other ABC importers were also hits in the STM screens, for example, the *ugp* glycerol-3-phosphate importer in the *B. tribocorum* screen (374).

In contrast, no apparent ABC exporters were essential for *Bartonella* virulence, but exporters of all kinds are inherently prone to extracellular complementation which could render them difficult to detect in an STM screen. Thus, some ABC export systems of *Bartonella* may somehow participate in pathogenicity, although experimental evidence is lacking (see "Other virulence factors" below). However, it is pointless to speculate about the contribution of particular systems as long as their substrates have not been identified. Type I secretion systems (T1SS) in other pathogens are known to secrete various virulence factors, such as adhesins (156) or surface layer proteins (416).

In addition to import or export functions, a third subgroup of ABC cassette proteins has been implicated in other contexts, e.g., UvrA as a prominent component of the DNA excision repair machinery (160). Similarly, the ChvD ABC protein is known to be involved in the regulation of virulence gene expression in *A. tumefaciens* (263) and was found to be essential for pathogenicity in the *B. tribocorum* STM screen (374), indicating that the *Bartonella* orthologs also contribute to the infection process.

Apart from ABC systems, other transporters were also revealed to be critical for *Bartonella* virulence in the STM screens (374,

427). One of them, the *pha* multicomponent K^+/H^+ antiporter, was shown to be crucial for pH adaptation and a host-associated lifestyle in other *Rhizobiales* (345).

Other virulence factors. Many studies have discovered other virulence factors of *Bartonella* that cannot be reasonably sorted into one of the categories used in this review or for which substantial knowledge on their function has not yet been determined.

The BatR/BatS two-component system was shown to be a master regulator of *Bartonella* virulence that guides the expression of a large regulon comprising various virulence genes and is induced at the slightly basic pH of human blood (347). Remarkably, a huge set of orthologous systems play key roles in the host interaction of other *Rhizobiales* (example in reference 28), and it is apparent that this vertically inherited transcriptional controller has assimilated horizontally acquired genes such as those coding for the VirB/D4 machinery into its regulon in *Bartonella*. Like the BatR/BatS system, other transcriptional regulators have been hit in the STM screens and may thus participate in coordinating the expression of the huge arsenal of *Bartonella* virulence factors. One of those, RosR (374), is well known to be essential for productive host interaction in other *Rhizobiales* such as *Sinorhizobium* (207).

OMP43 and OMP89, two outer membrane proteins of *Bartonella*, have been identified as fibronectin binders in addition to trimeric autotransporter adhesins and HbpA (108). The surface display of fibronectin binding proteins is a common theme among the infection strategies of many bacterial pathogens (reviewed in reference 175) and has been linked to endothelial invasion and inflammation, for example, in infective endocarditis (346) as a well-known complication of *Bartonella* infections. OMP43 of *Bartonella* is a porin-like protein homologous to OMP2b of *Brucella* (which is known to be a potent inhibitor of apoptosis [248]) and further exhibits considerable sequence similarity to the RopA protein of *Rhizobium leguminosarum*, whose expression is strongly repressed in bacteroids (65, 125). In addition to fibronectin binding, OMP43 was shown to bind HUVECs and thus was proposed to serve as a major adhesin during *Bartonella* infection (65, 162). The promoter of the *omp43* gene contains an H box that is indicative of transcriptional control by Irr (26), and a study of *B. henselae* found that OMP43 expression was downregulated during infection of endothelial cells *in vitro* (347). OMP89 is the *Bartonella* homolog of BamA/YaeT, the major component of the Gram-negative outer membrane protein assembly/biogenesis machinery (reviewed in reference 231). No further evidence beyond its property to bind fibronectin would indicate a direct role of this protein in *Bartonella* pathogenesis. Consistent with their localization on the cell surface, both OMP43 and OMP89 are highly immunogenic in infections with *Bartonella* (43, 84).

Amazingly, it is apparent that the bartonellae encode the full machinery required for synthesis and secretion of cyclic β-(1,2)-glucans, i.e., the respective synthetase (ChvB in *Agrobacterium tumefaciens* [79], BH00920 in *B. henselae*) and the dedicated ABC exporter (ChvA in *A. tumefaciens* [70], BH10210 in *B. henselae*) (6, 34). Cyclic β-(1,2)-glucans are circular oligosaccharides known to enforce the host interaction of both symbiotic and pathogenic *Rhizobiaceae* (comprehensively reviewed in reference 48). In *Brucella*, another genus of zoonotic pathogens within this taxon, cyclic β-(1,2)-glucans contribute to bacterial surface integrity and are essential to prevent lysosome fusion of the *Brucella*-containing vacuoles by somehow manipulating lipid rafts in host cells (14, 58). Despite the function of *Brucella* cyclic β-(1,2)-glucans in subverting defenses of a vertebrate host, the *B. abortus* cyclic β-(1,2)-glucan synthetase was sufficient to complement accordant mutants in *Rhizobium meliloti* as well as *A. tumefaciens* and restored the associated phenotypes (196), confirming that cyclic β-(1,2)-glucans are highly conserved among *Rhizobiales*. Although the presence of cyclic β-(1,2)-glucans has not been specifically examined for *Bartonella*, the conservation of the dedicated machinery and the abundance of these compounds as rhizobial host-interacting factors make it very likely that (i) *Bartonella* synthesizes cyclic β-(1,2)-glucans and (ii) they somehow play a role in *Bartonella*-host interaction. No gene related to cyclic β-(1,2)-glucans was found to be essential for virulence in the *Bartonella* STM screens (374, 427), but extracellular complementation of the secreted compound may have impeded detection. Consistently, none of the various STM screens in *Brucella* brought up any gene linked to cyclic β-(1,2)-glucans (except for one intergenic hit more than 200 base pairs downstream of an associated succinyltransferase gene) (144, 188, 255, 256), although they are known to be essential for intracellular survival of this pathogen (14).

Like *Brucella*, the bartonellae are known to evade the endocytic pathway and to establish a perinuclear niche inside their host cells (see above). Work with *B. henselae* showed that the bacterial factor(s) orchestrating this process is independent of both BadA and the VirB/D4 T4SS (246). Instead, a small-scale evaluation of transposon mutants revealed three peculiar proteins and HbpD as essential for this process. Although the contribution of these factors is not understood on a mechanistic level, their role in phagosomal escape could be confirmed by complementation analysis.

CONCLUDING REMARKS

It is striking that the leading symptoms of Carrion's disease, such as immune-mediated hemolytic anemia or pathological angiogenesis, are generally absent in reservoir host infections by the modern species but may occasionally arise in infections particularly of immunocompromised individuals and/or in incidental hosts. We therefore conclude that the bacterial factors responsible for these symptoms may be conserved over the whole genus *Bartonella*, especially when considering the virtual absence of large disparities in the arsenal of known virulence factors and the overall congruent course of infection. However, the activities of these factors are apparently tightly regulated and balanced with opposing activities and host responses in the modern species, thus allowing them to establish a controlled, silent course of infection that avoids elicitation of an immune response and favors vector transmission. Correspondingly, quiescent infections with persistent, asymptomatic bacteremia are prevalent in a certain proportion of individuals colonized by *B. bacilliformis*, confirming that the morbidity associated with Carrion's disease is not inherent to the infection cycle of this species.

We are convinced that the acquisition of type IV secretion systems in ancestors of the modern bartonellae, thanks to the highly modular nature of their virulence functions, opened up the opportunity to evolve a versatile cocktail of both cooperating and antagonistic activities for particularly fine-tuned host interaction. Decreased morbidity in combination with evolutionary versatility and at least partial redundancy of virulence functions may then have promoted host adaptability and thus the evolutionary success of the modern bartonellae. We find our hypothesis supported by the fact that the two adaptive radiations in lineages 3 and 4 were triggered only after the evolution of a diverse set of VirB/D4 effec-

tor proteins and the duplication and diversification of extracellular parts of the Trw T4SS.

The comprehensive listing and discussion of current knowledge on the molecular pathogenesis of *Bartonella* has demonstrated that the fragmentary and isolated nature of most knowledge on these remarkable pathogens is a major obstacle to drawing a coherent model of what underlies the diseases we observe in human patients. We thus recommend that future research should aim at combining our knowledge from cellular, clinical, microbiological, and veterinary research as well as the various models and strains used in the field. It seems particularly important to link the data obtained *in vitro* from infections with the Houston-1 and Marseille strains of *B. henselae*, but also with *B. quintana*, since these species are the most common cause of human *Bartonella* infections around the world and may serve as useful models for the other modern species. Furthermore, a comparison to the knowledge available on infections with *B. bacilliformis* seems desirable, especially in order to reveal the molecular mechanisms underlying its human host restriction, which may help to understand the zoonotic potential of *Bartonella*.

ACKNOWLEDGMENTS

We thank Maxime Quebatte for critically reading the manuscript.

This work was supported by grant 3100-061777 from the Swiss National Science Foundation (to C.D.) and grant 51RT 0_126008 (InfectX) in the frame of the SystemsX.ch Swiss Initiative for Systems Biology (to C.D.). A.H. is a fellow of the Werner Siemens Foundation.

We declare no conflicting interests relevant to the study.

REFERENCES

1. Abbott RC, et al. 1997. Experimental and natural infection with *Bartonella henselae* in domestic cats. Comp. Immunol. Microbiol. Infect. Dis. 20:41–51.
2. Abramson T, Kedem H, Relman DA. 2008. Modulation of the NF-kappaB pathway by *Bordetella pertussis* filamentous hemagglutinin. PLoS One 3:e3825.
3. Ades EW, et al. 1992. HMEC-1: establishment of an immortalized human microvascular endothelial cell line. J. Invest. Dermatol. 99:683–690.
4. Alexander B. 1995. A review of bartonellosis in Ecuador and Colombia. Am. J. Trop. Med. Hyg. 52:354–359.
5. Allison MJ, Pezzia A, Gerszten E, Mendoza D. 1974. A case of Carrion's disease associated with human sacrifice from the Huari culture of Southern Peru. Am. J. Phys Anthropol. 41:295–300.
6. Alsmark CM, et al. 2004. The louse-borne human pathogen *Bartonella quintana* is a genomic derivative of the zoonotic agent *Bartonella henselae*. Proc. Natl. Acad. Sci. U. S. A. 101:9716–9721.
7. Alvarez-Martinez CE, Christie PJ. 2009. Biological diversity of prokaryotic type IV secretion systems. Microbiol. Mol. Biol. Rev. 73:775–808.
8. Aly KA, Baron C. 2007. The VirB5 protein localizes to the T-pilus tips in *Agrobacterium tumefaciens*. Microbiology 153:3766–3775.
9. Amano A, Takeuchi H, Furuta N. 2010. Outer membrane vesicles function as offensive weapons in host-parasite interactions. Microbes Infect. 12:791–798.
10. Andersen-Nissen E, et al. 2005. Evasion of Toll-like receptor 5 by flagellated bacteria. Proc. Natl. Acad. Sci. U. S. A. 102:9247–9252.
11. Anderson B, Goldsmith C, Johnson A, Padmalayam I, Baumstark B. 1994. Bacteriophage-like particle of *Rochalimaea henselae*. Mol. Microbiol. 13:67–73.
12. Anderson B, et al. 1997. Analysis of 36-kilodalton protein (PapA) associated with the bacteriophage particle of *Bartonella henselae*. DNA Cell Biol. 16:1223–1229.
13. Andersson SG, Dehio C. 2000. *Rickettsia prowazekii* and *Bartonella henselae*: differences in the intracellular life styles revisited. Int. J. Med. Microbiol. 290:135–141.
14. Arellano-Reynoso B, et al. 2005. Cyclic beta-1,2-glucan is a *Brucella* virulence factor required for intracellular survival. Nat. Immunol. 6:618–625.
15. Arruda MA, Rossi AG, de Freitas MS, Barja-Fidalgo C, Graca-Souza AV. 2004. Heme inhibits human neutrophil apoptosis: involvement of phosphoinositide 3-kinase, MAPK, and NF-kappaB. J. Immunol. 173:2023–2030.
16. Arvand M, Ignatius R, Regnath T, Hahn H, Mielke ME. 2001. *Bartonella henselae*-specific cell-mediated immune responses display a predominantly Th1 phenotype in experimentally infected C57BL/6 mice. Infect. Immun. 69:6427–6433.
17. Avraamides CJ, Garmy-Susini B, Varner JA. 2008. Integrins in angiogenesis and lymphangiogenesis. Nat. Rev. Cancer 8:604–617.
18. Babic A, Lindner AB, Vulic M, Stewart EJ, Radman M. 2008. Direct visualization of horizontal gene transfer. Science 319:1533–1536.
19. Backert S, Selbach M. 2008. Role of type IV secretion in *Helicobacter pylori* pathogenesis. Cell. Microbiol. 10:1573–1581.
20. Backert S, Selbach M. 2005. Tyrosine-phosphorylated bacterial effector proteins: the enemies within. Trends Microbiol. 13:476–484.
21. Bai Y, Kosoy MY, Ray C, Brinkerhoff RJ, Collinge SK. 2008. Temporal and spatial patterns of *Bartonella* infection in black-tailed prairie dogs (*Cynomys ludovicianus*). Microb. Ecol. 56:373–382.
22. Bandara AB, Sriranganathan N, Schurig GG, Boyle SM. 2005. Carboxyl-terminal protease regulates *Brucella suis* morphology in culture and persistence in macrophages and mice. J. Bacteriol. 187:5767–5775.
23. Barbian KD, Minnick MF. 2000. A bacteriophage-like particle from *Bartonella bacilliformis*. Microbiology 146:599–609.
24. Batterman HJ, Peek JA, Loutit JS, Falkow S, Tompkins LS. 1995. *Bartonella henselae* and *Bartonella quintana* adherence to and entry into cultured human epithelial cells. Infect. Immun. 63:4553–4556.
25. Battisti JM, Sappington KN, Smitherman LS, Parrow NL, Minnick MF. 2006. Environmental signals generate a differential and coordinated expression of the heme receptor gene family of *Bartonella quintana*. Infect. Immun. 74:3251–3261.
26. Battisti JM, et al. 2007. Transcriptional regulation of the heme binding protein gene family of *Bartonella quintana* is accomplished by a novel promoter element and iron response regulator. Infect. Immun. 75:4373–4385.
27. Baumler AJ, Kusters JG, Stojiljkovic I, Heffron F. 1994. *Salmonella typhimurium* loci involved in survival within macrophages. Infect. Immun. 62:1623–1630.
28. Belanger L, Dimmick KA, Fleming JS, Charles TC. 2009. Null mutations in *Sinorhizobium meliloti* exoS and chvI demonstrate the importance of this two-component regulatory system for symbiosis. Mol. Microbiol. 74:1223–1237.
29. Beldomenico PM, et al. 2005. Environmental factors associated with *Bartonella vinsonii subsp. berkhoffii* seropositivity in free-ranging coyotes from northern California. Vector Borne Zoonotic Dis. 5:110–119.
30. Benjamin LE, Golijanin D, Itin A, Pode D, Keshet E. 1999. Selective ablation of immature blood vessels in established human tumors follows vascular endothelial growth factor withdrawal. J. Clin. Invest. 103:159–165.
31. Benson LA, Kar S, McLaughlin G, Ihler GM. 1986. Entry of *Bartonella bacilliformis* into erythrocytes. Infect. Immun. 54:347–353.
32. Berglund EC, et al. 2010. Genome dynamics of *Bartonella grahamii* in micro-populations of woodland rodents. BMC Genomics 11:152.
33. Berglund EC, et al. 2010. Rapid diversification by recombination in *Bartonella grahamii* from wild rodents in Asia contrasts with low levels of genomic divergence in Northern Europe and America. Mol. Ecol. 19:2241–2255.
34. Berglund EC, et al. 2009. Run-off replication of host-adaptability genes is associated with gene transfer agents in the genome of mouse-infecting *Bartonella grahamii*. PLoS Genet. 5:e1000546.
35. Bergonzelli GE, et al. 2006. GroEL of *Lactobacillus johnsonii* La1 (NCC 533) is cell surface associated: potential role in interactions with the host and the gastric pathogen *Helicobacter pylori*. Infect. Immun. 74:425–434.
36. Bermond D, et al. 2002. *Bartonella bovis* Bermond *et al.* sp. nov. and *Bartonella capreoli* sp. nov., isolated from European ruminants. Int. J. Syst. Evol. Microbiol. 52:383–390.
37. Berrich M, et al. 2011. Differential effects of *Bartonella henselae* on human and feline macro- and micro-vascular endothelial cells. PLoS One 6:e20204.
38. Bessman MJ, et al. 2001. The gene ygdP, associated with the invasiveness of *Escherichia coli* K1, designates a Nudix hydrolase, Orf176, active on

adenosine (5′)-pentaphospho-(5′)-adenosine (Ap5A). J. Biol. Chem. 276:37834–37838.
39. Bhutto AM, Nonaka S, Hashiguchi Y, Gomez EA. 1994. Histopathological and electron microscopical features of skin lesions in a patient with bartonellosis (verruga peruana). J. Dermatol. 21:178–184.
40. Billeter SA, et al. 2009. Infection and replication of *Bartonella* species within a tick cell line. Exp. Appl. Acarol. 49:193–208.
41. Blanc L, et al. 2010. Control of erythrocyte membrane-skeletal cohesion by the spectrin-membrane linkage. Biochemistry 49:4516–4523.
42. Bogdan C, Rollinghoff M, Diefenbach A. 2000. Reactive oxygen and reactive nitrogen intermediates in innate and specific immunity. Curr. Opin. Immunol. 12:64–76.
43. Boonjakuakul JK, et al. 2007. Proteomic and immunoblot analyses of *Bartonella quintana* total membrane proteins identify antigens recognized by sera from infected patients. Infect. Immun. 75:2548–2561.
44. Bouchouicha R, et al. 2009. Molecular epidemiology of feline and human *Bartonella henselae* isolates. Emerg. Infect. Dis. 15:813–816.
45. Boulouis HJ, et al. 2001. Kinetics of *Bartonella birtlesii* infection in experimentally infected mice and pathogenic effect on reproductive functions. Infect. Immun. 69:5313–5317.
46. Boulouis HJ, Chang CC, Henn JB, Kasten RW, Chomel BB. 2005. Factors associated with the rapid emergence of zoonotic *Bartonella* infections. Vet. Res. 36:383–410.
47. Bowers TJ, Sweger D, Jue D, Anderson B. 1998. Isolation, sequencing and expression of the gene encoding a major protein from the bacteriophage associated with *Bartonella henselae*. Gene 206:49–52.
48. Breedveld MW, Miller KJ. 1994. Cyclic beta-glucans of members of the family *Rhizobiaceae*. Microbiol. Rev. 58:145–161.
49. Breitschwerdt EB, Atkins CE, Brown TT, Kordick DL, Snyder PS. 1999. *Bartonella vinsonii* subsp. *berkhoffii* and related members of the alpha subdivision of the Proteobacteria in dogs with cardiac arrhythmias, endocarditis, or myocarditis. J. Clin. Microbiol. 37:3618–3626.
50. Breitschwerdt EB, et al. 2004. Clinicopathological abnormalities and treatment response in 24 dogs seroreactive to *Bartonella vinsonii* (*berkhoffii*) antigens. J. Am. Anim. Hosp. Assoc. 40:92–101.
51. Breitschwerdt EB, Kordick DL. 2000. *Bartonella* infection in animals: carriership, reservoir potential, pathogenicity, and zoonotic potential for human infection. Clin. Microbiol. Rev. 13:428–438.
52. Breitschwerdt EB, et al. 1995. Endocarditis in a dog due to infection with a novel *Bartonella* subspecies. J. Clin. Microbiol. 33:154–160.
53. Breitschwerdt EB, et al. 2007. *Bartonella* species in blood of immunocompetent persons with animal and arthropod contact. Emerg. Infect. Dis. 13:938–941.
54. Breitschwerdt EB, et al. 2010. *Bartonella vinsonii subsp. berkhoffii* and *Bartonella henselae* bacteremia in a father and daughter with neurological disease. Parasit. Vectors 3:29.
55. Breitschwerdt EB, Maggi RG, Nicholson WL, Cherry NA, Woods CW. 2008. *Bartonella* sp. bacteremia in patients with neurological and neurocognitive dysfunction. J. Clin. Microbiol. 46:2856–2861.
56. Breitschwerdt EB, et al. 2010. PCR amplification of *Bartonella koehlerae* from human blood and enrichment blood cultures. Parasit. Vectors 3:76.
57. Breitschwerdt EB, Maggi RG, Sigmon B, Nicholson WL. 2007. Isolation of *Bartonella quintana* from a woman and a cat following putative bite transmission. J. Clin. Microbiol. 45:270–272.
58. Briones G, et al. 2001. *Brucella abortus* cyclic beta-1,2-glucan mutants have reduced virulence in mice and are defective in intracellular replication in HeLa cells. Infect. Immun. 69:4528–4535.
59. Brouqui P, Lascola B, Roux V, Raoult D. 1999. Chronic *Bartonella quintana* bacteremia in homeless patients. N. Engl. J. Med. 340:184–189.
60. Brouqui P, Raoult D. 1996. *Bartonella quintana* invades and multiplies within endothelial cells *in vitro* and *in vivo* and forms intracellular blebs. Res. Microbiol. 147:719–731.
61. Buchmann AU, Kempf VA, Kershaw O, Gruber AD. 2010. Peliosis hepatis in cats is not associated with *Bartonella henselae* infections. Vet. Pathol. 47:163–166.
62. Buchmann AU, Kershaw O, Kempf VA, Gruber AD. 2010. Does a feline leukemia virus infection pave the way for *Bartonella henselae* infection in cats? J. Clin. Microbiol. 48:3295–3300.
63. Buckles EL, McGinnis Hill E. 2000. Interaction of *Bartonella bacilliformis* with human erythrocyte membrane proteins. Microb. Pathog. 29:165–174.
64. Burgess AW, Anderson BE. 1998. Outer membrane proteins of *Bartonella henselae* and their interaction with human endothelial cells. Microb. Pathog. 25:157–164.
65. Burgess AW, Paquet JY, Letesson JJ, Anderson BE. 2000. Isolation, sequencing and expression of *Bartonella henselae* omp43 and predicted membrane topology of the deduced protein. Microb. Pathog. 29:73–80.
66. Byam W, Lloyd L. 1920. Trench fever: its epidemiology and endemiology. Proc. R Soc. Med. 13:1–27.
67. Caceres-Rios H, et al. 1995. Verruga peruana: an infectious endemic angiomatosis. Crit. Rev. Oncog. 6:47–56.
68. Caceres AG, Galati EA, Le Pont F, Velasquez C. 1997. Possible role of *Lutzomyia maranonensis* and *Lutzomyia robusta* (Diptera: Psychodidae) as vectors of human bartonellosis in three provinces of region nor Oriental del Maranon, Peru. Rev. Inst. Med. Trop. Sao Paulo 39:51–52.
69. Callison JA, Battisti JM, Sappington KN, Smitherman LS, Minnick MF. 2005. Characterization and expression analysis of the groESL operon of *Bartonella bacilliformis*. Gene 359:53–62.
70. Cangelosi GA, et al. 1989. Role for [corrected] *Agrobacterium tumefaciens* ChvA protein in export of beta-1,2-glucan. J. Bacteriol. 171:1609–1615.
71. Capecchi B, et al. 2005. *Neisseria meningitidis* NadA is a new invasin which promotes bacterial adhesion to and penetration into human epithelial cells. Mol. Microbiol. 55:687–698.
72. Capo C, Amirayan-Chevillard N, Brouqui P, Raoult D, Mege JL. 2003. *Bartonella quintana* bacteremia and overproduction of interleukin-10: model of bacterial persistence in homeless people. J. Infect. Dis. 187:837–844.
73. Carithers HA, Margileth AM. 1991. Cat-scratch disease. Acute encephalopathy and other neurologic manifestations. Am. J. Dis. Child. 145:98–101.
74. Caro-Hernandez P, et al. 2007. Role of the Omp25/Omp31 family in outer membrane properties and virulence of *Brucella ovis*. Infect. Immun. 75:4050–4061.
75. Carroll JA, Coleman SA, Smitherman LS, Minnick MF. 2000. Hemin-binding surface protein from *Bartonella quintana*. Infect. Immun. 68:6750–6757.
76. Cartwright JL, Britton P, Minnick MF, McLennan AG. 1999. The IalA invasion gene of *Bartonella bacilliformis* encodes a (de)nucleoside polyphosphate hydrolase of the MutT motif family and has homologs in other invasive bacteria. Biochem. Biophys. Res. Commun. 256:474–479.
77. Cascales E, Christie PJ. 2003. The versatile bacterial type IV secretion systems. Nat. Rev. Microbiol. 1:137–149.
78. Castle KT, et al. 2004. Prevalence and diversity of *Bartonella* in rodents of northern Thailand: a comparison with *Bartonella* in rodents from southern China. Am. J. Trop. Med. Hyg. 70:429–433.
79. Castro OA, Zorreguieta A, Ielmini V, Vega G, Ielpi L. 1996. Cyclic beta-(1,2)-glucan synthesis in *Rhizobiaceae*: roles of the 319-kilodalton protein intermediate. J. Bacteriol. 178:6043–6048.
80. Cerimele F, et al. 2003. Infectious angiogenesis: *Bartonella bacilliformis* infection results in endothelial production of angiopoetin-2 and epidermal production of vascular endothelial growth factor. Am. J. Pathol. 163:1321–1327.
81. Chamberlin J, et al. 2002. Epidemiology of endemic *Bartonella bacilliformis*: a prospective cohort study in a Peruvian mountain valley community. J. Infect. Dis. 186:983–990.
82. Chang CC, et al. 2011. A comparative study of the interaction of *Bartonella henselae* strains with human endothelial cells. Vet. Microbiol. 149:147–156.
83. Chang CC, et al. 2002. Molecular epidemiology of *Bartonella henselae* infection in human immunodeficiency virus-infected patients and their cat contacts, using pulsed-field gel electrophoresis and genotyping. J. Infect. Dis. 186:1733–1739.
84. Chenoweth MR, Greene CE, Krause DC, Gherardini FC. 2004. Predominant outer membrane antigens of *Bartonella henselae*. Infect. Immun. 72:3097–3105.
85. Chenoweth MR, Somerville GA, Krause DC, O'Reilly KL, Gherardini FC. 2004. Growth characteristics of *Bartonella henselae* in a novel liquid medium: primary isolation, growth-phase-dependent phage induction, and metabolic studies. Appl. Environ. Microbiol. 70:656–663.
86. Chian CA, Arrese JE, Pierard GE. 2002. Skin manifestations of *Bartonella* infections. Int. J. Dermatol. 41:461–466.
87. Chinga-Alayo E, Huarcaya E, Nasarre C, del Aguila R, Llanos-Cuentas A. 2004. The influence of climate on the epidemiology of bartonellosis in Ancash, Peru. Trans. R. Soc. Trop. Med. Hyg. 98:116–124.

88. Chomel BB, et al. 1995. *Bartonella henselae* prevalence in domestic cats in California: risk factors and association between bacteremia and antibody titers. J. Clin. Microbiol. 33:2445–2450.
89. Chomel BB, et al. 2009. Ecological fitness and strategies of adaptation of *Bartonella* species to their hosts and vectors. Vet. Res. 40:29.
90. Chomel BB, Boulouis HJ, Maruyama S, Breitschwerdt EB. 2006. *Bartonella* spp. in pets and effect on human health. Emerg. Infect. Dis. 12:389–394.
91. Chomel BB, et al. 2002. Prevalence of *Bartonella* infection in domestic cats in Denmark. Vet. Res. 33:205–213.
92. Chomel BB, et al. 2009. Dogs are more permissive than cats or guinea pigs to experimental infection with a human isolate of *Bartonella rochalimae*. Vet. Res. 40:27.
93. Chomel BB, et al. 1996. Experimental transmission of *Bartonella henselae* by the cat flea. J. Clin. Microbiol. 34:1952–1956.
94. Chomel BB, et al. 2009. *Bartonella* endocarditis: a pathology shared by animal reservoirs and patients. Ann. N. Y. Acad. Sci. 1166:120–126.
95. Christie PJ, Atmakuri K, Krishnamoorthy V, Jakubowski S, Cascales E. 2005. Biogenesis, architecture, and function of bacterial type IV secretion systems. Annu. Rev. Microbiol. 59:451–485.
96. Clantin B, et al. 2007. Structure of the membrane protein FhaC: a member of the Omp85-TpsB transporter superfamily. Science 317: 957–961.
97. Cockerell CJ, LeBoit PE. 1990. Bacillary angiomatosis: a newly characterized, pseudoneoplastic, infectious, cutaneous vascular disorder. J. Am. Acad. Dermatol. 22:501–512.
98. Cockwill KR, Taylor SM, Philibert HM, Breitschwerdt EB, Maggi RG. 2007. *Bartonella vinsonii subsp. berkhoffii* endocarditis in a dog from Saskatchewan. Can. Vet. J. 48:839–844.
99. Coleman SA, Minnick MF. 2003. Differential expression of the invasion-associated locus B (ialB) gene of *Bartonella bacilliformis* in response to environmental cues. Microb. Pathog. 34:179–186.
100. Coleman SA, Minnick MF. 2001. Establishing a direct role for the *Bartonella bacilliformis* invasion-associated locus B (IalB) protein in human erythrocyte parasitism. Infect. Immun. 69:4373–4381.
101. Conyers GB, Bessman MJ. 1999. The gene, ialA, associated with the invasion of human erythrocytes by *Bartonella bacilliformis*, designates a nudix hydrolase active on dinucleoside 5′-polyphosphates. J. Biol. Chem. 274:1203–1206.
102. Cotter SE, Surana NK, Grass S, St Geme JW, III. 2006. Trimeric autotransporters require trimerization of the passenger domain for stability and adhesive activity. J. Bacteriol. 188:5400–5407.
103. Cotter SE, Surana NK, St Geme JW, III. 2005. Trimeric autotransporters: a distinct subfamily of autotransporter proteins. Trends Microbiol. 13:199–205.
104. Couper KN, Blount DG, Riley EM. 2008. IL-10: the master regulator of immunity to infection. J. Immunol. 180:5771–5777.
105. Cross AS. 2008. What is a virulence factor? Crit. Care 12:196.
106. Cyktor JC, Turner J. 2011. Il-10 and immunity against prokaryotic and eukaryotic intracellular pathogens. Infect. Immun. 79:2964–2973.
107. Dabo SM, Confer AW, Anderson BE, Gupta S. 2006. *Bartonella henselae* Pap31, an extracellular matrix adhesin, binds the fibronectin repeat III13 module. Infect. Immun. 74:2513–2521.
108. Dabo SM, Confer AW, Saliki JT, Anderson BE. 2006. Binding of *Bartonella henselae* to extracellular molecules: identification of potential adhesins. Microb. Pathog. 41:10–20.
109. Dautin N, Bernstein HD. 2007. Protein secretion in gram-negative bacteria via the autotransporter pathway. Annu. Rev. Microbiol. 61: 89–112.
110. Davidson AL, Chen J. 2004. ATP-binding cassette transporters in bacteria. Annu. Rev. Biochem. 73:241–268.
111. Davidson AL, Dassa E, Orelle C, Chen J. 2008. Structure, function, and evolution of bacterial ATP-binding cassette systems. Microbiol. Mol. Biol. Rev. 72:317–364.
112. Deguercy A, Hommel M, Schrevel J. 1990. Purification and characterization of 37-kilodalton proteases from *Plasmodium falciparum* and *Plasmodium berghei* which cleave erythrocyte cytoskeletal components. Mol. Biochem. Parasitol. 38:233–244.
113. Dehio C. 2005. *Bartonella*-host-cell interactions and vascular tumour formation. Nat. Rev. Microbiol. 3:621–631.
114. Dehio C. 2001. *Bartonella* interactions with endothelial cells and erythrocytes. Trends Microbiol. 9:279–285.
115. Dehio C. 2008. Infection-associated type IV secretion systems of *Bartonella* and their diverse roles in host cell interaction. Cell Microbiol. 10: 1591–1598.
116. Dehio C. 2004. Molecular and cellular basis of *Bartonella* pathogenesis. Annu. Rev. Microbiol. 58:365–390.
117. Dehio C. 2003. Recent progress in understanding *Bartonella*-induced vascular proliferation. Curr. Opin. Microbiol. 6:61–65.
118. Dehio C, et al. 2001. *Bartonella schoenbuchii* sp. nov., isolated from the blood of wild roe deer. Int. J. Syst. Evol. Microbiol. 51:1557–1565.
119. Dehio C, Meyer M. 1997. Maintenance of broad-host-range incompatibility group P and group Q plasmids and transposition of Tn5 in *Bartonella henselae* following conjugal plasmid transfer from *Escherichia coli*. J. Bacteriol. 179:538–540.
120. Dehio C, Meyer M, Berger J, Schwarz H, Lanz C. 1997. Interaction of *Bartonella henselae* with endothelial cells results in bacterial aggregation on the cell surface and the subsequent engulfment and internalisation of the bacterial aggregate by a unique structure, the invasome. J. Cell Sci. 110:2141–2154.
121. Dehio C, Sander A. 1999. *Bartonella* as emerging pathogens. Trends Microbiol. 7:226–228.
122. Dehio C, Sauder U, Hiestand R. 2004. Isolation of *Bartonella schoenbuchensis* from *Lipoptena cervi*, a blood-sucking arthropod causing deer ked dermatitis. J. Clin. Microbiol. 42:5320–5323.
123. Dehio M, Knorre A, Lanz C, Dehio C. 1998. Construction of versatile high-level expression vectors for *Bartonella henselae* and the use of green fluorescent protein as a new expression marker. Gene 215:223–229.
124. Dehio M, Quebatte M, Foser S, Certa U. 2005. The transcriptional response of human endothelial cells to infection with *Bartonella henselae* is dominated by genes controlling innate immune responses, cell cycle, and vascular remodelling. Thromb. Haemost. 94:347–361.
125. de Maagd RA, Mulders IH, Canter Cremers HC, Lugtenberg BJ. 1992. Cloning, nucleotide sequencing, and expression in *Escherichia coli* of a *Rhizobium leguminosarum* gene encoding a symbiotically repressed outer membrane protein. J. Bacteriol. 174:214–221.
126. Derrick SC, Ihler GM. 2001. Deformin, a substance found in *Bartonella bacilliformis* culture supernatants, is a small, hydrophobic molecule with an affinity for albumin. Blood Cells Mol. Dis. 27:1013–1019.
127. Dulak J, Deshane J, Jozkowicz A, Agarwal A. 2008. Heme oxygenase-1 and carbon monoxide in vascular pathobiology: focus on angiogenesis. Circulation 117:231–241.
128. Edelstein PH, et al. 2005. *Legionella pneumophila* NudA is a Nudix hydrolase and virulence factor. Infect. Immun. 73:6567–6576.
129. Edgell CJ, McDonald CC, Graham JB. 1983. Permanent cell line expressing human factor VIII-related antigen established by hybridization. Proc. Natl. Acad. Sci. U. S. A. 80:3734–3737.
130. Eitel J, Dersch P. 2002. The YadA protein of *Yersinia pseudotuberculosis* mediates high-efficiency uptake into human cells under environmental conditions in which invasin is repressed. Infect. Immun. 70:4880–4891.
131. Ellis BA, et al. 1999. An outbreak of acute bartonellosis (Oroya fever) in the Urubamba region of Peru, 1998. Am. J. Trop. Med. Hyg. 61:344–349.
132. El Tahir Y, Skurnik M. 2001. YadA, the multifaceted *Yersinia* adhesin. Int. J. Med. Microbiol. 291:209–218.
133. Engel P, Dehio C. 2009. Genomics of host-restricted pathogens of the genus *Bartonella*. Genome Dyn. 6:158–169.
134. Engel P, et al. 2011. Parallel evolution of a type IV secretion system in radiating lineages of the host-restricted bacterial pathogen *Bartonella*. PLoS Genet. 7:e1001296.
135. Erdem AL, Avelino F, Xicohtencatl-Cortes J, Giron JA. 2007. Host protein binding and adhesive properties of H6 and H7 flagella of attaching and effacing *Escherichia coli*. J. Bacteriol. 189:7426–7435.
136. Eremeeva ME, et al. 2007. Bacteremia, fever, and splenomegaly caused by a newly recognized *Bartonella* species. N. Engl. J. Med. 356: 2381–2387.
137. Facer CA. 1983. Merozoites of *P. falciparum* require glycophorin for invasion into red cells. Bull. Soc. Pathol. Exot. Filiales. 76:463–469.
138. Figueiredo RT, et al. 2007. Characterization of heme as activator of Toll-like receptor 4. J. Biol. Chem. 282:20221–20229.
139. Finkelstein JL, Brown TP, O'Reilly KL, Wedincamp J, Jr, Foil LD. 2002. Studies on the growth of *Bartonella henselae* in the cat flea (Siphonaptera: Pulicidae). J. Med. Entomol 39:915–919.
140. Finlay BB, McFadden G. 2006. Anti-immunology: evasion of the host immune system by bacterial and viral pathogens. Cell 124:767–782.
141. Fiori PL, Rappelli P, Addis MF, Mannu F, Cappuccinelli P. 1997.

Contact-dependent disruption of the host cell membrane skeleton induced by *Trichomonas vaginalis*. Infect. Immun. 65:5142–5148.
142. Fisman DN. 2000. Hemophagocytic syndromes and infection. Emerg. Infect. Dis. 6:601–608.
143. Florin TA, Zaoutis TE, Zaoutis LB. 2008. Beyond cat scratch disease: widening spectrum of *Bartonella henselae* infection. Pediatrics 121: e1413–1425.
144. Foulongne V, Bourg G, Cazevieille C, Michaux-Charachon S, O'Callaghan D. 2000. Identification of *Brucella suis* genes affecting intracellular survival in an in vitro human macrophage infection model by signature-tagged transposon mutagenesis. Infect. Immun. 68: 1297–1303.
145. Fournier PE, Minnick MF, Lepidi H, Salvo E, Raoult D. 2001. Experimental model of human body louse infection using green fluorescent protein-expressing *Bartonella quintana*. Infect. Immun. 69:1876–1879.
146. Frank AC, Alsmark CM, Thollesson M, Andersson SG. 2005. Functional divergence and horizontal transfer of type IV secretion systems. Mol. Biol. Evol. 22:1325–1336.
147. Franzoso S, et al. 2008. Human monocytes/macrophages are a target of *Neisseria meningitidis* adhesin A (NadA). J. Leukoc. Biol. 83:1100–1110.
148. Fuhrmann O, et al. 2001. *Bartonella henselae* induces NF-kappaB-dependent upregulation of adhesion molecules in cultured human endothelial cells: possible role of outer membrane proteins as pathogenic factors. Infect. Immun. 69:5088–5097.
149. Galdiero M, de l'Ero GC, Marcatili A. 1997. Cytokine and adhesion molecule expression in human monocytes and endothelial cells stimulated with bacterial heat shock proteins. Infect. Immun. 65:699–707.
150. Garcia FU, Wojta J, Broadley KN, Davidson JM, Hoover RL. 1990. *Bartonella bacilliformis* stimulates endothelial cells *in vitro* and is angiogenic *in vivo*. Am. J. Pathol. 136:1125–1135.
151. Garcia FU, Wojta J, Hoover RL. 1992. Interactions between live *Bartonella bacilliformis* and endothelial cells. J. Infect. Dis. 165:1138–1141.
152. Garcia-Caceres U, Garcia FU. 1991. Bartonellosis. An immunodepressive disease and the life of Daniel Alcides Carrion. Am. J. Clin. Pathol. 95:S58–66.
153. Garduno RA, Chong A, Nasrallah GK, Allan DS. 2011. The *Legionella pneumophila* chaperonin—an unusual multifunctional protein in unusual locations. Front. Microbiol. 2:122.
154. Gaywee J, Radulovic S, Higgins JA, Azad AF. 2002. Transcriptional analysis of *Rickettsia prowazekii* invasion gene homolog (invA) during host cell infection. Infect. Immun. 70:6346–6354.
155. Gazineo JL, et al. 2001. Bacillary angiomatosis: description of 13 cases reported in five reference centers for AIDS treatment in Rio de Janeiro, Brazil. Rev. Inst. Med. Trop. Sao Paulo 43:1–6.
156. Gerlach RG, et al. 2007. *Salmonella* pathogenicity island 4 encodes a giant non-fimbrial adhesin and the cognate type 1 secretion system. Cell. Microbiol. 9:1834–1850.
157. Gilmore RD, Jr, Bellville TM, Sviat SL, Frace M. 2005. The *Bartonella vinsonii* subsp. *arupensis* immunodominant surface antigen BrpA gene, encoding a 382-kilodalton protein composed of repetitive sequences, is a member of a multigene family conserved among bartonella species. Infect. Immun. 73:3128–3136.
158. Goel VK, et al. 2003. Band 3 is a host receptor binding merozoite surface protein 1 during the *Plasmodium falciparum* invasion of erythrocytes. Proc. Natl. Acad. Sci. U. S. A. 100:5164–5169.
159. Goodman RA, Breitschwerdt EB. 2005. Clinicopathologic findings in dogs seroreactive to *Bartonella henselae* antigens. Am. J. Vet. Res. 66: 2060–2064.
160. Goosen N, Moolenaar GF. 2001. Role of ATP hydrolysis by UvrA and UvrB during nucleotide excision repair. Res. Microbiol. 152:401–409.
161. Greene CE, McDermott M, Jameson PH, Atkins CL, Marks AM. 1996. *Bartonella henselae* infection in cats: evaluation during primary infection, treatment, and rechallenge infection. J. Clin. Microbiol. 34:1682–1685.
162. Greub G, Raoult D. 2002. *Bartonella*: new explanations for old diseases. J. Med. Microbiol. 51:915–923.
163. Gudlavalleti SK, Forsberg LS. 2003. Structural characterization of the lipid A component of *Sinorhizobium* sp. NGR234 rough and smooth form lipopolysaccharide. Demonstration that the distal amide-linked acyloxyacyl residue containing the long chain fatty acid is conserved in *Rhizobium* and *Sinorhizobium* sp. J. Biol. Chem. 278:3957–3968.
164. Gupta RS. 1995. Evolution of the chaperonin families (Hsp60, Hsp10 and Tcp-1) of proteins and the origin of eukaryotic cells. Mol. Microbiol. 15:1–11.
165. Guptill L, et al. 1997. Experimental infection of young specific pathogen-free cats with *Bartonella henselae*. J. Infect. Dis. 176:206–216.
166. Guptill L, et al. 2004. Prevalence, risk factors, and genetic diversity of *Bartonella henselae* infections in pet cats in four regions of the United States. J. Clin. Microbiol. 42:652–659.
167. Gurfield AN, et al. 2001. Epidemiology of *Bartonella* infection in domestic cats in France. Vet. Microbiol. 80:185–198.
168. Ha EM, et al. 2009. Coordination of multiple dual oxidase-regulatory pathways in responses to commensal and infectious microbes in drosophila gut. Nat. Immunol. 10:949–957.
169. Ha EM, et al. 2005. An antioxidant system required for host protection against gut infection in *Drosophila*. Dev. Cell 8:125–132.
170. Halling SM, et al. 2005. Completion of the genome sequence of *Brucella abortus* and comparison to the highly similar genomes of *Brucella melitensis* and *Brucella suis*. J. Bacteriol. 187:2715–2726.
171. Hanspal M, Dua M, Takakuwa Y, Chishti AH, Mizuno A. 2002. *Plasmodium falciparum* cysteine protease falcipain-2 cleaves erythrocyte membrane skeletal proteins at late stages of parasite development. Blood 100:1048–1054.
172. Heffernan EJ, Harwood J, Fierer J, Guiney D. 1992. The *Salmonella typhimurium* virulence plasmid complement resistance gene *rck* is homologous to a family of virulence-related outer membrane protein genes, including *pagC* and *ail*. J. Bacteriol. 174:84–91.
173. Heller R, et al. 1997. Prevalence of *Bartonella henselae* and *Bartonella clarridgeiae* in stray cats. J. Clin. Microbiol. 35:1327–1331.
174. Henderson B, Allan E, Coates AR. 2006. Stress wars: the direct role of host and bacterial molecular chaperones in bacterial infection. Infect. Immun. 74:3693–3706.
175. Henderson B, Nair S, Pallas J, Williams MA. 2011. Fibronectin: a multidomain host adhesin targeted by bacterial fibronectin-binding proteins. FEMS Microbiol. Rev. 35:147–200.
176. Henderson IR, Nataro JP. 2001. Virulence functions of autotransporter proteins. Infect. Immun. 69:1231–1243.
177. Henderson IR, Navarro-Garcia F, Desvaux M, Fernandez RC, Ala'Aldeen D. 2004. Type V protein secretion pathway: the autotransporter story. Microbiol. Mol. Biol. Rev. 68:692–744.
178. Hendrix LR. 2000. Contact-dependent hemolytic activity distinct from deforming activity of *Bartonella bacilliformis*. FEMS Microbiol. Lett. 182: 119–124.
179. Hendrix LR, Kiss K. 2003. Studies on the identification of deforming factor from *Bartonella bacilliformis*. Ann. N. Y. Acad. Sci. 990:596–604.
180. Henriquez C, et al. 2004. Report of an unusual case of persistent bacteremia by *Bartonella bacilliformis* in a splenectomized patient. Am. J. Trop. Med. Hyg. 71:53–55.
181. Hickey TB, Ziltener HJ, Speert DP, Stokes RW. 2010. *Mycobacterium tuberculosis* employs Cpn60.2 as an adhesin that binds CD43 on the macrophage surface. Cell. Microbiol. 12:1634–1647.
182. Hill EM, Raji A, Valenzuela MS, Garcia F, Hoover R. 1992. Adhesion to and invasion of cultured human cells by *Bartonella bacilliformis*. Infect. Immun. 60:4051–4058.
183. Hinnebusch BJ, Perry RD, Schwan TG. 1996. Role of the *Yersinia pestis* hemin storage (hms) locus in the transmission of plague by fleas. Science 273:367–370.
184. Hinode D, et al. 1998. The GroEL-like protein from *Campylobacter rectus*: immunological characterization and interleukin-6 and -8 induction in human gingival fibroblast. FEMS Microbiol. Lett. 167:1–6.
185. Hoiczyk E, Roggenkamp A, Reichenbecher M, Lupas A, Heesemann J. 2000. Structure and sequence analysis of *Yersinia* YadA and *Moraxella* UspAs reveal a novel class of adhesins. EMBO J. 19:5989–5999.
186. Holland IB, Schmitt L, Young J. 2005. Type 1 protein secretion in bacteria, the ABC-transporter dependent pathway. Mol. Membr. Biol. 22:29–39.
187. Holmes K, Roberts OL, Thomas AM, Cross MJ. 2007. Vascular endothelial growth factor receptor-2: structure, function, intracellular signalling and therapeutic inhibition. Cell Signal. 19:2003–2012.
188. Hong PC, Tsolis RM, Ficht TA. 2000. Identification of genes required for chronic persistence of *Brucella abortus* in mice. Infect. Immun. 68: 4102–4107.
189. Hotez PJ. 2008. Neglected infections of poverty in the United States of America. PLoS Negl. Trop. Dis. 2:e256.
190. Huang R, et al. 2011. *Bartonella quintana* infections in captive monkeys, China. Emerg. Infect. Dis. 17:1707–1709.
191. Huarcaya E, et al. 2011. Cytokines and T-lymphocyte count in patients

in the acute and chronic phases of *Bartonella bacilliformis* infection in an endemic area in Peru: a pilot study. Rev. Inst. Med. Trop. Sao Paulo 53:149–154.
192. Huarcaya E, Maguina C, Best I, Solorzano N, Leeman L. 2007. Immunological response in cases of complicated and uncomplicated bartonellosis during pregnancy. Rev. Inst. Med. Trop. Sao Paulo. 49:335–337.
193. Ihler GM. 1996. *Bartonella bacilliformis*: dangerous pathogen slowly emerging from deep background. FEMS Microbiol. Lett. 144:1–11.
194. Inatsuka CS, Julio SM, Cotter PA. 2005. *Bordetella* filamentous hemagglutinin plays a critical role in immunomodulation, suggesting a mechanism for host specificity. Proc. Natl. Acad. Sci. U. S. A. 102: 18578–18583.
195. Infante B, et al. 2008. BALB/c Mice resist infection with *Bartonella bacilliformis*. BMC Res. Notes. 1:103.
196. Inon de Iannino N, Briones G, Tolmasky M, Ugalde RA. 1998. Molecular cloning and characterization of cgs, the *Brucella abortus* cyclic beta(1-2) glucan synthetase gene: genetic complementation of *Rhizobium meliloti* ndvB and *Agrobacterium tumefaciens* chvB mutants. J. Bacteriol. 180:4392–4400.
197. Iredell J, et al. 2003. Characterization of the natural population of *Bartonella henselae* by multilocus sequence typing. J. Clin. Microbiol. 41:5071–5079.
198. Iredell J, McHattan J, Kyme P, Dillon B, Blanckenberg D. 2002. Antigenic and genotypic relationships between *Bartonella henselae* strains. J. Clin. Microbiol. 40:4397–4398.
199. Ishijima N, et al. 2011. BabA-mediated adherence is a potentiator of the *Helicobacter pylori* type IV secretion system activity. J. Biol. Chem. 286: 25256–25264.
200. Ismail TM, Hart CA, McLennan AG. 2003. Regulation of dinucleoside polyphosphate pools by the YgdP and ApaH hydrolases is essential for the ability of *Salmonella enterica* serovar *typhimurium* to invade cultured mammalian cells. J. Biol. Chem. 278:32602–32607.
201. Iwaki-Egawa S, Ihler GM. 1997. Comparison of the abilities of proteins from *Bartonella bacilliformis* and *Bartonella henselae* to deform red cell membranes and to bind to red cell ghost proteins. FEMS Microbiol. Lett. 157:207–217.
202. Jackson LA, Perkins BA, Wenger JD. 1993. Cat scratch disease in the United States: an analysis of three national databases. Am. J. Public Health 83:1707–1711.
203. Jackson LA, et al. 1996. Seroprevalence to *Bartonella quintana* among patients at a community clinic in downtown Seattle. J. Infect. Dis. 173: 1023–1026.
204. Jacob-Dubuisson F, et al. 2000. Molecular characterization of *Bordetella bronchiseptica* filamentous haemagglutinin and its secretion machinery. Microbiology 146:1211–1221.
205. Jacob-Dubuisson F, Locht C, Antoine R. 2001. Two-partner secretion in Gram-negative bacteria: a thrifty, specific pathway for large virulence proteins. Mol. Microbiol. 40:306–313.
206. Jameson P, et al. 1995. Prevalence of *Bartonella henselae* antibodies in pet cats throughout regions of North America. J. Infect. Dis. 172: 1145–1149.
207. Janczarek M, Kutkowska J, Piersiak T, Skorupska A. 2010. *Rhizobium leguminosarum bv. trifolii* rosR is required for interaction with clover, biofilm formation and adaptation to the environment. BMC Microbiol. 10:284.
208. Janka GE. 2007. Hemophagocytic syndromes. Blood Rev. 21:245–253.
209. Jay DG. 1996. Role of band 3 in homeostasis and cell shape. Cell 86: 853–854.
210. Jonson AB, Normark S, Rhen M. 2005. Fimbriae, pili, flagella and bacterial virulence. Contrib. Microbiol. 12:67–89.
211. Kabeya H, et al. 2002. Genomic variations among *Bartonella henselae* isolates derived from naturally infected cats. Vet. Microbiol. 89:211–221.
212. Kabeya H, Sase M, Yamashita M, Maruyama S. 2006. Predominant T helper 2 immune responses against *Bartonella henselae* in naturally infected cats. Microbiol. Immunol. 50:171–178.
213. Kabeya H, Tsunoda E, Maruyama S, Mikami T. 2003. Immune responses of immunocompetent and immunocompromised mice experimentally infected with *Bartonella henselae*. J. Vet. Med. Sci. 65:479–484.
214. Kabeya H, et al. 2009. Experimental infection of cats with *Bartonella henselae* resulted in rapid clearance associated with T helper 1 immune responses. Microbes Infect. 11:716–720.
215. Kabeya H, et al. 2007. Characterization of Th1 activation by *Bartonella henselae* stimulation in BALB/c mice: Inhibitory activities of interleukin-10 for the production of interferon-gamma in spleen cells. Vet. Microbiol. 119:290–296.
216. Kaiser PO, Riess T, O'Rourke F, Linke D, Kempf VA. 2011. *Bartonella* spp.: throwing light on uncommon human infections. Int. J. Med. Microbiol. 301:7–15.
217. Kaiser PO, et al. 2008. The head of *Bartonella* adhesin A is crucial for host cell interaction of *Bartonella henselae*. Cell. Microbiol. 10: 2223–2234.
218. Karem KL. 2000. Immune aspects of *Bartonella*. Crit. Rev. Microbiol. 26:133–145.
219. Karem KL, Dubois KA, McGill SL, Regnery RL. 1999. Characterization of *Bartonella henselae*-specific immunity in BALB/c mice. Immunology 97:352–358.
220. Karem KL, Paddock CD, Regnery RL. 2000. *Bartonella henselae*, *B. quintana*, and *B. bacilliformis*: historical pathogens of emerging significance. Microbes Infect. 2:1193–1205.
221. Kempf VA, Hitziger N, Riess T, Autenrieth IB. 2002. Do plant and human pathogens have a common pathogenicity strategy? Trends Microbiol. 10:269–275.
222. Kempf VA, et al. 2005. Activation of hypoxia-inducible factor-1 in bacillary angiomatosis: evidence for a role of hypoxia-inducible factor-1 in bacterial infections. Circulation 111:1054–1062.
223. Kempf VA, et al. 2005. *Bartonella henselae* inhibits apoptosis in Mono Mac 6 cells. Cell. Microbiol. 7:91–104.
224. Kempf VA, et al. 2000. Interaction of *Bartonella henselae* with endothelial cells results in rapid bacterial rRNA synthesis and replication. Cell. Microbiol. 2:431–441.
225. Kempf VA, et al. 2001. Evidence of a leading role for VEGF in *Bartonella henselae*-induced endothelial cell proliferations. Cell. Microbiol. 3:623–632.
226. Kirby JE, Nekorchuk DM. 2002. *Bartonella*-associated endothelial proliferation depends on inhibition of apoptosis. Proc. Natl. Acad. Sci. U. S. A. 99:4656–4661.
227. Kitchell BE, et al. 2000. Peliosis hepatis in a dog infected with *Bartonella henselae*. J. Am. Vet. Med. Assoc. 216:519–523,517.
228. Klein S, et al. 2002. Alpha 5 beta 1 integrin activates an NF-kappa B-dependent program of gene expression important for angiogenesis and inflammation. Mol. Cell. Biol. 22:5912–5922.
229. Knobloch J, Schreiber M. 1990. Bb65, a major immunoreactive protein of *Bartonella bacilliformis*. Am. J. Trop. Med. Hyg. 43:373–379.
230. Knobloch J, Solano L, Alvarez O, Delgado E. 1985. Antibodies to *Bartonella bacilliformis* as determined by fluorescence antibody test, indirect haemagglutination and ELISA. Trop. Med. Parasitol. 36:183–185.
231. Knowles TJ, Scott-Tucker A, Overduin M, Henderson IR. 2009. Membrane protein architects: the role of the BAM complex in outer membrane protein assembly. Nat. Rev. Microbiol. 7:206–214.
232. Koebnik R, Locher KP, Van Gelder P. 2000. Structure and function of bacterial outer membrane proteins: barrels in a nutshell. Mol. Microbiol. 37:239–253.
233. Koesling J, Aebischer T, Falch C, Schulein R, Dehio C. 2001. Antibody-mediated cessation of hemotropic infection by the intraerythrocytic mouse pathogen *Bartonella grahamii*. J. Immunol. 167:11–14.
234. Kordick DL, Breitschwerdt EB. 1995. Intraerythrocytic presence of *Bartonella henselae*. J. Clin. Microbiol. 33:1655–1656.
235. Kordick DL, Breitschwerdt EB. 1998. Persistent infection of pets within a household with three *Bartonella* species. Emerg. Infect. Dis. 4:325–328.
236. Kordick DL, Brown TT, Shin K, Breitschwerdt EB. 1999. Clinical and pathologic evaluation of chronic *Bartonella henselae* or *Bartonella clarridgeiae* infection in cats. J. Clin. Microbiol. 37:1536–1547.
237. Kordick DL, et al. 1997. *Bartonella clarridgeiae*, a newly recognized zoonotic pathogen causing inoculation papules, fever, and lymphadenopathy (cat scratch disease). J. Clin. Microbiol. 35:1813–1818.
238. Kordick DL, et al. 1995. Prolonged *Bartonella* bacteremia in cats associated with cat-scratch disease patients. J. Clin. Microbiol. 33:3245–3251.
239. Kosek M, et al. 2000. Natural history of infection with *Bartonella bacilliformis* in a nonendemic population. J. Infect. Dis. 182:865–872.
240. Kosoy M, et al. 2010. *Bartonella* spp. in bats, Kenya. Emerg. Infect. Dis. 16:1875–1881.
241. Kosoy M, Mandel E, Green D, Marston E, Childs J. 2004. Prospective studies of *Bartonella* of rodents. I. Demographic and temporal patterns in population dynamics. Vector Borne Zoonotic Dis. 4:285–295.
242. Kosoy MY, et al. 2000. Experimental evidence of host specificity of

Bartonella infection in rodents. Comp. Immunol. Microbiol. Infect. Dis. 23:221–238.
243. Kulp A, Kuehn MJ. 2010. Biological functions and biogenesis of secreted bacterial outer membrane vesicles. Annu. Rev. Microbiol. 64:163–184.
244. Kunz S, Oberle K, Sander A, Bogdan C, Schleicher U. 2008. Lymphadenopathy in a novel mouse model of *Bartonella*-induced cat scratch disease results from lymphocyte immigration and proliferation and is regulated by interferon-alpha/beta. Am. J. Pathol. 172:1005–1018.
245. Kyme P, Dillon B, Iredell J. 2003. Phase variation in *Bartonella henselae*. Microbiology 149:621–629.
246. Kyme PA, et al. 2005. Unusual trafficking pattern of *Bartonella henselae*-containing vacuoles in macrophages and endothelial cells. Cell. Microbiol. 7:1019–1034.
247. Laarmann S, Cutter D, Juehne T, Barenkamp SJ, St Geme JW. 2002. The *Haemophilus influenzae* Hia autotransporter harbours two adhesive pockets that reside in the passenger domain and recognize the same host cell receptor. Mol. Microbiol. 46:731–743.
248. Laloux G, Deghelt M, de Barsy M, Letesson JJ, De Bolle X. 2010. Identification of the essential *Brucella melitensis* porin Omp2b as a suppressor of Bax-induced cell death in yeast in a genome-wide screening. PLoS One 5:e13274.
249. Lamps LW, Scott MA. 2004. Cat-scratch disease: historic, clinical, and pathologic perspectives. Am. J. Clin. Pathol. 121(Suppl.):S71–S80.
250. Lang AS, Beatty JT. 2007. Importance of widespread gene transfer agent genes in alpha-proteobacteria. Trends Microbiol. 15:54–62.
251. La Scola B, et al. 2002. Genotypic characteristics of two serotypes of *Bartonella henselae*. J. Clin. Microbiol. 40:2002–2008.
252. Lawrenz MB, Lenz JD, Miller VL. 2009. A novel autotransporter adhesin is required for efficient colonization during bubonic plague. Infect. Immun. 77:317–326.
253. Leatham MP, et al. 2005. Mouse intestine selects nonmotile flhDC mutants of *Escherichia coli* MG1655 with increased colonizing ability and better utilization of carbon sources. Infect. Immun. 73:8039–8049.
254. LeBoit PE, et al. 1988. Epithelioid haemangioma-like vascular proliferation in AIDS: manifestation of cat scratch disease bacillus infection? Lancet i:960–963.
255. Lestrate P, et al. 2000. Identification and characterization of in vivo attenuated mutants of *Brucella melitensis*. Mol. Microbiol. 38:543–551.
256. Lestrate P, et al. 2003. Attenuated signature-tagged mutagenesis mutants of *Brucella melitensis* identified during the acute phase of infection in mice. Infect. Immun. 71:7053–7060.
257. Li A, Dubey S, Varney ML, Dave BJ, Singh RK. 2003. IL-8 directly enhanced endothelial cell survival, proliferation, and matrix metalloproteinases production and regulated angiogenesis. J. Immunol. 170: 3369–3376.
258. Liberto MC, et al. 2004. *Bartonella quintana*-induced apoptosis inhibition of human endothelial cells is associated with p38 and SAPK/JNK modulation and with stimulation of mitosis. Diagn. Microbiol. Infect. Dis. 50:159–166.
259. Lim HWG, Wortis M, Mukhopadhyay R. 2002. Stomatocyte-discocyte-echinocyte sequence of the human red blood cell: evidence for the bilayer-couple hypothesis from membrane mechanics. Proc. Natl. Acad. Sci. U. S. A. 99:16766–16769.
260. Linke D, Riess T, Autenrieth IB, Lupas A, Kempf VA. 2006. Trimeric autotransporter adhesins: variable structure, common function. Trends Microbiol. 14:264–270.
261. Litwin CM, Johnson JM. 2005. Identification, cloning, and expression of the CAMP-like factor autotransporter gene (cfa) of *Bartonella henselae*. Infect. Immun. 73:4205–4213.
262. Litwin CM, Rawlins ML, Swenson EM. 2007. Characterization of an immunogenic outer membrane autotransporter protein, Arp, of *Bartonella henselae*. Infect. Immun. 75:5255–5263.
263. Liu Z, Jacobs M, Schaff DA, McCullen CA, Binns AN. 2001. ChvD, a chromosomally encoded ATP-binding cassette transporter-homologous protein involved in regulation of virulence gene expression in *Agrobacterium tumefaciens*. J. Bacteriol. 183:3310–3317.
264. Lobov IB, Brooks PC, Lang RA. 2002. Angiopoietin-2 displays VEGF-dependent modulation of capillary structure and endothelial cell survival *in vivo*. Proc. Natl. Acad. Sci. U. S. A. 99:11205–11210.
265. Lund PA. 2001. Microbial molecular chaperones. Adv. Microb. Physiol. 44:93–140.
266. Lydy SL, et al. 2008. Isolation and characterization of *Bartonella bacilliformis* from an expatriate Ecuadorian. J. Clin. Microbiol. 46:627–637.
267. MacKichan JK, Gerns HL, Chen YT, Zhang P, Koehler JE. 2008. A SacB mutagenesis strategy reveals that the *Bartonella quintana* variably expressed outer membrane proteins are required for bloodstream infection of the host. Infect. Immun. 76:788–795.
268. Maeno N, et al. 1999. Live *Bartonella henselae* enhances endothelial cell proliferation without direct contact. Microb. Pathog. 27:419–427.
269. Maggi RG, Breitschwerdt EB. 2005. Isolation of bacteriophages from *Bartonella vinsonii subsp. berkhoffii* and the characterization of Pap31 gene sequences from bacterial and phage DNA. J. Mol. Microbiol. Biotechnol. 9:44–51.
270. Maggi RG, et al. 2008. *Bartonella henselae* in captive and hunter-harvested beluga (*Delphinapterus leucas*). J. Wildl. Dis. 44:871–877.
271. Maguina C, Garcia PJ, Gotuzzo E, Cordero L, Spach DH. 2001. Bartonellosis (Carrion's disease) in the modern era. Clin. Infect. Dis. 33:772–779.
272. Maguina C, Guerra H, and Ventosilla P. 2009. Bartonellosis. Clin. Dermatol. 27:271–280.
273. Manders SM. 1996. Bacillary angiomatosis. Clin. Dermatol. 14:295–299.
274. Mandle T, et al. 2005. Infection of human CD34+ progenitor cells with *Bartonella henselae* results in intraerythrocytic presence of *B. henselae*. Blood 106:1215–1222.
275. Marignac G, et al. 2010. Murine model for *Bartonella birtlesii* infection: new aspects. Comp. Immunol. Microbiol. Infect. Dis. 33:95–107.
276. Martin-Martin AI, Caro-Hernandez P, Orduna A, Vizcaino N, Fernandez-Lago L. 2008. Importance of the Omp25/Omp31 family in the internalization and intracellular replication of virulent *B. ovis* in murine macrophages and HeLa cells. Microbes Infect. 10:706–710.
277. Matera G, et al. 2008. The Janus face of *Bartonella quintana* recognition by Toll-like receptors (TLRs): a review. Eur. Cytokine Netw. 19:113–118.
278. Matera G, et al. 2003. *Bartonella quintana* lipopolysaccharide effects on leukocytes, CXC chemokines and apoptosis: a study on the human whole blood and a rat model. Int. Immunopharmacol. 3:853–864.
279. Matsumoto K, Berrada ZL, Klinger E, Goethert HK, Telford SR, III. 2008. Molecular detection of *Bartonella schoenbuchensis* from ectoparasites of deer in Massachusetts. Vector Borne Zoonotic Dis. 8:549–554.
280. Mayer DC, et al. 2009. Glycophorin B is the erythrocyte receptor of *Plasmodium falciparum* erythrocyte-binding ligand, EBL-1. Proc. Natl. Acad. Sci. U. S. A. 106:5348–5352.
281. Mazar J, Cotter PA. 2006. Topology and maturation of filamentous haemagglutinin suggest a new model for two-partner secretion. Mol. Microbiol. 62:641–654.
282. McCord AM, Burgess AW, Whaley MJ, Anderson BE. 2005. Interaction of *Bartonella henselae* with endothelial cells promotes monocyte/macrophage chemoattractant protein 1 gene expression and protein production and triggers monocyte migration. Infect. Immun. 73:5735–5742.
283. McCord AM, Cuevas J, Anderson BE. 2007. *Bartonella*-induced endothelial cell proliferation is mediated by release of calcium from intracellular stores. DNA Cell Biol. 26:657–663.
284. McCord AM, Resto-Ruiz SI, Anderson BE. 2006. Autocrine role for interleukin-8 in *Bartonella henselae*-induced angiogenesis. Infect. Immun. 74:5185–5190.
285. Mehock JR, Greene CE, Gherardini FC, Hahn TW, Krause DC. 1998. *Bartonella henselae* invasion of feline erythrocytes in vitro. Infect. Immun. 66:3462–3466.
286. Meng G, St Geme JW, III, Waksman G. 2008. Repetitive architecture of the *Haemophilus influenzae* Hia trimeric autotransporter. J. Mol. Biol. 384:824–836.
287. Mernaugh G, Ihler GM. 1992. Deformation factor: an extracellular protein synthesized by *Bartonella bacilliformis* that deforms erythrocyte membranes. Infect. Immun. 60:937–943.
288. Merrell DS, Falkow S. 2004. Frontal and stealth attack strategies in microbial pathogenesis. Nature 430:250–256.
289. Miller LH. 1994. Impact of malaria on genetic polymorphism and genetic diseases in Africans and African Americans. Proc. Natl. Acad. Sci. U. S. A. 91:2415–2419.
290. Miller SI, Bader M, Guina T. 2003. Bacterial vesicle formation as a mechanism of protein transfer to animals. Cell 115:2–3.
291. Miller SI, Ernst RK, Bader MW. 2005. LPS, TLR4 and infectious disease diversity. Nat. Rev. Microbiol. 3:36–46.
292. Minnick MF. 1994. Identification of outer membrane proteins of *Bartonella bacilliformis*. Infect. Immun. 62:2644–2648.
293. Minnick MF, Anderson B. 2006. The genus *Bartonella*, p 476–492. *In* Dworkin M, Falkow S, Rosenberg E, Schleifer K-H, Stackebrandt E (ed),

Proteobacteria: alpha and beta subclasses, 3rd ed, vol 5. Springer, New York, NY.
294. Minnick MF, Battisti JM. 2009. Pestilence, persistence and pathogenicity: infection strategies of *Bartonella*. Future Microbiol. 4:743–758.
295. Minnick MF, Mitchell SJ, McAllister SJ. 1996. Cell entry and the pathogenesis of *Bartonella* infections. Trends Microbiol. 4:343–347.
296. Minnick MF, et al. 2003. Five-member gene family of *Bartonella quintana*. Infect. Immun. 71:814–821.
297. Minnick MF, Smitherman LS, Samuels DS. 2003. Mitogenic effect of *Bartonella bacilliformis* on human vascular endothelial cells and involvement of GroEL. Infect. Immun. 71:6933–6942.
298. Mistry D, Stockley RA. 2006. IgA1 protease. Int. J. Biochem. Cell Biol. 38:1244–1248.
299. Mitchell SJ, Minnick MF. 1997. A carboxy-terminal processing protease gene is located immediately upstream of the invasion-associated locus from *Bartonella bacilliformis*. Microbiology 143:1221–1233.
300. Mitchell SJ, Minnick MF. 1995. Characterization of a two-gene locus from *Bartonella bacilliformis* associated with the ability to invade human erythrocytes. Infect. Immun. 63:1552–1562.
301. Mogollon-Pasapera E, Otvos L, Jr, Giordano A, Cassone M. 2009. *Bartonella*: emerging pathogen or emerging awareness? Int. J. Infect. Dis. 13:3–8.
302. Mohandas N, An X. 2006. New insights into function of red cell membrane proteins and their interaction with spectrin-based membrane skeleton. Transfus. Clin. Biol. 13:29–30.
303. Mohandas N, Gallagher PG. 2008. Red cell membrane: past, present, and future. Blood 112:3939–3948.
304. Mohle-Boetani JC, et al. 1996. Bacillary angiomatosis and bacillary peliosis in patients infected with human immunodeficiency virus: clinical characteristics in a case-control study. Clin. Infect. Dis. 22:794–800.
305. Molina-Cruz A, et al. 2008. Reactive oxygen species modulate *Anopheles gambiae* immunity against bacteria and *Plasmodium*. J. Biol. Chem. 283: 3217–3223.
306. Muller NF, et al. 2011. Trimeric autotransporter adhesin-dependent adherence of *Bartonella henselae*, *Bartonella quintana* and *Yersinia enterocolitica* to matrix components and endothelial cells under static and dynamic flow conditions. Infect. Immun. 79:2544–2553.
307. Munana KR, Vitek SM, Hegarty BC, Kordick DL, Breitschwerdt EB. 2001. Infection of fetal feline brain cells in culture with *Bartonella henselae*. Infect. Immun. 69:564–569.
308. Murphy SC, et al. 2007. Cytoplasmic remodeling of erythrocyte raft lipids during infection by the human malaria parasite *Plasmodium falciparum*. Blood 110:2132–2139.
309. Musso T, et al. 2001. Interaction of *Bartonella henselae* with the murine macrophage cell line J774: infection and proinflammatory response. Infect. Immun. 69:5974–5980.
310. Nagele V, et al. 2011. *Neisseria meningitidis* adhesin NadA targets beta1 integrins: Functional similarity to *Yersinia* invasin. J. Biol. Chem. 286: 20536–20546.
311. Namekata DY, et al. 2010. Oral shedding of *Bartonella* in cats: correlation with bacteremia and seropositivity. Vet. Microbiol. 146:371–375.
312. Nicholson TL, Brockmeier SL, Loving CL. 2009. Contribution of *Bordetella bronchiseptica* filamentous hemagglutinin and pertactin to respiratory disease in swine. Infect. Immun. 77:2136–2146.
313. Noguchi H. 1926. Etiology of Oroya fever. Iii. The behavior of *Bartonella bacilliformis* in *Macacus rhesus*. J. Exp. Med. 44:697–713.
314. Noinaj N, Guillier M, Barnard TJ, Buchanan SK. 2010. TonB-dependent transporters: regulation, structure, and function. Annu. Rev. Microbiol. 64:43–60.
315. Nor JE, et al. 2001. Up-regulation of Bcl-2 in microvascular endothelial cells enhances intratumoral angiogenesis and accelerates tumor growth. Cancer Res. 61:2183–2188.
316. Nystedt B, Frank AC, Thollesson M, Andersson SG. 2008. Diversifying selection and concerted evolution of a type IV secretion system in *Bartonella*. Mol. Biol. Evol. 25:287–300.
317. Ochman H, Lawrence JG, Groisman EA. 2000. Lateral gene transfer and the nature of bacterial innovation. Nature 405:299–304.
318. Ohl ME, Spach DH. 2000. *Bartonella quintana* and urban trench fever. Clin. Infect. Dis. 31:131–135.
319. Oliveira JH, et al. 2011. Blood meal-derived heme decreases ROS levels in the midgut of *Aedes aegypti* and allows proliferation of intestinal microbiota. PLoS Pathog. 7:e1001320.
320. Oliver KM, et al. 2009. Hypoxia activates NF-kappaB-dependent gene expression through the canonical signaling pathway. Antioxid. Redox. Signal. 11:2057–2064.
321. O'Reilly KL, Parr KA, Brown TP, Tedder-Ferguson B, Scholl DT. 2001. Passive antibody to *Bartonella henselae* protects against clinical disease following homologous challenge but does not prevent bacteremia in cats. Infect. Immun. 69:1880–1882.
322. O'Rourke F, Schmidgen T, Kaiser PO, Linke D, Kempf VA. 2011. Adhesins of *Bartonella* spp. Adv. Exp. Med. Biol. 715:51–70.
323. Ostberg Y, et al. 2004. Pleiotropic effects of inactivating a carboxyl-terminal protease, CtpA, in *Borrelia burgdorferi*. J. Bacteriol. 186: 2074–2084.
324. Otto BR, et al. 2005. Crystal structure of hemoglobin protease, a heme binding autotransporter protein from pathogenic *Escherichia coli*. J. Biol. Chem. 280:17339–17345.
325. Pachas P. 2000. Epidemiología de la Bartonelosis en el Peru. Oficina General de Epidemiología, Lima, Peru.
326. Padmalayam I, Karem K, Baumstark B, Massung R. 2000. The gene encoding the 17-kDa antigen of *Bartonella henselae* is located within a cluster of genes homologous to the virB virulence operon. DNA Cell Biol. 19:377–382.
327. Palanivelu DV, et al. 2011. Fic domain-catalyzed adenylylation: insight provided by the structural analysis of the type IV secretion system effector BepA. Protein Sci. 20:492–499.
328. Papadopoulos NG, et al. 2001. Circulating cytokines in patients with cat scratch disease. Clin. Infect. Dis. 33:e54–56.
329. Pappalardo BL, Brown T, Gebhardt D, Sontakke S, Breitschwerdt EB. 2000. Cyclic CD8+ lymphopenia in dogs experimentally infected with *Bartonella vinsonii* subsp. *berkhoffii*. Vet. Immunol. Immunopathol. 75: 43–57.
330. Pappalardo BL, Brown TT, Tompkins M, Breitschwerdt EB. 2001. Immunopathology of *Bartonella vinsonii* (*berkhoffii*) in experimentally infected dogs. Vet. Immunol. Immunopathol. 83:125–147.
331. Parrow NL, Abbott J, Lockwood AR, Battisti JM, Minnick MF. 2009. Function, regulation, and transcriptional organization of the hemin utilization locus of *Bartonella quintana*. Infect. Immun. 77:307–316.
332. Patel VP, Fairbanks G. 1986. Relationship of major phosphorylation reactions and MgATPase activities to ATP-dependent shape change of human erythrocyte membranes. J. Biol. Chem. 261:3170–3177.
333. Paulsen IT, et al. 2002. The *Brucella suis* genome reveals fundamental similarities between animal and plant pathogens and symbionts. Proc. Natl. Acad. Sci. U. S. A. 99:13148–13153.
334. Pawson T. 2004. Specificity in signal transduction: from phosphotyrosine-SH2 domain interactions to complex cellular systems. Cell 116:191–203.
335. Paziewska A, Harris PD, Zwolinska L, Bajer A, Sinski E. 2011. Recombination within and between species of the alpha proteobacterium *Bartonella* infecting rodents. Microb. Ecol. 61:134–145.
336. Perez C, Maggi RG, Diniz PP, Breitschwerdt EB. 2011. Molecular and serological diagnosis of *Bartonella* infection in 61 dogs from the United States. J. Vet. Intern. Med. 25:805–810.
337. Perry RD, Lucier TS, Sikkema DJ, Brubaker RR. 1993. Storage reservoirs of hemin and inorganic iron in *Yersinia pestis*. Infect. Immun. 61: 32–39.
338. Pinne M, Ostberg Y, Comstedt P, Bergstrom S. 2004. Molecular analysis of the channel-forming protein P13 and its paralogue family 48 from different Lyme disease *Borrelia* species. Microbiology 150:549–559.
339. Plettenberg A, et al. 2000. Bacillary angiomatosis in HIV-infected patients—an epidemiological and clinical study. Dermatology 201: 326–331.
340. Popa C, et al. 2007. *Bartonella quintana* lipopolysaccharide is a natural antagonist of Toll-like receptor 4. Infect. Immun. 75:4831–4837.
341. Postle K, Kadner RJ. 2003. Touch and go: tying TonB to transport. Mol. Microbiol. 49:869–882.
342. Prell J, et al. 2010. Role of symbiotic auxotrophy in the *Rhizobium*-legume symbioses. PLoS One 5:e13933.
343. Prell J, et al. 2009. Legumes regulate *Rhizobium* bacteroid development and persistence by the supply of branched-chain amino acids. Proc. Natl. Acad. Sci. U. S. A. 106:12477–12482.
344. Pugh CW, Ratcliffe PJ. 2003. Regulation of angiogenesis by hypoxia: role of the HIF system. Nat. Med. 9:677–684.
345. Putnoky P, et al. 1998. The pha gene cluster of *Rhizobium meliloti*

involved in pH adaptation and symbiosis encodes a novel type of K+ efflux system. Mol. Microbiol. 28:1091–1101.
346. Que YA, Moreillon P. 2011. Infective endocarditis. Nat. Rev. Cardiol. 8:322–336.
347. Quebatte M, et al. 2010. The BatR/BatS two-component regulatory system controls the adaptive response of *Bartonella henselae* during human endothelial cell infection. J. Bacteriol. 192:3352–3367.
348. Radford SE. 2006. GroEL: more than just a folding cage. Cell 125: 831–833.
349. Rahman MM, McFadden G. 2011. Modulation of NF-kappaB signalling by microbial pathogens. Nat. Rev. Microbiol. 9:291–306.
350. Raoult D, et al. 2006. Evidence for louse-transmitted diseases in soldiers of Napoleon's Grand Army in Vilnius. J. Infect. Dis. 193:112–120.
351. Raoult D, et al. 1996. Diagnosis of 22 new cases of *Bartonella* endocarditis. Ann. Intern. Med. 125:646–652.
352. Rearden A, Magnet A, Kudo S, Fukuda M. 1993. Glycophorin B and glycophorin E genes arose from the glycophorin A ancestral gene via two duplications during primate evolution. J. Biol. Chem. 268:2260–2267.
353. Reiling SA, et al. 2005. Prc protease promotes mucoidy in mucA mutants of *Pseudomonas aeruginosa*. Microbiology 151:2251–2261.
354. Reis C, et al. 2011. Vector competence of the tick *Ixodes ricinus* for transmission of *Bartonella birtlesii*. PLoS Negl. Trop. Dis. 5:e1186.
355. Resto-Ruiz SI, et al. 2002. Induction of a potential paracrine angiogenic loop between human THP-1 macrophages and human microvascular endothelial cells during *Bartonella henselae* infection. Infect. Immun. 70: 4564–4570.
356. Reynafarje C, Ramos J. 1961. The hemolytic anemia of human bartonellosis. Blood 17:562–578.
357. Rhomberg TA, et al. 2004. Proteomic analysis of the sarcosine-insoluble outer membrane fraction of the bacterial pathogen *Bartonella henselae*. Proteomics 4:3021–3033.
358. Rhomberg TA, Truttmann MC, Guye P, Ellner Y, Dehio C. 2009. A translocated protein of *Bartonella henselae* interferes with endocytic uptake of individual bacteria and triggers uptake of large bacterial aggregates via the invasome. Cell. Microbiol. 11:927–945.
359. Ricketts WE. 1948. *Bartonella bacilliformis* anemia (Oroya fever); a study of 30 cases. Blood 3:1025–1049.
360. Riess T, et al. 2004. *Bartonella* adhesin a mediates a proangiogenic host cell response. J. Exp. Med. 200:1267–1278.
361. Riess T, Raddatz G, Linke D, Schafer A, Kempf VA. 2007. Analysis of *Bartonella* adhesin A expression reveals differences between various *B. henselae* strains. Infect. Immun. 75:35–43.
362. Rodriguez-Barradas MC, et al. 1995. *In vitro* evaluation of the role of humoral immunity against *Bartonella henselae*. Infect. Immun. 63: 2367–2370.
363. Roggenkamp A, et al. 2003. Molecular analysis of transport and oligomerization of the *Yersinia enterocolitica* adhesin YadA. J. Bacteriol. 185:3735–3744.
364. Rojas CM, Ham JH, Deng WL, Doyle JJ, Collmer A. 2002. HecA, a member of a class of adhesins produced by diverse pathogenic bacteria, contributes to the attachment, aggregation, epidermal cell killing, and virulence phenotypes of *Erwinia chrysanthemi* EC16 on *Nicotiana clevelandii* seedlings. Proc. Natl. Acad. Sci. U. S. A. 99:13142–13147.
365. Rolain JM, et al. 2004. Recommendations for treatment of human infections caused by *Bartonella* species. Antimicrob. Agents Chemother. 48:1921–1933.
366. Rolain JM, Foucault C, Brouqui P, Raoult D. 2003. Erythroblast cells as a target for *Bartonella quintana* in homeless people. Ann. N. Y. Acad. Sci. 990:485–487.
367. Rolain JM, et al. 2002. *Bartonella quintana* in human erythrocytes. Lancet 360:226–228.
368. Rolain JM, Franc M, Davoust B, Raoult D. 2003. Molecular detection of *Bartonella quintana*, *B. koehlerae*, *B. henselae*, *B. clarridgeiae*, *Rickettsia felis*, and *Wolbachia pipientis* in cat fleas, France. Emerg. Infect. Dis. 9:338–342.
369. Rolain JM, La Scola B, Liang Z, Davoust B, Raoult D. 2001. Immunofluorescent detection of intraerythrocytic *Bartonella henselae* in naturally infected cats. J. Clin. Microbiol. 39:2978–2980.
370. Rolain JM, et al. 2003. Immunofluorescence detection of *Bartonella bacilliformis* flagella *in vitro* and *in vivo* in human red blood cells as viewed by laser confocal microscopy. Ann. N. Y. Acad. Sci. 990:581–584.
371. Roy CR, Mukherjee S. 2009. Bacterial FIC proteins AMP up infection. Sci. Signal. 2:pe14.
372. Sadarangani M, Pollard AJ, Gray-Owen SD. 2011. Opa proteins and CEACAMs: pathways of immune engagement for pathogenic *Neisseria*. FEMS Microbiol. Rev. 35:498–514.
373. Saenz HL, Dehio C. 2005. Signature-tagged mutagenesis: technical advances in a negative selection method for virulence gene identification. Curr. Opin. Microbiol. 8:612–619.
374. Saenz HL, et al. 2007. Genomic analysis of *Bartonella* identifies type IV secretion systems as host adaptability factors. Nat. Genet. 39:1469–1476.
375. Sakurai Y, Ohgimoto K, Kataoka Y, Yoshida N, Shibuya M. 2005. Essential role of Flk-1 (VEGF receptor 2) tyrosine residue 1173 in vasculogenesis in mice. Proc. Natl. Acad. Sci. U. S. A. 102:1076–1081.
376. Salvatore P, et al. 2008. Detrimental effects of *Bartonella henselae* are counteracted by L-arginine and nitric oxide in human endothelial progenitor cells. Proc. Natl. Acad. Sci. U. S. A. 105:9427–9432.
377. Sander A, Kretzer S, Bredt W, Oberle K, Bereswill S. 2000. Hemin-dependent growth and hemin binding of *Bartonella henselae*. FEMS Microbiol. Lett. 189:55–59.
378. Sander A, et al. 2000. Characterization of *Bartonella clarridgeiae* flagellin (FlaA) and detection of antiflagellin antibodies in patients with lymphadenopathy. J. Clin. Microbiol. 38:2943–2948.
379. Sasarman A, et al. 1968. Hemin-deficient mutants of *Escherichia coli* K-12. J. Bacteriol. 96:570–572.
380. Sasu S, LaVerda D, Qureshi N, Golenbock DT, Beasley D. 2001. *Chlamydia pneumoniae* and chlamydial heat shock protein 60 stimulate proliferation of human vascular smooth muscle cells via toll-like receptor 4 and p44/p42 mitogen-activated protein kinase activation. Circ. Res. 89:244–250.
381. Scheidegger F, et al. 2009. Distinct activities of *Bartonella henselae* type IV secretion effector proteins modulate capillary-like sprout formation. Cell Microbiol. 11:1088–1101.
382. Scheidegger F, Quebatte M, Mistl C, Dehio C. 2011. The *Bartonella henselae* VirB/Bep system interferes with vascular endothelial growth factor (VEGF) signalling in human vascular endothelial cells. Cell. Microbiol. 13:419–431.
383. Scherer DC, DeBuron-Connors I, Minnick MF. 1993. Characterization of *Bartonella bacilliformis* flagella and effect of antiflagellin antibodies on invasion of human erythrocytes. Infect. Immun. 61:4962–4971.
384. Schmid MC, et al. 2006. A translocated bacterial protein protects vascular endothelial cells from apoptosis. PLoS Pathog. 2:e115.
385. Schmid MC, et al. 2004. The VirB type IV secretion system of *Bartonella henselae* mediates invasion, proinflammatory activation and antiapoptotic protection of endothelial cells. Mol. Microbiol. 52:81–92.
386. Schmid Y, et al. 2004. *Yersinia enterocolitica* adhesin A induces production of interleukin-8 in epithelial cells. Infect. Immun. 72:6780–6789.
387. Schmiederer M, Anderson B. 2000. Cloning, sequencing, and expression of three *Bartonella henselae* genes homologous to the *Agrobacterium tumefaciens* VirB region. DNA Cell Biol. 19:141–147.
388. Schmitter T, et al. 2007. Opa proteins of pathogenic neisseriae initiate Src kinase-dependent or lipid raft-mediated uptake via distinct human carcinoembryonic antigen-related cell adhesion molecule isoforms. Infect. Immun. 75:4116–4126.
389. Schrier SL. 1987. Drug-induced endocytosis and entrapment in red cells and ghosts. Methods Enzymol. 149:260–270.
390. Schrier SL, Zachowski A, Devaux PF. 1992. Mechanisms of amphipath-induced stomatocytosis in human erythrocytes. Blood 79:782–786.
391. Schroder G, Schuelein R, Quebatte M, Dehio C. 2011. Conjugative DNA transfer into human cells by the VirB/VirD4 type IV secretion system of the bacterial pathogen *Bartonella henselae*. Proc. Natl. Acad. Sci. U. S. A. 108:14643–14648.
392. Schulein R, Dehio C. 2002. The VirB/VirD4 type IV secretion system of *Bartonella* is essential for establishing intraerythrocytic infection. Mol. Microbiol. 46:1053–1067.
393. Schulein R, et al. 2005. A bipartite signal mediates the transfer of type IV secretion substrates of *Bartonella henselae* into human cells. Proc. Natl. Acad. Sci. U. S. A. 102:856–861.
394. Schulein R, et al. 2001. Invasion and persistent intracellular colonization of erythrocytes. A unique parasitic strategy of the emerging pathogen *Bartonella*. J. Exp. Med. 193:1077–1086.
395. Schulte B, et al. 2006. *Bartonella quintana* variably expressed outer membrane proteins mediate vascular endothelial growth factor secretion but not host cell adherence. Infect. Immun. 74:5003–5013.
396. Schultz MG. 2010. Daniel Alcides Carrión [photo quiz]. Emerg. Infect. Dis. vol 16:1025–1027.

397. Schweyer S, Fayyazi A. 2002. Activation and apoptosis of macrophages in cat scratch disease. J. Pathol. 198:534–540.
398. Seki N, et al. 2007. Quantitative analysis of proliferation and excretion of *Bartonella quintana* in body lice, *Pediculus humanus* L. Am. J. Trop. Med. Hyg. 77:562–566.
399. Seki N, et al. 2006. Epidemiological studies on *Bartonella quintana* infections among homeless people in Tokyo, Japan. Jpn. J. Infect. Dis. 59:31–35.
400. Selbach M, et al. 2009. Host cell interactome of tyrosine-phosphorylated bacterial proteins. Cell Host Microbe 5:397–403.
401. Seubert A, Falch C, Birtles RJ, Schulein R, Dehio C. 2003. Characterization of the cryptic plasmid pBGR1 from *Bartonella grahamii* and construction of a versatile *Escherichia coli-Bartonella* spp. shuttle cloning vector. Plasmid 49:44–52.
402. Seubert A, Hiestand R, de la Cruz F, Dehio C. 2003. A bacterial conjugation machinery recruited for pathogenesis. Mol. Microbiol. 49: 1253–1266.
403. Seubert A, Schulein R, Dehio C. 2002. Bacterial persistence within erythrocytes: a unique pathogenic strategy of *Bartonella* spp. Int. J. Med. Microbiol. 291:555–560.
404. Sheetz MP, Singer SJ. 1974. Biological membranes as bilayer couples. A molecular mechanism of drug-erythrocyte interactions. Proc. Natl. Acad. Sci. U. S. A. 71:4457–4461.
405. Smalley JW, Birss AJ, Silver J. 2000. The periodontal pathogen *Porphyromonas gingivalis* harnesses the chemistry of the mu-oxo bishaem of iron protoporphyrin IX to protect against hydrogen peroxide. FEMS Microbiol. Lett. 183:159–164.
406. Smalley JW, Silver J, Marsh PJ, Birss AJ. 1998. The periodontopathogen *Porphyromonas gingivalis* binds iron protoporphyrin IX in the mu-oxo dimeric form: an oxidative buffer and possible pathogenic mechanism. Biochem. J. 331:681–685.
407. Smitherman LS, Minnick MF. 2005. *Bartonella bacilliformis* GroEL: effect on growth of human vascular endothelial cells in infected cocultures. Ann. N. Y. Acad. Sci. 1063:286–298.
408. Stanton TB. 2007. Prophage-like gene transfer agents-novel mechanisms of gene exchange for *Methanococcus*, *Desulfovibrio*, *Brachyspira*, and *Rhodobacter* species. Anaerobe 13:43–49.
409. Struyve M, Moons M, Tommassen J. 1991. Carboxy-terminal phenylalanine is essential for the correct assembly of a bacterial outer membrane protein. J. Mol. Biol. 218:141–148.
410. Sweger D, et al. 2000. Conservation of the 17-kilodalton antigen gene within the genus *Bartonella*. Clin. Diagn. Lab. Immunol. 7:251–257.
411. Sykes JE, Henn JB, Kasten RW, Allen C, Chomel BB. 2007. *Bartonella henselae* infection in splenectomized domestic cats previously infected with hemotropic *Mycoplasma* species. Vet. Immunol. Immunopathol. 116:104–108.
412. Sykes JE, Lindsay LL, Maggi RG, Breitschwerdt EB. 2010. Human coinfection with *Bartonella henselae* and two hemotropic mycoplasma variants resembling *Mycoplasma ovis*. J. Clin. Microbiol. 48:3782–3785.
413. Szczesny P, et al. 2008. Structure of the head of the *Bartonella* adhesin BadA. PLoS Pathog. 4:e1000119.
414. Tarazona-Santos E, et al. 2011. Population genetics of GYPB and association study between GYPB*S/s polymorphism and susceptibility to *P. falciparum* infection in the Brazilian Amazon. PLoS One 6:e16123.
415. Taylor CT. 2008. Interdependent roles for hypoxia inducible factor and nuclear factor-kappaB in hypoxic inflammation. J. Physiol. 586: 4055–4059.
416. Thompson SA, et al. 1998. *Campylobacter fetus* surface layer proteins are transported by a type I secretion system. J. Bacteriol. 180:6450–6458.
417. Ticona E, Huaroto L, Garcia Y, Vargas L, Madariaga MG. 2010. The pathophysiology of the acute phase of human bartonellosis resembles AIDS. Med. Hypotheses 74:45–49.
418. Tolia NH, Enemark EJ, Sim BK, Joshua-Tor L. 2005. Structural basis for the EBA-175 erythrocyte invasion pathway of the malaria parasite *Plasmodium falciparum*. Cell 122:183–193.
419. Truttmann MC, et al. 2011. *Bartonella henselae* engages inside-out and outside-in signaling via integrin β1 and talin1 during invasome-mediated bacterial uptake. J. Cell Sci. 124:3591–3602.
420. Truttmann MC, Rhomberg TA, Dehio C. 2011. Combined action of the type IV secretion effector proteins BepC and BepF promotes invasome formation of *Bartonella henselae* on endothelial and epithelial cells. Cell. Microbiol. 13:284–299.
421. Umemori E, Sasaki Y, Amano K, Amano Y. 1992. A phage in *Bartonella bacilliformis*. Microbiol. Immunol. 36:731–736.
422. Urick T, Arena ICCE, Xu W, Bessman MJ, Ruffolo CG. 2005. The pnhA gene of *Pasteurella multocida* encodes a dinucleoside oligophosphate pyrophosphatase member of the Nudix hydrolase superfamily. J. Bacteriol. 187:5809–5817.
423. Valentine KH, et al. 2007. *Bartonella* DNA in loggerhead sea turtles. Emerg. Infect. Dis. 13:949–950.
424. Van Audenhove A, Verhoef G, Peetermans WE, Boogaerts M, Vandenberghe P. 2001. Autoimmune haemolytic anaemia triggered by *Bartonella henselae* infection: a case report. Br. J. Haematol. 115:924–925.
425. van Putten JP, Duensing TD, Cole RL. 1998. Entry of OpaA+ gonococci into HEp-2 cells requires concerted action of glycosaminoglycans, fibronectin and integrin receptors. Mol. Microbiol. 29:369–379.
426. van Uden P, Kenneth NS, Rocha S. 2008. Regulation of hypoxia-inducible factor-1alpha by NF-kappaB. Biochem. J. 412:477–484.
427. Vayssier-Taussat M, et al. 2010. The Trw type IV secretion system of *Bartonella* mediates host-specific adhesion to erythrocytes. PLoS Pathog. 6:e1000946.
428. Verma A, Davis GE, Ihler GM. 2001. Formation of stress fibres in human endothelial cells infected with *Bartonella bacilliformis* is associated with altered morphology, impaired migration and defects in cell morphogenesis. Cell. Microbiol. 3:169–180.
429. Verma A, Davis GE, Ihler GM. 2000. Infection of human endothelial cells with *Bartonella bacilliformis* is dependent on Rho and results in activation of Rho. Infect. Immun. 68:5960–5969.
430. Verma A, Ihler GM. 2002. Activation of Rac, Cdc42 and other downstream signalling molecules by *Bartonella bacilliformis* during entry into human endothelial cells. Cell. Microbiol. 4:557–569.
431. Vermi W, et al. 2006. Role of dendritic cell-derived CXCL13 in the pathogenesis of *Bartonella henselae* B-rich granuloma. Blood 107: 454–462.
432. Vigil A, et al. 2010. Identification of the feline humoral immune response to *Bartonella henselae* infection by protein microarray. PLoS One 5:e11447.
433. Wai SN, et al. 2003. Vesicle-mediated export and assembly of pore-forming oligomers of the enterobacterial ClyA cytotoxin. Cell 115:25–35.
434. Walker TS, Winkler HH. 1981. *Bartonella bacilliformis*: colonial types and erythrocyte adherence. Infect. Immun. 31:480–486.
435. Wallden K, Rivera-Calzada A, Waksman G. 2010. Type IV secretion systems: versatility and diversity in function. Cell. Microbiol. 12: 1203–1212.
436. Wan YY, Flavell RA. 2009. How diverse—CD4 effector T cells and their functions. J. Mol. Cell Biol. 1:20–36.
437. Wang HY, Tang H, Shen CK, Wu CI. 2003. Rapidly evolving genes in human. I. The glycophorins and their possible role in evading malaria parasites. Mol. Biol. Evol. 20:1795–1804.
438. Werth N, et al. 2010. Activation of hypoxia inducible factor 1 is a general phenomenon in infections with human pathogens. PLoS One 5:e11576.
439. Williams-Bouyer NM, Hill EM. 1999. Involvement of host cell tyrosine phosphorylation in the invasion of HEp-2 cells by *Bartonella bacilliformis*. FEMS Microbiol. Lett. 171:191–201.
440. Xu YH, Lu ZY, Ihler GM. 1995. Purification of deformin, an extracellular protein synthesized by *Bartonella bacilliformis* which causes deformation of erythrocyte membranes. Biochim. Biophys. Acta 1234: 173–183.
441. Yager JA, et al. 2010. Bacillary angiomatosis in an immunosuppressed dog. Vet. Dermatol. 21:420–428.
442. Yamamoto K, et al. 1998. Homologous protection but lack of heterologous-protection by various species and types of *Bartonella* in specific pathogen-free cats. Vet. Immunol. Immunopathol. 65: 191–204.
443. Yamamoto K, et al. 2002. Experimental infection of domestic cats with *Bartonella koehlerae* and comparison of protein and DNA profiles with those of other *Bartonella* species infecting felines. J. Clin. Microbiol. 40: 466–474.
444. Yamamoto K, et al. 2003. Infection and re-infection of domestic cats with various *Bartonella* species or types: *B. henselae* type I is protective against heterologous challenge with *B. henselae* type II. Vet. Microbiol. 92:73–86.
445. Yoshiji H, et al. 2005. Angiopoietin 2 displays a vascular endothelial

growth factor dependent synergistic effect in hepatocellular carcinoma development in mice. Gut 54:1768–1775.
446. **Zahringer U, et al.** 1995. The lipopolysaccharide of *Legionella pneumophila* serogroup 1 (strain Philadelphia 1): chemical structure and biological significance. Prog. Clin. Biol. Res. 392:113–139.
447. **Zahringer U, Lindner B, Inamura S, Heine H, Alexander C.** 2008. TLR2—promiscuous or specific? A critical re-evaluation of a receptor expressing apparent broad specificity. Immunobiology 213:205–224.
448. **Zahringer U, et al.** 2004. Structure and biological activity of the short-chain lipopolysaccharide from *Bartonella henselae* ATCC 49882^T. J. Biol. Chem. 279:21046–21054.
449. **Zeng H, Sanyal S, Mukhopadhyay D.** 2001. Tyrosine residues 951 and 1059 of vascular endothelial growth factor receptor-2 (KDR) are essential for vascular permeability factor/vascular endothelial growth factor-induced endothelium migration and proliferation, respectively. J. Biol. Chem. 276:32714–32719.
450. **Zhang P, et al.** 2004. A family of variably expressed outer-membrane proteins (Vomp) mediates adhesion and autoaggregation in *Bartonella quintana*. Proc. Natl. Acad. Sci. U. S. A. 101:13630–13635.
451. **Zhang X, Yang X, Kumar M, Pal U.** 2009. BB0323 function is essential for *Borrelia burgdorferi* virulence and persistence through tick-rodent transmission cycle. J. Infect. Dis. 200:1318–1330.
452. **Zhao SQ, Cai YF, Zhu ZY.** 2005. Comparative proteomic analysis of *B. henselae* Houston and *B. henselae* Marseille by two-dimensional gel electrophoresis. Biomed. Environ. Sci. 18:341–344.
453. **Zimmermann R, Kempf VA, Schiltz E, Oberle K, Sander A.** 2003. Hemin binding, functional expression, and complementation analysis of Pap 31 from *Bartonella henselae*. J. Bacteriol. 185:1739–1744.

Alexander Harms obtained his M.Sc. degree in molecular microbiology at the Biozentrum, University of Basel, Switzerland, for a project investigating the functional diversification of *Bartonella* effector proteins. He continues his work as a Ph.D. student on a scholarship from the Werner Siemens Foundation and is now exploring the biochemical interactions with host factors that drove the remarkable parallel evolution of these effectors. His main research interest is the molecular evolution of *Bartonella*, particularly the biochemical and genetic mechanisms that underlie the exceptional success of the members of this genus as ubiquitous stealth pathogens.

Christoph Dehio received his Ph.D. in 1992 from the University of Cologne in Germany. From 1993 to 1995, he conducted postdoctoral research at the Institut Pasteur in Paris, France. From 1995 to 2000, he was a research group leader at the Max Planck Institute for Biology in Tübingen, Germany. Since 2000, he has been a research group leader at the Biozentrum of the University of Basel, Switzerland, where he holds the position of Associate Professor in molecular microbiology. Since 1995, he has devoted his research to the analysis of *Bartonella* pathogenesis. His current research focuses on studying the molecular, cellular, and evolutionary roles of type IV secretion systems in *Bartonella*-host interaction.

6.2.Unpublished results related to Review article I

A considerable number of studies on *Bartonella* have been published in the time between the finalization of *Review article I* and this work that have broadened our understanding of the molecular pathogenesis of *Bartonella*. In particular, the research on *Bartonella* evolution and phylogeny has progressed with remarkable speed so that new hypotheses and models need to be embraced as a basis for *Perspective* on the evolution of VirB/D4 T4SS and its effector proteins. I therefore use the opportunity to shortly summarize recent developments in the *Bartonella* field as an update of *Review article I*:

Bartonella infections in general

- In *Review article I* I had pointed out that it was disputed if the bartonellae represent true emerging pathogens or whether rather the awareness of *Bartonella* infections is emerging[320]. A new study now revealed that ecological alterations caused by human interventions can promote the prevalence of zoonotic pathogens like (specifically) *Bartonella* in nature[321]. Similarly, the research community concerned with Carrion's disease recently warned that the endemic area of this debilitating infection – so far generally confined to rural areas in the Andes highlands – is spreading, likely due to climate change and other anthropogenic factors influencing vector ecology[301].
- The remarkable adaptability of the radiating lineages of *Bartonella* (particularly L4) to new host species has been confirmed by the finding that – apart from mammals – not only reptiles like sea turtles, but also birds can be infected[293]. A newly identified species of *Bartonella* L2 confirms the ruminant-restricted host range of this lineage and is associated to camelids as its reservoir host[322].
- A pair of new studies showed that the host-interacting VirB/D4 T4SS of *B. henselae* can interact with the DNA processing and transfer machinery of enterobacterial R388 as well as a cryptic *Bartonella* plasmid and consequently transfer DNA into human cells where it may then integrate into the genome[323,324]. These findings reveal a remarkable conservation of the machinery providing the DNA substrate for bacterial conjugation and provide an interesting starting point to develop new tools for the genetic modification of eukaryotic cells.

Different virulence factors

- A recent study by Quebatte, Dick, *et al.* revealed that signaling of the BatR / BatS two-component system modulates *Bartonella* virulence gene expression in coordination with the stringent response to regulate the expression pattern of pathogenicity factors during different stages of the infection cycle[325]. Furthermore, several other studies exploring the transcriptional regulation of *Bartonella* virulence factors have been published, e.g., on the

influence of temperature (and therefore host or vector state of the infection) on the transcriptome of *B. quintana*[326].

- New data on the BadA TAA of *B. henselae* suggest that the stalk of BadA is responsible for fibronectin binding, while head and stalk together mediate adhesion to collagen and, most importantly, host cells for transcriptional reprogramming[327].
- A pair of high-coverage transcriptome and proteome analyses of *B. henselae* str. Houston-1 complements genomic annotations with data on subcellular localization and differential regulation under conditions mimicking the primary niche interaction with host cells. Notably, the authors catalogued all OMPs of *B. henselae* and suggest a massive reorganization of the membrane proteome regarding OMPs as well as type IV and type V secretion systems upon host interaction[328,329].
- *Review article I* had proposed based on according suggestions in the literature that some Hbps of *Bartonella* may form an antioxidant surface coat via heme acquisition. This model has been confirmed by two studies:
    - The Koehler lab showed that HbpC is secreted together with HbpA on outer membrane vesicles (OMVs) to protect the bacteria against toxic concentrations of heme[282]. They demonstrate for the first time that *Bartonella* is shedding OMVs and uses them in the context of infections (which had already been proposed in *Review article I*, albeit with a different reasoning). Thereby, they reveal a previous confusion between these structures and the phage-like particles of the gene transfer agent which had been mistakenly seen as a single entity before, causing HbpA to be first described as Pap31 (phage-associated protein of 31 kDa)[330].
    - A comparative study exploring the Hbps of *B. henselae* showed that these proteins can be functionally expressed in *E. coli* and promote the uptake of heme via a heterologous heme transporter. The authors reveal that *hbpA* is essential in *Bartonella* and that all Hbps contribute to the protection against oxygen radicals. Furthermore, they provide evidence that HbpA and HbpD may be involved in host cell invasion[331].

Type IV secretion systems

- The study by Deng *et al.* identified the host target of the Trw T4SS on erythrocytes as band 3 and showed its interaction with two copies of the TrwJ pilus component[306]. Band 3 had been mentioned in *Review article I* as a potential target of *Bartonella* manipulations on red blood cells since it is critical for their surface tightness by connecting the membrane to the underlying cytoskeleton (and a known interaction partner of *B. bacilliformis*) It will therefore be interesting to see if additional roles of band 3 for *Bartonella* infections on top of plain adhesion via the Trw T4SS may be discovered.

- New data on the biological functions of Beps secreted by the VirB/D4 T4SS of L4 have been published:
    - Truttmann *et al.* revealed that the anti-endocytic effect of BepC in combination with BepF requires the two BID domains of BepF which likely act via the manipulation of small GTPases in the host cell. Furthermore, the study showed that the tyrosine motifs of BepF are phosphorylated upon translocation into host cells but have no contribution to the anti-endocytic phenotype[224].
    - A study by Pulliainen, Pieles *et al.* found that the anti-apoptotic effect of the BID domain of BepA on host cells is mediated via a direct interaction with adenylyl cyclase (AC) and the Gα subunit of an AC-stimulating G protein causing an increase in cellular cAMP levels[312].
    - The work of Okujava *et al.* showed that BepE is required for the dissemination of *Bartonella* from the dermal inoculation site to the bloodstream *in vivo* and for the migration of infected dendritic cells through a lymphatic endothelial cell layer *in vitro*. Interestingly, BepE counteracts a cell fragmentation phenotype of BepC that is caused by impaired cell migration. The authors therefore reasonably speculate that “infected dermal dendritic cells may be involved in disseminating *Bartonella* towards the blood stream”. Furthermore, they propose to split the old model of a “primary niche” into a “dermal niche” comprising the initial steps upon *Bartonella* inoculation and a “bood seeding niche” where *Bartonella* is primed for erythrocyte infection[313].
- *Review article I* had highlighted the problematic situation that the two main virulence factors of *B. henselae*, the BadA TAA and the VirB/D4 T4SS, have so far primarily been investigated in strains that lacked functional expression of the respective other one. A study by Lu, Franz, Truttmann *et al.* now investigated the phenotypes associated with these virulence factors in a strain expressing both and found that the dense surface layer formed by BadA somehow interferes with type IV effector secretion, probably by impairing physical contact between VirB/D4 T4SS and the host cell. Consistently, BadA as a remarkably long, filamentous protein was not affected by the presence of the VirB/D4 T4SS. The authors therefore conclude that the expression of the VirB/D4 T4SS and (particularly) the TAAs may be coordinated in *Bartonella* to enable optimal manipulation of host cells during infections[332].

Open questions regarding the molecular pathogenesis of *Bartonella*

Despite considerable progress in the field, a number of research questions and elusive gaps in our understanding of the molecular pathogenesis of *Bartonella* are still open for investigation:

- the molecular functions of *iba* type autotransporters that appear to be essential for infection *in vivo*
- the molecular identity of the invasin(s) responsible for the zipper-like uptake of *Bartonella* into host cells at the primary niche
- the intracellular trafficking of *Bartonella* within nucleated cells (so far, only few elusive factors and HbpD have been shown to be essential for phagosomal escape in *B. henselae*[333])
- the molecular identity and mode of action of deformin
- the mechanism(s) of erythrocyte invasion using flagella or Trw T4SS
- the potential role of cyclic β-(1,2)-glucans as conserved host interaction factors of Rhizobiaceae[334] in *Bartonella* infections

It remains to be seen whether the dynamics of project development in the field will result in the exploration of one or more of these topics in the future.

***Bartonella* evolution and phylogeny**

- In *Review article I* I had discussed that *B. quintana*, being actually a clone that emerged out of *B. henselae*, is still in the process of adaptation to humans as its primary host based on the presence of discernable disease symptoms in immunocompetent patients. New studies now revealed that *B. quintana* infections are common among macaque monkeys where they cause “long-lasting chronic bacteremia without apparent clinical abnormalities”[335]. The authors further showed that only a subset out of the diversity of *B. quintana* strains found in macaques is likely able to infect humans[336]. Taken together one may be able to state with some justification that *B. quintana* is rather a zoonotic than a true human pathogen.
- The study by Guy *et al.*[284] followed up on previous work focusing on the gene-transfer agent in *Bartonella* (BaGTA)[318] whose importance and ubiquity had also been highlighted in *Review article I*. Importantly, the authors constructed a new phylogeny of *Bartonella* based on a considerable amount of new data and species that is partially not in line with the phylogeny published by Engel *et al.*[169] (see a summary under the next bullet point). Furthermore, they claim that the acquisition of BaGTA in combination with a phage-derived origin of run-off replication (ROR) by a common ancestor of all bartonellae was the original key innovation that kick-started the adaptive evolution of the genus. In their

model, the ROR origin serves to bias the exchange of chromosomal DNA via the BaGTA by amplification of a specific region of the genome that is accumulating various secretion systems and thereby prevents the emergence of cheaters that would lose these systems by enforcing constant re-acquisition. Like this, the BaGTA may constitute a true social trait and furthermore promote the horizontal exchange both of novel secretion systems as well as the evolution of established secretion systems (and other genes) via recombination. The results of this study readily explain old findings of remarkable diversity among *Bartonella* secretion systems and are confirmed by newer work showing widespread interspecies allelic recombination of various virulence factors in *Bartonella*[225,337-339]*.*

- The recent landmark study by Zhu *et al.*[267] also has to be seen in context of the work of Guy *et al.*[284] who hypothesized that "the plasticity given to [the ROR region containing various secretion systems] by the BaGTA has rescued *Bartonella* from the reductive evolutionary processes that are operating on host-specialized bacteria adapted to otherwise sterile intracellular environments". In short, Zhu *et al.* propose that *Bartonella* had been on an evolutionary track towards obligate intracellularity (likely in insects) but then turned around facilitated by the (re)acquisition of functions necessary for growth outside host cells. This view is strongly supported by studies reporting ancestral *Bartonella*-like bacteria as part of the microbiota that thrives within ants[340,341] or bees[342,343], though it is not finally known whether these represent symbionts, commensals, or pathogens. Furthermore, it was shown that bat flies are frequent carriers of *Bartonella* and that the four lineages of Engel *et al.*[169] are merely islands within the diversity of bat fly associated bartonellae[344]. Additionally, ancestral mammal-infecting species of *Bartonella* that clearly stand outside of this four-lineage system have been described with *B. australis*[345] (see phylogeny by Guy *et al.*[284]) and particularly *B. tamiae*. The latter species is apparently able to cause considerable sickness in infected hosts (including humans) and only distantly related to the other bartonellae, but was reported to be most closely related to the *Bartonella* bacteria found in bees[346,347]. The relations of these different species of *Bartonella* have been resolved by the congruent phylogenies published within the work of Guy *et al.*[284] and Zhu *et al.*[267] that confirmed the lineages described by Engel *et al.* (see figure 12). In short, the following picture is emerging regarding the bartonellae infecting mammal hosts (compare Figure 15):
    - *B. tamiae* holds an isolated position outside of the other species (for which Zhu *et al.* coined the term "eubartonellae")
    - within the eubartonellae, *B. australis* forms an ancestral lineage outside of a monophyletic group formed by the four lineages of Engel *et al.*[169]

- within this group, L1 with *B. bacilliformis* is not a deep-branching ancestral lineage, but the sister clade of ruminant-infecting L2, thereby forming a clade of bartonellae that lack host-interacting type IV secretion systems and are restricted to infect a very limited host range
- L3 is the sister clade of this group formed by L1 and L2 and not of L4, thus highlighting that the acquisitions of the VirB/D4 T4SS with a single primordial effector in common ancestors both of L3 and L4 were separate events
- ancestral *B. australis* harbors a Trw T4SS *at the same chromosomal locus* as L4 while *B. tamiae* does not (personal observation), suggesting that this machinery was acquired in a common ancestor of the eubartonellae and later lost in a common ancestor of L1-3, possibly due to evolutionary instability in combination with flagellation
- various representatives of L2-4 as well as *B. australis* (genomic copy) harbor a Vbh T4SS either plasmid-encoded and / or in form of a genomic island; in contrast, *B. bacilliformis* and the sequenced strains of *B. tamiae* lack such a machinery (personal observation; see also Figure 37 in the *Perspective* section)

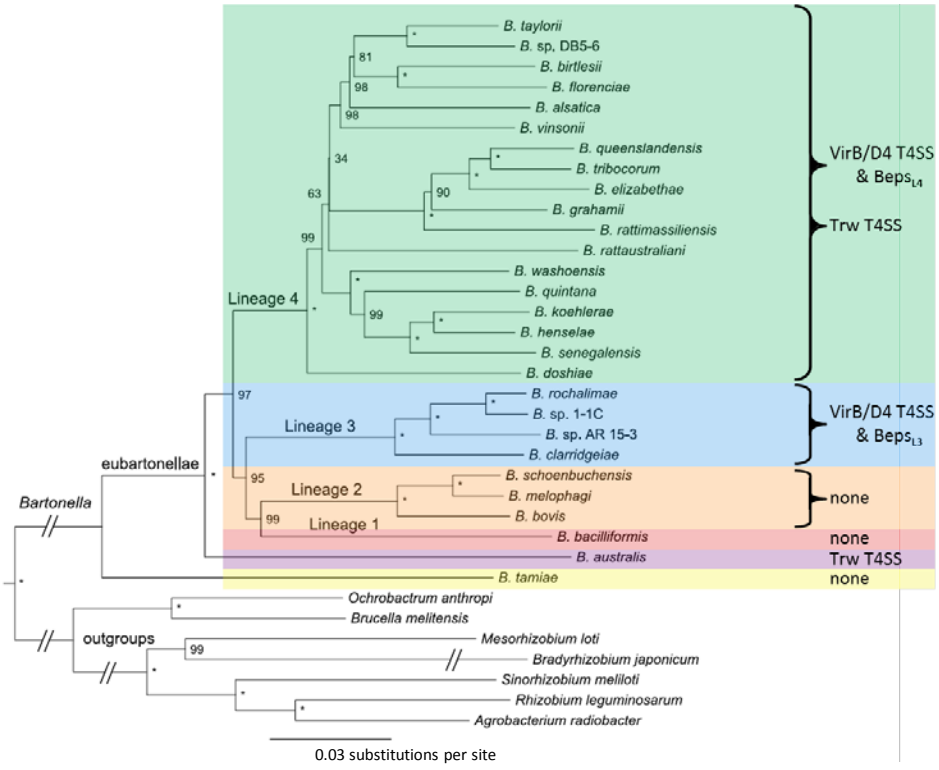

Figure 15: Current phylogeny of bartonellae infecting mammals. The phylogenic tree was adapted from Zhu *et al.*[267] and is congruent with the phylogeny published by Guy *et al.*[284]. I indicated presence and absence of the established host-interacting type IV secretion systems VirB/D4 and Trw and color-coded the different lineages of *Bartonella* as presented by Engel *et al.*[169] (compare Figure 12). The phylogeny had been constructed from a maximum likelihood analysis of "commonly used genetic markers of 28 *Bartonella* species, rooted to Rhizobiales". Node labels indicate bootstrap support values (of 100 replicates) with asterisks representing 100% support. Note that only known animal or human pathogens within *Bartonella* are shown in the tree and that the seemingly homogenous group of mammal-infecting bartonellae is paraphyletic with respect to insect-associated species (see details in the running text).

- Coming to the intracellularity of ancestors of *Bartonella*, the study by Zhu *et al.*[267] revealed that the *glpK* (glycerol kinase) gene had been lost together with the *glp* glycerol uptake system in a common ancestor of all bartonellae which firmly excludes the use of extracellular glycerol. In addition, a common ancestor of all eubartonellae lost the gene encoding GpsA (glycerol-3-phosphate (G3P) dehydrogenase), the protein that can regenerate G3P from the glycolysis. In consequence, the bacteria would have had to rely directly on the import of G3P which is a strictly intracellular metabolite, making it clear for the authors that all extant bartonellae evolved from ancestors with an obligate intracellular lifestyle. Conspicuously, *glpK* and *gpsA* have been re-acquired independently from each other in common ancestors of different clades of extant bartonellae from diverse sources: While *B. tamiae* regained *glpK*, the common ancestors of L4, of L1 and L2, as well as an ancestor of *B. australis* acquired *gspA.* Importantly, *B. bacilliformis* and L2 share the same heterologous allele of *gpsA* at the same locus which rules out an ancestral, isolated position of L1. The authors identified the sources of *glpK* and *gpsA* alleles acquired by *Bartonella* as different groups of proteobacteria that are mostly obligate endosymbionts of arthropods, especially keds and bat flies or aphids (suggesting horizontal transfer in a common arthropod host), while one *gpsA* was acquired from *Helicobacter* (suggesting horizontal transfer in a mammalian host). They therefore reasonably conclude that ancestral bartonellae lived in close association with arthropods that fed on mammal hosts.

  Interestingly, neither *glpK* nor *gpsA* has been regained in L3 of *Bartonella* which the authors use to explain the notoriously poor growth of these bacteria on artificial media.

In summary, these new studies exploring the phylogeny and evolution of *Bartonella* strongly confirm the general conclusions drawn from previous work of our laboratory[169,275] although some details now need to be seen from a different perspective. For example, the fact that L3 and L4 are not sister clades makes it much clearer that they acquired a primordial VirB/D4 T4SS with a single ancestral effector at two separate events. Furthermore, the newly structured phylogeny highlights the stark contrast between two species-rich clades L3 and L4 that infect a wide range of host species and another clade of species-poor eubartonellae formed by L1 and L2. Since only L3 and L4 harbor a VirB/D4 T4SS and because their explosive radiations had only been triggered after the parallel evolution of host-secreted effector cocktails in common ancestors of both lineages, the critical role of this machinery for host interaction and adaptation is now even more apparent.

6.3.Research article I (published)

"'If you want to understand function, study structure,' I was supposed to have said in my molecular biology days. (I believe I was sailing at the time.)
[…] In nature hybrid species are usually sterile, but in science the reverse is often true. Hybrid subjects are often astonishingly fertile, whereas if a scientific discipline remains too pure it usually wilts."

Francis Crick, English biologist and Nobel laureate, in "What Mad Pursuit: A Personal View of Scientific Discovery" (1988). Cited from page 150 of the paperback in the Alfred P. Sloan Foundation series (ISBN 0-465-09138-5)

Adenylylation control by intra- or intermolecular active-site obstruction in Fic proteins

Philipp Engel*, Arnaud Goepfert*, Frédéric V. Stanger, Alexander Harms, Alexander Schmidt, Tilman Schirmer, and Christoph Dehio

*These authors contributed equally to this work

Nature, Volume 482, Issue 7383, February 2012, 107-110.

Summary

Previous research on FIC domain proteins had frequently revealed deleterious phenotypes caused by their adenylylation activity such as host cell death via destruction of the cytoskeleton by different bacterial virulence factors or “filamentation induced by cAMP” of the *E. coli fic-1* allele. However, the absence of any obvious phenotype upon expression of wildtype *E. coli* Fic or human HypE (which shares the same biochemical activity as the cell-killing bacterial virulence factors) made clear that the potent activities of FIC domain proteins are tightly regulated, though the underlying mechanism had remained elusive.

During an investigation of a Bep-like protein of *B. schoenbuchensis* as a potential virulence factor we found that this protein (called VbhT) inhibited the growth of *E. coli* and *Bartonella* in dependence of the integrity of its FIC domain active site motif. This phenotype could be blocked by VbhA, a small protein encoded directly upstream of VbhT, and VbhA also inhibited the adenylylation activity of VbhT. We therefore concluded that VbhT causes bacterial growth inhibition via the adenylylation of cellular targets. A crystal structure of VbhT in complex with VbhA revealed that an α-helix of VbhA interacted with the active site of VbhT, indicating that VbhA interferes with the catalytic activity of toxin VbhT as a type II TA antitoxin. The tip of this inhibitory α-helix (α_{inh}) in VbhA homologs contains an (S/T)xxxE(G/N) motif with the invariant glutamate pointing into the active site.

Intriguingly, a comparison of the VbhTA complex with different FIC domain structures available in databases showed that an α_{inh} was generally present, but usually part of the same protein as the FIC domain. Based on the positioning of the α_{inh} either in a separate small protein or in the same polypeptide N- or C-terminally to the Fic core we categorized FIC domain proteins as class I, class II, or class III, respectively. For a deeper analysis, we predicted the structure of all FIC domain proteins listed in the Pfam database and analyzed the distribution of the three classes. Of all FIC domain proteins around 2/3 harbored a clearly recognizable α_{inh} with inhibition motif, and this proportion rose to 90% when only Fic proteins with an active site motif presumably capable of adenylylation were considered, suggesting co-evolution of activity and regulation. Based on analyses of Fic sequences and structures we defined the canonical adenylylation-competent active site motif as HxFx(D/E)GNGRxxR and concluded that conserved groups of FIC domain proteins harboring different active site motifs (like the Doc family) may have evolved different catalytic activities. Among the *bona fide* adenylylation-competent FIC domain proteins 80% belong to class II and roughly each 5% can be categorized as class I and class III. Furthermore, we performed an in-depth analysis of the phylogenetic distribution of FIC domain sequences which revealed that proteins assigned to classes I and III form monophyletic groups that arose as secondary

branches within a tree dominated by class II proteins. FIC domain proteins with degenerate active site motifs are found scattered all over the tree, suggesting that they have recurrently arisen from adenylylation-competent FIC domain proteins by sequence deterioration or adaptive evolution. The Doc family is an exception to this pattern since it lacks an adenylylation-competent active site motif and forms a large cluster of sequences that is separate from all other FIC domain proteins as a deep-branching lineage.

A comparative structural and biochemical analysis of different FIC domain mutants showed that the invariant glutamate of the (S/T)xxxE(G/N) motif interacts with an arginine at the active site that normally binds the γ-phosphate of the ATP substrate. This interaction displaces the γ-phosphate of the ATP and thereby causes a reorientation of the α-phosphate in a way that is not permissive for an in-line nucleophilic attack by the target residue, thus preventing adenylylation. Consistently, mutational abrogation of α_{inh}-mediated FIC domain inhibition in VbhTA of *B. schoenbuchensis*, SoFicT of *Shewanella oneidensis*, and NmFicT of *Neisseria meningitidis* as models for Fic classes I, II, and III, respectively, resulted in growth arrest upon ectopic expression in *E. coli*. In all cases, this growth inhibition correlated with an activation of the proteins' adenylylation activity regarding both auto-adenylylation and, for VbhT and NmFicT, detectable target adenylylation in *E. coli* lysates. While VbhT showed adenylylation of a ca. 80 kDa target, the NmFicT adenylylation activity resulted in three bands at 80 kDa, 100 kDa, and 150 kDa. Similarly, the abrogation of FIC domain inhibition boosted both auto-adenylylation and target adenylylation of human HypE.

In summary, the research presented in this article uncovered a regulatory mechanism that is broadly conserved among adenylylating FIC domain proteins and that controls their enzymatic activity by preventing the binding of ATP in an adenylylation-competent conformation. Our findings posed two major questions that may guide future research[a]:

- What are the enzymatic targets of the adenylylation activity of bacterial FIC domain proteins that results in bacterial growth arrest, and what is their biological function? While VbhTA shows features of type II TA modules, there is no easy hint at the biological role of class II and class III FIC domain proteins.
- What is the functional relevance of the auto-adenylylation activity that seems to be a universal feature of FIC domain proteins? We could map the auto-adenylylation of NmFicT to an invariant tyrosine of the α_{inh} in class III Fic proteins close to the (S/T)xxxE(G/N) motif, suggesting that auto-adenylylation 1) is inter-molecular (given its positioning relative to the active site) and 2) may have a regulatory role in relieving inhibition by the α_{inh}.

[a] Further results shedding light on the biological functions of FIC domain target adenylylation and auto-adenylylation are presented in *Research articles III* and *IV*.

Statement of the own participation

I contributed to this publication by the development of an adenylylation assay that greatly facilitated the explorative work on FIC domain proteins because it allowed to visualize both auto- and target adenylylation using processed lysates of ectopically expressing *E. coli* instead of purified proteins. I performed the majority of adenylylation assays shown in this publication. Furthermore, I analyzed diverse Fic protein constructs regarding their ability to inhibit *E. coli* growth. Additionally, I cloned a number of plasmid constructs and had established a protocol for site-directed mutagenesis in our laboratory that was instrumental for the construction of the vast amount of plasmid mutants used in this publication. The other authors performed all bioinformatic analyses and expressed and purified all recombinant protein constructs. They carried out all structural studies, performed the mass spectrometry analysis, and had discovered the mechanism of active-site obstruction. All authors contributed to experimental design, participated in data analysis, and wrote the manuscript.

LETTER

doi:10.1038/nature10729

Adenylylation control by intra- or intermolecular active-site obstruction in Fic proteins

Philipp Engel[1]†*, Arnaud Goepfert[1,2]*, Frédéric V. Stanger[1,2], Alexander Harms[1], Alexander Schmidt[3], Tilman Schirmer[2] & Christoph Dehio[1]

Fic proteins that are defined by the ubiquitous FIC (filamentation induced by cyclic AMP) domain are known to catalyse adenylylation (also called AMPylation); that is, the transfer of AMP onto a target protein. In mammalian cells, adenylylation of small GTPases through Fic proteins injected by pathogenic bacteria can cause collapse of the actin cytoskeleton and cell death[1,2]. It is unknown how this potentially deleterious adenylylation activity is regulated in the widespread Fic proteins that are found in all domains of life and that are thought to have critical roles in intrinsic signalling processes. Here we show that FIC-domain-mediated adenylylation is controlled by a conserved mechanism of ATP-binding-site obstruction that involves an inhibitory α-helix (α_{inh}) with a conserved (S/T)XXXE(G/N) motif, and that in this mechanism the invariable glutamate competes with ATP γ-phosphate binding. Consistent with this, FIC-domain-mediated growth arrest of bacteria by the VbhT toxin of *Bartonella schoenbuchensis* is intermolecularly repressed by the VbhA antitoxin through tight binding of its α_{inh} to the FIC domain of VbhT, as shown by structure and function analysis. Furthermore, structural comparisons with other bacterial Fic proteins, such as Fic of *Neisseria meningitidis* and of *Shewanella oneidensis*, show that α_{inh} frequently constitutes an amino-terminal or carboxy-terminal extension to the FIC domain, respectively, partially obstructing the ATP binding site in an intramolecular manner. After mutation of the inhibitory motif in various Fic proteins, including the human homologue FICD (also known as HYPE), adenylylation activity is considerably boosted, consistent with the anticipated relief of inhibition. Structural homology modelling of all annotated Fic proteins indicates that inhibition by α_{inh} is universal and conserved through evolution, as the inhibitory motif is present in ~90% of all putatively adenylylation-active FIC domains, including examples from all domains of life and from viruses. Future studies should reveal how intrinsic or extrinsic factors modulate adenylylation activity by weakening the interaction of α_{inh} with the FIC active site.

In two Fic proteins, IbpA and VopS, that are translocated by pathogenic bacteria into host cells, the ubiquitous FIC domain has been shown to catalyse adenylylation[1–4]. The crystal structure of the effector domain IbpA(FIC2) in complex with its adenylylated host target Cdc42 has been reported[5] and a catalytic mechanism has been proposed[5,6]. IbpA- or VopS-mediated adenylylation of Rho-family GTPases abolishes downstream signalling in human cells and, thus, causes actin cytoskeleton collapse and cell death[1,2]. By contrast, overexpression of a human Fic protein with similar target specificity, HYPE, had only a marginal effect[1]. This suggests that the potentially deleterious adenylylation activity is tightly regulated in HYPE and probably in most of the almost 3,000 Fic proteins that are proposed to have important roles in intrinsic signalling processes in bacteria, archaea and eukaryotes.

VbhT is a bacterial Fic protein of the mammalian pathogen *B. schoenbuchensis*[7,8]. It is composed of an N-terminal FIC domain and a C-terminal BID domain (Fig. 1a). The BID domain facilitates protein translocation into mammalian or bacterial target cells through a type IV secretion system or conjugation machinery[9], respectively, but the target cell and functional role of VbhT are unknown. VbhT arrests growth when expressed in *Escherichia coli* (Fig. 1c and Supplementary Fig. 1a). Growth arrest is repressed by mutation of histidine to alanine (VbhT(H136A)) in the conserved FIC motif HXFX(D/E)GNGRXXR. In other Fic proteins, this signature motif has been shown to be essential for target protein adenylylation activity[1,2,10], therefore suggesting that toxicity is related to adenylylation of endogenous proteins. Indeed, wild-type VbhT, but not VbhT(H136A), catalysed *in vitro* adenylylation of a putative *E. coli* target protein of approximately 80 kilodaltons (kDa) (Fig. 1d). Furthermore, *E. coli* cells showed filamentation after expression of wild-type VbhT, but not of VbhT(H136A) (Supplementary Fig. 2). A similar phenotype has been described for what is thought to be a hyperactive mutant of the *E. coli* Fic protein[11]. Co-expression of VbhT with VbhA, encoded by the small open reading frame *vbhA*

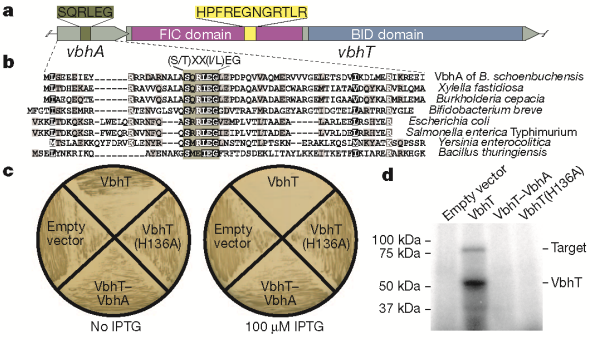

Figure 1 | The small protein VbhA represses the toxic effect (growth arrest) that is mediated by the adenylylation activity of VbhT in *E. coli*. **a**, Genetic organization of the type-IV-secretion-system-associated locus of *B. schoenbuchensis*, which is composed of the overlapping *vbhA* and *vbhT* genes. The FIC and BID domains that are encoded by *vbhT* are shown in different colours. Protein translations of the regions encoding the conserved motif of VbhA and the FIC motif of VbhT are depicted. **b**, Protein alignment of VbhA and a subset of the 158 homologues that are encoded upstream of *fic* loci in different bacteria (see also Supplementary Fig. 4). The most conserved region shows a (S/T)XX(I/L)EG consensus. Sequence accessions and strain designations are given in Supplementary Fig. 4. **c**, Growth of *E. coli* on lysogeny broth (LB) plates after IPTG-induced expression of different VbhT and VbhA constructs. Expression of VbhT shows a toxic effect, whereas bacterial growth is not affected when VbhT(H136A) is expressed or when VbhT and VbhA are co-expressed (VbhT–VbhA). All *E. coli* strains revealed normal growth without induction. Growth curve experiments in LB gave analogous results (Supplementary Fig. 1). **d**, Adenylylation assay with crude cell lysates of *E. coli* ectopically expressing the same constructs as in panel **c**.

[1]Focal Area Infection Biology, Biozentrum, University of Basel, CH-4056 Basel, Switzerland. [2]Core Program Structural Biology and Biophysics, Biozentrum, University of Basel, CH-4056 Basel, Switzerland. [3]Proteomics Core Facility, Biozentrum, University of Basel, CH-4056 Basel, Switzerland. †Present address: Department of Ecology and Evolutionary Biology, Yale University, New Haven, CT 06520-8106, USA. *These authors contributed equally to this work.

©2012 Macmillan Publishers Limited. All rights reserved

RESEARCH LETTER

immediately upstream of *vbhT* (Fig. 1a), completely repressed VbhT toxicity, as shown by wild-type-like bacterial growth, normal cell morphology, and inhibition of VbhT-dependent adenylylation (Fig. 1 and Supplementary Figs 1a and 2). We also observed VbhT-mediated toxicity and its repression by VbhA in *B. schoenbuchensis*, the natural carrier of this toxin and antitoxin, and in the related species *Bartonella henselae* (Supplementary Fig. 3).

The inhibitory action of VbhA on the VbhT toxin, and the genetic organization of the respective genes in an operon are reminiscent of toxin–antitoxin modules that are found in many bacterial genomes, often associated with mobile genetic elements[12]. A comprehensive analysis of the upstream region of FIC-domain-encoding genes (PFAM pf02661) identified 158 bacterial *vbhA* homologues that probably function as antitoxins. Although the sequences are rather diverse, a central (S/T)XX(I/L)EG motif is conspicuous (Fig. 1b and Supplementary Fig. 4). The high-resolution (1.5 Å) crystal structure of VbhA in complex with the FIC domain of VbhT (VbhT(FIC)) (Supplementary Table 1) shows that VbhA is folded into three anti-parallel helices that tightly embrace VbhT(FIC) (Fig. 2a) with the N-terminal helix (α_{inh}), adopting a location that is analogous but distinct to that of the antitoxin Phd in its complex with Doc[13] (Supplementary Fig. 5). Doc is a Fic protein with a degenerate, probably adenylylation-incompetent FIC motif[14] that may have adopted another toxic activity (Supplementary Information, section 1). The VbhA antitoxin motif locates to the C-terminal part of α_{inh} and is positioned close to the putative ATP-binding site[10] at the N-cap of the helix that follows the active loop of VbhT(FIC). This suggests that the antitoxin competes with ATP binding. VbhA residues Ser 20 and Glu 24 of the inhibitory motif form a hydrogen bond and a salt bridge, respectively, with the conserved Arg147 of VbhT following the active loop.

Intriguingly, structural comparison with other bacterial Fic proteins of known fold (Fic proteins from *S. oneidensis* (SoFic)[14,15] and from *N. meningitidis* (NmFic)[14] (Fig. 2b, c), and from *Bacteroides theataiotaomicron* (BtFic)[14] and from *Helicobacter pylori* (HpFic)[14] (Supplementary Fig. 6)) reveals that a structural equivalent of α_{inh} can be part of the FIC domain fold itself. Moreover, these proteins also show the SXXXE(G/N) inhibitory motifs that are, with respect to the FIC active site, arranged exactly as in the VbhA-VbhT(FIC) complex. Along the polypeptide chain, however, these α_{inh} occur at two distinct locations either in the N-terminal part (SoFic and BtFic) or at the C terminus (NmFic and HpFic). Thus, Fic proteins containing α_{inh} can be grouped into three classes (Fig. 2d) depending on whether α_{inh} is provided by an interacting antitoxin (class I) or whether it is part of the FIC fold as an N-terminal helix (class II) or a C-terminal helix (class III).

To investigate the distribution of class II and class III Fic proteins, we predicted the structures of all PFAM FIC domain entries by homology modelling (Supplementary Information, section 1). Including the class I proteins that are identified above, two-thirds of all Fic proteins were classified (Fig. 2e and Supplementary Table 2), with a strong dominance of class II, the class to which human HYPE belongs (Supplementary Tables 3 and 4). The proportion of classified Fic proteins increases to 90% when considering only adenylylation-competent Fic proteins that are defined by compliance with the HXFX(D/E)GNGRXXR motif (Supplementary Text). This suggests co-evolution of catalytic and inhibitory function. The inhibition motifs that are derived from Psi-Blast (class I) and structural predictions (classes II and III) are shown in Fig. 2f with the overall consensus being (S/T)XXXE(G/N). The strict conservation of the glutamate is striking and indicates that the observed ionic interaction with the second arginine of the conserved FIC motif (Figs 2a–c) is crucial for inhibition. Phylogenetic distribution of class I

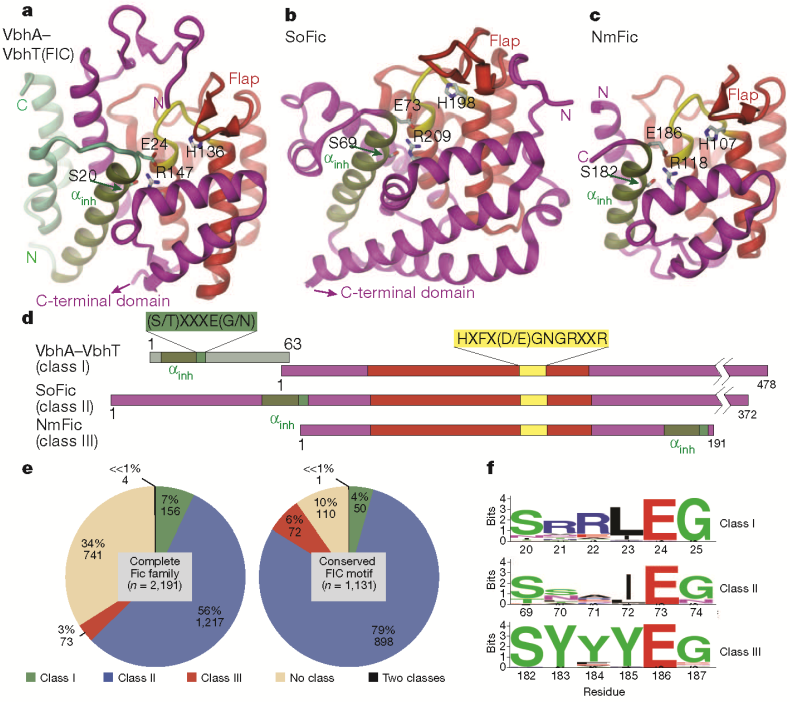

Figure 2 | Structures and classification of Fic proteins according to the position of the inhibitory motif along the polypeptide chain. Structures are shown in cartoon (FIC core as defined by PFAM, red; active site loop with histidine, yellow; inhibitory helix (α_{inh}) with SXXXE(G/N) motif, green) with important residues in full. **a**, Complex of VbhT(FIC) with antitoxin VbhA (green). **b**, SoFic (from *S. oneidensis*, PDB code 3EQX) with C-terminal domain omitted. **c**, NmFic (from *N. meningitidis*, PDB code 2G03). **d**, Linear organization of motifs in the proteins presented in panels **a**–**c**. **e**, Distribution of the three Fic protein classes for the entire family in the PFAM database (left) and the subset of Fic proteins with the conserved FIC motif HXFX[(D/E)GNGRXXR that is likely to convey adenylylation activity (right; see also Supplementary Information, section 1). **f**, Sequence profiles for the inhibition site of the three Fic protein classes.

©2012 Macmillan Publishers Limited. All rights reserved

and class III Fic proteins indicates that each is of monophyletic origin (Supplementary Fig. 7). Fic proteins with a degenerate FIC motif are dispersed over the tree, with the exception of the large cluster of Doc-like toxins. This suggests that there is recurrent degeneration of the conserved FIC motif with concomitant loss of adenylylation activity. Consistent with this, deterioration of the FIC motif seems to correlate with the absence of a recognizable inhibitory motif (Supplementary Fig. 7). Fic proteins with a degenerate FIC motif may display catalytic activities different from adenylylation, such as phosphocholination, as reported for the *Legionella pneumophila* effector AnkX[16].

Owing to our discovery of the prevalence of the inhibitory motif in Fic proteins, we carried out a detailed analysis of its functional and structural role. For this, NmFic (class III, Fig. 2c) was chosen, as it is the smallest active Fic family protein with known crystallization condition (Supplementary Table 1). As reported before[6], NmFic exhibits *in vitro* auto-adenylylation activity (Fig. 3d). The acceptor site was traced to Y183 of α_{inh} by mass spectrometry (Supplementary Information, section 1, and Supplementary Fig. 8). On the basis of the location of Y183 relative to the active site, auto-adenylylation is probably catalysed intermolecularly after partial unfolding or detachment of α_{inh}. Addition of *E. coli* lysate to NmFic did not reveal additional bands on the autoradiograph, and this indicated that there are no NmFic targets in *E. coli* or that the activity of NmFic is inhibited. The latter was shown to be correct as mutation of the inhibitory motif (S182A/E186A, NmFic(SE/AA)) resulted in transfer of radioactivity onto an ~80-kDa *E. coli* protein and enhanced auto-adenylylation with an additional acceptor site (Y188; Fig. 3d and Supplementary Fig. 9). Deletion of the entire α_{inh} helix (NmFic(Δ8)) led to similar target protein adenylylation, proving that the activity resides in the FIC domain core. However, only weak auto-adenylylation was apparent owing to the lack of the acceptor tyrosines in this deletion mutant (Fig. 3d and Supplementary Fig. 8c).

To investigate the inhibitory mechanism, crystals of NmFic proteins were soaked with the non-hydrolysable ATP analogue adenylyl imidodiphosphate (AMPPNP) (Supplementary Table 1). The NmFic–AMPPNP structure revealed nucleotide binding but with the γ-phosphate disordered (Fig. 3a). Notably, the orientation of the α-phosphate seems to be non-productive, as the position that is in line with the scissile Pα-O3α bond is occluded by H107 and N113 (Supplementary Fig. 10a and Supplementary Movie). To reveal the situation in an inhibition-relieved mutant, the structure of NmFic(SE/AA) was determined to 3.0 Å (Supplementary Fig. 11). Electron density was lacking for α_{inh}, indicating disorder, whereas the nucleotide conformation was well defined. In the NmFic(Δ8)–AMPPNP structure, the same nucleotide conformation was observed (Fig. 3b) and, owing to its high resolution (1.7 Å), the structural basis for the observed relief of inhibition in these mutants became evident. Whereas the adenosine moiety adopts the same position as in the wild-type, the γ-phosphate of the nucleotide is bound to R118, occupying the same position as the carboxylate of the inhibitory E186 in the wild type. As a consequence, the α-phosphate is found to be re-oriented, and the new orientation permits in line attack of a target side chain onto the α-phosphorus to accomplish AMP transfer (Fig. 3c, Supplementary Fig. 10 and Supplementary Movie).

The exact role of the inhibitory glutamate was investigated further by mutagenesis of Fic proteins from the three regulatory classes. In wild-type NmFic, Cα and Cβ of the glutamate are close to the position that is attained by the γ-phosphate position in NmFic(Δ8) (Fig. 3c). Still, an E to G single point mutant may provide sufficient space and main-chain flexibility to allow γ-phosphate binding. Indeed, similar to NmFic(Δ8)and NmFic(SE/AA), the mutant NmFic(E186G) resulted in growth inhibition of *E. coli* (Supplementary Fig. 1b). Likewise, co-expression of VbhT(FIC) and VbhA(E24G), as representatives for class I, caused *E. coli* growth defects (Supplementary Fig. 1a). We also included SoFic, a bacterial class II protein, in this analysis. Consistent with the effects of E to G single point mutants in NmFic and VbhA, mutant SoFic(E73G) revealed a negative effect on *E. coli* growth

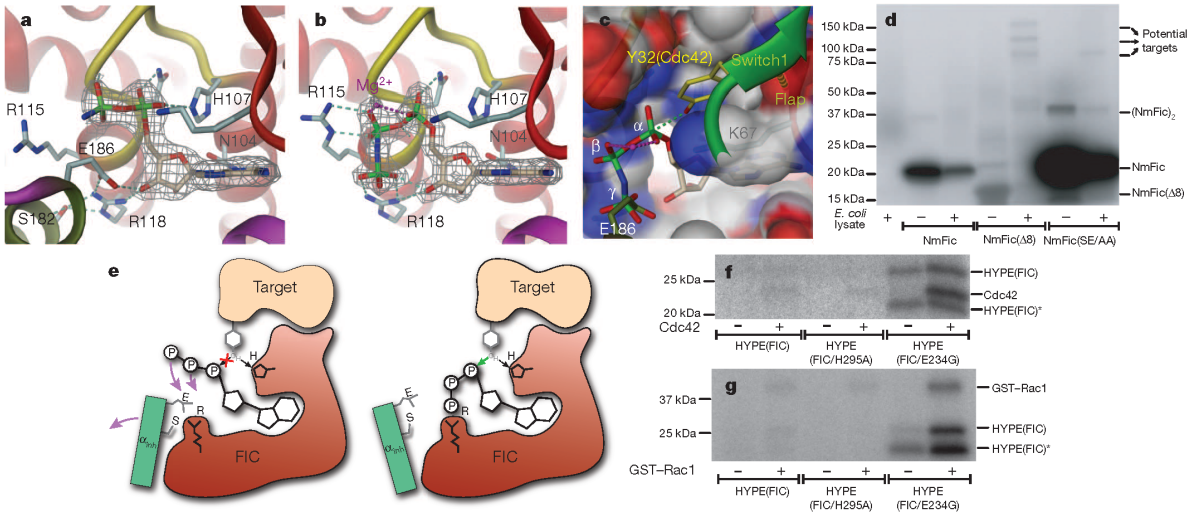

Figure 3 | Structure and function of wild-type and mutant NmFic reveals a general inhibition mechanism corroborated by HYPE protein analysis. **a**, Active site of NmFic with bound ATP analogue AMPPNP. The γ-phosphate seems to be disordered and has not been modelled. **b**, Active site of NmFic(Δ8) with bound AMPPNP and Mg^{2+}. The γ-phosphate occupies the position taken by E186 of the SXXXEG motif in the wild-type (as shown in **a**). Also shown are $2Fo - Fc$ maps that are contoured at 1.2σ and cover the ligands. **c**, Surface representation of the active site of NmFic(Δ8) with modifiable Y32 (yellow) of the Cdc42 switch1 loop (green) in a position that is obtained from a superposition of the active site loops of NmFic over the IbpA(FIC2)–Cdc42 complex[5]. **d**, Autoradiography of an SDS gel after incubation of wild-type and mutant NmFic with [α-^{32}P]ATP in the presence or absence of *E. coli* lysate. The mutants, but not the wild-type, catalyse AMP transfer onto *E. coli* target proteins. **e**, Scheme of a general inhibition mechanism for Fic proteins. The α_{inh} helix (green) with the (S/T)XXXE(G/N) motif prevents productive ATP binding. It is only after dissociation of the helix that the ATP γ-phosphate attains the position close to a conserved arginine (indicated by "R") of the FIC motif. This is accompanied by reorientation of the α-phosphate to allow in-line attack of the target hydroxyl side chain after proton transfer to the active histidine as proposed before[5]. **f**, **g**, Autoradiography after incubation of HYPE(FIC) with α-^{32}P-ATP in the presence or absence of Cdc42 (**f**) or GST-tagged Rac1 (GST–Rac1) (**g**). HYPE(FIC/E234G) shows enhanced auto-adenylylation and target adenylylation. HYPE(FIC)* denotes a degradation product of HYPE(FIC).

©2012 Macmillan Publishers Limited. All rights reserved

RESEARCH LETTER

(Supplementary Fig. 1c) and strongly enhanced auto-adenylylation (Supplementary Fig. 12). A similar marked effect on auto-adenylylation was observed after mutation of the corresponding residue in human HYPE (HYPE(FIC/E234G)), another class II protein (Fig. 3f, g). It is known that HYPE catalyses Cdc42 and Rac1 adenylylation[1,4]. The rather low adenylylation activity of wild-type HYPE on these substrates is markedly enhanced in the HYPE(FIC/E234G) mutant (Fig. 3f, g), demonstrating that the relief of inhibition by α_{inh} enhances not only auto-adenylylation but also AMP transfer onto bona fide protein targets.

From this study a general mechanism for the inhibition of the FIC-domain-mediated adenylylation has emerged that invokes a glutamate finger from α_{inh} to inter- or intramolecularly block part of the ATP binding site (Fig. 3e). Dissociation of the toxin–antitoxin complex (class I) or intramolecular loosening of the contact between α_{inh} and the FIC domain active site (classes II and III) allows ordered binding of the entire ATP moiety with the α-phosphate in an orientation that is productive for accepting an incoming target hydroxyl side chain.

Class I proteins might exert functions similar to the classical bacterial toxin–antitoxin modules[12], whereas class II and III Fic proteins seem to regulate intrinsic cellular functions that are related to physiological adaptation and cell homeostasis. Conservation of class II Fic proteins in all three kingdoms of life (Supplementary Table 2) emphasizes the important role of the regulatory mechanisms described here. How the adenylylation activity is activated by weakening the interaction of α_{inh} with the FIC active site in class II and class III Fic proteins is one of many important questions for future research. We also anticipate our study to be a starting point for rational approaches to modulate the adenylylation activities of Fic proteins—approaches that should aid in elucidating the diverse biological functions of these widespread signalling proteins.

METHODS SUMMARY

Toxicity experiments were performed with *E. coli* strain MG1655, which encodes an IPTG (isopropyl-β-D-thiogalactoside)-inducible T7 polymerase (strain AB472). Protein expression was controlled by the addition of either 100 μM IPTG (induction) or 1% glucose (repression). A PSI-BLAST search for homologues with VbhA of *B. schoenbuchensis* was conducted to identify Fic proteins belonging to class I. Class II and class III proteins were classified by structure predictions using the program HHpred[17]. We analysed all 2,189 proteins of the FIC PFAM family (pf02661, release 24). Adenylylation assays were carried out using bacterial crude cell lysates for VbhT constructs or purified proteins for NmFic, SoFic and HYPE constructs. For structure determination, VbhA and VbhT(FIC) were co-expressed in the BL21(DE3) strain of *E. coli*, and NmFic, SoFic(Δ8) and NmFic(SE/AA) in the BL21-AI strain of *E. coli*. VbhA-VbhT(FIC) and NmFic were purified by affinity chromatography followed by size exclusion chromatography. An additional anion exchange chromatography step was performed for NmFic(Δ8)and NmFic(SE/AA). Diffraction data were collected at beamline X06SA of the Swiss Light Source. For NmFic(Δ8)and NmFic(SE/AA), we obtained phases by molecular replacement using the NmFic structure (PDB code 2G03) as a search model. The VbhA–VbhT(FIC) complex was solved by molecular replacement using a fragment of BepA (PDB code 2JK8).

Full Methods and any associated references are available in the online version of the paper at www.nature.com/nature.

Received 4 July; accepted 24 November 2011.
Published online 22 January 2012.

1. Worby, C. A. *et al.* The fic domain: regulation of cell signaling by adenylylation. *Mol. Cell* **34,** 93–103 (2009).
2. Yarbrough, M. L. *et al.* AMPylation of Rho GTPases by *Vibrio* VopS disrupts effector binding and downstream signaling. *Science* **323,** 269–272 (2009).
3. Roy, C. R. & Mukherjee, S. Bacterial FIC proteins AMP up infection. *Sci. Signal.* **2,** pe14 (2009).
4. Mattoo, S. *et al.* Comparative analysis of *Histophilus somni* immunoglobulin-binding protein A (IbpA) with other Fic domain-containing enzymes reveals differences in substrate and nucleotide specificities. *J. Biol. Chem.* **286,** 32834–32842 (2011).
5. Luong, P. *et al.* Kinetic and structural insights into the mechanism of AMPylation by VopS Fic domain. *J. Biol. Chem.* **285,** 20155–20163 (2010).
6. Xiao, J., Worby, C. A., Mattoo, S., Sankaran, B. & Dixon, J. E. Structural basis of Fic-mediated adenylylation. *Nature Struct. Mol. Biol.* **17,** 1004–1010 (2010).
7. Dehio, C. *et al. Bartonella schoenbuchii* sp. nov., isolated from the blood of wild roe deer. *Int. J. Syst. Evol. Microbiol.* **51,** 1557–1565 (2001).
8. Engel, P. *et al.* Parallel evolution of a type IV secretion system in radiating lineages of the host-restricted bacterial pathogen *Bartonella*. *PLoS Genet.* **7,** e1001296 (2011).
9. Schulein, R. *et al.* A bipartite signal mediates the transfer of type IV secretion substrates of *Bartonella henselae* into human cells. *Proc. Natl Acad. Sci. USA* **102,** 856–861 (2005).
10. Palanivelu, D. V. *et al.* Fic domain-catalyzed adenylylation: insight provided by the structural analysis of the type IV secretion system effector BepA. *Protein Sci.* **20,** 492–499 (2011).
11. Utsumi, R., Nakamoto, Y., Kawamukai, M., Himeno, M. & Komano, T. Involvement of cyclic AMP and its receptor protein in filamentation of an *Escherichia coli* fic mutant. *J. Bacteriol.* **151,** 807–812 (1982).
12. Engelberg-Kulka, H., Amitai, S., Kolodkin-Gal, I. & Hazan, R. Bacterial programmed cell death and multicellular behavior in bacteria. *PLoS Genet.* **2,** e135 (2006).
13. Garcia-Pino, A. *et al.* Doc of prophage P1 is inhibited by its antitoxin partner Phd through fold complementation. *J. Biol. Chem.* **283,** 30821–30827 (2008).
14. Kinch, L. N., Yarbrough, M. L., Orth, K. & Grishin, N. V. Fido, a novel AMPylation domain common to Fic, Doc, and AvrB. *PLoS ONE* **4,** e5818 (2009).
15. Das, D. *et al.* Crystal structure of the Fic (Filamentation induced by cAMP) family protein SO4266 (gi|24375750) from *Shewanella oneidensis* MR-1 at 1.6 Å resolution. *Proteins* **75,** 264–271 (2009).
16. Mukherjee, S. *et al.* Modulation of Rab GTPase function by a protein phosphocholine transferase. *Nature* **477,** 103–106 (2011).
17. Söding, J., Biegert, A. & Lupas, A. N. The HHpred interactive server for protein homology detection and structure prediction. *Nucleic Acids Res.* **33,** W244–W248 (2005).

Supplementary Information is linked to the online version of the paper at www.nature.com/nature.

Acknowledgements We thank T. Glatter for mass spectrometry analysis of samples at the Core Proteomics facility. We thank the staff of beamline X06SA of the Swiss Light Source for assistance with data acquisition. We are grateful to G. Pluschke for providing the genomic DNA of *Neisseria meningitidis*, the ASU Biodesign Institute for providing the plasmid enclosing the *Shewanella oneidensis* Fic protein and S. Mattoo and J. Dixon for providing the pET-GSTX plasmids enclosing HYPE and HYPE(H295A). We also thank D. Bumann and A. Boehm for providing plasmid pC10E and *E. coli* strain AB472, respectively. This work was supported by grants 3100-061777 and 3100-138414 from the Swiss National Science Foundation (to C.D. and T.S., respectively), and grant 51RT 0_126008 (InfectX) in the frame of the SystemsX.ch Swiss Initiative for Systems Biology (to C.D.).

Author Contributions P.E., F.V.S. and A.H. cloned recombinant plasmids. P.E. discovered and physiologically characterized VbhT–VbhA as a toxin–antitoxin module and carried out the bioinformatic analysis. A.G. expressed, purified and crystallized VbhA–VbhT(FIC), NmFic(SE/AA) and NmFic(Δ8), and determined their structures. F.V.S. expressed, purified and crystallized NmFic with AMPPNP and determined the structure. A.G. and A.H. performed the adenylylation assays. A.H carried out the growth curve experiments. A.S. conducted the mass spectrometry analysis. All authors contributed to experimental design and data analysis. The manuscript was written by P.E., A.G., T.S. and C.D.

Author Information The atomic coordinates of VbhA–VbhT(FIC) and the complexes of NmFic, NmFic(SE/AA) and NmFic(Δ8) with AMPPNP have been deposited in the Protein Data Bank under accession codes 3SHG, 3S6A, 3SN9 and 3SE5, respectively. Reprints and permissions information is available at www.nature.com/reprints. The authors declare no competing financial interests. Readers are welcome to comment on the online version of this article at www.nature.com/nature. Correspondence and requests for materials should be addressed to C.D. (Christoph.Dehio@unibas.ch) or T.S. (Tilman.Schirmer@unibas.ch).

©2012 Macmillan Publishers Limited. All rights reserved

METHODS

Identification of VbhA homologues. VbhA of *B. schoenbuchensis* was queried against a database composed of translated open reading frames (>10 amino acids) identified in the 500-bp upstream region of all *fic* loci (PFAM release 24, 2,189 proteins). Nine rounds of Psi-Blast were performed and hits with an *E*-value <1 manually validated.

***E. coli* toxicity tests and cell filamentation.** *E. coli* AB472, a derivative of MG1655, was transformed with VbhT-expressing plasmids and always handled in LB containing 1% glucose. A single colony was picked, resuspended in 20 µl of LB and plated on LB plates containing 100 µM IPTG (induction) or 1% glucose (repression). Plates were incubated overnight at 37 °C. Growth curves were acquired by measuring optical density of liquid cultures in LB containing 100 µM IPTG that had been inoculated from overnight cultures of single colonies and were grown at 30 °C with continuous shaking. Cell filamentation was visualized by co-transformation of plasmid pC10E that constitutively expresses GFP and examined using fluorescence microscopy.

Conjugation experiments for VbhT toxicity tests in *Bartonella*. Plasmids were introduced into *Bartonella* strains by conjugation from *E. coli* using three-parental mating. *Bartonella* strains were grown for 36–48 h at 35 °C with 5% CO_2 on Columbia base agar plates supplemented with 5% defibrinated sheep blood and 100 µg ml^{-1} streptomycin. *E. coli* β2150 that harbours helper plasmid pRK2013, and *E. coli* β2150 that contains the VbhT-expressing plasmid were grown overnight at 37 °C in LB supplemented with 50 µg ml^{-1} kanamycin or 30 µg ml^{-1} chloramphenicol, respectively, and both media were also supplemented with diaminopimelic acid (DAP) and 1% glucose. After 16 h of incubation, *E. coli* strains were diluted 1:50 in fresh LB medium and grown to a opticial density (OD) at 595 nm (OD_{595nm}) of 0.4–0.8. Subsequently, each *E. coli* strain was diluted to OD_{595nm} of 0.25, washed once and resuspended in supplemented M199 medium (containing 10% FCS and 1% glucose). *Bartonella* strains were collected in 1 ml and resuspended in 60 µl of M199 (OD_{595nm} = 1). Each *Bartonella* suspension was mixed with 20 µl of *E. coli* β2150 that harbours pRK2013 and 20 µl of *E. coli* β2150 that harbours the VbhT-expressing plasmid. The conjugation mix was distributed on a conjugation filter on a columbia blood agar (CBA) plate supplemented with 150 µl DAP and 150 µl 1% glucose. After 6 h of incubation under *Bartonella* growth conditions as described before, the bacteria were washed off the filter with 1 ml supplemented M199. Dilutions of bacterial suspensions were plated on lysogeny broth agar (LA) supplemented with DAP, 1% glucose and 30 µg ml^{-1} chloramphenicol for selecting donors, on CBA supplemented with 1.2 µg ml^{-1} chloramphenicol for selecting transconjugants, and on CBA supplemented with 100 µg ml^{-1} streptomycin for selecting recipients. Agar plates were incubated under *Bartonella* growth conditions and colony-forming units were counted after 1 day for donors and after 7 days for recipients and transconjugants.

***In vitro* adenylylation assay.** Adenylylation activity of VbhT was assessed in an assay using lysates of ectopically expressing *E. coli*. Bacterial pellets were resuspended in reaction buffer (50 mM Tris-HCl pH 8.0, 150 mM NaCl, 0.1 mM EGTA, 15 mM $MgCl_2$, 140 µg ml^{-1} RNase A and protease inhibitor cocktail (Roche)) and lysed by sonication. After clearing lysates by centrifugation, supernatants were used for experimentation or stored at −20 °C.

Adenylylation reactions were prepared by supplementing 15 µl supernatant from expression cultures with 10 µCi [α-^{32}P]ATP (Hartmann Analytic) and 25 µl blank *E. coli* supernatant. Adenylylation activity of NmFic and SoFic constructs was assessed by incubating 60 µg purified protein with 10 µCi [α-^{32}P]ATP (Hartmann Analytic) and 25 µl blank *E. coli* supernatant. Reactions were incubated for 1 h at 30 °C, resolved by SDS–PAGE, and adenylylation was probed by autoradiography. For HYPE(FIC) assays, 15 ng of pure protein was incubated with 1.6 µg of purified GTPases.

Protein expression and purification. pFVS0011 vector (encoding VbhA and VbhT(FIC)) was transformed into *E.coli* BL21 (DE3). *E. coli* cultures were grown at 37 °C in LB medium supplemented with 50 µg ml^{-1} of kanamycin to an OD_{595nm} of 0.6 before induction with 0.3 mM IPTG for 16 h at 23 °C. Vectors pFVS0015 (carrying the *NmFic* gene), pFVS0016 (encoding NmFic(Δ8)), pFVS0037 (encoding NmFic(SE/AA)) were transformed into BL21-AI cells. Cells were incubated overnight in 750 ml LB medium that was supplemented with 50 µg ml^{-1} kanamycin and 1% glucose at 23 °C at 200 r.p.m. until OD_{595nm} of 2 was reached. Bacterial pellets were resuspended in terrific broth medium containing 50 µg ml^{-1} kanamycin to obtain an OD_{595nm} of approximately 1. Protein expression was induced at 23 °C with 0.1% arabinose and 0.5 mM IPTG for 23 h at 200 r.p.m. Plasmids harbouring *HYPE(FIC)* and *SoFic* constructs were transformed in *E. coli* Rosetta (DE3) cells and BL21-AI cells, respectively. The proteins were expressed as described for NmFic.

Cells containing overexpressed VbhA–VbhT(FIC) and NmFic were resuspended in lysis buffer containing 20 mM Tris (pH 7.5), 250 mM NaCl and 25 mM imidazole and disrupted using French press. Cell debris was pelleted by ultracentrifugation and the supernatant was applied to a His-Trap column (GE Healthcare). The stable complex was eluted with a gradient of elution buffer containing 20 mM Tris (pH 7.5), 250 mM NaCl and 500 mM imidazole. The protein was then concentrated and injected on a Superdex 75 16/60 gel filtration column (GE Healthcare) equilibrated with 10 mM Tris (pH 7.5) and 100 mM NaCl. The pure proteins were concentrated to 6 mg ml^{-1} for VbhA–VbhT(FIC) and 53 mg ml^{-1} for NmFic.

The same purification protocol was used for NmFic(Δ8) and NmFic (SE/AA), but with an additional intermediate purification step. After affinity purification, the proteins were adjusted to 20 mM Tris (pH 8.5), 25 mM NaCl, applied to a Resource-Q anion exchange column (Amersham Biosciences) and eluted with a linear gradient of NaCl. Peak fractions were concentrated and further purified by gel filtration chromatography. Purified proteins in 10 mM Tris (pH 7.8), 100 mM NaCl were concentrated to 30 mg ml^{-1} for NmFic(Δ8) and 51 mg ml^{-1} for NmFic(SE/AA). SoFic and SoFic(E73G) were purified as described previously[15]. HYPE(FIC), HYPE(FIC/H295A) and HYPE(FIC/E234G) were purified in the same way as NmFic. GST-tagged Cdc42 and Rac1 were expressed and purified as described previously[18,19].

Crystallization. All crystals were obtained at 20 °C (except for NmFic crystals, which were obtained at 4 °C) using the hanging-drop vapour diffusion method after mixing 1 µl protein solution with 1 µl reservoir solution. VbhA–VbhT(FIC) and NmFic(SE/AA) crystallized in 23% (w/v) PEG 3350 and 0.2 M di-ammonium tartrate, and were cryoprotected with 25% (w/v) PEG 3350, 0.2 M di-ammonium tartrate and 10% glycerol. NmFic crystallized in 5% 2-propanol, 0.1 M MES pH 6.0 and 0.1 M Ca-acetate, and was transferred into 8% 2-propanol, 0.1 M MES pH 6.0, 0.1 M Mg-acetate and 15% glycerol, then into 30% glycerol for cryoprotection. NmFic(Δ8) crystallized with 44% (v/v) PEG 600, 0.1 M Na-citrate pH 5.6. No cryoprotection was needed for data collection. In each case, the substrate analogue complex was produced by crystal soaking for 2 h with 10 mM AMPPNP, 10 mM $MgCl_2$.

Structure determination. Statistics of data collection and refinement are given in Supplementary Table 1. Diffraction data were collected at beamline X06SA (PXIII) of the Swiss Light Source (λ = 1.0 Å) at 100 K on a MAR CCD detector, processed using MOSFLM[20], and scaled with SCALA[21]. The structures were determined by molecular replacement (PHASER[22]) using a BepA fragment (PDB code 2JK8[10], residues 30–194) or the uncomplexed NmFic structure (PDB code 2G03, unpublished, Midwest Center for Structural Genomics) as models for structure solution of VbhA–VbhT(FIC) and the different NmFic proteins, respectively. A structure solution of wild-type and mutant NmFic in complex with AMPPNP was straightforward, whereas a weak solution (RFZ = 5.1, TFZ = 3.6) with poor phasing power was obtained for VbhA–VbhT(FIC). The partial model lacking VbhA was refined by rigid-body refinement using REFMAC5 (ref. 23) with three bodies to an R_{free} of 52%. Model extension using the module AutoBuild of the PHENIX package[24] yielded an almost complete model (R/R_{free} = 30.8%/35.2%). The remainder of the molecule was traced manually with COOT[25] and then by full refinement using PHENIX[24]. The Ramachandran plot showed that more than 99% of the residues are in favoured regions of the four structures. The figures were generated with Dino (http://www.dino3d.org).

Prediction of inhibition motif in Fic proteins. All Fic proteins (PFAM release 24, 2,189 proteins) were subjected to a profile-to-profile comparison with sequences from the PDB using HHpred[17]. HHpred builds an alignment of homologues for each query sequence by using iterations of PSI-BLAST searches against the non-redundant database. Secondary structures are then predicted on the PSI-BLAST alignment using PSIPRED[26]. On the basis of this data, a profile Hidden Markov Model (HMM) is generated. Each query profile is compared with the pre-computed HMMs of the proteins in the PDB to identify structural homologues. In terms of query profiles, the PDB profiles include secondary structure information derived from their three-dimensional structure. We analysed the pairwise profile alignments of each Fic protein with the eight different Fic family members deposited in the PDB. A Fic protein was predicted to belong to class II or class III if the templates' inhibitory motifs were aligned to a corresponding query sequence in the profile alignments (see Supplementary Information, section 1).

Phylogenetic analysis of Fic proteins. Phylogenetic trees of the Fic family were inferred with FastTree 2 (ref. 27) and RAxML 7.0.4 (ref. 28). Trees were built on the amino acid alignment provided by the PFAM database. Unaligned overhanging ends were trimmed off and identical sequences were reduced to one representative. We used local support values based on the Shimodaira–Hasegawa test to estimate the reliability of the tree inferred with FastTree2. The RaxML tree was inferred using the PROTMIXWAGF model and 25 rate categories.

Liquid chromatography–mass spectrometry analysis. 2.5 µM of purified NmFic, NmFic(Δ8) or NmFic(SE/AA) were incubated in reaction buffer (10 mM Tris, pH 8, 100 mM NaCl) in the presence or absence of 50 µM ATP and 50 µM $MgCl_2$ for 1 h. Proteins were reduced in 5 mM TCEP, alkylated in

©2012 Macmillan Publishers Limited. All rights reserved

RESEARCH LETTER

10 mM iodacetamid and digested with sequencing grade trypsin (Promega). The generated peptides were purified with C18 Microspin columns (Harvard Apparatus) and analysed using liquid chromatography–mass spectrometry (LC–MS) or MS on an easy nano-LC system coupled to an LTQ-Orbitrap-Velos mass spectrometer (both from Thermo-Fisher Scientific), as recently described[29] using a linear gradient from 95% solvent A (0.15% formic acid, 2% acetonitrile) and 5% solvent B (98% acetonitrile, 0.15% formic acid) to 35% solvent B over 40 min. The data acquisition mode was set to obtain one high-resolution MS scan in the Fourier Transform (FT) part of the mass spectrometer at a resolution of 60,000 (full width at half maximum) and MS–MS scans in the linear ion trap of the 20 most intense ions. The resulting MS2 scans were searched against a *N. meningitidis* protein database containing the target protein sequence, including NmFic and NmFic(SE/AA) sequences, that was obtained from EBI (http://www.ebi.ac.uk) using the SEQUEST search algorithm provided in the Proteome Discoverer software package (Thermo-Fisher Scientific). *In silico* trypsin digestion was performed after lysine and arginine (unless followed by proline), with a tolerance of two missed cleavages in fully tryptic peptides. Database search parameters were set to allow phosphoadenosine modification (+329.05252 Da) of threonine and tyrosine residues as variable modification and carboxyamidomethylation (+57.021464 Da) of cysteine residues as fixed modification. The fragment mass tolerance was set to 0.8 Da and the precursor mass tolerance to 15 p.p.m.

Strain construction. For toxicity experiments, the *vbhT* wild-type gene (FN645515) from *B. schoenbuchensis* R1 was cloned into pRSF-Duet1 (pPE0017, His_6-tagged *vbhT*). VbhT(H136A) (pPE0034) was constructed by introducing a two-base-pair point mutation in the FIC motif of *vbhT* of pPE0017, as described elsewhere[30]. Plasmid co-expressing VbhT and VbhA (VbhT/VbhA) was constructed by cloning *vbhA* (FN645515) amplified from *B. schoenbuchensis* R1 into pRSF-Duet1 (pPE0020, HA-tagged *vbhA*). *vbhT* was then cloned into pPE0020, resulting in pPE0021. To construct VbhT-expressing plasmids for *Bartonella*, *vbhT* from *B. schoenbuchensis* R1 was cloned into vector pMMB206 (ref. 31) (pVbhT, HA-tagged *vbhT*). pVbhT(H136A) was constructed from pVbhT as described before.

The in-frame deletion of the complete *vbhA/vbhT* operon in *B. schoenbuchensis* (*Bsch ΔvbhA/vbhT*) was generated as described previously by a two-step gene replacement procedure[9]. The mutagenesis vector pPE3005 was constructed by ligating a cassette with the flanking regions of the in-frame deletion into pTR1000[9].

For protein purification, the full-length *vbhA* gene and part of the *vbhT* gene encoding the FIC domain (*vbhT(FIC)*), amino acid residues 1–198, His_6-tagged) were amplified from plasmid pPE0021 and cloned into the pRSF-Duet1 vector (pFVS0011). VbhA(E24G)/VbhT(FIC) expression plasmid (pFVS0065) was generated by introducing a two-base-pair mutation in pFVS0011. The *NmFic* gene was amplified with an N-terminal His_6-tag from *N. meningitidis* from coding region of amino acid residues 11–191 and from coding region of amino acid residues 11–167 to generate plasmids expressing NmFic (pFVS0015) and NmFic(Δ8) (pFVS0016), respectively. The S182A/E186A double mutant construct (NmFic(SE/AA)) was generated by introducing two subsequent point mutations in pFVS0015. The E186G mutant construct (NmFic(E186G)) was generated by the same approach. The *SoFic* gene was amplified from plasmid (ASU biodesign institute, Clone ID SoCD00104192) and cloned with an N-terminal His_6-tag into pRSF-Duet1 (pFVS0040). The SoFic(E73G) plasmid (pFVS0058) was generated by introducing a two-base-pair point mutation in pFVS0040. GST–HYPE(E234G) (pFVS0064) was generated by introducing point mutations in the plasmid containing GST–HYPE. From these plasmids, shorter constructs (HYPE(FIC), HYPE(FIC/E234G) and HYPE(FIC/H295A)) only carrying the FIC domain of HYPE (from amino acids 187 to 437) were generated. For the expression of human Cdc42 and Rac1, the *Cdc42–Q61L* and *Rac1–Q61L* coding sequences were amplified from plasmid pRK5myc L61 Cdc42[32] and pRK5FLAG L61 Rac1 (ref. 32) and cloned into pGex6p1 with an N-terminal GST-tag, resulting in pAH088 and pAH060, respectively. The wild-type variants of Cdc42 and Rac1 were generated from the mutant constructs through polymerase chain reaction (PCR)-based site-directed mutagenesis[30] (resulting in pAH059 and pAH071). All primers and the resulting vectors are summarized in Supplementary Tables 5 and 6.

18. Self, A. J. & Hall, A. Purification of recombinant Rho/Rac/G25K from *Escherichia coli*. *Methods Enzymol.* **256,** 3–10 (1995).
19. Smith, S. J. & Rittinger, K. Preparation of GTPases for structural and biophysical analysis. *Methods Mol. Biol.* **189,** 13–24 (2002).
20. Leslie, A. G. The integration of macromolecular diffraction data. *Acta Crystallogr. D* **62,** 48–57 (2006).
21. Collaborative Computational Project, Number 4. The CCP4 suite: programs for protein crystallography. *Acta Crystallogr. D* **50,** 760–763 (1994).
22. McCoy, A. J. *et al.* Phaser crystallographic software. *J. Appl. Crystallogr.* **40,** 658–674 (2007).
23. Murshudov, G. N., Vagin, A. A. & Dodson, E. J. Refinement of macromolecular structures by the maximum-likelihood method. *Acta Crystallogr. D* **53,** 240–255 (1997).
24. Adams, P. D. *et al.* PHENIX: a comprehensive Python-based system for macromolecular structure solution. *Acta Crystallogr. D* **66,** 213–221 (2010).
25. Emsley, P. & Cowtan, K. Coot: model-building tools for molecular graphics. *Acta Crystallogr. D* **60,** 2126–2132 (2004).
26. Jones, D. T. Protein secondary structure prediction based on position-specific scoring matrices. *J. Mol. Biol.* **292,** 195–202 (1999).
27. Price, M. N., Dehal, P. S. & Arkin, A. P. FastTree 2—approximately maximum-likelihood trees for large alignments. *PLoS ONE* **5,** e9490 (2010).
28. Stamatakis, A. RAxML-VI-HPC: maximum likelihood-based phylogenetic analyses with thousands of taxa and mixed models. *Bioinformatics* **22,** 2688–2690 (2006).
29. Schmidt, A. *et al.* Absolute quantification of microbial proteomes at different states by directed mass spectrometry. *Mol. Syst. Biol.* **7,** 510 (2011).
30. Zheng, L., Baumann, U. & Reymond, J. L. An efficient one-step site-directed and site-saturation mutagenesis protocol. *Nucleic Acids Res.* **32,** e115 (2004).
31. Dehio, C. & Meyer, M. Maintenance of broad-host-range incompatibility group P and group Q plasmids and transposition of Tn5 in *Bartonella henselae* following conjugal plasmid transfer from *Escherichia coli*. *J. Bacteriol.* **179,** 538–540 (1997).
32. Rhomberg, T. A., Truttmann, M. C., Guye, P., Ellner, Y. & Dehio, C. A translocated protein of *Bartonella henselae* interferes with endocytic uptake of individual bacteria and triggers uptake of large bacterial aggregates via the invasome. *Cell. Microbiol.* **11,** 927–945 (2009).

©2012 Macmillan Publishers Limited. All rights reserved

SUPPLEMENTARY INFORMATION

doi:10.1038/nature10729

Content:

RESEARCH SUPPLEMENTARY INFORMATION

1. Supplementary Text

1.1 Defining an adenylylation competent FIC signature motif

Based on sequence conservation, previous mutagenesis results, and the structure of the competent NmFic(Δ8)/AMPPNP complex (Supplementary Fig. 10b), we have defined the HxFx[D/E]GNGRxxR profile as the crucial core motif for catalytically active Fic proteins with respect to adenylylation. The histidine residue (H) has been shown in several studies[1,2] to be essential for activity and probably acts as a general base for deprotonation of the target side-chain hydroxyl group[2,3]. The phenylalanine (F) is part of the hydrophobic core and important for correct positioning of the active loop. It remains unclear whether other hydrophobic residues could replace the phenylalanine. Strikingly, all Fic proteins so far shown to exhibit adenylylation activity harbour a phenylalanine at this position. The carboxylic side-chain of the aspartic/glutamic acid (D/E) probably coordinates the divalent cation (Mg^{2+} or Mn^{2+}) that is required for activity (data not shown). However, in the competent substrate complex structure (Supplementary Fig. 10b) it is partly disordered. As predicted before[2] and confirmed by the competent AMPPNP complex structure (Supplementary Fig. 10b), the three backbone amide nitrogens of GNG are involved in α- and β- phosphate binding. No other residue than a glycine is allowed for the two G positions, since side-chains would clash with the core of the protein or the ATP substrate, respectively. The asparagine side-chain is involved in positioning of the α-phosphate and establishes two H-bonds with the backbone amide and carbonyl group of the active site phenylalanine residue. Finally, the two arginines are forming a salt-bridge with the β- and γ-phosphate, respectively (Supplementary Fig. 10b). For all residues of the motif, single point mutants have been constructed except for the first glycine and first arginine that showed reduced or negligible auto-adenylylation and/or target adenylylation[1-5], thereby highlighting the

importance of these conserved residues. Thus, based on current structural and biochemical knowledge, we can assume that Fic proteins with a motif conforming to the consensus HxFx[D/E]GNGRxxR are likely to represent AMP transferases. In contrast, proteins divergent from this motif have most probably lost adenylylation activity.

1.2 Prediction and analysis of the three regulatory classes of Fic proteins

While class I proteins were identified by Psi-Blast for the detection of VbhA-homologous peptides encoded in the upstream region of *fic* loci, we used a structure based approach to detect class II and class III Fic proteins. The program HHpred predicts structures of distant homologs from proteins deposited in structure databases[6]. The analysis is based on a profile-to-profile comparison of Hidden Markov Models (HMMs) generated from Psi-Blast and secondary structure predictions (see Online Methods). We conducted an HHpred analysis for each protein in the FIC family (PFAM release 24, 2,189 proteins) using the protein structure database PDB. The PDB contains structures of FIC domains from eight different proteins: (i) 3dd7, DocH66Y of prophage P1 in complex with the C-terminal domain of Phd; (ii) 2jk8, BepA of *Bartonella henselae,* a type IV secretion system effector protein; (iii) 3n3u, IbpA of *Histophilus somni*, a protein secreted into host cells; (iv) 3let, VopS of *Vibrio parahaemolyticus*, a Type III secretion system effector protein; (v) 2f6s, Fic protein of *Helicobacter pylori* (HpFic); (vi) 2g03, Fic protein of *Neisseria meningitidis* (NmFic); (vii) 3eqx, Fic protein of *Shewanella oneidensis* (SoFic); (viii) 3cuc, Fic protein of *Bacteroides thetaiotaomicron* (BtFic). For all Fic proteins analyzed with HHpred, we detected significant structural homology with these eight FIC domain structures in the PDB. Based on the corresponding HHpred alignments, we validated each Fic protein for the presence of an N-terminal (class II) or C-terminal (class III) inhibition motif. Fic proteins were predicted to fall into one of these two classes, if the structural alignments with the two structural prototypes of

a class (for class II, SoFic and BtFic; for class III, NmFic and HpFic) included the region comprising their inhibition motif. The segment of the query sequence aligning with the inhibition motifs of a given class was then identified as the putative inhibition motif of the query protein. Only proteins for which both alignments predicted the same inhibition motif were categorized into the corresponding class.

Supplementary Tables 4a-e show that for most proteins, predicted to fall into one of the two classes, the corresponding template structures resulted in the highest homology scores among the eight Fic proteins in our HHpred analysis. Further, the inhibition motifs independently predicted from the two template structures, turned out to be the same for most Fic proteins. Finally, only four proteins were identified to belong to more than one of the three classes. Altogether, this demonstrates the high specificity of our analysis for the prediction of these regulatory features.

Strikingly, the consensus sequence of all motifs from class I, II, and III converges towards the general inhibition motif [S/T]xxxE[G/N]. The glutamate (E24 of VbhA), thereby, displays the most conserved amino acid, which is consistent with the presented mechanism of inhibition (Fig. 3).

As mentioned in the main text, in comparison to the entire family, the total number of proteins predicted to fall into one of the three regulatory classes is significantly increased in the subset of Fic proteins harbouring the adenylylation-competent FIC motif HxFx[D/E]GNGRxxR (see Supplementary Text 1.1). Thus, the inhibition motif seems to be a specific feature of proteins with adenylylation activity and indicates co-evolution of these two functional features. In contrast to this general trend, the relative number of class I proteins (regulated by an antitoxin-like protein) decreases in the subset of Fic proteins with a conserved FIC motif. This can be explained by the fact that a significant fraction of class I comprises proteins from *E. coli* and related species which harbour a serine instead of an

asparagine and a leucine instead of arginine (1st position) in the active loop. It remains to be elucidated whether HxFx[D/E]GSGLxxR either can still mediate adenylylation or has evolved another activity which is regulated by a similar mechanism as adenylylation.

Interestingly, class I and III are restricted to bacteria (which present 90% of all Fic proteins), while in archaea and eukaryotes only class II inhibition motifs were predicted (Supplementary Table 2). Most of the metazoan Fic proteins including the human homolog HYPE as well as some of the fungal Fic proteins are predicted to contain a class II regulatory motif suggesting that this regulatory mechanism of adenylylation activity is conserved in all domains of life.

1.3 Prediction of regulatory classes for selected Fic proteins

The classification based on the presence/absence of an inhibition motif is listed in Supplementary Table 3 for a subset of Fic proteins which were previously studied. For VopS, the effector protein of *Vibrio parahaemolyticus*, our analysis did not predict an inhibition motif. This is in agreement with the 3D structure of VopS[3], which does not reveal any regulatory helix positioned next to the FIC active site.

In case of the second bacterial virulence factor for which adenylylation activity in eukaryotic host cells was described, IbpA[4], our analysis predicted an N-terminal inhibition motif (class II). However, the 3D structure of IbpA does not show this predicted inhibition motif to be located in the active center of the FIC domain[1]. Thus, our prediction for IbpA may be a false positive. Both VopS and IbpA are translocated into eukaryotic host cells, where they adenylylate proteins of the Rho family GTPases. This leads to the collapse of the actin cytoskeleton and subsequently to cell death[4,5]. In general, effector proteins of bacterial pathogens that aim at killing or dramatically subverting the cells of their eukaryotic hosts (e.g.

immune cells) by adenylylation of cellular targets might not need to be regulated. Further, due to their specificity for eukaryotic targets, they may not be toxic for the bacterium before translocation and would thus not require an inhibited state.

However, for effector proteins of *Bartonella,* our Psi-Blast analysis identified homologs of VbhA located upstream of the effector gene loci. In contrast to VopS and IbpA, the effector proteins of *Bartonella* seem to have a much more subtle effect on host cells[7]. It remains to be elucidated whether for *Bartonella* effector proteins co-translocation of a VbhA-homolog into host cells allows regulation of adenylylation activity.

Like the bacterial virulence factors IbpA or VopS, the human Fic protein HYPE, was shown to adenylylate the GTPases RhoA, Rac1, and Cdc42[4]. The conserved N-terminal inhibition motif identified for HYPE and other mammalian Fic proteins might explain why HYPE, in contrast to IbpA or VopS, did not show any cytotoxic effect on mammalian cells[4]. Thus, the here-identified regulatory mechanism might be essential for the tight regulation of mammalian Fic proteins and their integration into key signaling pathways of mammals.

Doc proteins share the same structural fold as Fic proteins and are thus grouped into the FIC PFAM family (which is also referred to as Fic/Doc family). They constitute the toxins of toxin-antitoxin modules homologous to the post-segregational killing system Doc/Phd of Bacteriophage P1[8]. In our phylogenetic analysis (Supplementary Fig. 7), Doc proteins form a separate cluster clearly distinct from the remaining Fic proteins. Furthermore, their core motif (Supplementary Table 3) is highly divergent from the adenylylation competent motif as defined above (see Supplementary Text 1.1). Consistently, our HHpred and Psi-Blast analyses did not identify any adenylylation-inhibiting motif for Doc-related proteins. Nevertheless, Doc activity is inhibited by the antitoxin Phd which binds in a similar way as VbhA to VbhT (Supplementary Fig. 5). Doc-mediated toxicity on bacteria results from binding to the 30S ribosomal subunit, but the exact underlying mechanism of Doc-mediated toxicity remains

elusive and adenylylation activity has not been reported[9]. Still, inhibition of Doc toxicity by mutation of the histidine in the central motif of the FIC domain indicates its involvement in mediating the toxic effect[10]. For Doc as well as for other Fic proteins carrying a motif divergent from the adenylylation-competent consensus profile, the FIC domain could mediate other enzymatic activities[11]. Catalytic versatility of the FIC domain fold would further explain why this protein family is so abundant in a wide range of organisms.

1.4 Mass spectrometry (MS) results for the identification of the auto-adenylylation site of NmFic

In order to specifically pinpoint the location of the adenylylation in the FIC domain and to verify the results obtained for the adenylylation assay (Fig. 3d), a mass spectrometric analysis of the trypsinized NmFic protein samples was performed. As apparent from Supplementary Fig. 8a, the majority of the adenylylation could be identified at position Y6 in the displayed peptide sequence. Additional conformation was obtained by the identification of the same adenylylation site on the same peptide containing the C-terminal glycine as consequence of incomplete proteolysis (Supplementary Fig. 8b). However, due to the close proximity of the tyrosine residues, it cannot be excluded that Y7 or Y8 are also modified. Comparative analysis of the NmFic and NmFic(Δ8) mutant clearly indicates a strong increase in adenylylation for this domain (Supplementary Fig. 8c). Notably, we covered the whole protein sequence by MS analysis and could only identify adenylylation at the C-terminal tyrosine residues of this protein, indicating exclusive adenylylation of this protein at these sites and confirming the results obtained in Fig. 3d.

MS analysis of the NmFic(SE/AA) mutant revealed a higher degree of adenylylation, which is indicated by the identification of more and multiple adenylylated peptide species (Supplementary Fig. 9), again, confirming the observations made in Fig. 3d.

2. Supplementary Figures

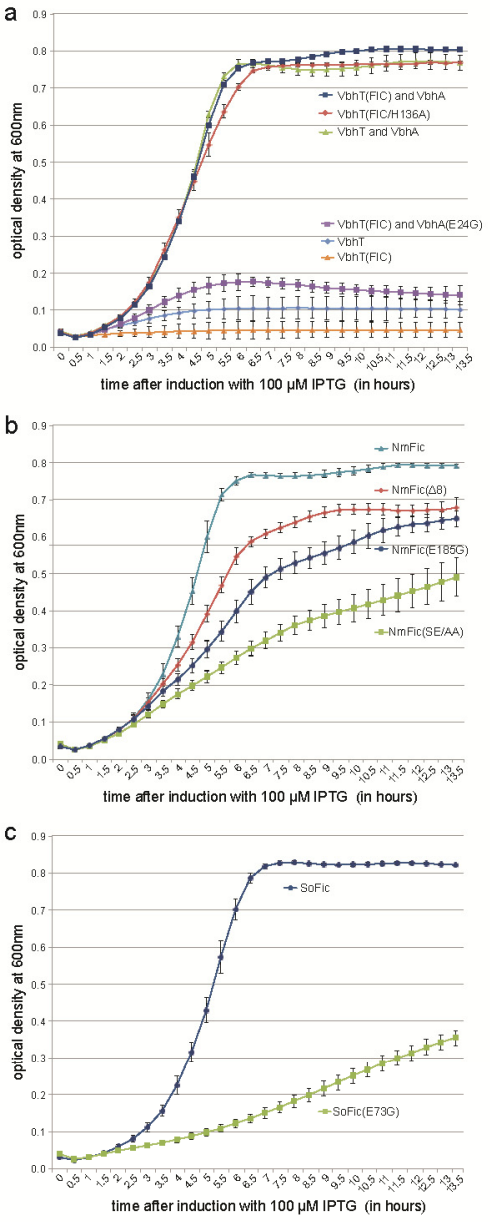

Supplementary Figure 1. Growth curves of *E. coli* MG1655 expressing different constructs of (a) VbhA-VbhT, (b) NmFic, or (c) SoFic. Cultures were inoculated with 5 µl

of an overnight culture and induced with 100 µM IPTG. Bacterial growth was measured by monitoring the optical density at 600 nm every 30 minutes. All experiments were carried out in quadruplicates.

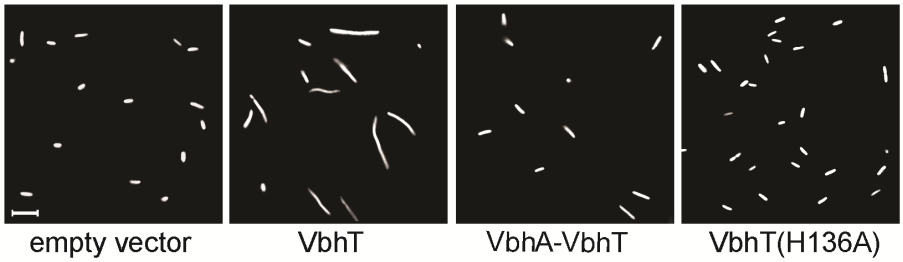

Supplementary Figure 2. Cell filamentation of *E. coli* upon expression of VbhT is repressed by co-expression of VbhA. Fluorescence microscopy of *E. coli* harbouring a GFP-reporter plasmid (pC10E) in addition to the same VbhA-VbhT-expression plasmids as presented in Fig. 1c (scale bar, 5 µm). Cell filamentation of *E. coli* observed upon VbhT expression is not evident for VbhT(H136A) or VbhA-VbhT.

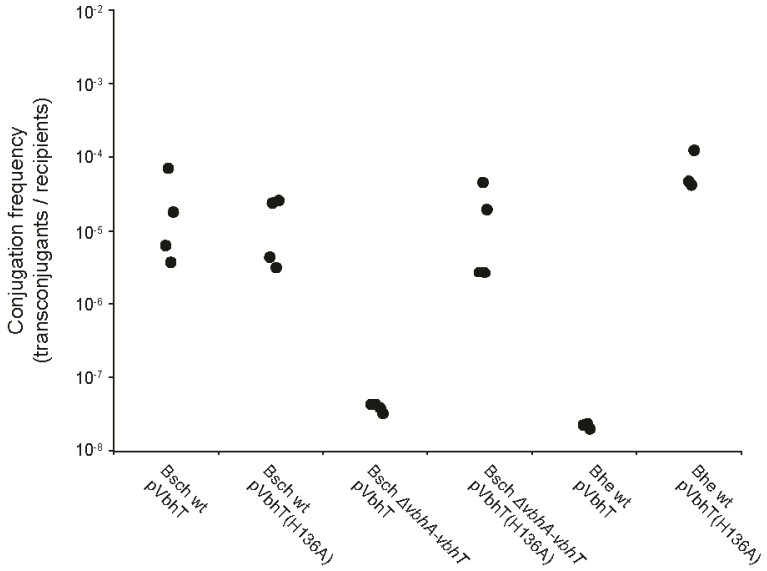

Supplementary Figure 3. Conjugation of VbhT expression plasmids into *Bartonella schoenbuchensis* and *Bartonella henselae* reveals toxicity of VbhT in the absence of *vbhA*. Conjugation frequencies are given by the number of transconjugants per recipient as determined by dilution plating and counting of colony forming units on media selective for either transconjugants or recipients. Conjugation of a plasmid expressing VbhT wild-type (pVbhT) into *B. schoenbuchensis* wild-type (Bsch wt) resulted in a conjugation frequency of about 10^{-5}. In contrast, conjugation of the same plasmid into *B. schoenbuchensis* harbouring a deletion of the complete *vbhA-vbhT* operon (Bsch Δ*vbhA-vbhT*) or into *B. henselae* wild-type (Bhe wt), which does not encode *vbhA*, gave no transconjugants in four and three independent experiments, respectively. This resulted in conjugation frequencies $< 10^{-7}$ (when taking the detection threshold in our experiments into account). The inability to conjugate the plasmid into these strains was dependent on a functional FIC motif: a plasmid expressing VbhT with an adenylylation-deficient FIC motif (pVbhT(H136A)) could be conjugated into Bsch Δ*vbhA-vbhT* and Bhe wt with a similar frequency as into Bsch wt.

RESEARCH SUPPLEMENTARY INFORMATION

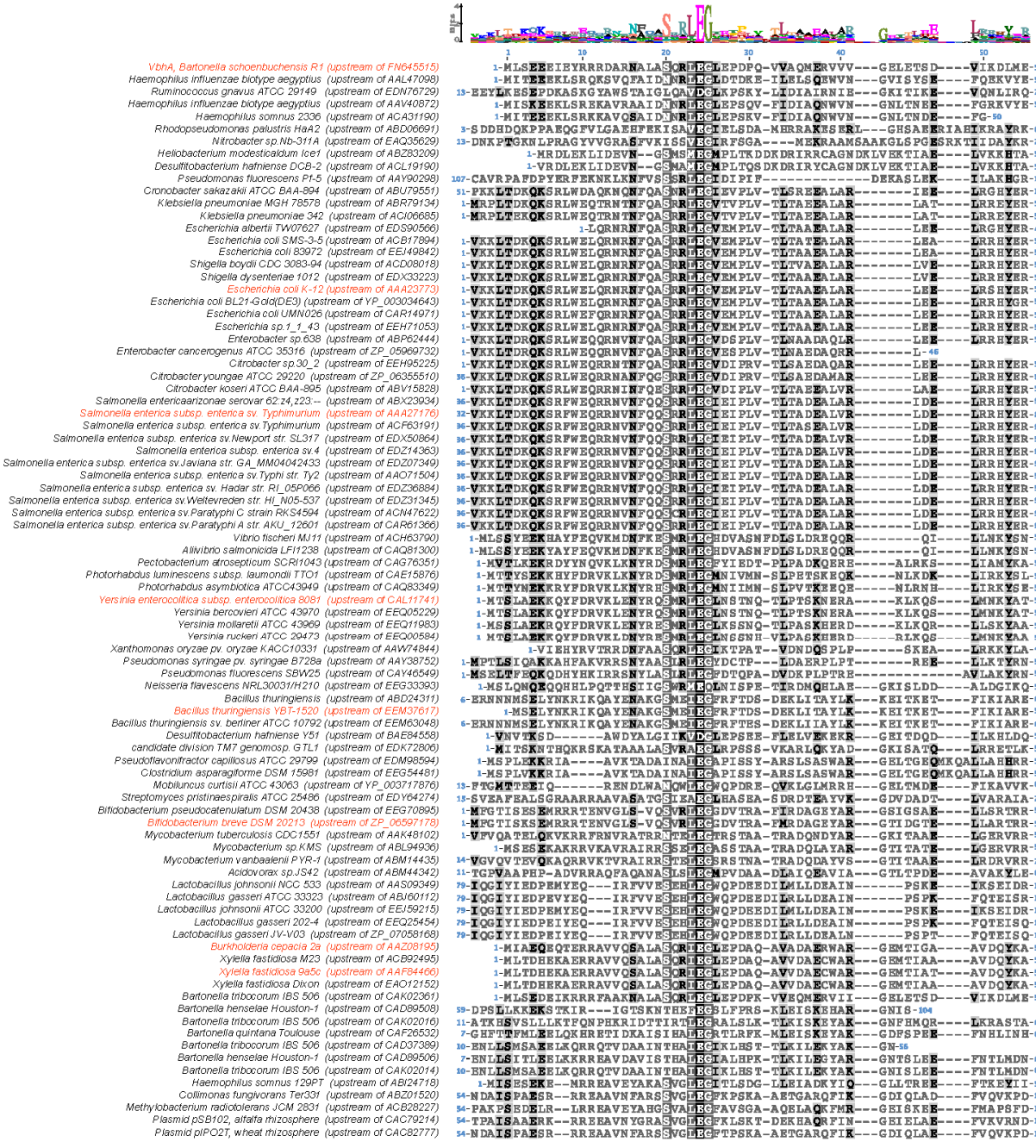

Supplementary Figure 4. Protein alignment of translated ORFs with homology to VbhA encoded in the upstream region *of fic* gene loci. We used Psi-Blast to query the VbhA protein sequence against all translated ORFs (>10 aa) found in the 500 bp upstream of loci

encoding Fic proteins. In total, this analysis identified 158 ORFs with homology to VbhA. 127 ORFs are overlapping with the corresponding *fic* gene, together constituting putative operons. From the remaining 31 ORFs, 20 are less than 100 bp away from the annotated start codon of the *fic* gene. In the depicted alignment, sequences identical to each other were reduced to one representative resulting in 87 aligned sequences including VbhA. Overhanging ends were trimmed. Start and end positions of the aligned sequences are indicated. The consensus sequence logo is depicted on top of the alignment indicating the conserved central motif. The alignment was generated with MUSCLE[12] (implemented in Geneious v5.3.6) and manually curated. Shading of amino acids indicates degree of conservation. Sequences used in the alignment of Fig. 1b are highlighted in red color.

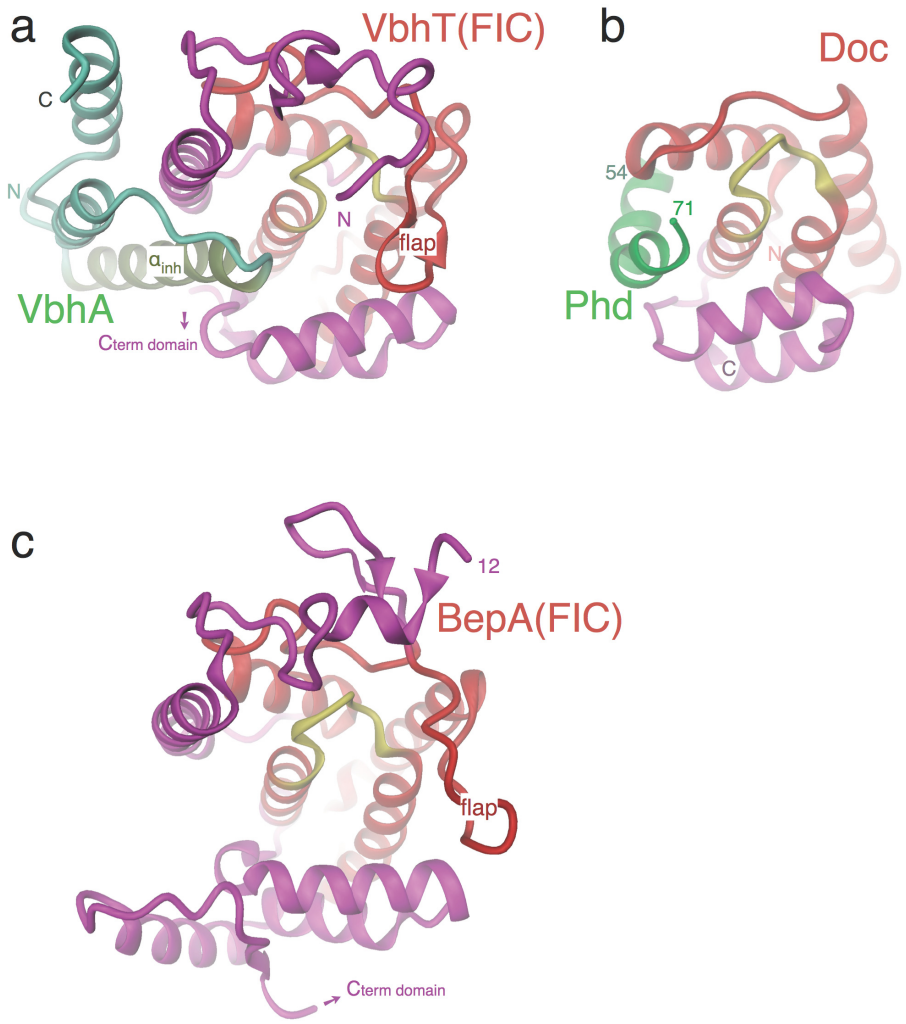

Supplementary Figure 5. Comparison of FIC domain folds and FIC/antitoxin interactions. a, VbhA-VbhT(FIC) from *B. schoenbuchensis*. The VbhT(FIC) structure is highly similar to that of BepA(FIC)[2] (rmsd of 1.6 Å for 169 C_α-positions, panel c). **b**, Doc/Phd from Bacteriophage P1[13], PDB code 3dd7). **c**, BepA(FIC) from *B. henselae*[2]. Representations of the structures as in Fig. 2.

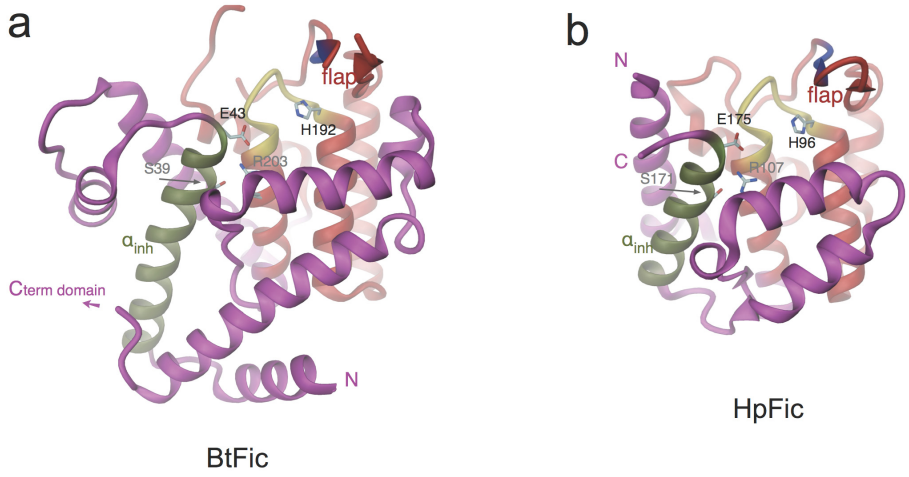

Supplementary Figure 6. Fic protein structures BtFic (BT2513 from *Bacteroides thetaiotaomicron*, PDB code 3CUC) (a) and HpFic (HP1159 from *Helicobacter pylori*, PDB code 2F6S) (b). Structures are shown in cartoon representation as in Fig. 2 (Fic core as defined by PFAM, red; active site loop with histidine, yellow; inhibitory helix (α_{inh}) with C-terminal SxxxEG motif, green; termini labeled with N and C) with important residues in full. Note that BtFic and HpFic are class II and III Fic proteins, respectively, and are close structural homologs of SoFic(Fig. 2b) and NmFic (Fig. 2c).

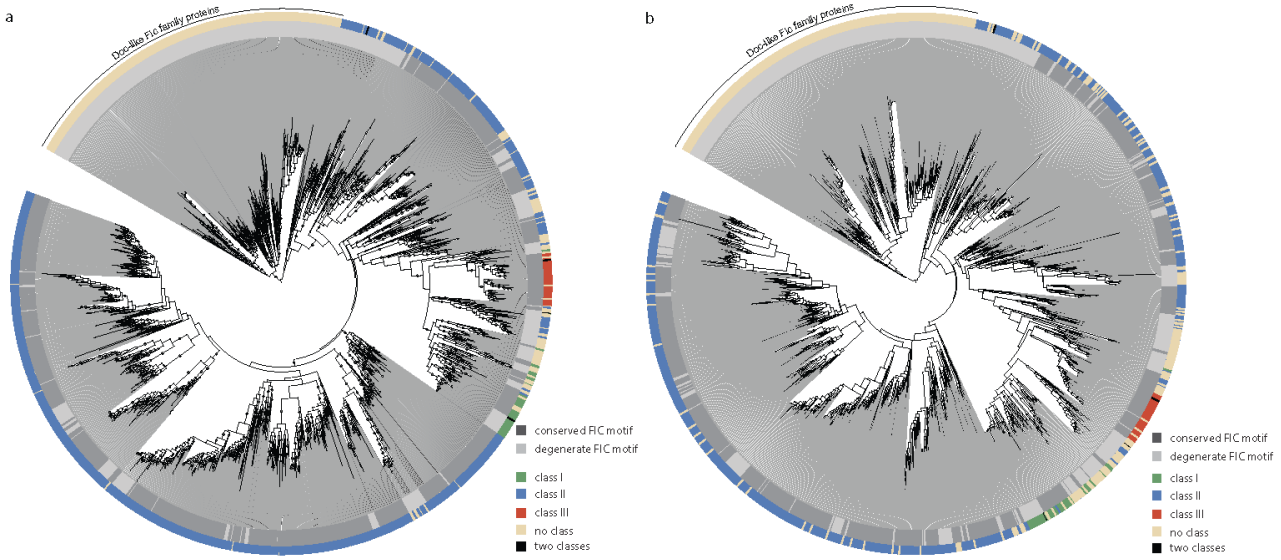

Supplementary Figure 7. **Phylogenetic trees of Fic proteins.** a, Approximately-maximum-likelihood tree inferred with FastTree2. Local support values were calculated as implemented in FastTree2[14] using the Shimodaira-Hasegawa test. Circles indicate branches with local support values > 0.9. b, Maximum-likelihood tree inferred with RAxML[15] using the PROTMIXWAG model. Dark and light grey coloring on the inner circle indicates the presence (conserved) or absence (degenerate) of the adenylylation competent motif, respectively. The outer circle depicts the class assigned to each Fic protein conforming the coloring of Fig. 2e. The large cluster of Doc-like proteins lacking the conserved FIC motif is indicated. An interactive version of the tree with species and accession number labels for each leaf can be accessed via the following link http://itol.embl.de/shared/Engel2011.

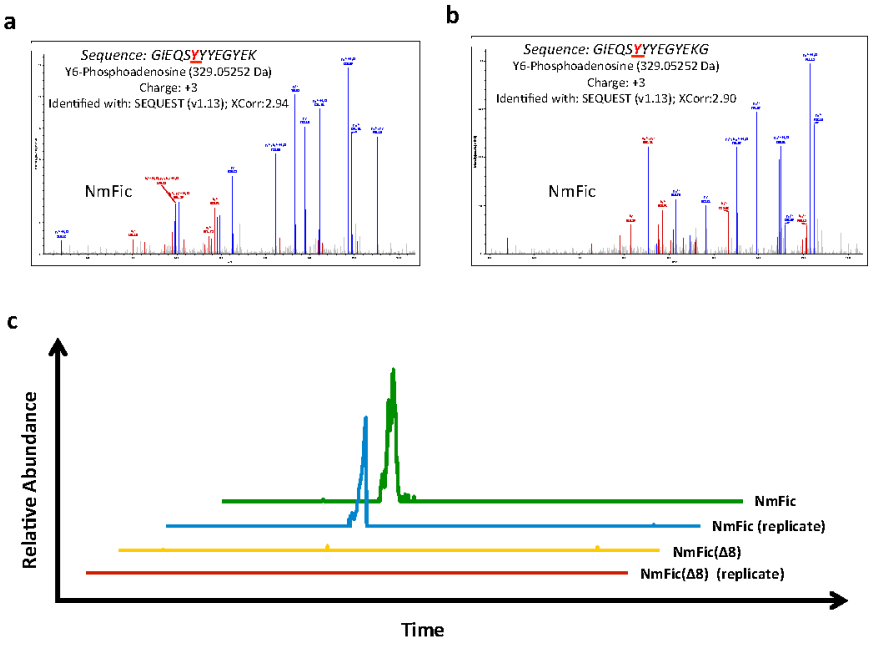

Supplementary Figure 8. LC-MS/MS analysis of adenylylated NmFic protein. a, MS/MS-spectrum of the fully cleaved peptide GIEQSYYYEGYEK at a charge state of 3 using CID. The identified adenylylation sites are underlined in the peptide sequence and indicated in red. All correctly assigned y- and b- fragment ions are indicated in blue and red, respectively, unassigned fragment ions are shown in gray. **b,** MS/MS-spectrum of the incompletely cleaved peptide GIEQSYYYEGYEKG showing the same modification. **c,** Extracted ion chromatograms of the fully cleaved peptide displayed in panel a for the different samples analyzed.

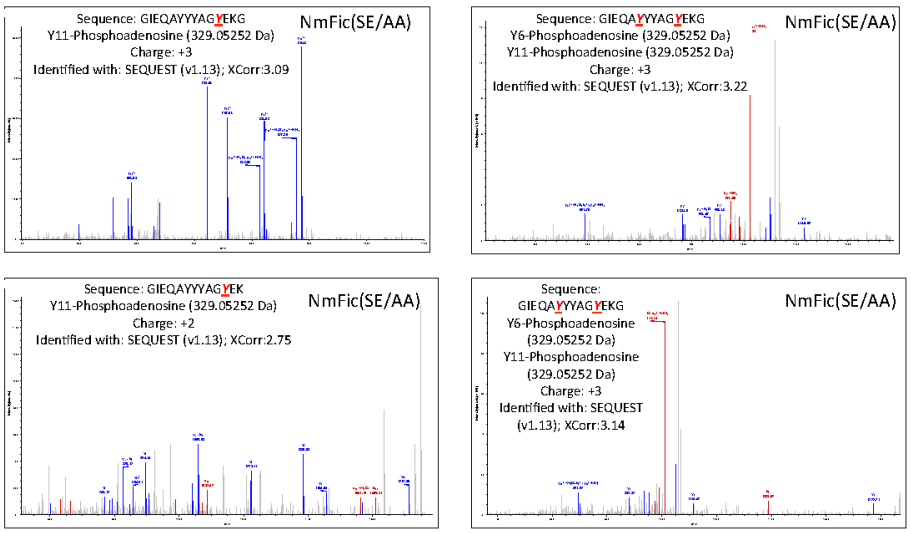

Supplementary Figure 9. LC-MS/MS analysis of adenylylated NmFic(SE/AA) protein. Four MS/MS-spectra are displayed showing the most significant adenylylated peptide sequences identified in the NmFic(SE/AA) mutant. The identified adenylylation sites are underlined in the peptide sequence and indicated in red. All correctly assigned y- and b-fragment ions are indicated in blue and red, respectively, unassigned fragment ions are shown in gray.

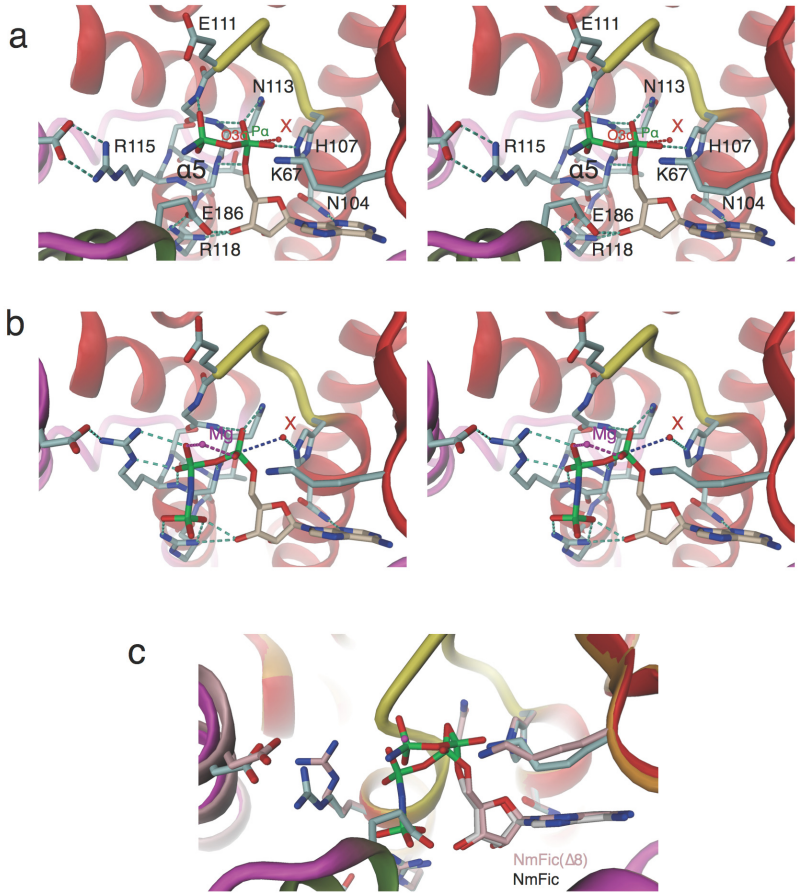

Supplementary Figure 10. AMPPNP binding to NmFic and NmFic(Δ8). The stereoviews of NmFic (a) and NmFic(Δ8) (b) show the detailed interactions of the nucleotide with the Fic active site with H-bonds marked by stippled lines in aquamarine. The structure represenations show similar views as in Figs 3a and b, but with the N-terminal end of helix α5 shown in full to visualize the capping interactions of the α- and β-phosphate with the helix. Additionally, the position that would have to be adopted by a target hydroxyl group for productive nucleophilic attack inline with the scissile Pα-O3α bond is indicated by a small red sphere (marked X) with the X - Pα distance set to 3.0 Å. (c) Superposition of NmFic (gray carbons) and NmFic(Δ8) (orange carbons).

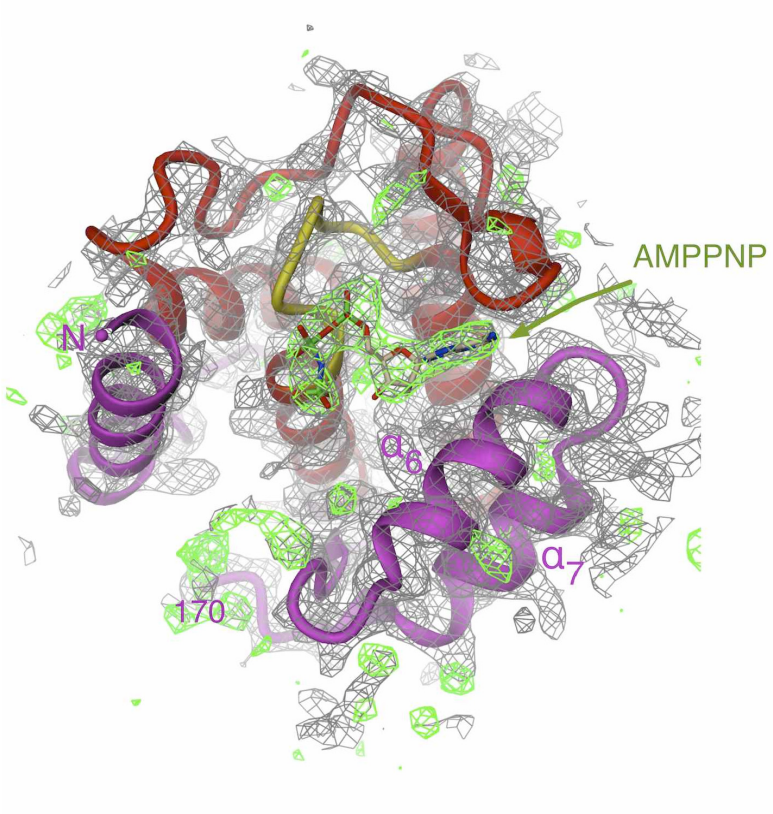

Supplementary Figure 11. Crystal structure of NmFic(SE/AA). The schematic cartoon of chain A is shown in the same representation as in Fig. 2a. Note that (as in all other 15 molecules of the asymmetric unit) helix α_{inh} which follows α7 is disordered as evidenced by missing electron density. The AMPPNP substrate analog, however, is fully resolved and found in the same conformation and orientation as in the corresponding NmFic(Δ8)/AMPPNP structure (Fig. 3b). The ligand has been omitted from phasing. The 2Fo-Fc density map is shown in grey (1.2 σ), the Fo-Fc map in green (3.0 σ).

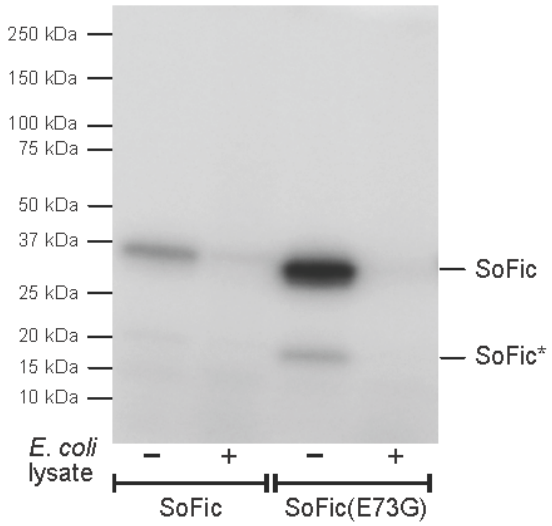

Supplementary Figure 12. Autoradiography of an SDS-gel after incubation of SoFic and SoFic(E73G) with α-^{32}P-ATP in the presence or absence of *E. coli* lysate. Auto-adenylylation is drastically increased in the SoFic(E73G) mutant. SoFic* indicates a truncated version of SoFic as evidenced by mass spectrometry. No target bands are revealed upon incubation with *E. coli* lysate. It is conceivable that the target is a small, unresolved peptide or DNA.

RESEARCH SUPPLEMENTARY INFORMATION

3. Supplementary Tables

Supplementary Table 1. Data collection and refinement statistics.

	VbhA-VbhT(FIC)	NmFic	NmFic(Δ8)	NmFic(SE/AA)
Data collection				
Space group	C2	$P6_422$	$P2_1$	$P2_1$
Cell dimensions				
a, *b*, *c* (Å)	106.34, 40.37, 73.79	148.96, 148.96, 75.80	73.94, 65.03, 75.99	110.31, 136.92, 114.66
α, β, γ (°)	90.00, 121.40, 90.00	90.00, 90.00, 120.00	90.00, 107.08, 90.00	90.00, 100.26, 90.00
Resolution (Å)	45.21-1.50(1.58-1.50) *	65.35-2.15(2.27-2.15) *	37.03-1.7(1.79-1.70) *	87.07-3.02(3.19-3.02) *
R_{sym} or R_{merge}	6.3(23.8)	9.3(46.9)	6.9(37.3)	11.2(35.2)
$I/\sigma I$	9.1(2.0)	18.5(4.0)	9.8(2.6)	6.9(2.2)
Completeness (%)	96.2(74.8)	99.1(93.9)	97.7(95.4)	89.0(43.1)
Redundancy	3.8(2.0)	13.6(8.8)	4.0(3.5)	3.8(2.1)
Refinement				
Resolution (Å)	15.0-1.50	15.0-2.15	15.0-1.7	15.0-3.02
No. reflections	41,211(4,622)	27,218(3,678)	73,865(10,470)	58,488(4,120)
R_{work}/ R_{free}	18.0/21.5	18.8/21.3	15.9/19.7	22.2/24.8
No. atoms				
Protein	2173	1681	5076	21120
Ligand/ion	2 TAR	1 ANP	4 ANP, 4 MG, 4 P6G	16 ANP
Water	255	189	424	-
B-factors				
Protein	22.1	37.2	18.4	66.4
Ligand/ion	22.2	44.8	34.6	36.5
Water	31.1	47.8	24.4	-
R.m.s deviations				
Bond lengths (Å)	0.012	0.012	0.010	0.009
Bond angles (°)	1.3	1.2	1.3	1.1

*Highest resolution shell is shown in parenthesis.

Supplementary Table 2. Distribution of Fic proteins from different domains of life in the three regulatory classes I to III.

	Data analyzed			Distribution of Fic proteins into the different regulatory classes I to III													
				class I[d]		class II[e]		class III[f]		no class		class I and II		class I and III		class II and III	
Domain	Dataset[a]	Proteins[b]	Domains[c]	#	%	#	%	#	%	#	%	#	%	#	%	#	%
All	FIC family	2189	2191	156	7.12	1217	55.55	73	3.33	741	33.82	1	0.05	1	0.05	2	0.09
	conserved FIC motif	1129	1131	50	4.42	898	79.40	72	6.37	110	9.73	0	0.00	0	0.00	1	0.09
Bacteria	FIC family	2072	2074	154	7.03	1146	52.30	73	3.33	697	31.81	1	0.05	1	0.05	2	0.09
	conserved FIC motif	1058	1059	50	4.42	834	73.74	72	6.37	102	9.02	0	0.00	0	0.00	1	0.09
Archaea	FIC family	49	49	0	0.00	30	1.37	0	0.00	19	0.87	0	0.00	0	0.00	0	0.00
	conserved FIC motif	26	26	0	0.00	26	2.30	0	0.00	0	0.00	0	0.00	0	0.00	0	0.00
Eukaryota	FIC family	59	59	0	0.00	38	1.73	0	0.00	21	0.96	0	0.00	0	0.00	0	0.00
	conserved FIC motif	40	40	0	0.00	35	3.09	0	0.00	5	0.44	0	0.00	0	0.00	0	0.00
Viruses	FIC family	5	5	0	0.00	2	0.09	0	0.00	3	0.14	0	0.00	0	0.00	0	0.00
	conserved FIC motif	4	4	0	0.00	2	0.18	0	0.00	2	0.18	0	0.00	0	0.00	0	0.00
Unclass[g]	FIC family	1	1	0	0.00	1	0.05	0	0.00	0	0.00	0	0.00	0	0.00	0	0.00
	conserved FIC motif	1	1	0	0.00	1	0.09	0	0.00	0	0.00	0	0.00	0	0.00	0	0.00
Other[g]	FIC family	3	3	2	0.09	0	0.00	0	0.00	1	0.05	0	0.00	0	0.00	0	0.00
	conserved FIC motif	1	1	0	0.00	0	0.00	0	0.00	1	0.09	0	0.00	0	0.00	0	0.00

[a] we analyzed the entire FIC PFAM family (PFAM release 24) as well as a subset of Fic proteins harbouring an adenylylation-competent core motif (conserved FIC motif, HxFx[D/E]GNGRxxR),
[b] number of proteins analyzed,
[c] number of domains analyzed; two proteins harbour two FIC domains,
[d] class I, antitoxin-like ORF harbouring inhibition motif,
[e] class II, N-terminal inhibition motif,
[f] class III, C-terminal inhibition motif,
[g] "Unclass" stands for unclassified Fic proteins, "Other" comprises three Fic proteins from plasmid sequences sampled from the environment

Supplementary Table 3. Prediction of class I, class II, and class III inhibition motifs for selected Fic proteins.

						HHpred results[d]																	
						class II structures						class III structures						Structures without class II or III regulatory features					
		predicted regulatory features (class I-III)[c]				SoFic (3eqx)			BtFic (3cuc)			NmFic (2g03)			HpFic (2f6s)			Doc (3dd7)		BepA (2jk8)		VopS (3let)		IbpA (3n3u)	
Fic protein[a]	FIC motif[b]	class I	class II	class III	none	rankff	score	motif	rankff	score	motif	rankff	score	motif	rankff	score	motif	rankff	score	rankff	score	rankff	score	rankff	score
BepA (CAD89506)	HPFREGNGRTQR	yes[e]	no	no	no	7	84	no	4	130	no	3	226	no	2	240	no	8	41	1	686	6	92	5	105
IbpA_FIC1 (BAC78649)	HPFAEGNGRMAR	no	yes	no	no	3	237	GSAVDD	2	250	GSAVDD	5	162	no	6	155	no	8	59	7	137	4	207	1	427
IbpA_FIC2 (BAC78649)	HPFAEGNGRMAR	no	yes[f]	no	no	4	210	TKVIED	3	228	TKVIED	6	163	no	7	149	no	9	57	8	129	5	194	1	488
VopS (BAC59949)	HGFTDGNGRMGR	no	no	no	no	4	48	no	3	50	no	2	52	no	6	43	no	8	24	7	41	1	426	5	47
Doc (CAA66833)	HIFNDANKRTAL	no	no	no	no	6	72	no	3	79	no	4	75	no	5	73	no	1	279	2	86	8	71	7	72
E.coli_Fic (AAA23773)	HPFRVGSGLAQR	yes[g]	no	no	no	6	170	no	4	197	no	3	233	no	2	240	no	8	60	1	326	7	141	5	178
Hype/FicD (AAQ89351)	HPFIDGNGRTSR	no	yes	no	no	4	267	TVAIEG	1	379	TVAIEG	5	226	no	6	209	no	8	81	7	193	2	366	3	292
SoFic (AAN57137)	HPFIDGNGRTGR	no	yes	no	no	1	616	SSEIEN	2	286	SSEIEN	4	171	no	6	156	no	8	58	7	150	5	169	3	270
BtFic (AAO77620)	HPFEDGNGRIAR	no	yes	no	no	2	283	SNHLEG	1	492	SNHLEG	5	216	no	6	193	no	8	77	7	180	4	242	3	269
NmFic (NP_273311)	HPFLEGNGRSTR	no	no	yes	no	6	150	no	4	193	no	1	363	SYYYEG	2	338	SYYYEG	8	61	3	218	7	143	5	171
HpFic (ACI27853)	HPFLEGNGRATR	no	no	yes	no	7	145	no	4	187	no	2	316	SYYYEG	1	348	SYYYEG	8	63	3	208	6	148	5	171

[a] protein name and genbank accession
[b] grey shading indicates conserved FIC motif (HxFx[D/E]GNGRxxR)
[c] based on Psi-Blast and HHpred analysis, class I: antitoxin-like ORF harbouring inhibition motif; class II: N-terminal inhibition motif; class III: C-terminal inhibition motif
[d] results of the HHpred alignments with each of the eight template structures from the FIC family, the rank of each alignment, the alignment score, and the presence of an inhibition motif for class II and class III are indicated.
[e] accession of the antitoxin-like ORF: YP_034061
[f] in the IbpA xtal structure (3n3u) the identified motif locates to a loop preceding a helix α6 that is roughly in the position of a canonical α_{inh} (see Supplementary Text)
[g] accession of the antitoxin-like ORF: NP_417821

Supplementary Table 4. Classification of all PFAM FIC domain-containing proteins according to the presence of an antitoxin or an intrinsic inhibition motif. Due to its bulkiness, the table is provided as an extra file in Excel format on http://www.nature.com/nature.

Supplementary Table 5. List of primers used in this study.

Primer name	Sequence (5'-3')
prPE484	CCGCTCGAGGTGAGGAAATATGAGGGTAGC
prPE485	CCGCTCGAGTTACCTTGTAATTCCCTTTGAAG
prPE500	CCGGAATTCAAGAAGGAGATATACATGAGACCATGGCCTACCCATAC
prPE501	CCGGAATTCTTACCTTGTAATTCCCTTTGAAG
prPE519	GGAAGATCTTCATATTTCCTCACGTTTTATCCG
prPE520	GGGAATTCCATATGGCCTACCCATACGATGTTCCAGATTACGCGGCCGCGATGTTGAGCGAGGAAGAAATC
prPE526	CGGGATCCAGCTGCACTTTATAATGTTCCTC
prPE527	ATTACATCTCCTTCAATTACCTA
prPE530	TAGGTAATTGAAGGAGATGTAATTAATTGCAATTATATTATTTCTTGAC
prPE517	CGGGATCCCATCAATGCTTGAAGGAATATGG
prAH095	CGGGATCCATGCAGACAATTAAGTGTGTTG
prAH097	CCGCTCGAGTTAGAATATACAGCACTTCCT
prAH106	CGGGATCCATGCAGGCCATCAAGTGTGT
prAH107	CCGCTCGAGTTACAACAGCAGGCATTTTC
prAH116	GAATGCGTTGGCCCCGTTTCGAGAAGGTAATGGACGTAC
prAH127	CCTTCTCGAAACGGGGCCAACGCATTCAATTCGCCCATG
prAH138	GGGATACAGCTGGACAGGAAGATTATGACAGATTACGCCCCC
prAH139	CTGTCATAATCTTCCTGTCCAGCTGTATCCCATAAGCCCAG
prAH181	CTTTTTGATACTGCAGGGCAAGAGGATTATGACAGATTACG
prAH182	CATAATCCTCTTGCCCTGCAGTATCAAAAAGTCCAAGAGTATATGG
prAG041	GCGCCCATGGTGTTGAGCGAGGAAGAAATCG
prAG042	CGCGGATCCTCATATTTCCTCACGTTTTATCC
prFVS037	GGGAATTCCATATGGTGAGGAAATATGAGGGTAGC
prFVS001	CGACCTCGAGTTAGTGATGGTGATGGTGATGTGTAAATTCAGTGAGGTTTCTAC
prFVS007	GGGAATTCCATATGCATCACCATCACCATCACATGAAATCCATAGACGAACAAAG
prFVS008	CGACCTCGAGTCAGCCTTTTTCATACCCTTCG
prFVS009	CGACCTCGAGTTAGTCAGTCAGGTTGTCCTTTAAC
prFVS010	CAGGCCTATTATTACGCAGGGTATGAAAAAG
prFVS011	CCTGCGTAATAATAGGCCTGCTCGATAC
prFVS026	GTATCGAGCAGGCGTATTATTACGCAGGGTATG
prFVS027	GTAATAATACGCCTGCTCGATACCTTTAAAGATG
prFVS032	GGGAATTCCATATGCATCACCATCACCATCACGAATGGCAAGCTGAACAAGC
prFVS033	CGACCTCGAGTTAAAGCGCATAACGGCTGAAC
prFVS063	CGTTTAGGCGGTTTGGAACCAGATCCACAAG
prFVS064	CTGGTTCCAAACCGCCTAAACGTTGACTAGC
prFVS067	CCAAGGCAGTAGCGAGATTGGCAATATCGTTACCACCAC
prFVS068	GATATTGCCAATCTCGCTACTGCCTTGGGCTTCGAGCAG
prFVS076	GTGGCCATCGGCGGCAACACCCTCACCCTCTC
prFVS077	GTGTTGCCGCCGATGGCCACTGTGTGGTAG
prFVS082	GTATTATTACGGCGGGTATGAAAAAGGCTGAC
prFVS083	CATACCCGCCGTAATAATACGACTGCTCG
prFVS088	GGGAATTCCATATGCATCACCATCACCATCACGTGGAAGAGATCGACCAGAG
prFVS089	CCGCTCGAGTCACGAGTACTCAGTTGTGGCAAAAAG

Supplementary Table 6. List of plasmids constructed in this study.

Plasmid name	Description	Primers used	
		fwd	rev
pPE0017	VbhT (MCS1) in pRSFDuet1	prPE484	prPE485
pPE0020	VbhA (MCS2) in pRSFDuet1	prPE520	prPE519
pPE0021	VbhT (MCS1) + VbhA (MCS2) in pRSFDuet1	-	-
pPE0034	VbhT His136Ala (MCS1) in pRSFDuet1	prAH116	prAH127
pPE1018	HA-VbhT in pMMB206 (pVbhT)	prPE500	prPE501
pPE1031	HA-VbhT(H136A) in pMMB206 (pVbhT(H136A))	prAH116	prAH127
pPE3005	VbhA-VbhT deletion fragment in pTR1000	prPE526	prPE517
pFVS0011	VbhA (MCS1) + VbhT 1-198 (MCS2) in pRSFDuet1	prAG037	prFVS001
pFVS0012	VbhT 1-198 (MCS2) in pRSFDuet1	prAG037	prFVS001
pFVS0015	NmFic 11-191 (MCS2) in pRSFDuet1	prFVS007	prFVS008
pFVS0016	NmFic 11-167 Δ8 (MCS2) in pRSFDuet1	prFVS007	prFVS009
pFVS0023	NmFic 11-191 Glu186Ala (MCS2) in pRSFDuet1	prFVS010	prFVS011
pFVS0037	NmFic 11-191 Ser182Ala Glu186Ala (MCS2) in pRSFDuet1	prFVS026	prFVS027
pFVS0040	SoFic 1-372 (MCS2) in pRSFDuet1	prFVS032	prFVS033
pFVS0058	SoFic 1-372 Glu73Gly (MCS2) in pRSFDuet1	prFVS067	prFVS068
pFVS0059	NmFic 11-191 Glu186Gly (MCS2) in pRSFDuet1	prFVS082	prFVS083
pFVS0065	VbhA Glu24Gly (MCS1) + VbhT 1-198 (MCS2) in pRSFDuet1	prFVS063	prFVS064
pFVS0080	VbhA Glu24Gly (MCS1) + VbhT 1-198 His136Ala (MCS2) in pRSFDuet1	prAH116	prAH127
GST-HypE	GST-HypE in pET-GSTx (kindly provided by Jack Dixon)	-	-
GST-HypE$_{H/A}$	GST-HypE His295Ala in pET-GSTx (kindly provided by Jack Dixon)	-	-
pFVS0064	GST-HypE Glu234Gly in pET-GSTx	prFVS076	prFVS077
pFVS0085	HypE(FIC) 187-437 (MCS2) in pRSFDuet1	prFVS088	prFVS089
pFVS0087	HypE(FIC) 187-437 His295Ala (MCS2) in pRSFDuet1	prFVS088	prFVS089
pFVS0091	HypE(FIC) 187-437 Glu234Gly (MCS2) in pRSFDuet1	prFVS088	prFVS089
pFVS0058	SoFic 1-372 Glu73Gly (MCS2) in pRSFDuet1	prFVS067	prFVS068
pAH059	GST-Cdc42 Gln61Leu		
pAH088	GST-Cdc42		
pAH060	GST-Rac1 Gln61Leu		
pAH071	GST-Rac1		

4. References

1 Xiao, J., Worby, C. A., Mattoo, S., Sankaran, B. & Dixon, J. E. Structural basis of Fic-mediated adenylylation. *Nat Struct Mol Biol* **17**, 1004-1010 (2010).

2 Palanivelu, D. V. *et al.* Fic domain-catalyzed adenylylation: insight provided by the structural analysis of the type IV secretion system effector BepA. *Protein Sci* **20**, 492-499 (2011).

3 Luong, P. *et al.* Kinetic and structural insights into the mechanism of AMPylation by VopS Fic domain. *J Biol Chem* **285**, 20155-20163 (2010).

4 Worby, C. A. *et al.* The fic domain: regulation of cell signaling by adenylylation. *Mol Cell* **34**, 93-103 (2009).

5 Yarbrough, M. L. *et al.* AMPylation of Rho GTPases by *Vibrio* VopS disrupts effector binding and downstream signaling. *Science* **323**, 269-272 (2009).

6 Soding, J., Biegert, A. & Lupas, A. N. The HHpred interactive server for protein homology detection and structure prediction. *Nucleic Acids Res* **33**, W244-248 (2005).

7 Schmid, M. C. *et al.* A translocated bacterial protein protects vascular endothelial cells from apoptosis. *PLoS Pathog* **2**, e115 (2006).

8 Lehnherr, H., Maguin, E., Jafri, S. & Yarmolinsky, M. B. Plasmid addiction genes of bacteriophage P1: doc, which causes cell death on curing of prophage, and phd, which prevents host death when prophage is retained. *J Mol Biol* **233**, 414-428 (1993).

9 Liu, M., Zhang, Y., Inouye, M. & Woychik, N. A. Bacterial addiction module toxin Doc inhibits translation elongation through its association with the 30S ribosomal subunit. *Proc Natl Acad Sci U S A* **105**, 5885-5890 (2008).

10 Magnuson, R. & Yarmolinsky, M. B. Corepression of the P1 addiction operon by Phd and Doc. *Journal of bacteriology* **180**, 6342-6351 (1998).

11 Mukherjee, S. *et al.* Modulation of Rab GTPase function by a protein phosphocholine transferase. *Nature* **477**, 103-106 (2011).

12 Edgar, R. C. MUSCLE: a multiple sequence alignment method with reduced time and space complexity. *BMC Bioinformatics* **5**, 113 (2004).

13 Garcia-Pino, A. *et al.* Doc of prophage P1 is inhibited by its antitoxin partner Phd through fold complementation. *J Biol Chem* **283**, 30821-30827 (2008).

14 Price, M. N., Dehal, P. S. & Arkin, A. P. FastTree 2--approximately maximum-likelihood trees for large alignments. *PLoS One* **5**, e9490 (2010).

15 Stamatakis, A. RAxML-VI-HPC: maximum likelihood-based phylogenetic analyses with thousands of taxa and mixed models. *Bioinformatics* **22**, 2688-2690 (2006).

Additional supplementary data are available online:

- a classification of all analyzed Pfam FIC domain proteins as class I, class II, or class III
- a movie that illustrates the mechanism of active site obstruction in FIC domains

6.4.Unpublished results related to Research article I

During the initial phase of my PhD project I generated a considerable amount of data related to *Research article I* that had not been published in this article but were instrumental for different follow-up projects such as *Research articles III* and *IV*. I therefore decided to present these data in the context of these later publications in order to make the progress of the different projects transparent.

Bacterial class II Fic proteins

Our research published in the frame of *Research article I* showed that only each around 5% of the (*bona fide* adenylylation-competent) FIC domain proteins belong to class I and class III that we investigated in more detail in *Research articles III* and *IV*, respectively. However, around 80% belong to class II (see Supplementary Figure 7 and Supplementary Table 2 in *Research article I*), but no coherent research project to investigate their molecular functions and biological roles had been initiated. Among these proteins are the metazoan orthologs of human HypE or CG9523 of *Drosophila* (see in the *Introduction* section), but these only make up a rather small part of the sequences.

My personal interest in class II Fic proteins arose when I realized that the far majority of them are bacterial proteins that share a common domain architecture with an N-terminal FIC domain (preceded by a regulatory subdomain with α_{inh}, called FicN[a]) linked to a C-terminal winged helix-turn-helix (wHTH) domain (Figure 16A). A typical representative of this protein family is SoFicT (NP_719793.1) that we used as a model class II Fic protein in *Research article I*. The crystal structure of SoFicT had been solved previously by a structural genomics consortium and revealed a (likely physiological) dimer in which FIC domain and wHTH domain of the monomers are connected by a long, α-helical linker that is positioned at the dimerization interface[179] (Figure 16B). The two wHTH domains are arranged in a way that is compatible with a joint dsDNA interaction similar to structurally related transcription factors, suggesting that SoFicT is a bifunctional protein capable of adenylylation and DNA binding.

[a] The N-terminal regulatory module containing the α_{inh} of these class II Fic proteins is present in the databases as Pfam PF13784 and InterPro IPR025758, respectively, but not consistently detected (personal observation).

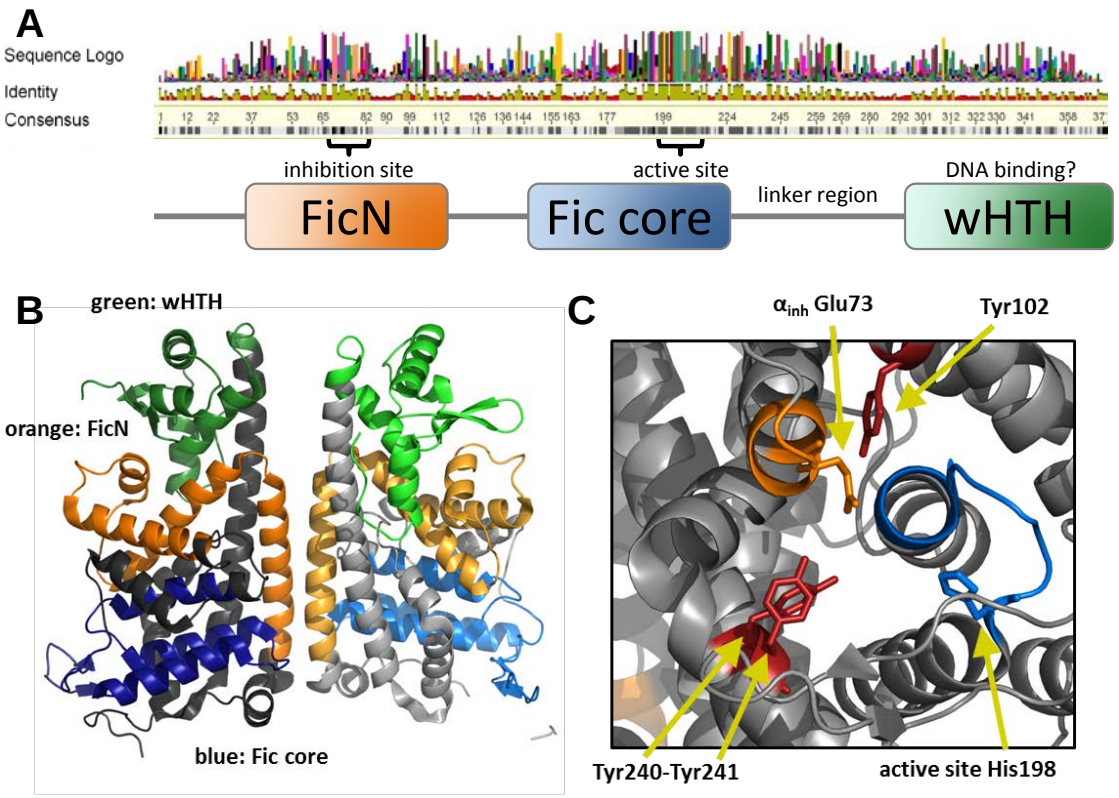

Figure 16: *In silico* analysis of structure-function relations in SoFicT Homologs. A) The alignment of some 1'000 class II Fic proteins with SoFicT as reference sequence[a] was created in Geneious (v.7.1.7., BioMatters) and sequence logo as well as consensus identity are represented graphically. All sequences have canonical active site and α_{inh} motifs, and the domain architecture predicted by InterPro (for SoFicT; FicN 30-111, Fic core 138-216) or deduced by Das *et al*.[179] from their structure (wHTH, 290-370) is indicated below. The alignment is by far not exhaustive for SoFicT homologs, and repeating it with any of the more distant hits results in completely different hit lists but the same overall picture. **B)** FicN, Fic core, and wHTH domains were highlighted in the structure of Das *et al*.[179] by color code as in the model depicted in (A). Note that the regulatory FicN domain connects the dimer interface with the active site of the Fic core. **C)** Three tyrosines are highly conserved among class II Fic proteins and never substituted by phenylalanines or histidines, indicating that they are possible auto-adenylylation sites. These tyrosines protrude towards α_{inh} and active site in a way that auto-adenylylation would likely abolish FicN inhibition and induce domain movements that could activate the Fic core. Furthermore, a threonine within the wHTH domains is universally conserved and could be an(other) auto-modification site. The protein structures in (B) and (C) were visualized using Pymol v1.4.1. (Schrödinger LLC).

In *Research article I* we showed that mutational activation of the SoFicT FIC domain results in growth inhibition in *E. coli*, but the biological relevance of these findings had remained unclear. The protein was expressed ectopically from a high-copy vector using a P_{T7} system, and the construct (that had also been used by the structural genomics consortium) carries a G109C substitution in the regulatory FicN domain. We also failed to detect any target adenylylation by the activated SoFicT_E73G construct, but this could as well be caused by a low-abundance or non-proteic target (compare target adenylylation in Figure 2A of *Research article III*).

[a] The alignment was created using a blastP search against the non-redundant NCBI protein database with maximal E-value of e^{-30}, gap cost (open / extended) of 7 / 2, and hits were aligned using the BLOSUM62 matrix. Columns with more than 75% gaps were hidden for simplicity. Coloring reflects amino acid similarity according to the cost matrix with black = 100% identity and white = <60% identity

SoFicT-like Fic proteins have remained largely uncharacterized, but a literature search revealed two articles with valuable contributions. In the first publication the authors show that the knockout of a *sofic*T homolog in *Sinorhizobium meliloti* is lethal, which – particularly in the light of our findings – made it likely that these proteins may be some kind of toxins that can impair bacterial cell functioning upon activation[348]. Furthermore, another study reported that homologs of SoFicT are frequently found genetically associated to type I restriction-modification systems and consequently established the nomenclature as MloA (methyltransferase-linked ORF A)[349]. I performed a large-scale sequence analysis which indeed confirmed a conspicuous accumulation of restriction-associated functions in the vicinity of genes homologous to *sofic*T including *sofic*T itself. However, the by far large majority of the several thousand homologs appear to be placed randomly in bacterial genomes with no signs of synteny or phylogenetic pattern, indicative of frequent horizontal gene transfer as part of the mobilome (see Figure 17). This analysis further revealed a lack of considerable differences in protein length and domain composition as well as a strong conservation of the canonical sequence motifs in Fic active site and α_{inh} despite major differences in overall primary sequence (see Figure 16A). In the absence of additional evidence it is therefore reasonable to accept the starting hypothesis that SoFicT homologs form one big protein family with shared molecular activities and biological functions.

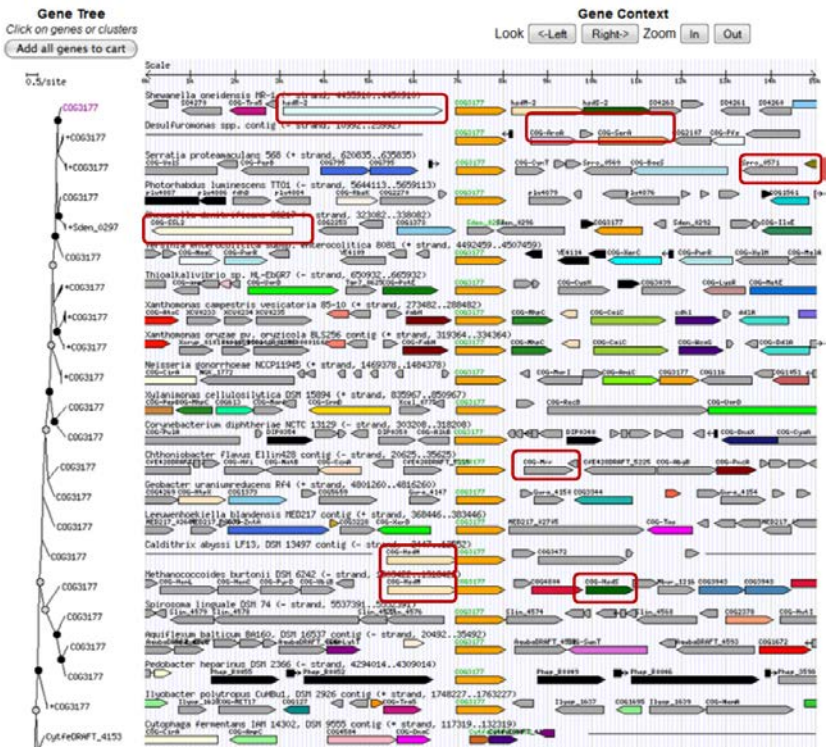

Figure 17: Genomic associations of SoFicT homologs. The illustration was created using the microbesonline resource (available at www.microbesonline.org) with SoFicT (SO_4266) as a query for the "tree browser" function. Representative loci encoding *sofic*T homologs (yellow, in center) are shown. A number of genes encoding restriction-modification functions can easily be spotted (red frames), but no systematic association or local syntenies are apparent. Various traces indicative of horizontal gene transfer such as transposases, integrases, and antibiotic resistance genes are found scattered around the *sofic*T homologs (not highlighted).

Generally, the ubiquity of *soficT* homologs in bacterial genomes is remarkable for a non-housekeeping gene family and points towards biological functions with high selective advantage, yet considerable gene evolution and turnover promoted by horizontal gene transfer. In my opinion such a pattern is indicative of a role in antiviral defense as a new type of abortive infection (Abi) system which is consistent with all available data. Already the "toxic" homolog in *Sinorhizobium meliloti* made the authors speculate that it may use the wHTH domains for transcriptional autoregulation as kind of a single-gene TA module[348]. It is easily conceivable that, in a default state, SoFicT homologs are dimers that control their own transcription and – upon receiving an unknown signal – switch towards a monomeric form that is active in target adenylylation and thereby impairs bacterial physiology. Such a mechanism of autoregulation would recapitulate the conditional cooperativity of class II toxin-antitoxin modules (Box 2) in a single protein. The results of Frédéric Stanger regarding the important role of auto-adenylylation for the activation of class III Fic proteins (see *Research article IV*) suggest that, analogously, the switch to a monomeric, active form of SoFicT homologs may depend on auto-adenylylation. Early attempts to identify the adenylylated sites in SoFicT have remained inconclusive (Frédéric Stanger, personal communication), but a number of hydroxyl residues are highly conserved among SoFicT homologs and may very well serve as molecular switches triggered by auto-modification (see Figure 16C).

Strikingly, the domain architecture of SoFicT homologs is similar to the AbiE / SanaTA family of abortive infection systems that act as a type IV TA module[19] (see *Table I* in the *Introduction* section). The AbiEii / SanaT toxins comprise an N-terminal nucleotidyltransferase domain analogous to FIC domains and a C-terminal helix-turn-helix domain, but – in contrast to what is known for SoFicT homologs – are encoded together with an antitoxin of unknown molecular function.

In order to evaluate the feasibility of a potential research project on the biological function of SoFicT homologs I chose two suitable model proteins encoded by organisms[a] more closely related to *E. coli* K-12. One of them, tentatively named UtiFicT (YP_543089), is encoded in the genome of *E. coli* UTI89[350], a uropathogenic isolate that I had worked on previously in the laboratory of Prof. Urs Jenal. The second one – tentatively named Y2FicT (YP_001008253) to avoid confusion with class I Fic protein YeFicT characterized in *Research article III* – is encoded in the genome of *Yersinia enterocolitica* strain *8081*[351]. While SoFicT and Y2FicT share 63.6% protein sequence identity, UtiFicT and SoFicT have largely divergent primary sequences (16.3% identity). Preliminary experiments could so far not detect an activity of class II Fic proteins as an Abi system (data not shown), but a dedicated study with a greater

[a] Interestingly, homologs of SoFicT are also found in *Bartonella* and typically encoded together with the "*tra*" T4SS system (see *Perspective* at the end of this work).

variety of bacteriophages, positive controls, and an array of different expression systems would be necessary to draw any conclusion. Interestingly, the ectopic expression even of wildtype SoFicT homologs from a single-copy vector caused considerable growth inhibition of *E. coli* (which is not uncommon for Abi proteins[352]) while the supposedly active E/G mutant in the α_{inh} did not (data not shown). These initial experiments clearly indicate that a more ample investigation of class II Fic proteins would be required to understand their molecular function(s) and biological role(s). It would be particularly helpful to identify the adenylylated target(s) – e.g., using the technique that we described in *Research article II* – which would allow to deduce the molecular mechanism of growth inhibition. Furthermore, one could use promoter-*gfp* fusions to demonstrate a potential transcriptional autoregulaton of SoFicT homologs, e.g., by flow cytometry.

6.5.Review article II (published)

"We believe that the order to which we would reduce our ideas has a foundation in the nature of things. And it is this belief that encourages us to reduce our knowledge of things into systematic order. The doing so is attended with many advantages. At the same time a spirit of systematizing may be carried too far. It is only in so far as it is in accordance with the order of nature that it can be useful or sound."

William Fleming, British philosopher, in "The vocabulary of philosophy, mental, moral, and metaphysical; with quotations and references; for the use of my students" (1857). The quotation was cited from p. 507 of an edition available online at the Internet Archive (https://archive.org/details/vocabularyofphil00fle; last accessed on November 19th, 2014)

Type II Toxin-Antitoxin Loci: The *fic* Family

Arnaud Goepfert, Alexander Harms, Tilman Schirmer, and Christoph Dehio

K. Gerdes (ed.), Prokaryotic Toxin-Antitoxins, Springer Berlin Heidelberg, 2013, 177-187.

Summary

Research in the field of FIC domain proteins had so far mostly focused on a few host-targeted virulence factors of bacterial pathogens, but recent publications showed that these had evolved secondarily out of a big pool of genuine bacterial Fic proteins of unknown function. Among these, VbhTA of *B. schoenbuchensis* displays features of a type II TA module. We therefore reviewed published literature on bacterial FIC domain proteins in general and formally described VbhTA and homologs as a new type II TA module.

Although a series of early research papers by Japanese groups had shown that a gain-of-function mutant of the *E. coli* K-12 Fic protein can suppress cell division as some kind of toxin, the underlying molecular mechanism had remained elusive and no follow-up studies had been published. Fresh impetus to the field was given only recently as research on a number of bacterial virulence factors with FIC domains established their conserved enzymatic activity as the adenylylation of target proteins, i.e., the covalent transfer of an adenosine 5'-monophosphate moiety.

A new study of our laboratory could show that the adenylylation activity of FIC domain proteins is generally regulated by a mechanism of active site obstruction in which a glutamate finger on the tip of a conserved inhibitory α-helix (α_{inh}) points into the active site (*Research article I*). This glutamate is strictly conserved as part of an (S/T)xxxE(G/N) motif and blocks adenylylation by forcing the ATP substrate to bind in a way is not permissive for an in-line nucleophilic attack of the target hydroxyl residue on the α-phosphate. Furthermore, we had classified FIC domain proteins depending on whether α_{inh} was present in a separate small protein (class I) or encoded together with the FIC domain in one polypeptide either N-terminally (class II) or C-terminally of the Fic core (class III).

As a model for class I FIC domain proteins we had described VbhT of *B schoenbuchensis* that satisfies the basic definition of a type II toxin-antitoxin module together with its partner VbhA (containing α_{inh}):

- the VbhT toxin inhibits bacterial growth via the adenylylation of unknown target(s)
- the VbhA protein inhibits VbhT via a direct protein-protein interaction
- VbhT and VbhA are encoded together in an operon structure where *vbhA* is upstream of *vbhT* with slight overlap

Of the typical features that have been described for functionality of a type II TA module only the transcriptional autoregulation via conditional cooperativity had not been addressed yet. Despite that, it was still apparent that class I Fic proteins should be considered a new family of type II TA modules with the toxins named "FicT" and the antitoxins named "FicA". We

identified 150 potential members of the FicTA family that included Fic of *E. coli* as a potential toxin (EcFicT) together with a small protein YhfG as a potential antitoxin (EcFicA).

The Doc toxin of the Doc-Phd type II TA module had been shown to inhibit bacterial growth by blocking translation elongation via an unknown mechanism. These earlier studies had also established that Doc represents a distinct type of FIC domain and features a non-canonical active site motif, though the invariant histidine is present and essential for growth inhibition. Furthermore, Doc was known have the same overall topology FIC domains *sensu stricto*, but it misses one α-helix that is generally found in all other Fic proteins and also lacks the β-hairpin flap that is considered to mediate target docking. We noted that its antitoxin Phd is largely different from FicA homologs and does not contain an α_{inh}, but binds Doc in an overall similar (though different) way. The DNA binding domain at the C-terminus of Phd had been shown to be essential for transcriptional autoregulation of the *phd-doc* locus by conditional cooperativity. We considered it plausible that Doc could carry out an enzymatic activity (not adenylylation) to modify cellular target(s) as the underlying cause of translation inhibition and therefore act conceptually similar to FicT toxins. Other FIC domain proteins had secondarily evolved phosphocholination of uridylylation as their primary enzymatic activities.

Our analyses indicated that the primordial FicTA module of *E. coli* K-12 seemed to be vertically inherited in Enterobacteriaceae which is not typical for type II TA modules, because these tend to be spread via horizontal gene transfer as it is also apparent for the FicTA family. Furthermore, the lack of an adenylylation-competent active site motif and the absence of detectable phenotypes with the wildtype protein raised suspicion whether it could act in a biochemically or biologically similar way as other FicTA modules. More generally, we concluded that class I Fic proteins act as a type II TA module and are likely activated via antitoxin degradation. However, it was unknown how class II or class III proteins could be activated *in vivo* or which biological functions they may have.

Summarizing, we described class I of FIC domain proteins as toxins of the new FicTA type II TA module and compared the FicTA family to the related Doc-Phd type II TA module. Future research may identify the enzymatic targets of FicT toxins and unravel if FicTA modules act in the context of bacterial persistence or abortive infection like most type II TA modules. Furthermore, elucidating the targets adenylylated by class II and class III Fic proteins may be a good starting point to find out their biological functions.

Statement of the own participation

I contributed to this publication by reviewing the literature regarding the biological functions of Fic proteins *sensu stricto* as well as the Doc-Phd toxin-antitoxin module and wrote the corresponding sections of text. Arnaud Goepfert focused on the structure-function relationship of FIC domain proteins and generated the figures with my occasional assistance. Prof. Christoph Dehio and Prof. Tilman Schirmer guided the construction of the publication. All authors participated in the finalization of the manuscript.

Chapter 10
Type II Toxin-Antitoxin Loci: The *fic* Family

Arnaud Goepfert, Alexander Harms, Tilman Schirmer and Christoph Dehio

Abstract FIC domain containing proteins (Fic proteins) are present in all domains of life but particularly widespread among prokaryotes. FIC domains with a fully conserved HxFx[D/E]GNGRxxR active site motif catalyze adenylylation (also known as AMPylation), the transfer of an adenosine 5′-monophosphate moiety onto target proteins. Adenylylation activity is tightly controlled by an inhibitory α-helix (α_{inh}) that can either be part of the Fic protein (intramolecular inhibition) or encoded on a different polypeptide chain (intermolecular inhibition), the latter constituting a novel class of type II toxin-antitoxin (TA) modules represented by VbhT-VbhA of *Bartonella schoenbuchensis* and FicT-FicA of *Escherichia coli*. The helix α_{inh} harbors a [S/T]xxxE[G/N] motif with the conserved glutamate partially obstructing the ATP-binding site and forcing ATP to bind in a catalytically incompetent conformation. Release of inhibition by removal of the antitoxin component or by mutation of the conserved glutamate in α_{inh} converts Fic proteins into toxins that severely impair bacterial growth.

10.1 Introduction

Fic proteins defined by carrying the conserved FIC domain are spread over all domains of life and are particularly abundant among prokaryotes, where several thousand of them have been identified in genome sequencing projects (PFAM

A. Goepfert · A. Harms · C. Dehio (✉)
Focal Area Infection Biology, Biozentrum, University of Basel,
Klingelbergstrasse 70, CH-4056 Basel, Switzerland
e-mail: christoph.dehio@unibas.ch

A. Goepfert · T. Schirmer
Focal Area Structural Biology and Biophysics, Biozentrum, University of Basel,
Klingelbergstrasse 70, CH-4056 Basel, Switzerland

K. Gerdes (ed.), *Prokaryotic Toxin-Antitoxins*,
DOI: 10.1007/978-3-642-33253-1_10, © Springer-Verlag Berlin Heidelberg 2013

pf02661). Only few of the bacterial Fic proteins present in the databases have known 3-D structures (Das et al. 2009; Luong et al. 2010; Xiao et al. 2010; Palanivelu et al. 2011), and very little is known about their biological role with the exception of some representatives that have secondarily evolved into virulence factors for the manipulation of eukaryotic host cells (Yarbrough et al. 2009; Worby et al. 2009).

The term *fic* (for "filamentation induced by cAMP") was first used by Utsumi et al. to describe the phenotype of an *Escherichia coli* mutant (Utsumi et al. 1982). This mutant showed a marked defect in cell division when grown at 43 °C and in the presence of cyclic AMP (cAMP) so that the bacteria appeared as long filaments under the light microscope. The mutant *fic-1* allele of the gene designated *fic* was found to code for a G55R substitution in the corresponding single-domain protein Fic that gave the name to the domain family (Kawamukai et al. 1989). Further experimentation revealed that a Δ*fic* deletion mutant strain was viable and showed no discernible phenotypes such as cell filamentation unless complemented with the *fic-1* allele in trans (Kawamukai et al. 1988), thus suggesting that *fic-1* is a gain-of-function mutation. However, though some potential links to carbon metabolism and cAMP signaling could be drawn, the biochemical and physiological basis of the *fic* phenotype has remained elusive until today.

Two decades after these initial studies, Yarbrough and coworkers reported that VopS, a type III secretion effector protein of *Vibrio parahaemolyticus* with two FIC domains, modifies small Rho family GTPases in the host cell by adenylylation, the covalent transfer of an adenosine 5′-monophosphate moiety (Yarbrough et al. 2009). The molecular mechanism involves a nucleophilic attack of the hydroxyl group of the modifiable target amino acid onto the α-phosphorous of ATP leading to transfer of the AMP moiety. Research in this context identified the consensus FIC signature sequence (HxFx[D/E]GNGRxxR) to form the active site motif of FIC domains with the histidine being essential for adenylylation activity. In addition, it was noted that Fic proteins usually exhibit autoadenylylation in addition to target protein adenylylation, even so the physiological role of this phenomenon remained elusive (Xiao et al. 2010; Kinch et al. 2009).

Although consecutive studies demonstrated activities virtually identical to those of VopS for the closely related FIC domains of host cell-translocated virulence factors of *Histophilus somni* and *Pasteurella multocida* (Mattoo et al. 2011), it is striking that the far majority of prokaryotic Fic proteins lack any obvious connection to virulence and therefore likely have a role in bacterial physiology. Exemplified by the VbhT-VbhA complex of *Bartonella schoenbuchensis*, it was recently demonstrated that the toxicity and adenylylation activity of a prokaryotic Fic protein can be specifically suppressed by complex formation with a cognate antitoxin, thus forming a toxin-antitoxin (TA) complex that shares several features of type II TA systems (Engel et al. 2012). In the following, we will briefly review our current knowledge on the evolution and the structure/function relation of this novel family of FIC domain-related TA modules, as well as the structural and functional conservation of the inhibitory mechanism in other Fic protein classes.

10.2 A Novel Class of FIC Domain-Associated Type II Toxin-Antitoxin Systems

Recently, we found that VbhT, a Fic protein of the ruminant-specific pathogen *Bartonella schoenbuchensis*, strongly inhibits bacterial growth when ectopically expressed in *E. coli*. This toxic effect was fully suppressed upon coexpression with VbhA, a small protein encoded by the *vbhA* gene located immediately upstream and likely transcriptionally/translationally coupled to *vbhT* (Engel et al. 2012). Toxicity of VbhT was apparently linked to adenylylation of *bona fide* target proteins in *E. coli* lysates and was dependent on the integrity of the FIC signature motif.

The VbhT-VbhA pair exhibits most of the features that qualify for a type II TA system (Yamaguchi et al. 2011) as shown by Engel et al. (2012).

- Endogenously expressed, VbhT is toxic to the cell.
- VbhA inhibits VbhT toxicity by forming a tight complex.
- VbhT and VbhA are encoded by an operon structure with an upstream antitoxin gene and a downstream toxin gene with presumable transcriptional and translational coupling.

Only transcriptional autoregulation by cooperative promoter binding, a salient feature of other type II TA systems, has not yet been addressed for the VbhT-VbhA module.

A search for *vbhA* homologs encoded immediately upstream of FIC domain-encoding genes identified approximately 150 genes (Engel et al. 2012). Alignment of these VbhA homologous revealed a consensus [S/TxxxE[G/N] motif with a strictly conserved glutamate (Fig. 10.1) that turned out to play a critical role in the inhibitory mechanism.

FicA from *E. coli* is one of the VbhA homologs and is encoded in front of the *fic* gene. In fact, FicA has recently been reported to physically interact with the *E. coli* Fic protein by tandem-affinity purification (Hu et al. 2009) and it was proposed that, indeed, the FicT-FicA module represents a novel TA system (Makarova et al. 2009). Whereas the presence of the [S/TxxxE[G/N] motif in FicA probably indicates a similar mode of inhibition as for the VbhA antitoxin, the slight degeneration of the consensus FIC motif (Fig. 10.1) leaves uncertain the catalytic activity of the toxin as is the case for other Fic proteins (see Sect. 10.7).

Taken together, we propose that VbhT-VbhA and FicT-FicA are the representative members of a novel class of the type II TA system.

Interestingly, gene pairs homologous to *vbhA-vbhT* and *FicT-FicA* are often genetically linked to mobile genetic elements, though this is not the case for the *E. coli ficA-ficT* and close homologs in the *Enterobacteriaceae* where syntenic loci in the chromosome are indicative of vertical transmission.

It is unknown today how the FIC domain-containing toxins of these TA systems get activated in the bacterial cell, but it is well conceivable that—just as described for other TA systems—VbhA-like antitoxins may be more labile than the Fic toxins or prone to faster elimination by intracellular proteases upon stress conditions or other physiological stimuli.

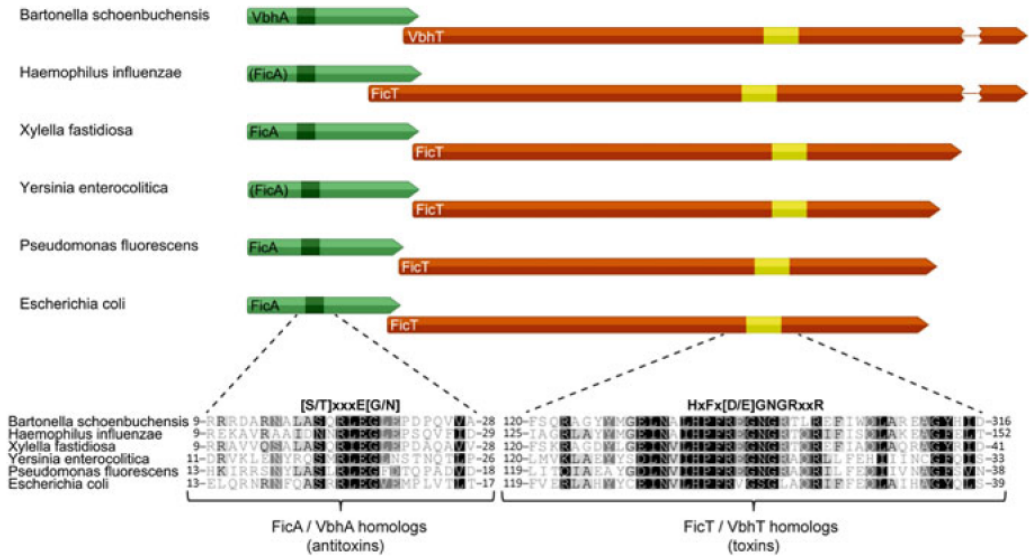

Fig. 10.1 Representatives of the VbhT-VbhA/FicT-FicA toxin-antitoxin family. The genetic organization of six representatives antitoxin-toxin operons (Sequences were taken from *Bartonella schoenbuchensis* R1 (*vbhT* is B11C_100026), *Haemophilus influenza* biotype *aegyptius* plasmid pF1947 (*ficT* is pF1947_03), *Xylella fastidiosa* 9a5c (*ficT* is XF1657), *Yersinia enterocolitica* subsp. *enterocolitica* 8081 (*ficT* is YE1667), *Pseudomonas fluorescens* SBW25 (*ficT* is PFLU0270), and *Escherichia coli* str. K-12 substr. MG1655 (*ficT* is b3661).) is shown at the *top* and the alignment of the signature motifs of VbhA/FicA-homologous antitoxins and VbhT/Fic-homologous toxins at the *bottom*. FicA homologs that were manually annotated are shown in *brackets*. Note that the active site of *Escherichia coli* FicT slightly diverges from the consensus

10.3 Crystal Structure of the VbhT-VbhA TA Module

Figure 10.2a shows the 1.5 Å structure of the FIC domain of VbhT [VbhT(FIC)] in a 1:1 complex with its cognate antitoxin VbhA (Engel et al. 2012). The core of the FIC domain, as defined by Pfam (Punta et al. 2012), is formed by a four-helix bundle (α2–α5). This fold is complemented by the N-terminal helix α1 and two antiparallel helices (α6 and α7) that are arranged perpendicularly to the bundle. Helices α4–α6 form the ATP-binding site. The FIC domain signature motif HxFx[D/E]GNGRxxR is located in the loop that follows helix α4 and extends to the N-cap of helix α5 (Fig. 10.2a). The histidine is indispensible for AMP transferase activity and most probably acts as the general base for the deprotonation of the target side-chain hydroxyl (Luong et al. 2010; Palanivelu et al. 2011). The phenylalanine of the motif is buried in the hydrophobic core of the protein and is important for the folding and the active loop conformation. The remaining residues accommodate the ATP triphosphate moiety. The carboxylic side-chain of the [D/E] residue interacts with a magnesium ion that, in turn, coordinates the α- and β-phosphates of ATP (Fig. 10.3b) (Engel et al. 2012). These two phosphates are

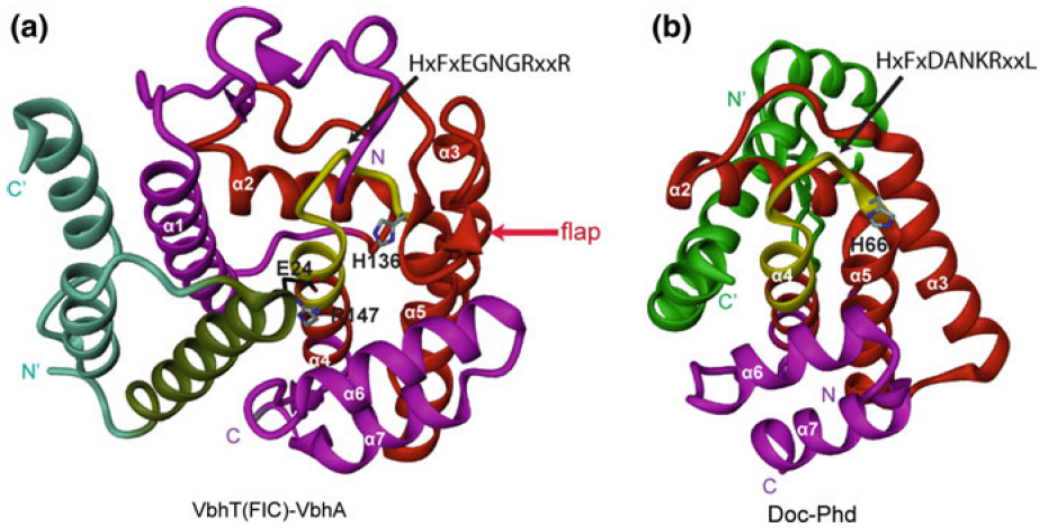

Fig. 10.2 Toxins VbhT (*left*) and Doc (*right*) and their interaction with cognate antitoxins VbhA and Phd, respectively. The toxins exhibit the FIC fold and are shown in *red* (FIC core as defined by PFAM (Punta et al. 2012)) and *magenta*. Their signature motif segments are highlighted in *yellow*. The antitoxins are shown in *green*. **a** Crystal structure of the complex of VbhT(FIC) with antitoxin VbhA (PDB code 3SHG) (Engel et al. 2012) with important residues in full. E24 of the inhibitory helix (α_{inh}, *dark green*) obstructs part of the ATP binding site by forming an intermolecular salt bridge with R147. **b** Crystal structure of the complex of Doc with antitoxin Phd (PDB code 3KH2) (Arbing et al. 2010). The C-terminal helix of Phd is located at a similar position relative to Doc as the N-terminal end of the VbhA helix α_{inh} in relation to VbhT. Thus, the Phd antitoxin may excert its inhibitory role analogously to VbhA, though the function of Doc is still unknown and binding of a substrate to its signature motif is hypothetical

bound to the compound anion binding nest (Watson and Milner-White 2002) at the N-cap of helix α5 with sequence GNGR and form several H-bonds with its main-chain amide groups. The first arginine of the motif interacts with the β-phosphate of ATP, whereas the second arginine serves as a binding site for the γ-phosphate. Furthermore, close to the active site, there is the so-called "flap", a β-hairpin or loop structure that closes onto the adenine ring and creates a suitable target docking site that allows the correct positioning of the modifiable target residue in the FIC active site via sequence-independent main chain–main chain interactions (Palanivelu et al. 2011).

VbhA is a small (62 residues) protein that folds into three anti-parallel helices and wraps around helix α1 of VbhT(FIC), mainly through hydrophobic interactions (Engel et al. 2012). Most relevant, the N-terminal α-helix (α_{inh}), that contains the [S/T]xxxE[G/N] motif is close to the FIC active site (as defined by its signature motif). In particular, residue glutamate E24, which is part of the [S/T]xxxE[G/N] signature motif (see below), forms an intermolecular salt bridge with the second arginine of the FIC motif.

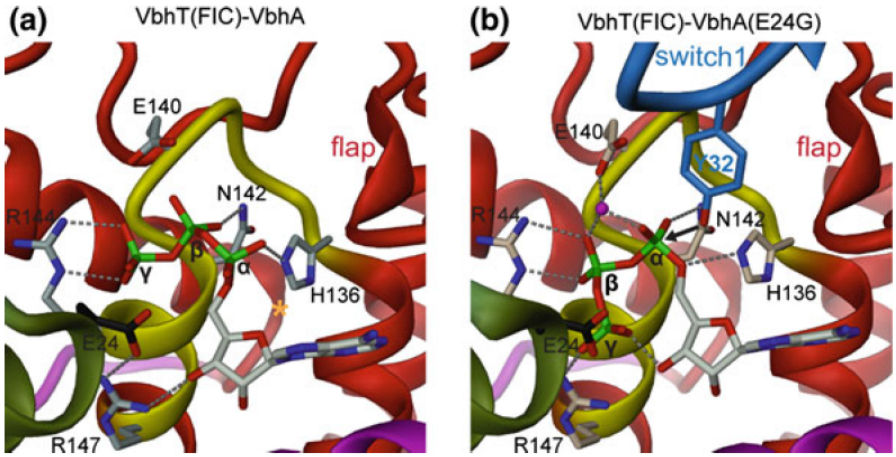

Fig. 10.3 Close-up view of ATP substrate binding to VbhT(FIC) in complex with wild-type VbhA (*left*) and the inhibition-relieved VbhA mutant E24G. Note that the position adopted by E24 of wild-type VbhA (*left*) is taken by the ATP γ-phosphate upon truncation of the glutamate finger (*right*). Furthermore, the location and orientation of the α-phosphate is distinct in the two complexes. In the wild-type situation (*left*), the position that would have to be adopted by a target hydroxyl group (*orange star*) is not accessible. Only in complex with the VbhA mutant (*right*), the α-phosphorous can be attacked in-line with the scissile bond as demonstrated by the superimposed model of the modifiable tyrosine 32 of the cdc42 target protein taken from Xiao et al. (2010). For further details and a movie see Engel et al. (2012)

10.4 VbhA Antitoxin Prevents Productive Binding of ATP to the Catalytic Site of VbhT

How VbhA inhibits the adenylylation activity of the VbhT toxin has been revealed by a detailed crystallographic investigation. It turned out that productive binding of the ATP substrate is impeded by the presence of the conserved glutamate of the antitoxin (E24) which forms an ionic interaction with the second FIC arginine (R147, see Fig. 10.3a).

Only upon truncation of the glutamate (mutant E24G), the ATP γ-phosphate attains the binding subsite close to the second arginine with concomitant rotation of the α-phosphate into an orientation competent for the in-line attack of the target side-chain hydroxyl (Fig. 10.3b). Obviously, the same productive mode of ATP binding is expected for isolated VbhT, explaining its toxicity. Thus, in summary, the antitoxin partly obstructs the nucleotide-binding site of the toxin which impedes competent ATP binding and accordingly inhibits the enzyme's action.

10.5 VbhT-VbhA is Structurally Related to Doc-Phd

The FIC domain fold is very similar to the structure of the well-known Doc toxin of the Doc-PhD type II TA system (see Chap. 9), and both protein families are classified together in the Pfam protein database (Punta et al. 2012) to form the Fic/

Doc family (Pfam: PF02661), also called Fido (Kinch et al. 2009). The Doc-Phd TA locus was discovered as a post-segregational killing system (PSK) that enforces stable maintenance of the P1 phage genome during lysogeny (Lehnherr et al. 1993). In the absence of inhibition by its PhD antitoxin, Doc inhibits translation elongation via an interaction with the ribosome (Liu et al. 2008), but details of the mechanism are not known.

Doc shows the same overall α-helical topology (α2–α7) as Fic proteins, but with helix α1 missing (Fig. 10.2). It has a divergent signature motif (HxFxDANKRxxL) but the histidine that is required for catalysis in Fic proteins is conserved in Doc and, in fact indispensible for its toxicity (Magnuson and Yarmolinsky 1998). Neither adenylylation nor any other enzymatic activity has yet been reported for Doc. However, based on the conservation of their particular active site motif, Doc family proteins are also likely to bind a small molecule substrate and/or catalyze a different enzymatic reaction. Furthermore, the absence of the flap that is essential for the positioning of target protein in the FIC active site and thus critical for adenylylation catalysis also suggests a distinct activity for Doc. Given the similar topology and functional active site location, Fic and Doc are likely to have a common origin and have adopted distinct functional properties later during evolution.

The relative arrangement of the Phd antitoxin with Doc is similar as between VbhA and VbhT (Fig. 10.2). This may indicate a similar mode of inhibition by partial active site obstruction. However, the absence of the [S/T]xxxE[G/N] inhibitory motif in Phd implies differences in the detailed mechanism. In addition to its C-terminal segment that neutralizes Doc activity, Phd carries an N-terminal DNA-binding domain involved in transcriptional regulation (Fig. 10.2b). In contrast, VbhA has no additional domain and a putative role in transcriptional autorepression remains to be elucidated (Fig. 10.2a).

10.6 The Versatile Arrangement of the Inhibitory Helix

Surprisingly, structural comparison of the VbhT-VbhA complex with the structures of other Fic proteins deposited in the PDB databank revealed that a structural equivalent of the inhibitory α-helix of VbhA including the inhibitory motif was present as part of the Fic polypeptide chain itself in several other structures (Engel et al. 2012) (Fig. 10.4). A comparative sequence analysis showed that in the far majority of potentially adenylylating Fic proteins (i.e., Fic proteins with a strictly conserved HxFx[D/E]GNGRxxR FIC active site motif), the inhibitory helix is not provided by a VbhA-like antitoxin but fused N-terminally to the FIC domain. Moreover, in some Fic proteins α_{inh} is found as a carboxy-terminal helix. We therefore proposed a tripartite classification system for Fic proteins: class I in which α_{inh} is contributed by an antitoxin, class II and III in which the inhibitory helix is part of the Fic protein itself as an N- or C-terminal extension of the FIC domain, respectively. We managed to construct inhibition-relieved and thus activated

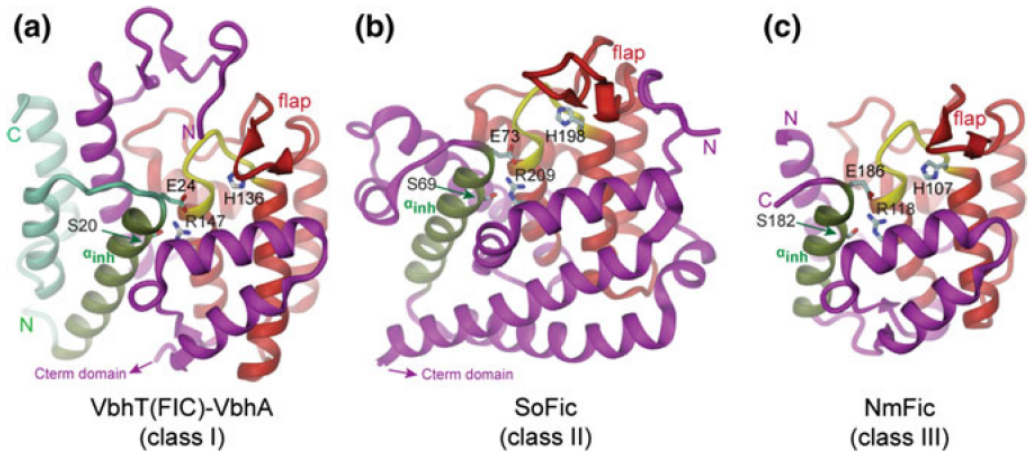

Fig. 10.4 The inhibitory motif can inhibit Fic-catalyzed adenylylation in an inter- (class I) or intra-molecular (class II and III) fashion. Representative crystal structures for **a** Class I, VbhT(FIC)-VbhA as shown in Fig. 10.2. **b** Class II, Fic protein of *S. oneidensis* (SoFic, PDB code 3EQX) (Das et al. 2009) with C-terminal domain omitted, **c** Class III, Fic protein of *N. meningitidis* (NmFic, PDB code 2G03). Whereas, in class I, the inhibitory helix (α_{inh}) with the glutamate finger is provided by a separate antitoxin protein, in class II and class III the helix is part of the FIC domain itself (Engel et al. 2012)

mutants of bacterial Fic proteins of all three classes and demonstrate that they exhibit considerable toxicity accompanied by cell filamentation in ectopically expressing *E. coli* (Engel et al. 2012). Hence, Fic proteins of class II and III—not being associated with a separate antitoxin—are not real TA systems, but could be seen as something conceptually related.

Fic proteins of class II typically display a two-domain architecture with an N-terminal FIC domain and a C-terminal DNA-binding domain, though several other domain architectures occur as well. Our model class II Fic protein So4266 of *Shewanella oneidensis* showed considerable toxicity and strongly increased autoadenylylation upon inactivation of the inhibitory helix, but no target adenylylation was detected (Engel et al. 2012). The authors of the initial publication on the crystal structure of this protein speculated that it may be a nuclease (Das et al. 2009), and it is conceivable to assume that autoadenylylation may induce conformational changes or modify the oligomeric state of the protein that would then trigger enzymatic activity. Other evidence for a function in the context of DNA is the finding that homologs of this Fic protein are often encoded within type I restriction loci (Miller et al. 2005). Like class II Fic proteins, those of class III also seem to act via the adenylylation of target proteins. But the presence of the inhibitory helix within the same polypeptide chain raises the question of how these proteins could be activated under physiological conditions in vivo.

10.7 Other Enzymatic Activities of Fic Proteins: Versatility in Function

Although adenylylation appears to be the prominent enzymatic activity of Fic proteins, other biochemical activities have been detected or suggested for members of this protein family. Whereas the majority of FIC domain-containing proteins seem to preferentially utilize ATP for target modification (Mattoo et al. 2011), VopS is capable of transferring GTP with virtually equal efficiency and may function as a guanylyl transferase. Yet, the FIC domain-containing type III secretion effector XopAC of the plant pathogen *Xanthomonas campestris* was found to specifically inactivate two host kinases by uridylylation, i.e., the transfer of an UMP moiety (Feng et al. 2012). AvrB, a type III secretion effector of *Pseudomonas syringae*, displays the canonical FIC fold and shares the same active site location as Fic proteins but with a highly degenerated FIC active site motif (MxDxRGSAAxxE). While it has been biologically characterized, the molecular mechanism underlying its function remains unknown though a possible kinase activity has been proposed (Desveaux et al. 2007). The *Legionella pneumophila* type IV secretion effector protein AnkX harbors an active site motif (HxFxDANGRxxV) slightly diverging from the canonical HxFx[D/E]GNGRxxR. This active site plasticity enables AnkX to bind CDP-choline at the active site and to catalyze phosphocholination of two small Rab GTPases in the host cell (Mukherjee et al. 2011).

10.8 Conclusions and Outlook

The VbhT-VbhA/FicT-FicA family shares several features characteristic of type II TA systems and is thus proposed to extend this class of TA systems. These novel TA system members are widespread among bacteria and are often associated with mobile DNA suggesting propagation by horizontal gene transfer. Based on the conservation of the canonical FIC active site motif in most Fic toxin components, they appear to mediate target protein adenylylation as exemplarily demonstrated for VbhT. Whether the *E. coli* Fic and close homologs in the Enterobacteriaceae that bear a slightly divergent active site motif also catalyze adenylylation or whether they exert other activities remains to be tested. The majority of Fic proteins do not belong to the VbhT-VbhA/FicT-FicA TA system and have no associated antitoxins. In fact, most of them are predicted to be autoregulated (Engel et al. 2012), i.e., inhibited intramolecularly by a mechanism analogous to that seen for the VbhT/VbhA members. Mutation of the strictly conserved glutamic acid of α_{inh} releaves the inhibition and thus provides a means to study Fic protein function. Future work on the large group of Fic proteins in general, and on FIC domain-related type II TA systems in particular should address the physiological modes of activation (stochastic and/or induced proteolysis), the nature of

the target molecules (proteins and possibly other macromolecules), and the nature of the inflicted post-translational modification (adenylylation, uridinylation, phosphocholination, etc.). In the context of the topic of this book, it will be particularly revealing to compare the molecular activities of the toxin components and their physiological regulation by the respective antitoxin components of the structurally closely related adenylylation-competent VbhT-VbhA module and the likely adenylylation incompetent FicT-FicA module, as well as representatives of the more distantly related Doc-PhD family.

References

Arbing, M.A., et al. (2010). Crystal structures of Phd-Doc, HigA, and YeeU establish multiple evolutionary links between microbial growth-regulating toxin-antitoxin systems. Structure 18, *8*, 996–1010.

Das, D. (2009). Crystal structure of the Fic (Filamentation induced by cAMP) family protein SO4266 (gi|24375750) from *Shewanella oneidensis* MR-1 at 1.6 A resolution. *Proteins, 75*(1), 264–271.

Desveaux, D., Singer, A. U., Wu, A. J., McNulty, B. C., Musselwhite, L., Nimchuk, Z., et al. (2007). Type III effector activation via nucleotide binding, phosphorylation, and host target interaction. *PLoS Pathogens, 3*(3), e48.

Engel, P., Goepfert, A., Stanger, F. V., Harms, A., Schmidt, A., Schirmer, T., et al. (2012). Adenylylation control by intra- or intermolecular active-site obstruction in Fic proteins. *Nature, 482*(7383), 107–110.

Feng, F., Yang, F., Rong, W., Wu, X., Zhang, J., Chen, S., et al. (2012). A Xanthomonas uridine 5′-monophosphate transferase inhibits plant immune kinases. *Nature, 485*(7396), 114–118.

Hu, P., et al. (2009). Global functional atlas of *Escherichia coli* encompassing previously uncharacterized proteins. *PLoS Biology, 7*(4), e96.

Kawamukai, M., Matsuda, H., Fujii, W., Nishida, T., Izumoto, Y., Himeno, M., et al. (1988). Cloning of the *fic-1* gene involved in cell filamentation induced by cyclic AMP and construction of a Δ*fic Escherichia coli* strain. *Journal of Bacteriology, 170*(9), 3864–3869.

Kawamukai, M., Matsuda, H., Fujii, W., Utsumi, R., & Komano, T. (1989). Nucleotide sequences of *fic* and *fic-1* genes involved in cell filamentation induced by cyclic AMP in *Escherichia coli*. *Journal of Bacteriology, 171*(8), 4525–4529.

Kinch, L. N., Yarbrough, M. L., Orth, K., & Grishin, N. V. (2009). Fido, a novel AMPylation domain common to fic, doc, and AvrB. *PloS one, 4*(6), e5818.

Lehnherr, H., Maguin, E., Jafri, S., & Yarmolinsky, M. B. (1993). Plasmid addiction genes of bacteriophage P1: Doc, which causes cell death on curing of prophage, and phd, which prevents host death when prophage is retained. *Journal of Molecular Biology, 233*(3), 414–428.

Liu, M., Zhang, Y., Inouye, M., & Woychik, N. A. (2008). Bacterial addiction module toxin Doc inhibits translation elongation through its association with the 30S ribosomal subunit. *Proceedings of the National academy of Sciences of the United States of America, 105*(15), 5885–5890.

Luong, P., Kinch, L. N., Brautigam, C. A., Grishin, N. V., Tomchick, D. R., & Orth, K. (2010). Kinetic and structural insights into the mechanism of AMPylation by VopS Fic domain. *The Journal of Biological Chemistry, 285*(26), 20155–20163.

Magnuson, R., & Yarmolinsky, M. B. (1998). Corepression of the P1 addiction operon by Phd and Doc. *Journal of Bacteriology, 180*(23), 6342–6351.

Makarova, K. S., Wolf, Y. I., & Koonin, E. V. (2009). Comprehensive comparative-genomic analysis of type 2 toxin-antitoxin systems and related mobile stress response systems in prokaryotes. *Biology Direct, 4*, 19.

Mattoo, S., Durrant, E., Chen, M. J., Xiao, J., Lazar, C. S., Manning, G., et al. (2011). Comparative analysis of *Histophilus somni* immunoglobulin-binding protein A (IbpA) with other fic domain-containing enzymes reveals differences in substrate and nucleotide specificities. *The Journal of Biological Chemistry, 286*(37), 32834–32842.

Miller, W. G., Pearson, B. M., Wells, J. M., Parker, C. T., Kapitonov, V. V., & Mandrell, R. E. (2005). Diversity within the *Campylobacter jejuni* type I restriction-modification loci. *Microbiology, 151*(Pt 2), 337–351.

Mukherjee, S., Liu, X., Arasaki, K., McDonough, J., Galan, J. E., & Roy, C. R. (2011). Modulation of Rab GTPase function by a protein phosphocholine transferase. *Nature, 477*(7362), 103–106.

Palanivelu, D. V., Goepfert, A., Meury, M., Guye, P., Dehio, C., & Schirmer, T. (2011). Fic domain-catalyzed adenylylation: Insight provided by the structural analysis of the type IV secretion system effector BepA. *Protein science : a publication of the Protein Society, 20*(3), 492–499.

Punta, M. et al. (2012). The Pfam protein families database. Nucleic acids research 40 (Database issue):D290–301.

Utsumi, R., Nakamoto, Y., Kawamukai, M., Himeno, M., & Komano, T. (1982). Involvement of cyclic AMP and its receptor protein in filamentation of an *Escherichia coli fic* mutant. *Journal of Bacteriology, 151*(2), 807–812.

Watson, J. D., & Milner-White, E. J. (2002). A novel main-chain anion-binding site in proteins: The nest. A particular combination of phi, psi values in successive residues gives rise to anion-binding sites that occur commonly and are found often at functionally important regions. *Journal of Molecular Biology, 315*(2), 171–182.

Worby, C. A., Mattoo, S., Kruger, R. P., Corbeil, L. B., Koller, A., Mendez, J. C., et al. (2009). The fic domain: Regulation of cell signaling by adenylylation. *Molecular Cell, 34*(1), 93–103.

Xiao, J., Worby, C. A., Mattoo, S., Sankaran, B., & Dixon, J. E. (2010). Structural basis of Fic-mediated adenylylation. *Nature Structural & Molecular Biology, 17*(8), 1004–1010.

Yamaguchi, Y., Park, J. H., & Inouye, M. (2011). Toxin-antitoxin systems in bacteria and archaea. *Annual Review of Genetics, 45*, 61–79.

Yarbrough, M. L., Li, Y., Kinch, L. N., Grishin, N. V., Ball, H. L., & Orth, K. (2009). AMPylation of Rho GTPases by *Vibrio* VopS disrupts effector binding and downstream signaling. *Science, 323*(5911), 269–272.

6.6.Unpublished results related to Review article II

I did not generate unpublished results directly in the context of my contribution to *Review article II* because all information regarding class I FIC domain proteins and their biological function in FicTA toxin-antitoxin modules is given in *Research article III* and the *Unpublished results related to Research article III*.

However, it appears necessary to me to correct the wrong claim in *Review article II* that VopS would have two FIC domains (it has only one – IbpA has two FIC domains).

6.7.Research article II (published)

"I once made the remark that two things disappeared in 1990: one was communism, the other was biochemistry, and that only one of these should be allowed to come back. Of course, biochemistry never really went away but continued to flourish in the thousands of unread pages of biochemical journals. Protein interactions will not be solved by proteomics or protein chips but by protein biochemistry. (…) We do not have to resurrect biochemistry, and it will flourish because it provides the only experimental basis for causal understanding of biochemical mechanisms."

Sydney Brenner, South African biologist and Nobel laureate, in "Biochemistry strikes back". Trends in Biochemical Sciences, Volume 25, Issue 12, December 1st 2000, page 584

An experimental strategy for the identification of AMPylation targets from complex protein samples

Kathrin Pieles*, Timo Glatter*, Alexander Harms, Alexander Schmidt, and Christoph Dehio

*These authors contributed equally to this work

Proteomics, Volume 14, Issue 9, May 2014, 1048-1052.

Summary

Facing the riddle that none of the Bep-related phenotypes of *Bartonella* infection could be traced back to any effector's FIC domain as the most prevalent and ancestral "effector module", we understood that it was necessary to identify their molecular targets as a starting point for functional analyses. In this publication we therefore developed a generic strategy to identify adenylylated proteins using stable-isotope labelled ATP substrates and show that the adenylylation target of Bep2 of *B. rochalimae* is vimentin.

Previous work had described the used of antibodies raised against adenylylated residues or click chemistry approaches to enrich and finally identify adenylylated proteins by mass spectrometry. However, these approaches are afflicted with technical difficulties and biases. We therefore developed a novel technique for the identification of adenylylated proteins in cell lysates that is technically easy and largely unbiased. As the core of our development we performed classical *in vitro* adenylylation assays by supplementing cell lysates known to contain the targets of adenylylation with the adenylylation donor of interest as well as a 3-plexed mix of heavy-isotope labelled ATP. This mix contained unlabeled ATP ($^{15}N_0{}^{13}C_0$-ATP), medium-labeled ATP ($^{15}N_5{}^{13}C_0$-ATP), and heavy-labeled ATP ($^{15}N_5{}^{13}C_{10}$-ATP) that we found to be used equally well by FIC domain proteins for adenylylation. The adenylylation of target proteins with this mix of isotopes results in three different adenylylated peptides with characteristic mass shifts relative to unmodified peptide (+ 329, + 334, + 344). The resulting pattern of peaks corresponding to these mass shifts could be detected by mass spectrometry and provided an additional level of information for the identification of adenylylation.

As a general proof-of-principle for our technique we analyzed the adenylylation of RhoA by the *V. parahaemolyticus* effector VopS which is known to target T35 on the small GTPase. The adenylylation with 3-plexed heavy-isotope labeled ATP resulted in the predicted ion triplet for a peptide encompassing the adenylylation site, and thorough inspection of the peptide fragment spectra confirmed T35 as the residue carrying the modification. Subsequently, we analyzed the adenylylation activity of Bep2 of *B. rochalimae* that targets an unknown host protein with an apparent molecular weight of approximately 50 kDa. For Bep2 we identified a triplet of adenylylation mass shifts on a peptide belonging to the intermediate filament protein vimentin, but could not unambiguously unravel the residue which is modified. Using a catalytically inactive mutant of Bep2 we demonstrated that it was indeed the *Bartonella* effector which caused the modification. Furthermore, we confirmed the adenylylation using recombinant Bep2 as well as vimentin with [α-^{32}P]-ATP in a classical *in vitro* adenylylation assay.

In summary, our results proved that a 3-plexed mix of heavy-labeled small molecule substrates can be used to trace biochemical reactions with high detectability and reliability particularly if the resulting protein modification is rare. Given the complexity of eukaryotic cells, it is the only prerequisite of our technique to know the apparent molecular weight of the adenylylated target(s) which allows to cut out specific areas of the cell lysate separated by SDS-PAGE. Our technique was of obvious relevance for the field of FIC domain proteins where no molecular target or biological function had been assigned to the far majority of representatives. The results obtained with Bep2 were interesting also from a more general point of view because we identified the first FIC domain adenylylation target that is not a small GTPase. However, any functional consequence of the adenylylation of vimentin as well as a possible biological role during *Bartonella* infection remained to be demonstrated.

Statement of the own participation

I contributed to this publication by showing that Bep2 of *B. rochalimae* displays an adenylylation activity dependent on the integrity of its FIC domain active site and that this adenylylation activity targets host protein(s) with an apparent molecular weight of approximately 50 kDa. As a prerequisite for these results I had adapted my previously published adenylylation assay using bacterial cell lysates (see *Research article I*) to mammalian cell lysates and developed a technique for their preparation. The other authors of this publication performed all other experiments, developed the biochemical procedure of adenylylation detection by ion triplets with heavy-labeled ATP, and wrote the manuscript.

1048 DOI 10.1002/pmic.201300470 *Proteomics* 2014, *14*, 1048–1052

TECHNICAL BRIEF

An experimental strategy for the identification of AMPylation targets from complex protein samples

Kathrin Pieles, Timo Glatter*, Alexander Harms, Alexander Schmidt and Christoph Dehio*

Biozentrum, University of Basel, Basel, Switzerland

AMPylation is a posttranslational modification (PTM) that has recently caught much attention in the context of bacterial infections as pathogens were shown to secrete Fic proteins that AMPylate Rho GTPases and thus interfere with host cell signaling processes. Although Fic proteins are widespread and found in all kingdoms of life, only a small number of AMPylation targets are known to date. A major obstacle to target identification is the limited availability of generic strategies allowing sensitive and robust identification of AMPylation events. Here, we present an unbiased MS-based approach utilizing stable isotope-labeled ATP. The ATP isotopes are transferred onto target proteins in crude cell lysates by in vitro AMPylation introducing specific reporter ion clusters that allow detection of AMPylated peptides in complex biological samples by MS analysis. Applying this strategy on the secreted Fic protein Bep2 of *Bartonella rochalimae*, we identified the filamenting protein vimentin as an AMPylation target that was confirmed by independent assays. Vimentin represents a new class of target proteins and its identification emphasizes our method as a valuable tool to systematically uncover AMPylation targets. Furthermore, the approach can be generically adapted to study targets of other PTMs that allow incorporation of isotopically labeled substrates.

Received: October 28, 2013
Revised: January 7, 2014
Accepted: January 29, 2014

Keywords:
Adenylylation / AMPylation / Fic proteins / Isotopic labeling / Microbiology / Vimentin

Additional supporting information may be found in the online version of this article at the publisher's web-site

Protein AMPylation (also known as adenylylation) is a PTM in which an AMP moiety is transferred onto a threonine or tyrosine residue of a target protein. AMPylation was discovered in the 1960s in the context of regulation of glutamine synthetase activity in *Escherichia coli* [1]. Recently, proteins belonging to the Fic family (filamentation induced by cAMP) were also shown to catalyze protein AMPylation. Fic proteins are found in all kingdoms of life and are conserved from bacteria to humans [2–4]. Although this protein family comprises thousands of proteins, the function of only two Fic proteins is understood in a physiological context. Yarbrough et al. were the first to demonstrate that a translocated bacterial Fic protein subverts host cell defense mechanisms within bacterial infection processes [5]. In particular, a type III secretion system effector from *Vibrio parahemolyticus*, VopS, is secreted into the host cell where it AMPylates a conserved threonine (T35) of Rho family GTPases. AMPylation impairs binding of GTPase interaction partners and thereby interferes with the host cell signaling machinery leading to cytoskeleton collapse and cell death [6]. Similarly, the surface antigen IbpA of *Histophilus somni* was shown by Worby et al. to target Rho GTPases. Though IbpA does not modify T35 but the neighboring tyrosine (Y32), it also impairs GTPase signaling leading to cytoskeleton collapse [7, 8]. Moreover, the human Fic protein HYPE was identified to target Rho GTPases in vitro, yet, its physiological role and potential in vivo targets remain elusive [7].

Despite this recent progress, comprehensive functional details into Fic protein-mediated AMPylation and its impact on cellular signaling events are still in its infancy. This is underlined by the fact that among the large number of existing Fic proteins only a handful are characterized as AMPylators

Correspondence: Professor Christoph Dehio, Biozentrum, University of Basel, Klingelbergstrasse 70, CH-4056 Basel, Switzerland
E-mail: christoph.dehio@unibas.ch
Fax: +41-61-267-21-18

*These authors contributed equally to this work.

© 2014 WILEY-VCH Verlag GmbH & Co. KGaA, Weinheim

[4] with small GTPases representing the only identified target class. The main reason for the limited insights into the biological role of Fic proteins and Fic-mediated target AMPylation is the limited availability of selective enrichment strategies specifically targeting the AMPylated moiety. This hampers the systematic analysis of AMPylation events and renders target identification a challenging task. Though target enrichment advanced with the introduction of an antibody raised against AMPylated threonine [9], tyrosine-modified peptides, and proteins would escape purification. Another promising step forward was recently presented by a strategy utilizing a functionalized ATP analog that can be trapped by an azide alkyne cycloaddition (also known as CLICK chemistry approach) to enrich for modified proteins [10, 11]. Yet, the modification of ATP goes along with changes in size and electron density of the substrate, which might impair binding to the substrate-binding site of Fic proteins [10]. Therefore, experimental strategies enabling unbiased and specific identification of AMPylated proteins are required to further elucidate the biological mechanism underlying protein AMPylation and its effect on cellular signaling. Here, we present an unbiased method to identify AMPylated targets from cell lysates building on in vitro activity assays using stable isotope-labeled ATP substrates. The in vitro reaction generates AMPylated peptide isotopes that can be detected as reporter ion clusters with defined mass shifts in MS analysis.

In the first step, an in vitro reaction of lysates of *E. coli* expressing an AMPylator and a eukaryotic cell extract is performed in the presence of α^{32}P-ATP to screen for possible AMPylation events (Fig. 1A). As AMPylation includes the transfer of the radioactive α-phosphate of the ATP, potential AMPylation targets, and their apparent molecular weight can be visualized by autoradiography. Once an AMPylation event is detected, an in vitro reaction is performed in which a 3-plexed labeled ATP mix is used as a substrate. The substrate mix contains unlabeled ATP ($^{15}N_0{}^{13}C_0$-ATP), medium-labeled ATP ($^{15}N_5{}^{13}C_0$-ATP), and heavy-labeled ATP ($^{15}N_5{}^{13}C_{10}$-ATP), which after AMP transfer will result in predictable mass shifts of the AMPylated peptides that are detectable by MS-analysis and serve as a reporter cluster specific for an AMPylation event. The AMPylated targets and modified residues are identified after an in-gel digest performed on excised gel bands corresponding to the known molecular weight of the target proteins followed by LC-MS analysis (Fig. 1A). Building on recently introduced experimental strategies that used a mix of isotope-labeled cross-linkers in postlysis reactions to ultimately increase specificity in cross-linked peptide identification [12, 13], we used a mixture of unlabeled and stable isotope-labeled forms of ATP to increase the specificity and reliability in detecting an AMPylation event on target proteins. Based on the MS-based sequencing information, the corresponding MS spectra can be inspected for the AMP-peptide isotopes that emerge as a reporter cluster displaying an additional level of information for AMPylation detection. Thus, the detection of these isotopic peptide ion triplets of AMP-peptides may also serve as a meaningful level of confidence of an AMPylation, in particular when MS-sequencing identification scores are close to a given significance threshold or when significance levels have to be lowered for obtaining preliminary peptide candidates. The use of peptide ion clusters improves target detectability and reliability even for low abundant target proteins. Subsequently, the fragment spectra of these triplets can be subjected to manual interpretation or the sample can be reanalyzed using optimized MS-parameters or different fragmentation techniques in combination with directed LC-MS analysis to increase the number of unambiguous identifications [14].

In order to evaluate our experimental strategy, we recapitulated the experiments done by Yarbrough et al. and incubated VopS with the purified small GTPase RhoA in the presence of 3-plexed ATP [5]. Following protein digestion by AspN and MS analysis, we identified the peptide DQFPVYVPTVFENYVA with increment masses matching to the three incorporated isotopically labeled substrates (+329, +334, +344) indicating an AMPylation event (Supporting Information Fig. 1). Closer inspection of the fragment spectra then indicated an AMPylation of RhoA on T35 by VopS as previously described by Yarbrough et al. This finding emphasizes the applicability of our experimental workflow in detecting AMPylation events.

In contrast to pathogens such as *V. parahaemolyticus* that secrete only one Fic protein, pathogens belonging to the genus *Bartonella* translocate a variety of FIC-domain containing effector proteins (Beps) into the host cell [15]. Yet, *Bartonella* infections are typically benign despite high pathogen load both on the cellular and organismic level [16]. This implies that *Bartonella* effectors likely target a variety of different host proteins for subtle alterations of host cell functions. In order to gain first insights into the target specificity of Beps, we applied our strategy on the effector Bep2 of *Bartonella rochalimae*.

To screen for possible AMPylation activity of Bep2, we performed in vitro AMPylation assays with bacterial lysates of *E. coli* cells expressing Bep2 and crude cell lysates derived from J774 mouse macrophages in the presence of α^{32}P-ATP. Following SDS-PAGE a protein band with an apparent molecular weight of 50 kDa was detected on the autoradiogram indicating that Bep2 indeed AMPylates a target protein in J774 mouse macrophages (Fig. 1B, lane 4). The molecular size estimation already indicates that the potential target is unlikely to fall in the class of small GTPases, which is the only known class of AMPylation targets and is represented by lower molecular weight [4].

In order to identify this protein, we performed trypsin in-gel digestion and LC-MS analysis of a parallel processed sample that underwent in vitro AMPylation reaction using the 3-plexed ATP mix. Upon LC-MS analysis and database search including the phospho-adenosine modification in all isotopic versions as a variable modification, we obtained a positive hit identifying a potential AMPylation on the peptide SLYSSSPGGAYVTR matching to the intermediate filament protein vimentin (Supporting Information Fig. 2).

© 2014 WILEY-VCH Verlag GmbH & Co. KGaA, Weinheim

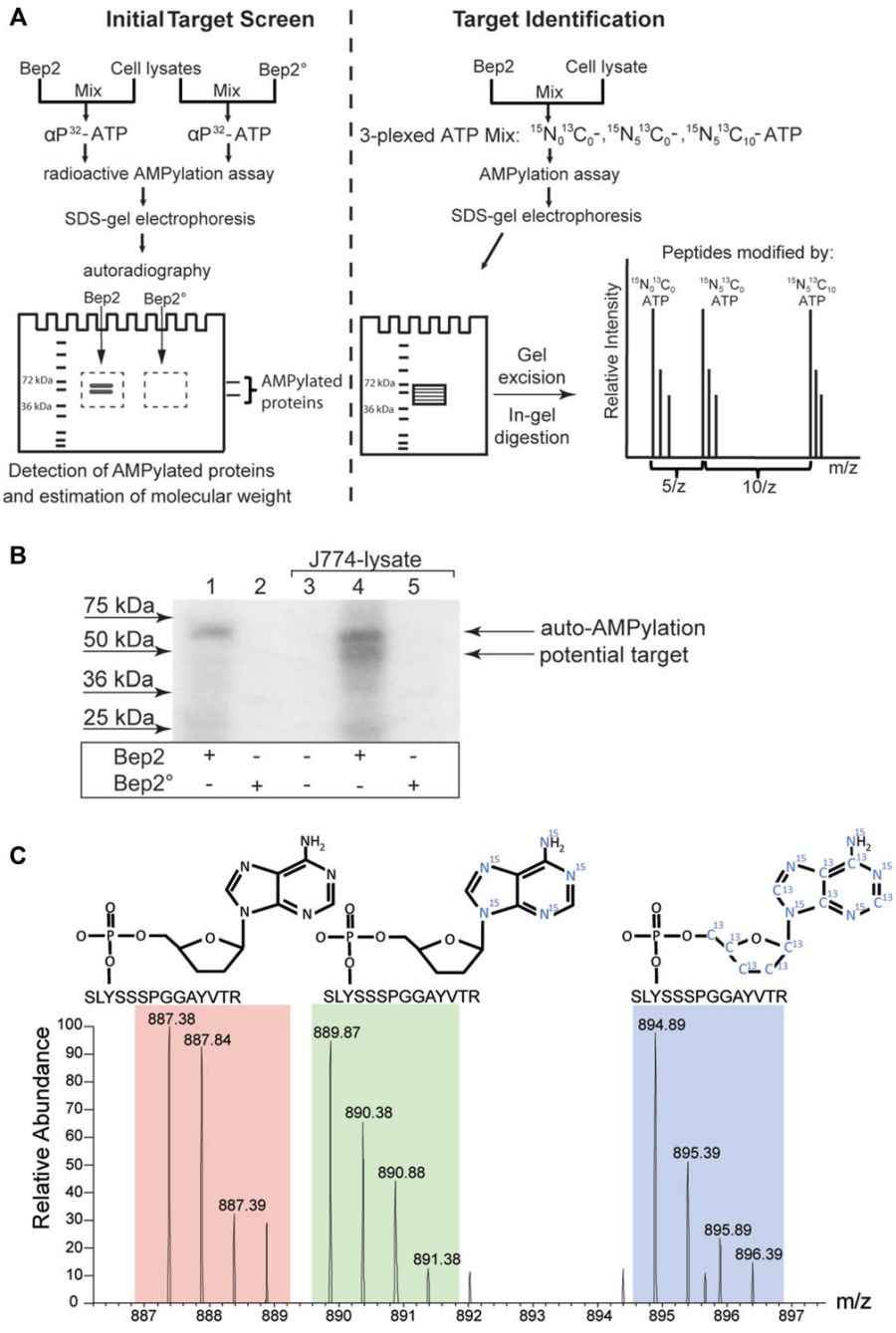

Figure 1. Workflow overview and target identification of *Bartonella rochalimae* effector protein Bep2. (A) Overview on the experimental workflow. Depicted is the workflow for identification of potential AMPylation targets on the example of Bep2. AMPylation assays are performed with radioactively labeled α^{32}P-ATP to estimate size of potential targets (left). In parallel, assays are performed with 3-plexed ATP ($^{15}N_0$ $^{13}C_0$-ATP, $^{15}N_5$-ATP, and $^{15}N_5{}^{13}C_{10}$-ATP), and the gel area at the running height of expected targets is excised and used for in-gel digestion and MS analysis (right). Preliminary candidate peptides are identified by MS/MS search and peptide AMPylation is specifically detected by the AMP-reporterion cluster characterized by specific mass shifts between the AMPylated peptide isotopes introduced by the 3-plexed ATP substrate mix. (B) Initial target screen by autoradiography. Representative autoradiogram of an in vitro AMPylation assay with active and inactive Bep2 is depicted. In vitro AMPylation assays were performed on wild-type and the inactive mutant of Bep2 (Bep2°) and mouse macrophage lysates in the presence of α^{32}P-ATP. After SDS-PAGE, AMPylated proteins were visualized via autoradiography. (C) Target identification by AMPylation specific reporter ion cluster. Samples derived from in vitro AMPylation assays with Bep2 using 3-plexed ATP were analyzed by in-gel digest and LC-MS/MS. The mass spectrum shows the *m/z* of the 3-plexed AMPylated peptide SLYSSSPGGAYVTR matching to the protein vimentin. The ions specifically encoding an AMPylation modification by their characteristic mass shift are highlighted by color shading.

Inspection of the search data revealed that all three AMP-modified peptide isotopes were identified with search scores slightly exceeding the score cut off that corresponds to a decoy false discovery rate of 1%. Although the search results already indicated an AMPylation event, we found further evidence confirming the AMPylation on this peptide when manually inspecting its isotopic distribution. As three isotopically labeled ATPs (unlabeled ATP, $^{15}N_5$-ATP, $^{15}N_5{}^{13}C_{10}$-ATP) were used for the AMP transfer reaction, we observed a peptide ion reporter cluster with three distinct peaks matching the expected mass shifts introduced by the different labels (Fig. 1C). Closer examination of the three AMP–peptide peaks showed that equal amounts of modified peptides were generated in the in vitro reaction emphasizing that no detectable

© 2014 WILEY-VCH Verlag GmbH & Co. KGaA, Weinheim

Proteomics 2014, *14*, 1048–1052

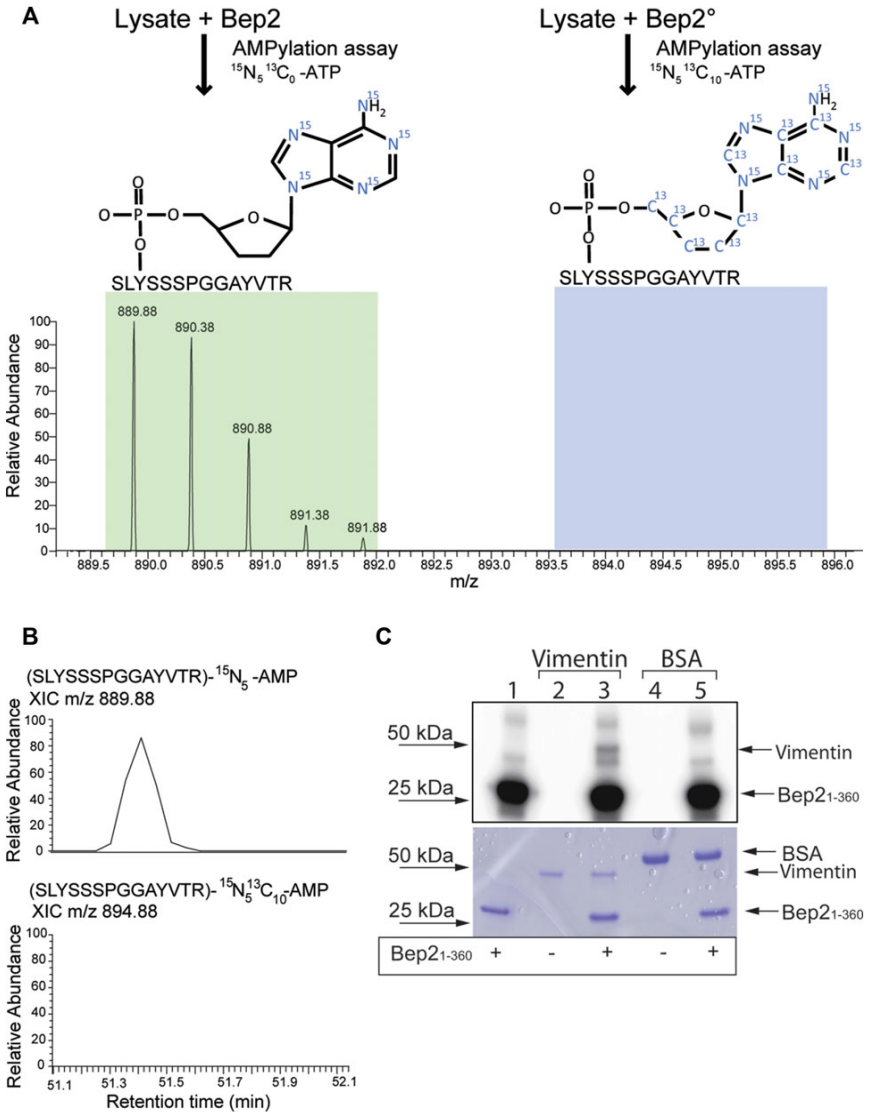

Figure 2. Validation of vimentin as an AMPylation target of Bep2. (A) Mass spectrum of AMP-reporter ions in the presence and absence of active Bep2. Samples derived from AMPylation assays with either Bep2 and $^{15}N_5{}^{13}C_0$-ATP or the inactive mutant of Bep2 (Bep2°) and $^{15}N_5{}^{13}C_{10}$-ATP were pooled and analyzed by LC-MS/MS. Depicted is a mass spectrum zoomed in on the *m/z* range of the reporter cluster. (B) Extracted-ion chromatogram (XIC) of samples derived from in vitro AMPylation assays. Assays were performed on wild-type Bep2 incubated with $^{15}N_5$-ATP and Bep2° incubated with $^{15}N_5{}^{13}C_{10}$-ATP. Samples were pooled and analyzed by LC-MS/MS. The XIC of AMPylated SLYSSSPGGAYVTR is shown for $^{15}N_5{}^{13}C_0$-AMP reporter channel for Bep2 (top) and $^{15}N_5{}^{13}C_{10}$-AMP for Bep2° (bottom). C) Validation experiments on vimentin as an AMPylation target of Bep2. In vitro AMPylation assays were performed with purified Bep2$_{1-360}$ in a complex with BiaA (E24G) and either buffer, vimentin, or BSA in the presence of α^{32}P-ATP. AMPylated proteins were visualized by autoradiography (top). The SDS-gel used for autoradiography was then stained with Coomassie to visualize all proteins (bottom).

background AMPylation by potential endogenous AMPylating proteins occurred.

In order to show that the observed AMPylation event is based on the activity of the FIC-domain, we generated a catalytically inactive Bep2 mutant (Bep2°) by replacing the histidine within the conserved Fic motif with an alanine (H161A). As the histidine is considered to act as general base to increase nucleophilicity of the AMPylation acceptor amino acid of the target, the replacement with alanine inhibits AMPylation as previously demonstrated for VopS and IbpA [5,7]. Then, wild-type and mutant Bep2 were separately incubated with J774 mouse macrophage lysates to perform in vitro AMPylation reaction using $^{15}N_5{}^{13}C_0$–ATP for wild-type and $^{15}N_5{}^{13}C_{10}$–ATP for mutant Bep2. Samples were pooled and proteins were separated by SDS-gel electrophoresis. Upon in-gel digestion and LC-MS analysis, we obtained SLYSSSPGGAYVTR to be AMPylated only with $^{15}N_5{}^{13}C_0$-ATP but not with $^{15}N_5{}^{13}C_{10}$-ATP. This indicates that in vitro reaction with wild-type Bep2, but not with the catalytically inactive Bep2-mutant protein, leads to AMPylation of SLYSSSPGGAYVTR, confirming that the reaction is specifically catalyzed by the active FIC-domain of Bep2 (Fig. 2A and B).

In order to confirm vimentin as a target protein of Bep2, we performed in vitro AMPylation assays with α^{32}P-ATP and purified proteins. To increase Bep2 solubility, we deleted the C-terminal BID domain of Bep2 that serves as a signal for translocation into the host cell via a type IV secretion system but apparently does not contribute to the AMPylation activity [17]. Solubility was further increased by coexpression of BiaA(E34G), a mutant of the Bep2-interacting antitoxin BiaA

© 2014 WILEY-VCH Verlag GmbH & Co. KGaA, Weinheim

of *B. rochalimae* that binds Bep2 without impairing AMPylation activity (Fig. 2C). Following purification by metal affinity and size exclusion chromatography, purified $Bep2_{1-360}$ complexed with BiaA(E34G) was used in AMPylation assays with α^{32}P-ATP and purified vimentin or BSA that was used as negative control. While there was no apparent AMPylation band in addition to the auto-AMPylation of Bep2 in the negative control, a clear AMPylation signal at the size of 50 kDa was detected in samples containing the Bep2-construct and vimentin confirming that vimentin is indeed a target protein of Bep2-mediated AMPylation (Fig. 2C, lane 3). Furthermore, as vimentin is a component of the cytoskeleton and shows no homology to small GTPases, it represents a new class of target proteins of Fic protein mediated AMPylation.

In our study, we presented an experimental strategy for the identification of protein AMPylation events in complex biological samples. We use stable isotope-labeled ATP in activity-based assays to introduce an AMP-reporter cluster to increase specificity of AMPylation target detection by MS. The relative intensity of peptide isotopes additionally allows us to distinguish between background signal of intrinsic AMPylation and specific target AMPylation of the introduced Fic protein. Certainly, peptides generated from proteolytic digests have to be within MS compatible size range. Therefore, it may be important to incorporate alternative digestion schemes in case in vitro AMPylation assays indicate a protein modification, but MS results do not reveal any significant hits. In addition, we anticipate that our strategy will improve the detection of AMPylation events on low-abundant proteins as the use of reporter clusters is largely independent of the known under-sampling effect in MS/MS based identification [18]. Although we established the procedure to specifically identify AMPylation targets, it is generally applicable to any protein modification for which isotope-labeled analogs are available and the modified peptides result in MS detectable reporter ion clusters.

Research was supported by grant 31003A-132979 of the Swiss National Science Foundation (SNSF), grant 51RT 0_126008 for the Research and Technology Development (RTD) project InfectX in the frame of SystemsX.ch (both to Christoph Dehio). Work of K. P. was supported by the International Ph.D. Program "Fellowships for Excellence" of the Biozentrum, University of Basel.

The authors have declared no conflict of interest.

References

[1] Brown, M. S., Segal, A., Stadtman, E. R., Modulation of glutamine synthetase adenylylation and deadenylylation is mediated by metabolic transformation of pii-regulatory protein. *Proc. Natl. Acad. Sci. U. S. A.* 1971, *68*, 2949–2953.

[2] Kinch, L. N., Yarbrough, M. L., Orth, K., Grishin, N. V., Fido, a novel AMPylation domain common to fic, doc, and AvrB. *PLoS One* 2009, *4*, e5818.

[3] Engel, P., Goepfert, A., Stanger, F. V., Harms, A. et al., Adenylylation control by intra- or intermolecular active-site obstruction in Fic proteins. *Nature* 2012, *482*, 107–110.

[4] Roy, C. R., Mukherjee, S., Bacterial FIC Proteins AMP Up Infection. *Sci. Signal.* 2009, *2*, pe14.

[5] Yarbrough, M. L., Li, Y., Kinch, L. N., Grishin, N. V. et al., AMPylation of Rho GTPases by Vibrio VopS disrupts effector binding and downstream signaling. *Science* 2009, *323*, 269–272.

[6] Higa, N., Toma, C., Koizumi, Y., Nakasone, N. et al., Vibrio parahaemolyticus effector proteins suppress inflammasome activation by interfering with host autophagy signaling. *PLoS Pathog.* 2013, *9*, e1003142.

[7] Worby, C. A., Mattoo, S., Kruger, R. P., Corbeil, L. B. et al., The fic domain: regulation of cell signaling by adenylylation. *Mol. Cell* 2009, *34*, 93–103.

[8] Mattoo, S., Durrant, E., Chen, M. J., Xiao, J. et al., Comparative analysis of *Histophilus somni* immunoglobulin-binding protein A (IbpA) with other fic domain-containing enzymes reveals differences in substrate and nucleotide specificities. *J. Biol. Chem.* 2011, *286*, 32834–32842.

[9] Hao, Y. H., Chuang, T., Ball, H. L., Luong, P. et al., Characterization of a rabbit polyclonal antibody against threonine-AMPylation. *J. Biotechnol.* 2011, *151*, 251–254.

[10] Grammel, M., Luong, P., Orth, K., Hang, H. C., A chemical reporter for protein AMPylation. *J. Am. Chem. Soc.* 2011, *133*, 17103–17105.

[11] Broncel, M., Serwa, R. A., Tate, E. W., A new Chemical handle for protein AMPylation at the host-pathogen interface. *Chembiochem* 2012, *13*, 183–185.

[12] Pimenova, T., Nazabal, A., Roschitzki, B., Seebacher, J. et al., Epitope mapping on bovine prion protein using chemical cross-linking and mass spectrometry. *J. Mass. Spectrom.* 2008, *43*, 185–195.

[13] Rinner, O., Seebacher, J., Walzthoeni, T., Mueller, L. et al., Identification of cross-linked peptides from large sequence databases (vol 5, pg 315, 2008). *Nat. Methods.* 2008, *5*, 748–748.

[14] Frese, C. K., Altelaar, A. F., Hennrich, M. L., Nolting, D. et al., Improved peptide identification by targeted fragmentation using CID, HCD and ETD on an LTQ-Orbitrap Velos. *J. Proteome. Res.* 2011, *10*, 2377–2388.

[15] Engel, P., Salzburger, W., Liesch, M., Chang, C. C. et al., Parallel evolution of a type IV secretion system in radiating lineages of the host-restricted bacterial pathogen *Bartonella*. *PLoS Genet.* 2011, *7*, e1001296.

[16] Harms, A., Dehio, C., Intruders below the radar: molecular pathogenesis of *Bartonella* spp. *Clin. Microbiol. Rev.* 2012, *25*, 42–78.

[17] Schulein, R., Guye, P., Rhomberg, T. A., Schmid, M. C. et al., A bipartite signal mediates the transfer of type IV secretion substrates of *Bartonella henselae* into human cells. *Proc. Natl. Acad. Sci. U. S. A.* 2005, *102*, 856–861.

[18] Nilsson, T., Mann, M., Aebersold, R., Yates, J. R., 3rd et al., Mass spectrometry in high-throughput proteomics: ready for the big time. *Nat. Methods* 2010, *7*, 681–685.

© 2014 WILEY-VCH Verlag GmbH & Co. KGaA, Weinheim

Supplementary data are available online

- a table listing all peptides detected by LC-MS analysis after in-gel digest (Table S1)
- a figure showing data that validate the workflow described in *Research article II* using the adenylylation of RhoA by VopS (Figure S1)
- a figure that shows ion series and MS/MS spectrum of the adenylylated vimentin peptide SLYSSSPGGGAYVTR (Figure S2)

6.8.Unpublished results related to Research article II

I did not generate unpublished results in the context of my contribution to *Research article II*. Additional data in the context of *Bartonella* effector proteins are summarized in the section *Appendix: Further results*.

6.9.Research article III (submitted)

“Chance favors the prepared mind.”

Louis Pasteur, French microbiologist, at his inaugural lecture as he was appointed dean of the new faculty of sciences at Lille University (December 5th 1854); original “(*dans les champs de l'observation,) le hasard ne favorise que les esprits préparés",* i.e., “(whenever observation is concerned,) chance favors the prepared mind”

Disruption of DNA topology via topoisomerase adenylylation –a new path to persistence

Alexander Harms, Frédéric Valentin Stanger, Patrick Daniel Scheu, Imke Greet de Jong, Timo Glatter, Kenn Gerdes, Tilman Schirmer, and Christoph Dehio

Submitted to *Cell*

NOTE ADDED IN PROOF - This manuscript has finally been published as

Alexander Harms, Frédéric V. Stanger, Patrick D. Scheu, Imke G. de Jong, Arnaud Goepfert, Timo Glatter, Kenn Gerdes, Tilman Schirmer, and Christoph Dehio (2015). Adenylylation of gyrase and topo IV by FicT toxins disrupts bacterial DNA topology. Cell Rep 12(9):1497-507.

Summary

One major function of toxin-antitoxin (TA) modules is to serve as a phenotypic switch that converts bacteria into multidrug tolerant persister cells. Interestingly, in all cases examined so far the activation of TA modules induced persistence by inhibiting translation or unsetting the proton-motive force. We previously described class I Fic proteins as toxins of the new FicTA toxin-antitoxin module that acts via the adenylylation of unknown targets (*Research article I* and *Review article II*).

In this study we comprehensively characterized the FicTA family of toxin-antitoxin modules and showed that they act by adenylylation and concomitant inactivation of DNA gyrase and topo IV which arrests bacterial growth and causes a phenotypic switch to persistence.

Using VbhT as a model toxin we found that this protein adenylylates GyrB and ParE, the B subunits of DNA gyrase and topo IV, at a conserved tyrosine in the ATP lid loop that borders the ATP binding site. Adenylylation fully blocked the signature activities of recombinant DNA gyrase as well as topo IV *in vitro*. Mechanistically, we found that the adenylylation of a GyrB ATPase model construct resulted in the inhibition of ATP hydrolysis which was sufficient to explain the inactivation of DNA gyrase and, by inference, topo IV.

We characterized the VbhTA system along with two other representatives of *Y. enterocolitica* (YeFicTA) and *P. aeruginosa* (PaFicTA) in which the FicT toxins are classical single domain class I Fic proteins, while VbhT harbors an additional BID domain. The expression of all FicT toxins suppressed *E. coli* growth which depended on the integrity of their FIC domain active site and could be abolished by the coexpression of cognate FicA antitoxins. We assessed changes in cellular DNA topology upon FicT toxin expression *in vivo* and could show that the expression of any FicT toxin causes a strong inhibition of topo IV, evidenced by chromosome segregation defects and considerable catenation as well as knotting of reporter plasmids. Interestingly, in our experimental system *in vivo* the expression of different FicT constructs was divergently potent in the inhibition of DNA gyrase activity which we assessed using flow cytometry with a relaxation-inducible *gfp* promoter fusion and by the topological analysis of reporter plasmids using chloroquine agarose gel electrophoresis. While PaFicT caused a strong inhibition of DNA gyrase, the expression of YeFicT or only the FIC domain of VbhT had at most a moderate effect, and VbhT in full length did not cause detectable gyrase inhibition. Genetic experiments confirmed severe distortions in cellular DNA topology upon FicT expression which appeared to greatly affect DNA replication.

Unlike the CcdB or ParE toxins that are part of post-segregational killing TA systems, topoisomerase targeting by FicT toxins does not result in poisoning of the enzymes and

consequent cell death. Instead, FicT toxins cause a reversible inhibition of their targets that results in bacterial growth arrest. Consistent with the role of toxin-antitoxin modules as major players in bacterial persister formation, we found that the ectopic expression of any FicT toxin converted *E. coli* into multidrug tolerant persister cells. We therefore concluded that the robust inhibition of topo IV – shared among all FicT toxins – is the primary driving force of the physiological effects of FicTA toxin-antitoxin modules. These results strongly suggested that the subversion of cellular DNA topology would be a new path of bacterial persister formation next to the inhibition of translation or the disruption of the proton-motive force. We therefore confirmed that also the treatment with novobiocin, a bacteriostatic inhibitor of DNA gyrase and topo IV, induced the formation of persister cells in *E. coli*. Similarly, the near-physiological activation of the genuine *yeficAT* locus upon antitoxin sequestration resulted in bacterial persistence.

In conclusion, our work revealed the molecular function and biological role of the FicTA toxin-antitoxin family and demonstrated that the disruption of cellular DNA topology is a new path to the persister state. We therefore expanded the understanding of the inherent physiological heterogeneity of persister cells formed in bacterial populations that may be a major obstacle to their complete eradication Furthermore, we anticipate that our results will help to understand the molecular basis of multidrug tolerance during different variants of the persister state and thereby provide new impulses for the development of dedicated treatments.

Statement of the own participation

I contributed to this publication by identifying DNA gyrase and topo IV as the molecular targets of the adenylylation activity of class I FIC domain proteins. Furthermore, I characterized the resulting inhibition of the topoisomerases *in vitro* and *in vivo* using various techniques to analyze changes in DNA topology. I generated various plasmid constructs and bacterial strains, and additional plasmids and strains were contributed by other authors. I discovered the biological function of class I Fic proteins in bacterial persister formation. The manuscript was primarily written by me, but all authors contributed ideas and advice at all stages. Other authors purified all protein constructs and investigated the ATPase activity of GyrB43 *in vitro,* assisted with the microscopy of *Escherichia coli* as well as the associated data processing, and performed the mass spectrometry analysis. Patrick Scheu and Prof. Kenn Gerdes joined the project with initial data on PaFicTA of *Pseudomonas aeruginosa*.

Research Article

Disruption of DNA topology via topoisomerase adenylylation –a new path to persistence

Alexander Harms[1], Frédéric Valentin Stanger[1,2], Patrick Daniel Scheu[3], Imke Greet de Jong[1], Timo Glatter[4], Kenn Gerdes[3,5], Tilman Schirmer[2] & Christoph Dehio[1]

[1]Focal Area Infection Biology, Biozentrum, University of Basel, CH-4056 Basel, Switzerland; [2]Focal Area Structural Biology and Biophysics, Biozentrum, University of Basel, CH-4056 Basel, Switzerland; [3]Centre for Cell & Molecular Biosciences, Newcastle University, NE2 4AX Newcastle upon Tyne, United Kingdom; [4]Proteomics Core Facility, Biozentrum, University of Basel, CH-4056 Basel, Switzerland; [5]Department of Biology, University of Copenhagen, DK-2200 Copenhagen, Denmark

Corresponding author:
Prof. Christoph Dehio
Biozentrum, University of Basel
Klingelbergstrasse 70
CH-4056 Basel, Switzerland
Tel.: +41-61-267 2140
Fax.: +41-61-267 2118
e-mail: christoph.dehio@unibas.ch

Summary

Bacterial persisters are multidrug tolerant cells generated from a phenotypic switch to dormancy that is typically exerted by toxin-antitoxin (TA) modules. All TA modules examined so far induce bacterial persistence by inhibiting translation or unsetting the proton-motive force. Here we characterize a group of FIC domain proteins as toxins of the conserved and abundant FicTA family of TA modules and reveal that they cause persister formation via a new mechanism, the disruption of DNA topology. FicT toxins act via the adenylylation and concomitant inactivation of DNA gyrase and topoisomerase IV (topo IV), the essential bacterial type IIA topoisomerases. Consequently, FicT activity results in major distortions of cellular DNA topology that cause reversible growth arrest and a phenotypic switch to the persister state. Our findings underline the inherent heterogeneity of persister cells formed by different types of TA modules that needs to be overcome by treatments aiming at complete eradication.

Highlights

- FicT toxins inhibit DNA gyrase and topoisomerase IV activities via adenylylation
- Topoisomerase adenylylation subverts cellular DNA topology and causes growth arrest
- FicT toxin activation causes formation of multidrug-tolerant persister cells
- Disruption of DNA topology is a newly identified path to bacterial persistence

eTOC blurb

Bacterial persister cells are notoriously multidrug-tolerant and generated by toxin-antitoxin modules; these were so far only known to act by inhibiting translation or unsetting the proton-motive force. Harms et al. present the disruption of cellular DNA topology as new way to persistence that is opened by the FicTA toxin-antitoxin module. FicT toxins inactivate gyrase and topoisomerase IV by adenylylation which causes the topological collapse of cellular DNA. These findings highlight the physiological diversity of bacterial persister cells.

Graphical Abstract

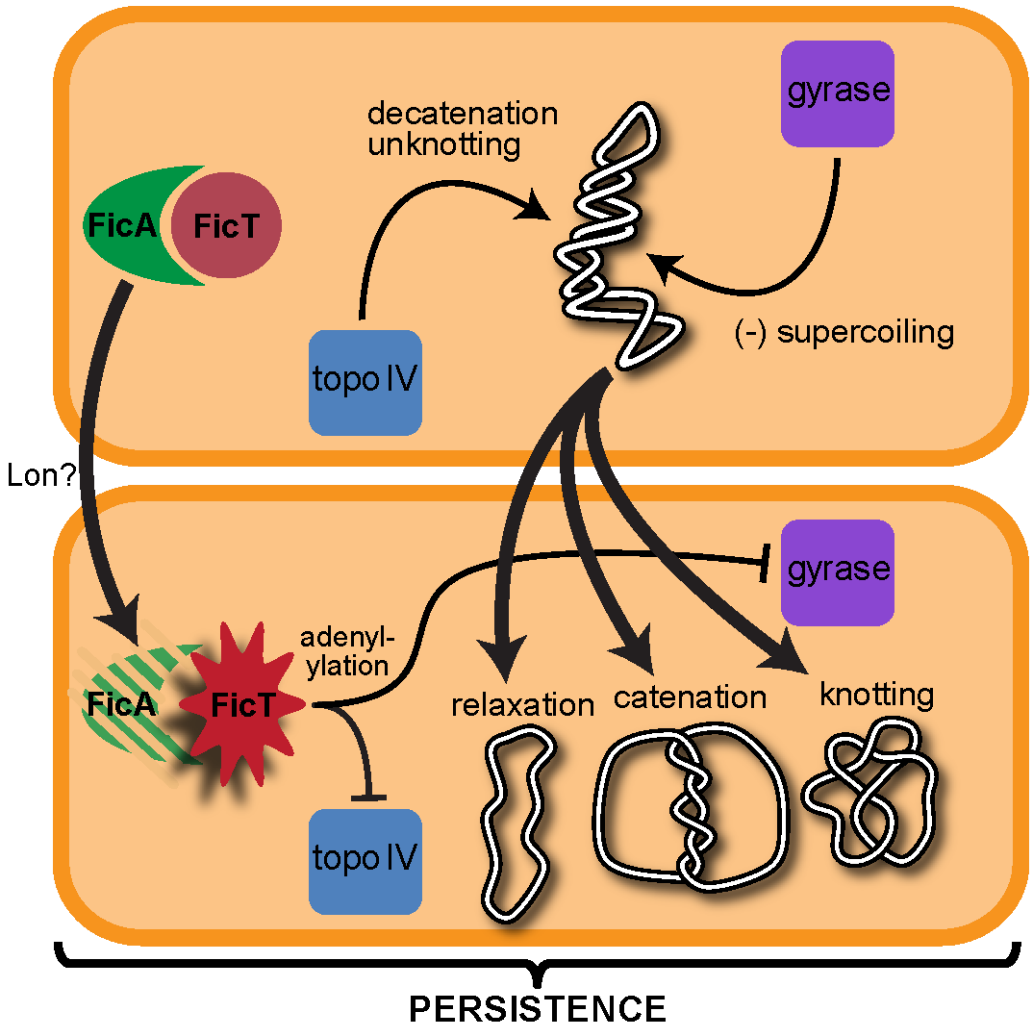

Introduction

Within a clonal population of bacterial cells, persisters are phenotypic variants that survive concentrations of antibacterials way above the minimal inhibitory concentration (MIC) and thus represent a major cause of treatment failure and relapse of bacterial infections (Balaban et al., 2013; Dhar and McKinney, 2007; Lewis, 2010). Unlike mere drug avoidance, persisters survive via real drug tolerance in a non-growing, non-dividing state that has been described as dormancy (Balaban et al., 2004; Maisonneuve et al., 2013). Therefore, unlike antibiotic resistance, bacterial persistence typically manifests in tolerance to various antimicrobials and may thus not be overcome by the development of new conventional drugs, although promising approaches to target these cells pharmacologically have been described in the literature (Conlon et al., 2013). Bacterial persistence is a non-inherited phenomenon, but genetically programmed in toxin-antitoxin modules (Keren et al., 2004; Maisonneuve et al., 2011).

Toxin-antitoxin (TA) modules comprise a toxin that blocks bacterial growth via the inactivation of essential cellular functions and an antitoxin that prevents functionality of the toxin. In the most abundant group of type II TA modules the antitoxin is a protein that inhibits the toxin via tight binding until it is degraded by proteases in response to cellular signaling (Brzozowska and Zielenkiewicz, 2013). Among other functions (reviewed by Unterholzner et al. (2013)), TA modules play a prominent role in persister formation where their activation serves as the phenotypic switch into dormancy (Balaban et al., 2004; Lewis, 2010; Maisonneuve and Gerdes, 2014). In the absence of extrinsic signals, stochastic stimuli cause the formation of a small subpopulation of persisters, e.g., via the fluctuation of ppGpp levels in *Escherichia coli* which control the activity of the protease Lon that activates a plethora of type II TA modules (Maisonneuve et al., 2013). This inherent heterogeneity ensures survival of bacterial populations in case of rare, unpredictable threats as a bet-hedging strategy

(Balaban et al., 2004). In addition to stochastic events, different stimuli can trigger the phenotypic switch to dormancy in a deterministic manner. For example, DNA damage can induce persister formation of *E. coli* (via the SOS response and type I TA toxin TisB; (Dörr et al., 2010; Tripathi et al., 2012)), and the uptake of *Salmonella* Typhimurium into phagocytic vacuoles induces persistence by activating a whole arsenal of TA modules (Helaine et al., 2014). Bacterial chromosomes usually encode multiple different TA modules that may display some redundancy, but often cumulatively contribute to persister formation (Helaine et al., 2014; Maisonneuve et al., 2013; Norton and Mulvey, 2012)

Despite considerable knowledge about the upstream signaling, the downstream processes initiated when TA modules flip the switch to dormancy and how they cause multidrug tolerance are not well understood (Maisonneuve and Gerdes, 2014). Conspicuously, although a multitude of different molecular targets have been described, the general concepts by which TA modules induce persister formation have so far been limited to the inhibition of translation or, in a few cases, the abrogation of the proton-motive force (Castro-Roa et al., 2013; Christensen and Gerdes, 2003; Unoson and Wagner, 2008; Wang et al., 2012; Winther et al., 2013). This remarkable limitation confirms that persisters are not just random non-growing bacteria and instead generated by dedicated mechanisms as specialized survivor cells (Keren et al., 2004). The extent of heterogeneity among persisters as a critical obstacle to their complete eradication has not yet been resolved, but it likely depends on the diversity of different physiological pathways available for persister formation (Balaban et al., 2013; Kester and Fortune, 2014). Here we describe the subversion of cellular DNA topology as a third and new path to the persister state and characterize a family of FIC (filamentation induced by cAMP) domain proteins as toxins of the FicTA type II toxin-antitoxin module that converts bacteria into persisters via dual topoisomerase inhibition.

Proteins containing FIC domains are found in all kingdoms of life and typically catalyze adenylylation (also known as AMPylation), the covalent transfer of an adenosine-5’

monophosphate (AMP) moiety onto target proteins (Engel, Goepfert et al., 2012; Kinch et al., 2009). Previous research on FIC domain proteins has focused on a few representatives that are host-targeted virulence factors of bacterial pathogens (Mukherjee et al., 2011; Yarbrough et al., 2009), but the far majority FIC domain proteins are genuine bacterial proteins of unknown function. We recently described the adenylylation activity of bacterial FIC domain proteins and discovered its inhibition by a conserved regulatory module that interferes with productive binding of the ATP substrate. Interestingly, we found the regulatory module of one group of bacterial FIC domain proteins to be part of a separate small protein that inhibits its cognate FIC domain via a tight interaction (Engel, Goepfert et al., 2012). Such a regulatory arrangement satisfies the core definition of type II toxin-antitoxin modules so that we introduced a new nomenclature and named the toxins "FicT" (for "FIC domain toxin") and their cognate antitoxins "FicA" (Engel, Goepfert et al., 2012; Goepfert et al., 2013). However, the enzymatic targets and biological functions of this new FicTA toxin-antitoxin module had remained elusive.

In this study, we characterize different representatives of the FicTA type II TA family and show that FicT toxins inactivate DNA gyrase and topoisomerase IV via adenylylation at their ATP binding site, causing reversible growth arrest. Using a wide range of different techniques we demonstrate that FicT toxin expression results in strong DNA knotting and catenation combined with a varying degree of DNA relaxation in *E. coli*, indicating that FicT toxins can inactivate both targets *in vivo*. Remarkably, we find that the disruption of cellular DNA topology upon activation of a FicTA module as well as by novobiocin, a chemical inhibitor of DNA gyrase and topo IV, converts bacteria into multidrug-tolerant persister cells. We therefore establish the subversion of DNA topology as a new mechanism to form persisters and believe that our findings will help to elucidate the molecular basis of multidrug tolerance as well as the inherent heterogeneity of these notoriously treatment-resistant cells.

Results

Ectopic expression of FicT toxins results in a reversible inhibition of bacterial growth

We previously established VbhTA of *Bartonella schoenbuchensis* as a model for the FicTA family and demonstrated that the antitoxin VbhA inhibits the adenylylation activity of the VbhT toxin and relieves the associated growth arrest in *Escherichia coli* (Engel, Goepfert et al., 2012). Since VbhT is unique among FicT homologs in that it harbors a C-terminal type IV secretion signal (called BID domain), we decided to investigate the molecular and biological functions of VbhT along with more typical representatives of *Yersinia enterocolitica* str. 8081 (YeFicTA module) and *Pseudomonas aeruginosa* PAO1 (PaFicTA module; see *Extended Results* in the Supplemental Information and Figure S1).

The expression of different FicT toxins from a single-copy vector in the absence of their cognate FicA antitoxins resulted in strong inhibition of *E. coli* growth (Figures 1A and 1B). This effect required the FicT toxins' adenylylation activity because mutation of the catalytic histidine within the FIC domain signature motif HXFX(D/E)GNGRXXR into alanine ("H/A" mutants) abolished the growth inhibition (Figure 1A). Subsequent expression of the cognate antitoxins reversed the growth inhibition (Figure 1C), demonstrating that FicT toxin activity leads to a classical bacteriostatic condition that is a common feature of many TA systems (Pedersen et al., 2002). We note that the ectopic expression of VbhT appears to be less potent in growth inhibition than that of YeFicT, PaFicT, or only the FIC domain of VbhT alone (VbhT(fic); Figure 1B), possibly due to differential expression of the constructs or because the BID domain of VbhT sterically reduces toxin activity.

FicT toxins adenylylate GyrB and ParE, the B subunits of DNA gyrase and topo IV

To unravel the molecular mechanism of the reversible growth inhibition caused by the FicT toxins' adenylylation activity we next aimed at uncovering the identity of the adenylylated target(s). For this purpose we performed *in vitro* adenylylation assays with lysates of *E. coli* that had expressed VbhT and used a pull-down approach similar to the one

published by Grammel et al. (2011) for target identification. Though we failed to achieve significant enrichment of potential targets, we serendipitously discovered an adenylylated peptide that belonged to GyrB of *E. coli* (data not shown). The theoretical molecular weight of GyrB (89.95 kDa) fits well with the apparent molecular weight of the *bona fide* endogenous target adenylylation detected by autoradiography in adenylylation assays with VbhT (Figure 2A and our previous work (Engel, Goepfert et al., 2012)) which we calculated to be approximately 90 kDa using the ImageQuant software (Molecular Dynamics). Ectopic expression of GyrB both of *E. coli* or *B. schoenbuchensis* unambiguously showed that these proteins are adenylylated by VbhT in bacterial lysates *in vitro* (Figure 2A). Given the very high similarity in sequence, structure, and function to GyrB (Bellon et al., 2004) we further suspected that its paralog ParE may also be targeted by VbhT. Indeed, like for GyrB, ectopic expression of ParE of *E. coli* and *B. schoenbuchensis* clearly demonstrated adenylylation by VbhT (Figure 2A). However, unlike for GyrB, no adenylylation of endogenous ParE is detectable by visual inspection of autoradiographs of our adenylylation experiments with cleared lysates of *E. coli* expressing VbhT (Figure 2A). We believe that this discrepancy is caused by largely different target abundances because *E. coli* cells contain approximately 10 times more molecules of GyrB than of ParE (Dr. Alexander Schmidt, personal communication).

GyrB and ParE are the B subunits of the two bacterial type IIA topoisomerases DNA gyrase and topoisomerase IV (topo IV) that control cellular DNA topology by maintaining negative supercoiling respectively removing DNA catenation and knotting (Sissi and Palumbo, 2010). Therefore, their activities are generally essential for all processes in bacterial cells that involve the manipulation of closed circular DNA such as chromosome replication, segregation, and transcription (Vos et al., 2011). Due to their remarkable conservation and essential functions the bacterial type IIA topoisomerases are targets of several groups of antimicrobials, bacteriocins, as well as the CcdBA and ParDE type II TA systems. These

toxins, the bacteriocins, as well as quinolone-based antimicrobials are poisons that prevent resealing of the DNA cleavage inherent to type II topoisomerase activity and ultimately result in cell death (Chen et al., 1996; Deghorain et al., 2013; Vos et al., 2011). In contrast, gyramide A and aminocoumarin drugs like novobiocin merely inactivate the enzymes as competitive inhibitors of their ATP hydrolysis activity which abrogates the cellular control of DNA topology but does not directly trigger cell death (Hardy and Cozzarelli, 2003; Rajendram et al., 2014).

Adenylylation at the ATP binding site inhibits DNA gyrase and topo IV *in vitro*

Using mass spectrometry, we found that VbhT adenylylates Y109 and its homolog Y105 in GyrB and ParE of *E. coli*, respectively (Figure S2). This highly conserved residue is part of the "ATP lid" and borders the ATP binding site (Brino et al., 2000). Since ATP hydrolysis is generally required for the cellular activities of DNA gyrase and topo IV (Bates et al., 2011), we assayed the hydrolysis of ATP by a GyrB ATPase model construct and found that adenylylation indeed completely inhibited the target's ATPase activity (Figure 2B). Subsequently, we used recombinant DNA gyrase and topo IV to assess the effect of adenylylation on the signature activities of both targets on suitable DNA substrates *in vitro*. As expected, adenylylation prevented supercoiling of a relaxed reporter plasmid by DNA gyrase and decatenation of kDNA, a meshwork of catenated DNA rings, by topo IV (Figure 2C).

FicT toxins cause varying levels of DNA gyrase inhibition *in vivo*

We then investigated whether FicT toxins also inactivate DNA gyrase and topo IV *in vivo*. Any inhibition of DNA gyrase would decrease the negative supercoiling of cellular DNA. We therefore used DNA of plasmid pAH160, a high-copy number vector originally designed for rhamnose-inducible protein expression, isolated from *E. coli* expressing FicT toxins to directly visualize changes in DNA topology via high-resolution agarose gel electrophoresis with chloroquine to resolve negative supercoiling (see *Experimental*

Procedures in the Supplemental Information). As expected, the treatment of *E. coli* with a high concentration of novobiocin that completely inactivates DNA gyrase resulted in collapse of the negative supercoiling (Figure 3A). However, a dose of VbhT, VbhT(fic), or YeFicT expression that strongly impaired bacterial growth (two hours of full induction; see Figure 1B) caused only a slight stretch of the topoisomer distribution towards DNA relaxation, while the expression of PaFicT resulted in full relaxation of the reporter plasmid (Figure 3A). These divergent findings lead us suspect that the transient nature of local DNA relaxation for the single topological domain of our simple reporter plasmid may have masked more prominent effects of a potential partial inhibition of DNA gyrase upon expression of our VbhT and YeFicT constructs. We therefore used another reporter plasmid encoding a relaxation-induced P*gyrB::gfpmut2* GFP promoter fusion to record any DNA gyrase inhibition inside single cells by flow cytometry. For validation, we confirmed that *E. coli* harboring this plasmid showed dose-dependent induction of GFP fluorescence upon inhibition of DNA gyrase with different concentrations of novobiocin (Figure 3B). In this system the expression of VbhT or YeFicT resulted in a rather weak, but detectable induction of GFP fluorescence, while VbhT(fic) elicited a stronger response and the expression of PaFicT had a similar effect as the highest concentrations of novobiocin (Figure 3B). Furthermore, we constructed a chromosomal P*gyrB::gfpmut2* reporter in order to directly assess the supercoiling of the nucleoid and avoid potential artifacts from analysing reporter plasmids which can be misleading (Rovinskiy, Agbleke et al., 2012). Like with the plasmid-based assay (Figure 3B), the treatment with different concentrations of novobiocin caused a dose-dependent induction of GFP fluorescence, while FicT toxin expression resulted in weak (VbhT and YeFicT), moderate (VbhT(fic)), or strong DNA relaxation (PaFicT; Figure 3C). These findings mirror our results from high resolution agarose gel electrophoresis and thus indicate that the expression of our VbhT and YeFicT constructs is unlikely to achieve levels of DNA gyrase inhibition *in vivo* that would greatly contribute to growth inhibition. The more prominent effect with VbhT(fic)

compared to VbhT in full length may be due to differences in expression or reflect an evolution of the VbhT FIC domain to stronger activity in order to partially compensate for the hindrance by its BID domain. Despite that, neither VbhT(fic) nor PaFicT are more potent toxins than YeFicT (Figure 1B), suggesting that DNA gyrase inhibition is not the primary driving force of FicT-mediated growth inhibition.

FicT toxins robustly inhibit topo IV *in vivo*

The inactivation of topo IV is known to result in DNA knotting and catenation which induce a classical phenotype called *par* hallmarked by cell filamentation and the sequestration of unsegregated DNA at the cell center (Kato et al., 1990). We therefore used fluorescence microscopy to study cell shape and DNA partitioning in *E. coli* expressing FicT toxins (Figure 4A). As expected from our biochemical data with VbhT, the expression of any FicT toxin greatly inhibited DNA segregation and bacterial cell division which was a first indication of topo IV inactivation *in vivo* (Figure 4A). In deviation from a classical *par* phenotype, the cells expressing VbhT(fic), YeFicT, and PaFicT – but not VbhT – displayed a highly condensed nucleoid morphology. These findings were immediately reminiscent of the phenotype that others had reported for gyramide A treatment, suggesting that the compaction was caused by DNA gyrase inhibition coming on top of the inactivation of topo IV (Rajendram et al., 2014). As an independent readout of topo IV inhibition *in vivo* we re-analyzed the pAH160 samples that we had used for the detection of DNA relaxation by high resolution agarose gel electrophoresis (see Figure 3A). After nicking to release all supercoiling, the samples were run on plain agarose gels to resolve DNA knotting and catenation. Plasmid isolated from *E. coli* that had expressed any of the FicT toxin constructs showed detectable DNA knots evidencing robust topo IV inhibition (Figure 4B). The seemingly weak extent of all DNA knotting with pAH160 is caused by the small size of this reporter plasmid (4359 bp) and hints at considerable knotting of the nucleoid, since the topological entanglement and size of chromosomal DNA greatly favors knotting and

complicates unknotting compared to small plasmids (Witz and Stasiak, 2010). Additionally, a clear ladder of catenanes with various node numbers is detected for VbhT and YeFicT as well as – more weakly – VbhT(fic), but not for PaFicT or the novobiocin treatment (dimeric catenanes appear between nicked monomeric and dimeric DNA; Figure 4B and see also Figure S3). The absence or reduction of catenation with VbhT(fic) and PaFicT compared to VbhT or YeFicT expression confirms the stronger gyrase inhibition that we detected earlier, because a concomitant inactivation of DNA gyrase and topo IV (but not the latter alone) causes a rapid arrest of DNA replication and therefore prevents the formation of catenanes (Khodursky et al., 2000).

In order to investigate the molecular mechanism of target inactivation by FicT toxins in more detail we next assayed whether the overexpression of GyrB and / or ParE could rescue the growth inhibition caused by FicT expression. Such reversion of the growth arrest would confirm a purely inhibitory mechanism for FicT toxins and has been shown, e.g., for the overexpression of GltX that is phosphorylated and concomitantly inactivated by the HipA toxin (Germain et al., 2013). In contrast, for the gyrase poison CcdB it was shown that the presence of a susceptible, wildtype gyrase is dominant over the co-expression of even a resistant mutant (Bernard and Couturier, 1992). Our results show that the growth inhibition caused by VbhT could be prevented by the overexpression of ParE, confirming an inhibitory mechanism (Figure 5). No effect was observed for the overexpression of GyrB, confirming our previous findings that the inactivation of DNA gyrase has no major contribution to growth inhibition by VbhT.

Topoisomerase inhibition by FicT toxins reveals a new path to the persister state

Our experiments investigating the effects of FicT toxin expression on DNA topology in bacterial cells strongly suggested that the obstruction of topological control upon topoisomerase inhibition was the cause of the growth arrest observed with FicT toxins. We therefore explored the consequences of FicT activity inside bacterial cells more deeply and

genetically confirmed that the expression of FicT toxins caused major problems with DNA processing, particularly chromosome replication, via the inhibition of replication fork progression and chromosome segregation (see Figure S4 and *Extended Results* in the Supplemental Information). In conclusion, the FicTA family constitutes the first TA module that inhibits bacterial growth via topoisomerase inhibition.

Toxin-antitoxin modules have long been recognized as the primary genetic basis of bacterial persistence but have so far only been shown to promote persister formation via the inhibition of translation or abrogation of the proton-motive force (Keren et al., 2004; Lewis, 2010; Maisonneuve et al., 2011). We therefore reasoned that the disruption of cellular DNA topology caused by FicT toxins could constitute a new way to trigger persister formation. To test this hypothesis, we treated *E. coli* with a high concentration of bacteriostatic novobiocin that inhibits DNA gyrase as well as topo IV and subsequently challenged the bacteria with either of three antibiotics (ciprofloxacin, kanamycin, or ampicillin) that kill via entirely different mechanisms. In all cases the treatment with novobiocin greatly increased the fraction of surviving persisters in the population (Figure 6A). Admittedly, others had shown before that a variety of treatments causing reversible growth inhibition in *E. coli* from bacteriostatic antimicrobials to the heterologous expression of different toxic proteins can induce multi-drug tolerance (Kwan et al., 2013; Vazquez-Laslop et al., 2006). The biological relevance of our results with novobiocin is therefore largely dependent on whether a natural TA module exploits this mechanism to induce bacterial persistence. We thus repeated the experiment described above and replaced the novobiocin treatment with the expression of FicT toxins to assay their effect on bacterial persistence. Remarkably, while the antibiotic challenge eliminated all but 1 in 10’000 of the cells in the vector control, 1 in 10 of the bacteria expressing FicT toxins survived any drug treatment (Figure 6B). This increase in the proportion of persisters was independent of the SOS response triggered by some FicT constructs (Figure S5) and quantitatively similar to the effects that others had observed upon

overexpression of toxins targeting translation or the proton-motive force (Dörr et al., 2010; Keren et al., 2004; Maisonneuve et al., 2011; Vazquez-Laslop et al., 2006).

Consequently, we asked whether the activation of a genuine *ficAT* locus instead of the ectopic expression of FicT could also induce bacterial persistence. For this purpose we cloned the *yeficAT* and *paficAT* loci including approximately 300 bp upstream of their start codon (to ensure control by their genuine promoter regions) on a low-copy plasmid. The functional expression of these TA modules in *E. coli* was tested via the co-expression of catalytically inactive FicT toxin mutants to titrate out the FicA antitoxin expressed from the *ficAT* locus (see model shown in Figure 7A). While we readily detected an activation of the *yeficAT* module, no significant growth inhibition was found with *paficAT*, suggesting that this TA module is not properly expressed in *E. coli* (Figure 7B). However, a comparable assay in its natural host organism *Pseudomonas aeruginosa* unambiguously detected an activation of PaFicT and thus functional expression of the *paficAT* module (Figure S6). We therefore chose *yeficAT* as our model FicTA module in *E. coli* and tested whether its activation via the overexpression of catalytically inactive YeFicT_H136A would trigger a phenotypic switch to bacterial persistence. Consistent with our earlier findings, the sequestration of YeFicA in the presence of an intact *yeficAT* module resulted in an increased fraction of persisters in the bacterial population (Figure 7C).

Under physiological conditions the activity of type II TA toxins is unleashed via protease-mediated antitoxin degradation in response to certain triggers or stochastically in a subpopulation of cells (Brzozowska and Zielenkiewicz, 2013; Maisonneuve et al., 2013). Thus, we finally asked whether any of the proteolytic systems of *E. coli* K-12 is able to target FicA antitoxins and thereby to activate *ficAT* modules. To address this question we took advantage of the observation that ectopic expression of the *yeficAT* module results in detectable growth inhibition, suggesting that one or more of the resident proteases in *E. coli* degrade part of the YeFicA pool inside the cells (Figure 7D; see *lamB* control). Since the

biochemical investigation of YeFicA degradation *in vivo* was not conclusive (data not shown), we tested *E. coli* deletion mutants lacking ClpP, HslV, or Lon protease for susceptibility to the ectopic expression of *yeficAT*. While no or only a partial attenuation of growth inhibition was observed in *clpP* and *hslV* mutants, the effect was completely absent in the *lon* mutant (Figure 7D; see also Figure S7). These results suggest that Lon is the primary protease targeting YeFicA in *E. coli* and are consistent with the role of Lon as the main player in TA module activation in *E. coli* and related bacteria (Brzozowska and Zielenkiewicz, 2013; Helaine et al., 2014; Maisonneuve et al., 2013).

Discussion

FicT adenylylates DNA gyrase and topo IV to promote persistence

In this study we characterized a diverse sample of TA modules belonging to the conserved and abundant FicTA family and determined their common molecular mechanism as the adenylylation and concomitant inactivation of DNA gyrase and topo IV. The expression of VbhT, YeFicT, and PaFicT toxins consistently caused a robust inhibition of topo IV activity in *E. coli*, but the extent of DNA gyrase inhibition differed, possibly reflecting divergent histories of host adaptation or a quantitative limitation of our single-copy expression system. Though a robust inhibition of topo IV alone is sufficient to inhibit bacterial growth, any additional inhibition of DNA gyrase aggravates this effect because both decatenation and unknotting activities of topo IV are guided by the gyrase-dependent negative supercoiling of the nucleoid (Witz and Stasiak, 2010). The other known topoisomerase-targeting TA systems CcdBA and ParDE are bactericidal plasmid addiction modules that trigger lethal DNA double-strand breaks by poisoning gyrase activity via non-covalent interaction with the A subunit (Bernard and Couturier, 1992; Deghorain et al., 2013). Conversely, the growth arrest caused by FicT toxins is largely reversible (Figure 1C) and relies on the covalent modification of the B subunit of both DNA gyrase and topo IV (Figure

2), resulting in mere target inactivation and not poisoning: Target overexpression could prevent the growth arrest caused by VbhT (Figure 5A), and we did not observe the appearance of diffuse nucleoids upon FicT expression that would have indicated DNA double-strand breaks ((Rajendram et al., 2014), see Figure 4A). This functional contrast between the FicTA family that promotes persister formation and gyrase-poisoning addiction modules reflects their opposing roles as life-saving and life-taking machineries, respectively. The addiction modules of mobile elements evolved to kill bacterial cells that have lost the respective replicon and therefore fail to replenish the pool of instable antitoxin (Deghorain et al., 2013)**.** Instead, FicTA modules are functionally more related to a variety of small proteins that inhibit gyrase by tight binding which blocks the DNA binding of the enzyme and thus prevents DNA damage caused by poisoning (Sengupta and Nagaraja, 2008; Tran and Jacoby, 2002). Mechanistically, FicT toxins resemble the structurally related Doc toxin that blocks translation via the phosphorylation of elongation factor EF-Tu and reversibly arrests bacterial growth (Castro-Roa et al., 2013).

The disruption of DNA topology is a new path to bacterial persistence

It is a main obstacle to the development of efficient strategies against bacterial persisters that we do not understand the meaning of "persistence" on the physiological or molecular level, i.e., how precisely bacteria can survive under a diversity of unrelated, clearly lethal conditions (Balaban et al., 2013). Initially, it was proposed that persisters evade killing via the direct inactivation of antimicrobial targets to prevent bactericidal poisoning (Keren et al., 2004), but this model appears to be too simplistic since it fails to explain why, e.g., TA modules that inhibit translation can protect cells from antibiotics that corrupt topoisomerases (Lewis, 2010; Maisonneuve et al., 2011). Nevertheless, the repeated finding that diverse bacteriostatic treatments can induce a multidrug-tolerant "persister-like state" in laboratory test tubes appeared to support the hypothesis that persistence may simply be the opposite of bacterial growth (Kwan et al., 2013; Vazquez-Laslop et al., 2006). On the other hand, the

intriguing limitation of TA modules to form persisters only via targeting the proton-motive force or, in most cases, inhibiting translation indicated that persisters may not be generated by accidental dormancy but rather by specialized mechanisms (Leplae et al., 2011; Unterholzner et al., 2013). Our discovery that the disruption of DNA topology constitutes a third path to the persister state does not generally change that notion. It is therefore important to stress that persisters are "not simply non-growing cells" but rather employ evolved strategies to survive lethal stress in a dedicated phenotypic state (Keren et al., 2004; Lewis, 2005). Furthermore, a number of recent studies have shown that persisters exhibit an inherent heterogeneity that is likely a consequence of the distinct molecular mechanisms employed by TA modules to induce dormancy (Helaine et al., 2014; Kester and Fortune, 2014; Norton and Mulvey, 2012). Additionally, it has been proposed that bacteria may be able to alternately activate TA modules even if they are wired to the same upstream signaling (Maisonneuve et al., 2011).

This inherent heterogeneity of persistence as a collection of divergent physiological states is important for the arising perspective of drugs designed to kill persister cells (Conlon et al., 2013) because it urges to ensure that these drugs can break both the stacking and the redundancy of the diverse TA modules that underlie persister formation. Therefore, we must explore the molecular mechanisms of different TA modules with regard to the downstream changes in cellular physiology that can all cause multidrug tolerance. The subversion of DNA topology as a third path to the persister state greatly widens the perspective of such a comparative analysis and brings us one step closer to understand how persister cells can survive antimicrobial treatment and – most importantly – how we can still kill them.

Experimental Procedures

Bacterial strains and plasmids

Bacterial strains and plasmids used and constructed over the course of this study are described in the Supplemental Information. All oligonucleotide primers are listed in Table S1. All vectors and details of their construction are listed in Table S2.

Toxicity tests

Unless stated differently, the effect of FicT toxin expression on bacterial viability was investigated in *E. coli* K-12 MG1655 Δ*ecficAT* (AHE573) and derivatives using a two-plasmid system with toxin genes under P*lac* control (pNDM220 derivatives) and antitoxin genes under P*ara* control (pBAD33 derivatives) as well as occasional other plasmids to co-express enzymatic targets or mutants of FicT toxins. Detailed procedures are described in the Supplemental Information.

Persister assays

The fraction of bacterial persisters in exponentially growing cultures of *E .coli* and the effect of different experimental interventions were quantified by forming the ratio of c.f.u. / ml after and before the exposure to lethal doses of antimicrobials. The procedures are described in detail in the Supplemental Information.

Protein expression and purification

Different VbhT constructs (Engel, Goepfert et al., 2012) and GyrB43 (Stanger et al., 2014), an N-terminal fragment of GyrB containing the ATPase domain (Ali et al., 1993), were expressed and purified as described previously. Further details on the expression and purification of VbhT constructs are given in the Supplemental Information.

ATP hydrolysis assay

The ATPase activity of GyrB43 was monitored by FPLC-based nucleotide quantification using the conditions described by Brino et al. (2000). For details, see the Supplemental Information.

Identification of AMPylation sites by LC-MS analysis

Recombinant *E. coli* DNA gyrase and topo IV (TopoGEN Inc.) were adenylylated *in vitro* with purified VbhT(fic)/VbhA(E/G), tryptically digested, C18-purified, and analysed by LC-MS/MS as described previously (Engel, Goepfert et al., 2012). Mass tolerance was set to 15 ppm for precursor ions and 0.6 Da for fragment ions. Converted MS data were searched using Mascot against a SwissProt *E. coli* decoy database containing target sequences of VbhTA. Search results were evaluated using Scaffold 3 (Proteome Software).

***In vitro* adenylylation assays**

The adenylylation activity of FicT constructs was assessed using cleared lysates of ectopically expressing *E. coli* and [α-^{32}P]-ATP (Hartmann Analytic) as described previously (Engel, Goepfert et al., 2012).

***In vitro* topoisomerase assays**

In vitro supercoiling or decatenation assays of recombinant DNA gyrase or topoisomerase IV of *E. coli* (TopoGEN Inc.) were performed according to the supplier's recommendations. Details of the experimental procedure are described in the Supplemental Information.

Flow cytometry with *gfp* promoter fusions

The response of P*gyrB* (for DNA relaxation (Menzel and Gellert, 1983)) and P*sulA* (for SOS induction) promoters to FicT toxin expression was probed using plasmid-encoded *gfpmut2*

promoter fusions of the collection created by Zaslaver et al. (2006) and pUA139, the parental plasmid without promoter, or chromosomal derivatives thereof (AHE1156 and AHE1158; see *Strain Construction* in the *Extended Experimental Procedures*). Experimental details are given in the Supplemental Information.

High-resolution agarose gel electrophoresis

Changes in cellular DNA topology upon FicT toxin expression were assessed using the pAH160 reporter plasmid isolated from snap-frozen samples of *E. coli* AHE938 cultures with the Wizard Plus SV Minipreps DNA Purification kit (Qiagen). Details of the experimental procedure for high-resolution agarose gel electrophoresis to resolve DNA supercoiling, knotting, and catenation are described in the Supplemental Information.

Fluorescence microscopy

E. coli AHE573 that had expressed FicT toxins for 2 hours were stained with membrane dye FM4-64 (Molecular Probes) ad 2.5 µg/ml and DNA dye DAPI (4',6'-diamidino-2-phenylindole, Roche) ad 5 µg/ml for 30 minutes in LB medium in the dark and then transferred onto microscopy slides coated with 1% agarose. Images were acquired using an Olympus IX71 microscope equipped with a CoolSnap HQ2 camera, LED illumination, and a 100x phase contrast objective (all from Applied Precision). Filter sets were Ex: 390/18, Em: 435/48 (DAPI) and Ex: 542/27, Em: 594/45 (TRITC). Snapshots were taken using SoftWorx 5.5 software and the pictures were adjusted for publication using ImageJ (http://rsbweb.nih.gov/ij/download.html) and Photoshop CS5 extended 12.0.4x64 (Adobe).

Authors Contributions

A.H., F.V.S., and P.D.S. cloned recombinant plasmids and constructed bacterial strains. F.V.S. expressed and purified protein constructs. A.H., F.V.S., P.D.S., and I.G.d.J. performed the experiments. T.G. conducted the mass spectrometry analysis. All authors participated in experimental design and data analysis. The manuscript was written by A.H., F.V.S., P.D.S., I.G.d.J, K.G., T.S., and C.D.

Acknowledgments

We are grateful to Guy Cornelis for genomic DNA of *Yersinia enterocolitica* strain 8081, Urs Jenal for genomic DNA of *Pseudomonas aeruginosa* PAO1, and Paul Williams (University of Nottingham) for *Pseudomonas aeruginosa* PAO1 bacteria. We thank Olin Silander for access to different *Escherichia coli* libraries and the Coli Genetic Stock Center (CGSC) for strains BW25113 and K996. Maxime Quebatte and Dirk Bumann are acknowledged for advice on flow cytometry. This work was supported by grants 3100-132979 and 3100-138414 from the Swiss National Science Foundation (to C.D. and T.S., respectively), ERC Advanced Investigator Grant FICModFun (340330) to C.D., ERC Advanced Investigator Grant PERSIST (294517) to K.G, and DFG grant SCHE1734/1-1 to P.D.S. A.H. is a fellow of the Fellowships for Excellence PhD program of the Biozentrum, University of Basel.

References

Ali, J.A., Jackson, A.P., Howells, A.J., and Maxwell, A. (1993). The 43-kilodalton N-terminal fragment of the DNA gyrase B protein hydrolyzes ATP and binds coumarin drugs. Biochemistry *32*, 2717-2724.

Balaban, N.Q., Gerdes, K., Lewis, K., and McKinney, J.D. (2013). A problem of persistence: still more questions than answers? Nat Rev Microbiol *11*, 587-591.

Balaban, N.Q., Merrin, J., Chait, R., Kowalik, L., and Leibler, S. (2004). Bacterial persistence as a phenotypic switch. Science *305*, 1622-1625.

Bates, A.D., Berger, J.M., and Maxwell, A. (2011). The ancestral role of ATP hydrolysis in type II topoisomerases: prevention of DNA double-strand breaks. Nucleic Acids Res *39*, 6327-6339.

Bellon, S., Parsons, J.D., Wei, Y., Hayakawa, K., Swenson, L.L., Charifson, P.S., Lippke, J.A., Aldape, R., and Gross, C.H. (2004). Crystal structures of *Escherichia coli* topoisomerase IV ParE subunit (24 and 43 kilodaltons): a single residue dictates differences in novobiocin potency against topoisomerase IV and DNA gyrase. Antimicrob Agents Chemother *48*, 1856-1864.

Bernard, P., and Couturier, M. (1992). Cell killing by the F plasmid CcdB protein involves poisoning of DNA-topoisomerase II complexes. J Mol Biol *226*, 735-745.

Brino, L., Urzhumtsev, A., Mousli, M., Bronner, C., Mitschler, A., Oudet, P., and Moras, D. (2000). Dimerization of *Escherichia coli* DNA-gyrase B provides a structural mechanism for activating the ATPase catalytic center. J Biol Chem *275*, 9468-9475.

Brzozowska, I., and Zielenkiewicz, U. (2013). Regulation of toxin-antitoxin systems by proteolysis. Plasmid *70*, 33-41.

Castro-Roa, D., Garcia-Pino, A., De Gieter, S., van Nuland, N.A., Loris, R., and Zenkin, N. (2013). The Fic protein Doc uses an inverted substrate to phosphorylate and inactivate EF-Tu. Nat Chem Biol *9*, 811-817.

Chen, C.R., Malik, M., Snyder, M., and Drlica, K. (1996). DNA gyrase and topoisomerase IV on the bacterial chromosome: quinolone-induced DNA cleavage. J Mol Biol *258*, 627-637.

Christensen, S.K., and Gerdes, K. (2003). RelE toxins from bacteria and Archaea cleave mRNAs on translating ribosomes, which are rescued by tmRNA. Mol Microbiol *48*, 1389-1400.

Conlon, B.P., Nakayasu, E.S., Fleck, L.E., LaFleur, M.D., Isabella, V.M., Coleman, K., Leonard, S.N., Smith, R.D., Adkins, J.N., and Lewis, K. (2013). Activated ClpP kills persisters and eradicates a chronic biofilm infection. Nature *503*, 365-370.

Deghorain, M., Goeders, N., Jové, T., and Melderen, L. (2013). Type II Toxin-Antitoxin Loci: The *ccdAB* and *parDE* Families. In Prokaryotic Toxin-Antitoxins, K. Gerdes, ed. (Springer Berlin Heidelberg), pp. 45-67.

Dhar, N., and McKinney, J.D. (2007). Microbial phenotypic heterogeneity and antibiotic tolerance. Curr Opin Microbiol *10*, 30-38.

Dörr, T., Vulic, M., and Lewis, K. (2010). Ciprofloxacin causes persister formation by inducing the TisB toxin in *Escherichia coli*. PLoS Biol *8*, e1000317.

Engel, P., Goepfert, A., Stanger, F.V., Harms, A., Schmidt, A., Schirmer, T., and Dehio, C. (2012). Adenylylation control by intra- or intermolecular active-site obstruction in Fic proteins. Nature *482*, 107-110.

Germain, E., Castro-Roa, D., Zenkin, N., and Gerdes, K. (2013). Molecular mechanism of bacterial persistence by HipA. Mol Cell *52*, 248-254.

Goepfert, A., Harms, A., Schirmer, T., and Dehio, C. (2013). Type II Toxin-Antitoxin Loci: The fic Family. In Prokaryotic Toxin-Antitoxins, K. Gerdes, ed. (Springer Berlin Heidelberg), pp. 177-187.

Grammel, M., Luong, P., Orth, K., and Hang, H.C. (2011). A chemical reporter for protein AMPylation. J Am Chem Soc *133*, 17103-17105.

Hardy, C.D., and Cozzarelli, N.R. (2003). Alteration of *Escherichia coli* topoisomerase IV to novobiocin resistance. Antimicrob Agents Chemother *47*, 941-947.

Helaine, S., Cheverton, A.M., Watson, K.G., Faure, L.M., Matthews, S.A., and Holden, D.W. (2014). Internalization of *Salmonella* by macrophages induces formation of nonreplicating persisters. Science *343*, 204-208.

Kato, J., Nishimura, Y., Imamura, R., Niki, H., Hiraga, S., and Suzuki, H. (1990). New topoisomerase essential for chromosome segregation in *E. coli*. Cell *63*, 393-404.

Keren, I., Shah, D., Spoering, A., Kaldalu, N., and Lewis, K. (2004). Specialized persister cells and the mechanism of multidrug tolerance in Escherichia coli. J Bacteriol *186*, 8172-8180.

Kester, J.C., and Fortune, S.M. (2014). Persisters and beyond: mechanisms of phenotypic drug resistance and drug tolerance in bacteria. Crit Rev Biochem Mol Biol *49*, 91-101.

Khodursky, A.B., Peter, B.J., Schmid, M.B., DeRisi, J., Botstein, D., Brown, P.O., and Cozzarelli, N.R. (2000). Analysis of topoisomerase function in bacterial replication fork movement: use of DNA microarrays. Proc Natl Acad Sci USA *97*, 9419-9424.

Kinch, L.N., Yarbrough, M.L., Orth, K., and Grishin, N.V. (2009). Fido, a novel AMPylation domain common to Fic, Doc, and AvrB. PloS One *4*, e5818.

Kwan, B.W., Valenta, J.A., Benedik, M.J., and Wood, T.K. (2013). Arrested protein synthesis increases persister-like cell formation. Antimicrob Agents Chemother *57*, 1468-1473.

Leplae, R., Geeraerts, D., Hallez, R., Guglielmini, J., Dreze, P., and Van Melderen, L. (2011). Diversity of bacterial type II toxin-antitoxin systems: a comprehensive search and functional analysis of novel families. Nucleic Acids Res *39*, 5513-5525.

Lewis, K. (2005). Persister cells and the riddle of biofilm survival. Biochemistry (Mosc) *70*, 267-274.

Lewis, K. (2010). Persister cells. Annu Rev Microbiol *64*, 357-372.

Maisonneuve, E., Castro-Camargo, M., and Gerdes, K. (2013). (p)ppGpp controls bacterial persistence by stochastic induction of toxin-antitoxin activity. Cell *154*, 1140-1150.

Maisonneuve, E., and Gerdes, K. (2014). Molecular mechanisms underlying bacterial persisters. Cell *157*, 539-548.

Maisonneuve, E., Shakespeare, L.J., Jørgensen, M.G., and Gerdes, K. (2011). Bacterial persistence by RNA endonucleases. Proc Natl Acad Sci USA *108*, 13206-13211.

Menzel, R., and Gellert, M. (1983). Regulation of the genes for *E. coli* DNA gyrase: homeostatic control of DNA supercoiling. Cell *34*, 105-113.

Mukherjee, S., Liu, X., Arasaki, K., McDonough, J., Galan, J.E., and Roy, C.R. (2011). Modulation of Rab GTPase function by a protein phosphocholine transferase. Nature *477*, 103-106.

Norton, J.P., and Mulvey, M.A. (2012). Toxin-antitoxin systems are important for niche-specific colonization and stress resistance of uropathogenic *Escherichia coli*. PLoS Pathog *8*, e1002954.

Pedersen, K., Christensen, S.K., and Gerdes, K. (2002). Rapid induction and reversal of a bacteriostatic condition by controlled expression of toxins and antitoxins. Mol Microbiol *45*, 501-510.

Rajendram, M., Hurley, K.A., Foss, M.H., Thornton, K.M., Moore, J.T., Shaw, J.T., and Weibel, D.B. (2014). Gyramides prevent bacterial growth by inhibiting DNA gyrase and altering chromosome topology. ACS Chem Biol *9*, 1312-1319.

Rovinskiy, N., Agbleke, A.A., Chesnokova, O., Pang, Z., and Higgins, N.P. (2012). Rates of gyrase supercoiling and transcription elongation control supercoil density in a bacterial chromosome. PLoS Genet *8*, e1002845.

Sengupta, S., and Nagaraja, V. (2008). YacG from *Escherichia coli* is a specific endogenous inhibitor of DNA gyrase. Nucleic Acids Res *36*, 4310-4316.

Sissi, C., and Palumbo, M. (2010). In front of and behind the replication fork: bacterial type IIA topoisomerases. Cell Mol Life Sci *67*, 2001-2024.

Stanger, F.V., Dehio, C., and Schirmer, T. (2014). Structure of the N-terminal Gyrase B fragment in complex with ADP·P_i reveals rigid-body motion induced by ATP hydrolysis. PloS One *9*, e107289.

Tran, J.H., and Jacoby, G.A. (2002). Mechanism of plasmid-mediated quinolone resistance. Proc Natl Acad Sci USA *99*, 5638-5642.

Tripathi, A., Dewan, P.C., Barua, B., and Varadarajan, R. (2012). Additional role for the *ccd* operon of F-plasmid as a transmissible persistence factor. Proc Natl Acad Sci USA *109*, 12497-12502.

Unoson, C., and Wagner, E.G. (2008). A small SOS-induced toxin is targeted against the inner membrane in *Escherichia coli*. Mol Microbiol *70*, 258-270.

Unterholzner, S.J., Poppenberger, B., and Rozhon, W. (2013). Toxin-antitoxin systems: Biology, identification, and application. Mob Genet Elements *3*, e26219.

Vazquez-Laslop, N., Lee, H., and Neyfakh, A.A. (2006). Increased persistence in *Escherichia coli* caused by controlled expression of toxins or other unrelated proteins. J Bacteriol *188*, 3494-3497.

Vos, S.M., Tretter, E.M., Schmidt, B.H., and Berger, J.M. (2011). All tangled up: how cells direct, manage and exploit topoisomerase function. Nat Rev Mol Cell Biol *12*, 827-841.

Wang, X., Lord, D.M., Cheng, H.Y., Osbourne, D.O., Hong, S.H., Sanchez-Torres, V., Quiroga, C., Zheng, K., Herrmann, T., Peti, W.*, et al.* (2012). A new type V toxin-antitoxin system where mRNA for toxin GhoT is cleaved by antitoxin GhoS. Nat Chem Biol *8*, 855-861.

Winther, K.S., Brodersen, D.E., Brown, A.K., and Gerdes, K. (2013). VapC20 of *Mycobacterium tuberculosis* cleaves the sarcin-ricin loop of 23S rRNA. Nat Commun *4*, 2796.

Witz, G., and Stasiak, A. (2010). DNA supercoiling and its role in DNA decatenation and unknotting. Nucleic Acids Res *38*, 2119-2133.

Yarbrough, M.L., Li, Y., Kinch, L.N., Grishin, N.V., Ball, H.L., and Orth, K. (2009). AMPylation of Rho GTPases by *Vibrio* VopS disrupts effector binding and downstream signaling. Science *323*, 269-272.

Zaslaver, A., Bren, A., Ronen, M., Itzkovitz, S., Kikoin, I., Shavit, S., Liebermeister, W., Surette, M.G., and Alon, U. (2006). A comprehensive library of fluorescent transcriptional reporters for *Escherichia coli*. Nat Methods *3*, 623-628.

Figure 1

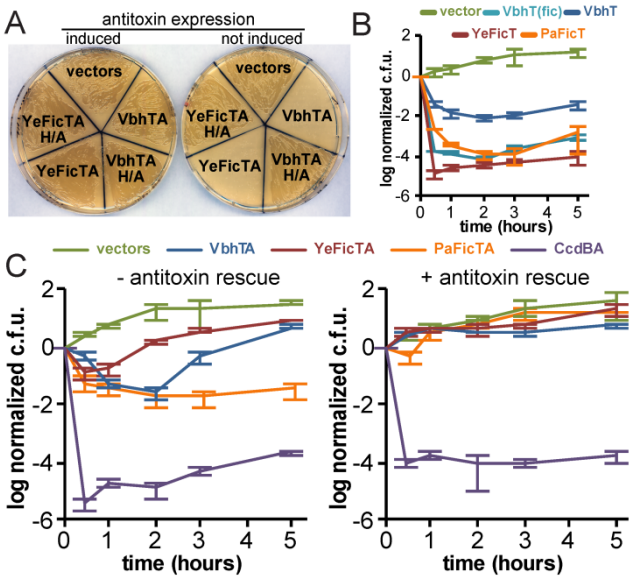
A
antitoxin expression
induced
not induced
vectors
VbhTA
YeFicTA H/A
YeFicTA
VbhTA H/A
B
vector
VbhT(fic)
VbhT
YeFicT
PaFicT
log normalized c.f.u.
time (hours)
C
vectors
VbhTA
YeFicTA
PaFicTA
CcdBA
- antitoxin rescue
+ antitoxin rescue
log normalized c.f.u.
time (hours)

Figure 1. FicT toxins reversibly inhibit bacterial growth

(A) FicT toxins, but not catalytically inactive mutants (”H/A” with a H136A substitution at the active site), inhibit *E. coli* growth on LB agar plates in the absence of cognate FicA antitoxins. The signature motifs of all FicTA modules investigated in this study are compared in Figure S1.

(B) We followed the colony forming units (c.f.u. / ml) of exponentially growing *E. coli* cultures in which FicT expression had been induced with 2000 μM of isopropyl β-D-thiogalactopyranoside (IPTG). The curves show a marked growth inhibition by YeFicT, PaFicT, or only the FIC domain of VbhT (VbhT(fic)) and a lower potency of VbhT.

(C) The c.f.u. / ml of exponentially growing *E. coli* cultures harboring plasmids for the expression of toxins under P*lac* and cognate antitoxins under P*ara* control were monitored over time after the induction of FicT expression by spotting on LB agar plates containing D-glucose (to inhibit toxin expression) or L-arabinose (to induce antitoxin expression). We find that the growth inhibition by FicT toxins, but not gyrase-poisoning toxin CcdB, is reversed by subsequent antitoxin expression. Weaker growth inhibition by FicT toxins in (C) compared to (B) is likely the consequence of leaky antitoxin expression.

All data points and error bars are mean and s.d. of biological triplicates.

Figure 2

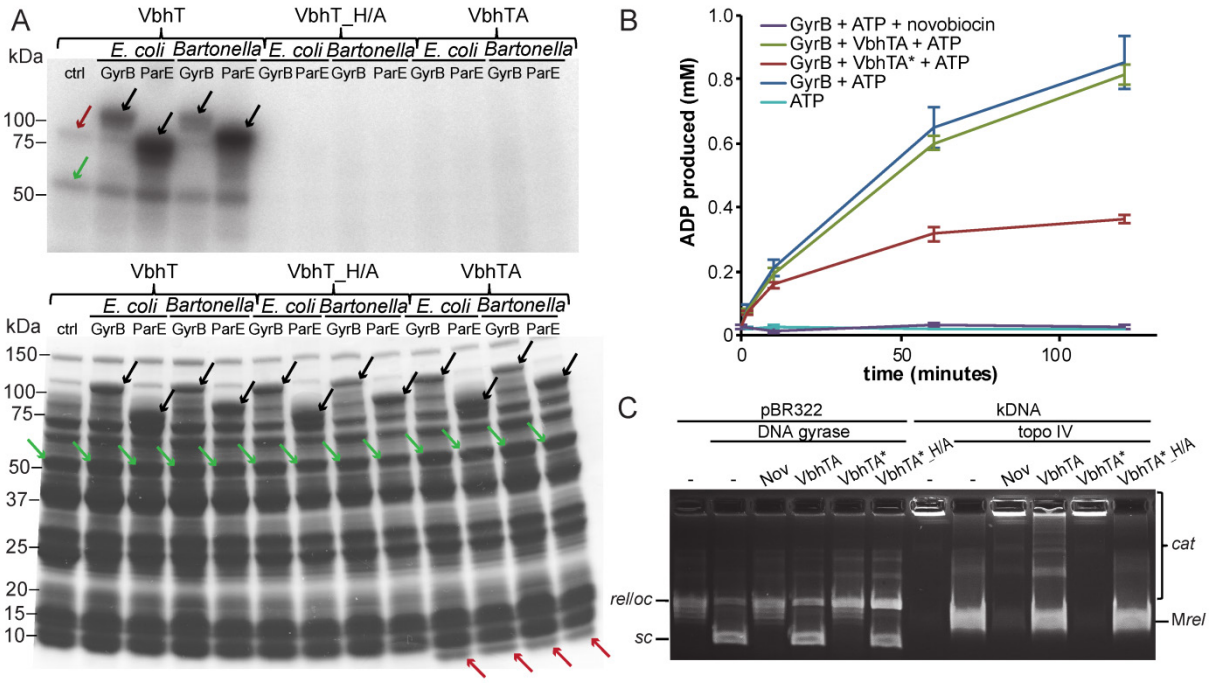
A
VbhT
VbhT_H/A
VbhTA
kDa
E. coli Bartonella E. coli Bartonella E. coli Bartonella
ctrl GyrB ParE GyrB ParE GyrB ParE GyrB ParE GyrB ParE GyrB ParE
100
75
50
VbhT
VbhT_H/A
VbhTA
E. coli Bartonella E. coli Bartonella E. coli Bartonella
kDa
ctrl GyrB ParE GyrB ParE GyrB ParE GyrB ParE GyrB ParE GyrB ParE
150
100
75
50
37
25
20
15
10
B
GyrB + ATP + novobiocin
GyrB + VbhTA + ATP
GyrB + VbhTA* + ATP
GyrB + ATP
ATP
ADP produced (mM)
1.0
0.8
0.6
0.4
0.2
0
0
50
100
time (minutes)
C
pBR322
DNA gyrase
kDNA
topo IV
- - Nov VbhTA VbhTA* VbhTA*_H/A - - Nov VbhTA VbhTA* VbhTA*_H/A
cat
rel/oc
sc
Mrel

Figure 2. FicT toxins adenylylate DNA gyrase and topo IV which results in target inhibition *in vitro*.

(A) Cleared lysates of *E. coli* that had expressed different VbhT (full length) constructs or target candidates were mixed, incubated with [α-^{32}P]-ATP to trace adenylylation, and then analyzed using SDS-PAGE and autoradiography.

The autoradiograph (top) shows VbhT auto-adenylylation (58 kDa; green arrow) and adenylylation of endogenous GyrB (90 kDa; red arrow) as well as ectopically expressed GST-fusions of GyrB and ParE of *E. coli* and *B. schoenbuchensis*, respectively (black arrows). The Coomassie stain (bottom) of the same gel shows the presence of all ectopically expressed proteins (green: VbhT, magenta: VbhA, black: GST-GyrB and GST-ParE). Using mass spectrometry we mapped the adenylylation sites to be tyrosine 109 in *E. coli* GyrB and tyrosine 105 in *E. coli* ParE (Figure S2).

(B) The curves represent ATP hydrolysis by a GyrB ATPase model construct as monitored by ADP production. Addition of the VbhT/VbhA complex (VbhTA) has no effect on GyrB-mediated ATP hydrolysis (compare blue and green curves), whereas adenylylation of GyrB by the VbhTA* construct (see below) progressively inhibits ATP hydrolysis, with full inactivation achieved after about one hour of incubation (red curve). Novobiocin immediately blocks ATP hydrolysis (purple curve). Data points and error bars are mean and s.d. of biological triplicates.

(C) The supercoiling and decatenation activities of recombinant DNA gyrase and topo IV were probed by monitoring the supercoiling (*sc*) of relaxed pBR322 (*rel*) and the decatenation of highly catenated kDNA (*cat*) into monomers (M*rel*) *in vitro*, respectively. The targets were pre-incubated with different VbhT constructs for one hour prior to the addition of DNA substrates. The agarose gel resolving the reaction products shows that both enzymes are fully inhibited by adenylylation as well as by novobiocin. *oc* = open circular (nicked) plasmid

In (B) and (C) VbhTA* as opposed to VbhTA indicates the presence of mutant VbhA(E24G) that is unable to inhibit VbhT, resulting in an active, adenylylation-competent construct (Engel, Goepfert et al., 2012); see also *Extended Experimental Procedures* in the Supplemental Information).

Figure 3

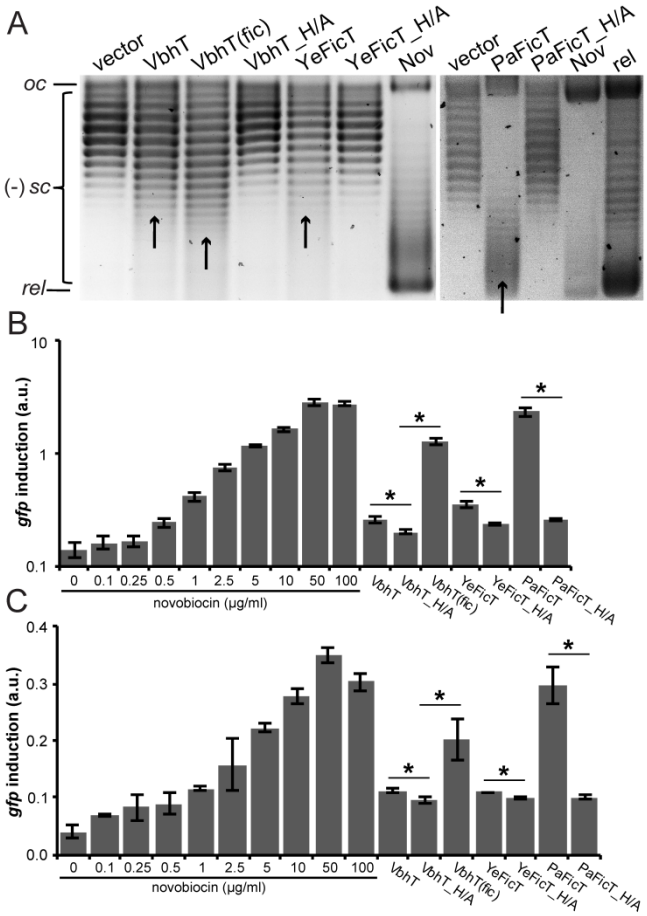
A
vector
VbhT
VbhT(fic)
VbhT_H/A
YeFicT
YeFicT_H/A
Nov
vector
PaFicT
PaFicT_H/A
Nov
rel
oc
(-) sc
rel
B
gfp induction (a.u.)
10
1
0.1
0 0.1 0.25 0.5 1 2.5 5 10 50 100
novobiocin (µg/ml)
VbhT
VbhT_H/A
VbhT(fic)
YeFicT
YeFicT_H/A
PaFicT
PaFicT_H/A
C
gfp induction (a.u.)
0.4
0.3
0.2
0.1
0.0
0 0.1 0.25 0.5 1 2.5 5 10 50 100
novobiocin (µg/ml)
VbhT
VbhT_H/A
VbhT(fic)
YeFicT
YeFicT_H/A
PaFicT
PaFicT_H/A

Figure 3. FicT toxins achieve only partial inhibition of DNA gyrase *in vivo*.

(A) Reporter plasmid pAH160 was analyzed by high resolution agarose gel electrophoresis (in presence of 12.5 µg/ml chloroquine to resolve negative supercoiling) following isolation from *E. coli* that had expressed different FicT constructs for two hours. The gel shows only a slight stretching of the pAH160 topoisomer distribution towards DNA relaxation with VbhT or YeFicT (arrows), indicative of weak inhibition of DNA gyrase, while high concentrations of novobiocin (Nov; 100 µg/ml) or the expression of PaFicT fully abrogate the negative supercoiling.

(B) The induction of a relaxation-sensitive P*gyrB::gfpmut2* module on a reporter plasmid was analyzed by flow cytometry in *E. coli* that had expressed different FicT constructs for two hours. As expected, the treatment with novobiocin elicited a dose-dependent response (10 µg/ml fully inhibit DNA gyrase in *acrA*-deficient *E. coli* (Khodursky et al., 2000)). Different FicT constructs induced weak (VbhT and YeFicT), intermediate (VbhT(fic)), or strong (PaFicT) expression of GFP ($p<0.01$, unequal variance t-test).

(C) A chromosomal P*gyrB::gfpmut2* module was used to assay nucleoid relaxation as described for the plasmid sensor in (B). Similarly, our set of FicT constructs differentially induced the expression of GFP (all ($p<0.05$, unequal variance t-test).

All data points and error bars are mean and s.d. of biological triplicates.

Figure 4

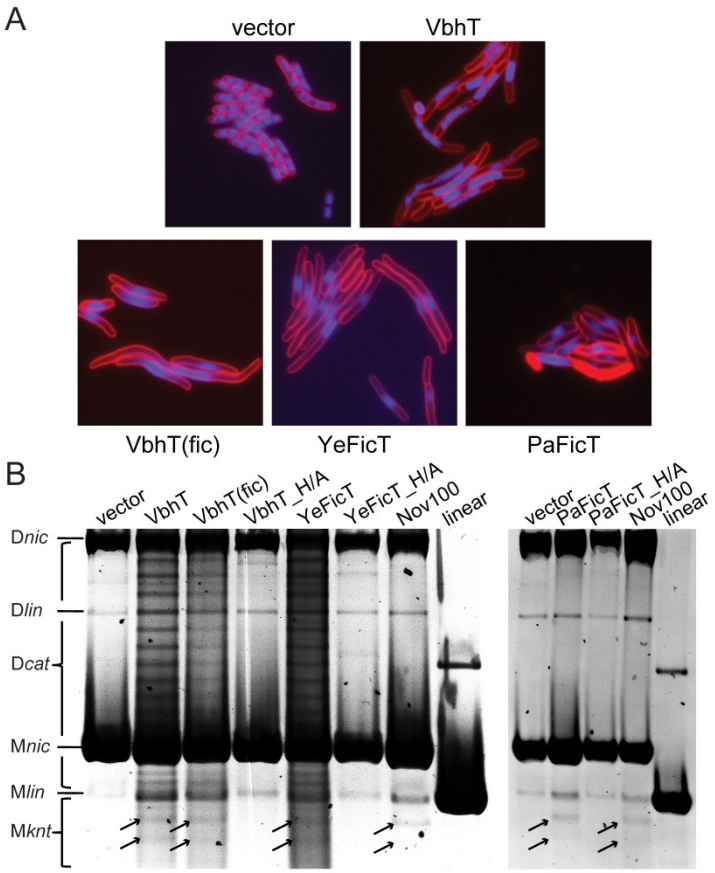
A
vector
VbhT
VbhT(fic)
YeFicT
PaFicT
B
vector
VbhT
VbhT(fic)
VbhT_H/A
YeFicT
YeFicT_H/A
Nov100
linear
vector
PaFicT
PaFicT_H/A
Nov100
linear
Dnic
Dlin
Dcat
Mnic
Mlin
Mknt

Figure 4. FicT expression results in robust inhibition of topo IV *in vivo.*

(A) *E. coli* cells that had expressed different FicT constructs for two hours were stained with FM4-64 (membranes; red) and DAPI (DNA, blue) and analyzed by fluorescence microscopy; representative images are shown. FicT toxin expression induces a "*par*" phenotype with cell filamentation and unsegregated nucleoids, indicative of strong topo IV inhibition. The nucleoid compaction observed with VbhT(fic), YeFicT, and PaFicT is likely a consequence of DNA gyrase inhibition (Rajendram et al., 2014).

(B) Nicking of the DNA samples used for Figure 3A separates nicked (*nic*) / linear (*lin*) dimers (*D*) and monomers (*M*) and reveals catenation (D*cat*) and knotting (M*knt*, arrows) upon FicT expression. High concentrations of novobiocin (100 µg/ml, *Nov100*) or PaFicT expression also inactivate DNA gyrase (note collapsed supercoiling in Figure 3A), leading primarily to DNA knotting in the absence of DNA replication. A lane plot that highlights the bands representing knotted topoisomers is shown in Figure S3.

Figure 5

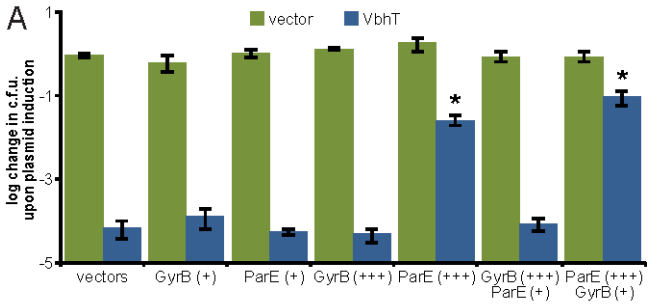
A
vector
VbhT
log change in c.f.u. upon plasmid induction
1
-1
-3
-5
*
*
vectors
GyrB (+)
ParE (+)
GyrB (+++)
ParE (+++)
GyrB (+++) ParE (+)
ParE (+++) GyrB (+)

Figure 5. VbhT-induced growth inhibition can be blocked by target overexpression

E. coli harboring plasmids for the expression of VbhT under P*lac* control as well as target(s) under P*ara* (low copy vectors, denoted by "+" expression level) or P*rha* (high copy vectors, denoted by "+++" expression level) control were spotted in serial dilutions onto different agar plates. The plates contained no inducer, 2000 μM IPTG, 0.2% L-arabinose and D-rhamnose (for P*ara* and P*rha*), or all inducers, and the bar diagram shows the difference in c.f.u. obtained between no inducer and all inducers conditions. It is apparent that a strong induction of ParE expression can prevent the growth inhibition caused by VbhT ($p<0.05$, unequal variance t-test against vector control of target expression). The data are in line with genetic findings that FicT toxins act via topoisomerase inhibition to subvert cellular DNA processing (Figure S4). Data points are mean values of three independent experiments with error bars denoting s.e.m.

Figure 6

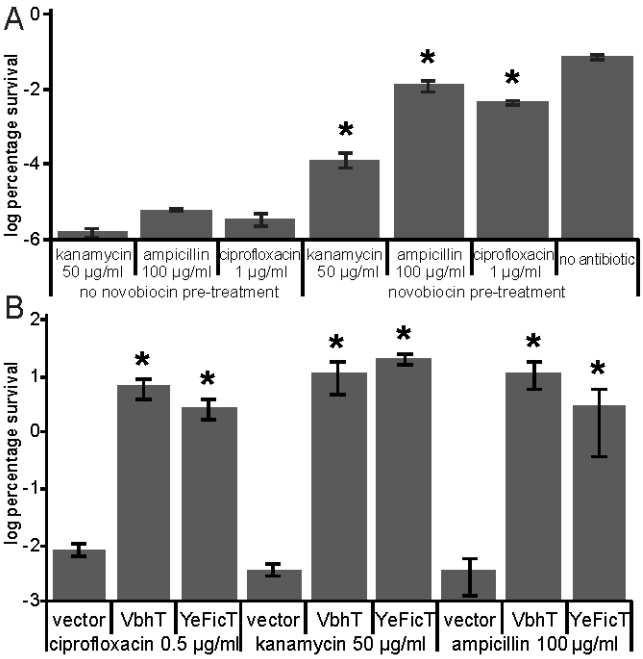
A
log percentage survival
0
-2
-4
-6
kanamycin 50 µg/ml
ampicillin 100 µg/ml
ciprofloxacin 1 µg/ml
kanamycin 50 µg/ml
ampicillin 100 µg/ml
ciprofloxacin 1 µg/ml
no antibiotic
no novobiocin pre-treatment
novobiocin pre-treatment
B
log percentage survival
2
1
0
-1
-2
-3
vector
VbhT
YeFicT
vector
VbhT
YeFicT
vector
VbhT
YeFicT
ciprofloxacin 0.5 µg/ml
kanamycin 50 µg/ml
ampicillin 100 µg/ml

Figure 6. The disruption of DNA topology by novobiocin or FicT expression induces bacterial persister formation

(A) Exponentially growing *E. coli* of strain AHE938 (novobiocin-sensitive due to *acrA* genotype) were treated with a high concentration of novobiocin for one hour (200 μg/ml) and then challenged with a lethal concentration of one of three different antibiotics for three more hours so that only persisters would survive. C.f.u. / ml were determined before and after drug challenge. The data show a 2-3 log increase in the proportion of persisters upon novobiocin treatment ($p<0.05$, unequal variance t-test against no-treatment control). This effect does not involve an activation of the SOS response, suggesting that it is caused by the disruption of cellular DNA topology itself (Figure S5D).

(B) Exponentially growing *E. coli* were induced to express FicT toxins for two hours and then challenged with a lethal concentration of one of three different antibiotics for three more hours so that only persisters would survive. C.f.u. / ml were determined before and after drug challenge; the data show a 1,000 fold increased proportion of persisters in *E. coli* expressing FicT toxins ($p<0.001$, unequal variance t-test). This effect is largely independent of the SOS activation caused by FicT expression (Figures S5A and S5E).

Figure 7

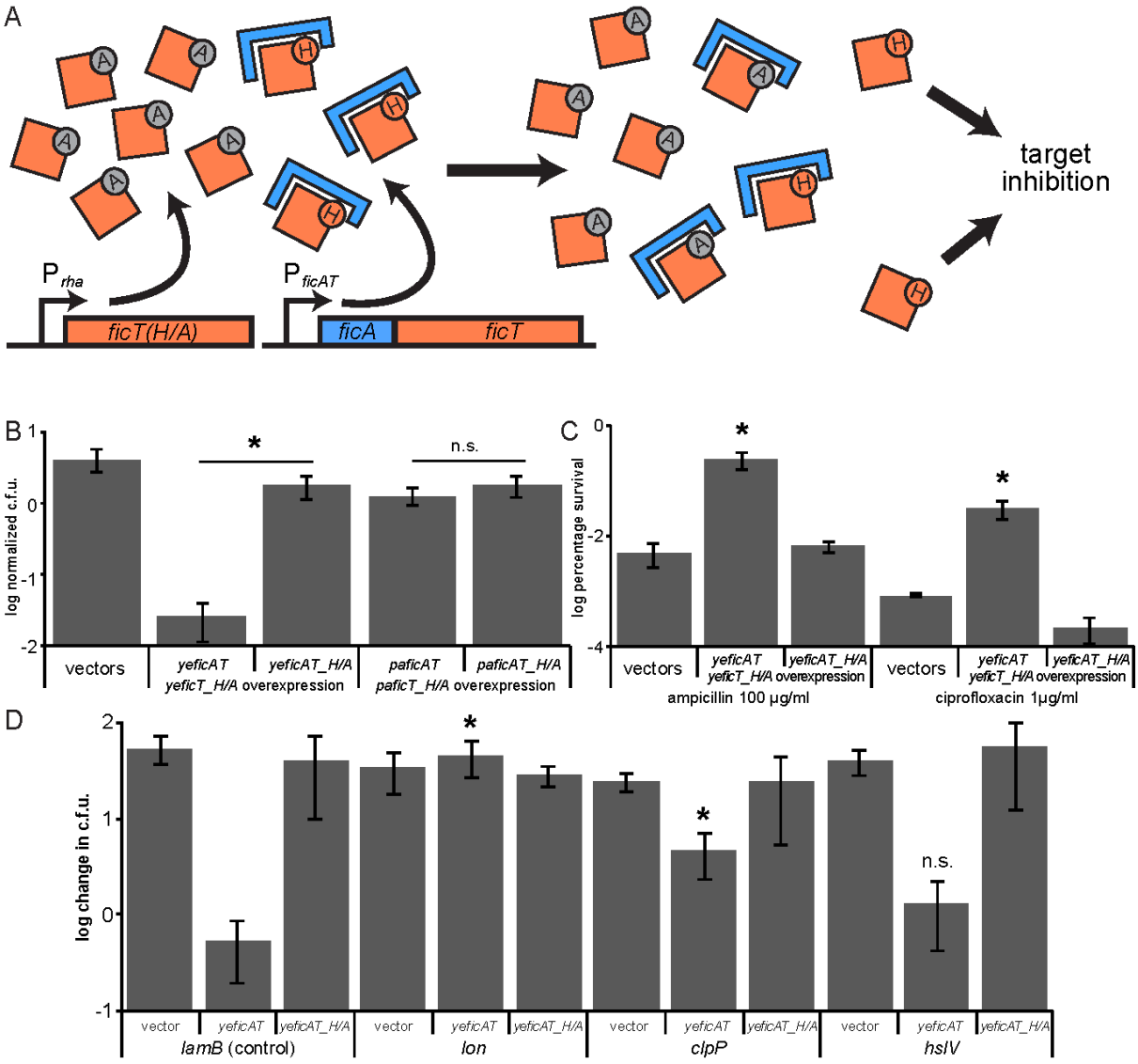
A
target inhibition
P rha
P ficAT
ficT(H/A)
ficA
ficT
B
log normalized c.f.u.
vectors
yeficAT
yeficT_H/A overexpression
yeficAT_H/A
paficAT
paficT_H/A overexpression
paficAT_H/A
n.s.
C
log percentage survival
vectors
yeficAT
yeficT_H/A overexpression
yeficAT_H/A
ampicillin 100 µg/ml
ciprofloxacin 1µg/ml
D
log change in c.f.u.
vector
yeficAT
yeficAT_H/A
lamB (control)
lon
clpP
hslV
n.s.

Figure 7. The *yeficAT* module can be activated by sequestration or Lon-mediated degradation of YeFicA and promotes persister formation

(A) The model illustrates the experimental activation of *ficAT* modules by antitoxin sequestration. Catalytically inactive FicT_H/A toxin mutants expressed from a high-copy vector upon D-rhamnose induction (left; with "A" instead of "H" in the stylized active site) titrate out cognate FicA antitoxins (blue) that are expressed together with wildtype FicT from a genuine *ficAT* locus on a low-copy vector. Free FicT toxins are active and cause bacterial growth inhibition via target adenylylation (see *Extended Experimental Procedures* in the Supplemental Information).

(B) *E. coli* harboring *yeficAT* or *paficAT* modules including their 300 bp upstream regions were induced to overexpress catalytically inactive FicT_H/A mutants for one hour (see A) and c.f.u. were recorded before and afterwards. The data show an activation of the intact *yeficAT* module upon antitoxin sequestration, but effects of *paficAT* were not significant (n.s.). A similar experiment in its natural host organism *Pseudomonas aeruginosa* PAO1 readily detected activation of *paficAT* (Figure S6).

(C) The genuine *yeficAT* module on a low-copy vector was activated by antitoxin sequestration as described in (A) and the bacteria were challenged with a lethal concentration of ampicillin or ciprofloxacin for three more hours so that only persisters would survive. C.f.u. / ml were determined before and after drug challenge, showing that this near-physiological activation of *yeficAT* significantly increases the proportion of persisters in the population ($p<0.05$ for unequal variance t-test against vector or H/A controls). This phenotype is largely independent of a potential SOS induction upon YeFicT activation (Figure S5F).

(D) *E. coli* protease mutants harboring a plasmid-encoded *yeficAT* module under P*lac* control were induced with 2000 µM IPTG and c.f.u. were recorded before and after two hours of expression. It is apparent that the ectopic co-expression of *yeficAT* from a heterologous promoter results in growth inhibition unless *lon* is inactivated, while the *clpP* mutant showed

only a partial rescue (both $p<0.05$ against *lamB* control, unequal variance t-test). The inactivation of *hslV* had no effect (n.s. = not significant). We confirmed that growth inhibition by YeFicT is not generally reduced in the *lon* mutant and did not detect a similar effect with *vbhAT(fic)* or *paficAT* (Figure S7A-C). All data points are mean values of three independent experiments with error bars denoting s.d.

Supplemental Information

Extended Results

Using a panel of diverse model proteins to study FicT toxins

We had previously shown that VbhT and VbhA of *Bartonella schoenbuchensis* fulfill the central definition of type II TA modules since the small VbhA protein inhibits both the adenylylation activity of FIC domain containing VbhT as well as the associated growth inhibition in *E. coli* via a direct protein-protein interaction (Engel, Goepfert et al., 2012). However, while the far majority of FicT homologs solely comprise a FIC domain, VbhT uniquely harbors a discernable type IV secretion signal at its C-terminus, a BID (Bep Intracellular Delivery) domain. BID domains are present in relaxases of a number of conjugation systems as well as the closely related host-targeted effectors of the genus *Bartonella* (Schulein et al., 2005), suggesting that VbhT may be secreted into a target cell (prokaryotic or eukaryotic) by the Vbh type IV secretion system (T4SS) encoded close-by. It was therefore possible that VbhT could have secondarily acquired a new function which may or may not rely on a different / altered biochemical activity than that of other FicT toxins. We therefore decided to study VbhTA along with more typical homologs to elucidate the molecular function and biological role FicTA modules.

The prototypic EcFicT protein of *Escherichia coli* was the first FIC domain protein to be described and the "filamentation induced by cAMP" phenotype of its *fic-1* allele gave the name to the domain family (Utsumi et al., 1982). Being a genuine *E. coli* protein, EcFicT would have been an ideal candidate for a biological characterization in this classical model organism along with VbhT. However, we found that EcFicT is unlikely to be representative of the bulk of FicT homologs because it belongs to an atypical subgroup that is only found in *Enterobacteria* and harbors a secondarily deteriorated FIC domain active site motif (Figure

S1). Consequently, EcFicT did not show adenylylation activity or inhibit bacterial growth (our unpublished results). However, we still used a Δ*ecficAT* derivative of *E. coli* str. K-12 substr. MG1655 for most experiments to exclude functional crosstalk of any kind between endogenous EcFicTA and our model systems.

Instead of EcFicTA we decided to characterize YeFicTA of *Yersinia enterocolitica* str. 8081, an organism closely related to *E. coli* (Thomson et al., 2006). YeFicT has 37% protein sequence identity to EcFicT and 32% protein sequence identity to the FIC domain of VbhT of *B. schoenbuchensis*. Most importantly, YeFicT appears to be an average FicT homolog with a conserved FIC domain active site motif. Though not originally annotated in genome of *Y. enterocolitica* str. 8081, we identified the small ORF *yeficA* encoded upstream of *yeficT* with slight overlap as a candidate antitoxin with inhibitory α-helix and identical length to *vbhA*.

Furthermore, we studied a rather distant relative of our other model proteins to assess whether our findings may apply to FicT homologs in general. For this purpose we chose PaFicT of *Pseudomonas aeruginosa* PAO1 with 22.1%, 16.6%, and 22.0% protein sequence identity in the conserved regions to YeFicT, EcFicT, and VbhT, respectively. Like for YeFicT, we identified the small ORF *paficA* encoded upstream of *paficT* with slight overlap that may serve as an antitoxin. Interestingly, the signature motifs of both the FIC domain in PaFicT (HXFX(D/E)GNGRXX**L** with a leucine instead of the final arginine) and PaFicA (SXXX**D**(G/N)) with an aspartate instead of the glutamate) slightly diverge from the canonical motifs as defined by Engel, Goepfert et al. (2012) (see Figure S1).

FicT expression impairs replication fork progression and DNA segregation

It is intuitive that the inhibition of chromosome decatenation upon topo IV inhibition by FicT would impair DNA segregation and cell division (Adams et al., 1992; Zechiedrich and Cozzarelli, 1995). Consistently, we found that the inactivation of topoisomerase III or

XerCD recombination which can both partially complement a topo IV deficiency in DNA segregation made *E. coli* hypersensitive to growth inhibition by FicT toxins (Figure S4A). Moreover, others have shown that the inactivation of topo IV results in an inhibition of DNA replication and transcription via DNA knotting as well as an impaired topological control of replication forks that is aggravated in different ways by DNA gyrase inhibition (Deibler et al., 2007; Khodursky et al., 2000; Lopez et al., 2012; Witz et al., 2011; Witz and Stasiak, 2010). DNA knots continuously arise in the tangled nucleoid from random strand passages that occur whenever cellular DNA handling cuts open the chromosome, e.g., during processes of replication, recombination, or repair, and they cannot be removed in the absence of functional topo IV (Deibler et al., 2001). Similarly, positive supercoiling arises ahead of DNA replication forks as well as transcription complexes and inhibits their progression unless it is continuously removed by DNA gyrase and topo IV (Chong et al., 2014; Khodursky et al., 2000). We therefore expected that the viability of bacteria expressing FicT toxins should depend on replication fork repair and restart via fork reversal and various recombination pathways. Indeed, we found that *E. coli* deficient in the *recABCD* or *ruvABC* machineries were hypersensitive to growth inhibition by FicT toxins (Figure S4A). Importantly, the same genes are also involved in a number of different DNA repair pathways on top of recombinational fork repair, e.g., the processing of double-strand breaks. We therefore verified that the single inactivation of *recA* (which is essential for double-strand break repair (Wigley, 2013)) does not abolish the reversibility of a FicT toxin-mediated growth arrest in our experimental system (Figure S4B). However, the dual inactivation of exonuclease V and homologous recombination which represent the two branches of replication fork restart after fork reversal results in detectable lethality upon FicT toxin expression (*recB* as well as *recDA* mutant in Figure S4B). We therefore conclude that frequent replication fork arrest impairs chromosome replication during growth arrest by FicT toxins (De Septenville et al., 2012). Fork arrest is a main trigger of the SOS response, a cascade of genes whose expression is

induced upon DNA damage (Erill et al., 2007). We indeed detected an activation of the SOS response upon FicT toxin expression that varied between the different constructs from not significant (VbhT) to similarly strong as with gyrase poisons ciprofloxacin or CcdB (VbhT(fic) and PaFicT) in rough correlation with the extent of DNA gyrase inhibition, but not growth arrest (Figure S5A; compare Figures 3 and 1B). These results are in line with previous work that demonstrated an activation of the SOS response with gyramide A, an inhibitor of ATP hydrolysis of DNA gyrase but not topo IV (Rajendram et al., 2014). Though most factors encoded by SOS genes are more or less directly involved in DNA repair, the SulA protein expressed in response to strong SOS induction blocks cell division via the inhibition of septation (Huisman et al., 1984), thus buying overtime for DNA repair functions. Irreversible blocks of cell division via SOS activation and SulA were proposed to be involved in a number of toxicity phenomena like thymineless death (Fonville et al., 2010). Similarly, we find that – at the relatively low level of FicT activity that we used in this experimental system – the inability to launch the SOS response (in a *lexA3* mutant) or the inactivation of *sulA* made the bacteria considerably more tolerant to FicT toxin expression than the control strain (Figure S4A). However, the contribution of the SOS response to growth inhibition is only minor at the higher levels of FicT activity that we generally used for phenotypic characterization (Figure S5B and S5C), suggesting that SulA-mediated growth inhibition is no necessary component of growth inhibition by FicT toxins. Furthermore, the SOS response was also not relevantly involved in the induction of persister formation upon the disruption of DNA topology by FicT toxins or novobiocin (Figure S5E-G).

Extended Experimental Procedures

Escherichia coli handling and growth conditions.

Escherichia coli was transformed with one or more plasmids using TSS transformation (Chung et al., 1989) and always handled in LB liquid or solid medium containing appropriate antibiotics as well as 1% w/v D-glucose to suppress basal expression of any construct prior to the inoculation of experimental cultures. Unless stated differently, experiments were performed with exponentially growing derivatives of *E. coli* K-12 harboring pNDM220 derivatives (encoding FicT toxin constructs under P*lac* control) and, whenever indicated, pBAD33 derivatives (encoding FicA antitoxins) as well as occasional other plasmids. Repeatedly, derivatives of pAH160 (encoding enzymatic targets or mutants of FicT toxins under P*rha* control) were used. For the enumeration of colony forming units (c.f.u.) bacterial cultures were serially diluted and spotted on LB agar plates which were thereafter incubated at 37°C for up to several days before counting. Selection for different genotypes or plasmid maintenance was performed with ampicillin ad 30 µg/ml (pNDM220 and derivatives) or 100 µg/ml (pGex-6p1 and derivatives), chloramphenicol ad 34 µg/ml, gentamicin ad 20 µg/ml, kanamycin ad 50 µg/ml, and tetracycline ad 12 µg/ml.

Plasmid Construction

Plasmids were constructed using standard procedures of restriction-based cloning or sequence- and ligation-independent cloning (SLIC) with enzymes obtained from New England Biolabs. For phenotypic analyses, toxin genes or *ficAT* modules were cloned into pNDM220 (Gotfredsen and Gerdes, 1998) under control of a particularly tight P*lac* (for pAH154 or pAH157 series, respectively) and antitoxin genes were cloned into pBAD33 under control of P*ara* (for pAH153 series), resulting in a two-plasmid expression system as it was used previously for the analysis of toxin-antitoxin interactions (Jørgensen et al., 2009).

Experiments investigating the effect of target (over)expression on growth inhibition by FicT toxins used *gyrB* and *parE* of *E. coli* cloned into pBAD33 (pAH153 series) and pAH160 backbones for P*ara* or P*rha* control, respectively. For the analysis of complete FicTA modules the *ficAT* loci including approximately 300 bp of upstream (promoter) region were cloned into pBAD33 (pAH176 series) and their activation by antitoxin sequestration was investigated using the co-expression of catalytically inactive FicT_H/A mutants from pAH160. For biochemical analyses and protein purification, toxins and / or antitoxins were cloned into pRSFDuet-1 (Novagen) and target candidates as glutathione S-transferase (GST) fusions into pGex-6p-1 (GE Healthcare).

The *yeficA* and *paficA* antitoxin genes were identified as ORFs encoded by nucleotides 1'867'230-1'867'042 and 1'480'066-1'479'788 in the genomes of *Yersinia enterocolitica* str. 8081 (NC_008800) and *Pseudomonas aeruginosa* PAO1 (NC_002516.2), respectively. YeFicT and PaFicT are proteins YP_001005954.1 and NP_250057.1. Point mutations and deletions were introduced via PCR into suitable template plasmids as described by Liu and Naismith (2008). Occasional sub-cloning of PCR products was performed using the StrataClone blunt PCR cloning kit (Agilent). Plasmid construction was always confirmed by DNA sequencing.

Strain Construction

E. coli strains used for phenotypic analyses were generated from *E. coli* str. K-12 substr. MG1655 and protein expression was performed in *E. coli* BL21 or derivatives. Strains were constructed using the method of Datsenko and Wanner (2000). For the deletion of *ecficAT* in *E. coli* K-12 MG1655 the original locus was amplified with prAH361/362, sub-cloned, and the deletion allele was produced via amplification with prAH359/360. Subsequent allelic replacement via a *kanR* / *sacB* cassette (amplified from pJM05 of MacKichan et al. (2008)

with prAH363/364) in the *ecficAT* locus resulted in strain AHE573 (*E. coli* str. K-12 substr. MG1655 Δ*ecficAT*. The deletion allele was constructed in a way to not affect expression of downstream gene *pabA* by leaving the last 55bp of the *ecficT* gene. The *lexA3* allele was moved via P1vir transduction from *E. coli* K996 (CGSC#: 7786) into AHE573 or, to yield a strain isogenic with the KEIO collection (Baba et al., 2006), into *E. coli* BW25113 (CGSC#: 7636) with selection for the *malE::tn10* marker close-by, resulting in AHE961 (*E. coli* K-12 Δec*ficAT lexA3 malE::tn10*) and AHE963 (*E. coli* BW25113 *lexA3 malE::tn10*). The *endA* gene in AHE573 was replaced by the inactive *endA** allele of BL21 (DE3) Gold (Agilent) to inactivate endonuclease I and improve the quality of isolated plasmids for high resolution agarose gel electrophoresis, resulting in AHE745 (*E. coli* K-12 Δec*ficAT endA**). Primers were prAH351/352 to amplify *endA* or *endA** and prAH366/367 for the locus-specific double-selectable cassette. The *acrA* gene in AHE745 was replaced with a gentamicin resistance cassette (amplified with prAH559/560 from pRS96 of Schulein et al. (2005)) to obtain a highly novobiocin-sensitive strain as it was used by Hardy and Cozzarelli (2003) (AHE938, *E. coli* K-12 Δ*ecficAT endA* acrA::genR*). An SOS-deficient derivative of AHE938 was created by P1 transduction from *E. coli* K996 as described above, resulting in strain AHE1263 (*E. coli* K-12 Δ*ecficAT endA* acrA::genR lexA3 malE::tn10*). For the construction of a chromosomal DNA relaxation sensor we first trimmed the promoter fragment of the pP*gyrB::gfpmut2* vector of Zaslaver *et al.* (2006) down to the P*gyrB* promoter as listed by RegulonDB (Salgado et al., 2013) by site-directed mutagenesis with primers prAH909/910, creating plasmid pP*gyrB::gfpmut2*_v1. A cassette containing a kanamycin cassette as well as the P*gyrB::gfpmut2* module was amplified from pP*gyrB::gfpmut2*_v1 using primers prAH925/926 and integrated into the *gapC* locus of AHE938 using lambda Red recombineering, creating strain AHE1158 (*E. coli* K-12 Δ*ecficAT endA* acrA::genR gapC::PgyrB::gfpmut2_v1*). A promoterless control was created analogously using plasmid pUA139 as the template for amplification, creating strain AHE1156 (*E. coli* K-12 Δ*ecficAT*

endA acrA::genR gapC::pUA139*). The construction of all strains was confirmed by DNA sequencing.

Toxicity tests

Experiments were generally performed with *E. coli* K-12 MG1655 Δ*ecficAT* (AHE573) and derivatives or, when indicated, single gene mutants of the KEIO collection (Baba et al., 2006). The growth of *E. coli* expressing FicT toxins was qualitatively assessed on LB agar plates inducing FicT toxin expression with 2000 µM of Isopropyl β-D-thiogalactopyranoside (IPTG) in presence or absence of 0.2% w/v L-arabinose to induce antitoxin expression. When indicated, *gyrB* and *parE* of *E. coli* where co-expressed from additional plasmids under P*ara* control (low-copy pBAD33 derivatives) and P*rha* control (high-copy pAH160 derivatives). For growth curves, FicT toxin expression was induced at t = 0 with 2000 µM of IPTG and the change in c.f.u. (on LB agar plates containing 1% D-glucose) was quantified by normalization to the c.f.u. at t = 0. When appropriate, the c.f.u. counts on plates containing 0.2% L-arabinose were enumerated in parallel. Differences in the susceptibility of various *E. coli* single gene mutants of the KEIO collection to growth inhibition by FicT toxins were assessed using the continuous expression of VbhT with 400 µM IPTG induction and the *lamB* mutant as an isogenic control. We chose this relatively low level of *lac* promoter induction and VbhT instead of YeFicT to avoid problems with saturating toxicity, leaky expression (especially in hypersensitive mutants), and an insufficient dynamic range to detect both increased and decreased susceptibility. The reversibility of FicT toxin expression by antitoxin induction upon plating on 0.2% L-arabinose with different *E. coli* mutants (Figure S4B) was tested after 90 minutes of FicT toxin induction to reliably detect both VbhT and YeFicT toxicity (see Figure 1C). We induced the near-natural activation of complete *ficAT* loci on low-copy vectors (pAH176 series) via the co-expression of according FicT_H/A mutants from high-

copy plasmids under P*rha* control (pAH160 derivatives). In this system, the pool of FicA antitoxin is sequestered by an excess of FicT_HA mutant which results in the activation of FicT toxins expressed from their natural promoter at the *ficAT* locus (see Figure 7A). Changes in c.f.u. / ml after one hour of FicT_H/A expression were quantified by plating on LB agar plates containing 1% D-glucose.

Persister assays

Generally, the proportion of persisters in exponentially growing cultures of *E. coli* was determined as the surviving fraction after lethal treatment with one of three different antibiotics (ciprofloxacin, kanamycin, or ampicillin). After drug challenge, the bacteria were washed extensively in sterile PBS, plated in serial dilutions on LB agar plates containing 1% D-glucose, and the c.f.u. counts were compared to those obtained with the same cultures before the addition of antibiotics.

The effects of changes in DNA topology and FicT activity on the fraction of persisters were assayed by specific treatments of the exponentially growing cultures prior to antibiotic challenge. A disruption of DNA topology was assayed in *E. coli* AHE938 (novobiocin-sensitive due to *acrA* genotype) in form of a pre-treatment with 200 µg/ml of novobiocin for one hour to inhibit both DNA gyrase and topo IV. Changes in the proportion of persisters caused by FicT activity were explored both by the expression of FicT toxins for two hours or the activation of complete *ficAT* loci by FicT_H/A overexpression for one hour in *E. coli* AHE573 (see above). In presence of pNDM220 and derivatives we added ampicillin in combination with 10 µg/ml clavulanate to inactivate the β-lactamase encoded on this vector (Vakulenko et al., 1998).

Protein Expression and Purification

All VbhT constructs were generally expressed and purified as described previously (Engel, Goepfert et al., 2012). For purification, VbhT was expressed in form of truncated constructs devoid of the BID domain and always together with its VbhA antitoxin for technical reasons (Engel, Goepfert et al., 2012). The asterisk in VbhTA* indicates the presence of mutant VbhA(E24G) that is unable to inhibit the adenylylation activity of VbhT, resulting in a construct representing active VbhT.

ATP hydrolysis assay

GyrB43, an N-terminal fragment of *E. coli* GyrB containing the ATPase domain (Ali et al., 1993), at a concentration of 50 µM was incubated with 1 mM ATP, 1 mM $MgCl_2$, and 10 µM of purified VbhTA constructs or 200 µM of novobiocin for up to 120 minutes. At 0, 2, 10, 60 and 120 minutes, an aliquot of each reaction was boiled for 5 minutes at 99°C and spun down at 16,000 *g* for 5 minutes to pellet the precipitated proteins. The supernatant composed of nucleotides was loaded on a Resource Q column (GE Healthcare) equilibrated with 5 mM ammonium bicarbonate pH 9.0. Nucleotides were eluted with a gradient of elution buffer containing 1 M ammonium bicarbonate pH 9.0. Samples were analyzed by FPLC and nucleotide peak areas were integrated using the Unicorn software (GE Healthcare). The ATPase activity of GyrB was visualized as the production of ADP over time.

***In vitro* topoisomerase assays**

Supercoiling and decatenation activities of recombinant type IIA topoisomerases of *E. coli* (TopoGEN Inc.) were performed according to the supplier's recommendations with one unit of enzyme per reaction and supplemented with novobiocin ad 5 µg/ml (to fully inhibit both topoisomerases) or 50 pmol of different purified constructs of VbhT(fic)A as indicated. Reactions were incubated for 30 minutes at 30°C and then 0.54 µg of relaxed pBR322 (DNA

gyrase / supercoiling assays) or kDNA (topo IV / decatenation assays) was added. After incubation at 37°C for one hour the reactions were stopped with Universal Stop Buffer and treated with proteinase K to resolve any potential DNA – protein linkages. The DNA was purified by chloroform – isoamyl alcohol extraction, resolved by electrophoresis in 1.1% agarose gels, stained with the GR Green Nucleic Acid Stain (Biolabo SA), and imaged at a Safe Imager (Invitrogen) equipped with an EOS 40D camera (Canon). Recombinant DNA gyrase and topo IV, DNA substrates, and 5x Universal Stop Buffer were obtained from TopoGEN Inc. (Columbus, Ohio).

Flow cytometry with *gfp* promoter fusions

GFP fluorescence (excited at 488 nm) and forward scatter of exponentially growing *E. coli* AHE938 (with plasmid reporters) or AHE1156 / AHE1158 (chromosomal reporters) were recorded with a FACSCalibur flow cytometer (Becton Dickinson) two hours after drug treatment or the induction of FicT toxin expression. Data of ca. 25'000 cells per sample were analyzed using the FlowJo software (Tree Star) to obtain mean GFP fluorescence and mean forward scatter values. Fluorescence values were corrected for background fluorescence at the given experimental condition (determined with *E coli* AHE938 harboring pUA139 or AHE1156). Subsequently, we removed distortions of apparent fluorescence caused by differences in cell size via normalization to the forward scatter because Renggli et al. (2013) recently demonstrated that the distortions of both values show a strong linear correlation.

High-resolution agarose gel electrophoresis

For the analysis of DNA supercoiling, topoisomers of our pAH160 plasmid reporter were separated in gels containing 1% of agarose (Eurogentec) and 12.5 µg/ml of chloroquine (AppliChem) at 1.5 V/cm in the dark. Gels were washed extensively in water to remove

chloroquine, stained with the GR Green Nucleic Acid Stain (Biolabo SA), and imaged at a Safe Imager (Invitrogen) equipped with an EOS 40D camera (Canon). As a control for DNA relaxation we treated reporter pAH160 with topoisomerase I (New England Biolabs) as suggested by the supplier. For the analysis of DNA catenation and knotting, plasmid supercoiling was removed by nicking with Nt.BbvCI (New England Biolabs) and topoisomers were resolved and visualized as described above without chloroquine. The presence of pNDM220 derivatives (size > 10'000 bp) in all samples did not impede analysis due to their low abundance and the huge size difference to pAH160 (4359 bp).

Investigation of *paficAT* in *Pseudomonas aeruginosa*

Pseudomonas aeruginosa PAO1 and derived strains were cultured on LB-Miller agar plates or in LB-Miller broth at 37°C. Derivatives of plasmid pHERDT30T (P*ara* vector / selection with gentamicin ad 20 µg/ml, (Qiu et al., 2008)) and pME6032 (P*lac* vector / selection with tetracycline ad 125 µg/ml, (Heeb et al., 2002)) were used for the expression of *paficT* and *paficA* constructs, respectively (see Table S2).

The *paficAT* module was deleted in *P. aeruginosa* PAO1 via allelic exchange with pPS16, a derivative of suicide plasmid pME3087 conferring tetracycline resistance (Voisard et al., 2007). pPS16 was constructed to contain fused homology sites corresponding to the sequence extending 500bp upstream and downstream of the *paficAT* module. The suicide vector was mobilized to *P. aeruginosa* PAO1 via conjugation with selection for chromosomal integration using tetracycline ad 125 µg/ml. The second crossover to loop-out the plasmid was selected by the susceptibility of deletion mutants to bacteriostatic tetracycline (20 µg/ml) via the killing of fast-growing resistant cells with 2 mg/ml of carbenicillin. Surviving cells were screened for tetracycline sensitivity and the clean deletion of *paficAT* was confirmed by PCR, resulting in strain *P. aeruginosa* PDS4 (*P. aeruginosa* PAO1 Δ*paficAT*).

For the microscopy experiment shown in Figure S6, exponentially growing cultures of *P. aeruginosa* PAO1 or PDS4 harboring plasmids for the expression of *paficT* and *paficA* constructs were induced with IPTG ad 1 mM or L-arabinose ad 0.2% w/v for 90 minutes. Subsequently, 10 µl of culture were stained with Hoechst 33342 (Invitrogen) and microscopy images were acquired using a Sony Cool-Snap HQ cooled CCD camera (Roper Scientific) attached to a Zeiss Axiovert 200 M microscope (Zeiss Ltd., Oberkochen, Germany). Image acquisition and analysis was performed using Metamorph (v6, Molecular Devices).

Figure S1

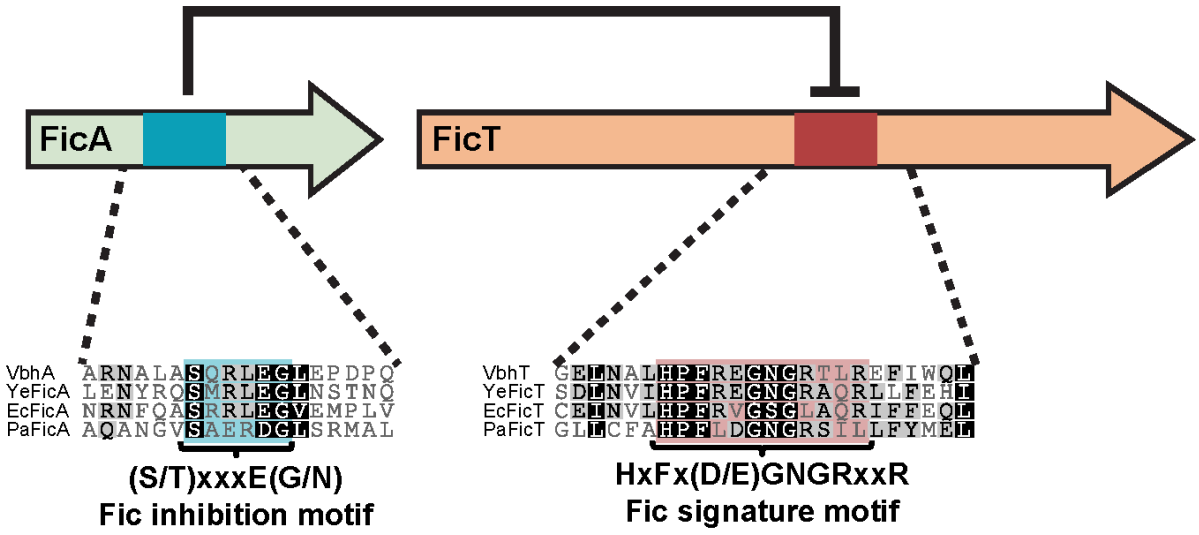
FicA
FicT
VbhA
YeFicA
EcFicA
PaFicA
VbhT
YeFicT
EcFicT
PaFicT
(S/T)xxxE(G/N)
Fic inhibition motif
HxFx(D/E)GNGRxxR
Fic signature motif

Figure S1. Comparison of FicA and FicT signature motifs of FicTA modules investigated in this study, Related to Figure 1

Protein sequences of FicA and FicT homologs were aligned using ClustalW (implemented in Geneious v.7.0.5), manually curated, and the signature motifs were extracted for illustration. Shading of amino acids indicates the degree of conservation according to the Blosum62 score matrix. The sequence alignments show that only EcFicT largely diverges from the canonical HXFX(D/E)GNGRXXR motif of FicT proteins as defined by Engel, Goepfert et al. (2012) and that PaFicT contains a leucine instead of the final arginine of the Fic signature motif (see also *Extended Results* in the Supplemental Information). All four FicA homologs contain an (S/T)XXXE(G/N) motif with the inhibitory glutamate being a chemically similar aspartate in PaFicA.

Figure S2

A

#1	b+	b2+	b3+	b4+	Seq.	y-	y2+	y3+	y4+	#2
1	148.07570	74.54149	50.03008	37.77438	F					26
2	263.10265	132.05496	88.37240	66.53112	D	2859.34223	1430.17475	953.78559	715.59102	25
3	378.12960	189.56844	126.71472	95.28786	D	2744.31528	1372.66128	915.44328	686.83429	24
4	492.17253	246.58990	164.72903	123.79859	N	2629.28833	1315.14780	877.10096	658.07754	23
5	579.20456	290.10592	193.73970	145.55660	S	2515.24540	1258.12634	839.08665	629.56661	22
6	1071.32040	536.16384	357.77832	268.58554	Y-Phosphoadenosine	2428.21337	1214.61032	810.07597	607.80680	21
7	1199.41537	600.21132	400.47664	300.60930	K	1936.09753	968.55240	646.03736	484.77984	20
8	1298.48379	649.74553	433.49945	325.37640	V	1808.00256	904.50492	603.33804	452.75610	19
9	1385.51582	693.26155	462.51912	347.13441	S	1708.93414	854.97071	570.31623	427.98999	18
10	1442.53729	721.77228	481.51728	361.38978	G	1621.90211	811.45469	541.30555	406.23099	17
11	1499.55876	750.28302	500.52444	375.64515	G	1564.88064	782.94396	522.29640	391.97562	16
12	1612.64283	806.82505	538.21913	403.91616	L	1507.85917	754.43322	503.29124	377.72025	15
13	1749.70174	875.35451	583.90543	438.18089	H	1394.77510	697.89119	465.59655	349.44923	14
14	1806.72321	903.86524	602.91259	452.43626	G	1257.71619	629.36173	419.91025	315.18451	13
15	1905.79163	953.39945	635.93539	477.20336	V	1200.69472	600.85100	400.90309	300.92914	12
16	1962.81310	981.91019	654.94255	491.45873	G	1101.62630	551.31679	367.88028	276.16203	11
17	2061.88152	1031.44440	687.96536	516.22584	V	1044.60483	522.80605	348.87313	261.90667	10
18	2148.91355	1074.96041	716.97603	537.98384	S	945.53641	473.27184	315.85232	237.13956	9
19	2247.98197	1124.49462	749.99684	562.75095	V	858.50438	429.75583	286.63964	215.38155	8
20	2347.05039	1174.02883	783.02165	587.51805	V	759.43596	380.22162	253.81684	190.61445	7
21	2461.09332	1231.05030	821.03596	616.02879	N	660.36754	330.68741	220.79403	165.84734	6
22	2532.13044	1266.56886	844.71500	633.78807	A	546.32461	273.66594	182.77972	137.33661	5
23	2645.21451	1323.11089	882.40969	662.05908	L	475.28749	238.14738	159.10068	119.57733	4
24	2732.24654	1366.62691	911.42036	683.81709	S	362.20342	181.60535	121.40599	91.30631	3
25	2860.30512	1430.65620	954.10656	715.83174	Q	275.17139	138.08933	92.39531	69.54331	2
26					K	147.11281	74.06004	49.70912	37.53366	1

C

#1	b+	b2+	b3+	Seq.	y-	y2+	y3+	#2
1	115.05021	58.02874	39.02159	N				21
2	607.16605	304.08666	203.06020	Y-Phosphoadenosine	2362.13405	1181.57066	788.04953	20
3	735.22463	368.11595	245.74639	Q	1870.01821	935.51274	624.01092	19
4	882.29305	441.65016	294.76920	F	1741.95963	871.48345	581.32473	18
5	969.32508	485.16618	323.77988	S	1594.89121	797.94424	532.30162	17
6	1026.34655	513.67691	342.78703	G	1507.85918	754.43323	503.29124	16
7	1083.36802	542.18765	361.79419	G	1450.83771	725.92249	484.28409	15
8	1196.45209	598.72968	399.48888	L	1393.81624	697.41176	465.27693	14
9	1333.51100	667.25914	445.17518	H	1280.73217	640.86972	427.58224	13
10	1390.53247	695.76987	464.18234	G	1143.67326	572.34027	381.89594	12
11	1489.60089	745.30408	497.20515	V	1086.65179	543.82953	362.88878	11
12	1546.62236	773.81482	516.21230	G	987.58337	494.29532	329.86597	10
13	1659.70643	830.35685	553.90699	I	930.56190	465.78459	310.85882	9
14	1746.73846	873.87287	582.91767	S	817.47783	409.24255	273.16413	8
15	1845.80688	923.40708	615.94048	V	730.44580	365.72654	244.15345	7
16	1944.87530	972.94129	648.96328	V	631.37738	316.19233	211.13064	6
17	2058.91823	1029.96275	686.97759	N	532.30896	266.65812	178.10784	5
18	2129.95535	1065.48131	710.65663	A	418.26603	209.63665	140.09353	4
19	2243.03942	1122.02335	748.35132	L	347.22891	174.11809	116.41449	3
20	2330.07145	1165.53936	777.36200	S	234.14484	117.57606	78.71980	2
21				K	147.11281	74.06004	49.70912	1

B

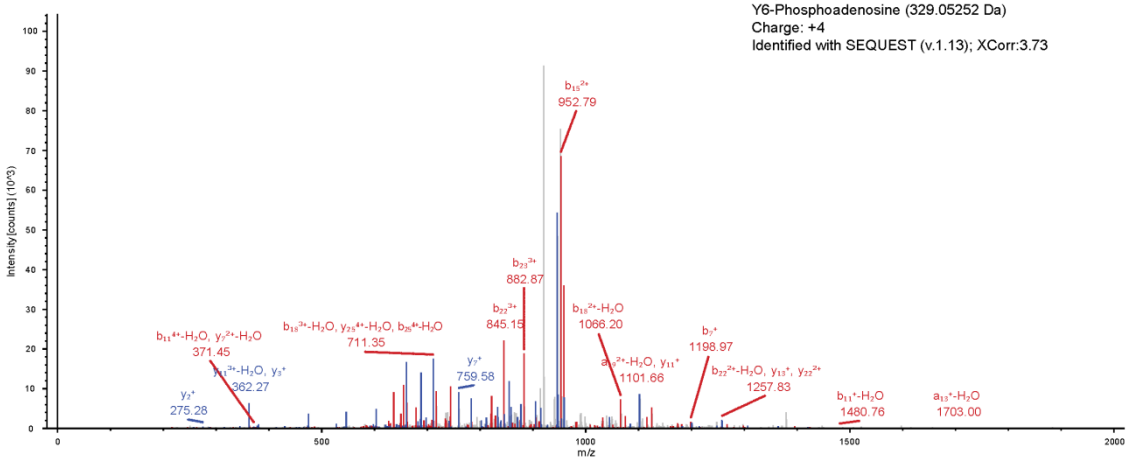

D

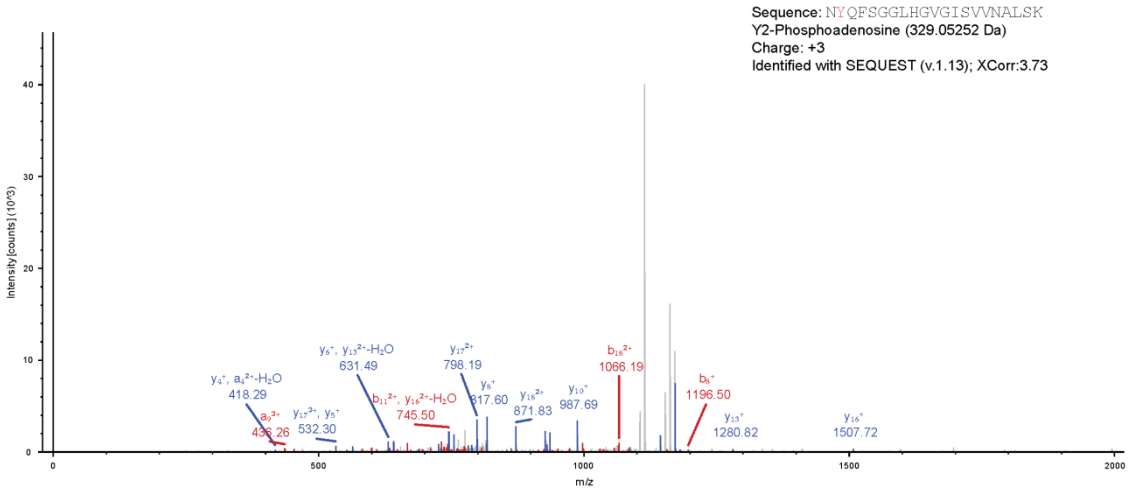

Figure S2. VbhT adenylylates Tyr109 and Tyr105 of *E. coli* GyrB and ParE, respectively, Related to Figure 2

Ion series and MS/MS spectra for detected adenylylated residues on GyrB (**A, B**) and ParE (**C, D**) are shown (see *Experimental Procedures*). The identified modified residue is marked in red. SEQUEST Xcorr search scores, peptide charge states and peptide sequence are shown in (B) and (D).

Figure S3

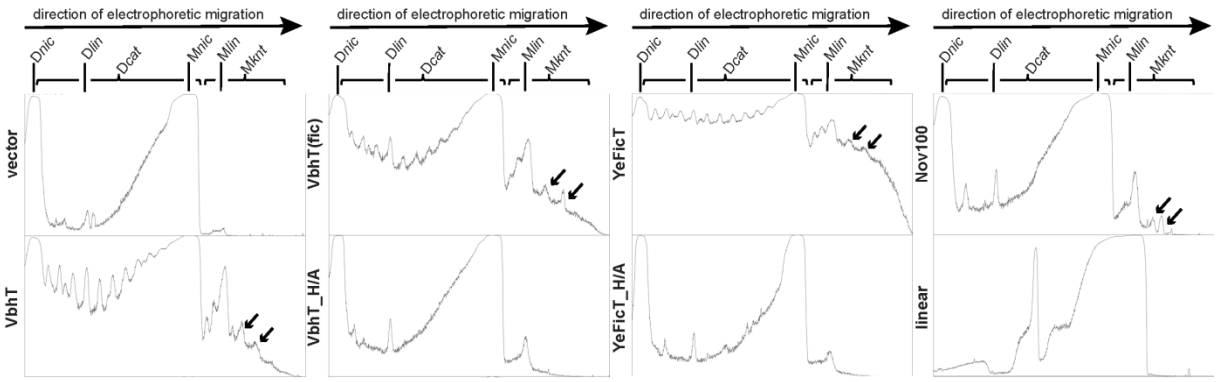
direction of electrophoretic migration
Dnic
Dlin
Dcat
Mnic
Mlin
Mknt
vector
VbhT
VbhT(fic)
VbhT_H/A
YeFicT
YeFicT_H/A
Nov100
linear

Figure S3. Lane plots of the nicked DNA agarose gel shown in Figure 4B, Related to Figure 4

A lane plot was created for the left agarose gel shown in Figure 4B using ImageJ (http://rsbweb.nih.gov/ij/download.html). Two bands of monomeric, knotted pAH160 reporter plasmid (arrows) are clearly visible for VbhT, VbhT(fic), and YeFicT expression as well as upon treatment with 100 µg/ml novobiocin (inhibiting topo IV) but are absent in controls.

Figure S4

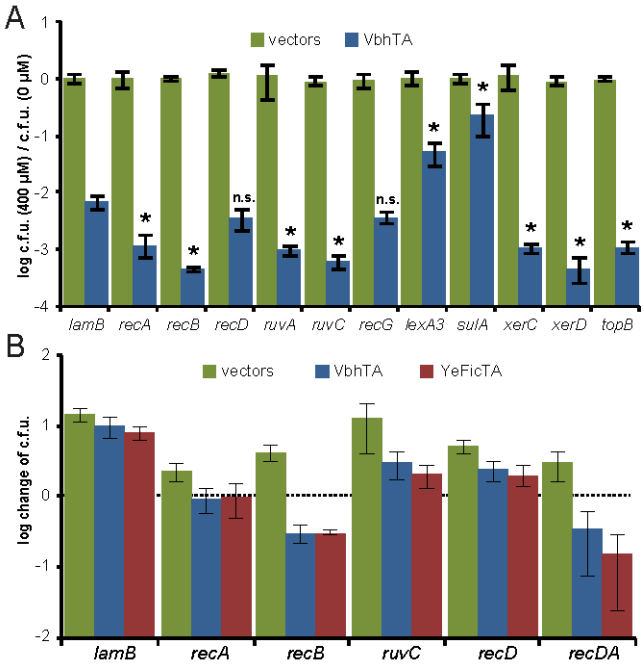
A
vectors
VbhTA
log c.f.u. (400 µM) / c.f.u. (0 µM)
1
0
-1
-2
-3
-4
n.s.
n.s.
*
lamB
recA
recB
recD
ruvA
ruvC
recG
lexA3
sulA
xerC
xerD
topB
B
vectors
VbhTA
YeFicTA
log change of c.f.u.
2
1
0
-1
-2
lamB
recA
recB
ruvC
recD
recDA

Figure S4. FicT expression impairs cellular DNA processing, Related to Figure 5

(A) The differential susceptibility of various *E. coli* K-12 single gene mutants and an isogenic *lexA3* strain harboring FicT toxin as well as FicA antitoxin vectors (to improve plasmid stability in hypersensitive strains via leaky expression) was quantified by forming the ratio of c.f.u. obtained on LB agar supplemented with 400 μM IPTG (to induce FicT expression) over those on LB agar without IPTG. We detect an increased sensitivity to VbhT expression in mutants defective for XerCD recombination (*xerC* / *xerD*) or topoisomerase III (*topB*) which can partially complement topo IV regarding decatenation (Cox et al., 2000; Grainge et al., 2007; Perez-Cheeks et al., 2012). Moreover, bacteria with defects in replication fork reversal, homologous recombination, and Holliday junction processing (*recA*, *recB*, *ruvA*, *ruvC*) are hypersensitive to VbhT expression, while the sole inactivation of *recD,* part of Exonuclease V, or *recG*, one of the factors that can drive replication fork reversal, did not have a clear effect. Conversely, the inability to induce the SOS response (*lexA3*) or suppress cell division following SOS induction (*sulA*) makes *E. coli* more tolerant under the conditions tested ($p<0.05$, unequal variance t-test). Data points are mean values of three independent experiments and s.d. is indicated by error bars. n.s. = not significant

(B) The reversibility of FicT-mediated growth inhibition (see Figure 1C) was assayed in different *E. coli* mutants by induction of antitoxin expression on LB agar plates subsequent to FicT toxin expression in liquid culture. FicT-mediated growth inhibition is reversible in the *lamB* control and *recA* / *recD* / *ruvC* single mutants (log change of c.f.u. ≥ 0), while dual inactivation of exonuclease V as well as homologous recombination activities in *recB* or *recDA* mutants results in detectable lethality (values ≤ 0), indicative of replication fork reversal driving fork repair after blockade (De Septenville et al., 2012). Data bars represent mean values of three independent experiments and error bars denote s.e.m.

Figure S5

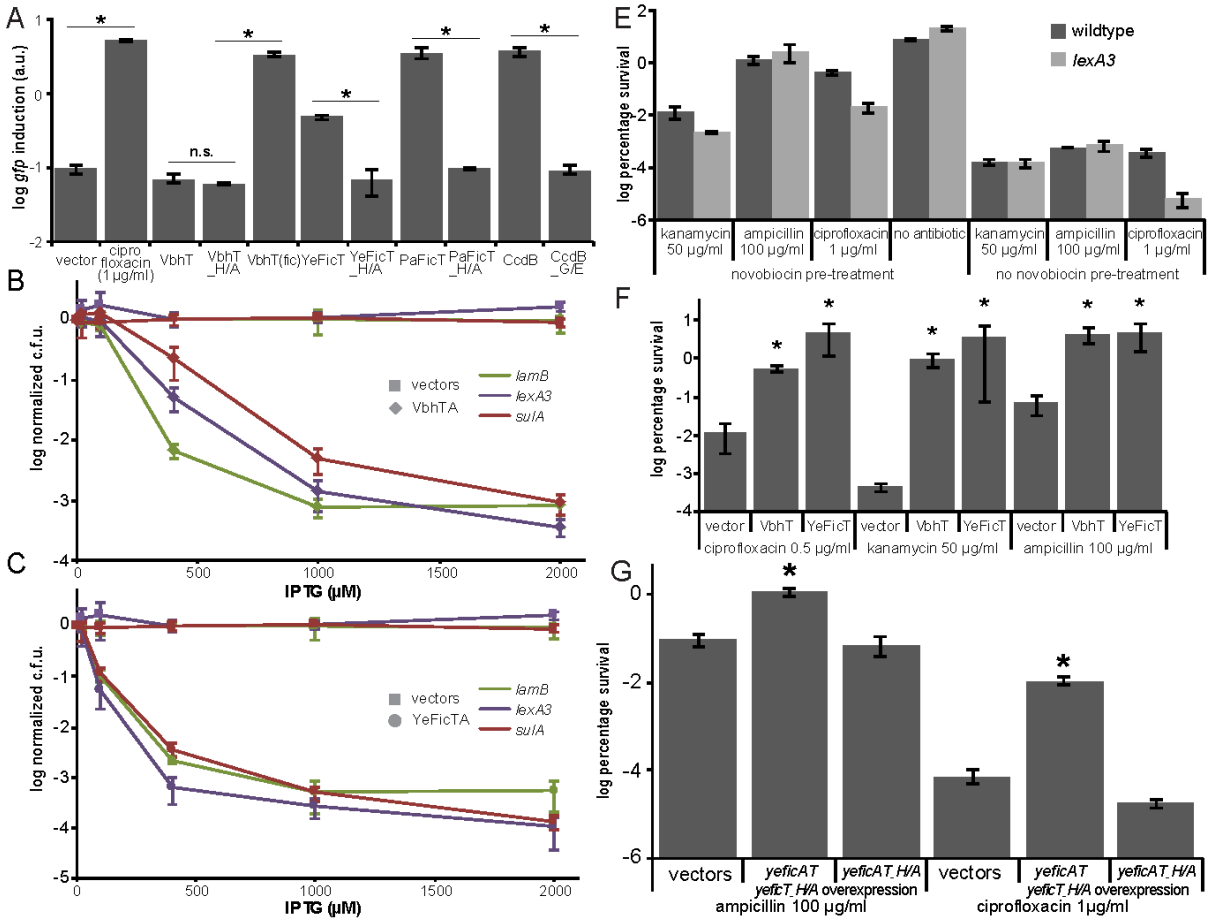
A
log gfp induction (a.u.)
vector
cipro floxacin (1 µg/ml)
VbhT
VbhT _H/A
VbhT(fic)
YeFicT
YeFicT _H/A
PaFicT
PaFicT _H/A
CcdB
CcdB _G/E
n.s.
B
log normalized c.f.u.
vectors
VbhTA
lamB
lexA3
sulA
IPTG (µM)
C
log normalized c.f.u.
vectors
YeFicTA
lamB
lexA3
sulA
IPTG (µM)
E
log percentage survival
wildtype
lexA3
kanamycin 50 µg/ml
ampicillin 100 µg/ml
ciprofloxacin 1 µg/ml
no antibiotic
novobiocin pre-treatment
no novobiocin pre-treatment
F
log percentage survival
vector
VbhT
YeFicT
ciprofloxacin 0.5 µg/ml
kanamycin 50 µg/ml
ampicillin 100 µg/ml
G
log percentage survival
vectors
yeficAT
yeficAT_H/A
yeficT_H/A overexpression
ampicillin 100 µg/ml
ciprofloxacin 1µg/ml

Figure S5. SOS induction upon topoisomerase inhibition by FicT toxins does not greatly contribute to growth inhibition or persister formation, Related to Figures 4, 6, and 7

(A) The destabilization of replication fork progression is a main trigger of the SOS response and therefore potentially involved in phenotypes related to FicT activity (see Figure S4 and *Extended Results* in the Supplemental Information). We therefore probed the activation of the SOS response upon FicT expression using flow cytometry recording fluorescence from a plasmid-encoded P*sulA::gfpmut2* module with a procedure identical to the detection of DNA relaxation via a P*gyrB::gfpmut2* reporter (Figure 3B). The results show that FicT expression results in divergent induction of the SOS response that is qualitatively similar to the DNA gyrase inhibition achieved (Figure 3). While SOS induction with VbhT is not significant (n.s.), VbhT(fic) and PaFicT cause levels of GFP expression similar to those observed with gyrase poisons CcdB or ciprofloxacin (all $p<0.05$, unequal variance t-test). The expression of inactive toxin mutants (FicT_H/A or CcdB_G100E) had no effect.

(B and C) We quantified the differential susceptibility of *E. coli lexA3* and *sulA* mutants as well as the *lamB* control to FicT expression by forming the ratio of c.f.u. obtained on LB agar supplemented with different concentrations of IPTG (to induce FicT expression) over those on LB agar without IPTG. Both for VbhT (B) and YeFicT (C) the data show that the SOS response contributes to growth inhibition only at low levels of FicT expression and plays no role at 2000 μM of IPTG that we generally used for phenotypic characterization.

(D, E, and F) The persister formation of a *lexA3* derivative of AHE938 (D) or AHE573 (E, F) was quantified as described for the parental strains (Figure 6 and Figure 7C) and still revealed greatly increased fractions of persister cells upon novobiocin treatment or FicT toxin expression, showing that an inability to launch the SOS response does not greatly affect the phenotype. We note an unexpectedly increased tolerance of the AHE573 *lexA3* vector control to ampicillin compared to the parental strain (see Figures 6B and 7C), but an identical effect

can also be seen in the data of Dörr et al. (2009) (figure 1, panel D) with the same concentration of ampicillin (100 µg/ml) and the same duration of drug challenge (3h).

All data points are mean values of three independent experiments with error bars denoting s.d. Stars indicate $p<0.05$ (unequal variance t-test).

Figure S6

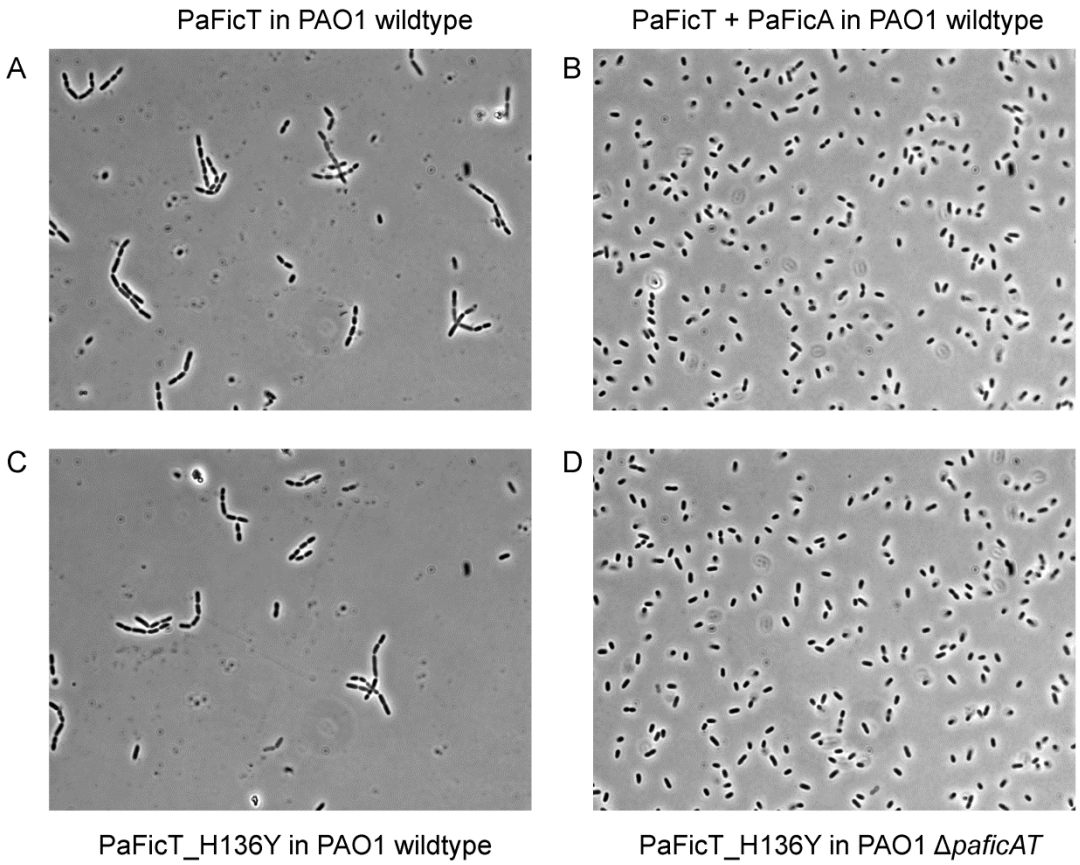
PaFicT in PAO1 wildtype
PaFicT + PaFicA in PAO1 wildtype
A
B
C
D
PaFicT_H136Y in PAO1 wildtype
PaFicT_H136Y in PAO1 Δ*paficAT*

Figure S6. Activation of the *paficAT* module by antitoxin sequestration results in growth inhibition of its natural host *Pseudomonas aeruginosa* PAO1, Related to Figure 7

Pseudomonas aeruginosa PAO1 wildtype (A, B, and D) or PDS4 (Δ*paficAT*) (C) expressing different PaFicT constructs were imaged by phase microscopy. As expected, the expression of PaFicT in *P. aeruginosa* wildtype cells inhibited cell division (A, leading to cell chain formation), while the co-expression of PaFicA and PaFicT had no discernible phenotype (B). The expression of catalytically inactive PaFicT_H136Y did not induce growth inhibition in *P. aeruginosa* Δ*paficAT* (D), but showed a phenotype similar to PaFicT expression in the wildtype strain. We therefore conclude that PaFicT_H136Y activates the endogenous *paficAT* module in *P. aeruginosa* by antitoxin sequestration.

Figure S7

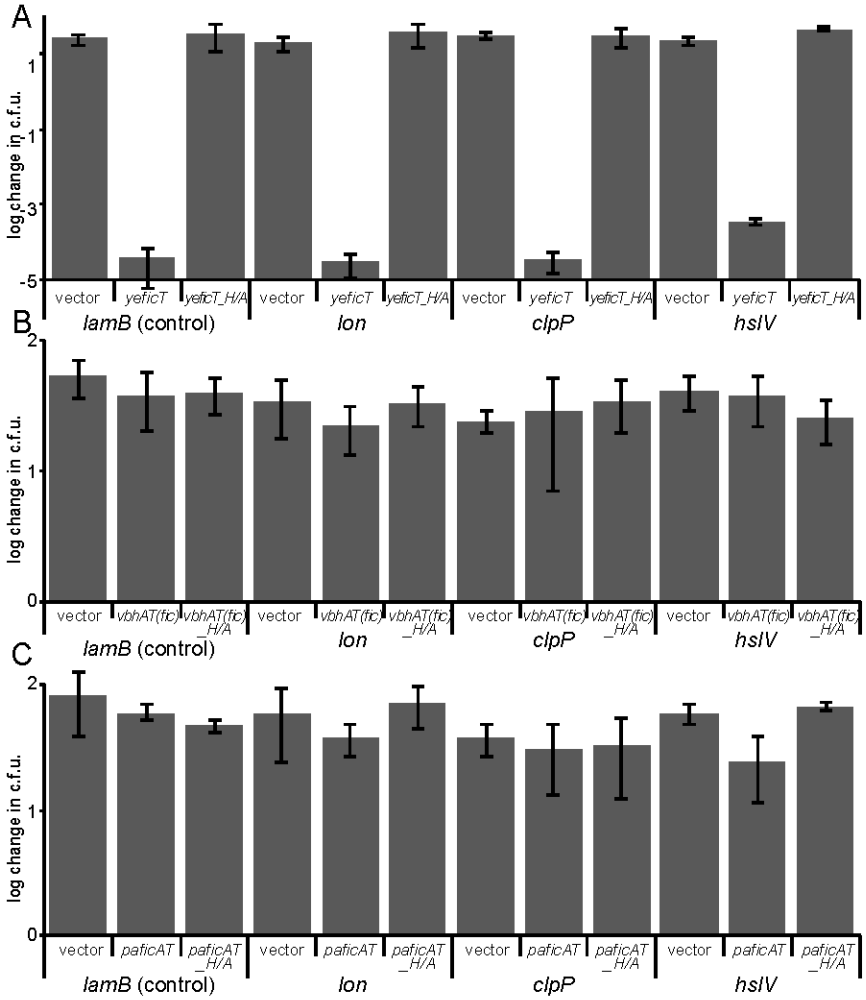
A
log change in c.f.u.
1
-1
-3
-5
vector
yeficT
yeficT_H/A
lamB (control)
lon
clpP
hslV
B
log change in c.f.u.
2
1
0
vbhAT(fic)
vbhAT(fic)_H/A
C
paficAT
paficAT_H/A

Figure S7. Additional results on FicT toxin activation by antitoxin degradation *in vivo*, Related to Figure 7

(A) The experiment of Figure 7D was repeated with *yeficT* instead of *yeficAT* expression. The data show that the *lon* mutant is not less susceptible to growth inhibition by FicT toxins than the other mutants.

(B and C) The experiment of Figure 7D was repeated with *vbhAT(fic)*(B) or *paficAT* (C) instead of *yeficAT*. No growth inhibition that would evidence toxin activation *in vivo* can be detected.

Supplemental References

Adams, D.E., Shekhtman, E.M., Zechiedrich, E.L., Schmid, M.B., and Cozzarelli, N.R. (1992). The role of topoisomerase IV in partitioning bacterial replicons and the structure of catenated intermediates in DNA replication. Cell *71*, 277-288.

Baba, T., Ara, T., Hasegawa, M., Takai, Y., Okumura, Y., Baba, M., Datsenko, K.A., Tomita, M., Wanner, B.L., and Mori, H. (2006). Construction of *Escherichia coli* K-12 in-frame, single-gene knockout mutants: the Keio collection. Mol Syst Biol *2*, 2006 0008.

Chong, S., Chen, C., Ge, H., and Xie, X.S. (2014). Mechanism of transcriptional bursting in bacteria. Cell *158*, 314-326.

Chung, C.T., Niemela, S.L., and Miller, R.H. (1989). One-step preparation of competent *Escherichia coli*: transformation and storage of bacterial cells in the same solution. Proc Natl Acad Sci USA *86*, 2172-2175.

Cox, M.M., Goodman, M.F., Kreuzer, K.N., Sherratt, D.J., Sandler, S.J., and Marians, K.J. (2000). The importance of repairing stalled replication forks. Nature *404*, 37-41.

Datsenko, K.A., and Wanner, B.L. (2000). One-step inactivation of chromosomal genes in *Escherichia coli* K-12 using PCR products. Proc Natl Acad Sci USA *97*, 6640-6645.

De Septenville, A.L., Duigou, S., Boubakri, H., and Michel, B. (2012). Replication fork reversal after replication-transcription collision. PLoS Genet *8*, e1002622.

Deibler, R.W., Mann, J.K., Sumners de, W.L., and Zechiedrich, L. (2007). Hin-mediated DNA knotting and recombining promote replicon dysfunction and mutation. BMC Mol Biol *8*, 44.

Deibler, R.W., Rahmati, S., and Zechiedrich, E.L. (2001). Topoisomerase IV, alone, unknots DNA in *E. coli*. Genes Dev *15*, 748-761.

Erill, I., Campoy, S., and Barbe, J. (2007). Aeons of distress: an evolutionary perspective on the bacterial SOS response. FEMS Microbiol Rev *31*, 637-656.

Fonville, N.C., Bates, D., Hastings, P.J., Hanawalt, P.C., and Rosenberg, S.M. (2010). Role of RecA and the SOS response in thymineless death in *Escherichia coli*. PLoS Genet *6*, e1000865.

Gotfredsen, M., and Gerdes, K. (1998). The *Escherichia coli relBE* genes belong to a new toxin-antitoxin gene family. Mol Microbiol *29*, 1065-1076.

Grainge, I., Bregu, M., Vazquez, M., Sivanathan, V., Ip, S.C., and Sherratt, D.J. (2007). Unlinking chromosome catenanes *in vivo* by site-specific recombination. EMBO J *26*, 4228-4238.

Heeb, S., Blumer, C., and Haas, D. (2002). Regulatory RNA as Mediator in GacA/RsmA-Dependent Global Control of Exoproduct Formation in *Pseudomonas fluorescens* CHA0. J Bacteriol *184*, 1046-1056.

Huisman, O., D'Ari, R., and Gottesman, S. (1984). Cell-division control in *Escherichia coli*: specific induction of the SOS function SfiA protein is sufficient to block septation. Proc Natl Acad Sci USA *81*, 4490-4494.

Jørgensen, M.G., Pandey, D.P., Jaskolska, M., and Gerdes, K. (2009). HicA of *Escherichia coli* defines a novel family of translation-independent mRNA interferases in bacteria and archaea. J Bacteriol *191*, 1191-1199.

Liu, H., and Naismith, J.H. (2008). An efficient one-step site-directed deletion, insertion, single and multiple-site plasmid mutagenesis protocol. BMC Biotechnol *8*, 91.

Lopez, V., Martinez-Robles, M.L., Hernandez, P., Krimer, D.B., and Schvartzman, J.B. (2012). Topo IV is the topoisomerase that knots and unknots sister duplexes during DNA replication. Nucleic Acids Res *40*, 3563-3573.

MacKichan, J.K., Gerns, H.L., Chen, Y.T., Zhang, P., and Koehler, J.E. (2008). A SacB mutagenesis strategy reveals that the *Bartonella quintana* variably expressed outer membrane proteins are required for bloodstream infection of the host. Infect Immun *76*, 788-795.

Perez-Cheeks, B.A., Lee, C., Hayama, R., and Marians, K.J. (2012). A role for topoisomerase III in *Escherichia coli* chromosome segregation. Mol Microbiol *86*, 1007-1022.

Qiu, D., Damron, F.H., Mima, T., Schweizer, H.P., and Yu, H.D. (2008). P_{BAD}-Based Shuttle Vectors for Functional Analysis of Toxic and Highly Regulated Genes in *Pseudomonas* and *Burkholderia* spp. and Other Bacteria. Appl Environ Microbiol *74*, 7422-7426.

Rajendram, M., Hurley, K.A., Foss, M.H., Thornton, K.M., Moore, J.T., Shaw, J.T., and Weibel, D.B. (2014). Gyramides prevent bacterial growth by inhibiting DNA gyrase and altering chromosome topology. ACS Chem Biol *9*, 1312-1319.

Renggli, S., Keck, W., Jenal, U., and Ritz, D. (2013). Role of autofluorescence in flow cytometric analysis of *Escherichia coli* treated with bactericidal antibiotics. J Bacteriol *195*, 4067-4073.

Salgado, H., Peralta-Gil, M., Gama-Castro, S., Santos-Zavaleta, A., Muniz-Rascado, L., Garcia-Sotelo, J.S., Weiss, V., Solano-Lira, H., Martinez-Flores, I., Medina-Rivera, A.*, et al.* (2013). RegulonDB v8.0: omics data sets, evolutionary conservation, regulatory phrases, cross-validated gold standards and more. Nucleic Acids Res *41*, D203-213.

Schulein, R., Guye, P., Rhomberg, T.A., Schmid, M.C., Schroder, G., Vergunst, A.C., Carena, I., and Dehio, C. (2005). A bipartite signal mediates the transfer of type IV secretion substrates of *Bartonella henselae* into human cells. Proc Natl Acad Sci USA *102*, 856-861.

Thomson, N.R., Howard, S., Wren, B.W., Holden, M.T., Crossman, L., Challis, G.L., Churcher, C., Mungall, K., Brooks, K., Chillingworth, T.*, et al.* (2006). The complete genome sequence and comparative genome analysis of the high pathogenicity *Yersinia enterocolitica* strain 8081. PLoS Genet *2*, e206.

Utsumi, R., Nakamoto, Y., Kawamukai, M., Himeno, M., and Komano, T. (1982). Involvement of cyclic AMP and its receptor protein in filamentation of an *Escherichia coli fic* mutant. J Bacteriol *151*, 807-812.

Vakulenko, S.B., Geryk, B., Kotra, L.P., Mobashery, S., and Lerner, S.A. (1998). Selection and characterization of β-lactam-β-lactamase inactivator-resistant mutants following PCR mutagenesis of the TEM-1 β-lactamase gene. Antimicrob Agents Chemother *42*, 1542-1548.

Voisard, C., Bull, C.T., Keel, C., Laville, J., Maurhofer, M., Schnider, U., Défago, G., and Haas, D. (2007). Biocontrol of Root Diseases by *Pseudomonas fluorescens* CHA0: Current Concepts and Experimental Approaches. In Molecular Ecology of Rhizosphere Microorganisms (Wiley-VCH Verlag GmbH), pp. 67-89.

Wigley, D.B. (2013). Bacterial DNA repair: recent insights into the mechanism of RecBCD, AddAB and AdnAB. Nat Rev Microbiol *11*, 9-13.

Witz, G., Dietler, G., and Stasiak, A. (2011). DNA knots and DNA supercoiling. Cell Cycle *10*, 1339-1340.

Zechiedrich, E.L., and Cozzarelli, N.R. (1995). Roles of topoisomerase IV and DNA gyrase in DNA unlinking during replication in *Escherichia coli*. Genes Dev *9*, 2859-2869.

Table S1. List of DNA oligonucleotides, Related to Experimental Procedures

⇨ only available digitally

Table S2. List of plasmids, Related to Experimental Procedures

⇨ only available digitally

6.10. Unpublished results related to Research article III

6.10.1. Towards the mechanism of type II topoisomerase inhibition upon adenylylation

In our publication we demonstrated that adenylylation of the B subunits inhibits the signature activities of recombinant DNA gyrase and topo IV holoenzymes *in vitro* (Figure 2C of *Research article III*) and causes corresponding phenotypes *in vivo* (Figures 3 and 4 of *Research article III*). Using VbhT of *B. schoenbuchensis* as a model we identified the adenylylation sites as conserved Tyr109 (*E. coli* GyrB) or Tyr105 (*E. coli* ParE) in the ATP lid loop at the ATP binding site (Figure S2 of *Research article III*). In this context we showed that the ATPase activity of an N-terminal fragment of GyrB ("GyrB43") comprising ATPase and transducer domains is inhibited upon adenylylation (Figure 2B of *Research article III*) which was sufficient to explain the inactivation of DNA gyrase and, by inference, topo IV.

However, preliminary biochemical and structural analyses of Frédéric Stanger indicate that an abrogation of the ATPase activity may not be generalized as the mechanism of target inhibition by FicT toxins, suggesting that adenylylation of the ATP lid loop must interfere with topoisomerase functioning in additional ways (Frédéric Stanger, unpublished). The generation of reasonable hypotheses that could explain the precise mode of target inhibition is hampered by the lack of a consistent, molecular understanding of the type II topoisomerase cycle despite recent advances in the field[214,215]. Generally, it is "assumed that the central DNA strand-passage mechanism is common to gyrase and non-supercoiling type IIA enzymes"[213] like topo IV, so that adenylylation may inactivate both targets in a similar way. It is the current model that ATP binding closes the N-gate between the ATPase domains and thereby encircles the T-segment inside the topoisomerase holoenzyme (Figure 10A). Subsequent ATP hydrolysis is likely coupled to strand passage, and the final ejection of ADP resets the enzyme. Previous studies showed that – despite its physical distance to the actual enzymatic center – the ATP lid loop is important for the catalytic function of DNA gyrase, probably via a role in the coupling of DNA remodeling and ATPase activities (see, e.g., the work of Lamour *et al.*[263] and literature cited therein). It is therefore easily conceivable that the adenylylation of the ATP lid loop by FicT toxins could directly inhibit the catalytic activity of gyrase and topo IV, but the molecular mechanism remains enigmatic.

Another interesting aspect is that the adenylylation by FicT toxins causes an inhibition of the catalytic activity of gyrase and topo IV without an inhibition of ATP binding (Frédéric Stanger, unpublished). Therefore, adenylylation could easily result in topoisomerase poisoning because the T-segment may pass through the N-gate and get trapped inside the holoenzyme. However, our findings do not support a locking of cleavable complexes on the

DNA, because the expression of VbhT (causing strong inhibition of topo IV, but not gyrase *in vivo*[a]) did not activate the SOS response as it would be expected for dsDNA break formation (Figure S5 in *Research article III*). Furthermore, we did not observe bacterial killing upon FicT toxin expression (see, e.g., Figures 1C and 5 in *Research article III*). It is interesting to note that YacG, a small proteic inhibitor of DNA gyrase, converts "the gyrase holoenzyme into an inactive, ATP-trapped configuration" similar to what our results indicate for adenylylated topoisomerases, but additionally prevents DNA binding by "sterically occluding the (…) DNA-binding site"[252]. These findings indicate that such a dual inhibition may be advantageous for a robust topoisomerase shut-off and urge to investigate whether adenylylation may also prevent DNA binding in some (likely indirect) way.

In order to draw firm conclusions on the molecular basis of topoisomerase inhibition by adenylylation future studies should use full gyrase and topo IV holoenzymes and investigate the properties of modified and unmodified enzymes *in vitro*. Most importantly, it would be interesting to see whether adenylylation affects DNA binding and which step of the catalytic cycle precisely is inhibited. For this purpose one could additionally use fluorescence resonance energy transfer (FRET) experiments to study domain movements within the topoisomerases as it has been reported previously by Lanz and Klostermeier[206] (see also the recent review by D. Klostermeier[353]).

6.10.2. The EcFicTA module is not functionally related to other FicTA modules

Several decades after the discovery of "filamentation induced by cAMP" the molecular basis of this phenotype and its causal connection to the *fic-1* allele of *ecficT* have still remained enigmatic (see *Introduction*). In *Research article III* we had initially planned to show a number of basic experiments with the EcFicTA module of *E. coli* str. K-12 substr. MG1655 in order to demonstrate that it is not part of the FicTA family of toxin-antitoxin modules. However, we later decided to omit these data in the final version for reasons of clarity.

[a] The data particularly with VbhT are relevant at this point, because a (considerable) inhibition of DNA gyrase always activates the SOS response due to replication fork stalling (independent of topoisomerase poisoning; see Box 1 and also the considerations in the *Extended Results* in the *Supplemental Information* of *Research article III*).

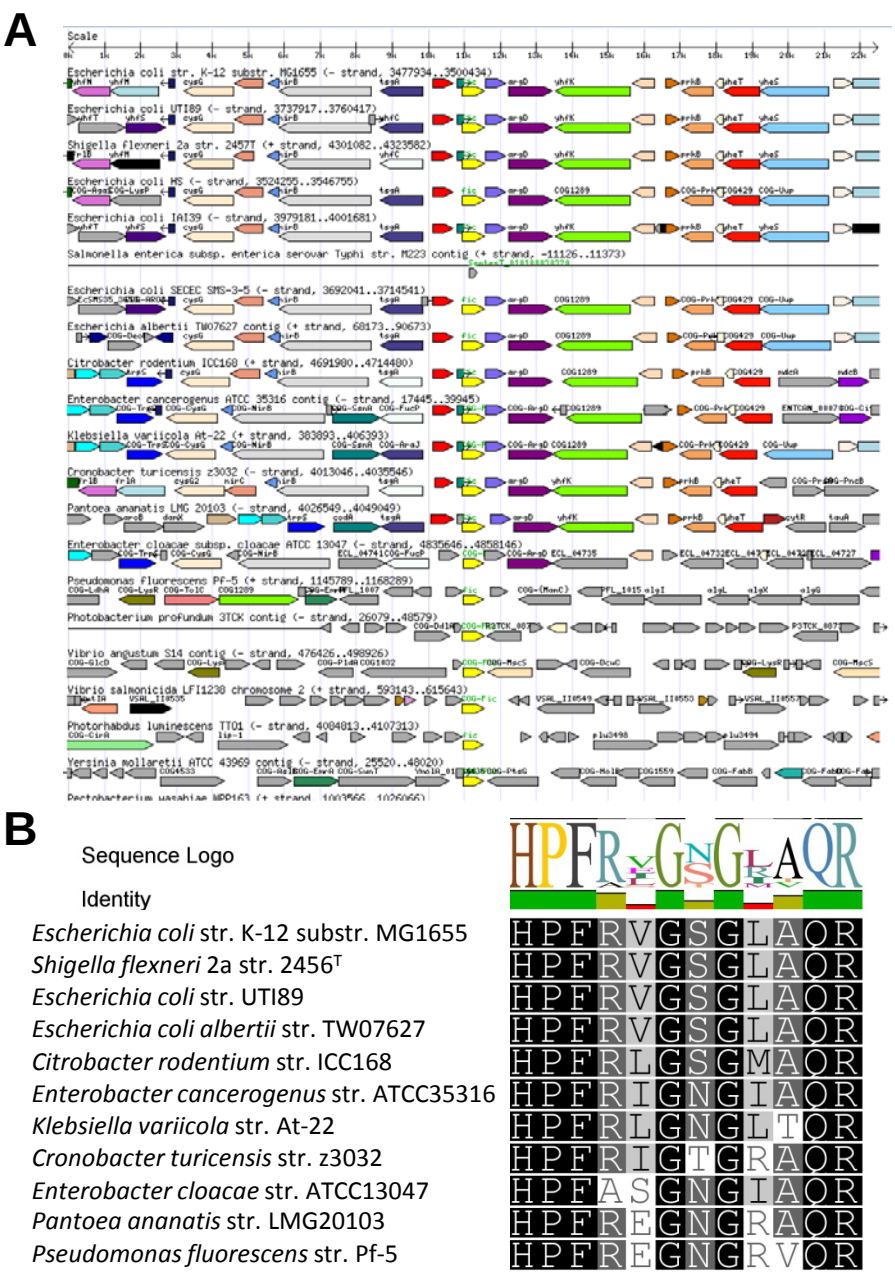

Figure 18: EcFicTA phylogeny and active site conservation of EcFicT orthologs. A) The "tree browser" function of microbesonline (www.microbesonline.org) was used to visualize the genomic environment of *ecficAT* and homologous loci (centered on *ecficT* in yellow). It is clear that species more closely related to *E. coli* (upper half) encode modules homologous to *ecficAT* at loci that are highly syntenic, suggesting vertical transmission within Enterobacteriales. On the other hand, more distant homologs are encoded in diverse genomic environments, suggesting frequent horizontal gene transfer as it is typical for FicTA modules. **B)** The Fic signature motifs of EcFicT and different homologs shown in (A) were aligned using ClustalW implemented in Geneious v7.1.7 with gap open / extend costs of 10 / 0.1 and a BLOSUM cost matrix. Coloring reflects amino acid similarity according to the cost matrix with black = 100% identity and white = <60% identity. A comparison of the sequences shows that the peculiar HxFxxGSGLxxR motif of EcFicT is conserved among relatives of *E. coli* (top), while homologs of more distantly related species display the canonical HxFxxGNGRxxR Fic signature motif (bottom). Note that *Pantoea ananatis* appears to encode a FicT-like protein with canonical active site motif in a locus syntenic with *ecficAT* loci of other Enterobacteriales (see (A)).

EcFicTA is different from other FicTA modules like YeFicTA of PaFicTA in that it appears to be vertically transmitted in the Enterobacteriales (Figure 18A) while the FicTA modules typically show strong signs of horizontal gene transfer. Furthermore, the FIC domain active

site motif of EcFicT deviates considerably from the canonical Fic signature sequence (see Figure S1 of *Research article III* and Figure 18B), suggesting that it may not be able to perform adenylylation. Consistently, I failed to detect any auto-adenylylation or target adenylylation activities of EcFicT (Figure 19A). The expression of EcFicT (and, similarly, of its *fic-1* derivative) did not result in detectable growth inhibition of *E. coli* Δ*ecficAT* which rules out that "filamentation induced by cAMP" could simply be caused by some kind of "activation" of EcFicT (Figure 19B).

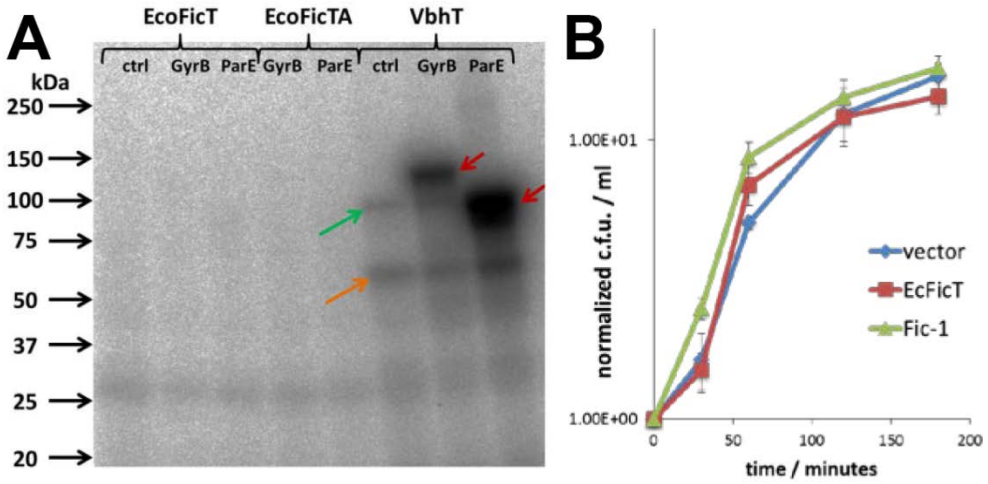

Figure 19: EcFicT does not display adenylylation activities or cause growth inhibition in *E. coli*. A) EcFicT, EcFicTA, or VbhT were expressed and tested for adenylylation in cleared lysates as described for full length VbhT in *Research article III* (Figure 2A). Different *ecficT* constructs were expressed from pPE0036 (*ecficT* in pRSFDuet-1) and pPE0038 (*ecficT* and *ecficA* in pRSFDuet-1) in BL21 (DE3) Δ*ecficAT* do avoid crosstalk with the endogenous EcFicTA module. The autoradiograph shows the adenylylation activity of VbhT (auto-adenylylation at orange arrow, endogenous GyrB adenylylation at green arrow, and GST-GyrB or GST-ParE of *E. coli* at red arrows), while no signal is detected for EcFicT. Note that the diffuse band above 25 kDa (close to the molecular weight of EcFicT) is often observed in adenylylation assays with bacterial lysates and does not point towards any activity of EcFicT. These results could be confirmed by Arnaud Goepfert using purified proteins (data not shown). **B)** The colony forming units (c.f.u.) of exponentially growing *E. coli* Δ*ecficAT* expressing *ecficT* or its *fic-1* derivative were monitored over time using an identical expression system and experimental procedure as it is described in *Research article III* (Figure 1B). No growth inhibition can be detected. Similarly, no effect of cAMP or 43°C on *E. coli* growth upon *ecficT* expression could be found (not shown).

In conclusion, we did not find evidence pointing towards the (or any) biological function of the EcFicTA module. Future studies may approach this problem from the biochemical site and try to identify a molecular activity of EcFicT as a starting point for further analyses. In my opinion, it is important to approach EcFicTA with an unbiased view, because the biological function of this module may very well be unrelated to "filamentation induced by cAMP" (see in the *Introduction* section). In order to unravel the molecular basis of this enigmatic phenotype it would probably be necessary to use exactly the same strains that showed "filamentation induced by cAMP" in previous studies and to determine their genome sequences. By comparison to the parental wildtype one may be able to identify mutations that could be involved in growth inhibition together with *fic-1* and help to resolve the cellular processes underlying the "fic" phenotype.

6.10.3. Another type of FicTA modules: Mobile Mystery Proteins

During our work on the characterization of class I Fic proteins as toxins of the FicTA toxin-antitoxin module others have published studies on FicT homologs of *Clostridium difficile* and *M. tuberculosis* but did not add substantial novelties to the field[354,355]. We had also performed a number of experiments on FicT of *M. tuberculosis* but failed to detect any growth inhibition in *E. coli*, suggesting that this protein is unable to target *E. coli* GyrB and / or ParE (sufficiently) or that it has a different molecular function (data not shown).

More relevantly, I uncovered that a subfamily of FicTA modules exists in which the antitoxins contain an additional helix-turn-helix (HTH) DNA binding domain. These proteins are found in the databases under the term “mobile mystery proteins” with the FicT homologs being “mobile mystery protein B” (InterPro family IPR013436) and the antitoxins being “mobile mystery protein A” (InterPro family IPR013435). There are around 100 different mobile mystery FicTA modules listed in the InterPro database, and their description concludes that these are “more often encoded within mobilisation-related contexts than not” and “always found together” in the classical genetic arrangement of *ficAT* loci (last accessed on November 11th, 2014). A comparative sequence analysis of all available FicT homologs of this family (“mobile mystery protein B”) revealed that they consistently contain a canonical Fic signature motif, suggesting adenylylation as their molecular function (see Figure 20). The antitoxins (“mobile mystery protein A”) cannot be reasonably aligned with classical FicA homologs and are much longer (typically around 150 aa compared to around 60 aa of FicA) due to their N-terminal HTH domain. In their C-terminal domain that supposedly acts to inhibit their cognate toxins I detected a conspicuous (S/T/N/H)MxLExQ motif with a universally conserved glutamate (Figure 20), indicating that they may regulate the toxins’ activity by active site obstruction similar to FicA antitoxins (see *Research article I*).

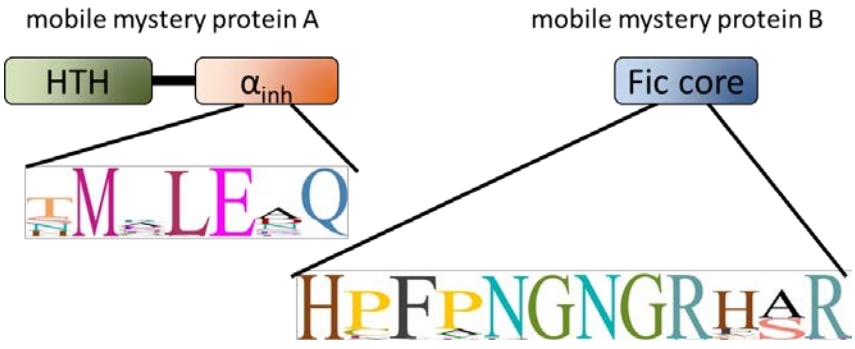

Figure 20: Domain architecture and signature motifs of mobile mystery proteins. The approximately 100 representatives of mobile mystery protein A and B families were each aligned using ClustalW implemented in Geneious v7.1.7 with gap open / extend costs of 10 / 0.1 and a BLOSUM cost matrix. For illustration, the sequence logos of the FicT signature motif (right) and a *bona fide* FicA-like inhibition motif (left) were extracted. It seems likely that mobile mystery B proteins act as FicT toxins via target adenylylation, while mobile mystery A proteins possibly inhibit their cognate toxins by active site obstruction with α_{inh}.

The presence of a HTH domain in the antitoxins of “mobile mystery” FicTA modules is a clear indication of transcriptional autoregulation via conditional cooperativity (see Box 2). It would therefore be interesting to see if also the classical FicTA modules investigated in *Research article III* exhibit such an autoregulation (either directly or indirectly, e.g., by influences of DNA topology), particularly because conditional cooperativity is instrumental for efficient recovery from the persister state into bacterial growth[6] (see also Box 2). Such experiments could easily be done, e.g., with *gfp* promoter fusions of *ficAT* modules and different combinations of antitoxins, toxins, or other stimuli. Furthermore, it would be interesting to investigate how mobile mystery A antitoxins bind and inhibit their cognate mobile mystery B toxins, i.e., if they really act via active site obstruction (see Figure 20) or via a different mechanism.

6.11. Research article IV (in preparation)

"As soon as you go into any biological process in any real detail, you discover it's open-ended in terms of what needs to be found out about it."

Joshua Lederberg, American geneticist and Nobel laureate, unsourced yet frequently attributed

Target adenylylation by class III Fic proteins is regulated by a double-lock mechanism: oligomerization and auto-adenylylation

Frédéric V. Stanger, Björn M. Burmann, Alexander Harms, Adam Mazur, Timothy Sharpe, Christoph Dehio, Sebstian Hiller, and Tilman Schirmer

In preparation

NOTE ADDED IN PROOF - This manuscript has finally been published as

Frédéric V. Stanger, Björn M. Burmann, Alexander Harms, Hugo Aragão, Adam Mazur, Timothy Sharpe, Christoph Dehio, Sebastian Hiller, and Tilman Schirmer (2016). Intrinsic regulation of FIC-domain AMP-transferases by oligomerization and automodification. Proc Natl Acad Sci U S A 113(5):E529-37

Summary

Fic proteins were previously shown to inhibit bacterial growth by target protein adenylylation which is controlled by a conserved mechanism of active site obstruction via a glutamate finger located at the tip of an inhibitory α-helix (α_{inh}; see *Research article I*). This inhibition was found to be relieved for some Fic proteins by the extrinsic proteolysis of a separate α_{inh}-containing polypeptide (*Research article III*). However, other Fic proteins like our model NmFicT of *Neisseria meningitidis* harbor the cognate α_{inh} at their own C-terminus and were therefore likely to be controlled by different molecular mechanisms.

In this research article we proposed that the adenylylation activity of NmFicT is regulated by a two-level control system that, upon signaling input, first unchains NmFicT from its storage in an inactive tetrameric form and then activates the monomers by auto-adenylylation. NmFicT activation causes bacterial growth inhibition via the inhibition of DNA gyrase.

Different crystal structures of NmFicT had consistently been obtained in a tetrameric form that comprised of “dimer of dimers” in which the four subunits made contact via two different interfaces on each monomer. Using size exclusion chromatography coupled to multi-angle laser light scattering (SEC-MALLS) we confirmed that NmFicT forms tetramers in solution. Structural studies revealed that these tetramers are catalytically inactive due to α_{inh}-mediated active site obstruction and because the active site as well as the β-hairpin flap are buried inside the complex. We therefore reasoned that oligomerization may be involved in the regulation of NmFicT and created mutants unable to oligomerize via either each one or both of the contact interfaces of the tetramer, thus primarily forming the two different dimers or monomeric NmFicT in solution. Further structural studies showed that the remaining subunit interface of each of the single-contact mutants was virtually identical to the same interface in the tetramer. The dissociation constants of oligomerization via either of the interfaces were found to be the same for a given interface in the dimer and the tetramer, indicating that there is no cooperativity in NmFicT oligomerization. Furthermore, we found that monomeric and tetrameric forms of wildtype NmFicT predominated in solution and were favored at low and high concentrations of the protein, respectively.

Mutationally activated NmFicT had previously been shown to cause bacterial growth inhibition and to adenylylate an unknown protein in *E. coli* lysates (*Research article I*). In this article we identified the target of NmFicT adenylylation as GyrB, the B subunit of DNA gyrase, while its paralog ParE was not targeted. We had previously demonstrated that VbhT, a Fic protein only distantly related to NmFicT, adenylylates GyrB (but also ParE) at the same residue as NmFicT and that this adenylylation causes target inactivation (*Research*

article III). Consistently, activated NmFicT was able to collapse the supercoiling of the cellular DNA in *E. coli* which is likely the underlying cause of the growth inhibition.

Interestingly, both growth inhibition and GyrB adenylylation were also observed with oligomerization-deficient mutants of NmFicT, but not the wildtype protein, which confirmed that the oligomerization of NmFicT is involved in its regulation. Furthermore, any mutational activation of NmFicT correlated with strongly increased auto-adenylylation which we had previously mapped to two tyrosines in the α_{inh}. Given that one of these was known to be positioned towards the inside of the Fic core in wildtype NmFicT, we reasoned that auto-adenylylation must involve conformational changes of the protein. The investigation of such effects by nuclear magnetic resonance (NMR) spectroscopy confirmed that auto-adenylylation caused movements of the α_{inh} as well as a neighboring helix and the β-hairpin flap. We therefore concluded that the auto-adenylylation of NmFicT relieves its active-site obstruction by repulsing the α_{inh} from the Fic core. Furthermore, we wondered whether this regulation was connected to the oligomerization that we had identified as another level of NmFicT regulation. Our experiments showed that the mutational abrogation of auto-adenylylation abolished growth inhibition by the activated NmFicT_E/G mutant in which the glutamate finger of α_{inh} was absent. These results proved a connection between the two layers of regulation of NmFicT. Consistently, the E/G mutation impaired the tetramerization of NmFicT, while an abrogation of auto-adenylylation favored oligomerization.

We therefore concluded that NmFicT may be controlled by a double-lock mechanism in which the protein is stored in an inactive form as a tetramer from which unknown stimuli could liberate the NmFicT monomers. These would then amplify their initially weak catalytic activity by intermolecular auto-adenylylation in order to alleviate α_{inh}-mediated active site obstruction and achieve robust inactivation of cellular DNA gyrase.

Statement of the own participation

I contributed to this publication by identifying GyrB as the adenylylated target of NmFicT and tested different GyrB orthologs and paralogs for adenylylation by NmFicT using lysate adenylylation assays. Furthermore, I analyzed changes in DNA supercoiling upon NmFicT expression by chloroquine-agarose gel electrophoresis of a reporter plasmid. The other authors conducted all structural as well as biophysical studies. Furthermore, they expressed and purified all protein constructs and performed all experiments using recombinant proteins. All authors contributed to design and analysis of the experiments and wrote the manuscript.

Target adenylylation by class III Fic proteins is regulated by a double-lock mechanism: oligomerization and auto-adenylylation

Frédéric V. Stanger[1,2], Björn M. Burmann[1], Alexander Harms[2], Adam Mazur[3], Timothy Sharpe[4], Christoph Dehio[2], Sebastian Hiller[1] and Tilman Schirmer[1]

[1]Focal Area Structural Biology and Biophysics, Biozentrum, University of Basel, Basel, Switzerland

[2]Focal Area Infection Biology, Biozentrum, University of Basel, Basel, Switzerland

[3]Research IT, Biozentrum, University of Basel, Basel, Switzerland

[4]Biophysics Facility, Biozentrum, University of Basel, Basel, Switzerland

Corresponding authors:

Prof. Tilman Schirmer	Prof. Sebastian Hiller	Prof. Christoph Dehio
Biozentrum, University of Basel		
Klingelbergstrasse 70		
CH-4056 Basel, Switzerland		
Tel.: +41-61-267-20-89	Tel.: +41-61-267-20-82	Tel.: +41-61-267-21-40
Fax.: +41-61-267-21-09	Fax.: +41-61-267-21-09	Fax.: +41-61-267-21-18
tilman.schirmer@unibas.ch	sebastian.hiller@unibas.ch	christoph.dehio@unibas.ch

Abstract

Fic proteins containing the HxFx[D/E]GNGRxxR motif catalyze adenylylation, the transfer of an AMP moiety from ATP onto target proteins. This activity has severe consequences on the cellular stability and thus has to be tightly controlled. Expression of the class III Fic protein NmFic of *Neisseria meningitidis* in *Escherichia coli* causes a severe growth defect. Recently, it has been shown that adenylylation-competent Fic proteins are specifically inhibited by an α-helix (α_{inh}), which can be found at different locations relative to the Fic active site. Mutation of the conserved glutamate of the inhibitory motif relieves the inhibition of Fic proteins. Yet, it has remained unclear how intrinsic and extrinsic factors contribute to the control of Fic protein activation.

Here, we report the structural and functional characterization of a Fic protein and its activation mechanism. We find that NmFic undergoes a monomer–tetramer equilibrium. Both the target binding site and the active site are located towards the center of this tetramer and are accessible only in the monomeric form. Consequently, mutation of crucial residues at the interfaces disrupts the tetramer formation and activates the protein. Furthermore, we show that trans-auto-adenylylation of NmFic leads to significant conformational changes and that the presence of the auto-adenylylated tyrosine Y183, part of the α_{inh} helix, is required for the activity of the Class III Fic protein. We also show that adenylylation of the bacterial target GyrB from the DNA gyrase complex by NmFic blocks the negative supercoiling and bacterial cell division.

Overall, these data provide the first intrinsic regulatory mechanism of a Fic protein via oligomerization and auto-adenylylation.

Introduction

Fic proteins containing FIC domains (pfam 02661) are found in all kingdoms of life as well as in viruses. They have originally been described to be involved in filamentation induced by cAMP (1), but until recently, their molecular role had remained elusive. Yarbrough *et al.* (2) deciphered the catalytic activity of the Type III effector protein VopS from *Vibrio parahaemolyticus* as adenylylation of the host cell Rho GTPases, resulting in collapse of the actin cytoskeleton and subsequent cell death. Enzymatically, Fic proteins containing the canonical HxFx[D/E]GNGRxxR motif catalyze adenylylation (or AMPylation), the covalent transfer of an AMP moiety from an ATP substrate onto a target protein (3, 4).

Fic proteins with an active site deriving from this consensus sequence likely catalyze other post-translational modifications. AnkX from *Legionella pneumophila* harbouring an HxFxDANGRxxV motif has been shown to catalyze the phosphocholination of the small GTPase Rab1 (5, 6). Doc of bacteriophage P1, a protein related to the Fic family proteins, contains the HxFxDANKRxxL active site motif, conferring a kinase activity and the phosphorylation of the translation elongation factor EF-Tu (7, 8).

The crystal structures of several FIC domain proteins have been determined (3, 9-12). Fic/Doc proteins contain a conserved central core of four helices that is flanked by additional Fic elements found in different positions (13). A loop joining the third and fourth helix of the Fic core forms the Fic active site motif. The complex structure of the Fic protein from *Histophilus somni* (IbpA) with its cognate target (Cdc42) reveals the stabilization of the modified residue by the β-hairpin region of the Fic protein, thus making the FLAP (or β-hairpin) a critical region of the Fic protein for target binding. The catalytic mechanism of Fic-mediated adenylylation has been inferred from this structure, where the catalytic histidine of the active site motif acts as a general base and deprotonates the attacking hydroxyl group, which in turn performs a nucleophilic attack on the α-phosphate of the ATP substrate. This results in the formation of a covalent phosphodiester bond between the AMP moiety and the modified amino acid.

The activity of Fic proteins is tightly regulated. A conserved inhibition motif, part of an inhibitory alpha-helix (α_{inh}), is located in the close vicinity of the active site (3). It has been demonstrated that the strictly conserved glutamate of this motif plays a key role in obstructing the γ-phosphate position of the ATP substrate, therefore inhibiting competent substrate binding in adenylylating Fic proteins. Interestingly, this inhibition motif is either found on a separate small protein that forms a tight complex with the Fic protein, or at the N-terminus or C-terminus compared to the Fic active site within the same polypeptide chain (3, 12). These three possibilities lead to a classification of Fic proteins into class I, II and III,

respectively (3, 12). The mutation of this glutamate residue to glycine relieves the inhibition of Fic proteins, thus increasing the adenylylation activity (3, 12).

Yet, the intrinsic or extrinsic factors that affect the conformation of this inhibitory α-helix and therefore the catalytic activity have not been investigated. This regulation may depend on additional domains found in multi-domain Fic proteins or localization of Fic proteins fused to a signal sequence. For the single domain class III Fic proteins, scattered through all classes of proteobacteria likely due to horizontal gene transfer, the regulation mechanism is most probably inherent. Interestingly, the class III Fic protein NmFic from *Neisseria meningitidis* (*N. meningitidis*) is auto-adenylylated on two tyrosine residues, Y183 and Y188, located in the vicinity of the inhibition motif (3). The strictly conserved tyrosine Y183 is buried, pointing towards the Fic core. Modeling of auto-adenylylation of this residue results in steric clashes, suggesting a conformational change upon auto-adenylylation.

Recently, it has been shown that Fic proteins also target bacterial proteins (3) which results in bacterial growth arrest. ParE of the topoIV complex and GyrB of the DNA gyrase complex are adenylylated by the Class I Fic protein VbhT from *Bartonella schoenbuchensis* (Harms *et al., in preparation*).

We here show that the class III Fic protein NmFic, containing the α_{inh} helix at the C-terminus, specifically adenylylates GyrB, resulting in growth arrest. We report the structure-function characterization of the regulation mechanism of the class III Fic protein NmFic via a new double-lock mechanism. Interestingly, NmFic forms a tetramer with the active site and target binding-site buried in the center of the tetramer, inaccessible for target binding. NmFic undergoes a monomer-tetramer equilibrium where the active and target binding sites are accessible in the monomeric form. Disruption of the tetramer by repellant mutations results in bacterial growth arrest by activation of the Fic protein. Ultimately, we show that auto-adenylylation of the conserved tyrosine Y183 leads to drastic conformational changes, e.g. of the α_{inh} helix, that are crucial for the class III Fic protein activity. We anticipate that this double-lock mechanism by oligomerization and auto-adenylylation is conserved through all class III Fic proteins.

Material and Methods

Plasmid construction

pRSF-Duet1 derivatives were cloned as described previously (3) and used for over-expression of proteins for purification. For phenotypic analyses, *nmfic* genes were cloned into pNMD220 (14) under the control of a particularly tight P*lac*. Site-directed mutagenesis was performed following the protocol described by Zheng *et al.* (15). A list of used plasmids and respective oligonucleotides can be found in Table S1 and Table S2.

Expression – Isotope labeling – Purification

Plasmids pFVS0015, pFVS0051, pFVS0083, pFVS0109, pFVS0135, pFVS0137, pFVS0138, pFVS0143 were transformed into *E. coli* BL21 (λDE3) cells. Plasmids pFVS0059, pFVS0125, pFVS0126 and pFVS0134 were transformed into *E. coli* BL21 AI cells. NmFic and GyrB43 (residues 1-392) proteins were expressed and purified as described previously in (3) or (16), respectively. For NMR analysis, [*U*-^{13}C,^{15}N]-labeled NmFic was obtained by growing the expression cells in M9 minimal media (17) supplemented with ($^{15}NH_4$)Cl (Cambridge Isotope Labs) and D-[^{13}C]-glucose (Sigma Aldrich) using standard NmFic expression and purification conditions.

SEC-MALLS analysis

Size exclusion chromatography coupled to multi-angle laser light scattering (SEC-MALLS) was employed for the determination of the oligomeric state and elution concentration of NmFic wild-type and various mutants at different concentrations. SEC-MALLS analysis was performed as described previously (18). The column was equilibrated in 10 mM Tris pH 7.6 and 100 mM NaCl at 4°C.

SEC-MALLS derived apparent mass values (MW^{app}) for $NmFic_{wt}$, $NmFic_{E102R}$ (mutant 1) and $NmFic_{E156R}$ (mutant 2) measured in a range of various elution concentrations were fitted simultaneously to obtain the dimerization affinities (K_{D1} and K_{D2}), assuming that both interaction interfaces are independent. Therefore, $NmFic_{E102R}$ and $NmFic_{E156R}$ are assumed to form only dimers, as one of the interfaces was mutated, and $NmFic_{wt}$ is in monomer-tetramer equilibrium, which involves both interfaces. The equilibria were modeled as fast-exchange processes with respect to the timescale of chromatographic separation, since all the samples yielded a single MALLS peak. The theoretical MW^{app} values were calculated from mass concentrations ($c_{m,i}$) and molecular weights (MW_i) of populated species (monomer and dimer for the interface mutants; monomer, dimers, trimer and tetramer for the other NmFic variants):

$$MW^{app} = \frac{\sum_i c_{m,i} MW_i}{\sum_i c_{m,i}} \quad (1)$$

The global non-linear least-squares fitting was performed using Levenberg-Marquardt algorithm (19, 20). All routines were implemented in the Python language using NumPy and SciPy numerical libraries (21).

Monomer-tetramer equilibrium analysis

The equilibrium concentrations of individual species for $NmFic_{wt}$ were calculated using numerical solution of the set of mass action law equations (22) describing the monomer-tetramer oligomerization scheme (Fig. S3). The reaction extents were used as state variables and inequality constraints were imposed to ensure the correctness of the results. Optimization of reaction extents values was accomplished using Sequential Least SQuares Programming (SLSQP) method (23) as implemented in the SciPy library (21).

Spotting experiment

Escherichia coli K-12 MG1655 were transformed with pNDM220 derivative plasmids using TSS transformation (24) and handled in LB liquid medium containing appropriate antibiotics as well as 1% (w/v) D-glucose to suppress basal expression before the inoculation of experimental cultures. For the counting of colony forming units (CFU/mL), bacterial cultures were serially diluted and spotted on LB agar plates containing 0, 50 µM, 100 µM, 250 µM, 500 µM, 1000 µM or 2000 µM of isopropyl β-D-thiogalactopyranoside (IPTG) and 30 µg/mL ampicillin which were then incubated at 37°C.

***In vitro* adenylylation assay**

Adenylylation assays were performed using crude cell lysate of ectopically expressing *E. coli* as described previously (3) or using purified proteins as described in (12). Adenylylation activity of NmFic was assessed by incubating 5 µM NmFic protein with 10 µCi [α-^{32}P]-ATP (Hartmann analytic) and 25 µM GyrB43. In addition to radioactively labeled ATP, 62.5 µM of cold ATP was added and 200 µM of novobiocin, a potent inhibitor of GyrB43 to prevent immediate hydrolysis of ATP by GyrB43.

***In vivo* Supercoiling assay**

In vivo supercoiling assays were performed as described previously (Harms *et al.*, *in preparation*).

NMR spectroscopy

NMR experiments were performed on a Bruker AscendII 700 MHz spectrometer running Topspin 3.0 and equipped with a cryogenically cooled triple-resonance probe. All experiments were performed in NMR-buffer (25 mM MES, 150 mM NaCl, pH 6.5) at 25°C. For the sequence-specific backbone resonance assignments of NmFic and adenylylated-NmFic, the following experiments were recorded: 2D ^{15}N-^{1}H TROSY-HSQC (25), 3D HNCA (26, 27), 3D HNCACB (26-28), 3D HNCO (29), and 3D HN(CA)CO (30). For the analysis of the dynamic properties of NmFic and adenylylated-NmFic the following experiments were measured: ^{15}N{^{1}H}-NOE (31), T_1(^{15}N) (32), TRACT (33). NMR data were processed with PROSA (34) and analyzed with CARA, XEASY (35), and Topspin3.0 (Bruker Biospin). Nonlinear least-square fits of relaxation data were done with Matlab (MathWorks). R_2(^{15}N) values were derived from R_α(^{15}N) and R_β(^{15}N). Error bars for R_1(^{15}N), R_α(^{15}N), and R_β(^{15}N) were calculated by a statistical bootstrapping scheme and error bars for the ^{15}N{^{1}H}-NOE from the spectral noise. Secondary chemical shifts were calculated relative to the random-coil values of Kjaergaard and Poulsen (36).

The chemical shift changes of the amide moiety upon ATP were fitted by non-linear regression analysis to Equation 2 by using standard software. Δ_{obs} corresponds to the chemical shift difference at a given titration point and Δ_{max} is the maximal chemical shift difference at the last titration point.

$$\Delta_{obs} = \Delta_{max} \frac{(K_D + [ATP]_0 + [NmFic]_0) - \sqrt{(K_D + [ATP]_0 + [NmFic]_0)^2 - (4[NmFic]_0[ATP]_0)}}{2[NmFic]_0} \quad (2)$$

Crystallization

NmFic$_{E156R}$ and NmFic$_{E156R,Y183F}$ (10 and 8 mg/mL, respectively) crystallized in 500 µL of precipitant solution containing 10 mM Tris pH 7.8 and 100 mM NaCl using the batch crystallization method at 4°C.

All other crystals were obtained using the sitting-drop vapor-diffusion method by mixing 0.2 µL protein solution with 0.2 µL reservoir solution equilibrating against a reservoir of 80 µL at 20°C except NmFic$_{wt}$ (tetramer form) that crystallized in 7% (v/v) 2-propanol, 0.1 M MES pH 6.0, 0.05 M calcium acetate at 4°C. NmFic$_{E102R}$ crystallized after one month in 8% (v/v) Tacsimate pH 6.0, 20% (w/v) PEG 3350 and NmFic$_{E102R,E156R}$ crystallized after ten days in 8% (v/v) Tacsimate pH 5.0, 30% (w/v) PEG 1500. NmFic$_{Y183F,E186G}$ crystallized in 0.1 M Tris pH 8.0, 30% (w/v) Jeffamine M-600 pH 7.0. For data collection, crystals were cryoprotected by soaking into a reservoir solution supplemented with 15-30% glycerol and subsequently flash-frozen in liquid nitrogen.

Structure determination

X-ray data were collected at the Swiss Light Source (Villigen, Switzerland) on beamline X06SA (PXI) or X06DA (PXIII) at 100 K and a wavelength of 1.000 Å or 0.800 Å (Table 1). Diffraction data were indexed and integrated using iMosflm (37) or XDS (38) and subsequently merged and scaled using XSCALE (38) or aimless (39). $NmFic_{wt}$ diffracted to 3.10 Å. $NmFic_{E156R}$, $NmFic_{E102R}$ and $NmFic_{E102R,E156R}$ diffracted to 0.99 Å, 2.35 Å and 1.90 Å, respectively. $NmFic_{Y183F,E186G}$ and $NmFic_{E156R,Y183F}$ respectively diffracted to 2.20 Å and 1.00 Å. Data collection and processing statistics are summarized in Table 1. Structures were determined by molecular replacement using Phaser (40) with $NmFic_{wt}$ (PDB: 3S6A (3)), devoid from ligand or ordered solvent, as search model. Several rounds of model building and refinement were performed using Coot (41) and Refmac5 (42) or phenix.refine (43). 5% of the data were excluded from refinement and used for cross-validation. The geometry of the final model was assessed using MolProbity (44) showing > 99% of the residues in the core and allowed regions of the Ramachandran plot. Final refinement yielded NmFic models with reasonable R_{work}/R_{free} values for their respective resolution ranges (45). Refinement statistics are summarized in Table 2.

Figures were prepared with Dino (A. Philippsen unpublished, http://www.dino3d.org).

Results

NmFic undergoes a monomer–tetramer equilibrium

Crystals of $NmFic_{wt}$ grown at high protein concentration belong to the space group $P6_5$ and contain four molecules per asymmetric unit. These four molecules form a non-crystallographic 222 tetramer that contains two equivalent dimers (Fig. 1 *(a,b)* and Fig. S1 *(b)*). The same tetramer form is observed for $NmFic_{\Delta 8}$, a deletion mutant of the α_{inh} helix (α8) that had been previously determined from non-isomorphous crystals (3). Isologous contacts are observed at the interfaces of $NmFic_{wt}$ between subunits A-B, C-D and A-D, B-C, respectively (Fig. 1). The first interface (buried surface area of 420.3 +/- 1.1 $Å^2$) forms hydrophobic interactions and two symmetrical salt-bridges between residues R149 and E156 of two neighboring monomers (Fig. 1 *(d)*). The second interface (826.1 +/- 11.3 $Å^2$) forms the same type of interactions, with salt-bridges between residues R71 and E102 (Fig. 1 *(c)*). The residues involved in these interfaces are conserved in class III Fic proteins as shown by the multiple sequence alignment (Fig. S2). Consequently, analysis of the oligomeric state of $NmFic_{wt}$ in solution revealed the presence of multimeric forms in a concentration dependent manner Fig. S1 *(a)*). Size exclusion chromatography coupled to multi-angle laser light scattering (SEC-MALLS) was performed, revealing a single peak that varies in elution volume and apparent molar mass (from 22 kDa to 88 kDa) with varying total protein concentration. This shows that the protein is in a monomer–tetramer equilibrium in fast exchange with respect to the timescale of chromatographic separation (Fig. 2 *(a)*).

The Fic active site is located in the center of the tetramer and the β-hairpin forming the target-binding site (FLAP) is deeply buried (Fig. 1 *(a,b,e)*, yellow and light blue, respectively). Modeling of the binding of a small target fragment based on the superimposition of the IbpA/Cdc42 complex structure (PDB: 4ITR (10)) on the FLAP region of NmFic reveals several steric clashes (depicted by stars on Fig. 1 *(e)*). It is therefore well conceivable that NmFic in this tetrameric form is incompetent for target binding and that a lower oligomeric state, i.e. monomer or dimer, is the active species.

To test this hypothesis, we engineered variants of NmFic carrying single amino acid mutations (glutamic acid to arginine) of the salt-bridges formed at both dimerization interfaces, $NmFic_{E102R}$ and $NmFic_{E156R}$. The crystallographic structures of $NmFic_{E102R}$ and $NmFic_{E156R}$ were determined (Tables 1-2). These structures reveal that the dimerization interfaces are maintained as in the tetrameric wild-type protein (Fig. 3). The interface areas for $NmFic_{E102R}$ and $NmFic_{E156R}$ are 418.6 $Å^2$ and 779.4 $Å^2$, respectively, and thus virtually identical to the tetramer (420.3 ± 1.1 $Å^2$ and 826.1 ± 11.3 $Å^2$, respectively). Residue E102 is involved in a salt-bridge with E71 of the FLAP in the wild-type protein and the mutation

$NmFic_{E102R}$ leads to an increase in flexibility of the FLAP region as evidenced by the lack of electron density for residues 62–77. The high-resolution structure (0.99 Å) of $NmFic_{E156R}$ reveals the exact same dimer as observed within the tetrameric crystal form (RMSD of 0.989 Å for Cα atoms).

The multimerization equilibrium of these two proteins, as well as the double mutant, was assessed by SEC-MALLS. As expected, these mutants do not form a tetrameric species, but undergo a monomer–dimer equilibrium (22 kDa – 44 kDa) via the remaining interface (Fig. 2 *(a)*). The combination of both mutations in $NmFic_{E102R,E156R}$ reveals a constant mass of 22 kDa (monomer) at various protein concentration (Fig. 2 *(a)*). From these data, the dimerization constants (K_d) for $NmFic_{E102R}$ (mutant 1) and $NmFic_{E156R}$ (mutant 2) were determined to K_{d1} = 7.4 ± 1.4 µM and K_{d2} = 59.9 ± 11.8 µM, respectively. Note that the smaller dimerization interface features the higher affinity. The independent global fitting of the monomer–dimer–tetramer equilibrium of the wild-type protein yielded 7.6 ± 1.1 µM and 61.3 ± 8.8 µM for K_{D1} and K_{D2}, respectively (Fig. S3, Fig. 2 *(a)* and Table 3). These values are virtually identical in the precision of the experiment, indicating directly that the two interfaces are not connected by cooperativity. Based on the dissociation constants, the concentration-dependences of monomeric, dimeric, trimeric and tetrameric species of $NmFic_{wt}$ were calculated (Fig. 2 *(b)*). At total NmFic concentrations below 2 µM, NmFic is mostly present as monomers, whereas above this threshold, tetrameric species populate. Importantly, since most protein is sequestered as tetramers, the monomer concentration reaches a value of just 5 µM at a total NmFic concentration of 1 mM (Fig. 2 *(b)*). In contrast, the monomer concentrations in the Fic mutants are much larger, with 60 µM and 150 µM for mutant 1 ($NmFic_{E102R}$) and mutant 2 ($NmFic_{E156R}$) respectively at 1 mM total concentration (Fig. 2 *(c) and* S4). As monomer and tetramer are the predominant species, the monomer-tetramer equilibrium of $NmFic_{wt}$ can also be fitted with a single effective dissociation constant K_{Def} of 21.8 ± 1.0 µM (Table 3).

NmFic targets GyrB of the DNA gyrase complex

As the next step, we aimed to identify the target of NmFic within *E. coli*. VbhT, a Fic protein from the α-proteobacteria *Bartonella schoenbuchensis* adenylylates its own ParE and GyrB, as well as the homologous proteins from *E. coli* (Harms *et al., in preparation*). In turn, though VbhT adenylylates both proteins, the *in vivo* supercoiling activity of GyrB is only faintly affected by VbhT when the decatanation activity of ParE is drastically inhibited by the expression of the Fic protein VbhT. Because of the similar growth defect phenotype of *E. coli* induced by expression of VbhT and the inhibition-relieved mutant of NmFic ($NmFic_{E186G}$) (3, 12), we tested the adenylylation of *E. coli* GyrB and ParE by $NmFic_{E186G}$. Interestingly, this

inhibition-relieved mutant of the class III Fic protein from *N. meningitidis* (3, 12) specifically adenylylates *E. coli* GyrB but not ParE, suggesting a different mechanism of the bacterial growth inhibition (Fig. 4 *(a)*). Furthermore, $NmFic_{E186G}$ adenylylates GyrB of *N. meningitidis* stronger than the homologous in *E. coli* (Fig. 4 *(a)*). Mutation of the adenylylated tyrosine 109 from *E. coli* GyrB (to alanine or phenylalanine) completely abolishes the adenylylation of GyrB, showing that GyrB is specifically adenylylated on this residue. The tyrosine 109 from GyrB is located in the N-terminal ATPase domain of GyrB and conserved in bacterial topoisomerases. This residue is part of the ATP lid-loop (46) and involved in a weak contact with the N3 of the adenine ring of the ATP substrate of GyrB (47). The adenylylation of GyrB results in the inhibition of ATP hydrolysis (Harms *et al.*, *in preparation*), which is required for the DNA supercoiling activity of DNA gyrase that is essential for bacterial growth (48, 49).

Like novobiocin at the high concentration of 100 µg/mL, the expression of $NmFic_{E186G}$ in *E. coli* results in collapse of the negative supercoiling of a reporter plasmid (Fig. 4 *(b)*). No effect can be observed with the catalytically inactive $NmFic_{H107A,E186G}$ mutant, showing that the observed loss of supercoiling activity directly results from the adenylylation of GyrB by the inhibition-relieved mutant $NmFic_{E186G}$ (Fig. 4 *(b)*). This is in contrast with the effect of VbhT on GyrB, which does not inhibit the *in vivo* supercoiling activity of GyrB (Harms *et al.*, *in preparation*).

Tetramerization deficient mutants induce growth defects and adenylylate GyrB

Knowledge of the target enabled us to evaluate the activity of NmFic mutants of the dimerization interfaces *in vitro* by adenylylation assay. For *in vivo* characterization (*E. coli* model), bacteria (*E. coli* K12 MG1655) were transformed with plasmids containing *nmfic* genes, grown in liquid culture, and serial dilutions of exponentially growing bacteria were spotted on LB-agar plates supplemented with increasing amounts of IPTG (form none to 2 mM) (Fig. 5 *(a)*). Colony forming units were counted allowing the quantification of bacterial growth defect upon expression of the different NmFic mutants. Compared to the wild-type or the catalytically inactive mutant in which the first histidine of the Fic active site motif has been mutated (2), $NmFic_{E102R}$ (mutant 1), $NmFic_{E156R}$ (mutant 2) and $NmFic_{E102R,E156R}$ (monomer) mutants show a severe growth defect in dependence of the induction level (Fig. 5 *(a,b)*). This growth defect was quantified for each mutant, resulting in the loss of 1.5, 3.0, and 1.5 log10 CFU/mL of viability for $NmFic_{E102R}$, $NmFic_{E156R}$ and $NmFic_{E102R,E156R}$, respectively. In addition to the loss in colony number, the colonies exhibited a drastically smaller size (Fig. 5 *(a)*). Furthermore, expression of the combination of the dimerization interface mutants with the H107A mutation (catalytically inactive) abolishes the growth defect of *E. coli*, similarly to the expression of wild-type tetrameric NmFic (Fig. 5 *(a,b)*). These observations evidence that the

catalytic activity of NmFic is responsible for the growth defect of bacteria expressing the dimerization interface mutants. *In vitro*, an adenylylation assay revealed that purified NmFic mutants of the dimerization interface adenylylate the target GyrB (N-terminal fragment containing the ATPase and transducer domains). These results are in agreement with the *in vivo* results, clearly showing that the catalytically inactive mutants are unable to transfer radioactively labeled α-^{32}P-AMP on GyrB (Fig. 5 *(c)* and Fig. S5). These observations rely so far on the total concentration of NmFic proteins expressed for *in vivo* quantification or the total concentration of pure protein in the *in vitro* assays.

It is interesting to compare the growth defect to the NmFic monomer concentration rather than the total concentration. For that purpose, a conversion factor (ratio) between IPTG and total NmFic concentration was applied, with a concentration of 100 µM of inducer (IPTG) leading to 1 µM of total NmFic protein (Fig. 6 *(a)*), based on different IPTG/NmFic$_{total}$ ratios that were tested graphically (Fig. 6 (b) and Fig. S6 *(a-c)*). At this ratio, the concentration of monomer in the NmFic$_{wt}$ (forming tetramer) stays rather low (< 1 µM) at a total NmFic concentration of 10-20 µM. This is in contrast with the mutant 1, mutant 2 and monomer mutant, in which the monomer concentration is very close to the total NmFic concentration. Fig. 6 *(b)* shows that for NmFic$_{wt}$, a sufficient concentration of monomeric Fic protein cannot be achieved with the maximal level of induction that can be used experimentally. This points towards a threshold level of NmFic that can be tolerated by the cell and here not obtained in wild-type NmFic, where the tetramer acts as a sponge that stores the active NmFic species. Taken together, these results reveal a first level of regulation of NmFic by oligomerization.

Structural investigation of auto-adenylylated NmFic by NMR

To understand the effect of auto-adenylylation of NmFic, we investigated the changes induced by auto-modification of a catalytically inactive monomer mutant (NmFic$_{E102R,H107A,E156R}$) in solution using high-resolution nuclear magnetic resonance (NMR). NmFic is auto-adenylylated on two tyrosines positioned in the close vicinity of the conserved inhibitory glutamate, that is part of the α_{inh} helix (helix 8) (3). Modeling of auto-adenylylation on tyrosine 183 and 188 results in steric clashes with the Fic core, suggesting a putative conformational change upon auto-adenylylation of NmFic. Intriguingly, tyrosine Y183 is strictly conserved in class III Fic proteins. We obtained well-dispersed NMR spectra for a native and an auto-adenylylated sample (inactive monomer mutant that was adenylylated by the addition of trace amounts of hyperactive NmFic$_{\Delta 8}$, Fig. S7). Sequence-specific resonance assignments were obtained for 95% and 93% for native and adenylylated NmFic$_{E102R,H107A,E156R}$, respectively. Analysis of the chemical shift changes upon auto-adenylylation revealed that the helix 1, the inhibitory helix 8 (α_{inh}) and the FLAP region (Fig.

7) are the most affected regions upon adenylylation. The changes in the helix 1 are highly likely a direct result of the auto-adenylylation of helix 8 possibly leading repulsion of both helices from the Fic core. This movement will then lead to the activation of NmFic by active-site opening, with auto-adenylylation being the intrinsic factor that expulses the inhibition motif from the ATP binding site, relieving the inhibition of class III Fic proteins. We used the chemical shifts of the backbone $^{13}C\alpha$ and $^{13}C\beta$ nuclei to identify the secondary-structure elements of both NmFic forms in solution. NmFic features eight α-helices in solution, that corresponds in their number and positioning to the crystalline structure (Fig. S8). In addition, residues 62–66 of the FLAP region, exhibit a small β-sheet. These secondary elements remain upon adenylylation, showing only a slight decrease of about 15% percent of helical content in helix 1.

The opening of the γ-phosphate binding site upon adenylylation, leads to a two-fold increase of the affinity of ATP binding compared to the native unadenylylated form, with respective dissociation constants of 4.0 ± 1.2 mM and 7.8 ± 1.1 mM (Table 4 and Fig. S9). These constants are rather high, but are in excellent agreement with similar observations for Doc, the toxin of bacteriophage P1 that phosphorylates EF-Tu, with a K_D of 7.2 mM for an ATP analog in the absence of target. Strikingly, upon pre-formation of a Doc–EF-Tu complex, the affinity for the substrate increases by ~ 10^5-fold to 0.26 µM (7). This effect can be deduced to the fact that the FLAP region is responsible for target binding but also needs to provide important residues for ATP binging and the base-binding pocket. We observed a high degree of flexibility in the FLAP-region on the picosecond–nanosecond timescale by measurement of $^{15}N\{^1H\}$-NOE measurements. This dynamic behavior was further evidenced by a reduction in the T_1-relaxation time as well as by the absence of electron density in this region in crystal structures. Therefore a significant increase of the substrate affinity upon GyrB binding and subsequent stabilization of the FLAP to enhance ATP binding in-line with the Doc–EF-Tu interaction can be expected.

Presence of the auto-adenylylated tyrosine 183 of NmFic is required for activity

To investigate further the role of auto-adenylylation, we mutated the tyrosine 183 and tested the effect *in vivo*. Since $NmFic_{wt}$ is known to be inhibited by a tight tetramer formation, we investigated the effect of Y183 on the inhibition-relieved mutant $NmFic_{E186G}$ (3, 12). Comparison of $NmFic_{E186G}$ to $NmFic_{Y183F,E186G}$ shows that the growth defect phenotype of $NmFic_{E186G}$ is completely abolished by the Y183F mutation (Fig. 8 *(a)*). To rule out any significant structural changes upon Y183F mutation, we compared the crystal structures of both aforementioned proteins. Both structures are very similar, with root mean square deviation (RMSD) of 0.306 Å for the Cα atoms (0.684 Å for all atoms) after superimposition

(50) (Fig. 8 *(b)*). These *in vivo* and structural results clearly indicate that the auto-adenylylation of residue Y183 is crucial for the activity of the protein. Additionally, the combination of mutants of the dimerization interface (mutant 1, mutant 2 and monomer mutant) with the mutation of Y183 also re-established normal growth of *E. coli* cells (Fig. 8 *(a)*), while leading to no structural changes as evidenced by the RMSD of 0.228 Å for the Cα atoms (0.428 Å for all atoms) for the mutant 2 ($NmFic_{E156R}$) and the mutant 2 Y183F ($NmFic_{E156R,Y183F}$) obtained at 1.0 Å resolution (Fig. 8 *(c)*).

The SEC-MALLS analysis of the inhibition-relieved $NmFic_{E186G}$ mutant reveals a less stable tetramer that $NmFic_{wt}$ (Fig. 9 *(a)* and Table 3) with a tetramerization K_{Def} of 190.0 ± 9.5 µM ($NmFic_{E186G}$) compared to 21.8 ± 1.0 µM ($NmFic_{wt}$), albeit the mutation is far away from oligomerization interfaces. A double mutation Y183F,E186G has an opposite effect, making the tetramer much tighter (Table 3). There may be an effect of auto-adenylylation on the lower affinity of $NmFic_{E186G}$ since the purified protein is expected to be partially auto-modified, as revealed by an increased A_{260}/A_{280} ratio (data not shown). The monomer concentration of the E186G mutant compared to the total concentration reveals that this mutant, even though still forming a tetramer, has monomer levels very close to the dimer mutants (Fig. 9 *(b)*).
Altogether, combination of solution NMR analysis, crystallographic analysis and *in vivo* growth analysis reveals that the auto-adenylylation of NmFic is a required mechanism of relief of inhibition in class III Fic proteins. This layer of control is accompanied by the regulation through tetramerization to tightly control the adenylylation of the target GyrB.

Discussion

Fic proteins need to be tightly regulated due to their highly toxic activity both in the prokaryotic and eukaryotic cells (2, 3) (Harms *et al.*, *in preparation*). The crystal structure shows that tetrameric Fic can not be competent for target binding, due to burying of the target binding site in the core of the tetramer. On a first level of regulation, disassembly of the tetrameric state is thus essential for activation of the Fic protein. Our activation model assumes that the cell can compensate for the deleterious effects of a small intracellular concentration of monomeric NmFic, up to a level at which the inhibition of DNA gyrase by NmFic is not bacteriostatic. *In vitro* oligomerization analysis yields a maximal level of 2 µM for monomeric Fic. This value could be modulated *in vivo*, due to molecular crowding effects in the cytosol or additional binding partners that would facilitate the tetramer formation. A level of 1-2 µM of monomer, corresponding to 600-1200 molecules per bacteria, would be sufficient to inhibit the 1300 GyrB molecules (A. Schmidt, personal communication), thus the DNA gyrase machinery and negative supercoiling in the cell, resulting in cell growth arrest.

Dimers and monomers of NmFic are toxic for *E. coli*, but the toxicity does not accumulate from dimers to monomer (Fig. 5). At rather low concentration, the concentration of monomer is very close to the total protein concentration (Fig. 2 *(c)*), and therefore no significant difference is expected. The mutant 1 and monomer are less toxic than the mutant 2, which can not be rationalized from the interfaces. Nonetheless, both mutant 1 and monomer mutant harbor the E102R mutation, residue that is located below the target binding site (FLAP) and may contribute to target binding, since it is unlikely that three main chain–main chain hydrogen bonds of the FLAP are sufficient for target binding and specificity. Alternatively, this mutation may also slightly alter GyrB binding. We can not exclude that a dimer (mutant 1, mutant 2 or both) is/are also active in a natural environment. Nonetheless, the low abundance of these species within the monomer-tetramer equilibrium of wild-type NmFic (Fig. 2 *(b)*) makes it highly unlikely that the dimers have a major role in the activity of NmFic in the cell.

The neutralization of toxic proteins is a common scheme in biology. Binding of antitoxins to toxins is a quite common way to neutralize toxins of all kind prior to their intended activation in time or location. The *E. coli* relB/RelE protein complex is a characteristic example of such a toxin-antitoxin system (14). The relBE toxin-antitoxin system acts as transcriptional autoregulation system. In the case of nutritional starvation, transcription from the relBE operon gets dramaticaly increased and the level of RelB antitoxin is reduced by Lon-dependent proteolysis, a common mechanism of antitoxin degradation (51). The liberation of the RelE toxin results in cellular growth arrest (52). Keeping a protein in an inactivated oligomeric state, like tetramerization for NmFic, is an elegant way to control protein function

that can be activated directly by an external trigger. In this case, the protein acts as its own antitoxin. Similar activation mechanism can also be found for the bacterial chaperone trigger factor, directly interacting in the monomeric form with a large variety of nascent chains on the ribosome (53), which is in the cytosol in a monomer-dimer equilibrium that can be modulated depending on the growth conditions (54, 55). Trigger factor dimerizes with an apparent K_D of 18 µM, in the same range as the effective K_{Def} of $NmFic_{wt}$ (21.8 ± 1.0 µM). Furthermore, the plant Ultraviolet-B radiation photoreceptor UVR8, responsible for adaptation to UV, is inactive as a dimer but active as a monomer. In the ground state, inactive, UVR8 is present as a homodimer that monomerizes within seconds of UV-B irradiation (56). The active monomer then interacts with COP1, resulting in changes in gene expression, acclimation and UV-B tolerance (57).

A second level of control is provided by auto-adenylylation of NmFic. We propose that this auto-adenylylation is the intrinsic factor that expulses the strictly conserved glutamate of the inhibition motif, thus relieving the inhibition of class III Fic proteins. This is evidenced by *in vivo* effects of the mutation of the strictly conserved Y183 within class III Fic proteins. Additionally, the investigation of the auto-adenylylation in solution by NMR reveals chemical shifts changes of residues belonging to the α_{inh} helix, the helix that is responsible for the inhibition of competent ATP binding (3, 12). Changes in the chemical shifts of the helix α1 are likely an effect of the movement of helix α8, since this is the adjacent helix that will be affected by the introduction of the adenylylation on Y183. The observed changes within the FLAP is likely due to the binding of the target in the auto-adenylylated form, whereas the target here is the intermolecular helix α8.

Is there a link between the oligomerization and auto-adenylylation? First, it is worth noting that a target cannot bind to the tetrameric form of NmFic, i.e. here the helix 8 acting as an intermolecular target. Auto-adenylylation occurs via binding of the helix α8 (α_{inh}) on the FLAP of another monomer and covalent transfer of AMP on the tyrosine 183. Once auto-adenylylated, the helix α8 cannot fold back to its original inhibitory position, relieving the auto-inhibition. Interestingly, the $NmFic_{E186G}$ mutant of the inhibitory glutamate has a much lower affinity for both forms of dimers within the tetramer as observed by the shifted monomer-tetramer equilibrium towards higher concentration (Table 3). The helix α8 lies on the surface of the tetramer and is not involved in dimerization interfaces. Additionally, $NmFic_{E186G}$ is found endogenously auto-adenylylated. This observation indicates a putative link between oligomerization and auto-adenylylation, where adenylylation has an enhancing effect on monomerization. The auto-adenylylation of the mutant 1, mutant 2 and monomer mutant are required for the activity of these proteins, as evidenced by the experimental *in vivo* growth data. The monomer and dimer mutants are also active, showing that the auto-

adenylylation is not only involved in disrupting the oligomer but rather in an own activity. Altogether, the information obtained on auto-adenylylation show that the auto-adenylylation *per se* is required for the activity of the protein, expulsing the inhibitory helix from the ATP binding site, but most likely needs the monomerization of NmFic beforehand. Commonly, auto-adenylylation has been observed for most Fic proteins investigated so far (10, 11, 13, 58-60) but its putative role within the functional cycle of these proteins was not yet addressed. Therefore, the regulatory function of auto-adenylylation for class III Fic proteins may indicate that auto-modification is also involved in the control of catalytic activities of class I and class II FIC domains and could thus be a general feature of Fic proteins.

In summary, our experiments suggest a model for Fic activation (Fig. 10). Upon an initiation signal that remains still elusive, the NmFic tetramer is disrupted which liberates the FLAP, enabling target binding. The disruption of the tetramer is followed by a second layer of regulation, auto-adenylylation. This modification of monomers leads to full activation of the protein by expulsion of the inhibitory alpha helix. Once a certain level of auto-adenylylated monomer is present in the cell, adenylylation of GyrB from the DNA gyrase subunit blocks efficiently the bacterial growth, resulting in a bacteriostatic effect. Our study revealed the tight two-step regulation of class III Fic proteins and identified its biological role as a negative regulator of the DNA-gyrase machinery.

Author contribution

F.V.S. and A.H. cloned recombinant plasmids. F.V.S. expressed, purified, crystallized and determined the X-ray structure of protein constructs and analyzed the *E. coli* growth upon expression of NmFic. A.H. discovered the target of NmFic, performed adenylylation and supercoiling assay. B.M.B. conducted the NMR analysis of NmFic. F.V.S., A.M. and T.Sh. performed and analyzed the SEC-MALLS experiments. All authors participated in experimental design, data analysis and wrote the manuscript.

Acknowledgments

We thank the staff of beam-lines X06DA and X06SA of the Swiss Light Source (Villigen, Switzerland) for excellent support. We gratefully acknowledge Gerd Pluschke for kindly providing the genomic DNA of *Neisseria meningitidis*. This work was supported by the ERC Advanced Investigator Grant (ERC-2013-AdG) FICModFun 340330 (to C.D.), and SNF grants 3100-132979 (to C.D.) and 31003A-138414 (to T.S.).

Table 1. Data collection statistics.

	wt	E102R	E156R	E102R-E156R	Y183F-E186G	E156R-Y183F
X-ray source	SLS X06DA (PXIII)	SLS X06SA (PXI)	SLS X06DA (PXIII)	SLS X06DA (PXIII)	SLS X06DA (PXIII)	SLS X06DA (PXIII)
X-ray detector	MAR225 CCD	Pilatus 6M	Pilatus 2M	Pilatus 2M	Pilatus 2M	Pilatus 2M
Wavelength (Å)	1.00853547/6	1.000	0.800	1.000	1.000	0.800
Space group	P 6_5	P 2 2_1 2_1	P 2 2_1 2_1	P 2 2_1 2_1	P 6_4 2 2	P 2 2_1 2_1
Cell dimensions (Å) a, b, c	131.92, 131.92, 167.74	48.56, 81.91, 97.53,	35.33, 50.54, 130.14	35.40, 39.75, 132.75	148.64 148.64 75.98	35.38 50.70 129.78
Matthews coeff. (Å^3/Da)	5.06	2.53	2.73	2.45	5.84	2.74
Solvent content (%)	75.50	50.98	54.67	49.39	78.79	54.79
Mol. per asym. unit	4	2	1	1	1	1
Resolution limits (Å)	14.95 - 3.10 (3.21 - 3.10)	62.72 - 2.35 (2.43 - 2.35)	47.15 - 0.99 (1.02 - 0.99)	66.37 - 1.50 (1.55 - 1.50)	53.13 - 2.20 (2.28 - 2.20)	32.91 - 1.00 (1.04 - 1.00)
Total reflections	58397 (5680)	120000 (12268)	839576 (79738)	53547 (2947)	560845 (53518)	784149 (73569)
Unique reflections	29964 (2991)	16808 (1666)	129866 (12557)	8894 (474)	25596 (2494)	122935 (11501)
Multiplicity	1.9 (1.9)	7.1 (7.4)	6.5 (6.4)	6.0 (6.2)	21.9 (21.5)	6.4 (6.4)
Completeness (%)	99.74 (99.70)	99.89 (100.00)	99.47 (97.58)	74.68 (99.57)	99.93 (99.76)	96.84 (91.52)
Mosaicity	1.22	0.19	0.10	0.27	0.47	0.21
⟨ I/σ(I) ⟩	11.08 (3.35)	21.93 (4.57)	29.81 (3.47)	26.97 (19.17)	20.95 (1.91)	25.42 (3.43)
R_{merge} † (%)	6.35 (24.31)	7.52 (47.95)	3.16 (54.76)	4.59 (5.64)	16.73 (212.70)	3.90 (49.68)
R_{meas} ‡ (%)	8.98	8.12	3.43	5.03	17.13	4.26
$CC_{1/2}$ (%)	99.0 (84.4)	99.9 (93.0)	100.0 (86.9)	99.9 (99.9)	99.9 (84.1)	100.0 (85.0)
CC* (%)	99.7 (95.7)	100.0 (98.2)	100.0 (96.4)	100.0 (100.0)	100.0 (95.6)	100.0 (95.9)

Number in parentheses belong to the outer shell.

† $R_{merge} = \sum_{hkl}\sum_i |I_i(hkl) - \langle I(hkl)\rangle| / \sum_{hkl}\sum_i I_i(hkl)$, where $I_i(hkl)$ is the observed intensity for a reflection and $\langle I(hkl)\rangle$ is the average intensity obtained from multiple observations of symmetry-related reflections.

‡ $R_{meas} = \sum_{hkl} [N/(N-1)]^{1/2} \sum_i |I_i(hkl) - \langle I(hkl)\rangle| / \sum_{hkl}\sum_i I_i(hkl)$, where $I_i(hkl)$ is the observed intensity for a reflection, $\langle I(hkl)\rangle$ is the average intensity obtained from multiple observations of symmetry-related reflections and N is the number of observations of intensity I(hkl).

Table 2. Refinement statistics.

	wt	E102R	E156R	E102R-E156R	Y183F-E186G	E156R-Y183F
PDB code	N/A	N/A	N/A	N/A	N/A	N/A
Resolution limits (Å)	14.95 - 3.10 (3.21 - 3.10)	62.72 - 2.35 (2.43 - 2.35)	47.15 - 0.99 (1.02 - 0.99)	66.37 - 1.50 (1.55 - 1.50)	53.13 - 2.20 (2.28 - 2.20)	32.91 - 1.00 (1.04 - 1.00)
R_{work} * (%)	18.20 (23.94)	21.43 (23.08)	12.24 (16.21)	20.83 (25.58)	17.31 (31.92)	14.65 (18.21)
R_{free} ** (%)	22.82 (30.82)	25.84 (26.76)	13.13 (16.98)	25.59 (36.61)	20.97 (34.82)	15.50 (19.19)
Number of non-H atoms	5967	2705	1848	1449	1608	1847
- macromolecules	5860	2685	1619	1342	1459	1618
- ligands	107	-	8	-	31	8
- water	-	20	221	107	118	221
Protein residues	712	326	181	162	178	181
RMSD bond lengths (Å)	0.014	0.014	0.026	0.019	0.012	0.028
RMSD bong angles (°)	1.79	1.46	2.22	1.80	1.28	2.45
Ramachandran favored/allowed * (%)**	96.7 / 99.7	99.7 / 100.0	100.0 / 100.0	99.4 / 100.0	100.0 / 100.0	100.0 / 100.0
Ramachandran outliers * (%)**	0.3	0.0	0.0	0.0	0.0	0.0
Clashscore ***	1.79	1.87	6.61	3.73	5.10	6.26
Wilson B-factor	34.97	33.80	8.36	16.72	34.72	7.95
Average B values ($Å^2$)	29.90	37.50	12.00	22.10	46.10	11.40
- macromolecules	29.20	37.60	10.80	21.50	45.50	10.10
- ligands	71.00	-	18.30	-	45.40	18.60
- solvent	-	28.00	20.90	28.70	54.00	20.50

Numbers in parentheses refer to the outer shell.

* $R_{work} = \sum_{hkl} || F_{obs}| - |F_{calc} || / \sum_{hkl} |F_{obs}|$
** R_{free} is the R value calculated for 5% of the data set that was not included in the refinement.
*** Molprobity

Table 3. Dissociation constants for the dimerization of NmFic *via* the interface 1 (K_{D1}) or interface 2 (K_{D2}).

		K_{D1} [µM]	K_{D2} [µM]	Effective K_D [µM] **
$NmFic_{E102R}$	Local fitting	7.4 ± 1.1	-	-
	Global fitting	7.6 ± 1.1	-	-
$NmFic_{E156R}$	Local fitting	-	59.9 ± 11.8	-
	Global fitting	-	61.3 ± 8.8	-
$NmFic_{wt}$		7.6 ± 1.1	61.3 ± 8.8	21.8 ± 1.0
$NmFic_{Y183F}$ *		7.2 ± N/A	56.2 ± 2.7	20.4 ± 1.0
$NmFic_{E186G}$ *		66.1 ± N/A	511.9 ± 25.9	190.0 ± 9.5
$NmFic_{Y183F,E186G}$ *		3.6 ± N/A	28.1 ± 1.9	10.3 ± 0.7

* Both dissociation constants were not fitted individually, but with a ratio of $K_{D2} = 7.74 * K_{D1}$, assuming both interfaces are affected similarly by the mutations that are not part of the interface.

** The effective K_D (K_{Def}) represents a value of the dissociation constant where $K_{D1} = K_{D2}$.

Table 4. Dissociation constants for the interaction of NmFic or auto-adenylylated NmFic with ATP for selected residues.

Residue	Native NmFic K_D [mM]	Auto-adenylylated NmFic K_D [mM]
K140	7.0 ± 0.7	5.7 ± 0.8
T141	9.0 ± 1.4	4.8 ± 1.3
I105	6.7 ± 0.3	3.0 ± 0.9
G69	9.0 ± 0.4	3.2 ± 0.4
G68	7.3 ± 0.7	3.2 ± 0.5
Median	**7.8 ± 1.1**	**4.0 ± 1.2**

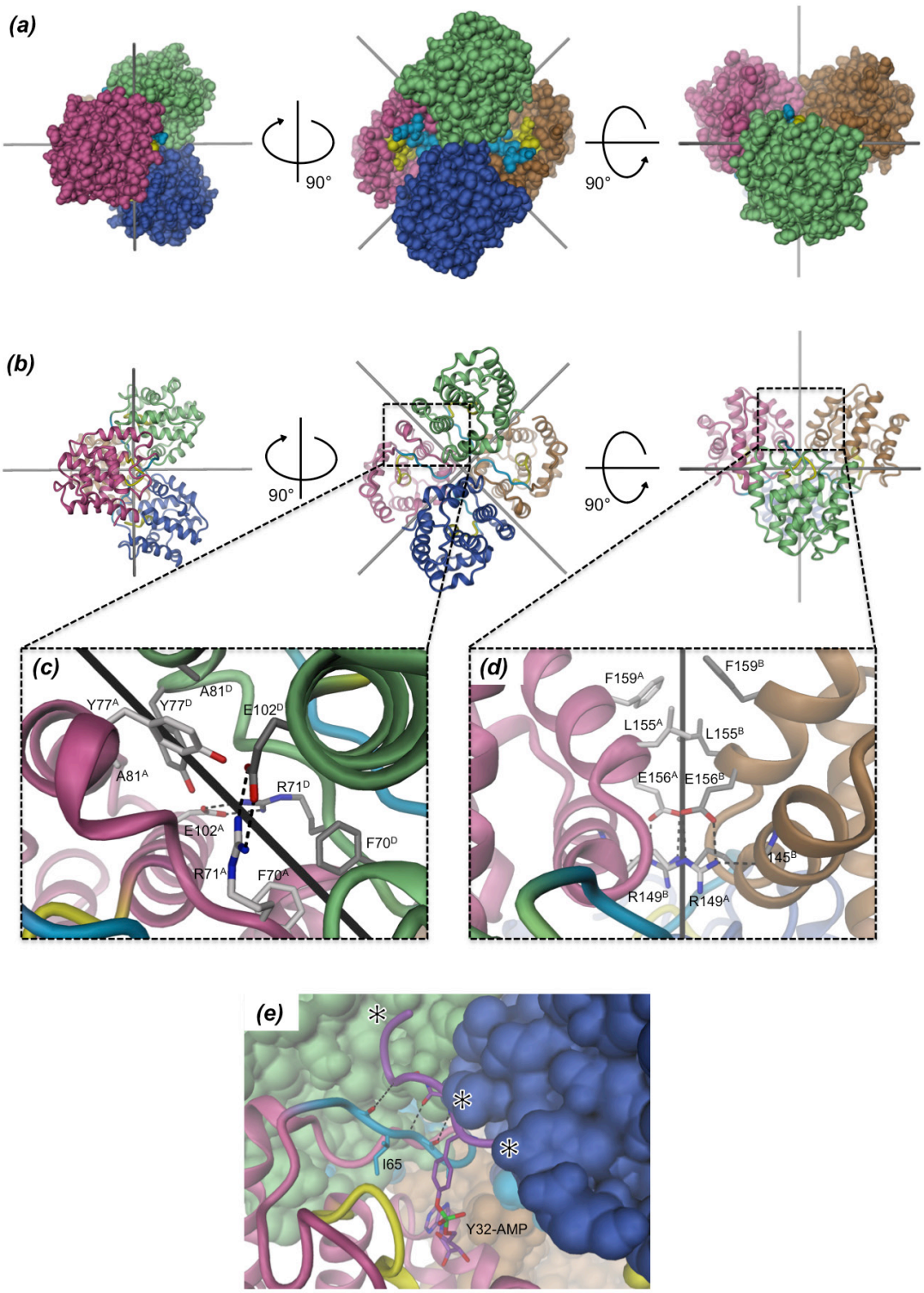

Figure 1. Tetrameric structure of the class III Fic protein NmFic. *(a)* Crystal structure of the NmFic 222 tetramer in $P6_5$ crystal form shown in surface representation. Local symmetry axes are indicated by black lines: monomer A in pink, B in brown, C in blue and D in green. The Fic active site motif is highlighted in yellow and the FLAP in light blue. Equivalent dimers within the tetramer are formed by AB, CD and AD, BC *(b)* Cartoon representation as in *(a)*.

(c) Close-up view of the AD dimerization interface, with contact area of ~ 826 Å^2. *(d)* Close-up view of the AB dimerization interface, with contact area of ~ 421 Å^2. Hydrogen-bonds are depicted as dashed black lines. Indices of the labeled residues refer to the respective monomers. *(e)* Superimposition of the switch 1 region of cdc42 (violet) on NmFic based on the IbpA/cdc42 complex structure (PDB: 4ITR (10)). The main-chain of the target sterically clashes with the other subunits (shown as blue and green surfaces) of the NmFic tetramer (clashes indicated by black stars).

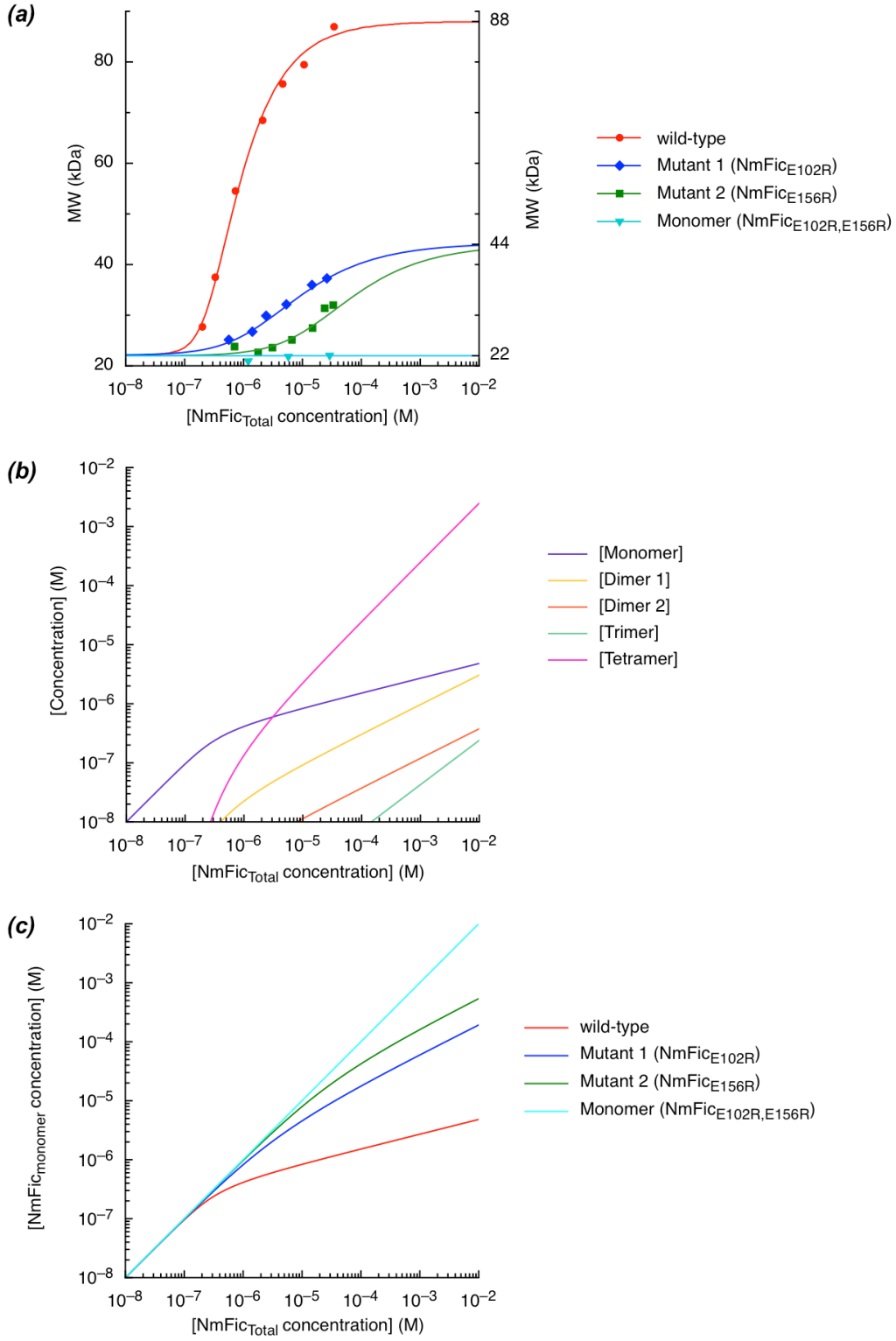

Figure 2. Dynamic monomer–oligomer equilibrium of NmFic. *(a)* Concentration dependence of the effective molecular weight as determined by MALLS for different variants of NmFic. The points are experimental data points, the lines are the result of a non-linear fit of the monomer–oligomer model of Figure S3. The resulting dissociation constants are

shown in Table 3. *(b)* Molecular concentrations of oligomeric species of $NmFic_{wt}$ as a function of the total protein concentration, as calculated from the dissociation constants K_{D1} and K_{D2}. *(c)* Concentration of monomeric protein as a function of total protein concentration for different variants of NmFic, as indicated.

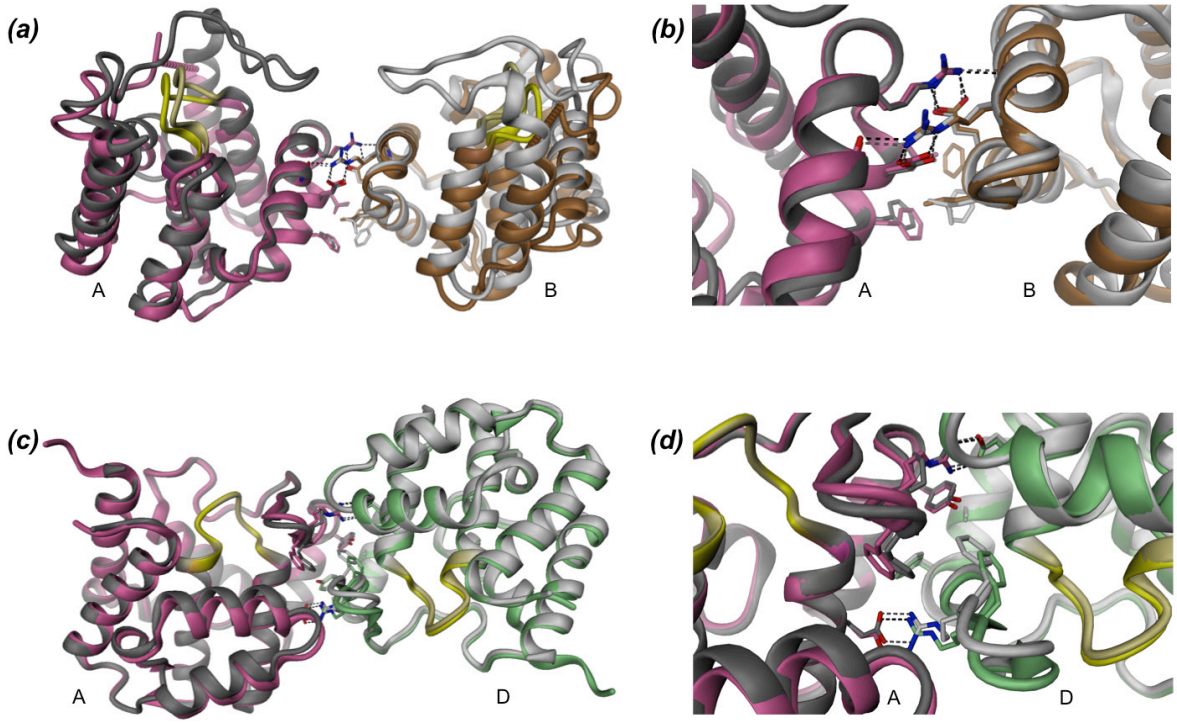

Figure 3. Crystal structures of NmFic$_{E102R}$ and NmFic$_{E156R}$. *(a)* Structure of NmFic$_{E102R}$ (pink/orange) superimposed with the AB dimer as part of the NmFic$_{wt}$ tetramer (dark/light gray). The active site is colored in yellow in both structures. The FLAP region is not observed in the crystal structure due its flexibility and absence of crystal contacts (top). Only the corresponding molecules are shown for clarity. *(b)* Close-up view of the conserved hydrophobic and hydrophilic interactions between the tetramer form and the NmFic$_{E102R}$ form. *(c)* Structure of NmFic$_{E156R}$ (pink/green) superimposed with the AD dimer as part of the NmFic$_{wt}$ tetramer (dark/light gray). *(d)* Details of the conserved interaction site.

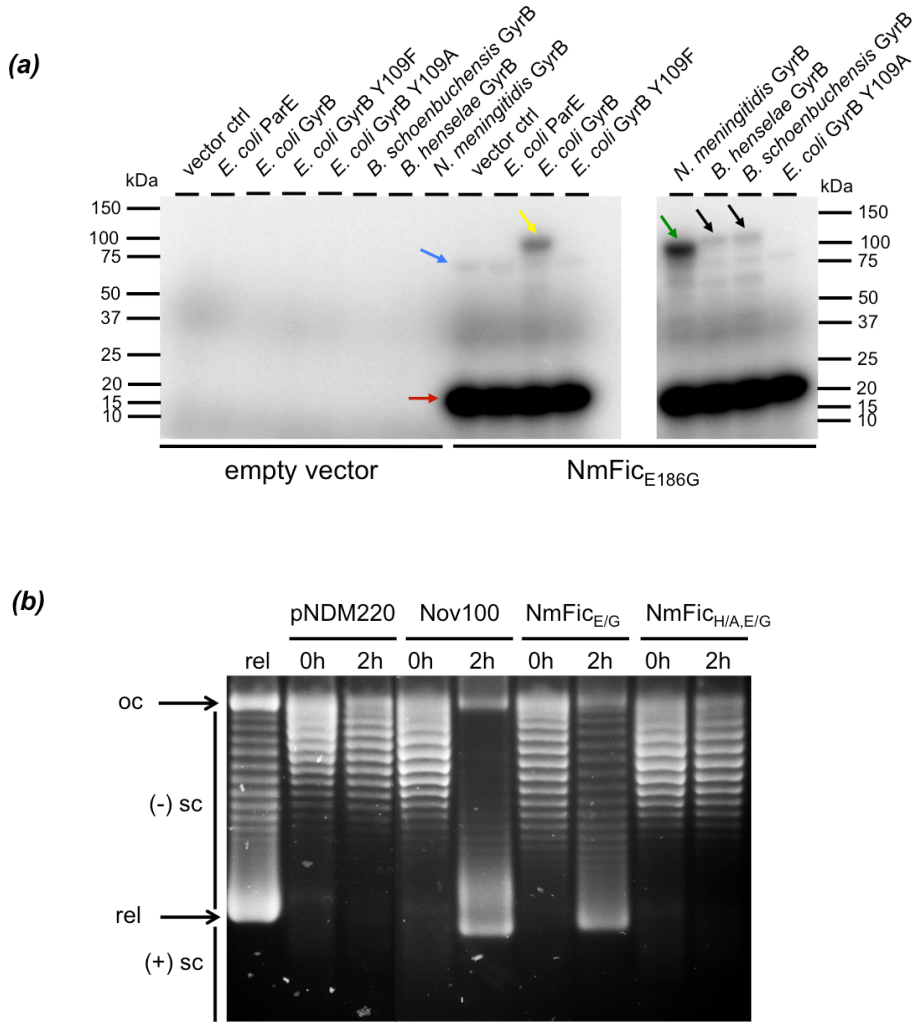

Figure 4. *In vitro* adenylylation of DNA gyrase by NmFic and *in vivo* inhibition of negative supercoiling. *(a)* Autoradiogram of *in vitro* adenylylation assay using α-^{32}P-ATP with crude cell lysates of *E. coli* ectopically expressing full-length and GST-tagged GyrB or ParE constructs from various organisms, incubated with pure inhibition-relieved NmFic$_{E186G}$. The red arrow indicates the auto-adenylylation of NmFic, the blue arrow the adenylylation of endogenously expressed GyrB, the yellow arrow the adenylylation of GST-tagged GyrB from *E. coli*, the green arrow the adenylylation of GST-GyrB from *N. meningitidis* and black arrows the adenylylation of GST-GyrB from *Bartonella* species . *(b)* Complete *in vivo* inhibition of the negative supercoiling ((-)sc) activity of DNA gyrase by the inhibition-relieved NmFic$_{E186G}$ protein at a similar level as the potent inhibitor novobiocin revealed by chloroquine agarose gel electrophoresis.

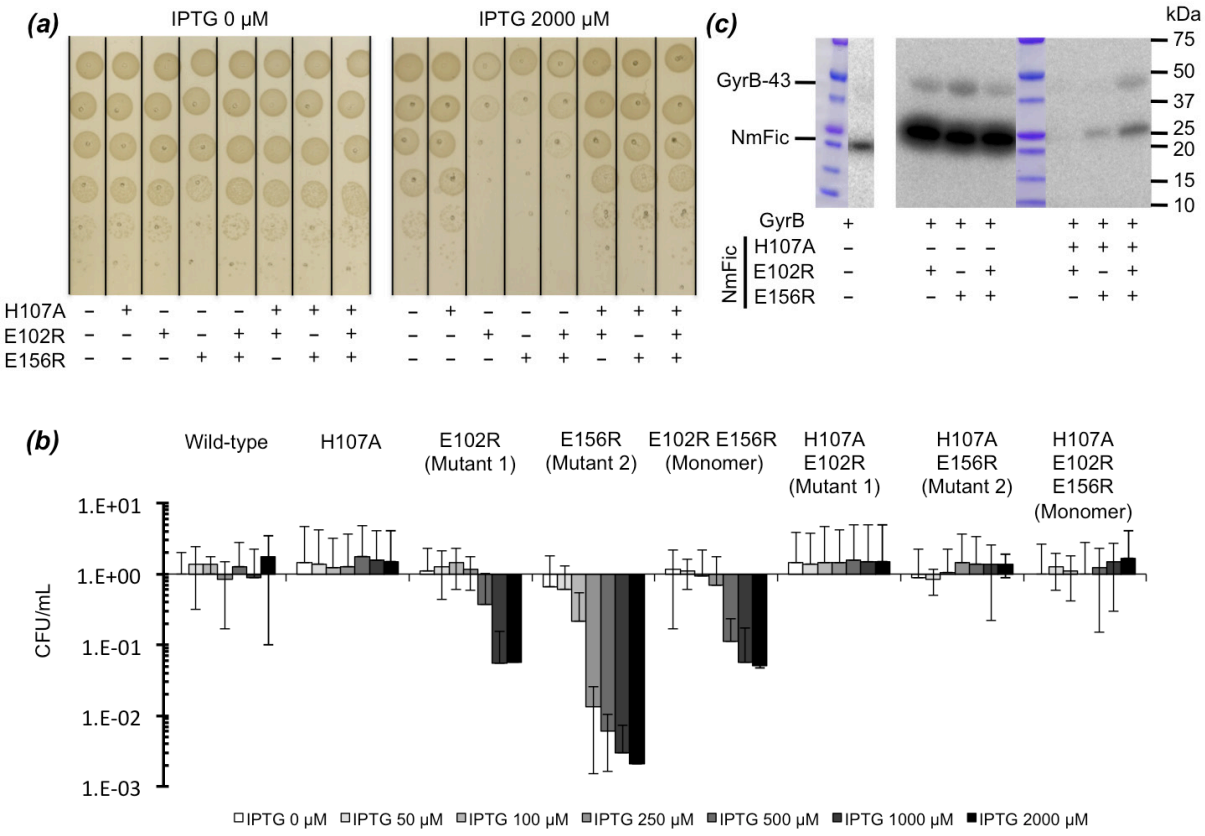

Figure 5. Growth defect of *E. coli* expressing NmFic variants. *(a)* Spotting experiment of *E. coli* MG1655 (λDE3) expressing NmFic derivatives on plates containing 0 or 2000 µM of the expression inducer IPTG. Note the remarkable growth defect, both in colony number and colony size, of the $NmFic_{E102R}$, $NmFic_{E156R}$ and $NmFic_{E102R,E156R}$ mutants. *(b)* Quantification of *E. coli* growth defect. The bars represent the average of three independent experiments and the error bars represent the standard deviation. *(c) In vitro* adenylylation assay with purified NmFic proteins and purified GyrB43 (N-terminal 43-kDa fragment comprising the ATPase and transducer domains).

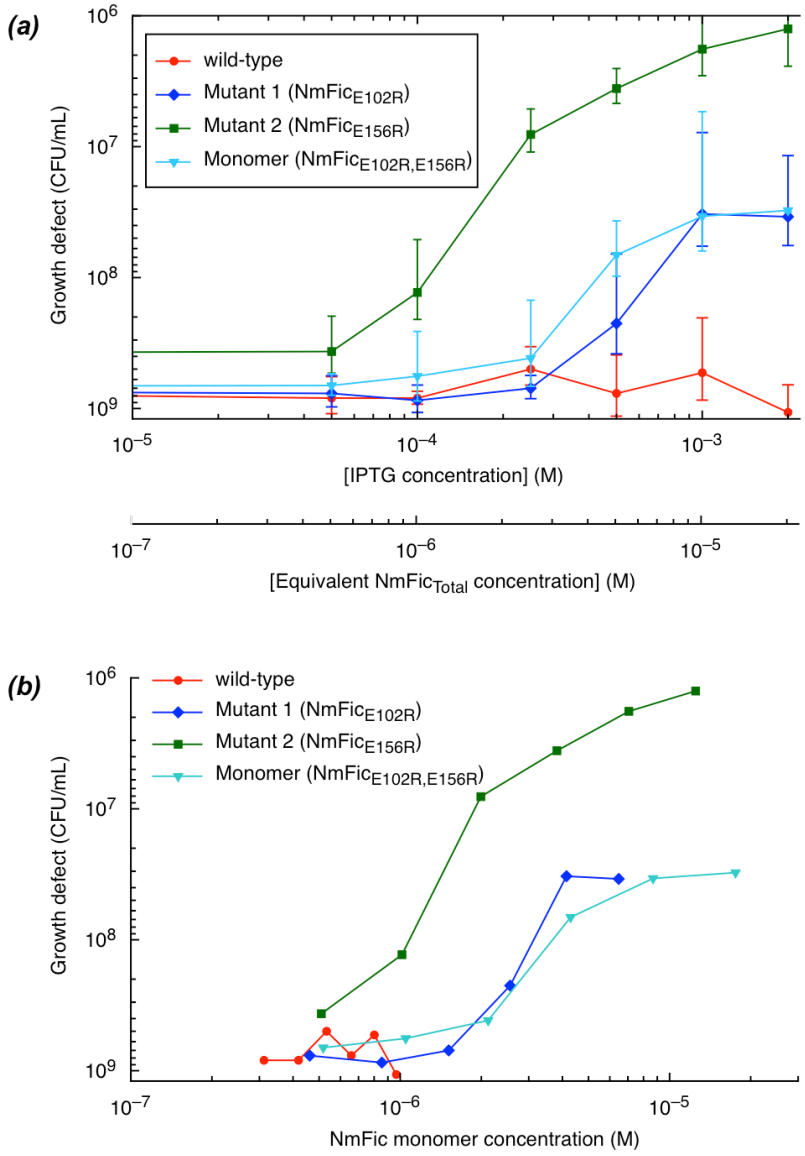

Figure 6. Bacterial growth defect correlates with the concentration of monomeric NmFic. *(a) E. coli* growth defect depending on IPTG concentration or equivalent of NmFic total concentration, assuming 100 µM IPTG correspond to 1 µM NmFic total protein (2nd horizontal axis). *(b) E. coli* growth defect depending on the monomer concentration of NmFic, assuming the same ratio as in *(a)*.

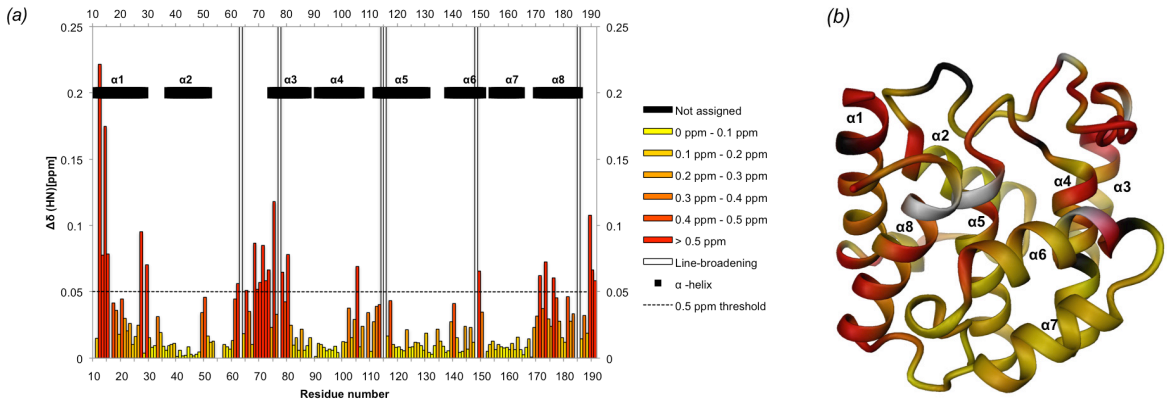

Figure 7. Structural perturbations of NmFic by auto-adenylylation. *(a)* Combined chemical shifts difference of the backbone amide moiety, $\Delta\delta$(HN) between unmodified and auto-adenylylated $NmFic_{E102R,H107A,E156R}$ as function of the residue number. Unassigned residues are colored in black and residues exhibiting significant line-broadening in the adenylylated form are depicted in white. *(b)* Plot of the same chemical shift differences on the structure of monomeric NmFic using the same color code as in panel *(a).* The largest chemical shift differences cluster in helices α1 and α8 (α_{inh}), and in the FLAP region.

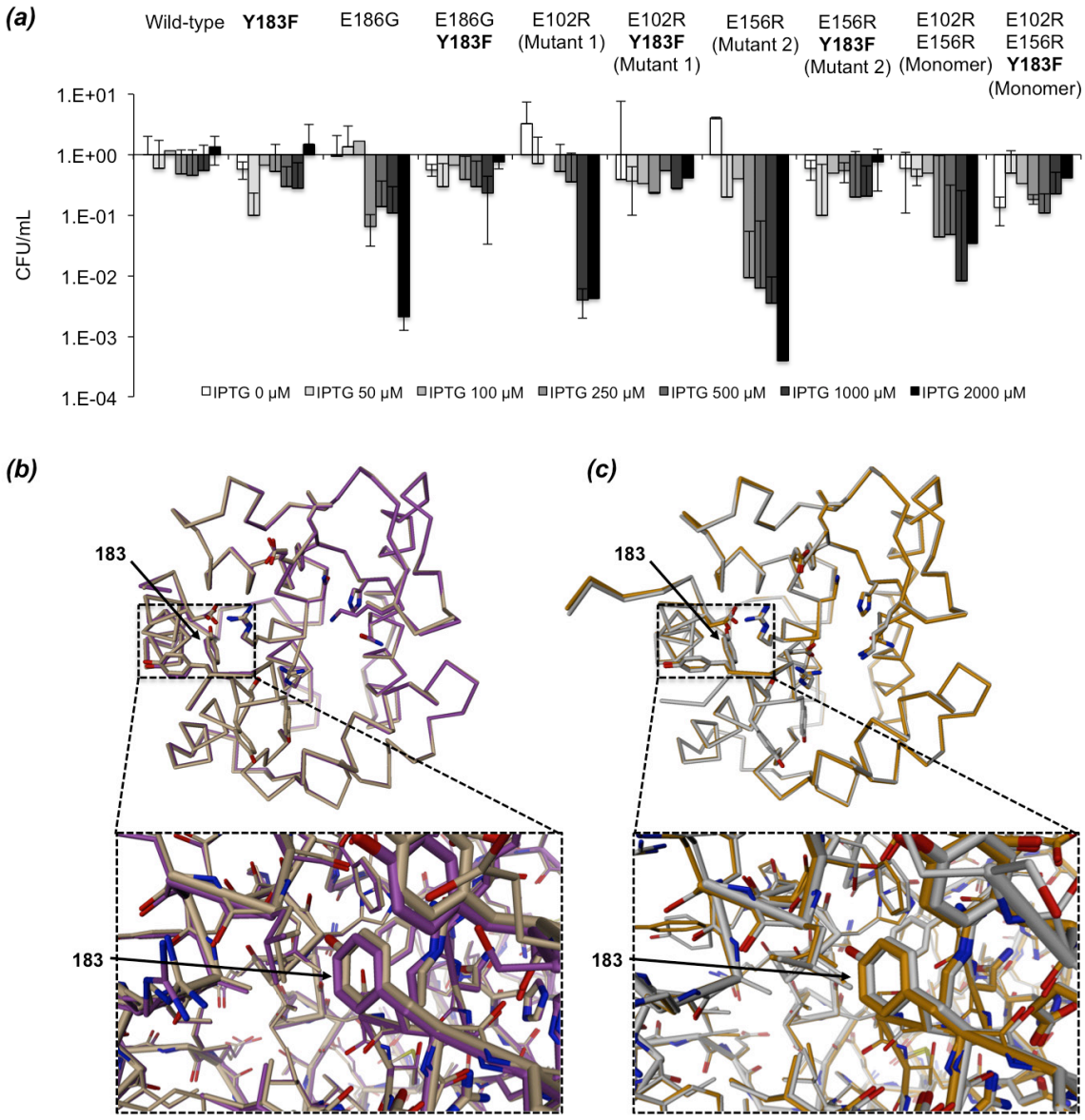

Figure 8. **Mutation of Y183 abolishes the growth defect of NmFic without affecting the local protein structure.** *(a)* Quantification of the *E. coli* growth defect. The bars represent the average of two independent experiments and the error bars the standard deviation. *(b)* Superimposition of $NmFic_{E186G}$ (beige) and $NmFic_{Y183F,E186G}$ (violet) with an RMSD of 0.306 Å for the Cα positions. *(c)* Superimposition of $NmFic_{E156R}$ (light gray) and $NmFic_{E156R,Y183F}$ (orange), with an RMSD of 0.228 Å for the Cα positions.

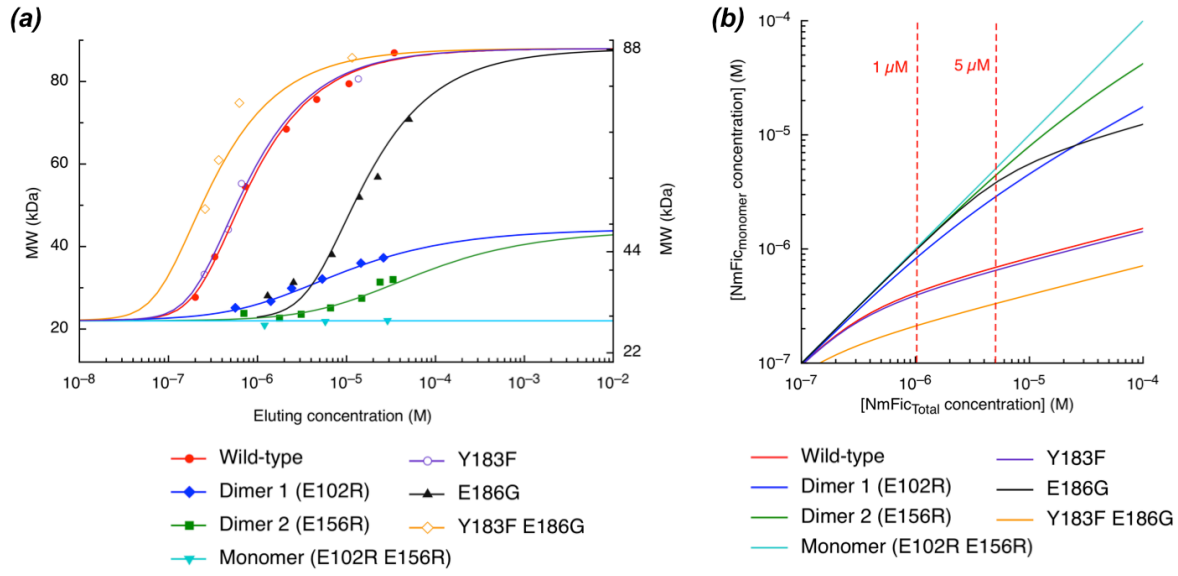

Figure 9. Dynamic monomer–oligomer equilibrium of NmFic mutants. *(a)* SEC-MALLS analysis of the oligomeric state of NmFic mutants of the auto-adenylylated tyrosine (Y183F, purple), of the inhibitory glutamate (E186G, black) or combination of both mutations (Y183F E186G, yellow). Respective dissociation constants are reported in Table 3. For comparison, wild-type, mutant 1, mutant 2, and monomer mutant are shown in the same colors as in Fig. 2. *(b)* Comparison of the monomer concentration ($NmFic_{monomer}$) versus total protein concentration ($NmFic_{Total}$) for the wild-type protein and mutants of the dimerization interface or of the auto-adenylylated tyrosine 183, using the same color code as in panel *(a)*.

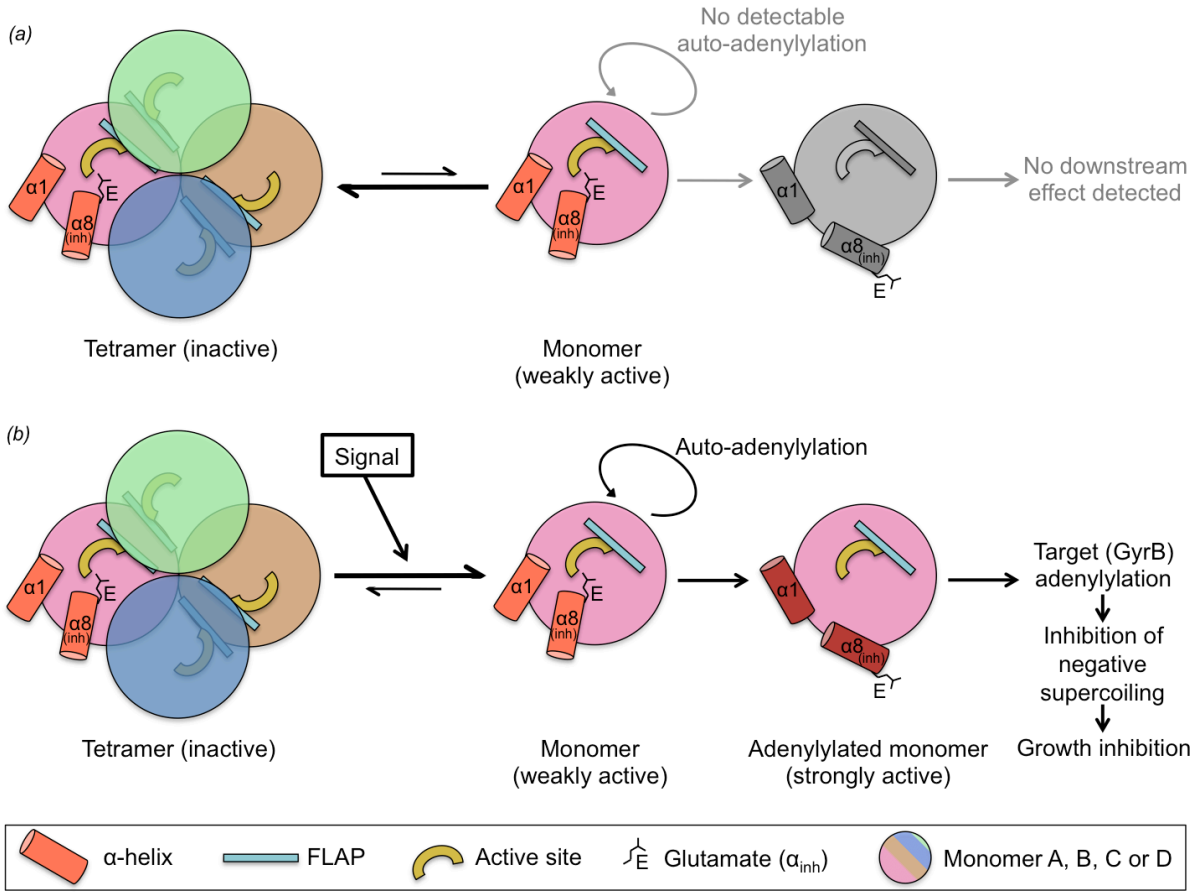

Figure 10. Regulation mechanism of class III Fic proteins. *(a)* In normal conditions, the monomer-tetramer equilibrium is in favor of the tetramer formation. *(b)* Upon a certain signal, the monomer-tetramer equilibrium is pushed towards the monomer. The monomer is then auto-adenylylated, which results in a conformational change of the helix α8 (α_{inh}) and the neighboring helix α1. The Fic protein is now active and able to adenylylate its target GyrB, leading to the inhibition of negative supercoiling and inhibition of bacterial growth.

Table S1. List of Plasmids.

Plasmid	Backbone	Description	Primer (fw)	Primer (rv)	Restriction sites	Source
pRSF-Duet1	pRSF-Duet1	Empty vector (RSF1030 *ori*, P*T7*)				Novagen
pFVS0015	pRSF-Duet1	$NmFic_{wt}$				Engel *et al*.
pFVS0051	pRSF-Duet1	$NmFic_{H107A}$	prFVS149	prFVS150		this study
pFVS0059	pRSF-Duet1	$NmFic_{E186G}$				Goepfert *et al.*
pFVS0083	pRSF-Duet1	$NmFic_{Y183F,E186G}$	prFVS096	prFVS092		this study
pFVS0109	pRSF-Duet1	*E. coli* GyrB 1-392 N_{ter} His_6-tag	prFVS107	prFVS114	NdeI/XhoI	this study
pFVS0117	pRSF-Duet1	$NmFic_{H107A,E186G}$	prFVS082	prFVS083		this study
pFVS0125	pRSF-Duet1	$NmFic_{E102R}$	prFVS119	prFVS120		this study
pFVS0126	pRSF-Duet1	$NmFic_{E156R}$	prFVS121	prFVS122		this study
pFVS0134	pRSF-Duet1	$NmFic_{E102R,E156R}$	prFVS119	prFVS120		this study
pFVS0135	pRSF-Duet1	$NmFic_{E156R,Y183F}$	prFVS091	prFVS092		this study
pFVS0137	pRSF-Duet1	$NmFic_{E102R,H107A}$	prFVS149	prFVS150		this study
pFVS0138	pRSF-Duet1	$NmFic_{H107A,E156R}$	prFVS149	prFVS150		this study
pFVS0143	pRSF-Duet1	$NmFic_{E102R,H107A,E156R}$	prFVS149	prFVS150		this study
pNMD220	pNDM220	Empty vector (mini-R1 ori, PLac)				Gotfredsen *et al.*
pAH154_NmFic_wt	pNDM220	$NmFic_{wt}$	prAH525	prAH526	BamHI/EcoRI	this study
pAH154_NmFic_E186G	pNDM220	$NmFic_{E186G}$	prAH537	prAH538		this study
pFVS0146	pNDM220	$NmFic_{Y183F}$	prFVS091	prFVS092		this study
pFVS0147	pNDM220	$NmFic_{Y183F,E186G}$	prFVS096	prFVS092		this study
pFVS0149	pNDM220	$NmFic_{E102R}$	prFVS119	prFVS120		this study
pFVS0150	pNDM220	$NmFic_{E156R}$	prFVS121	prFVS122		this study
pFVS0151	pNDM220	$NmFic_{H107A}$	prFVS149	prFVS150		this study
pFVS0173	pNDM220	$NmFic_{E102R,E156R}$	prFVS119	prFVS120		this study
pFVS0174	pNDM220	$NmFic_{E102R,Y183F}$	prFVS091	prFVS092		this study

Plasmid	Backbone	Description	Primer (fw)	Primer (rv)	Restriction sites	Source
pFVS0175	pNDM220	$NmFic_{E156R,Y183F}$	prFVS091	prFVS092		this study
pFVS0177	pNDM220	$NmFic_{E102R,H107A}$	prFVS149	prFVS150		this study
pFVS0178	pNDM220	$NmFic_{E102R,E156R,Y183F}$	prFVS091	prFVS092		this study
pFVS0179	pNDM220	$NmFic_{H107A,E156R}$	prFVS149	prFVS150		this study
pFVS0197	pNDM220	$NmFic_{E102R,H107A,E156R}$	prFVS149	prFVS150		this study

Table S2. List of DNA oligonucleotides and their respective sequences.

Primer	Sequence (5'-3')
prFVS082	GTATTATTACGGCGGGTATGAAAAAGGCTGAC
prFVS083	CATACCCGCCGTAATAATACGACTGCTCG
prFVS091	GAGCAGTCGTTTTATTACGAAGGGTATGAAAAAG
prFVS092	GTAATAAAACGACTGCTCGATACCTTTAAAG
prFVS096	GAGCAGTCGTTTTATTACGGCGGGTATGAAAAAG
prFVS107	GGGAATTCCATATGCATCACCATCACCATCACTCGAATTCTTATGACTCCTCCAG
prFVS114	CGACCTCGAGTTAGGTCATTTCACGCGCGCGACG
prFVS119	CAAATATGTTCGTATGAACATTGCCCATCC
prFVS120	CAATGTTCATACGAACATATTTGGCGATGATTTC
prFVS121	CAACGATTTACGUCTGCGCTTTTTGTTAAAG
prFVS122	CAAAAAGCGCAGACGTAAATCGTTGACGGGGCTG
prFVS149	GAACATTGCCGCCCCGTTTTTGGAGGGTAATGGCAG
prFVS150	CAAAAACGGGGCGGCAATGTTCATTTCAACATATTTG
prAH525	GAGCGGGGATCCATAGGAGGAACAATTTTATGAAATCCATAGACGAACAAAG
prAH526	CTCCCGCGAATTCTCAGCCTTTTTCATACCCTTC
prAH537	TTATTACGGCGGGTATGAAAAAGGCTGAGAA
prAH538	TTCATACCCGCCGTAATAATACGACTGCTCG

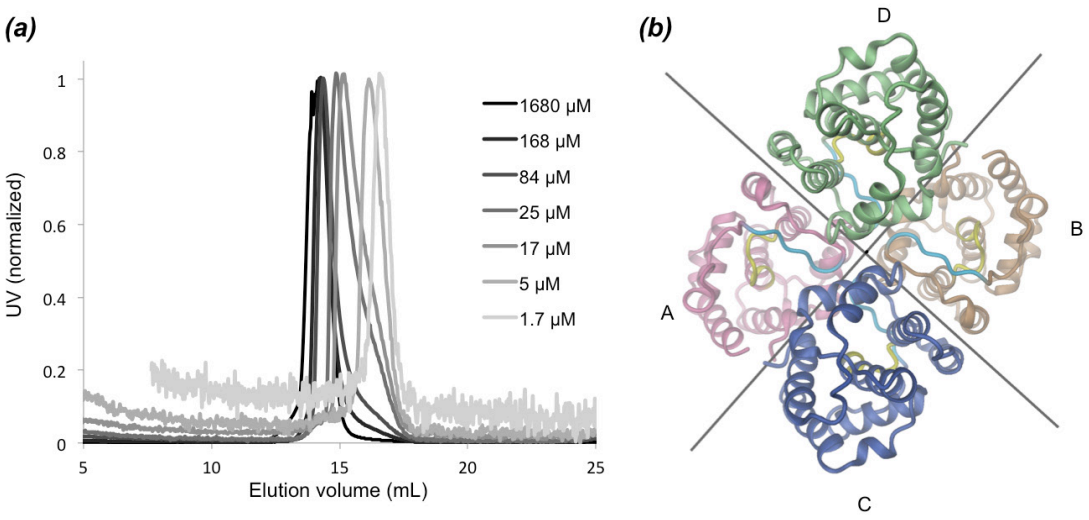

Figure S1. Dynamic equilibrium of $NmFic_{wt}$ from monomer to tetramer. *(a)* Dynamic equilibrium of $NmFic_{wt}$ on the time-scale of the Size Exclusion Chromatography (SEC) experiment. SEC analysis using an analytical S75 16/60 column (GE Healthcare) with a flowrate of 0.5 mL/min loaded with 50 µL of wild-type NmFic at various loading concentrations (gray-scale from dark-gray [1680 µM] to light-gray [1.7 µM]). *(b)* The NmFic 222 tetramer observed in the $P6_5$ crystal form shown as ribbon representation (same as Fig. 1).

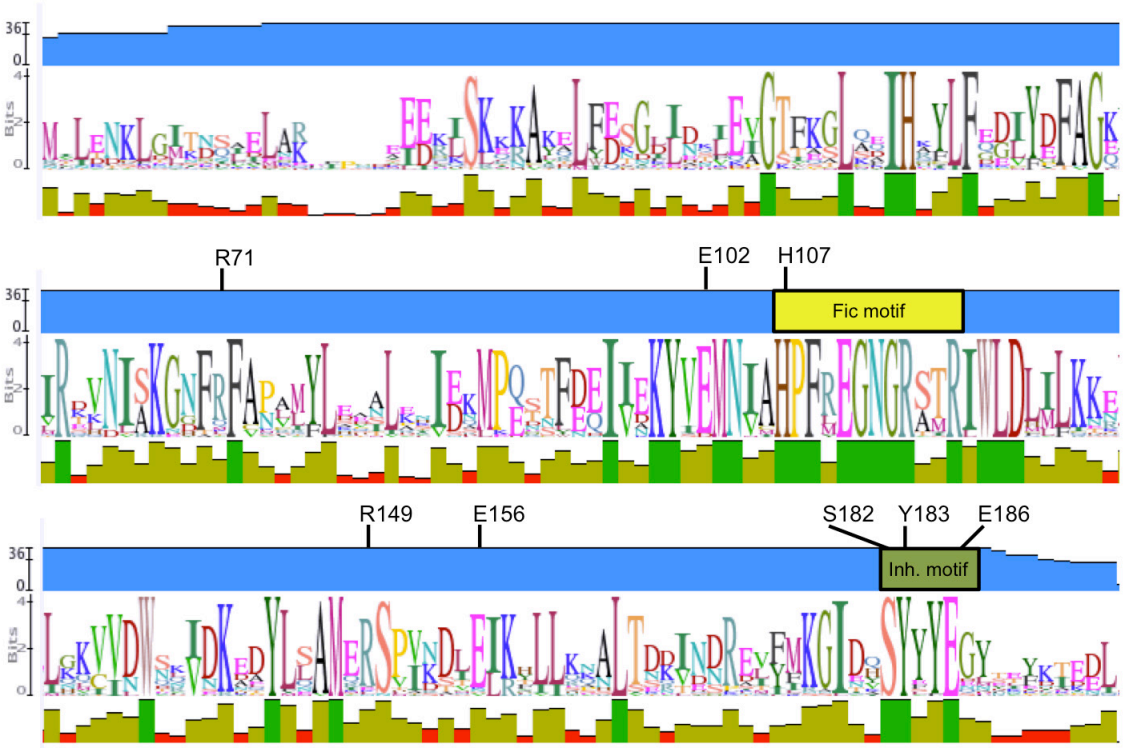

Figure S2. Amino acid conservation in class III Fic proteins. The alignment contains one representative sequence for each of 41 organisms. The alignment was calculated using MUSCLE (Multiple Sequence Comparison by Log-Expectation) (61) (http://www.geneious.com).

(a)

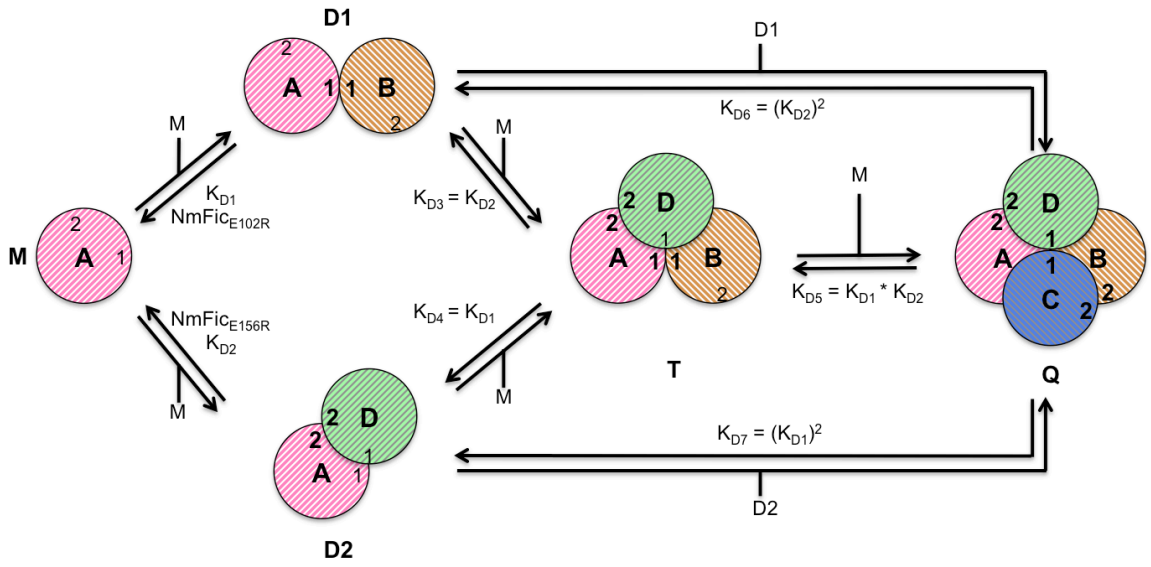

(b)

$$2 * M \leftrightarrows D1 \qquad K_{D1} = \frac{[D1]}{[M]^2} \qquad (3)$$

$$2 * M \leftrightarrows D2 \qquad K_{D2} = \frac{[D2]}{[M]^2} \qquad (4)$$

$$M + D1 \leftrightarrows T \qquad K_{D3} = K_{D2} \qquad (5)$$

$$M + D2 \leftrightarrows T \qquad K_{D4} = K_{D1} \qquad (6)$$

$$M + T \leftrightarrows Q \qquad K_{D5} = K_{D1} * K_{D2} \qquad (7)$$

$$2 * D1 \leftrightarrows Q \qquad K_{D6} = (K_{D2})^2 \qquad (8)$$

$$2 * D2 \leftrightarrows Q \qquad K_{D7} = (K_{D1})^2 \qquad (9)$$

Figure S3. Thermodynamic model of NmFic multimerization. *(a)* Schematic view of the equilibrium and *(b)* set of mass action law equations. (M = monomer, D1 = dimer 1, D2 = dimer 2, T = trimer, Q = tetramer).

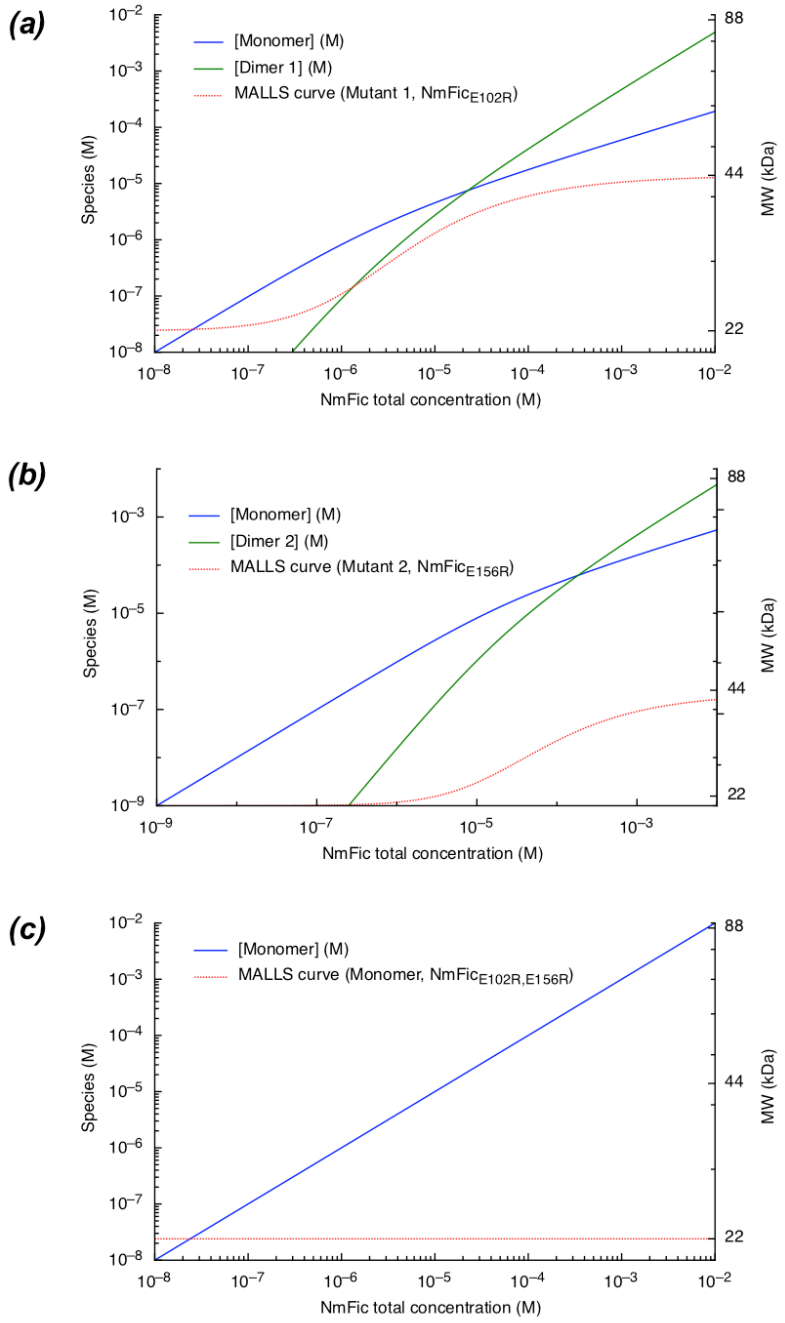

Figure S4. Dynamic equilibrium of NmFic tetramerization-deficient mutants. Species profile calculated with the equilibrium constants *(a)* K_{D1} for NmFic$_{E102R}$, *(b)* K_{D2} for NmFic$_{E156R}$ and *(c)* NmFic$_{E102R,E156R}$. The red curves represent the fitted experimental MALLS data.

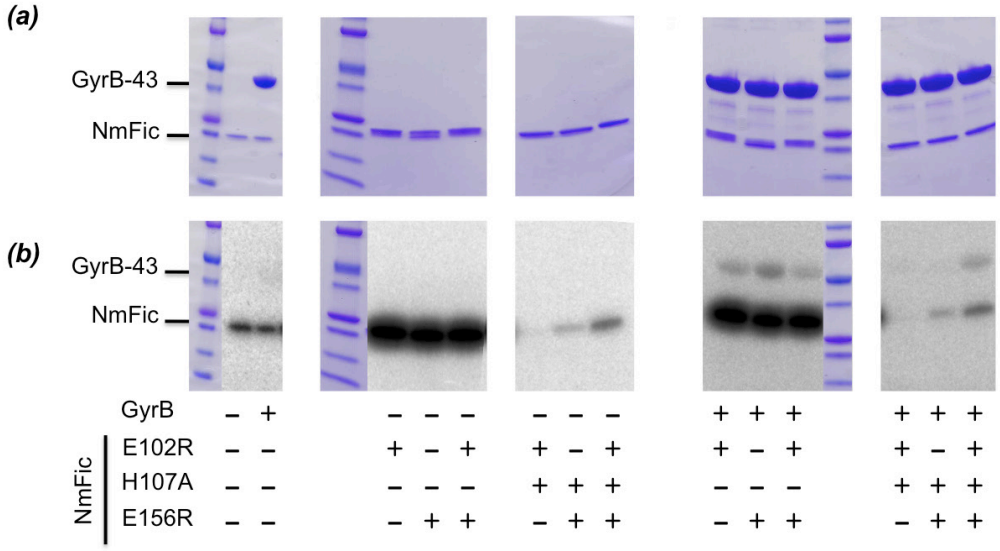

Figure S5. Adenylylation assay with pure NmFic proteins and pure GyrB43. *(a)* SDS-PAGE and *(b)* autoradiography of the SDS-PAGE gel after incubation of NmFic variants with [α-^{32}P]-ATP and pure GyrB proteins. The dimerization interface mutants catalyze the adenylylation of the target protein GyrB.

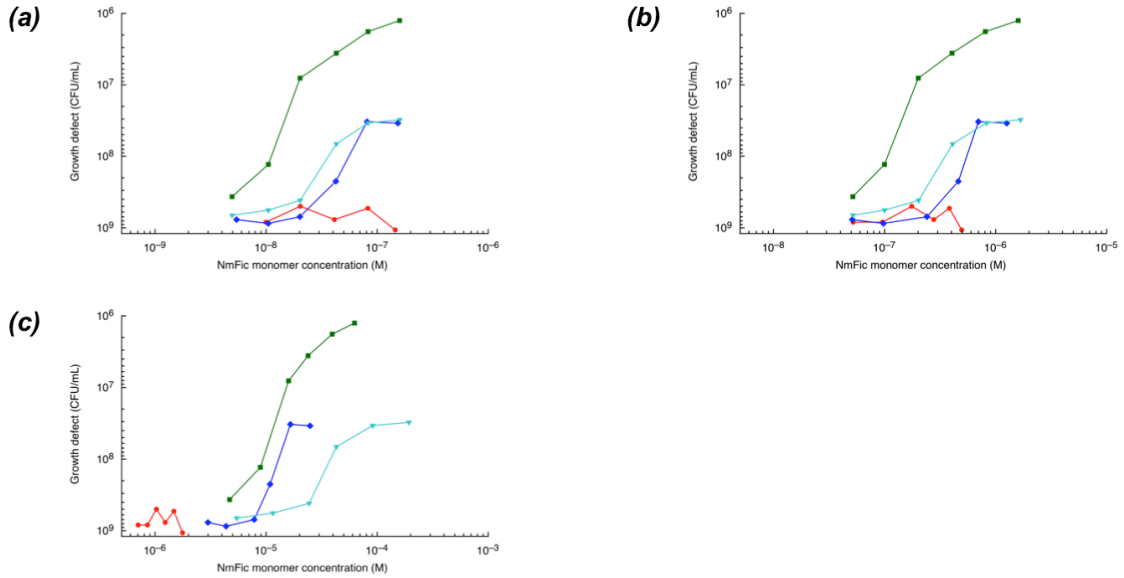

Figure S6. Calculated IPTG/[NmFic$_{monomer}$] ratios. Different equivalence and the resulting plots as in Figure 6 *(b)*, with *(a)* 100 µM IPTG = 0.01 µM NmFic, *(b)* 100 µM IPTG = 0.1 µM NmFic and *(c)* 100 µM IPTG = 10 µM NmFic.

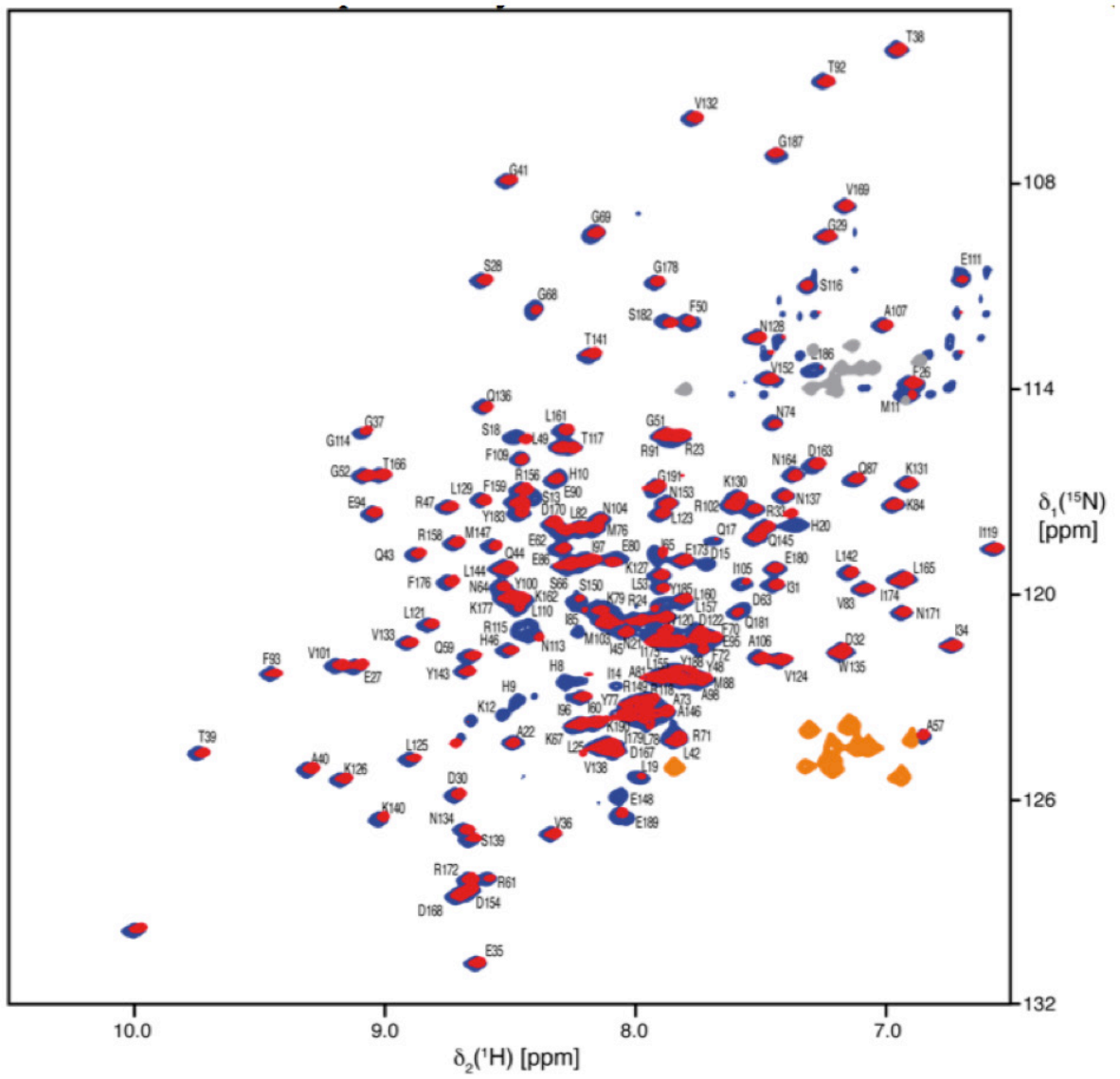

Figure S7. NMR fingerprint spectra of unmodified and auto-adenylylated NmFic. Overlay of 2D [^{15}N,^{1}H]-HSQC spectra of 0.5 mM [*U*-^{13}C,^{15}N]-labelled monomeric, inactive NmFic (NmFic$_{E102R,H107A,E156R}$) (blue) and of 0.25 mM [*U*-^{13}C,^{15}N]-labelled adenylylated monomeric inactive NmFic (NmFic$_{E102R,H107A,E156R}$) (red). Measurements were performed at 700 MHz in 25 mM MES assignment is indicated.

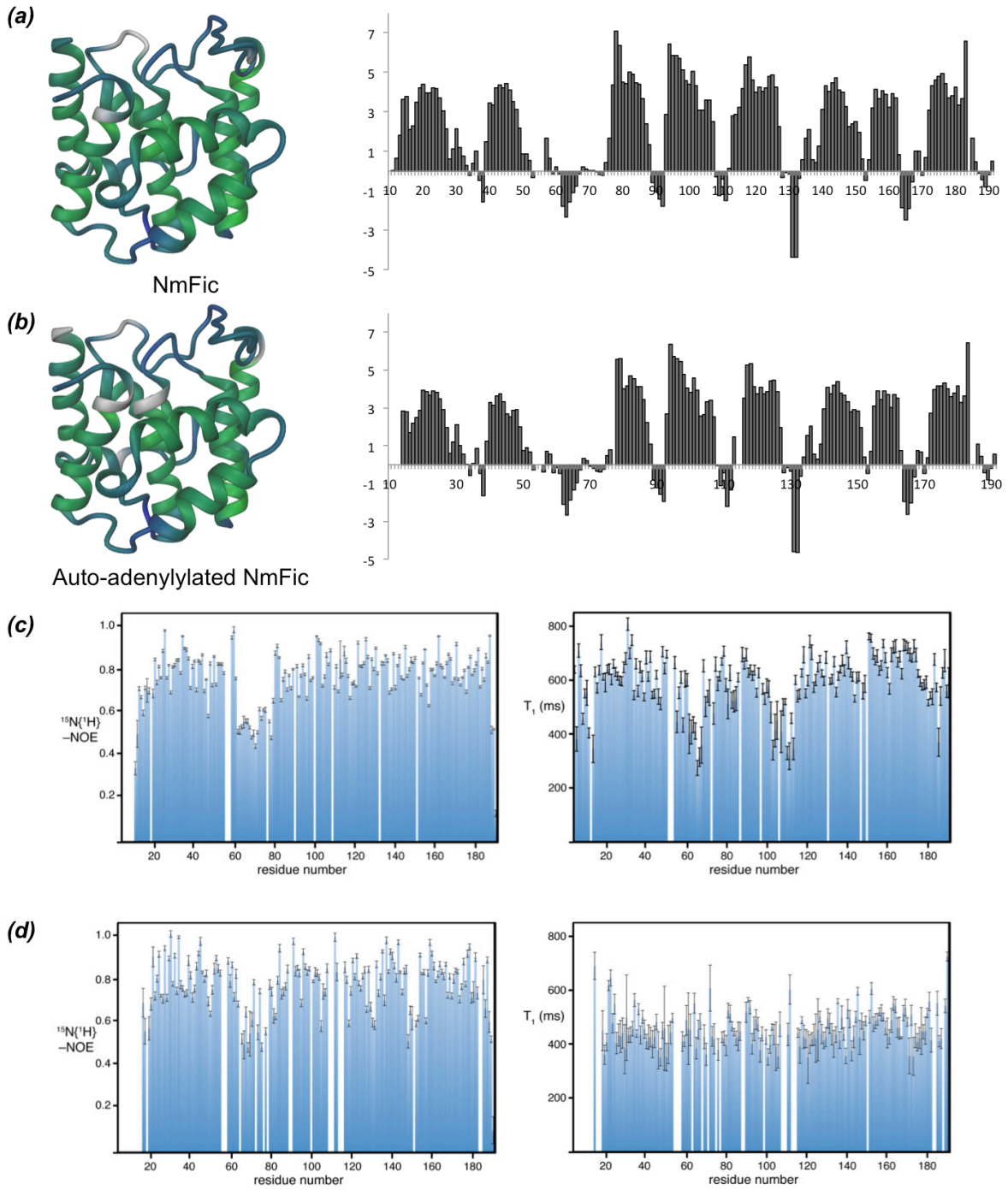

Figure S8. Secondary structure analysis of unmodified and adenylylated NmFic. Combined secondary chemical shifts for $^{13}C\alpha$ and 13Cβ of (a) unmodified and (b) adenylylated $NmFic_{E102R,H107A,E156R}$, plotted against the amino acid residue number. A 1–2–1 weighting function for residues (*i*-1) – *i* – (*i*+1) has been applied to the raw data. Consecutive stretches of positive and negative values indicate α-helix and β-sheet secondary structure elements, respectively. Heteronuclear NOE (left) and T_1 relaxation (right) experiment of (c) unmodified NmFic and *(d)* auto-adenylylated NmFic.

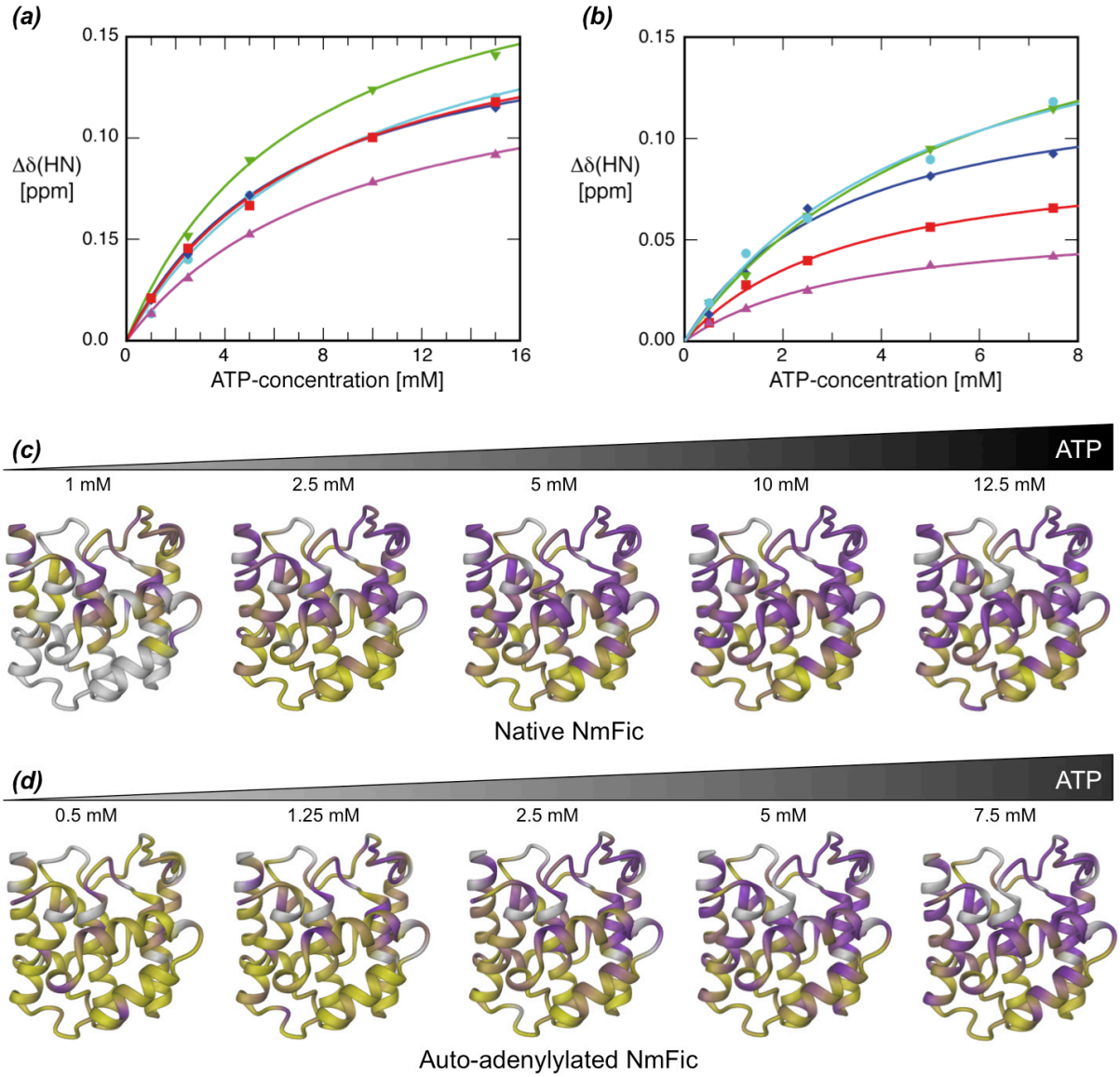

Figure S9. Effect of ATP binding on the NmFic monomer. Backbone amide chemical shift perturbations for selected residues upon titrating of *(a)* ATP to [*U*-^{13}C,^{15}N]–NmFic$_{E102R,H107A,E156R}$ (starting concentration 500 µM) and *(b)* ATP to adenylylated [*U*-^{13}C,^{15}N]–NmFic$_{E102R,H107A,E156R}$ (starting concentration 250 µM). The lines represent nonlinear least–squares best–fits of the normalized changes in the ^{1}H and ^{15}N chemical shifts using a bimolecular equilibrium binding model. The optimized value of the equilibrium dissociation constant is 7.8 ± 1.2 mM for *(a)* and 4.0 ± 1.1 mM for *(b)*. Chemical shift differences of the amide moiety of *(c)* native monomeric NmFic and *(d)* auto-adenylylated monomeric NmFic with Δδ(HN) as a function of the ATP concentration, relative to apo NmFic with a gradient from yellow (unchanged chemical shift) to purple (chemical shift change of 0.05 ppm and above). *(c)* Native monomeric NmFic and *(d)* auto-adenylylated monomeric NmFic.

References

1. Utsumi, R., Nakamoto, Y., Kawamukai, M., Himeno, M., and Komano, T. (1982) Involvement of cyclic AMP and its receptor protein in filamentation of an Escherichia coli fic mutant. J Bacteriol 151, 807–812
2. Yarbrough, M. L., Li, Y., Kinch, L. N., Grishin, N. V., Ball, H. L., and Orth, K. (2009) AMPylation of Rho GTPases by Vibrio VopS disrupts effector binding and downstream signaling. Science 323, 269–272
3. Engel, P., Goepfert, A., Stanger, F. V., Harms, A., Schmidt, A., Schirmer, T., and Dehio, C. (2012) Adenylylation control by intra- or intermolecular active-site obstruction in Fic proteins. Nature 482, 107–110
4. Garcia-Pino, A., Zenkin, N., and Loris, R. (2014) The many faces of Fic: structural and functional aspects of Fic enzymes. Trends in Biochemical Sciences 39, 121–129
5. Mukherjee, S., Liu, X., Arasaki, K., McDonough, J., Galán, J. E., and Roy, C. R. (2011) Modulation of Rab GTPase function by a protein phosphocholine transferase. Nature 477, 103–106
6. Campanacci, V., Mukherjee, S., Roy, C. R., and Cherfils, J. (2013) Structure of the Legionella effector AnkX reveals the mechanism of phosphocholine transfer by the FIC domain. EMBO J 32, 1469–1477
7. Castro-Roa, D., Gieter, S. D., Nuland, N. A. J. V., Loris, R., Garcia-Pino, A., and Zenkin, N. (2013) The Fic protein Doc uses an inverted substrate to phosphorylate and inactivate EF-Tu. Nat Chem Biol, 1–9
8. Cruz, J. W., Rothenbacher, F. P., Maehigashi, T., Lane, W. S., Dunham, C. M., and Woychik, N. A. (2014) Doc toxin is a kinase that inactivates elongation factor tu. J Biol Chem 289, 7788–7798
9. Luong, P., Kinch, L. N., Brautigam, C. A., Grishin, N. V., Tomchick, D. R., and Orth, K. (2010) Kinetic and structural insights into the mechanism of AMPylation by VopS FIC domain. Journal of Biological Chemistry 285, 20155
10. Xiao, J., Worby, C. A., Mattoo, S., Sankaran, B., and Dixon, J. E. (2010) Structural basis of Fic-mediated adenylylation. Nat Struct Mol Biol 17, 1004–1010
11. Palanivelu, D. V., Goepfert, A., Meury, M., Guye, P., Dehio, C., and Schirmer, T. (2011) Fic domain-catalyzed adenylylation: insight provided by the structural analysis of the type IV secretion system effector BepA. Protein science : a publication of the Protein Society 20, 492–499
12. Goepfert, A., Stanger, F. V., Dehio, C., and Schirmer, T. (2013) Conserved inhibitory mechanism and competent ATP binding mode for adenylyltransferases with fic fold. PLoS ONE 8, e64901
13. Kinch, L. N., Yarbrough, M. L., Orth, K., and Grishin, N. V. (2009) Fido, a novel AMPylation domain common to fic, doc, and AvrB. PLoS ONE 4, e5818
14. Gotfredsen, M., and Gerdes, K. (1998) The Escherichia coli relBE genes belong to a new toxin-antitoxin gene family. Mol Microbiol 29, 1065–1076
15. Zheng, L., Baumann, U., and Reymond, J.-L. (2004) An efficient one-step site-directed and site-saturation mutagenesis protocol. Nucleic Acids Res 32, e115
16. Brino, L., Urzhumtsev, A., Mousli, M., Bronner, C., Mitschler, A., Oudet, P., and Moras, D. (2000) Dimerization of Escherichia coli DNA-gyrase B provides a structural mechanism for activating the ATPase catalytic center. J Biol Chem 275, 9468–9475
17. Sambrook, J., Fritsch, E. F., and Maniatis, T. (1989) Molecular Cloning: A Laboratory Manual, 2nd Ed, Cold Spring Harbor Laboratory
18. Sundriyal, A., Massa, C., Samoray, D., Zehender, F., Sharpe, T., Jenal, U., and Schirmer, T. (2014) Inherent regulation of EAL domain-catalyzed hydrolysis of second

messenger cyclic di-GMP. J Biol Chem 289, 6978–6990

19. Levenberg, K. (1944) A method for the solution of certain non-linear problems in least squares. Quarterly Journal of Applied Mathmatics II, 164–168
20. Marquardt, D. W. (1963) An Algorithm for Least-Squares Estimation of Nonlinear Parameters. Journal of the Society for Industrial and Applied Mathematics 11, 431–441
21. van der Walt, S., Colbert, S. C., and Varoquaux, G. (2011) The NumPy Array: A Structure for Efficient Numerical Computation. Computing in Science & Engineering 13, 22–30
22. Paz-García, J. M., Johannesson, B., Ottosen, L. M., Ribeiro, A. B., and Rodríguez-Maroto, J. M. (2013) Computing multi-species chemical equilibrium with an algorithm based on the reaction extents. Computers & Chemical Engineering 58, 135–143
23. Kraft, D. (1994) Algorithm 733: TOMP–Fortran modules for optimal control calculations. ACM Transactions on Mathematical Software (TOMS) 20, 262–281
24. Chung, C. T., Niemela, S. L., and Miller, R. H. (1989) One-step preparation of competent Escherichia coli: transformation and storage of bacterial cells in the same solution. Proc Natl Acad Sci USA 86, 2172–2175
25. Pervushin, K., Riek, R., Wider, G., and Wüthrich, K. (1997) Attenuated T2 relaxation by mutual cancellation of dipole-dipole coupling and chemical shift anisotropy indicates an avenue to NMR structures of very large biological macromolecules in solution. Proc Natl Acad Sci USA 94, 12366–12371
26. Grzesiek, S., and Bax, A. (1992) Improved 3D Triple-Resonance NMR Techniques Applied to a 31-kDa Protein. Journal of Magnetic Resonance 96, 432–440
27. Kay, L. E., Ikura, M., Tschudin, R., and Bax, A. (2011) Three-dimensional triple-resonance NMR Spectroscopy of isotopically enriched proteins. 1990. J. Magn. Reson. 213, 423–441
28. Bax, A., and Ikura, M. (1991) An efficient 3D NMR technique for correlating the proton and 15N backbone amide resonances with the alpha-carbon of the preceding residue in uniformly 15N/13C enriched proteins. J. Biomol. NMR 1, 99–104
29. Grzesiek, S., Anglister, J., Ren, H., and Bax, A. (1993) 13C line narrowing by 2H decoupling in 2H/13C/15N enriched proteins. Application to triple resonance 4D J connectivity of sequential amides. J Am Chem Soc 115, 4369–4370
30. Clubb, R. T., Thanabal, V., and Wagner, G. (1992) A constant-time three-dimensional triple-resonance pulse scheme to correlate intraresidue 1HN, 15N, and 13C' chemical shifts in 15N-13C-labelled proteins. Journal of Magnetic Resonance 97, 213–217
31. Zhu, G., Xia, Y., Nicholson, L. K., and Sze, K. H. (2000) Protein Dynamics Measurements by TROSY-Based NMR Experiments. Journal of Magnetic Resonance 143, 423–426
32. Zhu, L., Sharp, J. D., Kobayashi, H., Woychik, N. A., and Inouye, M. (2010) Noncognate Mycobacterium tuberculosis toxin-antitoxins can physically and functionally interact. J Biol Chem 285, 39732–39738
33. Lee, D., Hilty, C., Wider, G., and Wüthrich, K. (2006) Effective rotational correlation times of proteins from NMR relaxation interference. Journal of Magnetic Resonance 178, 72–76
34. Güntert, P., Dötsch, V., Wider, G., and Wüthrich, K. (1992) Processing of multi-dimensional NMR data with the new software PROSA. J. Biomol. NMR 2, 619–629
35. Bartels, C., Xia, T.-H., Billeter, M., Güntert, P., and Wüthrich, K. (1995) The program XEASY for computer-supported NMR spectral analysis of biological macromolecules. J. Biomol. NMR 6, 1–10
36. Kjaergaard, M., and Poulsen, F. M. (2011) Sequence correction of random coil

chemical shifts: correlation between neighbor correction factors and changes in the Ramachandran distribution. J. Biomol. NMR 50, 157–165

37. Battye, T. G. G., Kontogiannis, L., Johnson, O., Powell, H. R., and Leslie, A. G. W. (2011) iMOSFLM: a new graphical interface for diffraction-image processing with MOSFLM. Acta Crystallogr D Biol Crystallogr 67, 271–281
38. Kabsch, W. (2010) XDS. Acta Crystallogr D Biol Crystallogr 66, 125–132
39. Evans, P. R., and Murshudov, G. N. (2013) How good are my data and what is the resolution? Acta Crystallogr D Biol Crystallogr 69, 1204–1214
40. McCoy, A. J., Grosse-Kunstleve, R. W., Adams, P. D., Winn, M. D., Storoni, L. C., and Read, R. J. (2007) Phaser crystallographic software. J Appl Crystallogr 40, 658–674
41. Emsley, P., Lohkamp, B., Scott, W. G., and Cowtan, K. (2010) Features and development of Coot. Acta Crystallogr D Biol Crystallogr 66, 486–501
42. Murshudov, G. N., Skubák, P., Lebedev, A. A., Pannu, N. S., Steiner, R. A., Nicholls, R. A., Winn, M. D., Long, F., and Vagin, A. A. (2011) REFMAC5 for the refinement of macromolecular crystal structures. Acta Crystallogr D Biol Crystallogr 67, 355–367
43. Adams, P. D., Afonine, P. V., Bunkóczi, G., Chen, V. B., Davis, I. W., Echols, N., Headd, J. J., Hung, L.-W., Kapral, G. J., Grosse-Kunstleve, R. W., McCoy, A. J., Moriarty, N. W., Oeffner, R., Read, R. J., Richardson, D. C., Richardson, J. S., Terwilliger, T. C., and Zwart, P. H. (2010) PHENIX: a comprehensive Python-based system for macromolecular structure solution. Acta Crystallogr D Biol Crystallogr 66, 213–221
44. Chen, V. B., Arendall, W. B., Headd, J. J., Keedy, D. A., Immormino, R. M., Kapral, G. J., Murray, L. W., Richardson, J. S., and Richardson, D. C. (2010) MolProbity: all-atom structure validation for macromolecular crystallography. Acta Crystallogr D Biol Crystallogr 66, 12–21
45. Urzhumtseva, L., Afonine, P. V., Adams, P. D., and Urzhumtsev, A. (2009) Crystallographic model quality at a glance. Acta Crystallogr D Biol Crystallogr 65, 297–300
46. Dutta, R., and Inouye, M. (2000) GHKL, an emergent ATPase/kinase superfamily. Trends in Biochemical Sciences 25, 24–28
47. Wigley, D. B., Davies, G. J., Dodson, E. J., Maxwell, A., and Dodson, G. (1991) Crystal structure of an N-terminal fragment of the DNA gyrase B protein. Nature 351, 624–629
48. Gross, C. H., Parsons, J. D., Grossman, T. H., Charifson, P. S., Bellon, S., Jernee, J., Dwyer, M., Chambers, S. P., Markland, W., Botfield, M., and Raybuck, S. A. (2003) Active-site residues of Escherichia coli DNA gyrase required in coupling ATP hydrolysis to DNA supercoiling and amino acid substitutions leading to novobiocin resistance. Antimicrob Agents Chemother 47, 1037–1046
49. Bates, A. D., Berger, J. M., and Maxwell, A. (2011) The ancestral role of ATP hydrolysis in type II topoisomerases: prevention of DNA double-strand breaks. Nucleic Acids Res 39, 6327–6339
50. Kleywegt, G. J. (1996) Use of non-crystallographic symmetry in protein structure refinement. Acta Crystallogr D Biol Crystallogr 52, 842–857
51. Li, G.-Y., Zhang, Y., Inouye, M., and Ikura, M. (2008) Structural mechanism of transcriptional autorepression of the Escherichia coli RelB/RelE antitoxin/toxin module. J Mol Biol 380, 107–119
52. Christensen, S. K., and Gerdes, K. (2003) RelE toxins from bacteria and Archaea cleave mRNAs on translating ribosomes, which are rescued by tmRNA. Mol Microbiol 48, 1389–1400
53. Oh, E., Becker, A. H., Sandikci, A., Huber, D., Chaba, R., Gloge, F., Nichols, R. J., Typas, A., Gross, C. A., Kramer, G., Weissman, J. S., and Bukau, B. (2011) Selective

ribosome profiling reveals the cotranslational chaperone action of trigger factor in vivo. Cell 147, 1295–1308

54. Kaiser, C. M., Chang, H.-C., Agashe, V. R., Lakshmipathy, S. K., Etchells, S. A., Hayer-Hartl, M., Hartl, F. U., and Barral, J. M. (2006) Real-time observation of trigger factor function on translating ribosomes. Nature 444, 455–460
55. Patzelt, H., Kramer, G., Rauch, T., Schönfeld, H.-J., Bukau, B., and Deuerling, E. (2002) Three-state equilibrium of Escherichia coli trigger factor. Biol. Chem. 383, 1611–1619
56. Rizzini, L., Favory, J.-J., Cloix, C., Faggionato, D., O'Hara, A., Kaiserli, E., Baumeister, R., Schäfer, E., Nagy, F., Jenkins, G. I., and Ulm, R. (2011) Perception of UV-B by the Arabidopsis UVR8 protein. Science 332, 103–106
57. Heijde, M., and Ulm, R. (2012) UV-B photoreceptor-mediated signalling in plants. Trends in Plant Science 17, 230–237
58. Pieles, K., Glatter, T., Harms, A., Schmidt, A., and Dehio, C. (2014) An experimental strategy for the identification of AMPylation targets from complex protein samples. Proteomics 14, 1048–1052
59. Feng, F., Yang, F., Rong, W., Wu, X., Zhang, J., Chen, S., He, C., and Zhou, J.-M. (2012) A Xanthomonas uridine 5′-monophosphate transferase inhibits plant immune kinases. Nature 485, 114–118
60. Goody, P. R., Heller, K., Oesterlin, L. K., Müller, M. P., Itzen, A., and Goody, R. S. (2012) Reversible phosphocholination of Rab proteins by Legionella pneumophila effector proteins. EMBO J 31, 1774–1784
61. Edgar, R. C. (2004) MUSCLE: multiple sequence alignment with high accuracy and high throughput. Nucleic Acids Res 32, 1792–1797

6.12. Unpublished results related to Research article IV

Over the course of my PhD project I generated different sets of data that are related to *Research article IV* but have so far not been included in any manuscript.

6.12.1. A "cold" adenylylation assay using biotinylated ATP

Adenylylation assays using [α-^{32}P]-ATP are not convenient and inflexible due to restrictions caused by radioactivity, and the radioactive labeling of adenylylation is also not easily compatible with downstream applications that could, e.g., identify adenylylated target proteins. Therefore, it seemed reasonable to investigate different forms of labeled ATP that would allow to visualize AMP transfer more effectively. At the beginning of my PhD project I examined whether biotinylated ATP could be an alternative to radioactivity, because the resulting biotinylation of adenylylated target proteins would be easy to detect in a procedure technically similar to Western Blotting and could also be used for pulldown experiments aimed at target identification[a]. Two compounds were tested based on a structural analysis of Arnaud Goepfert and Tilman Schirmer, EDA-ATP-biotin (labelled at the hydroxyl groups of the ribose) and N^6-(6-Amino)hexyl-ATP-biotin (labeled at the adenine ring; see molecular structures in Figure 21A).

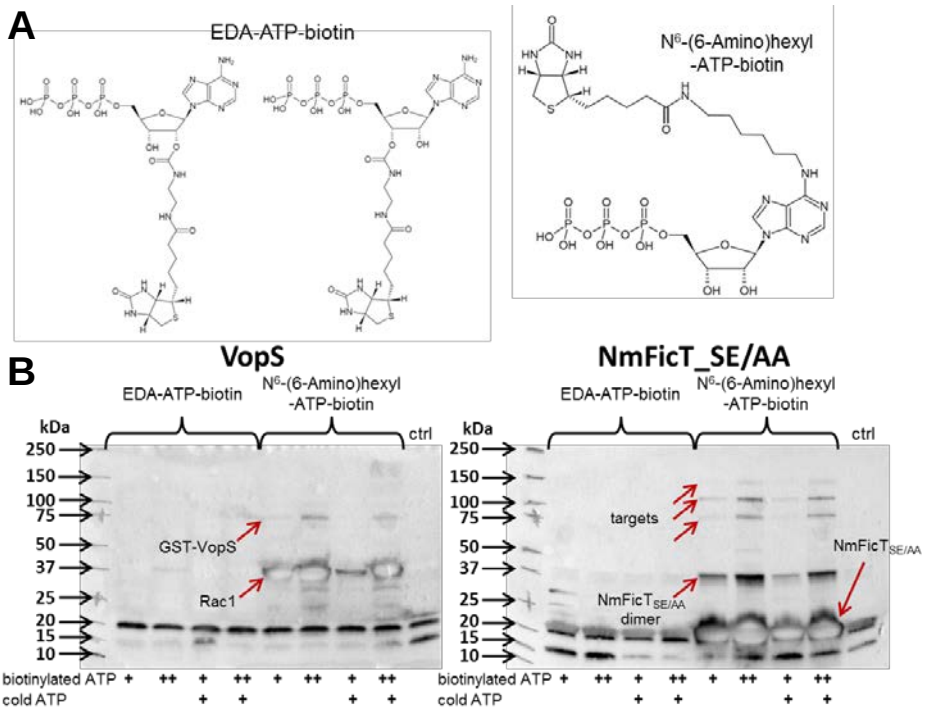

Figure 21: A "cold" adenylylation assay with biotinylated ATP. A) EDA-ATP-biotin and N^6-(6-Amino)hexyl-ATP-biotin are biotinylated at the hydroxyl groups of the ribose or at the adenine ring, respectively (adapted from the website of Jena Bioscience, www.jenabioscience.de. **B)** Classical adenylylation assays with *E. coli* lysates (like, e.g., in Figure 2A of *Research article III*) were performed with GST-VopS and Rac1-Q61L (left) or NmFicT_SE/AA and plain *E. coli* lysate (right). NmFicT_SE/AA had been obtained as purified protein from Frédéric Stanger and was added to reactions ad 0.3 µg/µl. Reactions were supplemented with cold ATP ad 150 µM (or not) and biotinylated ATP at 7.5 µM ("+") or 75 µM ("++") and incubated at 30°C for 1h. Subsequently, they were separated by SDS-PAGE and proteins were transferred on nitrocellulose membranes (semi-dry).

[a] These experiments had been performed before the adenylylated targets of VbhT or NmFicT were identified.

Biotinylation was detected using HRP-coupled streptavidin (Thermo Scientific) and visualized by chemoluminescence. The blots clearly show that only N^6-(6-Amino)hexyl-ATP-biotin was successfully used by Fic proteins for auto- and target adenylylation (arrows). It appears that 75 μM of labeled ATP in the absence of cold ATP is the optimal reaction condition. Background bands at 15 kDa and 20 kDa are also present in the absence of labeled ATP ("ctrl" reactions) and likely represent *E. coli* proteins that are biotinylated as part of cellular processes.

In my initial experiments I performed classical adenylylation assays using cleared lysates of *E. coli* that had expressed well-known VopS or NmFicT_SE/AA, a NmFicT construct that had previously been shown to adenylylate unknown targets in *E. coli* lysates (*Research article I*). While no biotinylation could be detected with EDA-ATP-biotin, N^6-(6-Amino)hexyl-ATP-biotin readily labeled the targets both of VopS as well as NmFicT_SE/AA with a clarity that had rarely been achieved using radioactivity (see Figure 21B). Unfortunately, VbhT or *Bartonella* effector proteins were apparently unable to use biotinylated ATP as a substrate for adenylylation (data not shown), but the success with NmFicT_SE/AA should pave the way towards the identification of the adenylylated targets of bacterial Fic proteins.
Interestingly, the improved sensitivity of detection of adenylylation with biotinylated ATP compared to radioactivity showed that not only NmFicT_Δ8, but also NmFicT_SE/AA adenylylates several different target proteins in *E. coli* lysates (compare Figure 3D of *Research article I* to Figure 21B).

6.12.2. Target adenylylation and biological function of NmFicT

Independent of their biological relevance, it was interesting to identify the diverse target proteins adenylylated by NmFicT in *E.coli* because they would provide valuable information on the target recognition of FIC domain proteins. Furthermore, both NmFicT as well as VbhT caused the adenylylation of a protein that we initially estimated to be of ca. 80 kDa molecular weight (see *Research article I*, but compare the analysis in Figure 22), indicating that the identification of targets adenylylated by NmFicT may also promote the research on VbhT which was not directly accessible for assays with biotinylated ATP.

Using NmFicT_Δ8, the construct that appeared to have the largest target range, I therefore performed adenylylation reactions with N^6-(6-Amino)hexyl-ATP-biotin in order to identify the target proteins by enrichment in subsequent biotin-streptavidin pulldown experiments. The visualization of input adenylylation reactions allowed to quantify the apparent molecular weight of the target proteins as a reference for the results of the pulldown experiments (Figure 22). For unknown reasons, I never achieved any reliable and reproducible enrichment of any protein in the pulldown experiments, but the mass spectrometry analyses repeatedly detected adenylylated peptides of different *E. coli* proteins. These were cloned and tested in *E. coli* lysate adenylylation assays, confirming that NmFicT_Δ8 adenylylates AtpD (ATP synthase F_1 complex β subunit), GyrB (DNA gyrase B subunit), and RpoB/C (RNA polymerase β and β' subunits). However, the far majority of targets adenylylated by

this protein have still remained elusive (see Figure 22B). Parallel experiments that tried to exploit the minimal adenylylation activity of VbhT with N^6-(6-Amino)hexyl-ATP-biotin also identified an adenylylated peptide of GyrB (not shown; see *Research article I*).

A

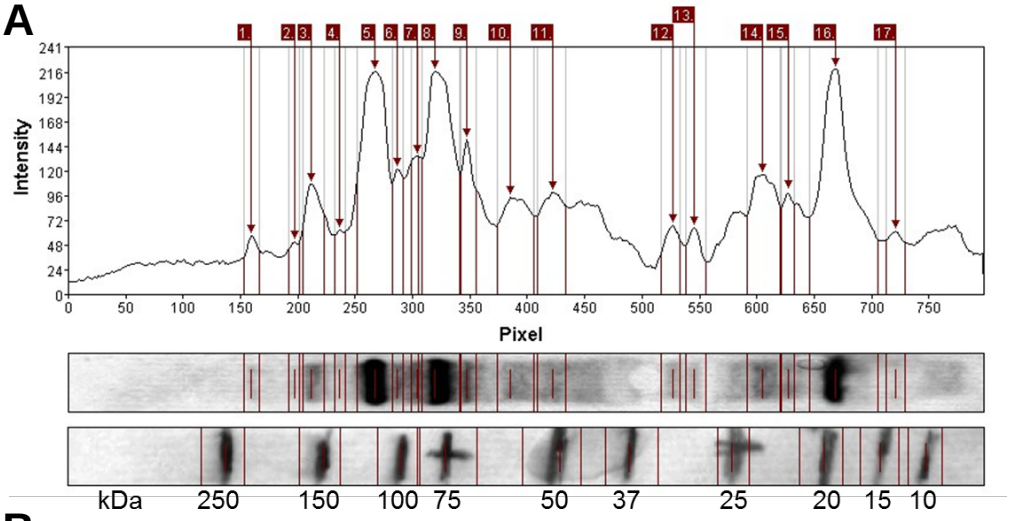

B

band	predicted Mw (kDa)	identity
1.	230	???
2.	184	???
3.	**168**	**RpoB / RpoC (151 / 155 kDa)**
4.	145	???
5.	**121**	**???**
6.	107	???
7.	98	???
8.	**89**	**GyrB (90 kDa)**

band	predicted Mw (kDa)	identity
9.	77	???
10.	62	???
11.	51	AtpD (50 kDa)
12.	31	
13.	28	??? ???
14.	22	background
15.	21	???
16.	**18**	**NmFicT_Δ8 (19 kDa)**
17.	16	background

Figure 22: NmFicT_Δ8 adenylylates a wide range of targets in *E. coli*. A) An adenylylation reaction with N^6-(6-Amino)hexyl-ATP-biotin was processed as described for Figure 21B. I analyzed the apparent molecular weight of the different adenylylation bands using the GelAnalyzer software (available at www.gelanalyzer.com) by fitting a logarithmic calibration curve on the bands of the molecular weight marker. **B)** Seventeen bands were clearly detected, and the three major target adenylylation bands visible in Figure 21B as well as the auto-adenylylation of NmFicT_Δ8 are highlighted in grey. Additional experiments (accidental detection of adenylylated peptides by mass spectrometry and / or the analysis of candidate proteins in lysate adenylylation assays) confirmed a number of proteins as adenylylation targets of NmFicT_Δ8, but the majority has remained unknown.

Interestingly, a series of follow-up experiments showed that the most wildtype-like construct NmFicT_E/G exclusively adenylylates GyrB of *E. coli* and not AtpD, RpoB/C, or any of the multiple unknown proteins targeted by NmFicT_Δ8. Because the latter construct is not more toxic than NmFicT_E/G (see Supplementary Figure 1B of *Research article I*) it seems likely that the various targets of NmFicT_Δ8 are not biologically relevant and rather simply reflect a relaxed target specificity upon deletion of the complete α_{inh} helix.

In contrast, it is of much greater biological relevance whether the NmFicT protein really evolved to target only GyrB (which, in *E. coli*, causes only mild growth inhibition; see Supplementary Figure 1B of *Research article I* and Figures 5 and 8 of *Research article IV*). I therefore tested a panel of type II topoisomerase B subunits in *E. coli* lysates for

adenylylation by VbhT (known to target both GyrB and ParE; see *Research article III*) and NmFicT_E/G (Figure 23).

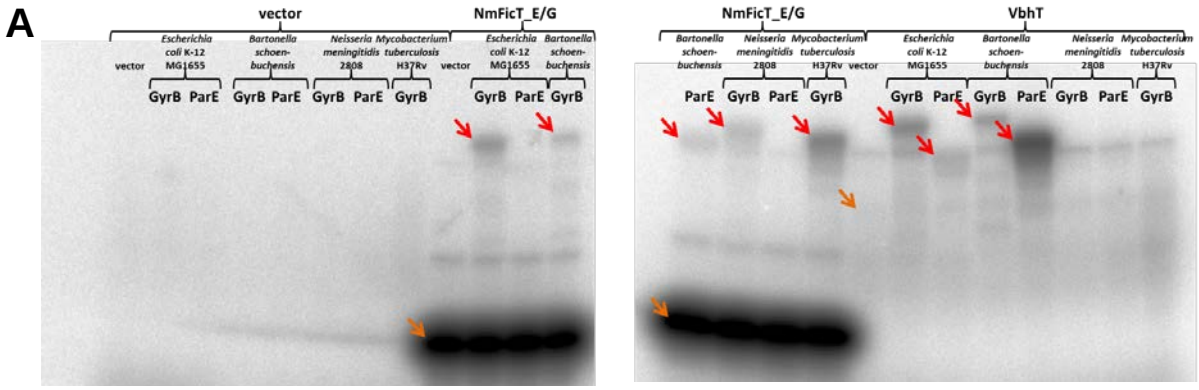

Figure 23: Target and host specificity of NmFicT_E/G and VbhT. The autoradiographs of a lysate adenylylation assay with NmFicT_E/G, VbhT, and different type II topoisomerase B subunits show that NmFicT_E/G adenylylates all GyrB orthologs that were tested, but ParE only of *B. schoenbuchensis*. VbhT adenylylates GyrB and ParE of *E. coli* and *B. schoenbuchensis*, but not of *N. meningitidis* or *M. tuberculosis* (the latter organism lacks topoisomerase IV). The experiment has been performed just as described for the lysate adenylylation assay in Figure 2A of *Research article III*. Target proteins (as GST fusions) are highlighted with red arrows, and Fic proteins are highlighted with orange arrows. The presence of all protein constructs was confirmed by Coomassie staining (not shown).

The results strongly suggest that NmFicT_E/G does *not* target ParE of its host organism *Neisseria meningitidis*, but this notion would need to be confirmed with purified proteins for certainty. While a biological function similar class I Fic proteins may be expected for the dual targeting of GyrB and ParE (see *Research article III*), a sole inhibition of DNA gyrase would point towards a role in the protection against DNA damage similar to, e.g., the GyrI protein of *E. coli*[356]. However, preliminary experiments so far failed to detect such an effect of NmFicT expression, while it was readily observed with GyrI. Nevertheless, future studies should focus on this aspect and test different experimental techniques as well as possibly other class III Fic proteins on top of NmFicT to thoroughly assess a potential function in DNA protection.

Closely linked to the question of its biological function is the search for a physiological trigger that would activate NmFicT *in vivo* as proposed in *Research article IV*. The GyrI protein of *E. coli* and a number of similar factors are typically controlled by the SOS response that is induced upon detection of DNA damage (see Box 1), but *N. meningitidis* appears to lack this signal transduction pathway[357]. Assuming a role in DNA damage protection, it is therefore more likely that NmFicT may somehow directly sense DNA damage without mediating cellular signaling, e.g., via effects on a potential transcriptional or translational autoregulation which could very well affect the monomer-tetramer equilibrium. Future studies should therefore investigate the activity of the *nmficT* promoter or homologous sequences in response to, e.g., DNA damage caused by mitomycin C or ciprofloxacin. Furthermore, it would be interesting to see if NmFicT interacts with parts of the cellular core machinery that could also provide signaling input.

6.13. Appendix: Further results

Over the course of my PhD work I generated data that cannot be directly linked to any *Research article* in the *Results* section. Furthermore, I shortly recapitulate some unpublished findings that I had already included in my Master thesis but that are nevertheless relevant for the *Perspective* developed further below.

6.13.1. *Bartonella* encodes FicTA toxin-antitoxin modules closely related to VbhTA

Early in my PhD work I discovered that *Bartonella* encodes classical FicTA modules (with single domain FicT toxins) that are closely related to VbhT. Interestingly, they are typically encoded together with Vbh type IV secretion machineries (see also Figure 38 in the *Perspective* section), suggesting that these FicTA modules may represent an evolutionary state preceding the acquisition of a type IV secretion signal by an ancestor of VbhTA. A sequence analysis revealed canonical Fic signature and Fic inhibition motifs and high overall primary sequence similarity among each other and also to other FicTA modules like YeFicTA (Figure 24A). Therefore, it was likely from the beginning that these FicTA modules would act as a toxin-antitoxin system targeting GyrB and ParE by adenylylation.

As a model for further investigation I chose BtrFicTA, a FicTA module encoded on the chromosome of *Bartonella tribocorum* CIP 105476 together with the remnants of a Vbh T4SS and a number of plasmid-associated genes[a], suggesting that the whole locus originates from the collapse of pVbh-like conjugative plasmid (see Figure 38). Like VbhT (Figure 2A in *Research article III*), BtrFicT adenylylates both GyrB and ParE of *E. coli* (Figure 24B) and of *Bartonella* (not shown).The expression of *btrficT* in *E. coli* results in growth arrest that depends on the toxin's adenylylation activity and can be inhibited by co-expression of the cognate antitoxin *btrficA* (see Figure 24C).

[a] BtrFicT had independently been disovered by Marius Liesch who described it in a side note of his Master thesis as a "FIC-encoding hypothetical protein of *B. tribocorum* (BT2350) which is encoded downstream of the Vbh T4SS […] but not coupled to a BID domain"[319].

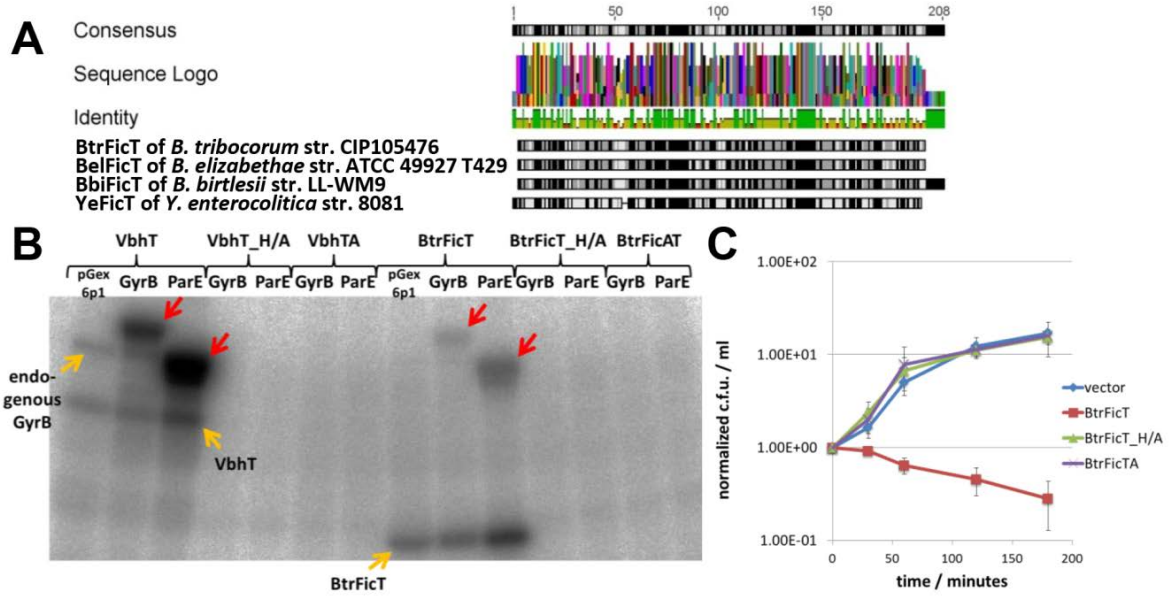

Figure 24: FicTA modules in *Bartonella* and the activities of BtrFicTA. A) Three putative FicTA modules were identified in *B. tribocorum* (BtrFicT is YP_001610356.1), *B. elizabethae* (BelFicT is WP_005774621), and *B. birtlesii* (BbiFicT is WP_006590445.1) by tblastn with different FicT toxins against several databases. An incomplete sequence of a homologous module was obtained for *B. washoensis* (not shown). The sequence alignment of the FicT homologs of *Bartonella* with YeFicT reveals high sequence similarity among the *Bartonella* FicT proteins (> 70% shared primary sequence) and considerable similarity to YeFicT (approximately 35% primary sequence identity). All FicT proteins display a canonical Fic signature motif and all cognate FicA homologs display a canonical Fic inhibition motif (not shown). This alignment was created using ClustalW implemented in Geneious v7.1.7 with gap open / extend costs of 10 / 0.1 and a BLOSUM cost matrix. Coloring reflects amino acid similarity according to the cost matrix with black = 100% identity and white = <60% identity. **B)** The adenylylation activity of BtrFicT was tested in a lysate adenylylation assay as shown in, e.g., Figure 2A of *Research article III*. It is clear from the autoradiograph that auto-adenylylation is detectable for both VbhT and BtrFicT, but no clear adenylylation of endogenous targets can be seen with BtrFicT (orange arrows). Ectopically expressed GST-GyrB and GST-ParE (of *E. coli*) are adenylylated both by VbhT and BtrFicT (red arrows). Adenylylation activities of VbhT and BtrFicT are consistently abolished in H/A active site mutants or in presence of cognate FicA antitoxins. **C)** The growth inhibition by BtrFicT was assayed in an experiment similar to the one described in Figure 1B of *Research article III*. While the expression of BtrFicT from a single-copy plasmid impairs the growth of *E. coli* Δ*ecficAT*, no such effect can be observed with the H/A active site mutant or upon co-expression of the cognate BtrFicA antitoxin.

In conclusion, my preliminary characterization of BtrFicTA made it apparent that FicTA modules in *Bartonella* are typical representatives of the FicTA toxin-antitoxin family just like YeFicTA or PaFicTA that I characterized in *Research article III*. From another perspective, they strongly resemble VbhT with the difference that they lack a type IV secretion signal.

6.13.2. Bep-associated FicA antitoxins in *Bartonella* and potential functions

Technically, it is relevant to mention that I continuously failed to obtain detectable amounts of BtrFicT in the "soluble" fraction of the cleared *E. coli* lysates that I typically used for adenylylation assays (Figure 25A). It had long been noted in our laboratory that the co-expression of cognate FicA antitoxins greatly improved the expression and solubility of FicT toxins or Beps with FIC domains, but this of course complicates the functional analysis of any adenylylation activity of these proteins.

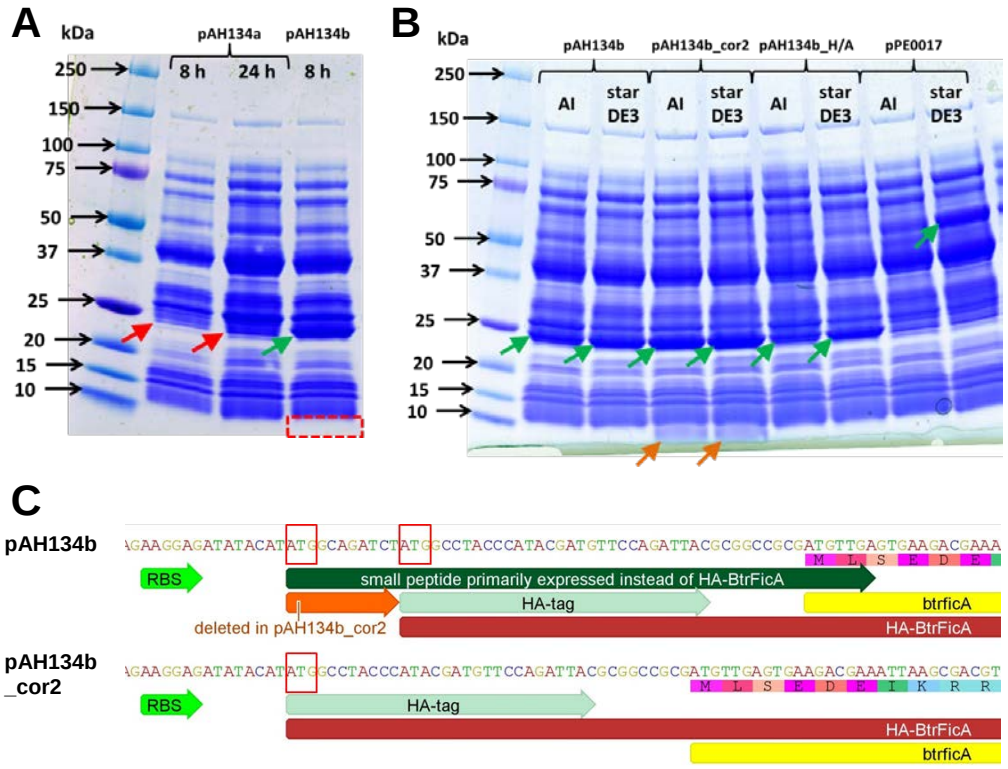

Figure 25: Improved expression of BtrFicT with BtrFicA under "restrained expression". A) The expression of *btrficT* alone (pAH134a) for different periods of time does not result in detectable BtrFicT in the cleared *E. coli* lysate as observed by Coomassie staining, while *btrficT* supposedly expressed together with *btrficA* (pAH134b) yields a considerable amount of BtrFicT (compare band at green arrow to the red arrows). However, no BtrFicA can be detected (red box). **B)** This expression experiment compared different *btrficTA* constructs (pAH134 series) with *vbhT* expressed from the isogenic pPE0017 plasmid in BL21-AI ("AI") or BL21-star (DE3) ("star DE3"). As expected from previous experiments (not shown), the yield of "soluble" VbhT in the cleared lysates is superior with BL21-star (DE3) (green arrow to the right). Similar to the result shown in (A), plasmid pAH134b (encoding *btrficT* and *btrficA*) results in considerable expression of BtrFicT but not BtrFicA, and the same is true for the catalytically inactive derivative pAH134b_H/A (green arrows). The deletion of a few base pairs in pAH134b restores expression of BtrFicA (in pAH134b_cor2; orange arrows) and abolishes growth inhibition (not shown). Active "BtrFicT" as well as "BtrFicT_H/A" shown in Figure 24 have been expressed from pAH134b vectors, while lysates generated with original pAH134a did not result in detectable adenylylation activity (not shown). **C)** Plasmid pAH134b encodes a start codon directly upstream of the HA-*btrficA* construct that causes translation of a small peptide of different frame (start codons are highlighted in red boxes). Because translation initiation at the ribosome binding site (RBS) typically uses the first available start codon, the translation of HA-BtrFicA in pAH134b is highly inefficient (see also the absence of detectable BtrFicA with this plasmid in (A) and (B)). Plasmid pAH134b_cor2 has been created by deletion of a few base pairs and linked the start codon of HA-*btrficA* to the ribosome binding site.

Interestingly, my first attempt to co-express *btrficT* and *btrficA* from the two multiple cloning sites of pRSFDuet-1 (as we did it, e.g., for the lysate adenylylation assays with VbhTA in *Research articles I* and *III*) resulted in a plasmid that caused growth inhibition comparable the absence of *btrficA* (data not shown). I was therefore not surprised to see that no BtrFicA was detectable by visual inspection of Coomassie stains of lysates obtained from these cultures, but quite excited by the considerable amount of BtrFicT (Figure 25B). A thorough analysis of the sequence of this co-expression plasmid (pAH134b) revealed a cloning mistake that resulted in an aberrant start codon a few base pairs upstream of the start codon of the antitoxin construct, but not in frame (Figure 25C). This genetic arrangement would allow only occasional expression of *btrficA* whenever a ribosome accidentally skips the first start codon, explaining both the growth inhibition and the absence of detectable BtrFicA.

Consistently, the repair of this cloning mistake abolished the growth inhibition and resulted in typical amounts of BtrFicA in cleared lysates (Figure 25B). In order to investigate the biochemical properties of BtrFicT I made use of the improved expression of this toxin under "restrained expression" of *btrficA* and routinely used plasmid pAH134b for the expression of "active" BtrFicT and analogously BtrFicT_H136A. The lysates generated from these expressions were later used to demonstrate auto-adenylylation and target adenylylation of BtrFicT (see above in Figure 24B).

From a general point of view, these results indicate that FicA antitoxins may aid the folding of FicT toxins, e.g., by preventing their aggregation via transient binding to some hydrophobic patches on their surface. Such a function could also explain why *Bartonella* effector proteins with FIC domains – in their majority not exhibiting any "toxicity" (personal observation) – are accompanied by at least one FicA-like antitoxin in all species (see Figure 26 for a comparison) that may act as a chaperone similar to effector chaperones in type III secretion (recently reviewed by Thomas *et al.*[358]). The *bona fide* effector "antitoxins" in *Bartonella* are generally not encoded directly together with any *bep* gene in a similar genetic arrangement as *ficAT* loci, but are found at a separate locus which may indicate that their expression level is adjusted to serve for the chaperoning of several or all Beps with FIC domains. In addition to effector binding, it is easily conceivable that the sequestration by FicA antitoxins inside *Bartonella* would also keep the Bep FIC domains in an inactive state, thereby preventing futile ATP hydrolysis prior to secretion into the host cell. Future studies should investigate the competitive index of *Bartonella ficA* mutants (including deletions of potential *ficAT* toxin-antitoxin modules) *in vivo* and try to unravel the precise biological function of these conserved proteins, e.g., upon challenge with different levels of stress in *in vitro* infections.

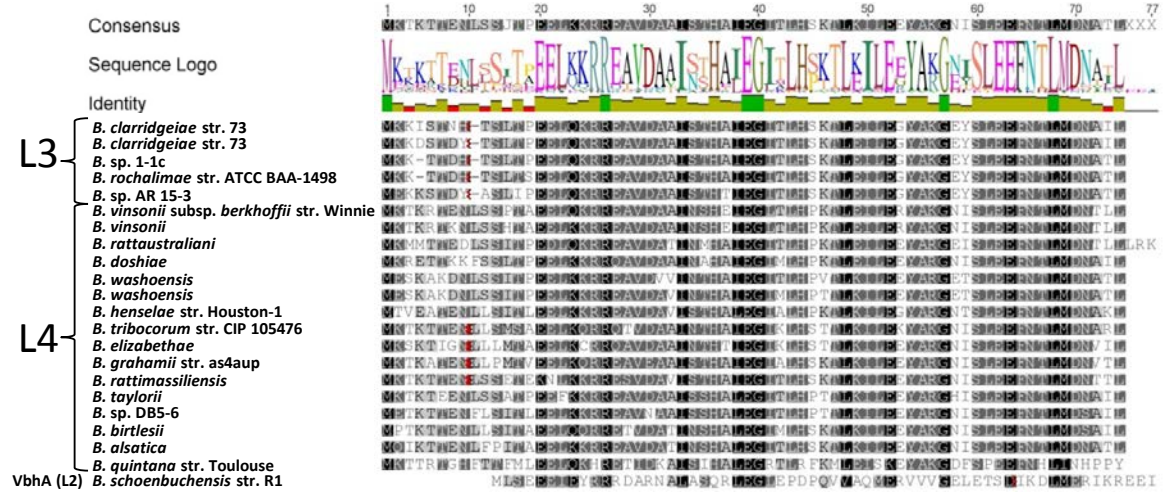

Figure 26: Sequence alignment of effector "antitoxins" in *Bartonella*. FicA homologs were identified by blastp with the ortholog of *B. rochalimae* that I had investigated in my Master project[359]. The sequences were aligned with VbhA of *B. schoenbuchensis* using ClustalW implemented in Geneious v7.1.7 with gap open / extend costs of 10 / 0.1 and a BLOSUM cost matrix. Coloring reflects amino acid similarity according to the cost matrix with black = 100% identity and white = <60% identity. Columns with >75% gaps were hidden (red). The far majority of sequences displays a canonical (S/T)xxxE(G/N) inhibition motif (see the invariant glutamate at position 39).

6.13.3. The OB-fold in Beps and VbhT was acquired *en bloc* with the BID domain

Bartonella effector proteins typically contain an OB-fold (oligonucleotide / oligosaccharide binding) between the FIC domain and the BID domain that has so far not been assigned to any function and whose origin had remained elusive[152]. Interestingly, my *in silico* analyses showed that the VbhT homologs of *B. grahamii* also contain an OB-fold, while VbhT of *B. schoenbuchensis* seems to lack the corresponding primary sequence (Figure 27). Over the course of additional sequence comparisons I discovered that not only *Bartonella* effector proteins, but also conjugative relaxases encode an OB-fold ahead of their BID domain (Figure 27). Given that these proteins are likely the evolutionary source of the type IV secretion signal of *Bartonella* effector proteins[311] it is plausible that the common ancestor of extant VbhT proteins and all Beps has been generated by a single sequence reshuffling event that fused an OB-BID module of a conjugative relaxase *en bloc* to the 3' end of a *ficT* gene (see further considerations in the *Perspective* at the end of this work).

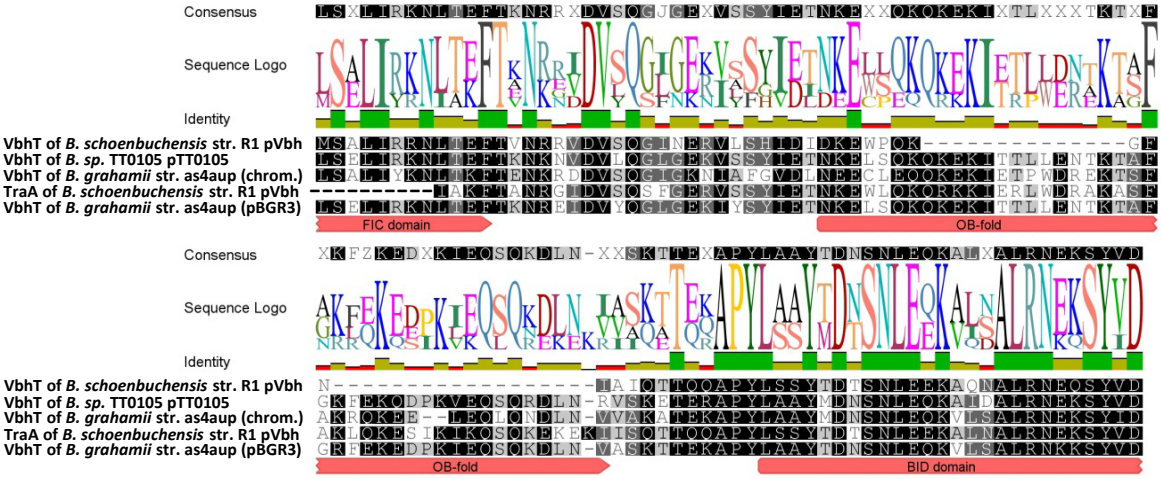

Figure 27: Alignment of the OB-fold region in VbhT homologs and a conjugative relaxase. The protein sequences of four VbhT homologs and the C-terminus of the TraA relaxase of *B. schoenbuchensis* R1 were aligned using ClustalW implemented in Geneious v7.1.7 with gap open / extend costs of 10 / 0.1 and a BLOSUM cost matrix. Coloring reflects amino acid similarity (ignoring gaps) according to the cost matrix with black = 100% identity and white = <60% identity. Protein domains were assigned by comparison to Bep domain annotations performed by Philipp Engel and Arnaud Goepfert in our laboratory. The alignment clearly shows that the protein sequence of the OB-fold in VbhT homologs is homologous to the corresponding sequence in the TraA relaxase. VbhT homologs and relaxase can be aligned continuously from the end of the FIC domain down to the C-termini of the proteins, suggesting that OB-fold and BID domain were acquired *en bloc* by a FicT-like ancestor of VbhT from a conjugative relaxase. Curiously, the primary sequence corresponding to the OB-fold is missing in VbhT of *B. schoenbuchensis* R1.

6.13.4. Broad analysis of *Bartonella* effector proteins

During my Master project I performed an extensive *in silico* analysis of *Bartonella* effector proteins and compared the Bep orthologs of four species of L3 and four species of L4 to get an overview of the conservation of critical residues as a basis for the subsequent functional investigation (Figure 28)[359].

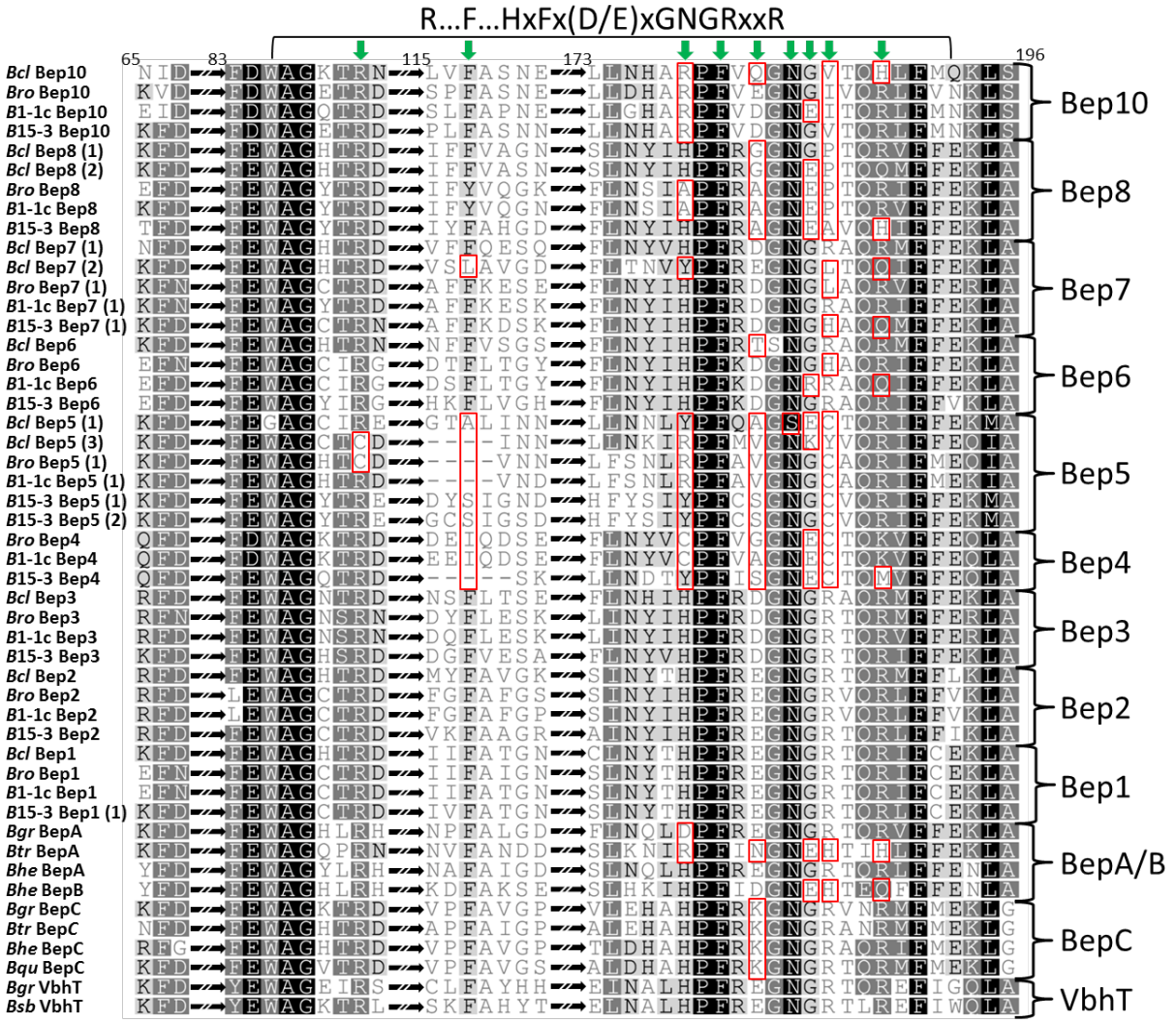

Figure 28: Bep FIC domain show mutations at particular positions and confined to certain orthologous groups. The FIC domains of *Bartonella* effector proteins were aligned using ClustalW implemented in Geneious as described in the original work and residues critical for adenylylation were indicated by green arrows (Figure 32 in my previous work[359]). Red boxes highlight deviations of Bep sequences at such positions, and it is apparent that these are distributed highly unevenly between the different orthologous groups. *Bartonella* species are indicated with a short three-letter code (*Bcl* = *B. clarridgeiae*, *Bro* = *B. rochalimae*, *B*11c = *B.* sp. 1-1c, *B*15-3 = *B.* sp. AR15-3, *Bgr* = *B. grahamii*, *Btr* = *B. tribocorum*, *Bhe* = *B. henselae*, *Bqu* = *B. quintana*). The results are summarized up and discussed in the running text.

In short, my analysis showed that no ortholog of VbhT or Bep1, Bep2, and Bep3 families deviates from the canonical Fic signature sequence, indicating that these proteins might have a conserved function in target adenylylation (Figure 28). The situation is completely different for the other groups of effectors[a] that display alternative sequence motifs at the active site which are often conserved among orthologs. It is well possible that at least some of these divergent active site motifs may have evolved to perform novel catalytic activities as it was shown, e.g., for Doc and AnkX (see in the *Introduction* section).

[a] However, I explicitly do not exclude that single orthologs of other Bep families that contain a canonical Fic active site motif might act via target adenylylation, e.g., for Bep clades 6 and 7.

As model species for a biochemical analysis of *Bartonella* effectors with FIC domains I chose well investigated *B. henselae* str. Houston-1 for L4 and *B. rochalimae* for L3[a]. Host-targeted effectors of all orthologous groups could be detectably expressed into the cleared lysates that I used for adenylylation assays throughout my Master project (not shown). I therefore investigated potential adenylylation activities but failed to detect any adenylylation with all effectors except for Bep1 and Bep2. Bep1 caused the adenylylation of small target proteins in host cell lysates (approximately 20 kDa) that I later identified as Rac1 and a few closely related small GTPases (Figure 29A). Interestingly, Bep1 targets Rac1 at the same residue as IbpA (Tyr32) but displays considerable specificity compared to VopS or IbpA in that it does not adenylylate RhoA or Cdc42 (Figure 29B). While all orthologs of Bep1 seem to target Rac1, its paralog Bep2 was found to adenylylate a different target of approximately 50 kDa molecular weight (Figure 29C; later identified as vimentin in *Research article II*).

[a] *B. rochalimae* was chosen because initial experiments had found superior expression of some of its effectors in *E. coli* compared to orthologs of other species (not shown).

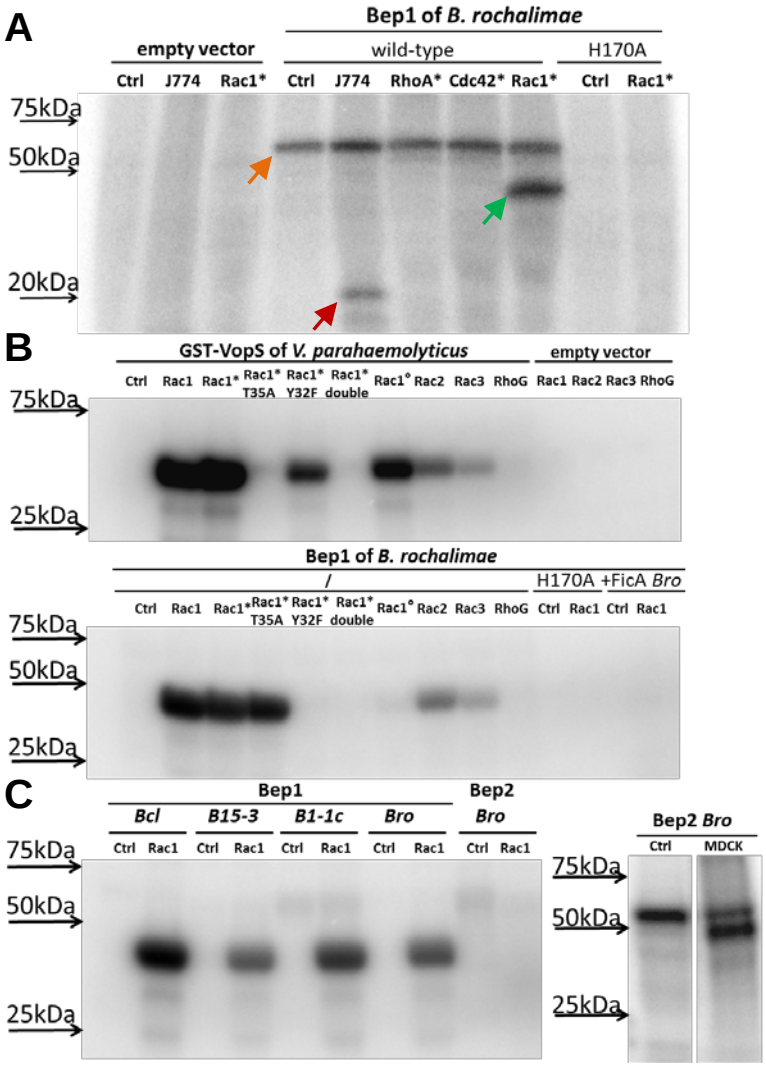

Figure 29: Specificity and diversification of the adenylylation activities of Bep1 and Bep2. The adenylylation activity of FIC domain proteins was investigated using cleared lysates of *E. coli* expressing different constructs with a procedure that we later published for VbhT (see, e.g., Figure 2A in *Research article I*). Targets were supplied either ectopically expressed as GST-fusions in *E. coli* lysates or in form of host cell lysates (see the protocol described in *Research article II*). **A)** Bep1 of *B. rochalimae* shows auto-adenylylation (orange arrows) and causes a double band of target adenylylation around 20 kDa in host cell lysates (here: J774 mouse macrophage; red arrow). Such a double band is characteristic of the electrophoretic migration of small GTPases that were shown to be adenylylated by distantly related FIC domain proteins IbpA and VopS. I therefore cloned different small GTPases as GST-fusions (with "*" indicating constitutively active mutants) and tested their adenylylation by Bep1. Unlike VopS or IbpA, Bep1 only adenylylates Rac1 and not Cdc42 or RhoA (green arrow). **B)** Bep1 targets Tyr32 of Rac1 since it is unable to adenylylate a Y32F mutant, while VopS (targeting T35) can adenylylate this construct. Different Rac1 constructs ("°" denoting the dominant-negative T17N mutant) were tested for adenylylation together with Rac2, Rac3, and RhoG that are closely related to Rac1. All these constructs were adenylylated by Bep1 (not visible for RhoG in this experiment due to weak expression). Generally, the adenylylation activity of Bep1 depended on the integrity of its active site motif (catalytic histidine mutated in H170A) and was inhibited by the FicA homolog of *B. rochalimae.* **C)** The four orthologs of Bep1 all adenylylate Rac1 while its paralog Bep2 does not and instead targets a protein of approximately 50 kDA in host cell lysates (here: MDCK dog cells for technical reasons). Figure panels were adapted from Figures 25-27 of my previous work[359].

No adenylylation was detected for any effector except for VbhT (see *Research article I*), Bep1, and Bep2 (not shown). These results are in line with the predictions of my *in silico* analysis, though an adenylylation activity of Bep3 would have been expected. I therefore investigated the protein sequence of Bep3 orthologs in more detail and discovered that the

extended N-termini characteristic of this family of effectors (as well as most orthologs of Bep4 and Bep5) contain FicA-like modules with α_{inh}-like sequences (Figure 30). From an evolutionary perspective, the fact that FicA orthologs and Beps are typically encoded together in the genomes of *Bartonella* makes it easily conceivable that a simple point mutation in a stop codon of *ficA* would result in a fusion protein similar to Bep3-5.

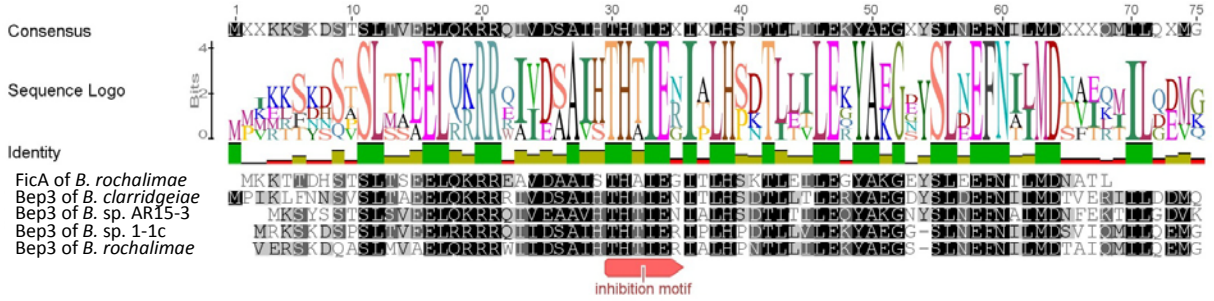

Figure 30: The N-terminus of Bep3-5 contains a FicA-like module. FicA of *B. rochalimae* was aligned to the N-termini of four Bep3 orthologs using ClustalW implemented in Geneious v7.1.7 with gap open / extend costs of 10 / 0.1 and a BLOSUM cost matrix. Coloring reflects amino acid similarity according to the cost matrix with black = 100% identity and white = <60% identity. It is clear that the N-terminus of Bep3 is homologous to FicA antitoxins, and all orthologs display a canonical (S/T)xxxE(G/N) inhibition motif (highlighted below the alignment; see the invariant glutamate at position 34). A similar alignment can be created with most orthologs of Bep4 and Bep5 (not shown).

It is likely that my failure to detect any adenylylation activity with Bep3 was caused by the FicA-like module of this effector which may either – as a conservative hypothesis – control the FIC domain similar to FicA antitoxins or – given that the α_{inh} manipulates substrate binding – rather modulate the enzymatic activity. The biological and biochemical role of these FicA-like modules in Bep3-5 could be investigated by future studies using targeted protein mutants and classical protein biochemistry. Notably, a similar module has been described for the RalF family of host-targeted effectors of *Legionella pneumophila* and *Rickettsia prowazekii*. In these proteins the GEF activity of the N-terminal "effector domain" is controlled by a C-terminal "capping domain" that also serves to localize the effector to divergent target pools inside the host cell in order to promote different biological functions[360].

The remarkable specificity and diversification of *Bartonella* effector proteins despite a high protein sequence similarity in their FIC domains raises the question how the target recognition of these proteins is mediated on the molecular level. *Bartonella* effector proteins lack obvious, large accessory modules like the arm sub-domain of VopS or IbpA[153], but my *in silico* analyses uncovered two sequence elements that appear to be candidates for a role in target recognition. First, I found that the FIC domains of *Bartonella* effectors contain a (nearly) Bep-specific β-hairpin adjacent to the "flap" that I had deliberately named "Bep-element" in my previous work[359] (highlighted in cyan in Figure 31). Second, the "flap" itself greatly differs in protein sequence and contains insertions of difference size (highlighted in violet in Figure 31). The considerable sequence conservation among Bep elements of

effector paralogs in *Bartonella* makes it unlikely that this region is directly involved in divergent target recognition, but the length and primary sequence of the β-hairpin flap differs between paralogous groups of Beps (Figure 31D). Future studies should therefore investigate the contribution of Bep-element and flap region to the target recognition of *Bartonella* effector proteins in more detail. For example, it would be interesting to exchange these modules between orthologs and paralogs of Bep1 and Bep2 for which the target spectrum is known (see above and in *Research article II*).

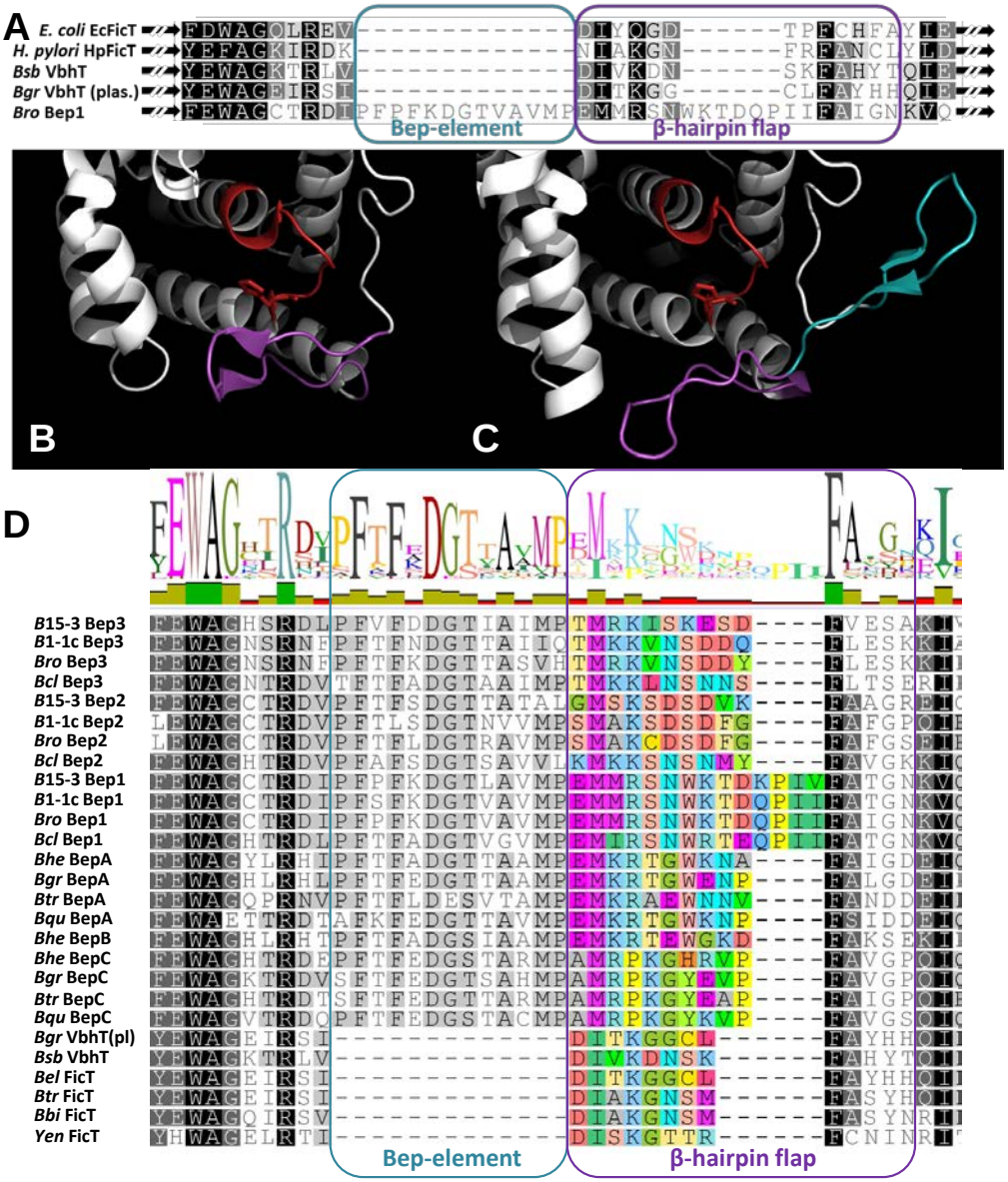

Figure 31: Two sequence features of *Bartonella* effector proteins that could be involved in target recognition. A) The FIC domains of five different proteins had been aligned to visualize the nearly Bep-specific "Bep-element" (cyan) and a Bep-specific elongation of the flap (violet). In (**B**) and (**C**) I highlighted the structural correlates of Bep-element (cyan) and β-hairpin flap (violet) on the structures of HpFicT and BepA of *B. henselae*, respectively. The active site loop of the FIC domains is shown in red for orientation. This figure was adapted from my Master thesis that contains additional details regarding the technical analysis[359]. **D)** FIC domain containing Beps of L4 as well as presumably adenylylation-competent effector clades of L3 (see Figure 28) were aligned using ClustalW implemented in Geneious v7.1.7 with gap open / extend costs of 10 / 0.1 and a BLOSUM cost matrix. Coloring reflects amino acid similarity according to the cost matrix with black = 100% identity and white = <60% identity. Bep element and the β-hairpin flap are highlighted in cyan and violet as shown in (A). The alignment makes clear that the primary sequence of the Bep element is very similar between Beps, while the N-terminal side of the flap as well as Bep-specific insertions at its tip are highly conserved among orthologous

groups, but differ among paralogs (amino acid sequence highlighted in color). By comparison, it is clear that VbhT and *Bartonella* FicT homologs as well as YeFicT lack the Bep-element and contain only a relatively short flap. Species names were abbreviated like in Figure 28 (*Bel* = *B. elizabethae*, *Bbi* = *B. birtlesii*, *Yen* = *Y. enterocolitica*). Only one of the two copies of Bep1 in *B.* sp. 15-3 is shown, and a six-amino-acid insertion after the variable region of the flap in Bep3 of *B.* sp. 15-3 was omitted for reasons of clarity. Additional data on the Bep-element are illustrated in Figure 43 that is part of the *Perspective* section.

6.13.5. Developing new tools for *Bartonella* genetics and microbiology

Over the course of my PhD project our laboratory repeatedly encountered problems with the plasmid-driven expression of toxic constructs in *Bartonella*. Together with Simone Eicher I discovered that these issues were caused by a pair of direct repeats flanking the P_{lac} promoter region of the most common plasmid backbones that were used for gene expression in *Bartonella*, and Maxime Quebatte identified additional repeats that greatly aggravated the instability of these vectors (not shown). In short, the considerable leaky expression of genes cloned into these plasmids selected for the emergence of clones which lacked the promoter region as a consequence of recombination events.

Maxime Quebatte therefore decided to repair the well-established plasmid backbone pCD341[361] and systematically modified the P_{lac} promoter to remove the repeat regions and at the same time achieve lower leaky expression. Using flow cytometry with a *gfp*-encoding derivative of pCD341, he could show that his construct with promoter variant #5 displayed very weak background expression and a smooth dose-dependent response to the inducer isopropyl-β-D-thiogalactopyranoside (IPTG) on the single-cell level (Maxime Quebatte, unpublished). The availability of such a superior tool motivated me to add another modification to it, because the use of the pCD341 backbone had so far been limited due to inherent problems with molecular cloning caused by topological peculiarities and its large size (>10'000 base pairs). In order to overcome this obstacle I cloned a *ccdB* toxin gene into the end of the multiple cloning site of the vector created by Maxime Quebatte and added a second multiple cloning site that I had designed *de novo* behind it, resulting in plasmid pBZ485_a. (Figure 32A). The CcdB toxin causes the formation of double-strand breaks in the cellular DNA[41] which is lethal already at low levels in *E. coli* cloning strains that are technically *recA*-deficient and therefore greatly impaired in double-strand break repair[a] (see Box 1 and in the *Extended Results* in the *Supplemental Information* of *Research article III*). The directional cloning of an insert using restriction sites in both multiple cloning sites replaces *ccdB*, so that a transformation of the ligation reaction allows the formation of colonies only for clones that obtained the desired ligation product and not uncut or re-ligated vector backbone. This strategy of negative selection has been first described more than twenty years ago[362] and is widely used in high-throughput cloning kits. As a proof-of-principle I transformed commercially available chemocompetent *E. coli* with 100 ng of uncut

[a] For this reason, the vector backbone with *ccdB* needs to be propagated in *E. coli* DB3.1 that is resistant against CcdB due to the *gyrA462* genotype.

pBZ485_a (i.e., an amount of backbone that is typically the upper limit used for ligations) and reproducibly obtained no colonies. Others have started to use pBZ485_a for their experiments and could confirm the convenience of cloning with *ccdB* counterselection as well as reliable expression of insert genes in *Bartonella* (not shown). One potential risk of pBZ485_a is that it encodes the mobilization functions of plasmid RSF1010 which are known to inhibit the function of a number of different type IV secretion systems[a], but no such effects have so far been observed in *Bartonella* with its ancestors that are isogenic in this respect (Maxime Quebatte, personal communication).

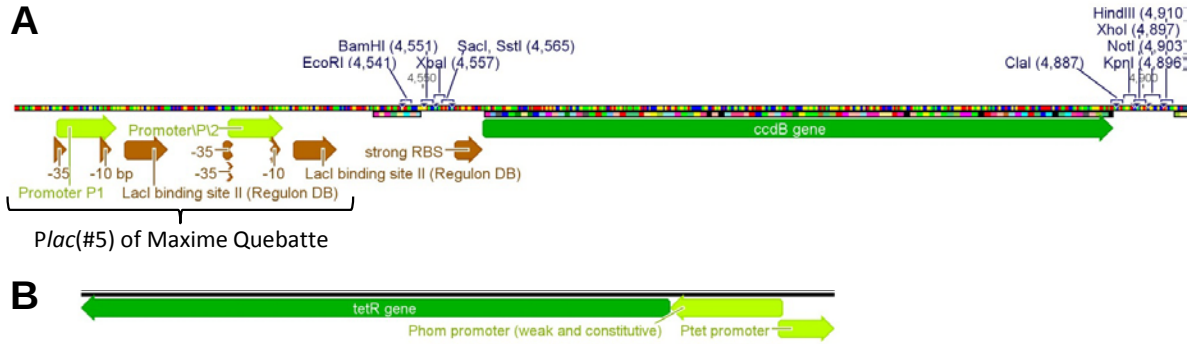

Figure 32: New gene expression vectors for *Bartonella*. A) The figure shows part of plasmid pBZ485_a with the P*lac*(#5) promoter created by Maxime Quebatte upstream of the *ccdB* gene which his flanked by two multiple cloning sites. **B)** The *tetR* / P*tet* module described by Nakashima and Tamura[367] contains the *terR* gene under the control of a weak, constitutive promoter facing opposite of P*tet*.

Encouraged by the success of pBZ485_a, Maxime Quebatte and I came to the conclusion that it would be useful to create a second expression plasmid as a replacement for previously used pPG100[311] that should be compatible with pBZ485_a. Furthermore, we decided to use a different promoter system than P_{lac} in order to enable the divergent expression of two genes in *Bartonella.* Preliminary experiments with L-arabinose-inducible P_{ara} or L-rhamnose-inducible P_{rha} promoters that I had cloned as *rfp* promoter fusions did not detect inducible expression in *Bartonella*, while the constructs were functional as predicted in *E. coli* (Maxime Quebatte, unpublished). Since we reasoned that this may be caused by the reluctance of *Bartonella* use (and import?) sugars as a carbon source[368], I decided to use a tetracycline-inducible P_{tet} system instead. A suitable module encoding P*tet* together with *tetR* that, in this system, acts as the inducer of the promoter, had previously been published by Nakashima and Tamura[367] (Figure 32B). In this study the authors showed that their P*tet* construct was far superior to other promoters with regard to the inducibility of the system (four orders of magnitude between expression in the absence and presence of induction). I have therefore

[a]RSF1010 is a mobilizable broad-host range plasmid that parasitizes a wide range of type IV secretion systems for its own conjugation[363]. However, it also interacts with host-targeting type IV secretion machineries to an extent that it impairs the secretion of their genuine substrates by blocking the coupling protein as shown for the *Agrobacterium tumefaciens* VirB/D4 T4SS[364] and validly proposed for the *Legionella pneumophila* Dot/Icm T4SS[365]. Furthermore, RSF1010 seems to impair plasmid transfer by the AvhB conjugation system of *Agrobacterium* tumefaciens that is closely related to the *Bartonella* VirB/D4 T4SS[366] (see below).

begun to create a vector (deliberately named pBZ485_b) using the backbone of well-established pPG100 that would contain the P_{tet} module upstream of the multiple cloning sites of pBZ485_a flanking *ccdB*. Like this, the same insert could be cloned into pBZ485_a and pBZ485_b using the same restriction sites.

7. Perspective

“Evolution does not produce novelties from scratch. It works on what already exists, either transforming a system to give it new functions or combining several systems to produce a more elaborate one. (...) New functions developed as new proteins appeared. But these were merely variations on previous themes. (…)

(Therefore, it) is not biochemical novelties that generated diversification of organisms. In all likelihood, it worked the other way around. It is the selective pressure resulting from changes in behavior or in ecological niches that led to biochemical adjustments and changes in molecular types. (...) The few big steps of evolution required acquisition of new information. But specialization and diversification occurred by using differently the same structural information.

(For that reason, all) living organisms are historical structures: literally creations of history. They represent, not a perfect product of engineering, but a patchwork of odd sets pieced together when and where opportunities arose.”

François Jacob, French biologist and Nobel laureate, in “Evolution and tinkering”. Science, Volume 196, Number 4295, 10 June 1977, 1161-1166 (continuation of the quote ahead of this work).

My work builds up on previous research of Henri Saenz and Philipp Engel who had greatly advanced our understanding of the co-evolution of the VirB/D4 T4SS and its host-targeted effectors with *Bartonella*[169,275]. It is their "shoulders of giants" like in Newton's famous quote that I could step upon and look back deeper into evolutionary history. Together, our studies suggest a model that describes – in a plausible way – the adaptive path from an ancestral conjugative machinery and an originally unrelated toxin-antitoxin module to the extant host-interacting type IV secretion system with a diversified effector repertoire. Importantly, the model suggests that the emergence of an interbacterial type IV secreted effector was critical as an evolutionary "missing link" between bacterial conjugation and host interaction.

In the words of Francis Crick[369],

> "A good model in biology (…) not only should address the problem in hand but if at all possible should serve to unite evidence from several different approaches so that various sorts of tests can be made of it. This may not always be possible to do straight away – the theory of natural selection could not immediately be tested at the cellular and the molecular level – but a theory will always command more attention if it is supported by unexpected evidence, particularly evidence of a different *kind*."

I will therefore present and discuss the evolutionary model in this *Perspective* section from different angles and continuously refer to the underlying evidence and the contributions of others. Furthermore, I will indicate whenever the model generates testable hypotheses at important steps and outline how these could be addressed experimentally to confirm, refine, or refute it.

7.1.Evolution of bacterial secretion systems

Bacterial secretion denotes the transport of biomolecules (typically proteins) across membranes from the inside of the cell to a compartment located further outside or into the extracellular milieu. So far, seven main types of dedicated bacterial protein secretion systems have been described (exhaustively reviewed in a recent special issue of Biochimica et Biophysica Acta[370,371]), and a number of additional mechanisms like secretion via outer membrane vesicles has not yet been included in this systematic catalog[372]. Many of these machineries comprise representatives that serve genuine bacterial functions as well as others that have been exapted for host interaction in symbiotic, commensal, or pathogenic contexts. The two most well studied secretion systems that can have critical roles in host interaction are the type III and type IV machineries which are analogous in the aspect that they typically secrete effector proteins from the bacterial cytoplasm into the host cytosol where these manipulate cellular signaling in favor of the bacterium[373,374]. However, while type

III secretion systems evolved from the flagellar machinery that was exapted for host-targeted effector secretion only once[375], host-interacting type IV secretion systems have repeatedly and independently evolved from bacterial conjugation systems[303]. This difference implies that the type IV secretion machinery may somehow be inherently prone to such an evolutionary event, likely because it already mediates the intercellular (yet inter-*bacterial*) transfer of (nucleo)protein complexes that can easily be modulated by adaptive tinkering[a]. The model presented in this *Perspective* describes the exaptation of a classical conjugative type IV secretion system into a host-interacting machinery in *Bartonella* with particular focus on the *de novo* evolution of its secreted effector proteins.

[a] The other known machinery that mediates direct interbacterial DNA transfer, mycobacterial type VII secretion systems[382,383], can also act as a virulence factor that delivers effector proteins into eukaryotic host cells, but the evolutionary connections have not yet been resolved (see the recent review by Houben *et al.*[376]).

7.2.Step I: Origin in bacterial conjugation systems

7.2.1. Conjugative type IV secretion mediates DNA transfer

Bacterial conjugation denotes the interbacterial transfer of DNA via type IV secretion, typically in the form of plasmids. Conjugative plasmid transfer has been suggested to be the most frequent mechanism of horizontal gene transfer that promotes the spread of diverse fitness traits such as antibiotic resistance, metabolic pathways, and machineries both for microscopic warfare as well as symbiotic, commensal, or pathogenic host interaction (recently reviewed by Guglielmini *et al.*[377]).

Conjugative machineries consist of a type IV secretion system (T4SS) that constitutes the "mating pair formation" (Mpf) complex, and a "DNA transfer replication" (Dtr) module that provides and processes the DNA substrate. Mpf and Dtr are physically and functionally linked by the so-called type IV coupling protein (T4CP). The molecular mechanism of conjugative plasmid transfer has been extensively reviewed, but most knowledge comes from a few model systems like the machineries of plasmid RSF1010 or the *E. coli* F-plasmid[304,363,378-380] (see a model in Figure 33). In short, the conjugation process is initiated in the donor cell upon receiving a dedicated signal that may be based on intercellular contact with potential recipients via the pilus of the Mpf machinery (1). Subsequently, the coupling protein docks to the type IV secretion machinery and recruits a Dtr / DNA complex that is called relaxasome. The relaxasome consists of a few accessory factors and a protein called relaxase that specifically binds to a DNA sequence called *oriT* ("origin of transfer") where it cuts a single strand at the *nic* site. Subsequently, conjugative transfer begins with the assembly of Dtr, Mpf, and coupling protein, and essentially denotes the translocation[a] of the relaxase that stays attached to the 5' end of the cleaved DNA single strand (2). Subsequently, this DNA strand is continuously pumped into the recipient cells (3), while the donor performs parallel "strand replacement synthesis" to substitute for it. DNA transfer itself is very fast (around 800 bp / s for the F-plasmid[379]). Because the ssDNA transfer into the recipient is initiated at the 5' end, complementary strand synthesis resembles the discontinuous "lagging strand" during dsDNA replication with repeated initiation and DNA replication in short bursts (see Box 3 below). However, the molecular mechanism of complementary strand synthesis is not well understood. At the end of plasmid transfer, the

[a] It has remained a major riddle whether conjugative transfer occurs through the lumen of the pilus itself or whether the pilus merely establishes contact between donor and recipient cells. Though this riddle has remained unresolved in general, the field seems to favor a function of F-pili (found in, e.g., conjugation of the F-plasmid) as a conduit for conjugative transfer, while this seems not to be the case for P-pili found e.g., with the *Agrobacterium* VirB/D4 T4SS or the RP4 machinery[379,381]. This issue has been recently reviewed together with the molecular mechanism of bacterial conjugation in general[382].

second half of the *oriT* enters the recipient cell and the plasmid is recircularized at *nic* by the relaxase (4).

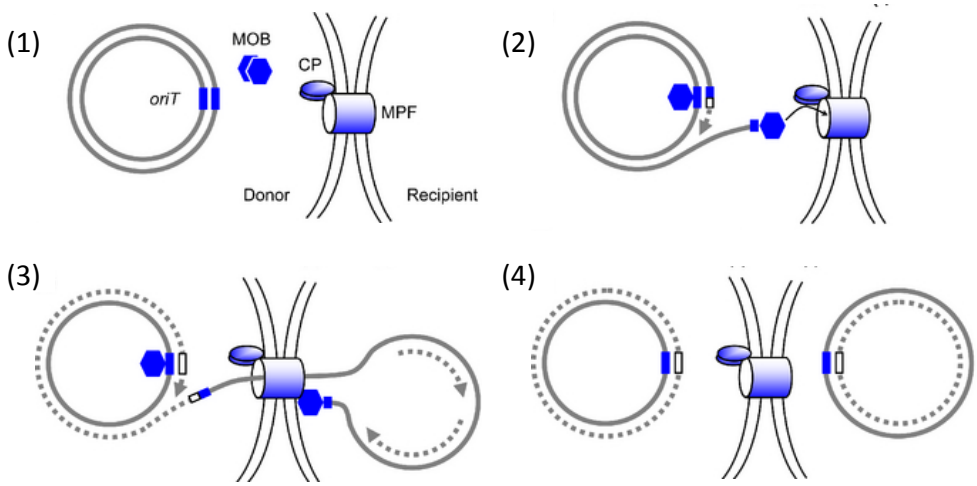

Figure 33: Simple model of bacterial conjugation. The process is explained in the running text from (1) to (4). Note that in this model the relaxase (MOB) is shown as staying attached to the channel of DNA transfer which has not been unambiguously demonstrated. The illustration was adapted from Bellanger *et al.*[383].

Conjugation generally either transfers plasmids or the plasmid-like state of integrative conjugative elements but, if a chromosomal *oriT* and dedicated mobilization functions are available, can also transfer whole bacterial chromosomes into the recipient[384,385]. Integrative conjugative elements (ICEs) are genomic islands encoding a conjugative type IV secretion system and can excise from the genome typically by site-specific recombination. After circularization, they conjugate in a transiently plasmid-like state (recently reviewed by Bellanger *et al.*[383]). There is no principal separation between ICEs and conjugative plasmids, but they are "essentially short-term variants of otherwise identical backbone elements"[377,386]. In contrast to conjugative "self-transmissible" entities, *mobilizable* plasmids or ICEs do not encode their own Mpf machinery but typically have dedicated Dtr functions. A recent study showed that mobilizable plasmids and ICEs outnumber conjugative ones[386].

7.2.2. Relatives of *Bartonella* plasmids and type IV machineries in Rhizobiales

The maintenance of sometimes quite a number of extrachromosomal replicons ranging from small cryptic plasmids to secondary chromosomes as well as the presence of both conjugative and / or host-interacting type IV secretion systems is characteristic of the α-proteobacterial order of Rhizobiales[387-389]. In this respect, *Bartonella* is a rather typical representative of this group, and it is not difficult to construct links between rhizobial relatives and the Vbh or VirB/D4 type IV secretion systems as well as the plasmids often encoding the Vbh machinery. It had already been noted by Saenz, Engel *et al.* that the Vbh T4SS is not only closely related to the VirB/D4 T4SS, but that the pVbh Mpf and Dtr functions are very similar to counterparts encoded on a particular family of rhizobial plasmids in, e.g.,

A. tumefaciens (pAT), *Rhizobium etli* (p42d), or *Sinorhizobium meliloti* (pSymA)[275] (see examples in Figure 34). The conjugative function of the Vbh-like type IV secretion systems on these plasmids has been well documented[366,390,391], and pSymA of *S. meliloti* as well as p42d of *R. etli* are classical symbiotic plasmids that carry genes important for plant interaction[392,393]. The pAT plasmid of *A. tumefaciens* appears not to have a critical role in the pathogenesis of this organism[a] and instead encodes various functions that confer a competitive advantage in soil[395,396]. According to a nomenclature that has been recently proposed, the Dtr functions of these plasmids (as well as pVbh) belong to type II of rhizobial conjugation systems[387], and their relaxase is a classical representative of the Mob_Q family[397]. Marius Liesch had already noted earlier that the relaxase of pVbh in *B. schoenbuchensis* str. R1 is very similar to those of these other rhizobial plasmids but differs from them in that it contains only one and not two BID domains at its C-terminus[319] (Figure 34A). *oriT* and *nic* of the relaxase encoded by p42d have been identified biochemically and were almost identical to obviously homologous sequences on other rhizobial plasmids of this group[397] including pVbh of *B. schoenbuchensis* R1[319] (Figure 34B).

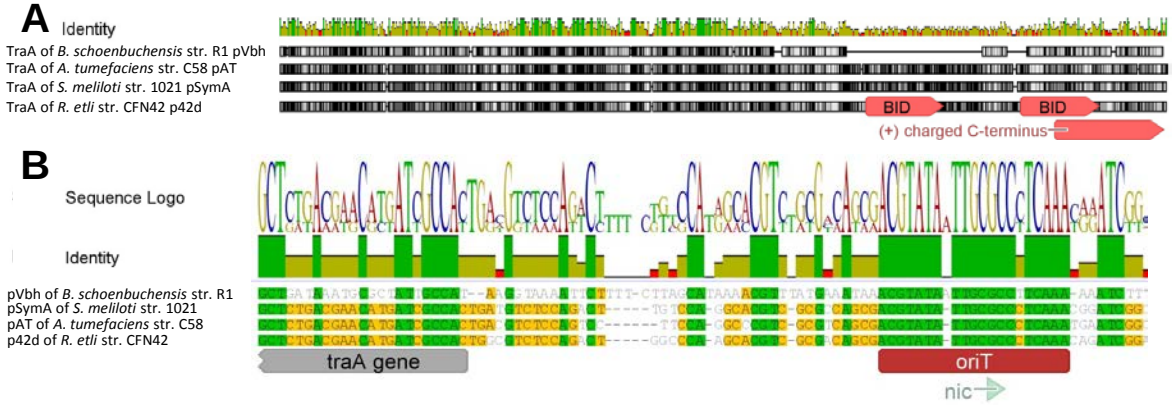

Figure 34: Similarity between conjugation functions of pVbh and rhizobial plasmids. A) TraA relaxase proteins of pVbh of *B. schoenbuchensis* R1 and the three rhizobial plasmids mentioned above have been aligned using ClustalW implemented in Geneious v7.1.7 with gap open / extend costs of 10 / 0.1 and a BLOSUM cost matrix. The alignment was manually curated and BID domains as well as positively charged C-termini were annotated as described by Pérez-Mendoza *et al.*[397]. Coloring reflects amino acid similarity according to the cost matrix with black = 100% identity and white = <60% identity. It is clear that TraA of *B. schoenbuchensis* lacks one BID domain and adjacent sequence that is present in the other relaxase proteins. Alignment of the sequence present in TraA of *B. schoenbuchensis* str. R1 with the distal C-terminal region of the other relaxases consistently yielded the best results. **B)** The *oriT* region of p42d of *R. etli* as described by Pérez-Mendoza *et al.*[397] was aligned to the corresponding sequence of pVbh and other rhizobial plasmids using a similar procedure as described for the protein alignment above (green = 100% identity). As already observed by Mariues Liesch[319], the putative *oriT* of pVbh and related rhizobial plasmids are almost identical.

[a] Two major plasmids are co-resident in *A. tumefaciens*, pAT and pTi. While pAT is a conjugative plasmid and encodes functions that are mostly advantageous in an environmental lifestyle (see running text), pTi encodes the T-DNA that is transferred by the VirB/D4 T4SS into plant cells where it integrates into the host genome and promotes tumor formation. Secretion of the Ti-DNA is accompanied by a set of effector proteins that primarily guide its way into the nucleus as well as its genomic integration (recently reviewed by A. Pitzschke[394]. Additionally, pTi also encodes a second, conjugative type IV secretion system (see below).

The conjugative type IV secretion system encoded on the three rhizobial plasmids mentioned above belongs to the MPF_T family and is therefore distantly related to the archetypal VirB/D4 T4SS of the Ti-plasmid of *A. tumefaciens* and other family members like RP4 or R388[380]. A recent phylogeny published by Guy *et al.* confirmed that the VirB/D4 and Vbh type IV secretion systems of *Bartonella* form a monophyletic group that is the sister clade of a group containing the conjugation systems of *A. tumefaciens*, *R. etli*, and *S. meliloti*[284] (shown in Figure 35). Therefore, one can say that backbone and conjugation functions of the pVbh plasmid in *Bartonella* have no features that would distinguish it from a typical conjugative plasmid of Rhizobiales which may simply have entered the genus via bacterial conjugation.

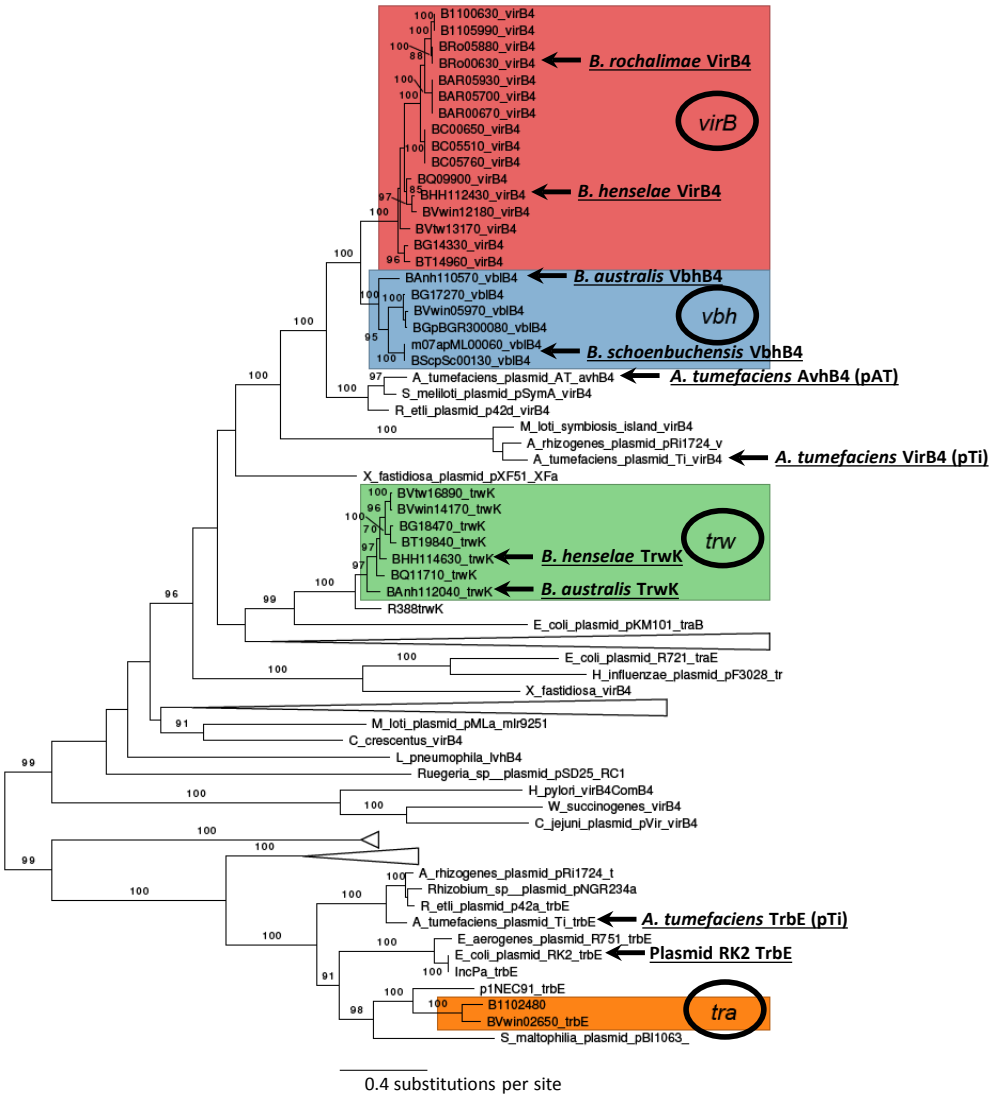

Figure 35: Phylogeny illustrating the evolutionary connections between type IV secretion systems of *Bartonella*. The phylogeny had been constructed on an alignment of VirB4 homologs and bootstrap support values higher than 90% of 100 are indicated at the branche. The four type IV secretion systems of *Bartonella* are indicated by color code and representative species are indicated. It is clearly apparent that VirB/D4 (*virB*, red) and Vbh (*vbh*, blue) machineries of *Bartonella* constitute a monophyletic group that is most closely related to a number of rhizobial conjugation systems mentioned in the running text. It is therefore likely that the VirB/D4 T4SS evolved in the genus *Bartonella* from a Vbh-like ancestor. Furthermore, the phylogeny illustrates the close relationship of the Trw T4SS (*trw*, green) to the machinery of conjugative plasmid R388 and the separate position of the *B. australis* Trw T4SS compare to those of L4 (see also *Unpublished results related to Review article I*). Another, rather elusive T4SS ("*tra*", orange) encoded in genomic islands of some bartonellae (see below) is only

distantly related to the other machineries of *Bartonella*. Note that the phylogeny also shows complex relationships between type IV secretion systems of other Rhizobiales. For example, the host-interacting VirB/D4 T4SS of the *A. tumefaciens* plasmid pT is rather closely related to Vbh and VirB/D4 machineries of *Bartonella*, but the conjugative AvhB T4SS of the *A. tumefaciens* pAT plasmid is even closer. Furthermore, the *conjugative* Trb T4SS encoded on the Ti-plasmid is rather distantly related to all these machineries and instead shares a more recent ancestry with the (RP4) T4SS encoded on the *E. coli* RK2 plasmid and the *tra* machinery of *Bartonella*. The phylogeny was adapted from Guy *et al.*[284].

From a functional point of view, it has been shown that the relaxase of the conjugative AvhB T4SS encoded on pAT of *A. tumefaciens* is secreted by the VirB/D4 machinery of *B. henselae*, suggesting that secretion signals may be generally compatible among the type IV secretion systems discussed in this section[311]. Not unexpectedly, Marius Liesch found that pVbh of *B. schoenbuchensis* str. R1 can conjugate into *B. henselae* with considerable efficiency (around 10^{-3} per recipient in the experimental setup that was used). Though it has been argued that the Vbh T4SS – being the only type IV secretion system in L2 – could have a role in virulence, Mariues Liesch failed to detect any positive evidence for this idea. For example, the Vbh T4SS could not complement a *B. henselae* mutant lacking the VirB/D4 machinery for effector secretion despite likely compatibility of secretion signals[319]. It is therefore not clear if the pVbh plasmid (at least in L2) has a direct function in *Bartonella* pathogenicity. An *in silico* analysis did not reveal obvious virulence factors on the pVbh plasmid of *B. schoenbuchensis* str. m07a (Figure 36), though a number of genes could not be conclusively assigned to any function. However, it appears that pVbh plasmids tend to harbor a considerable arsenal of toxin-antitoxin modules that may control persister formation at some point of the infection cycle similar to, e.g., TA modules of other pathogens[33,39,94]. Additionally, conjugative type IV secretion systems typically promote biofilm formation[398] which could also promote the colonization of niches in (arthropod or mammal) hosts. For example, it has been proposed that the ability to form biofilms in the flea fore gut was crucial for a *Y. enterocolitica* - like ancestor of *Y. pestis* to become transmitted by these vectors[399].

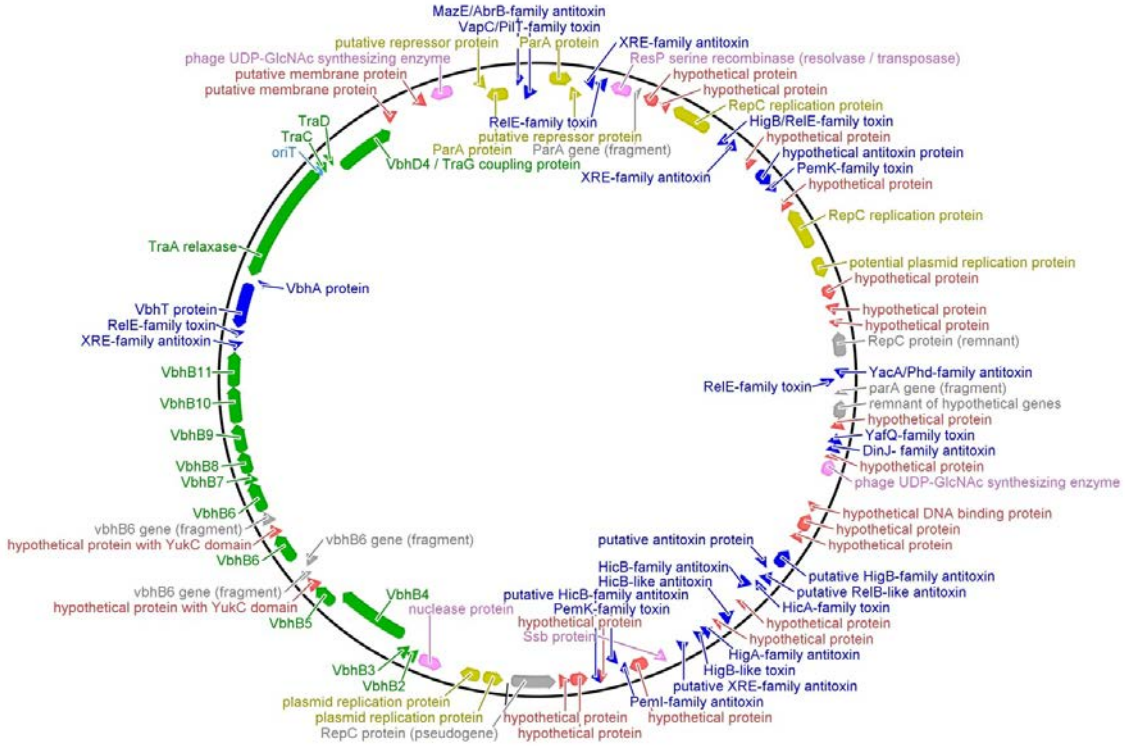

Figure 36: Full annotation of pVbh of *B. schoenbuchensis* str. m07a. Plasmid pVbh of *B. schoenbuchensis* str. m07a had been sequenced by Guy *et al.*[284] as "pML". The plasmid is nearly identical to pVbh of *B. schoenbuchensis* str. R1 that had been sequenced, yet not fully assembled, previously in our laboratory[319]. Importantly, pVbh of strain R1 is the source of the *vbhAT* module that has been characterized in *Research articles I* and *III*, but pVbh of strain m07a encodes genes with almost identical sequence. I manually annotated every gene on pVbh using different variants of BLAST, sequence comparisons, and literature mining. The plasmid encodes a complete conjugation system with Mpf, Dtr, and T4CP functions (highlighted in green), though the *vbh* locus encoding the T4SS contains a number of gene fragments (generally indicated by grey color). Similarly, pseudogenes that are obviously derived from other genes encoded on pVbh like *repC* or the partitioning functions can be found scattered over the plasmid in multiple copies. A surprising number of toxin-antitoxin modules (shown in blue) is scattered over the plasmid with sometimes unexpected combinations of toxin and antitoxin families, but the flexibility of these associations has been well described (see Figure 1C in the *Introduction* section). Genes encoding proteins involved in plasmid replication and partitioning are highlighted in yellow. Of those genes typically involved in replication via a *repABC* mechanism only *repC* could be safely identified. However, it has been shown that RepC alone is necessary and sufficient for plasmid replication, while RepA and RepB have rather accessory roles[400]. A number of genes could not be assigned to any function (shown in red). Five genes could be identified that are neither necessary for the functioning of a conjugative plasmid nor part of toxin-antitoxin modules (highlighted in magenta). Two copies of an apparently phage-derived UDP-GlcNAC synthesizing enzyme are encoded on pVbh. This gene is found in all bartonellae except for *B. tamiae* and *B. australis*, often in several copies and in chromosomal phage loci (personal observation). A ResP serine site-specific recombinase is present on pVbh and all homologous replicons in *Bartonella*. It is possible that this protein is involved in plasmid multimer resolution, but it may also promote the frequent genomic integrations that are observed for *vbh* replicons as it is common among ICE recombinases[386] (but see below). Furthermore, an elusive nuclease protein is encoded directly upstream of *vbhB2* and conserved among the far majority of *vbh* as well as *virB* loci of *Bartonella*[275]. The function of this gene is unclear, but it could be involved in the functionality of the T4SS because both Vbh and VirB/D4 machineries lack the (not essential) VirB1 lytic transglycosylase that is involved in pilus biogenesis[401]. Plasmid pVbh also encodes an *ssb* single-strand binding protein that could be involved in complementary strand synthesis in the recipient cell as described for other conjugative plasmids[402] (but see below).

Plasmid pVbh or chromosomal derivatives can be found in the majority of *Bartonella* species (Figure 37). While the plasmid copies in *B. schoenbuchensis* or *B. grahamii* (called pBGR3[318]) reveal the presence of an intact conjugative machinery, it has already been noted earlier by Saenz, Engel *et al.*[275] that most chromosomal copies have been subject to considerable sequence deterioration and are obviously inactive with regard to bacterial

conjugation. These authors also revealed that – at an earlier state of their evolutionary history – additional species like *B. quintana* harbored a chromosomal *vbh* locus that has been largely reduced in the extant genomes. It is therefore highly unlikely that plasmid pVbh exhibits a facultatively ICE-like behavior as could have been imagined from the high frequency of genomic integration. Instead, pVbh appears to be a genuine conjugative plasmid that may simply suffer from genetic instability and inadvertent chromosomal integrations, e.g., due to recombinogenic sequences or regions with strong homologies to the chromosome like the Mpf locus (compare Figure 36).

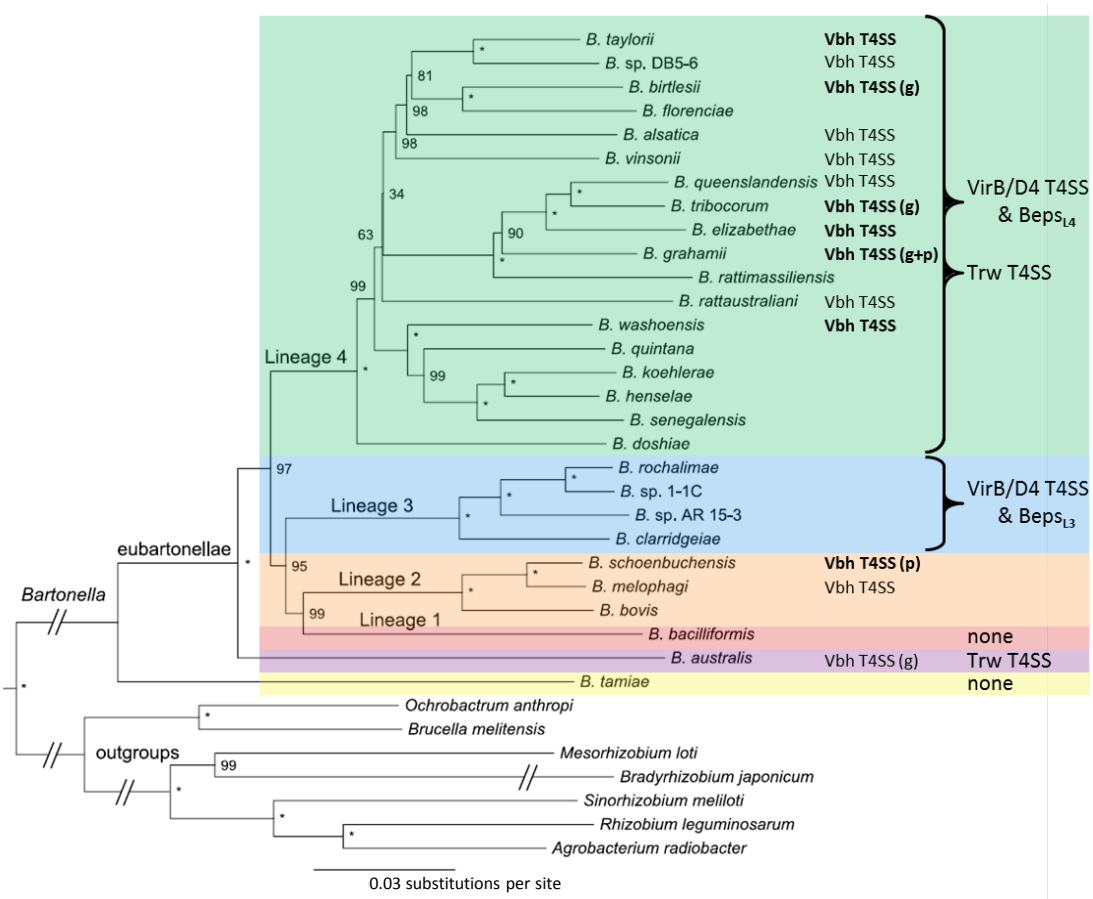

Figure 37: The distribution of chromosomal and extrachromosomal copies of pVbh in *Bartonella*. The phylogenetic tree (see details in Figure 15) illustrates the phylogenetic distribution of the Vbh T4SS in *Bartonella* (compare Figure 35 for their phylogenetic relations). Presence of absence of the Vbh T4SS was assessed by BLAST searches with the nucleotide sequence of the full *vbh* locus of *B. schoenbuchensis* str. R1 pVbh against the genus *Bartonella*. BLAST hits were manually inspected to determine whether the *vbh* locus forms a genomic island (g) or is encoded on a plasmid (p), but in many cases no clear result was obtained for *vbh* loci on small contigs. Note that – in contrast to previous findings of Saenz, Engel, *et al*.[275] that were based on PCR amplification – I failed to detect any evidence of a *vbh* locus in any strain of *B. bovis* , suggesting that the sequences submitted to the databases may be incomplete or that a potential pVbh plasmid may have been omitted in genome sequencing. The presence of FIC domain proteins associated to the *vbh* locus is indicated by bold font (see also Figure 24 and linked running text in *Appendix: Further results*). While *vbh* loci in plasmids typically encode seemingly intact Mpf, Dtr, and T4CP, chromosomal loci are usually deteriorated and lack Dtr functions as well as T4CP in addition to deletions and pseudogenization of Mpf genes. All chromosomal copies are surrounded by homologs of plasmid replication or partitioning genes as well as scattered toxin-antitoxin modules that are all also found on pVbh, suggesting that chromosomal *vbh* loci are derived from the integration of a pVbh plasmid.

In addition to pVbh a number of *Bartonella* species contain small, cryptic plasmids that encode not much more than essential replication functions and a relaxase (e.g., pBGR1 of *B. grahamii*[403] or pMS of *B. schoenbuchensis* str. m07a[284]). Furthermore, genomic islands encoding an type IV secretion machinery that is related to the conjugative Trb T4SS of the *A. tumefaciens* virulence plasmid pTi have been described by Guy *et al.*[284] as the "*tra*" T4SS (compare Figure 35). While the *tra* locus of *B.* sp. 1-1c has undergone considerable deterioration, more extended loci can be found in the genomes of *B. vinsonii* subsp. *berkhoffii* str. Winnie, *B. rattimassiliensis* str. 15908, and particularly in *B. alsatica* strain IBS 382 (personal observation). Interestingly, these loci often encode a class II Fic protein that displays the characteristic FicN-FIC-wHTH domain architecture discussed in the *Unpublished results related to Research article I*. Furthermore, a number of additional replicons are found with a more restricted distribution among the bartonellae. For example, plasmid pNH4 was isolated from *B rattaustraliani* and encodes no Mpf functions, but a Dtr locus that is very similar to the pVbh Dtr region. pNH4 can therefore be seen as a mobilizable derivative of pVbh and encodes only few additional genes including, e.g., another class II Fic protein. Interestingly, it has been claimed that the conjugation of pNH4 into *B. henselae* resulted in bacteria that had the ability to replicate in amoeba[404], though the genetic basis of this phenomenon is unclear.

With regard to the biological function of pVbh it would be interesting to follow up on early experiments of Marius Liesch and try to establish the bovine endothelial cell infection model of Guy *et al.*[284] in our laboratory. Since they readily observed infection of these cells with *B. bovis*, it is tempting to speculate that closely related *B. schoenbuchensis* may also be able to invade these cells and traffic to the typical vacuolar niche of *Bartonella* (see *Review article I*). Such an *in vitro* infection model would allow to investigate whether the pVbh plasmid has a role in virulence and, if yes, which factors encoded on this replicon are involved in pathogenesis.

7.3.Step II: A FIC domain protein enters the scene

In the previous section I presented compelling evidence that a Vbh-like plasmid may have entered *Bartonella* from other Rhizobiales simply by conjugation using its own dedicated machinery and that such a plasmid may or may not have already promoted *Bartonella* virulence in one or the other way. However, none of the rhizobial plasmids that are closely related to pVbh encodes any FIC domain protein that would be particularly similar to the FIC domains of *Bartonella* effector proteins, while I could show that genomic islands derived from pVbh plasmids encode a FicTA toxin-antitoxin module that is closely related to the Beps (Figure 38A; see also Figure 24 in *Appendix: Further results*). The closest relatives of this FicTA module outside *Bartonella* are found in environmental proteobacteria, e.g., in a phage

island in the genome of plant-infecting γ–proteobacterium *Xylella fastidiosa* or on a family of conjugative plasmids isolated from soil-dwelling β-proteobacteria (Figure 38B). These plasmids comprise, e.g., pEST4011 of *Achromobacter denitrificans* or pIJB1 of *Burkholderia cepacia* and belong to the IncP-1 group of replicons[405]. Interestingly, the conjugative machinery encoded on these plasmids does not display considerable sequence similarity to the Vbh T4SS, but is more closely related to the *tra* machinery or the Trb T4SS of the *A. tumefaciens* virulence plasmid pTi (personal observation). In addition to a number of metabolic functions, pEST4011 and related replicons are loaded with insertion sequences and transposases, and vectors of the IncP-1 family are generally known as broad-host plasmids with highly mosaic accessory content that frequently engage in recombination[406]. It is therefore appealing that an ancestral FicTA module may have entered *Bartonella* not together with pVbh but rather on a different conjugative plasmid that was later largely lost from the genus, while the toxin-antitoxin module thrived in association with the Vbh T4SS (see below).

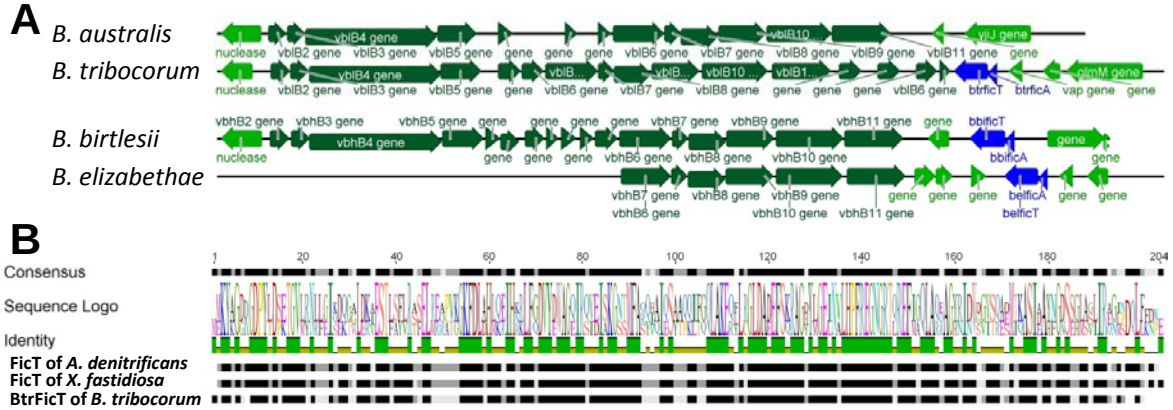

Figure 38: Chromosomal FicTA modules in *Bartonella* and their relatives. A) Representative genomic islands containing a *vbh* locus are shown with Mpf functions highlighted in dark green (including pseudogenes) and other genes shown in green. FicTA modules are colored in blue. Note that *ficAT* loci are invariably found directly downstream of the Mpf machinery at the same position where the *vbhAT* genes are encoded on pVbh (compare Figure 36). FicTA homologs were only found at the *vbh* loci of *B. tribocorum*, *B. elizabethae*, *B. birtlesii* and, in form of a pseudogene, in *B. washoensis* (see Figure 24 in *Appendix: Further results* for a direct comparison of these proteins). Generally, the *vbh* loci in the chromosomes of *Bartonella* were never found to encode any Dtr functions and seem to be in different states of deterioration. **B)** BtrFicT was aligned to FicT homologs of *Achromobacter denitrificans* plasmid pEST4011 (NP_990877.1) and *Xylella fastidiosa* str. 9a5c (NP_298946.1) using ClustalW implemented in Geneious v7.1.7 with gap open / extend costs of 10 / 0.1 and a BLOSUM cost matrix. Coloring reflects amino acid similarity according to the cost matrix with black = 100% identity and white = <60% identity. The overall primary sequence identity between BtrFicT and any of the other proteins is >50%, while these exhibit more than 80% of sequence identity among each other.

Generally, the presence of toxin-antitoxin modules on conjugative plasmids is a common feature of these and other mobile elements[21,66,407] (see also the *Introduction* section). It is more difficult to determine whether they have a particular biological function in the organism that hosts these mobile elements, e.g., in persister formation, or whether they primarily act in post-segregational killing (PSK). The accumulation of PSK toxin-antitoxin modules on plasmids has been considered as a “Mafia trait” that prevents the emergence of plasmid-less

cheaters if the plasmid provides a public good like secreted virulence factors[408]. However, our limited knowledge on potential pathogenicity functions encoded on pVbh does not support hypotheses in this direction to explain the crowding of TA modules including an ancestral FicTA system.

It would be possible to assess experimentally if the FicTA loci encoded in some bartonellae can act in post-segregational killing and / or bacterial persistence, but exhaustive experimentation in *Bartonella* could also be cut short by clarifying whether *Escherichia coli* may be a similarly suitable model organism. FicTA modules in general as well as the *Bartonella* BtrFicTA module in particular have already been studied in *Research article III* and in experiments shown in *Appendix: Further results*.

7.4.Step III: *de novo* evolution of an intra-kingdom effector

The last two sections illustrated how both components which later converged in the evolution of a primordial VirB/D4 T4SS of *Bartonella* probably entered the genus via horizontal gene transfer in form of bacterial conjugation, though likely not together. Genetic reshuffling via different recombination events may have created a state as it is represented by the *vbh* loci in the chromosomes of different *Bartonella* species, i.e., with a *ficAT* toxin-antitoxin module encoded downstream of the *vbh* T4SS locus adjacent to the relaxase of the system. A simple comparison of the primary sequences of BtrFicT, VbhT, *Bartonella* effector proteins, and a pVbh relaxase suggests that this genetic arrangement created the evolutionary opportunity to transfer a type IV secretion signal from the relaxase onto the toxin of such an ancestral FicTA module in a way reminiscent of "terminal reassortment"[409] (Figure 39). Conspicuously, VbhT proteins are encoded at the same locus downstream of the Mpf machinery like the *Bartonella* FicT toxins, exhibit high sequence similarity to them in the FIC domain, and display a FIC-BID domain architecture as it would be the result of such a fusion. It is therefore reasonable to assume that VbhT homologs may be extant representatives of ancestral FicT-BID proteins as some kind of a "living fossil" that may provide unparalleled insight into the evolution of type IV secretion systems and their effectors in *Bartonella*. The primary sequences of the type IV secretion signal in VbhT and associated conjugative relaxases are nearly identical, and Marius Liesch showed that the VirB/D4 T4S of *B. henselae* translocates proteins based on the secretion signal of VbhT[319]. One can therefore safely assume that VbhT is secreted by the Vbh T4SS into recipient cells during bacterial conjugation and thus constitutes the first example of an interbacterial type IV secretion effector protein (see Figure 40 and below)[a].

[a] All these considerations imply that VbhA is not secreted alongside VbhT. It seems likely that VbhA is stripped off from VbhT during substrate unfolding prior to translocation which appears to be a general feature of type IV

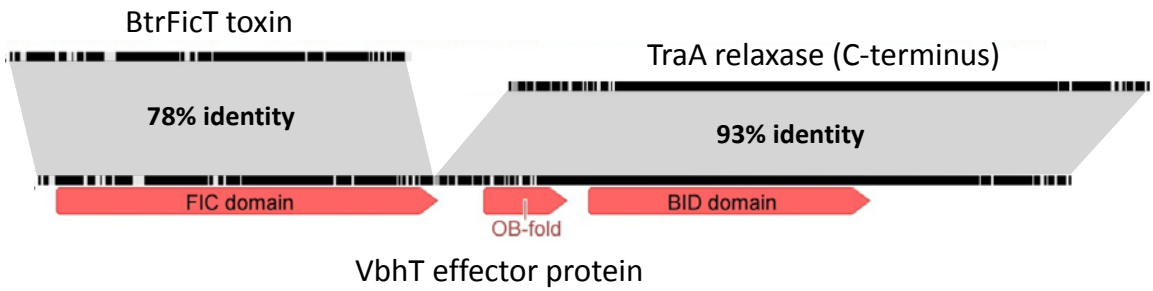

Figure 39: A single sequence reshuffling event created an ancestral VbhT effector. The illustration was created from a protein sequence alignment of BtrFicT of *B. tribocorum* (see Figure 24) and the VbhT effector as well as the (C-terminus of the) TraA relaxase encoded on pBGR3 of *B. grahamii* str. as4aup. Note that the full length of VbhT can be aligned both to BtrFicT (FIC domain) or the TraA relaxase (OB-BID module) with very high protein sequence identity. It is evident that the striking similarity between the bipartite secretion signal of VbhT and its cognate TraA relaxase may be the result of co-evolutionary forces and / or the adaptation to their common T4CP, because the sequence identity shared between VbhT of pBGR3 and the OB-BID module of TraA of pVbh of *B. schoenbuchensis* str. R1 is much lower (67%; not shown). Different direct homologs to VbhT of pVbh or pBGR3 are encoded in an identical genetic setup (see Figure 36) at the chromosomal *vbh* locus of *B. grahamii* str. as4aup and on plasmid pTT0105 (that is very similar to pBGR3). Another homolog can be found in *B. taylorii*, but it is unclear if this sequence constitutes a pseudogene because the open reading frame is terminated by an assembly gap (*B. taylorii* str. 8TBB contig 1.80). Unexpectedly, I failed to detect a homologous sequence to VbhT of pVbh in *B. melophagi*, another species of L2. Close inspection of the *vbh* locus of *B. melophagi* (contig 1.32 of strain K-2C, accession AIMA01000032) revealed a deletion between *vbhB9* and *traA* that apparently removed *vbhAT* and some *vbh* genes (not shown). Importantly, Schulein *et al.* showed that BID domain and positively charged C-terminus of *Bartonella* effectors are sufficient as a secretion signal for the VirB/D4 type IV secretion system[311]. These results leave no room for an important function of the OB-fold in the context of protein translocation together with the BID domain and raise the possibility that the OB-fold was carried along in Bep evolution as a "hitchhiking" stretch of primary sequence. However, it is easily conceivable that the OB-fold between FIC domain and BID domain could serve as a linker supporting protein dynamics or that the OB-fold has secondarily acquired a functional role in host cell manipulation in some groups of *Bartonella* effectors.

It is important to highlight that the terminal reassortment which likely generated an ancestral secreted FicT toxin was not some kind of an accelerated gradual evolution, but rather a random quantum leap without any original adaptive component[409]. One may therefore argue that – despite its plausibility given the genetic arrangement of *vbh* loci with single-domain Fic proteins – such an event would be highly unlikely and violate the principle of parsimony. However, while "Occam's razor is a useful tool in the physical sciences, it can be very dangerous to implement in biology."[369] Much more important than the isolated probability of such a sequence reshuffling event is therefore whether natural selection could favor and propagate the result. More precisely, it is the critical question whether a secreted FicT toxin – a primordial VbhT protein – could be advantageous for a conjugative plasmid or its host bacterium.

secretion[382]. Note that, similar to VbhT (*Research articles I* and *III*), the adenylylation of host targets by Bep1 of *B. rochalimae* was found to be inhibited by its cognate FicA homolog (*Appendix: Further results*), suggesting that these are generally not translocated.

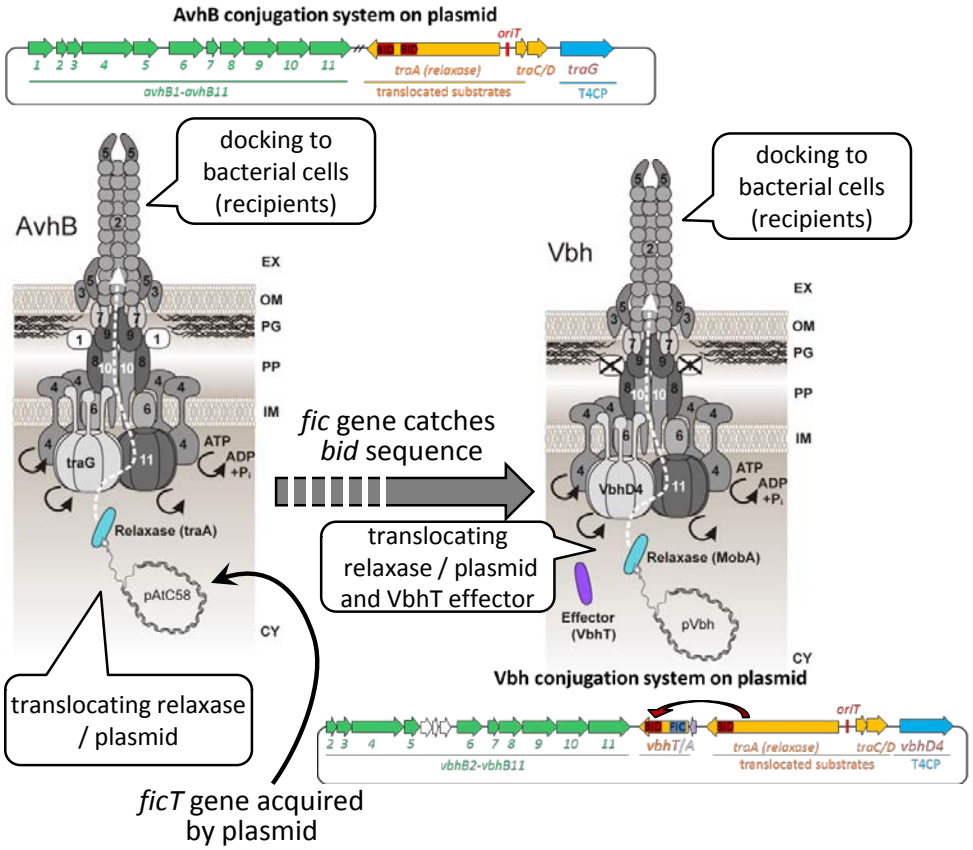

Figure 40: *de novo* evolution of a type IV secreted effector protein. The figure illustrates the evolutionary model that is presented in the running text. In short, an ancestral Vbh-like conjugation system and an ancestral *ficT* toxin gene likely entered the genus *Bartonella* separately via horizontal gene transfer, and a primordial FicTA module was acquired by a pVbh-like plasmid at a locus between its Mpf and Dtr functions. Subsequently, a sequence reshuffling event transferred a type IV secretion signal from the Vbh relaxase to the FicT toxin. It is tempting to speculate that the presence of only one BID domain in the relaxases of pVbh-like plasmids compared to two BID domains in rhizobial homologs is causally connected to this reshuffling event. The conservation of VbhT homologs among pVbh-like plasmids suggests that the FicT-OB-BID fusion proved to be useful as a type IV secreted interbacterial effector protein. The original conjugation system is illustrated as the AvhB machinery of the *A. tumefaciens* plasmid pAT that is closely related to the Vbh T4SS.

7.4.1. Conjugative protein transfer, complementary strand synthesis, and SOS induction

Generally, protein secretion via type IV secretion is obviously not a new concept, though it has been largely restricted to host-targeted effectors of bacterial pathogens that evolved to subvert signaling of the eukaryotic host cell in favor of the bacterium in a multitude of ways (recently reviewed by Voth *et al.*[410]). By analogy, it is the most trivial hypothesis that a secreted FicT toxin like VbhT could be used to damage other bacteria in a way similar to, e.g., contact-dependent inhibition systems (recently reviewed by Hayes *et al.*[411]) or type VI secretion systems active in microbial warfare[412,413]. However, one can nearly exclude this hypothesis for Vbh T4SS / VbhT because FicT toxins including VbhT are strictly bacteriostatic (see *Research article III*) and could therefore at most transiently affect potential target cells. Furthermore, in the context of bacterial conjugation it would be counterproductive for the mobile replicon to harm the recipient and thereby deliberately limit its own spread. Additionally, only a small subpopulation of bacteria harboring conjugative

plasmids functionally express the type IV machinery because the expression of Mpf functions is very costly (recently discussed by Koraimann and Wagner[414]), so that the secondary use of a conjugative T4SS for niche competition would be highly inefficient. Taken together, these considerations strongly suggest that the biological function of an ancestral secreted FicT or extant VbhT must be found in a different context.

So far, the secretion of proteins on top of the relaxase (nucleo)protein complex during bacterial conjugation has only been demonstrated for a single factor, though in diverse arrangements. The primase encoded by IncP plasmid RP4 does not only promote vegetative plasmid replication, but is also transferred into recipient cells during conjugation and required for maximal conjugation efficiency into a broad panel of distinct species[415,416]. These results have been reproduced by others with plasmids of the IncQ family that encode a relaxase-primase fusion protein[417,418], and it has been found that different IncQ plasmids harbor different variants of such a fusion, indicating that they have evolved independently[419-424]. Furthermore, conjugative transfer of a primase protein was also shown for plasmids of the IncI family[425]. Potential biological functions of this apparently rather widespread phenomenon have been reviewed by R. Meyer who concluded that the secretion of primase activities may facilitate complementary strand synthesis (see also Box 3) after transfer by physically "tethering" a primase close to the priming sites on the conjugated DNA single-strand[363]. He noted that in case of an RSF1010-like IncQ family model plasmid the primase domain fused to the relaxase as well as cognate priming sites were not required for conjugative transfer via the highly permissive RP4 machinery between *E. coli* cells. However, both were critical for the rather inefficient mobilization by an F-like conjugation system in isogenic experiments and also greatly improved conjugative transfer via RP4 into the heterologous recipient *Salmonella*[426]. It has therefore been suggested that the transfer of plasmid-encoded primase and cognate recognition sites on the plasmid are "an obvious adaptation for broad-host-range plasmids (while) narrow-host-range plasmids, such as F and ColE1, (would) probably use cellular mechanisms of priming" of the recipient[419]. This hypothesis is consistent with the fact that broad host-range machineries like the conjugation systems of IncQ or RP4, but not the narrow-host-range F-plasmid of *E. coli* secrete primase activities[416]. In the words of R. Meyer, the primase might serve as a "back-up system" for heterologous recipients that lack a maximally compatible machinery for the initiation of complementary strand synthesis[363]. Like this, the repeated initiation of Okazaki fragment synthesis would be performed by a cognate primase that is physically located close to the translocon which could make the conjugation process more tolerant to heterologous DNA replication machineries.

Another line of evidence for the importance of efficient complementary strand synthesis during bacterial conjugation has been generated by a more recent, originally unrelated study. In this work, Baharoglu *et al.* systematically confirmed the long-standing assumption that plasmid conjugation generally results in a transient activation of the SOS response[427] (Figure 41A). This transcriptional program responds to exposed single-stranded DNA[9] as it is typically transferred during bacterial conjugation[370,417] (see also Box 1). Thus, a robust activation of the SOS response is an obvious consequence of inefficient complementary strand synthesis and either results in recombinatory absorption of the transferred DNA into the recipient genome or its degradation, particularly by the RecBCD (Exconuclease V) complex[427-430]. The SOS response is therefore both an indicator of problems with plasmid accommodation in the recipient cell as well as an obstacle to it. Furthermore, the lytic program of lysogenic phages is typically wired to the SOS response in a wide range of bacteria[431-433]. The failure to efficiently manage complementary strand synthesis during bacterial conjugation may therefore kill the recipient as well as a potentially susceptible donor and, in consequence, also eliminate the plasmid.

Box 3: Discontinuous DNA synthesis. Due to the antiparallel orientation of the two strands of dsDNA, only one of them (the „leading strand“) can be synthesized continuously because DNA polymerases are limited to elongate DNA strands in 5‘-3‘ direction. The other strand (the „lagging strand“) is synthesized discontinuously – and opposite to replication fork movement – in form of short Okazaki fragments (1000-2000 base pairs) that are finally assembled to a full DNA strand (recently reviewed by Kurth and O’Donnell[8]). Generally, it is the function of primase to initiate DNA synthesis by producing short RNA “primers” at dedicated initiation sites. These primers are critical for assembly and function of the replisome, because DNA polymerase itself is also unable to initiate DNA synthesis. Therefore, primase is particularly important for lagging strand synthesis where DNA replication needs to be repeatedly re-initiated for each Okazaki fragment (recently reviewed by Corn and Berger[10]).

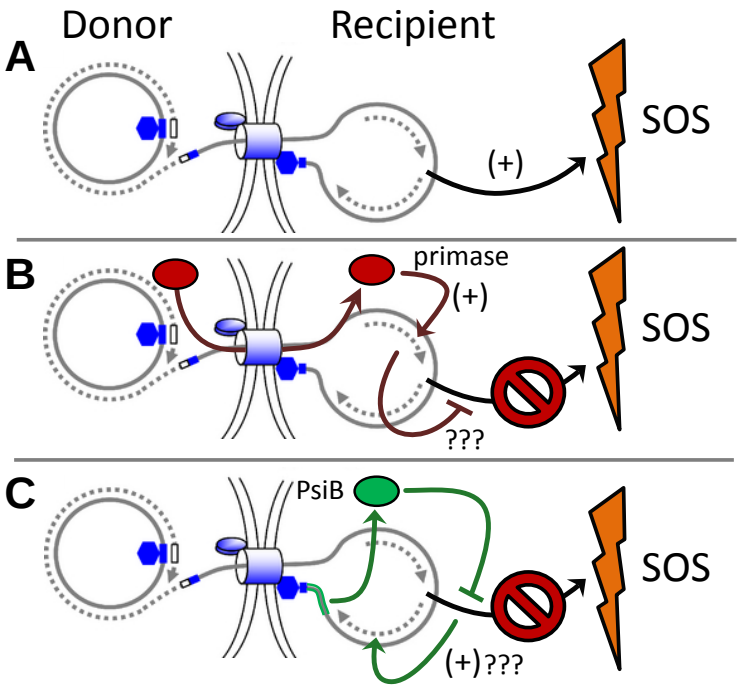

Figure 41: Secreted primases and PsiB during bacterial conjugation. A) Bacterial conjugation activates the SOS response which can be greatly amplified by problems with complementary strand synthesis. **B)** Secreted primase of the donor is thought to promote complementary strand synthesis in the recipient and should therefore prevent or minimize SOS induction. **C)** The *psiB* gene is expressed from the plasmid leader region in the recipient and inhibits SOS induction, thereby likely buying overtime for complementary strand synthesis. The original illustration was adapted from Bellanger *et al.*[383].

Consistently, conjugative plasmids have evolved dedicated factors to inhibit SOS induction like the PsiB protein that is expressed from the leading region of numerous *E. coli* plasmids[427,434,435] (Figure 41B). Baharoglu *et al.* further reported that the conjugation of plasmid RP4 (lacking *psiB*) resulted in an only weak activation of the SOS response both in *E. coli* and in *Vibrio* as a heterologous host[427]. Conspicuously, RP4 was the only plasmid with a primase-secreting conjugation machinery that they tested, suggesting a causal connection between primase activity and only marginal SOS induction (Figure 41C), and it has been shown repeatedly in *E. coli* that a lack of primase activity triggers the SOS response[436-438]. I therefore propose to unite previous studies on primase secretion and SOS inhibitors because exposed ssDNA of the conjugated plasmids is likely the inducer of the SOS response during conjugation. It seems clear that both the secretion of a primase and the action of plasmidic SOS inhibitors promote complementary strand synthesis either by direct facilitation of that process or by the prevention of adverse effects if it is inefficient, respectively[a] (compare Figures 41B and 41C). While such a function for primase secretion is

[a] Given the critical role of complementary strand synthesis for bacterial conjugation it seems likely that additional mechanisms on top of primase secretion or SOS inhibition may have evolved to increase its efficiency. For example, it has been shown that plasmid R46 of *Salmonella* Typhimurium and related pKM101 of *E. coli* encode a MucB lesion bypass DNA polymerase that seems to be activated by SOS induction[439]. Because this system is encoded close to the *oriT* of these vectors and thus presumably expressed early on in recipient

well established, others have proposed that an activation of the SOS response may have no negative effect on conjugation frequencies[427]. However, early work had clearly demonstrated that the deletion of *psiB* from the F-plasmid detectably decreased its ability to conjugate even among *E. coli*[402], suggesting that it may even have a stronger effect in heterologous hosts.

7.4.2. The biological function of VbhT in bacterial conjugation

In the last section I proposed that the mechanisms of primase secretion or SOS inhibition by which bacterial conjugation systems promote productive plasmid transfer converge in improved complementary strand synthesis under unfavorable conditions such as conjugation into heterologous hosts. None of these factors to enhance the efficiency of plasmid transfer is found on pVbh and homologous replicons[a]. It is therefore easily conceivable that the evolution of VbhT as a secreted FicT toxin may represent an independent solution to the problem that complementary strand synthesis is probably the most critical step in bacterial conjugation, but inherently out of reach for the donor cell and the conjugative machinery. Due to its type IV secretion signal VbhT would be secreted along with relaxase and ssDNA into the recipient where it could act until the *vbhAT* locus is transferred and VbhA is produced in the transconjugant. The position of *vbhAT* close to the *oriT* and opposite of the leading region on pVbh (see Figure 36) ensures that VbhT would be active throughout the whole process of conjugative DNA transfer and could thus promote complementary strand synthesis until the plasmid is recircularized in the recipient cell.

Mechanistically, it is conceivable that VbhT as a strong inhibitor of topoisomerase IV may impair the progression of replication fork complexes on the recipient cell chromosome and thereby free additional resources for complementary strand synthesis (Figure 42; see also *Research article III*). In *E. coli* there are not more than 50-100 molecules of primase per cell that must be recycled for the synthesis of each and every primer during chromosome replication (compiled by Corn and Berger[10]). Similarly, various components of the replisome are present in only small numbers[440,441], and the processivity of DNA polymerase (in *E: coli*) typically replicates 80-90 kilobases per initiation event[442] which greatly limits the instances where competition between replication initiation on the incoming plasmid and the chromosome could take place at all. In contrast to this remarkable processivity on the chromosome, the synthesis of the complementary strand during conjugation relies entirely on Okazaki fragments and therefore needs to be re-initiated every one or two kilobases of plasmid sequence (Box 3). It is critical to note that the incoming plasmid itself would be the

cells (personal observation) it may also act to promote complementary strand synthesis, though this has not been demonstrated experimentally.

[a] The orphan *ssb* on pVbh of *B. schoenbuchensis* str. m07a could potentially have a function in this context by shielding ssDNA as it was shown for homologs encoded together with *psiB*[435]. However, such an activity seems unlikely for pVbh because *ssb* is not encoded in the leading region and not found on homologous replicons such as pBGR3of *B. grahamii* str. as4aup[318].

only DNA molecule in the recipient that is not disturbed by the activity of VbhT because it is not topologically closed (see the section on DNA topoisomerases in the *Introduction*). Instead, it seems likely that complementary strand synthesis would be greatly favored by access to a big pool of replication functions. In the absence of opposing evidence I therefore propose that it is the function of VbhT to promote complementary strand synthesis in the recipient cell analogous to the secretion of primase by other conjugative plasmids. However, VbhT is unique in its function as a real secreted effector protein because its activity is not confined to the replicating DNA itself but relies on the manipulation of the recipient's DNA synthesis machinery (Figure 42). The remarkable conservation of the molecular target of VbhT may help it to expand the conjugative host range of the plasmids that it is encoded on (*Research article III*).

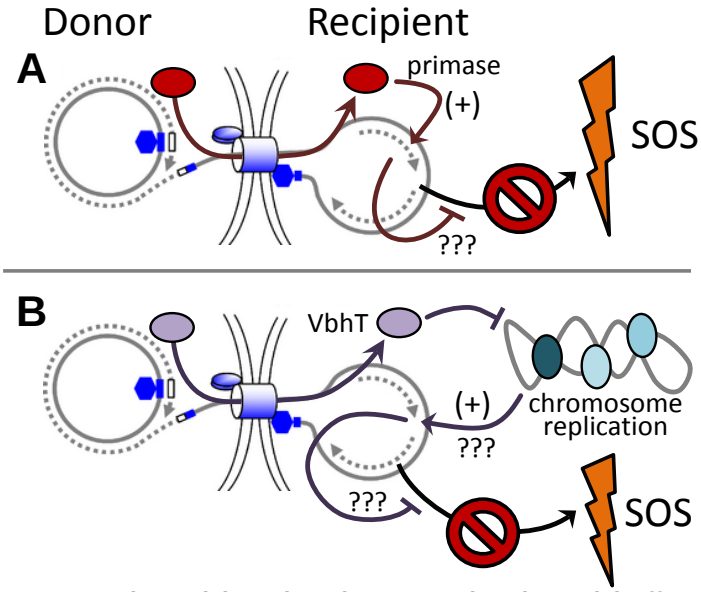

Figure 42: VbhT may promote bacterial conjugation as an interbacterial effector protein. A) Bacterial conjugation critically relies on efficient complementary strand synthesis in the recipient cell. The failure to rapidly complete this process causes a robust activation of the SOS response and has a number of detrimental consequences (see running text). The secretion of primase activities by a number of conjugative plasmids evolved to promote complementary strand synthesis which should counteract SOS induction. **B)** I propose that the secretion of VbhT by the Vbh T4SS is an independent evolutionary solution to the problem of complementary strand synthesis. VbhT could act as an interbacterial effector protein that targets the recipient's DNA topology in order to redirect the DNA synthesis machinery (cyan; on schematic nucleoid) to the incoming plasmid. Consequently, VbhT would favor complementary strand synthesis and act against SOS induction. The figure was adapted from Bellanger *et al.*[383].

One may ask whether there could be evolutionary intermediates in the evolution from FicT toxins to VbhT. For example, it would be conceivable that a FicT toxin could be expressed in the recipient cell from the leading region of a conjugative plasmid similar to SOS inhibitor PsiB (see above) or plasmidic anti-restriction proteins[443]. However, the *ficAT* loci of fossil *vbh* plasmids in the chromosomes of *Bartonella* are invariably encoded downstream of the Vbh T4SS at the same position as *vbhT* on pVbh (Figure 38A). This position is exactly opposite to the leading region and would therefore be transferred *last* into the recipient cell (see above).

Furthermore, the association of *ficT* toxins with a *ficA* antitoxin gene in tight genetic coupling makes it difficult to imagine that an excess of toxin could be produced in the absence of targeted antitoxin degradation.

7.4.3. Experimental approaches to study the biological function of VbhT

A possible role of VbhT in complementary strand synthesis during bacterial conjugation is accessible via a wide range of experimental approaches. A dedicated study would be highly fruitful with regard to originality and impact, because VbhT is likely the first interbacterial type IV secreted effector protein and may represent a "missing link" in the evolution of a host-interacting bacterial T4SS. However, one could think about making such a study even more attractive by trying to establish a functional link between primase secretion, SOS inhibition, and ultimately VbhT, in bacterial conjugation.

For this purpose I propose to repeat a few critical experiments of Baharoglu *et al.*[427] and test whether a deletion of the primase gene on plasmid RP4 relieves the inhibition of SOS induction upon conjugation of this plasmid. Furthermore, one could use plasmid pCD341, a derivative of RSF1010[361], as a model for IncQ vectors that encode a relaxase-primase fusion. It would be interesting to test whether the deletion of this primase module causes increased SOS induction in recipient cells and restricts the conjugative host range as described by others (see above). In case any such phenotype could be detected or reproduced, one may be tempted to see if a FicT toxin fused to the pCD341 relaxase instead of its primase domain could restore at least part of the original host range and / or dampen SOS induction.

Most importantly, it will be necessary to demonstrate the effect of VbhT on the conjugation of the plasmid that it is originally encoded on. For these assays I propose to use pBGR3 of *B. grahamii*[318] as a model system. pBGR3 is nearly identical to pVbh of *B. schoenbuchensis* and encodes an intact *vbhAT* locus, but lacks a considerable number of TA modules as well as the numerous repeats of pseudogenes, so that it is only half the size of the latter replicon (28 kb). Simply tagging this plasmid with an antibiotic resistance gene should allow to determine conjugation frequencies of different mutant vectors under different experimental conditions. In order to increase the experimental throughput it would be desirable to use *E. coli* as a model donor species. Marius Liesch had already tried and failed to establish pVbh of *B.schoenbuchensis* str. R1 in *E. coli*[319], but I propose that these attempts cannot be taken as evidence against the ability of pVbh or the Vbh T4SS to replicate and conjugate in *E. coli*, respectively. pVbh had been tagged with a transposon cassette that contained an R6K *oriV* which would promote plasmid replication to a highly unphysiological copy number in the DH5α (λpir) strain of *E. coli* that was used as a recipient. Considering the size of pVbh (58 kb), the expected increase in copy number would likely interfere with *E. coli* growth, and

the R6K *oriV* may also greatly compromise plasmid stability in case the genuine *repBAC* replication system of pVbh was active in *E. coli*, because dual replication initiation would cause repeated replication fork collisions. Additionally, DH5α (λpir) encodes the McrAB and Mrr type IV restriction systems that are known to recognize and cut a large number of adenine and cytosine methylation[444], possibly including the methylation patterns genuine to *B. schoenbuchensis*. The general feasibility of DNA transfer into *E. coli* via the VbhT4SS is supported by the finding that the closely related *B. henselae* VirB/D4 T4SS can translocate a derivative of enterobacterial plasmid R388 into *E.coli*[323]. I am therefore confident that pBGR3 will be able to replicate and conjugate in *E. coli* without major problems. However, in case of failure to obtain a genuine pVbh-like plasmid that is functional in *E. coli*, one could possibly substitute the replication functions for an analogous system of *E. coli* (e.g., of the F-plasmid). Additionally, one could probably functionally replace the Vbh T4SS with another MPF machinery. Mob_Q family Dtr modules are known to be quite promiscuous and, e.g., efficiently conjugated by the *E. coli* RP4 machinery (recently reviewed by Loftie-Eaton and Rawlings[445]).

Technically, it is possible to follow the process of bacterial conjugation using fluorescence microscopy which could provide a valuable and highly vivid experimental readout. Others have shown previously that complementary strand synthesis during conjugation can be directly monitored using a SeqA-YFP translational fusion[a,447]. The quantification of bacterial conjugation may be easiest via an antibiotic resistance cassette and the counting of colony forming units. However, different assays using flow cytometry have been reported that are permissive for high-throughput experimentation or heterogeneous mixtures of recipients[448,449] and would also allow to monitor different physiological features of donors, recipients, and transconjugants in parallel. Furthermore, it would be essential as part of a dedicated study on VbhT to directly demonstrate the translocation of this protein into recipient cells. Suitable experimental systems for this purpose would be a bacterial derivative of the CRAfT (Cre Reporter Assay for Translocation)[450] or possibly more novel, analogous systems that use the machinery of CRISPR[451] (Clustered Regularly Interspaced Short Palindromic Repeats, originally an adaptive immunity system of bacteria[452]). Alternatively, one may use direct labeling with fluorescent protein fusions or via bimolecular fluorescence complementation that has both been used successfully to visualize the translocation of host-targeted effectors via the VirB/D4 T4SS of *A. tumefaciens*[453].

[a] Unfortunately, this system requires the recipient cells to be *dam*-deficient which is known to result in a modest constitutive activation of the SOS response by itself[446]. One may therefore have to optimize this model by genetic tinkering for our particular experimental needs.

7.4.4. VbhT and conjugation – a unique association?

If VbhT really represents an independent evolutionary solution to a critical problem in bacterial conjugation, it is valid to ask whether functionally related Fic proteins could exist associated to conjugative type IV secretion systems outside of *Bartonella*. Conspicuously, I identified a number of different FIC domain proteins that are encoded together with type IV secretion systems and may constitute translocated substrates. It has previously been described that different type IV secretion systems can use highly diverse translocation signals that are often poorly understood. However, they are almost always found at the C-terminus of the protein and include stretches with net positive charge (see the recent study of Alperi *et al*.[454] and literature cited therein).

Consistently, a group of FIC domain proteins that are genetically associated to *bona fide* conjugative type IV secretion systems on rhizobial plasmids harbor a C-terminal extension that is approximately 150 aa long and, at the distal site, aligns well with the highly positively charged C-terminus of the respective conjugative relaxase (not shown). It is therefore likely that these proteins are secreted effectors, though target cell and biological function remain unclear. Furthermore, they are not encoded together with FicA homologs and do not contain an (S/T)xxxE(G/N) motif in their FIC domain, suggesting that they are regulated very differently from other Fic proteins or do not act as toxins in any sense. Their FIC domain active site motifs are unremarkable, suggesting adenylylation as their molecular function. Intriguingly, it appears that these proteins contain a short sequence stretch at the position of the "Bep-element" in host-targeted effectors of *Bartonella* (Figure 43A) that is missing in all other Fic proteins. The overall sequence identity upon alignment to the FIC domains of Beps, VbhT, or BtrFicT is not high (approximately 25%), suggesting that these rhizobial Fic proteins are not ancestrally related to FIC domains in *Bartonella* (not shown). Consequently, they either must have evolved a Bep-element by convergent evolution or a gene conversion event must have transferred this sequence insert between an ancestor of these proteins and a common ancestor of all Beps, but not VbhT (see Figure 43A).

Furthermore, two FIC domain proteins encoded together with a type IV secretion system at a genomic island of *Campylobacter fetus* subsp. *veneralis* were proposed to be secreted effector proteins. The type IV machinery was shown to be capable of acting as an Mpf complex in bacterial conjugation[455] but also clearly contributed to cytotoxicity in host cells[456]. However, so far no significant evidence for a secretion of the two Fic proteins into eukaryotic or bacterial target cells could be found.

Finally, plasmid p1METDI of the environmental Rhizobium *Methylobacterium extorquens* str. DM4 encodes a FIC domain protein together with a putative antitoxin in a *ficAT*-like arrangement, though the antitoxin obviously lacks a canonical (S/T)xxxE(G/N) inhibition

motif. The Fic protein contains a C-terminal extension of more than 200 aa of which the distal region does not align to the far C-terminus of the relaxase, but is clearly homologous to another region in the C-terminal half of that protein (not shown). Although the overall sequence similarity of this *Methylobacterium* Fic protein to FIC domains in *Bartonella* is low, the genetic arrangement together with the *traA* relaxase and the other Dtr genes is precisely identical (Figure 43B).

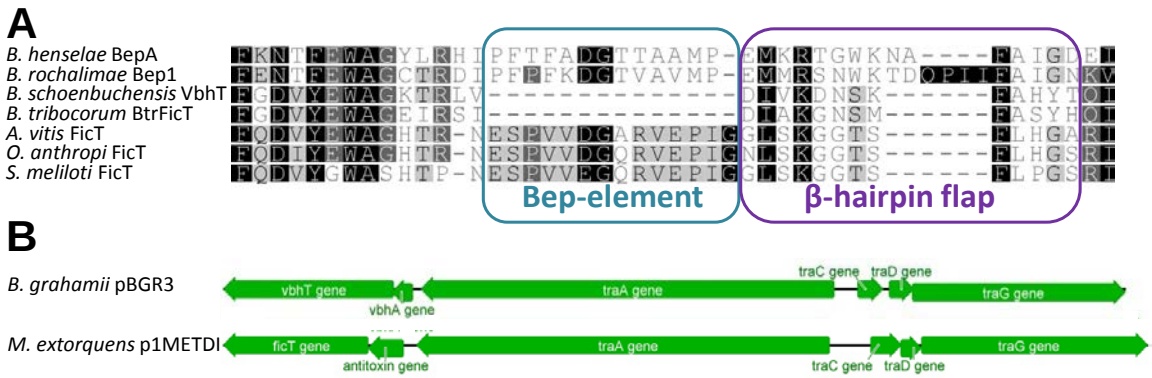

Figure 43: Potential conjugative effector proteins of other type IV secretion systems. A) A family of plasmid-encoded FIC domain proteins of Rhizobiales (e.g., YP_006962993.1 of *S. meliloti* plasmid pHRC017, YP_002546551.1 on *Agrobacterium vitis* str. S4 plasmid pATS4a, or YP_001373060.1 of *Ochrobactrum anthropi* str. ATCC 49188 plasmid pOANT01) harbor a sequence stretch at the position of the Bep-element of host-targeted effectors of *Bartonella*. The Fic proteins were aligned using ClustalW implemented in Geneious v7.1.7 with gap open / extend costs of 10 / 0.1 and a BLOSUM cost matrix. Coloring reflects amino acid similarity according to the cost matrix with black = 100% identity and white = <60% identity (ignoring gaps). Note that – although the overall sequence similarity of this region to *Bartonella* proteins is very low – the glutamate-glycine pair that is at the tip of the Bep-element-hairpin and universally conserved among Beps (Figure 31D) is also found in these rhizobial sequences. **B)** The genetic arrangement of the *vbhAT* locus on pBGR3 of *B. grahamii* str. as4aup and the *bona fide ficAT* locus on p1METDI of *M. extorquens* str. DM4 are precisely identical, but the antitoxin of *M. extorquens* is not homologous to the FicA family.

Taken together, it is therefore apparent that good candidates for other type IV secreted FIC domain effectors exist that may have a function in bacterial conjugation either similar to the proposed role of VbhT or in a completely different context. In any case, the poor sequence similarity to *Bartonella* Fic proteins strongly suggests that other potential interbacterial FIC domain effectors must have evolved by convergent evolution, i.e., that they originated from an independent terminal reassortment event. Although it would not make much sense to focus on these proteins in any way, it could be interesting to test one or more of them for comparison once a biological function of VbhT in bacterial conjugation has been firmly established.

7.5.Step IV: From intra-kingdom to inter-kingdom effectors

In the previous sections I described how an interbacterial effector protein may have been created *de novo* by a domain reshuffling event that fused a FicT toxin to a type IV secretion signal. Furthermore, I proposed that this effector – a prototypic VbhT protein – was the

translocated substrate of an ancestral Vbh-like conjugation system and served to promote plasmid transfer under adverse conditions. Importantly, the functional and genetic arrangement of this peculiar machinery is only a short step away from a host-interacting, effector secreting type IV secretion system.

7.5.1. First contact: From bacterial conjugation to host interaction

Intuitively, a physical interaction of the type IV secretion pilus with host cells is a necessary prerequisite for the evolution of host-targeted effector secretion. Such an interaction does not require substantial adaptation of a bacterial conjugation system, because the broad classes of molecular structures that are known to be targeted by interbacterial mating pair formation - lipids, sugars, and proteins[457-461] – are obviously also present on eukaryotic cells. Consistently, type IV secretion systems are rather promiscuous in their target cell range and can conjugate DNA not only into other bacteria, but also into yeast[462] as well as human, fungal, and plant cells[463]. It was even shown for the VirB/D4 T4SS of *B. henselae* that this machinery does not only secrete Beps[311], but also supports the relaxase-dependent transfer of plasmids into human cells[323,324]. Intriguingly, the same type IV secretion system was also reported to be capable of conjugation into *E. coli*[323]. It seems therefore appropriate to adopt the view of type IV secretion as a "drilling machine"[460] that requires little cooperation of the recipient and can easily be exapted for intercellular protein transfer in diverse functional contexts. A primordial Vbh-like conjugation system with an ancestral VbhT-like interbacterial effector may thus already have had the inherent capability of at least a basic interaction with host cells or could have easily reached this potential. Though a direct evolution into a host-interacting, effector-secreting machinery could be imagined, I do not wish to exclude the possibility of an intermediate, at least secondary function of the type IV secretion machinery itself in host interaction, e.g., by binding to some receptor on the cell surface. Such an interaction would open three evolutionary paths for an ongoing adaptation to host interaction: It is clear that a focused specialization in host cell interaction via the T4SS pilus could result in the loss of Dtr and T4CP functions, while components of the extracellular core machinery may be shaped by adaptive evolution. Such a scenario apparently happened for the Trw T4SS of *Bartonella* that evolved from a conjugative, R388-like machinery into an adhesin for red blood cells[276,307]. Alternatively, the type IV secretion machinery could adapt the conjugation process to host interaction and use the concept of DNA secretion to promote virulence like *A. tumefaciens* with its Ti DNA[394]. Furthermore, one could imagine that the type IV secretion machinery may lose its Dtr and DNA transfer functions but instead specialize in effector secretion, possibly along with an original direct function in host cell interaction via the pilus. One example of this evolutionary path is the Cag T4SS of *H. pylori* that does not only secrete the effector CagA, but also stimulates integrins on the cell surface in an effector-independent manner to manipulate cellular signaling[464].

Similarly, the obvious link between *Bartonella* FicT toxins, VbhT, and Beps (Figure 39) strongly suggests that the conjugative machinery ancestral to the *Bartonella* VirB/D4 T4SS adapted to effector secretion in some way. It is tempting to speculate that this evolutionary path may have been favored by the availability of a pre-evolved, interbacterial effector as raw material for adaptive "tinkering" that should have made the machinery even more prone to exaptation for protein secretion than it is anyhow already typical for type IV secretion systems[303]. Furthermore, the highly flexible nature of the FIC domain as a tunable enzymatic machinery must have greatly facilitated the adaptation of an original, VbhT-like effector to the manipulation of host proteins, because only few aspects of the Fic function are really hard-coded in the catalytic core. This flexibility is also illustrated by the plethora of largely divergent host-targeted virulence factors that rely on the function of FIC domains (see a compilation in the *Introduction*).

7.5.2. Copy & Paste as an adaptive strategy

It is clear that the evolution of an originally interbacterial, VbhT-like effector protein into a host-targeted, prototypical Bep almost closes the gap to the analyses of Henri Saenz and Philipp Engel who demonstrated that all *Bartonella* effector proteins evolved from one single common ancestor with a FIC-BID domain architecture[169,275]. With regard to this evolutionary state one may ask whether the cognate type IV secretion system of this effector was already encoded as a genomic island like the extant VirB/D4 T4SS or, similar to the extant conjugative Vbh T4SS, on a plasmid. Several lines of evidence argue for the second scenario that essentially postulates a pVbh-related virulence plasmid in *Bartonella* similar to the diverse plasmids with symbiotic or pathogenic functions of other Rhizobiales. An early study on the genomic environment of the VirB/D4 T4SS in L4 indicated that it is encoded in a region which is likely a remnant of such a large replicon[271,319]. Consistently, the VirB/D4 T4SS of L3 and L4 had integrated independently and into different loci of the genomes of common ancestors of these two lineages[169]. Given that, in the light of new phylogenetic studies[267,284], these common ancestors must have been rather distantly related to each other, this dual integration is best explained with a circulating virulence plasmid that may have been similarly prone to chromosomal integration as pVbh is (see above).

The evolutionary processes that link the acquisition of a primordial VirB/D4 T4SS and its single ancestral effector to the extant machineries with diversified effector cocktails have been described by others and were already summarized in the *Introduction* section (see also Figure 44). However, I still decided to shortly highlight the most important points at the end of this *Perspective* (see the work of Henri Saenz and Philipp Engel and literature cited therein[169,275]).

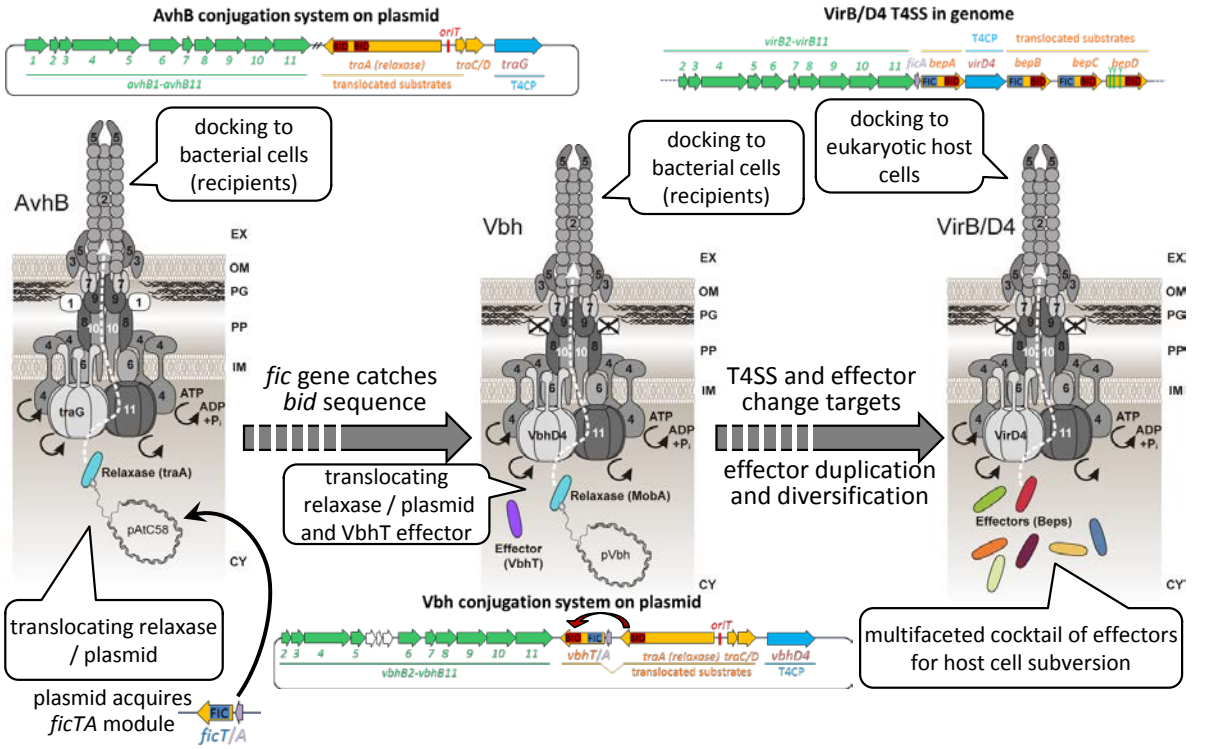

Figure 44: From one intra-kingdom effector to multiple inter-kingdom effectors. This illustration builds up on Figure 40 and now also illustrates the second major step in the evolution of the VirB/D4 T4SS and its host-secreted effectors according to the model presented in the running text. In short, an interbacterial effector protein as an evolutionary "missing link" possibly constituted a pre-adaptation which greatly favored the exaptation of an ancestral Vbh-like T4SS to a host-interacting machinery. While the changes in mating pore formation between bacterial and eukaryotic target cell are trivial, the evolution of a prototypic Bep that targets host proteins instead of bacterial proteins by adenylylation may have been favored by the inherently flexible enzymatic core machinery of FIC domains. Subsequently, a series of effector gene duplication and diversification shaped the extant repertoires of L3 and L4.

It is likely that the original duplications of an ancestral effector may have served to optimize its expression via simple gene dosage effects, but also provided the raw material for further adaptive evolution in different steps. A comparison of the effector phylogenies of L3 and L4 (Figure 14A) shows effectors with adenylylation activity (BepA and Bep1) as the most deep branching lineages, confirming that this was likely the original state. Initial gene duplication and diversification events may have created adenylylating effectors with different molecular targets as, e.g., apparent from Bep1 and Bep2 of L3 (Figure 29). It seems likely that the emergence of extended sequence motifs in the β-hairpin flap (Figure 31) or other, yet unrecognized accessory modules were instrumental to guide the remarkable target specificity and diversification of these effectors. Subsequent steps of Bep evolution likely intervened more heavily with the typical FIC domain functioning, as can be seen by the loss of *bona fide* adenylylation-competent active site motifs in L4 and beyond Bep3 in L3 (compare Figures 14A and 28). It is likely that the emergence of effectors with FicA-like "caps" at the N-terminus in Bep3-5 has to be seen in a similar context (Figure 30). Though one may speculate that at least some effectors may employ FIC domains with non-canonical active site motifs for novel (catalytic?) activities similar to, e.g., Doc or AnkX (see in the

Introduction), this hypothesis remains to be tested experimentally. Furthermore, the remarkable conservation of FicA-like antitoxins at *virB/D4* loci in both lineages (Figure 26) suggests that these may play an important role in effector functioning, e.g., as molecular chaperones (see above). As a second level of effector evolution it has been shown that (at least in L4) the BID domains of many Beps acquired direct functions in host interaction which also resulted in effectors with several BID domains. Finally, in both lineages independently a novel type of effector emerged in which the FIC domain had been replaced by tyrosine-containing motifs that get phosphorylated upon translocation into the host cell (Bep9 in L3 and BepD/E/F/H in L4; Figure 14A). It seems likely that the evolution of different effector types which do not critically rely on the enzymatic activity of FIC domains reflects intrinsic limitations of the original FIC-BID domain architecture. For example, it is easily conceivable that the effectors with tandem-repeated tyrosine-containing motifs may act as signaling HUBs in the host cell and therefore be superior to FIC domains with regard to the manipulation of whole signaling networks.

It is important to note that all this diversification of the effector repertoires likely occurred prior to the onset of the adaptive radiations of L3 and L4, because the different species within one lineage generally have very similar sets of effectors. The obvious conceptual parallelism in the evolution of the effector repertoires of L3 and L4 is a strong indication of comparable selective pressures imposed by the shared infection strategy of the bartonellae. It will therefore be interesting to see – as more and more effectors of both lineages are being investigated in detail – in which respect this parallel evolution left traces in the molecular activities of *Bartonella* effectors.

7.6.Concluding remarks

I chose to highlight two remarkable points about this work that deserve a few last words. First, the data presented throughout this study strongly suggest that an ancestral, VbhT-like interbacterial effector protein and the associated Vbh-like T4SS constitute an evolutionary "missing link" that connects the host-interacting, effector secreting VirB/D4 T4SS to its conjugative ancestors. It is the nature of such an evolutionary intermediate that it displays characteristic features of both of the two states that it connects. In this particular case, the conjugative Vbh-like T4SS of this intermediate state likely still performed bacterial conjugation as its central function just like the classical machineries from which it evolved. However, it had acquired a VbhT-like interbacterial effector protein by terminal reassortment that probably served to promote bacterial conjugation as an accessory factor (see Figures 44 and 45). Though rather a gimmick than a revolution with view to the original conjugation system, this interbacterial effector was likely a pre-adaptation of the type IV secretion machinery to efficient host manipulation and made the Vbh-like T4SS prone to exaptation

into a plain protein-secreting and host-interacting machinery (see above). The importance of such evolutionary intermediates lies in the fact that they make adaptive processes transparent[a], particularly if these are not easily conceivable from the original and the derived states alone. In this case the presence of a VbhT-like effector in the missing link establishes the concept of interbacterial effector secretion via type IV machineries which had never been observed before (see above) and could act as a "stepping stone" in the evolution of host-interacting type IV secretion systems. Furthermore, the remarkable sequence similarity of extant *Bartonella* FicT toxins, VbhT, and the TraA relaxase (Figure 39) strongly supports the idea that these proteins are ancestrally related to the different players of this evolutionary process. In particular, VbhT may be seen as a "living fossil" that can not only reveal new perspectives on the mechanism of bacterial conjugation, but could also be instrumental to understand early stages in the evolution of the host-interacting Vir/D4 T4SS.

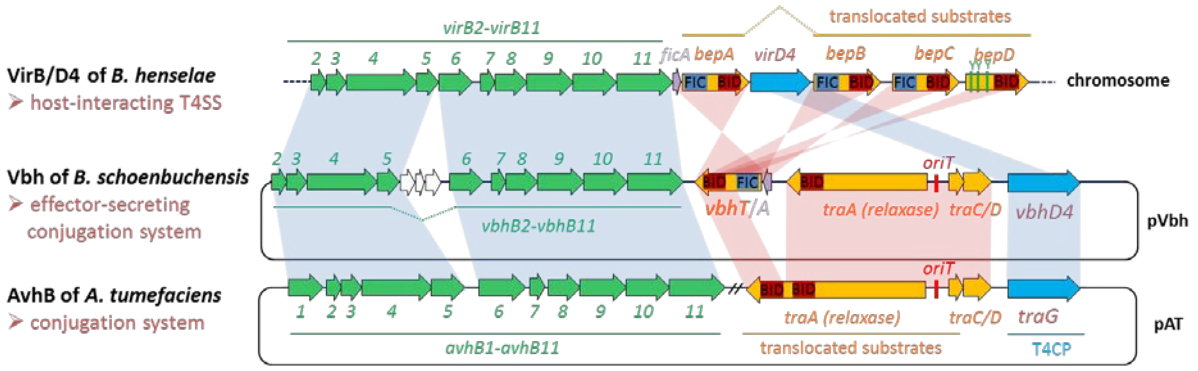

Figure 45: The Vbh T4SS with VbhT represents a "missing link". The illustration schematically compares the VirB/D4 T4SS of *B. henselae*, the Vbh T4SS of *B. schoenbuchensis*, and the AvhB T4SS of *A. tumefaciens* (as a representative of related classical conjugation systems). Note that the type IV machinery itself (green) as well as the T4CP (blue) are highly conserved in all three system, but that the region encoding substrates / Dtr functions (yellow) differs in a way that highlights the position of the Vbh T4SS as an evolutionary missing link: Like the conjugative AvhB system, the Vbh T4SS harbors a cognate Dtr region with a relaxase and *oriT* and is plasmid-encoded. Similar to the host-interacting VirB/D4 T4SS, the Vbh T4SS encodes an effector protein with FIC-BID domain architecture. FicA homologs are indicated in pale magenta. It is tempting to speculate that the reduction of the relaxase to a singe BID domain (compare Figure 34A) for the Vbh T4SS may be causally connected to the terminal reassortment event that transferred one such domain onto an ancestral *ficT* gene. The illustration was adapted from a drawing of Philipp Engel.

Second, the evolutionary history of the VirB/D4 T4SS in *Bartonella* is different from many other complex bacterial virulence factors in that it had not been acquired as a ready-to-use package via horizontal gene transfer but appears to have evolved from an ancestral conjugation system within *Bartonella* itself. It is likely that this phenomenon is connected to

[a] Another example for a "missing link" in microbiology is the organism *Bordetella petrii* that bridges between pathogenic and host-restricted bordetellae like *B. bronchiseptica* on one side and related free-living, environmental β-proteobacteria like *Achromobacter* on the other side[465]. Like the latter, *B. petrii* displays metabolic versatility and is a facultative anaerobe, while it encodes a considerable arsenal of virulence factors including autotransporters and fimbriae and was reported to be an opportunistic pathogen. Therefore, *B. petrii* marks a stepping stone on a plausible adaptive path in which originally environmental ancestors acquired virulence factors by horizontal gene transfer and progressively lost metabolic capabilities with increasing host association.

the lifestyle of *Bartonella*: While other pathogens can have extended environmental stages or thrive in multi-species communities like the skin or gut flora that are hotspots of horizontal gene transfer[466-468], *Bartonella* may at most be able to participate in genetic exchange during passage through the arthropod vector. Consequently, it has been repeatedly shown that bacterial pathogens can acquire pre-evolved pathogenicity islands encoding full secretion machineries[469] via horizontal gene transfer and may even receive occasional upgrades in the form of separate effector genes[470-472]. One example of such an organism is *Salmonella* where the pathogenic lifestyle is apparently driven "to a large extent by mobile or laterally acquired genetic elements"[473]. Conversely, I conclude that the evolution of the VirB/D4 T4SS in *Bartonella* has to be seen in exactly the opposite context. Though originally acquired horizontally as a conjugation system, the machinery evolved stepwise via series of effector gene duplication and diversification that were likely driven by constant selective pressure originating from the *Bartonella* infection strategy. Therefore, even the emergence of a full-blown VirB/D4 machinery with a diversified effector cocktail in extant species of L3 and L4 did not result in marked changes of the overall strategy. Instead, the modularity of the type IV secretion system and the evolvability inherent to the effector genes rather refined the ability of *Bartonella* to manipulate its host at the different stages of the infection cycle. It seems likely that this flexibility may greatly contribute to the increased host adaptability of bartonellae in L3 and L4. Furthermore, it will be interesting to see what kind of subtle differences in host interaction may be revealed in future studies with bartonellae of L4, L3, and species of the more host-restricted lineages L1 and L2.

8. Acknowledgments

This work was carried out in the group of Prof. Christoph Dehio in the Focal a of Infection Biology at the Biozentrum of the University of Basel.

I am particularly grateful to Prof. Christoph Dehio who has always supported me with valuable suggestions, challenging criticism, and trust. The freedom and independence that I had with my research in his laboratory were for sure instrumental to the success of this work.

Furthermore, I wish to thank Prof. Urs Jenal and Prof. Tilman Schirmer who completed my thesis committee. The vivid lecturing of Prof. Jenal was clearly involved in my original decision to study microbiology and gave me a lot to learn about how to give good talks. Prof. Tilman Schirmer and his enthusiasm about the link between protein structure and function were a major driving force of my research throughout this project and greatly expanded my understanding of protein evolution.

Before anybody else, I am grateful to Maxime Québatte with whom I enjoyed all these years in R485. He taught me most of the basic microbiological skills that were essential for the development of my project, and he was always willing and patient enough to share his experience with me.

Special thanks also to Prof. Philipp Engel who mentored my first steps in science and whom I still owe to unravel the biological function of VbhT. As you can see, I'm on it.

Special thanks also to all the close collaborators without whom this work would not have been possible and many of whom have become friends. In particular, the talent of Dr. Frédéric Stanger was essential for the success of many things that I simply could not have done, and I will never forget how science once paid us a lobster buffet. Dr. Arnaud Goepfert is to be thanked for his inspiring optimism even when he faced dramatic opponents like good old Yoda. Jonas Körner was my Master student and successfully completed a challenging project due to his endless perseverance and dedication. I am proud to see him now standing firm on both feet with his own research.

I would further like to thank Dr. Nikolaus Schmitz, Dr. Christoph Schmutz, and Dr. Isabel Sorg who recently joined our team in R485 and who gave me the opportunity to learn from their unique abilities and to enjoy their gentleness as colleagues.

I wish to express special gratitude to Prof. Kenn Gerdes and Dr. Patrick Scheu who joined my research at a critical moment and contributed unique insight and advice.

In addition to those mentioned above I would like to thank all present and past members of the Dehio group for the cooperative and friendly atmosphere in the lab. I wish to thank in particular Dr. Alain Casanova, Dr. Raquel Conde, Dr. Simone Eicher, Marco Faustmann, Marius Liesch, Claudia Mistl, and Dr. Sabrina Siamer. I am particularly grateful to bacteriophage T1 who awakened my interest in bacterial virology. Along these lines I would also like to thank various members of other research groups, particularly Beatrice Claudi, Dr. Airat Gubaev, Dr. Lucie Hosch, Dr. Simon Ittig, Dr. Tina Jäger, Dr. Imke de Jong, Dr. Nina Link, Christian Lori, Dr. Alain Mazé, Alberto Reinders, Dr. Francesco Renzi, and Dr. Samuel Steiner.

Many special thanks to the technical and administrative staff for their invaluable support. I wish to thank Marina Kuhn-Rüfenacht, Patric Hänni, and Roger Sauer for managing the infrastructure in a way that all the problems and complications typically stayed invisible for me. I owe many thanks to the ladies in the media kitchen without whom I could not have worked nearly as efficient and smooth

for all these years. Similarly, I wish to thank Claudia Erbel-Sieler, Michaela Hanisch, Dr. Anne-Cécile Hiebel, and Angie Klarer for their continuous help with all the paperwork.

I would like to thank my close friends for all the good time that we had together. I am particularly grateful to Dimitri Bieli, Philipp Bless, Vasco Campos, Loic Sauteur, Stefan Heiler, Thomas Schubert, all the Laufental gang, and of course my two expatriate comrades, the Züri-MJ and Nils the farmer.

I am very grateful to my girlfriend Julia for all her patience and understanding over the last years that helped me keep the balance. Finally, I wish to thank my parents who have supported me so warmly for now more than 27 years.

And – at the end – big thanks to those that I forgot to mention. I am sorry for that.

9. Curriculum Vitae

Name: Alexander Joscha Heinrich Harms

Date of birth: 25.06.1987

Place of birth: Berlin, Germany

Citizenship: German

Address	**Office:**	**Private:**
	Biozentrum University of Basel Infection Biology Klingelbergstrasse 50/70 CH-4056 Basel Switzerland Phone: +41-61-267 2138 Email: alexander.harms@unibas.ch	Hebelstrasse 65 CH-4056 Basel Switzerland Phone: +41-61-261 19 87 Mobile: +41-79-870 49 76

Education and Research experience:

2011 – 2015 **PhD Thesis**

Focal area Infection Biology, Biozentrum, University of Basel CH

Supervisor: Prof. Christoph Dehio

Committee Members: Prof. Urs Jenal and Prof. Tilman Schirmer

Fellow of the “Opportunities for Excellence” program

Title: “FIC domain toxins are the origin of intra- and inter-kingdom effectors of *Bartonella*”

2013 **Phage Task Force**

Co-director together with Dr. Nina Link

Biozentrum, University of Basel CH

Project: Identification, surveillance, and eradication of a bacteriophage T1 contamination

2009 - 2011 **Graduate studies**

Awarded M.Sc. in Molecular Biology (final grade 6.0)

Focal area Infection Biology, Biozentrum, University of Basel CH

Supervisor: Prof. Christoph Dehio

Title: “FIC domains of *Bartonella* effector proteins – AMPylation and beyond”

2009 **3-month internship at Actelion Pharmceuticals**

Pharmacokinetics / Pharmacodynamics

Laboratory of Dr. Peter Seiler, Anti-Infectives Pharmacology,

Actelion Pharmaceuticals Ltd., Allschwil, Switzerland

2006 - 2009	**Undergraduate studies** Awarded B.Sc. in Biology (final grade 5.8) Major studies in Molecular Biology University of Basel CH
1997 - 2006	**Abitur** University entrance diploma (final grade 1.0) St. Ursula Gymnasium, Dorsten, Germany

Teaching experience:

2013 – 2014	Supervision of a master student Focal area Infection Biology, Biozentrum, University of Basel CH
2009 – present	Assistant and tutor for undergraduate students in practical courses “Microbiology” once a year Focal area Infection Biology, Biozentrum, University of Basel CH

Oral presentations:

2014	Short presentation at the Swiss Society for Microbiology (Annual Assembly 2014) in Fribourg, Switzerland Title: “Fic toxins subvert DNA topology by AMPylation of topoisomerases to promote persistence”
2014	Short presentation at the Biozentrum PhD retreat 2014 in Engelberg, Switzerland Title: “Fic toxins subvert DNA topology by AMPylation of topoisomerases to promote persistence”
2014	Presentation at the EMBO workshop on stalked α-proteobacteria and relatives in Marburg, Germany Title: “FIC toxins AMPylate topoisomerases to subvert DNA topology and promote persistence”
2013	Presentation at the Biozentrum Symposium in Basel, Switzerland Title: “Fic toxins reveal the evolutionary origin of bacterial effector proteins”
2012	Presentation at the Evolutionary Biology Meeting in Marseille, France Title: “Parallel evolution of type IV secretion effector repertoires in radiating lineages of the bacterial pathogen *Bartonella*”

Poster presentations:

2014 Poster at the Gordon Research Conference on DNA Topoisomerases in Biology & Medicine in Newry ME; United States
Title: “Fic toxins manipulate DNA topology via topoisomerase inhibition and shed light on *Bartonella* effector evolution”

2014 Poster at the EMBO workshop on stalked α-proteobacteria and relatives in Marburg, Germany
Title: “FIC toxins AMPylate topoisomerases to subvert DNA topology and promote persistence”

2012 Poster at the International Conference on *Bartonella* as Animal and Human Pathogens in Raleigh NC, United States
Title: “Specificity and diversification: New insight into biology and evolution of *Bartonella* effector proteins”

Publications:

1. Alexander Harms and Christoph Dehio (2012) Intruders below the radar: molecular pathogenesis of *Bartonella* spp. Clin Microbiol Rev. 25(1):42-78.

2. Philipp Engel, Arnaud Goepfert, Frédéric V. Stanger, Alexander Harms, Alexander Schmidt, Tilman Schirmer, Christoph Dehio (2012) Adenylylation control by intra- or intermolecular active-site obstruction in Fic proteins. Nature. 482(7383):107-10.

3. Arnaud Goepfert, Alexander Harms, Tilman Schirmer, Christoph Dehio (2013) Type II Toxin-Antitoxin Loci: The *fic* Family. K. Gerdes (ed.), Prokaryotic Toxin-Antitoxins, Springer Berlin Heidelberg, 2013, 177-187.

4. Kathrin Pieles, Timo Glatter, Alexander Harms, Alexander Schmidt, Christoph Dehio (2014) An experimental strategy for the identification of AMPylation targets from complex protein samples. Proteomics. 14 (9):1048-52.

5. Alexander Harms, Frédéric Valentin Stanger, Patrick Daniel Scheu, Imke Greet de Jong, Timo Glatter, Kenn Gerdes, Tilman Schirmer, Christoph Dehio. Disruption of DNA topology via topoisomerase adenylylation –a new path to persistence. Submitted to *Cell*.

6. Frédéric V. Stanger, Björn M. Burmann, Alexander Harms, Adam Mazur, Timothy Sharpe, Christoph Dehio, Sebastian Hiller, Tilman Schirmer. Target adenylylation by class III Fic proteins is regulated by a double-lock mechanism: oligomerization and auto-adenylylation. In preparation.

10. References

1 Overgaard, M., Borch, J., Jørgensen, M. G. & Gerdes, K. Messenger RNA interferase RelE controls relBE transcription by conditional cooperativity. *Mol Microbiol* **69**, 841-857 (2008).

2 Afif, H., Allali, N., Couturier, M. & Van Melderen, L. The ratio between CcdA and CcdB modulates the transcriptional repression of the ccd poison-antidote system. *Mol Microbiol* **41**, 73-82 (2001).

3 Winther, K. S. & Gerdes, K. Regulation of enteric vapBC transcription: induction by VapC toxin dimer-breaking. *Nucleic Acids Res* **40**, 4347-4357 (2012).

4 Gelens, L., Hill, L., Vandervelde, A., Danckaert, J. & Loris, R. A general model for toxin-antitoxin module dynamics can explain persister cell formation in *E. coli*. *PLoS Comput Biol* **9**, e1003190 (2013).

5 Cataudella, I., Sneppen, K., Gerdes, K. & Mitarai, N. Conditional cooperativity of toxin - antitoxin regulation can mediate bistability between growth and dormancy. *PLoS Comput Biol* **9**, e1003174 (2013).

6 Cataudella, I., Trusina, A., Sneppen, K., Gerdes, K. & Mitarai, N. Conditional cooperativity in toxin-antitoxin regulation prevents random toxin activation and promotes fast translational recovery. *Nucleic Acids Res* **40**, 6424-6434 (2012).

7 Baharoglu, Z. & Mazel, D. SOS, the formidable strategy of bacteria against aggressions. *FEMS Microbiol Rev* **38**, 1126-1145 (2014).

8 Kurth, I. & O'Donnell, M. New insights into replisome fluidity during chromosome replication. *Trends Biochem Sci* **38**, 195-203 (2013).

9 Erill, I., Campoy, S. & Barbe, J. Aeons of distress: an evolutionary perspective on the bacterial SOS response. *FEMS Microbiol Rev* **31**, 637-656 (2007).

10 Corn, J. E. & Berger, J. M. Regulation of bacterial priming and daughter strand synthesis through helicase-primase interactions. *Nucleic Acids Res* **34**, 4082-4088 (2006).

11 Smith, K. C. Recombinational DNA repair: the ignored repair systems. *Bioessays* **26**, 1322-1326 (2004).

12 Faridani, O. R., Nikravesh, A., Pandey, D. P., Gerdes, K. & Good, L. Competitive inhibition of natural antisense Sok-RNA interactions activates Hok-mediated cell killing in *Escherichia coli*. *Nucleic Acids Res* **34**, 5915-5922 (2006).

13 Vogel, J., Argaman, L., Wagner, E. G. & Altuvia, S. The small RNA IstR inhibits synthesis of an SOS-induced toxic peptide. *Curr Biol : CB* **14**, 2271-2276 (2004).

14 Li, G. Y., Zhang, Y., Inouye, M. & Ikura, M. Inhibitory mechanism of *Escherichia coli* RelE-RelB toxin-antitoxin module involves a helix displacement near an mRNA interferase active site. *J Biol Chem* **284**, 14628-14636 (2009).

15 Garcia-Pino, A. *et al.* Doc of prophage P1 is inhibited by its antitoxin partner Phd through fold complementation. *J Biol Chem* **283**, 30821-30827 (2008).

16 Fineran, P. C. *et al.* The phage abortive infection system, ToxIN, functions as a protein-RNA toxin-antitoxin pair. *Proc Natl Acad Sci U S A* **106**, 894-899 (2009).

17 Blower, T. R. *et al.* Identification and classification of bacterial Type III toxin-antitoxin systems encoded in chromosomal and plasmid genomes. *Nucleic Acids Res* **40**, 6158-6173 (2012).

18 Masuda, H., Tan, Q., Awano, N., Wu, K. P. & Inouye, M. YeeU enhances the bundling of cytoskeletal polymers of MreB and FtsZ, antagonizing the CbtA (YeeV) toxicity in *Escherichia coli*. *Mol Microbiol* **84**, 979-989 (2012).

19 Dy, R. L., Przybilski, R., Semeijn, K., Salmond, G. P. & Fineran, P. C. A widespread bacteriophage abortive infection system functions through a Type IV toxin-antitoxin mechanism. *Nucleic Acids Res* **42**, 4590-4605 (2014).

20 Wang, X. *et al.* A new type V toxin-antitoxin system where mRNA for toxin GhoT is cleaved by antitoxin GhoS. *Nat Chem Biol* **8**, 855-861 (2012).

21 Leplae, R. *et al.* Diversity of bacterial type II toxin-antitoxin systems: a comprehensive search and functional analysis of novel families. *Nucleic Acids Res* **39**, 5513-5525 (2011).

22 Schuster, C. F. & Bertram, R. Toxin-antitoxin systems are ubiquitous and versatile modulators of prokaryotic cell fate. *FEMS Microbiol Lett* **340**, 73-85 (2013).

23 Van Melderen, L. & Saavedra De Bast, M. Bacterial toxin-antitoxin systems: more than selfish entities? *PLoS Genet* **5**, e1000437 (2009).

24 Unterholzner, S. J., Poppenberger, B. & Rozhon, W. Toxin-antitoxin systems: Biology, identification, and application. *Mob Genet Elements* **3**, e26219 (2013).

25 Yamaguchi, Y., Park, J. H. & Inouye, M. Toxin-antitoxin systems in bacteria and archaea. *Annu Rev Genet* **45**, 61-79 (2011).

26 Gerdes, K. & Maisonneuve, E. Bacterial persistence and toxin-antitoxin loci. *Annu Rev Microbiol* **66**, 103-123 (2012).

27 Christensen, S. K. & Gerdes, K. RelE toxins from bacteria and Archaea cleave mRNAs on translating ribosomes, which are rescued by tmRNA. *Mol Microbiol* **48**, 1389-1400 (2003).

28 Zhang, Y. & Inouye, M. The inhibitory mechanism of protein synthesis by YoeB, an *Escherichia coli* toxin. *J Biol Chem* **284**, 6627-6638 (2009).

29 Jørgensen, M. G., Pandey, D. P., Jaskolska, M. & Gerdes, K. HicA of *Escherichia coli* defines a novel family of translation-independent mRNA interferases in bacteria and archaea. *J Bacteriol* **191**, 1191-1199 (2009).

30 Zhang, Y. *et al.* MazF cleaves cellular mRNAs specifically at ACA to block protein synthesis in *Escherichia coli*. *Mol Cell* **12**, 913-923 (2003).

31 Yamaguchi, Y., Park, J. H. & Inouye, M. MqsR, a crucial regulator for quorum sensing and biofilm formation, is a GCU-specific mRNA interferase in *Escherichia coli*. *J Biol Chem* **284**, 28746-28753 (2009).

32 Lehnherr, H., Maguin, E., Jafri, S. & Yarmolinsky, M. B. Plasmid addiction genes of bacteriophage P1: doc, which causes cell death on curing of prophage, and phd, which prevents host death when prophage is retained. *J Mol Biol* **233**, 414-428 (1993).

33 Helaine, S. *et al.* Internalization of *Salmonella* by macrophages induces formation of nonreplicating persisters. *Science* **343**, 204-208 (2014).

34 Castro-Roa, D. *et al.* The Fic protein Doc uses an inverted substrate to phosphorylate and inactivate EF-Tu. *Nat Chem Biol* **9**, 811-817 (2013).

35 Germain, E., Castro-Roa, D., Zenkin, N. & Gerdes, K. Molecular mechanism of bacterial persistence by HipA. *Mol Cell* **52**, 248-254 (2013).

36 Winther, K. S. & Gerdes, K. Enteric virulence associated protein VapC inhibits translation by cleavage of initiator tRNA. *Proc Natl Acad Sci U S A* **108**, 7403-7407 (2011).

37 Winther, K. S., Brodersen, D. E., Brown, A. K. & Gerdes, K. VapC20 of *Mycobacterium tuberculosis* cleaves the sarcin-ricin loop of 23S rRNA. *Nat Commun* **4**, 2796 (2013).

38 Zhang, Y. & Inouye, M. RatA (YfjG), an *Escherichia coli* toxin, inhibits 70S ribosome association to block translation initiation. *Mol Microbiol* **79**, 1418-1429 (2011).

39 Norton, J. P. & Mulvey, M. A. Toxin-antitoxin systems are important for niche-specific colonization and stress resistance of uropathogenic *Escherichia coli*. *PLoS Pathog* **8**, e1002954 (2012).

40 Gerdes, K. *et al.* Mechanism of postsegregational killing by the hok gene product of the parB system of plasmid R1 and its homology with the relF gene product of the *E. coli* relB operon. *EMBO J* **5**, 2023-2029 (1986).

41 Bernard, P. & Couturier, M. Cell killing by the F plasmid CcdB protein involves poisoning of DNA-topoisomerase II complexes. *J Mol Biol* **226**, 735-745 (1992).

42 Jiang, Y., Pogliano, J., Helinski, D. R. & Konieczny, I. ParE toxin encoded by the broad-host-range plasmid RK2 is an inhibitor of *Escherichia coli* gyrase. *Mol Microbiol* **44**, 971-979 (2002).

43 Sberro, H. *et al.* Discovery of functional toxin/antitoxin systems in bacteria by shotgun cloning. *Mol Cell* **50**, 136-148 (2013).

44 Dy, R. L., Richter, C., Salmond, G. P. C. & Fineran, P. C. Remarkable Mechanisms in Microbes to Resist Phage Infections. *Annu Rev Virol* **1**, 307-331 (2014).

45 Samson, J. E., Spinelli, S., Cambillau, C. & Moineau, S. Structure and activity of AbiQ, a lactococcal endoribonuclease belonging to the type III toxin-antitoxin system. *Mol Microbiol* **87**, 756-768 (2013).

46 Blower, T. R. *et al.* A processed noncoding RNA regulates an altruistic bacterial antiviral system. *Nat Struct Mol Biol* **18**, 185-190 (2011).

47 Mutschler, H., Gebhardt, M., Shoeman, R. L. & Meinhart, A. A novel mechanism of programmed cell death in bacteria by toxin-antitoxin systems corrupts peptidoglycan synthesis. *PLoS Biol* **9**, e1001033 (2011).

48 Masuda, H., Tan, Q., Awano, N., Yamaguchi, Y. & Inouye, M. A novel membrane-bound toxin for cell division, CptA (YgfX), inhibits polymerization of cytoskeleton proteins, FtsZ and MreB, in *Escherichia coli*. *FEMS Microbiol Lett* **328**, 174-181 (2012).

49 Aakre, C. D., Phung, T. N., Huang, D. & Laub, M. T. A bacterial toxin inhibits DNA replication elongation through a direct interaction with the beta sliding clamp. *Mol Cell* **52**, 617-628 (2013).

50 Yamaguchi, Y. & Inouye, M. Regulation of growth and death in *Escherichia coli* by toxin-antitoxin systems. *Nat Rev Microbiol* **9**, 779-790 (2011).

51 Brzozowska, I. & Zielenkiewicz, U. Regulation of toxin-antitoxin systems by proteolysis. *Plasmid* **70**, 33-41 (2013).

52 Maisonneuve, E., Castro-Camargo, M. & Gerdes, K. (p)ppGpp controls bacterial persistence by stochastic induction of toxin-antitoxin activity. *Cell* **154**, 1140-1150 (2013).

53 Kim, Y. *et al. Escherichia coli* toxin/antitoxin pair MqsR/MqsA regulate toxin CspD. *Environ Microbiol* **12**, 1105-1121 (2010).

54 Diago-Navarro, E., Hernandez-Arriaga, A. M., Kubik, S., Konieczny, I. & Diaz-Orejas, R. Cleavage of the antitoxin of the parD toxin-antitoxin system is determined by the ClpAP protease and is modulated by the relative ratio of the toxin and the antitoxin. *Plasmid* **70**, 78-85 (2013).

55 Lehnherr, H. & Yarmolinsky, M. B. Addiction protein Phd of plasmid prophage P1 is a substrate of the ClpXP serine protease of *Escherichia coli*. *Proc Natl Acad Sci U S A* **92**, 3274-3277 (1995).

56 Koga, M., Otsuka, Y., Lemire, S. & Yonesaki, T. *Escherichia coli* rnlA and rnlB compose a novel toxin-antitoxin system. *Genetics* **187**, 123-130 (2011).

57 Prysak, M. H. *et al.* Bacterial toxin YafQ is an endoribonuclease that associates with the ribosome and blocks translation elongation through sequence-specific and frame-dependent mRNA cleavage. *Mol Microbiol* **71**, 1071-1087 (2009).

58 Donegan, N. P., Thompson, E. T., Fu, Z. & Cheung, A. L. Proteolytic regulation of toxin-antitoxin systems by ClpPC in *Staphylococcus aureus*. *J Bacteriol* **192**, 1416-1422 (2010).

59 Brzozowska, I. & Zielenkiewicz, U. The ClpXP protease is responsible for the degradation of the Epsilon antidote to the Zeta toxin of the streptococcal pSM19035 plasmid. *J Biol Chem* **289**, 7514-7523 (2014).

60 Ogura, T. & Hiraga, S. Mini-F plasmid genes that couple host cell division to plasmid proliferation. *Proc Natl Acad Sci U S A* **80**, 4784-4788 (1983).

61 Jensen, R. B., Grohmann, E., Schwab, H., Diaz-Orejas, R. & Gerdes, K. Comparison of ccd of F, parDE of RP4, and parD of R1 using a novel conditional replication control system of plasmid R1. *Mol Microbiol* **17**, 211-220 (1995).

62 Cooper, T. F. & Heinemann, J. A. Postsegregational killing does not increase plasmid stability but acts to mediate the exclusion of competing plasmids. *Proc Natl Acad Sci U S A* **97**, 12643-12648 (2000).

63 Cooper, T. F., Paixao, T. & Heinemann, J. A. Within-host competition selects for plasmid-encoded toxin-antitoxin systems. *Proc Biol Sci* **277**, 3149-3155 (2010).

64 Dao-Thi, M. H. *et al.* Molecular basis of gyrase poisoning by the addiction toxin CcdB. *J. Mol. Biol.* **348**, 1091-1102 (2005).

65 Shao, Y. *et al.* TADB: a web-based resource for Type 2 toxin-antitoxin loci in bacteria and archaea. *Nucleic Acids Res* **39**, D606-611 (2011).

66 Pandey, D. P. & Gerdes, K. Toxin-antitoxin loci are highly abundant in free-living but lost from host-associated prokaryotes. *Nucleic Acids Res* **33**, 966-976 (2005).

67 Bertram, R. & Schuster, C. F. Post-transcriptional regulation of gene expression in bacterial pathogens by toxin-antitoxin systems. *Front Cell Infect Microbiol* **4**, 6 (2014).

68 Wang, X. & Wood, T. K. Toxin-antitoxin systems influence biofilm and persister cell formation and the general stress response. *Appl Environ Microbiol* **77**, 5577-5583 (2011).

69 Stern, A. & Sorek, R. The phage-host arms race: shaping the evolution of microbes. *Bioessays* **33**, 43-51 (2011).

70 Hyman, P. & Abedon, S. T. Bacteriophage host range and bacterial resistance. *Adv Appl Microbiol* **70**, 217-248 (2010).

71 Labrie, S. J., Samson, J. E. & Moineau, S. Bacteriophage resistance mechanisms. *Nat Rev Microbiol* **8**, 317-327 (2010).

72 Snyder, L. & McWilliams, K. The rex genes of bacteriophage lambda can inhibit cell function without phage superinfection. *Gene* **81**, 17-24 (1989).

73 Parma, D. H. *et al.* The Rex system of bacteriophage lambda: tolerance and altruistic cell death. *Genes Dev* **6**, 497-510 (1992).

74 Fukuyo, M., Sasaki, A. & Kobayashi, I. Success of a suicidal defense strategy against infection in a structured habitat. *Sci Rep* **2**, 238 (2012).

75 Otsuka, Y. & Yonesaki, T. Dmd of bacteriophage T4 functions as an antitoxin against *Escherichia coli* LsoA and RnlA toxins. *Mol Microbiol* **83**, 669-681 (2012).

76 Skorupski, K., Tomaschewski, J., Ruger, W. & Simon, L. D. A bacteriophage T4 gene which functions to inhibit *Escherichia coli* Lon protease. *J Bacteriol* **170**, 3016-3024 (1988).

77 Engelberg-Kulka, H. *et al. rexB* of bacteriophage lambda is an anti-cell death gene. *Proc Natl Acad Sci U S A* **95**, 15481-15486 (1998).

78 Blower, T. R., Evans, T. J., Przybilski, R., Fineran, P. C. & Salmond, G. P. Viral evasion of a bacterial suicide system by RNA-based molecular mimicry enables infectious altruism. *PLoS Genet* **8**, e1003023 (2012).

79 Samson, J. E., Magadan, A. H., Sabri, M. & Moineau, S. Revenge of the phages: defeating bacterial defences. *Nat Rev Microbiol* **11**, 675-687 (2013).

80 Pecota, D. C. & Wood, T. K. Exclusion of T4 phage by the hok/sok killer locus from plasmid R1. *J Bacteriol* **178**, 2044-2050 (1996).

81 Hazan, R. & Engelberg-Kulka, H. *Escherichia coli* mazEF-mediated cell death as a defense mechanism that inhibits the spread of phage P1. *Mol Genet Genomics* **272**, 227-234 (2004).

82 Maisonneuve, E. & Gerdes, K. Molecular mechanisms underlying bacterial persisters. *Cell* **157**, 539-548 (2014).

83 Gardner, A., West, S. A. & Griffin, A. S. Is bacterial persistence a social trait? *PLoS One* **2**, e752 (2007).

84 Dhar, N. & McKinney, J. D. Microbial phenotypic heterogeneity and antibiotic tolerance. *Curr Opin Microbiol* **10**, 30-38 (2007).

85 Balaban, N. Q., Gerdes, K., Lewis, K. & McKinney, J. D. A problem of persistence: still more questions than answers? *Nat Rev Microbiol* **11**, 587-591 (2013).

86 Lewis, K. Persister cells. *Annu Rev Microbiol* **64**, 357-372 (2010).

87 Lewis, K. Persister cells and the riddle of biofilm survival. *Biochemistry. Biokhimiia* **70**, 267-274 (2005).

88 Cohen, N. R., Lobritz, M. A. & Collins, J. J. Microbial persistence and the road to drug resistance. *Cell Host Microbe* **13**, 632-642 (2013).

89 Mulcahy, L. R., Burns, J. L., Lory, S. & Lewis, K. Emergence of *Pseudomonas aeruginosa* Strains Producing High Levels of Persister Cells in Patients with Cystic Fibrosis. *J Bacteriol* **192**, 6191-6199 (2010).

90 Hazan, R., Maura, D., Que, Y. A. & Rahme, L. G. Assessing *Pseudomonas aeruginosa* Persister/antibiotic tolerant cells. *Methods Mol Biol (Clifton, N.J.)* **1149**, 699-707 (2014).

91 Maisonneuve, E., Shakespeare, L. J., Jørgensen, M. G. & Gerdes, K. Bacterial persistence by RNA endonucleases. *Proc Natl Acad Sci U S A* **108**, 13206-13211 (2011).

92 De la Cruz, M. A. *et al.* A toxin-antitoxin module of *Salmonella* promotes virulence in mice. *PLoS Pathog* **9**, e1003827 (2013).

93 Ren, D., Kordis, A. A., Sonenshine, D. E. & Daines, D. A. The ToxAvapA toxin-antitoxin locus contributes to the survival of nontypeable *Haemophilus influenzae* during infection. *PLoS One* **9**, e91523 (2014).

94 Ren, D., Walker, A. N. & Daines, D. A. Toxin-antitoxin loci vapBC-1 and vapXD contribute to survival and virulence in nontypeable *Haemophilus influenzae*. *BMC Microbiol* **12**, 263 (2012).

95 Ramage, H. R., Connolly, L. E. & Cox, J. S. Comprehensive functional analysis of *Mycobacterium tuberculosis* toxin-antitoxin systems: implications for pathogenesis, stress responses, and evolution. *PLoS Genet* **5**, e1000767 (2009).

96 Sala, A., Bordes, P. & Genevaux, P. Multiple toxin-antitoxin systems in *Mycobacterium tuberculosis*. *Toxins* **6**, 1002-1020 (2014).

97 Balaban, N. Q., Merrin, J., Chait, R., Kowalik, L. & Leibler, S. Bacterial persistence as a phenotypic switch. *Science* **305**, 1622-1625 (2004).

98 Rotem, E. *et al.* Regulation of phenotypic variability by a threshold-based mechanism underlies bacterial persistence. *Proc Natl Acad Sci U S A* **107**, 12541-12546 (2010).

99 Kussell, E. & Leibler, S. Phenotypic diversity, population growth, and information in fluctuating environments. *Science* **309**, 2075-2078 (2005).

100 Fasani, R. A. & Savageau, M. A. Molecular mechanisms of multiple toxin-antitoxin systems are coordinated to govern the persister phenotype. *Proc Natl Acad Sci U S A* **110**, E2528-2537 (2013).

101 Tripathi, A., Dewan, P. C., Barua, B. & Varadarajan, R. Additional role for the *ccd* operon of F-plasmid as a transmissible persistence factor. *Proc Natl Acad Sci U S A* **109**, 12497-12502 (2012).

102 Dörr, T., Vulic, M. & Lewis, K. Ciprofloxacin causes persister formation by inducing the TisB toxin in *Escherichia coli*. *PLoS Biol* **8**, e1000317 (2010).

103 Wang, X. *et al.* Antitoxin MqsA helps mediate the bacterial general stress response. *Nat Chem Biol* **7**, 359-366 (2011).

104 Spoering, A. L. & Lewis, K. Biofilms and Planktonic Cells of *Pseudomonas aeruginosa* Have Similar Resistance to Killing by Antimicrobials. *Journal of Bacteriology* **183**, 6746-6751 (2001).

105 Willenborg, J., Willms, D., Bertram, R., Goethe, R. & Valentin-Weigand, P. Characterization of multi-drug tolerant persister cells in *Streptococcus suis*. *BMC microbiology* **14**, 120 (2014).

106 Fozo, E. M. *et al.* Abundance of type I toxin-antitoxin systems in bacteria: searches for new candidates and discovery of novel families. *Nucleic Acids Res* **38**, 3743-3759 (2010).

107 Georgiades, K. & Raoult, D. Genomes of the most dangerous epidemic bacteria have a virulence repertoire characterized by fewer genes but more toxin-antitoxin modules. *PLoS One* **6**, e17962 (2011).

108 Carolin Frank, A., Amiri, H. & Andersson, S. E. Genome deterioration: loss of repeated sequences and accumulation of junk DNA. *Genetica* **115**, 1-12 (2002).

109 Tan, Q., Awano, N. & Inouye, M. YeeV is an *Escherichia coli* toxin that inhibits cell division by targeting the cytoskeleton proteins, FtsZ and MreB. *Mol Microbiol* **79**, 109-118 (2011).

110 Van Acker, H., Sass, A., Dhondt, I., Nelis, H. J. & Coenye, T. Involvement of toxin-antitoxin modules in *Burkholderia cenocepacia* biofilm persistence. *Pathog Dis* **71**, 326-335 (2014).

111 Prax, M. & Bertram, R. Metabolic aspects of bacterial persisters. *Front Cell Infect Microbiol* **4** (2014).

112 Bigger, J. TREATMENT OF STAPHYLOCOCCAL INFECTIONS WITH PENICILLIN BY INTERMITTENT STERILISATION. *The Lancet* **244**, 497-500 (1944).

113 Keren, I., Shah, D., Spoering, A., Kaldalu, N. & Lewis, K. Specialized persister cells and the mechanism of multidrug tolerance in Escherichia coli. *J Bacteriol* **186**, 8172-8180 (2004).

114 Shah, D. *et al.* Persisters: a distinct physiological state of *E. coli*. *BMC Microbiol* **6**, 53 (2006).

115 Keren, I., Minami, S., Rubin, E. & Lewis, K. Characterization and transcriptome analysis of *Mycobacterium tuberculosis* persisters. *mBio* **2**, e00100-00111 (2011).

116 Shi, W. & Zhang, Y. PhoY2 but not PhoY1 is the PhoU homologue involved in persisters in *Mycobacterium tuberculosis*. *J Antimicrob Chemother* **65**, 1237-1242 (2010).

117 Li, Y. & Zhang, Y. PhoU is a persistence switch involved in persister formation and tolerance to multiple antibiotics and stresses in *Escherichia coli*. *Antimicrob Agents Chemother* **51**, 2092-2099 (2007).

118 Vazquez-Laslop, N., Lee, H. & Neyfakh, A. A. Increased persistence in Escherichia coli caused by controlled expression of toxins or other unrelated proteins. *J Bacteriol* **188**, 3494-3497 (2006).

119 Spoering, A. L., Vulic, M. & Lewis, K. GlpD and PlsB participate in persister cell formation in *Escherichia coli*. *J Bacteriol* **188**, 5136-5144 (2006).

120 Hu, Y., Kwan, B. W., Osbourne, D. O., Benedik, M. J. & Wood, T. K. Toxin YafQ increases persister cell formation by reducing indole signalling. *Environ Microbiol* (2014).

121 Leszczynska, D., Matuszewska, E., Kuczynska-Wisnik, D., Furmanek-Blaszk, B. & Laskowska, E. The formation of persister cells in stationary-phase cultures of *Escherichia coli* is associated with the aggregation of endogenous proteins. *PLoS One* **8**, e54737 (2013).

122 Yildiz, F. H. & Schoolnik, G. K. Role of rpoS in stress survival and virulence of *Vibrio cholerae*. *J Bacteriol* **180**, 773-784 (1998).

123 Murakami, K. *et al.* Role for rpoS gene of *Pseudomonas aeruginosa* in antibiotic tolerance. *FEMS Microbiol Lett* **242**, 161-167 (2005).

124 Kim, Y. & Wood, T. K. Toxins Hha and CspD and small RNA regulator Hfq are involved in persister cell formation through MqsR in *Escherichia coli*. *Biochem Biophys Res Commun* **391**, 209-213 (2010).

125 Luidalepp, H., Joers, A., Kaldalu, N. & Tenson, T. Age of inoculum strongly influences persister frequency and can mask effects of mutations implicated in altered persistence. *J Bacteriol* **193**, 3598-3605 (2011).

126 Allison, K. R., Brynildsen, M. P. & Collins, J. J. Heterogeneous bacterial persisters and engineering approaches to eliminate them. *Curr Opin Microbiol* **14**, 593-598 (2011).

127 Kester, J. C. & Fortune, S. M. Persisters and beyond: mechanisms of phenotypic drug resistance and drug tolerance in bacteria. *Crit Rev Biochem Mol Biol* **49**, 91-101 (2014).

128 Johnson, P. J. & Levin, B. R. Pharmacodynamics, population dynamics, and the evolution of persistence in *Staphylococcus aureus*. *PLoS Genet* **9**, e1003123 (2013).

129 Allison, K. R., Brynildsen, M. P. & Collins, J. J. Metabolite-enabled eradication of bacterial persisters by aminoglycosides. *Nature* **473**, 216-220 (2011).

130 Barraud, N., Buson, A., Jarolimek, W. & Rice, S. A. Mannitol Enhances Antibiotic Sensitivity of Persister Bacteria in *Pseudomonas aeruginosa* Biofilms. *PLoS One* **8**, e84220 (2013).

131 Orman, M. A. & Brynildsen, M. P. Dormancy is not necessary or sufficient for bacterial persistence. *Antimicrob Agents Chemother* **57**, 3230-3239 (2013).

132 Kwan, B. W., Valenta, J. A., Benedik, M. J. & Wood, T. K. Arrested protein synthesis increases persister-like cell formation. *Antimicrob Agents Chemother* **57**, 1468-1473 (2013).

133 Unoson, C. & Wagner, E. G. A small SOS-induced toxin is targeted against the inner membrane in *Escherichia coli*. *Mol Microbiol* **70**, 258-270 (2008).

134 Conlon, B. P. *et al.* Activated ClpP kills persisters and eradicates a chronic biofilm infection. *Nature* **503**, 365-370 (2013).

135 Utsumi, R., Nakamoto, Y., Kawamukai, M., Himeno, M. & Komano, T. Involvement of cyclic AMP and its receptor protein in filamentation of an *Escherichia coli fic* mutant. *J Bacteriol* **151**, 807-812 (1982).

136 Kawamukai, M. *et al.* Cloning of the *fic-1* gene involved in cell filamentation induced by cyclic AMP and construction of a delta fic *Escherichia coli* strain. *J Bacteriol* **170**, 3864-3869 (1988).

137 Kawamukai, M., Matsuda, H., Fujii, W., Utsumi, R. & Komano, T. Nucleotide sequences of *fic* and *fic-1* genes involved in cell filamentation induced by cyclic AMP in *Escherichia coli*. *J Bacteriol* **171**, 4525-4529 (1989).

138 Komano, T., Utsumi, R. & Kawamukai, M. Functional analysis of the *fic* gene involved in regulation of cell division. *Res Microbiol* **142**, 269-277 (1991).

139 Salgado, H. *et al.* RegulonDB v8.0: omics data sets, evolutionary conservation, regulatory phrases, cross-validated gold standards and more. *Nucleic Acids Res* **41**, D203-213 (2013).

140 Makarova, K. S., Wolf, Y. I. & Koonin, E. V. Comprehensive comparative-genomic analysis of type 2 toxin-antitoxin systems and related mobile stress response systems in prokaryotes. *Biology direct* **4**, 19 (2009).

141 Hu, P. *et al.* Global functional atlas of *Escherichia coli* encompassing previously uncharacterized proteins. *PLoS Biol* **7**, e96 (2009).

142 Utsumi, R. *et al.* Stationary phase-specific expression of the *fic* gene in *Escherichia coli* K-12 is controlled by the *rpoS* gene product (σ38). *FEMS microbiology letters* **113**, 273-278 (1993).

143 Utsumi, R. *et al.* Identification of a membrane protein induced concurrently with cell filamentation by cyclic AMP in an *Escherichia coli* K-12 *fic* mutant. *J Bacteriol* **155**, 398-401 (1983).

144 Cruz, J. W. & Woychik, N. A. Teaching Fido New ModiFICation Tricks. *PLoS Pathog* **10**, e1004349 (2014).

145 Casselli, T., Lynch, T., Southward, C. M., Jones, B. W. & DeVinney, R. *Vibrio parahaemolyticus* inhibition of Rho family GTPase activation requires a functional chromosome I type III secretion system. *Infect Immun* **76**, 2202-2211 (2008).

146 Zekarias, B. *et al. Histophilus somni* IbpA DR2/Fic in virulence and immunoprotection at the natural host alveolar epithelial barrier. *Infect Immun* **78**, 1850-1858 (2010).

147 Woolery, A. R., Yu, X., LaBaer, J. & Orth, K. AMPylation of Rho GTPases subverts multiple host signaling processes. *J Biol Chem* (2014).

148 Mattoo, S. *et al.* Comparative analysis of *Histophilus somni* immunoglobulin-binding protein A (IbpA) with other fic domain-containing enzymes reveals differences in substrate and nucleotide specificities. *J Biol Chem* **286**, 32834-32842 (2011).

149 Yu, X. *et al.* Copper-catalyzed azide-alkyne cycloaddition (click chemistry)-based Detection of Global Pathogen-host AMPylation on Self-assembled Human Protein Microarrays. *Molecular & Cellular Proteomics* **13**, 3164-3176 (2014).

150 Yarbrough, M. L. *et al.* AMPylation of Rho GTPases by *Vibrio* VopS disrupts effector binding and downstream signaling. *Science* **323**, 269-272 (2009).

151 Luong, P. *et al.* Kinetic and structural insights into the mechanism of AMPylation by VopS Fic domain. *J Biol Chem* **285**, 20155-20163 (2010).

152 Palanivelu, D. V. *et al.* Fic domain catalyzed adenylylation: insight provided by the structural analysis of the type IV secretion system effector BepA. *Protein Sci* (2010).

153 Xiao, J., Worby, C. A., Mattoo, S., Sankaran, B. & Dixon, J. E. Structural basis of Fic-mediated adenylylation. *Nat Struct Mol Biol* **17**, 1004-1010 (2010).

154 Campanacci, V., Mukherjee, S., Roy, C. R. & Cherfils, J. Structure of the *Legionella* effector AnkX reveals the mechanism of phosphocholine transfer by the FIC domain. *EMBO J* **32**, 1469-1477 (2013).

155 Woolery, A. R., Luong, P., Broberg, C. A. & Orth, K. AMPylation: Something old is new again. *Front Microbiol* **1** (2010).

156 Feng, F. *et al.* A *Xanthomonas* uridine 5'-monophosphate transferase inhibits plant immune kinases. *Nature* **485**, 114-118 (2012).

157 Pan, X., Luhrmann, A., Satoh, A., Laskowski-Arce, M. A. & Roy, C. R. Ankyrin repeat proteins comprise a diverse family of bacterial type IV effectors. *Science* **320**, 1651-1654 (2008).

158 Roy, C. R. & Mukherjee, S. Bacterial FIC Proteins AMP Up Infection. *Sci Signal* **2**, pe14 (2009).

159 Mukherjee, S. *et al.* Modulation of Rab GTPase function by a protein phosphocholine transferase. *Nature* **477**, 103-106 (2011).

160 Goody, P. R. *et al.* Reversible phosphocholination of Rab proteins by *Legionella pneumophila* effector proteins. *The EMBO journal* **31**, 1774-1784 (2012).

161 Kinch, L. N., Yarbrough, M. L., Orth, K. & Grishin, N. V. Fido, a novel AMPylation domain common to fic, doc, and AvrB. *PLoS One* **4**, e5818 (2009).

162 Desveaux, D. *et al.* Type III effector activation via nucleotide binding, phosphorylation, and host target interaction. *PLoS Pathog* **3**, e48 (2007).

163 Cui, H. *et al. Pseudomonas syringae* effector protein AvrB perturbs *Arabidopsis* hormone signaling by activating MAP kinase 4. *Cell Host Microbe* **7**, 164-175 (2010).

164 Liu, J., Elmore, J. M., Lin, Z. J. & Coaker, G. A receptor-like cytoplasmic kinase phosphorylates the host target RIN4, leading to the activation of a plant innate immune receptor. *Cell Host Microbe* **9**, 137-146 (2011).

165 Wu, L., Chen, H., Curtis, C. & Fu, Z. Q. Go in for the kill: How plants deploy effector-triggered immunity to combat pathogens. *Virulence* **5** (2014).

166 Chung, E. H., El-Kasmi, F., He, Y., Loehr, A. & Dangl, J. L. A Plant Phosphoswitch Platform Repeatedly Targeted by Type III Effector Proteins Regulates the Output of Both Tiers of Plant Immune Receptors. *Cell Host Microbe* **16**, 484-494 (2014).

167 Lee, C. C. *et al.* Crystal structure of the type III effector AvrB from *Pseudomonas syringae*. *Structure* **12**, 487-494 (2004).

168 Innes, R. W. Activation of plant nod-like receptors: how indirect can it be? *Cell Host Microbe* **9**, 87-89 (2011).

169 Engel, P. *et al.* Parallel evolution of a type IV secretion system in radiating lineages of the host-restricted bacterial pathogen *Bartonella*. *PLoS Genet* **7**, e1001296 (2011).

170 Garcia-Pino, A., Zenkin, N. & Loris, R. The many faces of Fic: structural and functional aspects of Fic enzymes. *Trends Biochem Sci* **39**, 121-129 (2014).

171 Liu, M., Zhang, Y., Inouye, M. & Woychik, N. A. Bacterial addiction module toxin Doc inhibits translation elongation through its association with the 30S ribosomal subunit. *Proc Natl Acad Sci U S A* **105**, 5885-5890 (2008).

172 Finn, R. D. *et al.* The Pfam protein families database. *Nucleic Acids Res* **38**, D211-222 (2010).

173 Worby, C. A. *et al.* The fic domain: regulation of cell signaling by adenylylation. *Mol Cell* **34**, 93-103 (2009).

174 Rahman, M. *et al.* Visual neurotransmission in Drosophila requires expression of Fic in glial capitate projections. *Nature neuroscience* **15**, 871-875 (2012).

175 Ham, H. *et al.* Unfolded protein response-regulated dFic reversibly AMPylates BiP during endoplasmic reticulum homeostasis. *J Biol Chem* (2014).

176 Lewallen, D. M. *et al.* Inhibiting AMPylation: a novel screen to identify the first small molecule inhibitors of protein AMPylation. *ACS Chem Biol* **9**, 433-442 (2014).

177 Engel, P. *et al.* Adenylylation control by intra- or intermolecular active-site obstruction in Fic proteins. *Nature* **482**, 107-110 (2012).

178 Goepfert, A., Stanger, F. V., Dehio, C. & Schirmer, T. Conserved inhibitory mechanism and competent ATP binding mode for adenylyltransferases with Fic fold. *PLoS One* **8**, e64901 (2013).

179 Das, D. *et al.* Crystal structure of the Fic (Filamentation induced by cAMP) family protein SO4266 (gi|24375750) from *Shewanella oneidensis* MR-1 at 1.6 A resolution. *Proteins* **75**, 264-271 (2009).

180 Itzen, A., Blankenfeldt, W. & Goody, R. S. Adenylylation: renaissance of a forgotten post-translational modification. *Trends Biochem Sci* **36**, 221-228 (2011).

181 Deweese, J. E., Osheroff, M. A. & Osheroff, N. DNA Topology and Topoisomerases: Teaching a "Knotty" Subject. *Biochem Mol Biol Educ* **37**, 2-10 (2008).

182 Koster, D. A., Crut, A., Shuman, S., Bjornsti, M. A. & Dekker, N. H. Cellular strategies for regulating DNA supercoiling: a single-molecule perspective. *Cell* **142**, 519-530 (2010).

183 Liu, L. F. & Wang, J. C. Supercoiling of the DNA template during transcription. *Proc Natl Acad Sci U S A* **84**, 7024-7027 (1987).

184 Schvartzman, J. B. & Stasiak, A. A topological view of the replicon. *EMBO Rep* **5**, 256-261 (2004).

185 Postow, L., Hardy, C. D., Arsuaga, J. & Cozzarelli, N. R. Topological domain structure of the *Escherichia coli* chromosome. *Genes Dev* **18**, 1766-1779 (2004).

186 de Vries, R. DNA condensation in bacteria: Interplay between macromolecular crowding and nucleoid proteins. *Biochimie* **92**, 1715-1721 (2010).

187 Rovinskiy, N., Agbleke, A. A., Chesnokova, O., Pang, Z. & Higgins, N. P. Rates of gyrase supercoiling and transcription elongation control supercoil density in a bacterial chromosome. *PLoS Genet* **8**, e1002845 (2012).

188 Baxter, J. "Breaking Up Is Hard to Do": The Formation and Resolution of Sister Chromatid Intertwines. *J Mol Biol*.

189 Schvartzman, J. B., Martinez-Robles, M. L., Hernandez, P. & Krimer, D. B. The benefit of DNA supercoiling during replication. *Biochem Soc Trans* **41**, 646-651 (2013).

190 Cozzarelli, N. R., Cost, G. J., Nollmann, M., Viard, T. & Stray, J. E. Giant proteins that move DNA: bullies of the genomic playground. *Nat Rev Mol Cell Biol* **7**, 580-588 (2006).

191 Pommier, Y., Leo, E., Zhang, H. & Marchand, C. DNA Topoisomerases and Their Poisoning by Anticancer and Antibacterial Drugs. *Chemistry & Biology* **17**, 421-433 (2010).

192 Vos, S. M., Tretter, E. M., Schmidt, B. H. & Berger, J. M. All tangled up: how cells direct, manage and exploit topoisomerase function. *Nat Rev Mol Cell Biol* **12**, 827-841 (2011).

193 Schoeffler, A. J. & Berger, J. M. DNA topoisomerases: harnessing and constraining energy to govern chromosome topology. *Q Rev Biophys* **41**, 41-101 (2008).

194 Forterre, P. & Gadelle, D. Phylogenomics of DNA topoisomerases: their origin and putative roles in the emergence of modern organisms. *Nucleic Acids Res* **37**, 679-692 (2009).

195 DiNardo, S., Voelkel, K. A., Sternglanz, R., Reynolds, A. E. & Wright, A. *Escherichia coli* DNA topoisomerase I mutants have compensatory mutations in DNA gyrase genes. *Cell* **31**, 43-51 (1982).

196 Masse, E. & Drolet, M. Relaxation of transcription-induced negative supercoiling is an essential function of *Escherichia coli* DNA topoisomerase I. *J Biol Chem* **274**, 16654-16658 (1999).

197 Perez-Cheeks, B. A., Lee, C., Hayama, R. & Marians, K. J. A role for topoisomerase III in *Escherichia coli* chromosome segregation. *Mol Microbiol* **86**, 1007-1022 (2012).

198 Lopez, C. R. *et al.* A role for topoisomerase III in a recombination pathway alternative to RuvABC. *Mol Microbiol* **58**, 80-101 (2005).

199 Terekhova, K., Marko, J. F. & Mondragon, A. Single-molecule analysis uncovers the difference between the kinetics of DNA decatenation by bacterial topoisomerases I and III. *Nucleic Acids Res*(2014).

200 Bergerat, A., Gadelle, D. & Forterre, P. Purification of a DNA topoisomerase II from the hyperthermophilic archaeon *Sulfolobus shibatae*. A thermostable enzyme with both bacterial and eucaryal features. *J Biol Chem* **269**, 27663-27669 (1994).

201 Dutta, R. & Inouye, M. GHKL, an emergent ATPase/kinase superfamily. *Trends Biochem Sci* **25**, 24-28 (2000).

202 Manjunatha, U. H. *et al.* Functional characterisation of mycobacterial DNA gyrase: an efficient decatenase. *Nucleic Acids Res* **30**, 2144-2153 (2002).

203 Gubaev, A. & Klostermeier, D. The mechanism of negative DNA supercoiling: a cascade of DNA-induced conformational changes prepares gyrase for strand passage. *DNA Repair (Amst)* **16**, 23-34 (2014).

204 Liu, L. F. & Wang, J. C. DNA-DNA gyrase complex: the wrapping of the DNA duplex outside the enzyme. *Cell* **15**, 979-984 (1978).

205 Brown, P. O. & Cozzarelli, N. R. A sign inversion mechanism for enzymatic supercoiling of DNA. *Science* **206**, 1081-1083 (1979).

206 Lanz, M. A. & Klostermeier, D. The GyrA-box determines the geometry of DNA bound to gyrase and couples DNA binding to the nucleotide cycle. *Nucleic Acids Res* **40**, 10893-10903 (2012).

207 Ward, D. & Newton, A. Requirement of topoisomerase IV *parC* and *parE* genes for cell cycle progression and developmental regulation in *Caulobacter crescentus*. *Mol Microbiol* **26**, 897-910 (1997).

208 Papillon, J. *et al.* Structural insight into negative DNA supercoiling by DNA gyrase, a bacterial type 2A DNA topoisomerase. *Nucleic Acids Res* **41**, 7815-7827 (2013).

209 Corbett, K. D., Schoeffler, A. J., Thomsen, N. D. & Berger, J. M. The structural basis for substrate specificity in DNA topoisomerase IV. *J Mol Biol* **351**, 545-561 (2005).

210 Vos, S. M., Lee, I. & Berger, J. M. Distinct regions of the *Escherichia coli* ParC C-terminal domain are required for substrate discrimination by topoisomerase IV. *J Mol Biol* **425**, 3029-3045 (2013).

211 Sissi, C. & Palumbo, M. In front of and behind the replication fork: bacterial type IIA topoisomerases. *Cell Mol Life Sci* **67**, 2001-2024 (2010).

212 Bates, A. D. & Maxwell, A. The role of ATP in the reactions of type II DNA topoisomerases. *Biochem Soc Trans* **38**, 438-442 (2010).

213 Bates, A. D., Berger, J. M. & Maxwell, A. The ancestral role of ATP hydrolysis in type II topoisomerases: prevention of DNA double-strand breaks. *Nucleic Acids Res* **39**, 6327-6339 (2011).

214 Basu, A., Schoeffler, A. J., Berger, J. M. & Bryant, Z. ATP binding controls distinct structural transitions of *Escherichia coli* DNA gyrase in complex with DNA. *Nat Struct Mol Biol* **19**, 538-546, s531 (2012).

215 Stanger, F. V., Dehio, C. & Schirmer, T. Structure of the N-terminal Gyrase B fragment in complex with ADPPi reveals rigid-body motion induced by ATP hydrolysis. *PLoS One* **9**, e107289 (2014).

216 Witz, G. & Stasiak, A. DNA supercoiling and its role in DNA decatenation and unknotting. *Nucleic Acids Res* **38**, 2119-2133 (2010).

217 Khodursky, A. B. *et al.* Analysis of topoisomerase function in bacterial replication fork movement: use of DNA microarrays. *Proc Natl Acad Sci U S A* **97**, 9419-9424 (2000).

218 Zechiedrich, E. L. & Cozzarelli, N. R. Roles of topoisomerase IV and DNA gyrase in DNA unlinking during replication in *Escherichia coli*. *Genes Dev* **9**, 2859-2869 (1995).

219 Chong, S., Chen, C., Ge, H. & Xie, X. S. Mechanism of transcriptional bursting in bacteria. *Cell* **158**, 314-326 (2014).

220 Deibler, R. W., Rahmati, S. & Zechiedrich, E. L. Topoisomerase IV, alone, unknots DNA in *E. coli*. *Genes Dev.* **15**, 748-761 (2001).

221 Deibler, R. W., Mann, J. K., Sumners de, W. L. & Zechiedrich, L. Hin-mediated DNA knotting and recombining promote replicon dysfunction and mutation. *BMC Mol Biol* **8**, 44 (2007).

222 Witz, G., Dietler, G. & Stasiak, A. DNA knots and DNA supercoiling. *Cell cycle* **10**, 1339-1340 (2011).

223 Witz, G., Dietler, G. & Stasiak, A. Tightening of DNA knots by supercoiling facilitates their unknotting by type II DNA topoisomerases. *Proc Natl Acad Sci U S A* **108**, 3608-3611 (2011).

224 Truttmann, M. C., Guye, P. & Dehio, C. BID-F1 and BID-F2 domains of *Bartonella henselae* effector protein BepF trigger together with BepC the formation of invasome structures. *PLoS One* **6**, e25106 (2011).

225 Guy, L. *et al.* A genome-wide study of recombination rate variation in *Bartonella henselae*. *BMC Evol Biol* **12**, 65 (2012).

226 Classen, S., Olland, S. & Berger, J. M. Structure of the topoisomerase II ATPase region and its mechanism of inhibition by the chemotherapeutic agent ICRF-187. *Proc Natl Acad Sci U S A* **100**, 10629-10634 (2003).

227 Rimsky, S. & Travers, A. Pervasive regulation of nucleoid structure and function by nucleoid-associated proteins. *Curr Opin Microbiol* **14**, 136-141 (2011).

228 Carter, S. D. & Sjogren, C. The SMC complexes, DNA and chromosome topology: right or knot? *Crit Rec Biochem Mol Biol* **47**, 1-16 (2012).

229 Travers, A. & Muskhelishvili, G. Bacterial chromatin. *Curr Opin Genet Dev* **15**, 507-514 (2005).

230 Nicolas, E. *et al.* The SMC complex MukBEF recruits topoisomerase IV to the origin of replication region in live *Escherichia coli*. *mBio* **5**, e01001-01013 (2014).

231 Lindow, J. C., Britton, R. A. & Grossman, A. D. Structural maintenance of chromosomes protein of *Bacillus subtilis* affects supercoiling *in vivo*. *J Bacteriol* **184**, 5317-5322 (2002).

232 Malik, M., Bensaid, A., Rouviere-Yaniv, J. & Drlica, K. Histone-like protein HU and bacterial DNA topology: suppression of an HU deficiency by gyrase mutations. *J Mol Biol* **256**, 66-76 (1996).

233 Howard, M. T., Neece, S. H., Matson, S. W. & Kreuzer, K. N. Disruption of a topoisomerase-DNA cleavage complex by a DNA helicase. *Proc Natl Acad Sci U S A* **91**, 12031-12035 (1994).

234 Pommier, Y. Drugging topoisomerases: lessons and challenges. *ACS Chem Biol* **8**, 82-95 (2013).

235 Tse-Dinh, Y.-C. Bacterial topoisomerase I as a target for discovery of antibacterial compounds. *Nucleic Acids Res* **37**, 731-737 (2009).

236 Collin, F., Karkare, S. & Maxwell, A. Exploiting bacterial DNA gyrase as a drug target: current state and perspectives. *Appl Microbiol Biotechnol* **92**, 479-497 (2011).

237 Gellert, M., O'Dea, M. H., Itoh, T. & Tomizawa, J. Novobiocin and coumermycin inhibit DNA supercoiling catalyzed by DNA gyrase. *Proc Natl Acad Sci U S A* **73**, 4474-4478 (1976).

238 Sugino, A., Higgins, N. P., Brown, P. O., Peebles, C. L. & Cozzarelli, N. R. Energy coupling in DNA gyrase and the mechanism of action of novobiocin. *Proc Natl Acad Sci U S A* **75**, 4838-4842 (1978).

239 Hardy, C. D. & Cozzarelli, N. R. Alteration of *Escherichia coli* topoisomerase IV to novobiocin resistance. *Antimicrob Agents Chemother* **47**, 941-947 (2003).

240 Edwards, M. J. *et al.* A crystal structure of the bifunctional antibiotic simocyclinone D8, bound to DNA gyrase. *Science* **326**, 1415-1418 (2009).

241 Nakada, N., Gmunder, H., Hirata, T. & Arisawa, M. Characterization of the binding site for cyclothialidine on the B subunit of DNA gyrase. *J Biol Chem* **270**, 14286-14291 (1995).

242 Oram, M. *et al.* Mode of action of GR122222X, a novel inhibitor of bacterial DNA gyrase. *Antimicrob Agents Chemother* **40**, 473-476 (1996).

243 Osburne, M. S. Characterization of a cinodine-resistant mutant of *Escherichia coli*. *J Antibiot (Tokyo)* **48**, 1359-1361 (1995).

244 P, S. H. *et al.* Optimization of pyrrolamides as mycobacterial GyrB ATPase inhibitors: structure-activity relationship and in vivo efficacy in a mouse model of tuberculosis. *Antimicrob Agents Chemother* **58**, 61-70 (2014).

245 Rajendram, M. *et al.* Gyramides prevent bacterial growth by inhibiting DNA gyrase and altering chromosome topology. *ACS Chem Biol* **9**, 1312-1319 (2014).

246 Nakanishi, A., Oshida, T., Matsushita, T., Imajoh-Ohmi, S. & Ohnuki, T. Identification of DNA gyrase inhibitor (GyrI) in *Escherichia coli*. *J Biol Chem* **273**, 1933-1938 (1998).

247 Chatterji, M. & Nagaraja, V. GyrI: a counter-defensive strategy against proteinaceous inhibitors of DNA gyrase. *EMBO Rep* **3**, 261-267 (2002).

248 Sengupta, S. & Nagaraja, V. Inhibition of DNA gyrase activity by *Mycobacterium smegmatis* MurI. *FEMS Microbiol Lett* **279**, 40-47 (2008).

249 Tran, J. H., Jacoby, G. A. & Hooper, D. C. Interaction of the plasmid-encoded quinolone resistance protein Qnr with *Escherichia coli* DNA gyrase. *Antimicrob Agents Chemother* **49**, 118-125 (2005).

250 Tran, J. H., Jacoby, G. A. & Hooper, D. C. Interaction of the plasmid-encoded quinolone resistance protein QnrA with *Escherichia coli* topoisomerase IV. *Antimicrob Agents Chemother* **49**, 3050-3052 (2005).

251 Sengupta, S. & Nagaraja, V. YacG from *Escherichia coli* is a specific endogenous inhibitor of DNA gyrase. *Nucleic Acids Res* **36**, 4310-4316 (2008).

252 Vos, S. M. *et al.* Direct control of type IIA topoisomerase activity by a chromosomally encoded regulatory protein. *Genes Dev* **28**, 1485-1497 (2014).

253 Drlica, K. *et al.* Quinolones: action and resistance updated. *Curr Top Med Chem* **9**, 981-998 (2009).

254 Sugino, A., Peebles, C. L., Kreuzer, K. N. & Cozzarelli, N. R. Mechanism of action of nalidixic acid: purification of *Escherichia coli nalA* gene product and its relationship to DNA gyrase and a novel nicking-closing enzyme. *Proc Natl Acad Sci U S A* **74**, 4767-4771 (1977).

255 Wohlkonig, A. *et al.* Structural basis of quinolone inhibition of type IIA topoisomerases and target-mediated resistance. *Nat Struct Mol Biol* **17**, 1152-1153 (2010).

256 Pan, X. S., Dias, M., Palumbo, M. & Fisher, L. M. Clerocidin selectively modifies the gyrase-DNA gate to induce irreversible and reversible DNA damage. *Nucleic Acids Res* **36**, 5516-5529 (2008).

257 Richter, S. N. *et al.* Clerocidin interacts with the cleavage complex of *Streptococcus pneumoniae* topoisomerase IV to induce selective irreversible DNA damage. *Nucleic Acids Res* **34**, 1982-1991 (2006).

258 Hashimi, S. M., Wall, M. K., Smith, A. B., Maxwell, A. & Birch, R. G. The phytotoxin albicidin is a novel inhibitor of DNA gyrase. *Antimicrob Agents Chemother* **51**, 181-187 (2007).

259 Pierrat, O. A. & Maxwell, A. Evidence for the role of DNA strand passage in the mechanism of action of microcin B17 on DNA gyrase. *Biochemistry* **44**, 4204-4215 (2005).

260 Bernard, P. *et al.* The F plasmid CcdB protein induces efficient ATP-dependent DNA cleavage by gyrase. *J Mol Biol* **234**, 534-541 (1993).

261 Deghorain, M., Goeders, N., Jové, T. & Melderen, L. in *Prokaryotic Toxin-Antitoxins* (ed Kenn Gerdes) Ch. 4, 45-67 (Springer Berlin Heidelberg, 2013).

262 Bax, B. D. *et al.* Type IIA topoisomerase inhibition by a new class of antibacterial agents. *Nature* **466**, 935-940 (2010).

263 Lamour, V., Hoermann, L., Jeltsch, J.-M., Oudet, P. & Moras, D. An Open Conformation of the *Thermus thermophilus* Gyrase B ATP-binding Domain. *J Biol Chem* **277**, 18947-18953 (2002).

264 Scheirer, K. E. & Higgins, N. P. The DNA Cleavage Reaction of DNA Gyrase: COMPARISON OF STABLE TERNARY COMPLEXES FORMED WITH ENOXACIN AND CcdB PROTEIN. *Journal of Biological Chemistry* **272**, 27202-27209 (1997).

265 Shah, S. & Heddle, J. G. Squaring up to DNA: pentapeptide repeat proteins and DNA mimicry. *Applied microbiology and biotechnology* (2014).

266 Li, T. K. & Liu, L. F. Modulation of gyrase-mediated DNA cleavage and cell killing by ATP. *Antimicrob Agents Chemother* **42**, 1022-1027 (1998).

267 Zhu, Q., Kosoy, M., Olival, K. J. & Dittmar, K. Horizontal Transfers and Gene Losses in the Phospholipid Pathway of *Bartonella* Reveal Clues about Early Ecological Niches. *Genome Biol Evol* **6**, 2156-2169 (2014).

268 Chomel, B. B. *et al.* Ecological fitness and strategies of adaptation of *Bartonella* species to their hosts and vectors. *Vet Res* **40**, 29 (2009).

269 Pulliainen, A. T. & Dehio, C. Persistence of *Bartonella* spp. stealth pathogens: from subclinical infections to vasoproliferative tumor formation. *FEMS Microbiol Rev* **36**, 563-599 (2012).

270 Breitschwerdt, E. B., Maggi, R. G., Chomel, B. B. & Lappin, M. R. Bartonellosis: an emerging infectious disease of zoonotic importance to animals and human beings. *J Vet Emerg Crit Care (San Antonio)* **20**, 8-30 (2010).

271 Alsmark, C. M. *et al.* The louse-borne human pathogen *Bartonella quintana* is a genomic derivative of the zoonotic agent *Bartonella henselae*. *Proc Natl Acad Sci U S A* **101**, 9716-9721 (2004).

272 Kaiser, P. O., Riess, T., O'Rourke, F., Linke, D. & Kempf, V. A. *Bartonella* spp.: throwing light on uncommon human infections. *Int J Med Microbiol* **301**, 7-15 (2011).

273 Maguina, C., Guerra, H. & Ventosilla, P. Bartonellosis. *Clin Dermatol* **27**, 271-280 (2009).

274 Angelakis, E. & Raoult, D. Pathogenicity and treatment of *Bartonella* infections. *Int J Antimicrob Agents* **44**, 16-25 (2014).

275 Saenz, H. L. *et al.* Genomic analysis of *Bartonella* identifies type IV secretion systems as host adaptability factors. *Nature Genet* **39**, 1469-1476 (2007).

276 Vayssier-Taussat, M. *et al.* The Trw type IV secretion system of *Bartonella* mediates host-specific adhesion to erythrocytes. *PLoS Pathog* **6**, e1000946 (2010).

277 Minnick, M. F. & Battisti, J. M. Pestilence, persistence and pathogenicity: infection strategies of *Bartonella*. *Future Microbiol* **4**, 743-758 (2009).

278 Minnick, M. F., Smitherman, L. S. & Samuels, D. S. Mitogenic effect of *Bartonella bacilliformis* on human vascular endothelial cells and involvement of GroEL. *Infect Immun* **71**, 6933-6942 (2003).

279 Derrick, S. C. & Ihler, G. M. Deformin, a substance found in *Bartonella bacilliformis* culture supernatants, is a small, hydrophobic molecule with an affinity for albumin. *Blood Cells Mol Dis* **27**, 1013-1019 (2001).

280 Riess, T. *et al. Bartonella* adhesin a mediates a proangiogenic host cell response. *J Exp Med* **200**, 1267-1278 (2004).

281 Zhang, P. *et al.* A family of variably expressed outer-membrane proteins (Vomp) mediates adhesion and autoaggregation in *Bartonella quintana*. *Proc Natl Acad Sci U S A* **101**, 13630-13635 (2004).

282 Roden, J. A., Wells, D. H., Chomel, B. B., Kasten, R. W. & Koehler, J. E. Hemin binding protein C is found in outer membrane vesicles and protects *Bartonella henselae* against toxic concentrations of hemin. *Infect Immun* **80**, 929-942 (2012).

283 Nystedt, B., Frank, A. C., Thollesson, M. & Andersson, S. G. Diversifying selection and concerted evolution of a type IV secretion system in *Bartonella*. *Mol Biol Evol* **25**, 287-300 (2008).

284 Guy, L. *et al.* A gene transfer agent and a dynamic repertoire of secretion systems hold the keys to the explosive radiation of the emerging pathogen *Bartonella*. *PLoS Genet* **9**, e1003393 (2013).

285 Burgess, A. W. & Anderson, B. E. Outer membrane proteins of *Bartonella henselae* and their interaction with human endothelial cells. *Microb Pathog* **25**, 157-164 (1998).

286 Liu, M. & Biville, F. Managing iron supply during the infection cycle of a flea borne pathogen, *Bartonella henselae*. *Front Cell Infect Microbiol* **3**, 60 (2013).

287 Kirby, J. E. & Nekorchuk, D. M. *Bartonella*-associated endothelial proliferation depends on inhibition of apoptosis. *Proc Natl Acad Sci U S A* **99**, 4656-4661 (2002).

288 Breitschwerdt, E. B. Bartonellosis: one health perspectives for an emerging infectious disease. *ILAR J* **55**, 46-58 (2014).

289 Breitschwerdt, E. B., Maggi, R. G., Cadenas, M. B. & de Paiva Diniz, P. P. A groundhog, a novel *Bartonella* sequence, and my father's death. *Emerg Infect Dis* **15**, 2080-2086 (2009).

290 Mascarelli, P. E. *et al. Bartonella henselae* infection in a family experiencing neurological and neurocognitive abnormalities after woodlouse hunter spider bites. *Parasit Vectors* **6**, 98 (2013).

291 Erol, E. *et al. Bartonella bovis* isolated from a cow with endocarditis. *J Vet Diagn Invest* **25**, 288-290 (2013).

292 Billeter, S. A., Sangmaneedet, S., Kosakewich, R. C. & Kosoy, M. Y. *Bartonella* species in dogs and their ectoparasites from Khon Kaen Province, Thailand. *Southeast Asian J Trop Med Public Health* **43**, 1186-1192 (2012).

293 Mascarelli, P. E., McQuillan, M., Harms, C. A., Harms, R. V. & Breitschwerdt, E. B. *Bartonella henselae* and *B. koehlerae* DNA in birds. *Emerg Infect Dis* **20**, 490-492 (2014).

294 Diatta, G. *et al.* Prevalence of *Bartonella quintana* in patients with fever and head lice from rural areas of Sine-Saloum, Senegal. *Am J Trop Med Hyg* **91**, 291-293 (2014).

295 Billeter, S. A. *et al.* Infection and replication of *Bartonella* species within a tick cell line. *Exp Appl Acarol* **49**, 193-208 (2009).

296 Palmero, J. *et al.* Experimental infection of horses with *Bartonella henselae* and *Bartonella bovis*. *J Vet Intern Med* **26**, 377-383 (2012).

297 Chomel, B. B. *et al.* Experimental infection of dogs with various *Bartonella* species or subspecies isolated from their natural reservoir. *Vet Microbiol* **168**, 169-176 (2014).

298 Colton, L., Kabeya, H. & Kosoy, M. Experimental infection of three laboratory mouse stocks with a shrew origin *Bartonella elizabethae* strain: an evaluation of bacterial host switching potential. *Infect Ecol Epidemiol* **2** (2012).

299 Dehio, C. *Bartonella*-host-cell interactions and vascular tumour formation. *Nat Rev Microbiol* **3**, 621-631 (2005).

300 Dehio, C. Infection-associated type IV secretion systems of *Bartonella* and their diverse roles in host cell interaction. *Cell Microbiol* **10**, 1591-1598 (2008).

301 Minnick, M. F. *et al.* Oroya fever and verruga peruana: bartonelloses unique to South America. *PLoS Negl Trop Dis* **8**, e2919 (2014).

302 Hotez, P. J. Neglected Infections of Poverty in the United States of America. *PLoS Negl Trop Dis* **2**, e256 (2008).

303 Frank, A. C., Alsmark, C. M., Thollesson, M. & Andersson, S. G. Functional divergence and horizontal transfer of type IV secretion systems. *Mol Biol Evol* **22**, 1325-1336 (2005).

304 Cabezón, E., Ripoll-Rozada, J., Peña, A., de la Cruz, F. & Arechaga, I. Towards an integrated model of bacterial conjugation. *FEMS Microbiol Rev* (2014).

305 Seubert, A., Hiestand, R., de la Cruz, F. & Dehio, C. A bacterial conjugation machinery recruited for pathogenesis. *Mol Microbiol* **49**, 1253-1266 (2003).

306 Deng, H. K., Le Rhun, D., Le Naour, E., Bonnet, S. & Vayssier-Taussat, M. Identification of *Bartonella* Trw host-specific receptor on erythrocytes. *PLoS One* **7**, e41447 (2012).

307 Nystedt, B., Frank, A. C., Thollesson, M. & Andersson, S. G. E. Diversifying Selection and Concerted Evolution of a Type IV Secretion System in *Bartonella*. *Mol Biol Evol* **25**, 287-300 (2008).

308 Sander, A. *et al.* Characterization of *Bartonella clarridgeiae* flagellin (FlaA) and detection of antiflagellin antibodies in patients with lymphadenopathy. *J Clin Microbiol* **38**, 2943-2948 (2000).

309 Rolain, J. M. *et al.* Immunofluorescence detection of *Bartonella bacilliformis* flagella *in vitro* and in vivo in human red blood cells as viewed by laser confocal microscopy. *Ann N Y Acad Sci* **990**, 581-584 (2003).

310 Andersen-Nissen, E. *et al.* Evasion of Toll-like receptor 5 by flagellated bacteria. *Proc Natl Acad Sci U S A* **102**, 9247-9252 (2005).

311 Schulein, R. *et al.* A bipartite signal mediates the transfer of type IV secretion substrates of *Bartonella henselae* into human cells. *Proc Natl Acad Sci U S A* **102**, 856-861 (2005).

312 Pulliainen, A. T. *et al.* Bacterial effector binds host cell adenylyl cyclase to potentiate Galphas-dependent cAMP production. *Proc Natl Acad Sci U S A* **109**, 9581-9586 (2012).

313 Okujava, R. *et al.* A translocated effector required for bartonella dissemination from derma to blood safeguards migratory host cells from damage by co-translocated effectors. *PLoS Pathog* **10**, e1004187 (2014).

314 Siamer, S. & Dehio, C. New insights into the role of *Bartonella* effector proteins in pathogenesis. *Curr Opin Microbiol* ***in press*** (2015).

315 Merrell, D. S. & Falkow, S. Frontal and stealth attack strategies in microbial pathogenesis. *Nature* **430**, 250-256 (2004).

316 O'Boyle, N. & Boyd, A. Manipulation of intestinal epithelial cell function by the cell contact-dependent type III secretion systems of *Vibrio parahaemolyticus*. *Front Cell Infect Microbiol* **3**, 114 (2014).

317 Corbeil, L. B. *Histophilus somni* host-parasite relationships. *Anim Health Res Rev***8**, 151-160 (2007).

318 Berglund, E. C. *et al.* Run-off replication of host-adaptability genes is associated with gene transfer agents in the genome of mouse-infecting *Bartonella grahamii*. *PLoS Genet* **5**, e1000546 (2009).

319 Liesch, M. *Bartonella schoenbuchensis genome assembly and functional characterization of the VirB-homologous (Vbh) type IV secretion system* Master of Science thesis, University of Basel, (2008).

320 Mogollon-Pasapera, E., Otvos, L., Jr., Giordano, A. & Cassone, M. *Bartonella*: emerging pathogen or emerging awareness? *Int J Infect Dis* **13**, 3-8 (2009).

321 Young, H. S. *et al.* Declines in large wildlife increase landscape-level prevalence of rodent-borne disease in Africa. *Proc Natl Acad Sci U S A* **111**, 7036-7041 (2014).

322 Rasis, M., Rudoler, N., Schwartz, D. & Giladi, M. *Bartonella dromedarii* sp. nov. Isolated from Domesticated Camels (*Camelus dromedarius*) in Israel. *Vector Borne Zoonot Dis* **14**, 775-782 (2014).

323 Fernandez-Gonzalez, E. *et al.* Transfer of R388 derivatives by a pathogenesis-associated type IV secretion system into both bacteria and human cells. *J Bacteriol* **193**, 6257-6265 (2011).

324 Schroder, G., Schuelein, R., Quebatte, M. & Dehio, C. Conjugative DNA transfer into human cells by the VirB/VirD4 type IV secretion system of the bacterial pathogen *Bartonella henselae*. *Proc Natl Acad Sci U S A* **108**, 14643-14648 (2011).

325 Quebatte, M., Dick, M. S., Kaever, V., Schmidt, A. & Dehio, C. Dual input control: activation of the *Bartonella henselae* VirB/D4 type IV secretion system by the stringent sigma factor RpoH1 and the BatR/BatS two-component system. *Mol Microbiol* **90**, 756-775 (2013).

326 Abromaitis, S. *et al. Bartonella quintana* deploys host and vector temperature-specific transcriptomes. *PLoS One* **8**, e58773 (2013).

327 Kaiser, P. O., Linke, D., Schwarz, H., Leo, J. C. & Kempf, V. A. Analysis of the BadA stalk from *Bartonella henselae* reveals domain-specific and domain-overlapping functions in the host cell infection process. *Cell Microbiol* **14**, 198-209 (2012).

328 Stekhoven, D. J., Omasits, U., Quebatte, M., Dehio, C. & Ahrens, C. H. Proteome-wide identification of predominant subcellular protein localizations in a bacterial model organism. *J Proteomics* **99**, 123-137 (2014).

329 Omasits, U. *et al.* Directed shotgun proteomics guided by saturated RNA-seq identifies a complete expressed prokaryotic proteome. *Genome Res* **23**, 1916-1927 (2013).

330 Bowers, T. J., Sweger, D., Jue, D. & Anderson, B. Isolation, sequencing and expression of the gene encoding a major protein from the backteriophage (*sic!*) associated with *Bartonella henselae*. *Gene* **206**, 49-52 (1998).

331 Liu, M. *et al.* Heme binding proteins of *Bartonella henselae* are required when undergoing oxidative stress during cell and flea invasion. *PLoS One* **7**, e48408 (2012).

332 Lu, Y. Y. *et al. Bartonella henselae* trimeric autotransporter adhesin BadA expression interferes with effector translocation by the VirB/D4 type IV secretion system. *Cell Microbiol* **15**, 759-778 (2013).

333 Kyme, P. A. *et al.* Unusual trafficking pattern of *Bartonella henselae* -containing vacuoles in macrophages and endothelial cells. *Cell Microbiol* **7**, 1019-1034 (2005).

334 Breedveld, M. W. & Miller, K. J. Cyclic β-glucans of members of the family Rhizobiaceae. *Microbiological reviews* **58**, 145-161 (1994).

335 Li, H. *et al.* Transmission and maintenance cycle of *Bartonella quintana* among rhesus macaques, China. *Emerg Infect Dis* **19**, 297-300 (2013).

336 Li, H. *et al.* Genetic diversity of *Bartonella quintana* in macaques suggests zoonotic origin of trench fever. *Mol Ecol* **22**, 2118-2127 (2013).

337 Paziewska, A., Sinski, E. & Harris, P. D. Recombination, diversity and allele sharing of infectivity proteins between *Bartonella* species from rodents. *Microb Ecol* **64**, 525-536 (2012).

338 Berglund, E. C. *et al.* Genome dynamics of *Bartonella grahamii* in micro-populations of woodland rodents. *BMCGgenomics* **11**, 152 (2010).

339 Berglund, E. C. *et al.* Rapid diversification by recombination in *Bartonella grahamii* from wild rodents in Asia contrasts with low levels of genomic divergence in Northern Europe and America. *Mol Ecol* **19**, 2241-2255 (2010).

340 Larson, H. K. *et al.* Distribution and dietary regulation of an associated facultative Rhizobiales-related bacterium in the omnivorous giant tropical ant, *Paraponera clavata*. *Naturwissenschaften* **101**, 397-406 (2014).

341 Russell, J. A. *et al.* Bacterial gut symbionts are tightly linked with the evolution of herbivory in ants. *Proc Natl Acad Sci U S A* **106**, 21236-21241 (2009).

342 Martinson, V. G. *et al.* A simple and distinctive microbiota associated with honey bees and bumble bees. *Mol Ecol* **20**, 619-628 (2011).

343 Ahn, J. H. *et al.* Pyrosequencing analysis of the bacterial communities in the guts of honey bees *Apis cerana* and *Apis mellifera* in Korea. *J Microbiol* **50**, 735-745 (2012).

344 Morse, S. F. *et al.* Global distribution and genetic diversity of *Bartonella* in bat flies (Hippoboscoidea, Streblidae, Nycteribiidae). *Infect Genet Evol* **12**, 1717-1723 (2012).

345 Fournier, P. E. *et al. Bartonella australis* sp. nov. from kangaroos, Australia. *Emerg Infect Dis* **13**, 1961-1962 (2007).

346 Kosoy, M. *et al. Bartonella tamiae* sp. nov., a newly recognized pathogen isolated from three human patients from Thailand. *J Clin Microbiol* **46**, 772-775 (2008).

347 Colton, L., Zeidner, N., Lynch, T. & Kosoy, M. Y. Human isolates of *Bartonella tamiae* induce pathology in experimentally inoculated immunocompetent mice. *BMC Infect Dis* **10**, 229 (2010).

348 Milunovic, B., diCenzo, G. C., Morton, R. A. & Finan, T. M. Cell growth inhibition upon deletion of four toxin-antitoxin loci from the megaplasmids of *Sinorhizobium meliloti*. *J Bacteriol* **196**, 811-824 (2014).

349 Miller, W. G. *et al.* Diversity within the *Campylobacter jejuni* type I restriction–modification loci. *Microbiology* **151**, 337-351 (2005).

350 Chen, S. L. *et al.* Identification of genes subject to positive selection in uropathogenic strains of *Escherichia coli*: a comparative genomics approach. *Proc Natl Acad Sci U S A* **103**, 5977-5982 (2006).

351 Thomson, N. R. *et al.* The complete genome sequence and comparative genome analysis of the high pathogenicity *Yersinia enterocolitica* strain 8081. *PLoS Genet* **2**, e206 (2006).

352 Chopin, M.-C., Chopin, A. & Bidnenko, E. Phage abortive infection in lactococci: variations on a theme. *Curr Opin Microbiol* **8**, 473-479 (2005).

353 Klostermeier, D. Single-molecule FRET reveals nucleotide-driven conformational changes in molecular machines and their link to RNA unwinding and DNA supercoiling. *Biochem Soc Trans* **39**, 611-616 (2011).

354 Welner, D. *et al.* Protein expression, characterization, crystallization and preliminary X-ray crystallographic analysis of a Fic protein from *Clostridium difficile*. *Acta Crystallogr F Struct Biol Commun* **70**, 827-831 (2014).

355 Mishra, S. *et al.* Cloning, expression, purification, and biochemical characterisation of the FIC motif containing protein of *Mycobacterium tuberculosis*. *Protein Expr Purif* **86**, 58-67 (2012).

356 Chatterji, M., Sengupta, S. & Nagaraja, V. Chromosomally encoded gyrase inhibitor GyrI protects *Escherichia coli* against DNA-damaging agents. *Arch Microbiol* **180**, 339-346 (2003).

357 Davidsen, T., Tuven, H. K., Bjøras, M., Rødland, E. A. & Tønjum, T. Genetic interactions of DNA repair pathways in the pathogen *Neisseria meningitidis*. *J Bacteriol* **189**, 5728-5737 (2007).

358 Thomas, N. A., Ma, I., Prasad, M. E. & Rafuse, C. Expanded roles for multicargo and class 1B effector chaperones in type III secretion. *J Bacteriol* **194**, 3767-3773 (2012).

359 Harms, A. *FIC domains of Bartonella effector proteins - AMPylation and beyond* Master of Science thesis, University of Basel, (2010).

360 Alix, E. *et al.* The capping domain in RalF regulates effector functions. *PLoS Pathog* **8**, e1003012 (2012).

361 Dehio, M., Knorre, A., Lanz, C. & Dehio, C. Construction of versatile high-level expression vectors for *Bartonella henselae* and the use of green fluorescent protein as a new expression marker. *Gene* **215**, 223-229 (1998).

362 Bernard, P., Gabant, P., Bahassi, E. M. & Couturier, M. Positive-selection vectors using the F plasmid *ccdB* killer gene. *Gene* **148**, 71-74 (1994).

363 Meyer, R. Replication and conjugative mobilization of broad host-range IncQ plasmids. *Plasmid* **62**, 57-70 (2009).

364 Cascales, E., Atmakuri, K., Liu, Z., Binns, A. N. & Christie, P. J. *Agrobacterium tumefaciens* oncogenic suppressors inhibit T-DNA and VirE2 protein substrate binding to the VirD4 coupling protein. *Mol Microbiol* **58**, 565-579 (2005).

365 Segal, G. & Shuman, H. A. Intracellular multiplication and human macrophage killing by *Legionella pneumophila* are inhibited by conjugal components of IncQ plasmid RSF1010. *Mol Microbiol* **30**, 197-208 (1998).

366 Chen, L., Chen, Y., Wood, D. W. & Nester, E. W. A new type IV secretion system promotes conjugal transfer in *Agrobacterium tumefaciens*. *J Bacteriol* **184**, 4838-4845 (2002).

367 Nakashima, N. & Tamura, T. Gene silencing in *Escherichia coli* using antisense RNAs expressed from doxycycline-inducible vectors. *Lett Appl Microbiol* **56**, 436-442 (2013).

368 Chenoweth, M. R., Somerville, G. A., Krause, D. C., O'Reilly, K. L. & Gherardini, F. C. Growth characteristics of *Bartonella henselae* in a novel liquid medium: primary isolation, growth-phase-dependent phage induction, and metabolic studies. *Appl Environ Microbiol* **70**, 656-663 (2004).

369 Crick, F. *What mad pursuit : a personal view of scientific discovery*. (Basic Books, 1988).

370 Kuhn, A. Introduction to special issue on protein trafficking and secretion. *Biochim Biophys Acta* **1843**, 1429-1432 (2014).

371 Economou, A. & Dalbey, R. E. Preface to special issue on protein trafficking and secretion in bacteria. *Biochim Biophys Acta* **1843**, 1427 (2014).

372 Bonnington, K. E. & Kuehn, M. J. Protein selection and export via outer membrane vesicles. *Biochim Biophys Acta* **1843**, 1612-1619 (2014).

373 Christie, P. J., Whitaker, N. & Gonzalez-Rivera, C. Mechanism and structure of the bacterial type IV secretion systems. *Biochim Biophys Acta* **1843**, 1578-1591 (2014).

374 Raymond, B. *et al.* Subversion of trafficking, apoptosis, and innate immunity by type III secretion system effectors. *Trends Microbiol* **21**, 430-441 (2013).

375 Abby, S. S. & Rocha, E. P. The non-flagellar type III secretion system evolved from the bacterial flagellum and diversified into host-cell adapted systems. *PLoS Genet* **8**, e1002983 (2012).

376 Houben, E. N. G., Korotkov, K. V. & Bitter, W. Take five — Type VII secretion systems of Mycobacteria. *Biochim Biophys Acta* **1843**, 1707-1716 (2014).

377 Guglielmini, J., de la Cruz, F. & Rocha, E. P. C. Evolution of Conjugation and Type IV Secretion Systems. *Mol Biol Evol* **30**, 315-331 (2013).

378 de la Cruz, F., Frost, L. S., Meyer, R. J. & Zechner, E. L. Conjugative DNA metabolism in Gram-negative bacteria. *FEMS Microbiol Rev* **34**, 18-40 (2010).

379 Arutyunov, D. & Frost, L. S. F conjugation: back to the beginning. *Plasmid* **70**, 18-32 (2013).

380 Smillie, C., Garcillán-Barcia, M. P., Francia, M. V., Rocha, E. P. C. & de la Cruz, F. Mobility of Plasmids. *Microbiol Mol Biol Rev* **74**, 434-452 (2010).

381 Alvarez-Martinez, C. E. & Christie, P. J. Biological diversity of prokaryotic type IV secretion systems. *Microbiol Mol Biol Rev* **73**, 775-808 (2009).

382 Cabezón, E., Ripoll-Rozada, J., Peña, A., de la Cruz, F. & Arechaga, I. Towards an integrated model of bacterial conjugation. *FEMS Microbiol Rev*, n/a-n/a (2014).

383 Bellanger, X., Payot, S., Leblond-Bourget, N. & Guédon, G. Conjugative and mobilizable genomic islands in bacteria: evolution and diversity. *FEMS Microbiol Rev* **38**, 720-760 (2014).

384 Cavalli-Sforza, L. L. Forty years ago in "Genetics": the unorthodox mating behavior of bacteria. *Genetics* **132**, 635-637 (1992).

385 Ferrieres, L. *et al.* Silent mischief: bacteriophage Mu insertions contaminate products of *Escherichia coli* random mutagenesis performed using suicidal transposon delivery plasmids mobilized by broad-host-range RP4 conjugative machinery. *J Bacteriol* **192**, 6418-6427 (2010).

386 Guglielmini, J., Quintais, L., Garcillán-Barcia, M. P., de la Cruz, F. & Rocha, E. P. C. The Repertoire of ICE in Prokaryotes Underscores the Unity, Diversity, and Ubiquity of Conjugation. *PLoS Genet* **7**, e1002222 (2011).

387 Ding, H. & Hynes, M. F. Plasmid transfer systems in the rhizobia. *Can J Microbiol* **55**, 917-927 (2009).

388 Lopez-Guerrero, M. G. *et al.* Rhizobial extrachromosomal replicon variability, stability and expression in natural niches. *Plasmid* **68**, 149-158 (2012).

389 Landeta, C. *et al.* Plasmids with a chromosome-like role in rhizobia. *J Bacteriol* **193**, 1317-1326 (2011).

390 Jones, K. M., Lloret, J., Daniele, J. R. & Walker, G. C. The type IV secretion system of *Sinorhizobium meliloti* strain 1021 is required for conjugation but not for intracellular symbiosis. *J Bacteriol* **189**, 2133-2138 (2007).

391 Perez-Mendoza, D. *et al.* Identification of functional *mob* regions in *Rhizobium etli*: evidence for self-transmissibility of the symbiotic plasmid pRetCFN42d. *J Bacteriol* **186**, 5753-5761 (2004).

392 Gonzalez, V. *et al.* The mosaic structure of the symbiotic plasmid of *Rhizobium etli* CFN42 and its relation to other symbiotic genome compartments. *Genome Biol* **4**, R36 (2003).

393 Barnett, M. J. *et al.* Nucleotide sequence and predicted functions of the entire *Sinorhizobium meliloti* pSymA megaplasmid. *Proc Natl Acad Sci U S A* **98**, 9883-9888 (2001).

394 Pitzschke, A. *Agrobacterium infection* and plant defense—transformation success hangs by a thread. *Frontiers in plant science* **4**, 519 (2013).

395 Morton, E. R., Platt, T. G., Fuqua, C. & Bever, J. D. Non-additive costs and interactions alter the competitive dynamics of co-occurring ecologically distinct plasmids. *Proc Biol Sci* **281**, 20132173 (2014).

396 Nair, G. R., Liu, Z. & Binns, A. N. Reexamining the role of the accessory plasmid pAtC58 in the virulence of *Agrobacterium tumefaciens* strain C58. *Plant physiology* **133**, 989-999 (2003).

397 Perez-Mendoza, D. *et al.* The relaxase of the *Rhizobium etli* symbiotic plasmid shows nic site cis-acting preference. *J Bacteriol* **188**, 7488-7499 (2006).

398 Ghigo, J. M. Natural conjugative plasmids induce bacterial biofilm development. *Nature* **412**, 442-445 (2001).

399 Sun, Y. C., Jarrett, C. O., Bosio, C. F. & Hinnebusch, B. J. Retracing the evolutionary path that led to flea-borne transmission of *Yersinia pestis*. *Cell Host Microbe* **15**, 578-586 (2014).

400 Pinto, U. M., Pappas, K. M. & Winans, S. C. The ABCs of plasmid replication and segregation. *Nat Rev Microbiol* **10**, 755-765 (2012).

401 Berger, B. R. & Christie, P. J. Genetic complementation analysis of the *Agrobacterium tumefaciens virB* operon: *virB2* through *virB11* are essential virulence genes. *J Bacteriol* **176**, 3646-3660 (1994).

402 Jones, A. L., Barth, P. T. & Wilkins, B. M. Zygotic induction of plasmid *ssb* and *psiB* genes following conjugative transfer of Incl1 plasmid Collb-P9. *Mol Microbiol* **6**, 605-613 (1992).

403 Seubert, A., Falch, C., Birtles, R. J., Schulein, R. & Dehio, C. Characterization of the cryptic plasmid pBGR1 from *Bartonella grahamii* and construction of a versatile *Escherichia coli-Bartonell*a spp. shuttle cloning vector. *Plasmid* **49**, 44-52 (2003).

404 Saisongkorh, W., Robert, C., La Scola, B., Raoult, D. & Rolain, J.-M. Evidence of Transfer by Conjugation of Type IV Secretion System Genes between *Bartonella* Species and *Rhizobium radiobacter* in Amoeba. *PLoS One* **5**, e12666 (2010).

405 Sen, D. *et al.* Comparative genomics of pAKD4, the prototype IncP-1δ plasmid with a complete backbone. *Plasmid* **63**, 98-107 (2010).
406 Norberg, P., Bergstrom, M., Jethava, V., Dubhashi, D. & Hermansson, M. The IncP-1 plasmid backbone adapts to different host bacterial species and evolves through homologous recombination. *Nature Commun* **2**, 268 (2011).
407 Guglielmini, J. & Van Melderen, L. Bacterial toxin-antitoxin systems: Translation inhibitors everywhere. *Mobil Genet Elements* **1**, 283-290 (2011).
408 Madsen, J. S., Burmolle, M., Hansen, L. H. & Sorensen, S. J. The interconnection between biofilm formation and horizontal gene transfer. *FEMS Immunol Med Microbiol* **65**, 183-195 (2012).
409 Stavrinides, J., Ma, W. & Guttman, D. S. Terminal reassortment drives the quantum evolution of type III effectors in bacterial pathogens. *PLoS Pathog* **2**, e104 (2006).
410 Voth, D. E., Broederdorf, L. J. & Graham, J. G. Bacterial Type IV secretion systems: versatile virulence machines. *Future Microbiol* **7**, 241-257 (2012).
411 Hayes, C. S., Koskiniemi, S., Ruhe, Z. C., Poole, S. J. & Low, D. A. Mechanisms and biological roles of contact-dependent growth inhibition systems. Cold Spring Harb Persp Med **4** (2014).
412 Ma, L. S., Hachani, A., Lin, J. S., Filloux, A. & Lai, E. M. *Agrobacterium tumefaciens* deploys a superfamily of type VI secretion DNase effectors as weapons for interbacterial competition in planta. *Cell Host Microbe* **16**, 94-104 (2014).
413 Murdoch, S. L. *et al.* The opportunistic pathogen *Serratia marcescens* utilizes type VI secretion to target bacterial competitors. *J Bacteriol* **193**, 6057-6069 (2011).
414 Koraimann, G. & Wagner, M. A. Social behavior and decision making in bacterial conjugation. *Front Cell Infect Microbiol* **4**, 54 (2014).
415 Lanka, E. & Barth, P. T. Plasmid RP4 specifies a deoxyribonucleic acid primase involved in its conjugal transfer and maintenance. *J Bacteriol* **148**, 769-781 (1981).
416 Rees, C. E. & Wilkins, B. M. Protein transfer into the recipient cell during bacterial conjugation: studies with F and RP4. *Mol Microbiol* **4**, 1199-1205 (1990).
417 Parker, C. & Meyer, R. Mechanisms of Strand Replacement Synthesis for Plasmid DNA Transferred by Conjugation. *J Bacteriol* **187**, 3400-3406 (2005).
418 Parker, C. & Meyer, R. J. The R1162 relaxase/primase contains two, type IV transport signals that require the small plasmid protein MobB. *Mol Microbiol* **66**, 252-261 (2007).
419 Henderson, D. & Meyer, R. The MobA-Linked Primase Is the Only Replication Protein of R1162 Required for Conjugal Mobilization. *J Bacteriol* **181**, 2973-2978 (1999).
420 Tietze, E. Nucleotide Sequence and Genetic Characterization of the Novel IncQ-like Plasmid pIE1107. *Plasmid* **39**, 165-181 (1998).
421 Kehrenberg, C., Wallmann, J. & Schwarz, S. Molecular analysis of florfenicol-resistant *Pasteurella multocida* isolates in Germany. *J Antimicrob Chemother* **62**, 951-955 (2008).
422 Whittle, G., Katz, M. E., Clayton, E. H. & Cheetham, B. F. Identification and Characterization of a Native *Dichelobacter nodosus* Plasmid, pDN1. *Plasmid* **43**, 230-234 (2000).
423 Rohrer, J. & Rawlings, D. E. Sequence analysis and characterization of the mobilization region of a broad-host-range plasmid, pTF-FC2, isolated from *Thiobacillus ferrooxidans*. *J Bacteriol***174**, 6230-6237 (1992).
424 Bönemann, G., Stiens, M., Pühler, A. & Schlüter, A. Mobilizable IncQ-Related Plasmid Carrying a New Quinolone Resistance Gene, qnrS2, Isolated from the Bacterial Community of a Wastewater Treatment Plant. *Antimicrob Agents Chemother* **50**, 3075-3080 (2006).
425 Wilkins, B. M. & Thomas, A. T. DNA-independent transport of plasmid primase protein between bacteria by the I1 conjugation system. *Mol Microbiol* **38**, 650-657 (2000).
426 Henderson, D. & Meyer, R. J. The primase of broad-host-range plasmid R1162 is active in conjugal transfer. *J Bacteriol* **178**, 6888-6894 (1996).
427 Baharoglu, Z., Bikard, D. & Mazel, D. Conjugative DNA transfer induces the bacterial SOS response and promotes antibiotic resistance development through integron activation. *PLoS Genet* **6**, e1001165 (2010).

428 Delmas, S. & Matic, I. Interplay between replication and recombination in *Escherichia coli*: Impact of the alternative DNA polymerases. *Proc Natl Acad Sci U S A* **103**, 4564-4569 (2006).

429 Amarir-Bouhram, J., Goin, M. & Petit, M. A. Low efficiency of homology-facilitated illegitimate recombination during conjugation in *Escherichia coli*. *PLoS One* **6**, e28876 (2011).

430 Zaman, M. M. & Boles, T. C. Plasmid recombination by the RecBCD pathway of *Escherichia coli*. *J Bacteriol* **178**, 3840-3845 (1996).

431 Waldor, M. K. & Friedman, D. I. Phage regulatory circuits and virulence gene expression. *Curr Opin Microbiol* **8**, 459-465 (2005).

432 Lemire, S., Figueroa-Bossi, N. & Bossi, L. Bacteriophage crosstalk: coordination of prophage induction by trans-acting antirepressors. *PLoS Genet* **7**, e1002149 (2011).

433 Selva, L. *et al.* Killing niche competitors by remote-control bacteriophage induction. *Proc Natl Acad Sci U S A* **106**, 1234-1238 (2009).

434 Bagdasarian, M. *et al.* PsiB, and anti-SOS protein, is transiently expressed by the F sex factor during its transmission to an *Escherichia coli K-12* recipient. *Mol Microbiol* **6**, 885-893 (1992).

435 Golub, E., Bailone, A. & Devoret, R. A gene encoding an SOS inhibitor is present in different conjugative plasmids. *J Bacteriol* **170**, 4392-4394 (1988).

436 Ingmer, H., Miller, C. & Cohen, S. N. The RepA protein of plasmid pSC101 controls *Escherichia coli* cell division through the SOS response. *Mol Microbiol* **42**, 519-526 (2001).

437 Versalovic, J. & Lupski, J. R. Missense mutations in the 3' end of the Esch*erichia coli dnaG gene* do not abolish primase activity but do confer the chromosome-segregation-defective (par) *ph*enotype. *Microbiology* **143**, 585-594 (1997).

438 Norris, V., Alliotte, T., Jaffe, A. & D'Ari, R. DNA replication termination in *Escherichia coli parB* (a *dnaG* allele), *parA*, and *gyrB* mutants affected in DNA distribution. *J Bacteriol* **168**, 494-504 (1986).

439 Goldsmith, M., Sarov-Blat, L. & Livneh, Z. Plasmid-encoded MucB protein is a DNA polymerase (pol RI) specialized for lesion bypass in the presence of MucA', RecA, and SSB. *Proc Natl Acad Sci U S A* **97**, 11227-11231 (2000).

440 Taniguchi, Y. *et al.* Quantifying *E. coli* Proteome and Transcriptome with Single-Molecule Sensitivity in Single Cells. *Science* **329**, 533-538 (2010).

441 Reyes-Lamothe, R., Sherratt, D. J. & Leake, M. C. Stoichiometry and architecture of active DNA replication machinery in *Escherichia coli*. *Science* **328**, 498-501 (2010).

442 Georgescu, R. E., Yao, N. Y. & O'Donnell, M. Single-molecule analysis of the *Escherichia coli* replisome and use of clamps to bypass replication barriers. *FEBS Lett* **584**, 2596-2605 (2010).

443 Althorpe, N. J., Chilley, P. M., Thomas, A. T., Brammar, W. J. & Wilkins, B. M. Transient transcriptional activation of the IncI1 plasmid anti-restriction gene (*ardA*) and SOS inhibition gene (*psiB*) early in conjugating recipient bacteria. *Mol Microbiol* **31**, 133-142 (1999).

444 Loenen, W. A. & Raleigh, E. A. The other face of restriction: modification-dependent enzymes. *Nucleic Acids Res* **42**, 56-69 (2014).

445 Loftie-Eaton, W. & Rawlings, D. E. Diversity, biology and evolution of IncQ-family plasmids. *Plasmid* **67**, 15-34 (2012).

446 Løbner-Olesen, A., Marinus, M. G. & Hansen, F. G. Role of SeqA and Dam in *Escherichia coli* gene expression: a global/microarray analysis. *Proc Natl Acad Sci U S A* **100**, 4672-4677 (2003).

447 Babić, A., Lindner, A. B., Vulić, M., Stewart, E. J. & Radman, M. Direct Visualization of Horizontal Gene Transfer. *Science* **319**, 1533-1536 (2008).

448 Shintani, M. *et al.* Single-cell analyses revealed transfer ranges of IncP-1, IncP-7, and IncP-9 plasmids in a soil bacterial community. *Appl Environ Microbiol* **80**, 138-145 (2014).

449 del Campo, I. *et al.* Determination of conjugation rates on solid surfaces. *Plasmid* **67**, 174-182 (2012).

450 den Dulk-Ras, A., Vergunst, A. C. & Hooykaas, P. J. Cre Reporter Assay for Translocation (CRAfT): a tool for the study of protein translocation into host cells. *Methods Mol Biol* **1197**, 103-121 (2014).

451 Ji, W. *et al.* Specific Gene Repression by CRISPRi System Transferred through Bacterial Conjugation. *ACS Synth Biol* (2014).

452 Barrangou, R. & Marraffini, L. A. CRISPR-Cas systems: Prokaryotes upgrade to adaptive immunity. *Mol Cell* **54**, 234-244 (2014).

453 Sakalis, P. A., van Heusden, G. P. & Hooykaas, P. J. Visualization of VirE2 protein translocation by the *Agrobacterium* type IV secretion system into host cells. *MicrobiologyOpen* **3**, 104-117 (2014).

454 Alperi, A. *et al.* A Translocation Motif in Relaxase TrwC Specifically Affects Recruitment by Its Conjugative Type IV Secretion System. *J Bacteriol* **195**, 4999-5006 (2013).

455 Kienesberger, S. *et al.* Interbacterial macromolecular transfer by the *Campylobacter fetus* subsp. *venerealis* type IV secretion system. *J Bacteriol* **193**, 744-758 (2011).

456 Gorkiewicz, G. *et al.* A genomic island defines subspecies-specific virulence features of the host-adapted pathogen *Campylobacter fetus* subsp. *venerealis*. *J Bacteriol* **192**, 502-517 (2010).

457 Gyohda, A., Furuya, N., Ishiwa, A., Zhu, S. & Komano, T. Structure and function of the shufflon in plasmid r64. *Adv Biophys* **38**, 183-213 (2004).

458 Anthony, K. G., Sherburne, C., Sherburne, R. & Frost, L. S. The role of the pilus in recipient cell recognition during bacterial conjugation mediated by F-like plasmids. *Mol Microbiol* **13**, 939-953 (1994).

459 Watanabe, T., Arai, T. & Hattori, T. Effects of cell wall polysaccharide on the mating ability of *Salmonella typhimurium*. *Nature* **225**, 70-71 (1970).

460 Perez-Mendoza, D. & de la Cruz, F. *Escherichia coli* genes affecting recipient ability in plasmid conjugation: are there any? *BMC Genomics* **10**, 71 (2009).

461 Manoil, C. & Rosenbusch, J. P. Conjugation-deficient mutants of *Escherichia coli* distinguish classes of functions of the outer membrane OmpA protein. *Mol Gen Genet* **187**, 148-156 (1982).

462 Mizuta, M. *et al.* Screening for yeast mutants defective in recipient ability for transkingdom conjugation with *Escherichia coli* revealed importance of vacuolar ATPase activity in the horizontal DNA transfer phenomenon. *Microbiol Res* **167**, 311-316 (2012).

463 Lacroix, B., Tzfira, T., Vainstein, A. & Citovsky, V. A case of promiscuity: *Agrobacterium*'s endless hunt for new partners. *Trends Genet* **22**, 29-37 (2006).

464 Kwok, T. *et al. Helicobacter* exploits integrin for type IV secretion and kinase activation. *Nature* **449**, 862-866 (2007).

465 Gross, R. *et al.* The missing link: *Bordetella petrii* is endowed with both the metabolic versatility of environmental bacteria and virulence traits of pathogenic Bordetellae. *BMC Genomics* **9**, 449 (2008).

466 Aminov, R. I. Horizontal gene exchange in environmental microbiota. *Front Microbiol* **2**, 158 (2011).

467 McCarthy, A. J. *et al.* Extensive Horizontal Gene Transfer during *Staphylococcus aureus* Co-colonization *In Vivo*. *Genome Biol Evol* **6**, 2697-2708 (2014).

468 Coyne, M. J., Zitomersky, N. L., McGuire, A. M., Earl, A. M. & Comstock, L. E. Evidence of extensive DNA transfer between *Bacteroidales* species within the human gut. *mBio* **5**, e01305-01314 (2014).

469 Gal-Mor, O. & Finlay, B. B. Pathogenicity islands: a molecular toolbox for bacterial virulence. *Cell Microbiol* **8**, 1707-1719 (2006).

470 Boyd, E. F. Bacteriophage-encoded bacterial virulence factors and phage-pathogenicity island interactions. *Adv Virus Res* **82**, 91-118 (2012).

471 Lopez, C. A. *et al.* Phage-mediated acquisition of a type III secreted effector protein boosts growth of *salmonella* by nitrate respiration. *mBio* **3** (2012).

472 Ma, W., Dong, F. F., Stavrinides, J. & Guttman, D. S. Type III effector diversification via both pathoadaptation and horizontal transfer in response to a coevolutionary arms race. *PLoS Genet* **2**, e209 (2006).

473 Mebrhatu, M. T., Cenens, W. & Aertsen, A. An overview of the domestication and impact of the *Salmonella* mobilome. *Crit Rev Microbiol* **40**, 63-75 (2014).